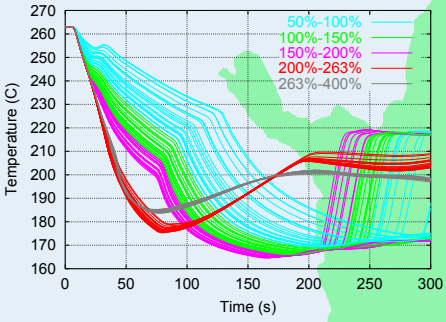

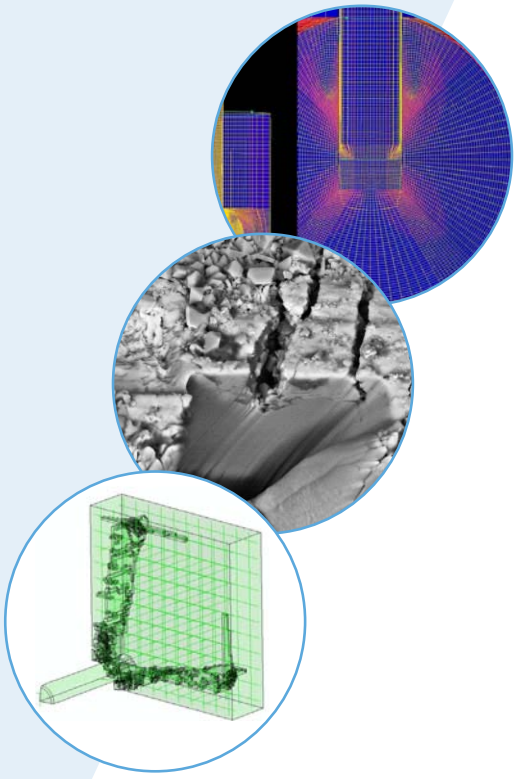

SAFIR2010, The Finnish Research Programme on Nuclear Power Plant Safety 2007–2010

Final Report

VTT TIEDOTTEITA – RESEARCH NOTES 2571

SAFIR2010

The Finnish Research Programme on Nuclear Power Plant Safety 2007–2010

Final Report

Eija Karita Puska & Vesa Suolanen (Eds.)

ISBN 978-951-38-7689-0 (soft back ed.)
ISSN 1235-0605 (soft back ed.)

ISBN 978-951-38-7690-6 (URL: http://www.vtt.fi/publications/index.jsp)
ISSN 1455-0865 (URL: http://www.vtt.fi/publications/index.jsp)

JULKAISIJA – UTGIVARE – PUBLISHER

VTT, Vuorimiehentie 5, PL 1000, 02044 VTT
puh. vaihde 020 722 111, faksi 020 722 7001

VTT, Bergsmansvägen 5, PB 1000, 02044 VTT
tel. växel 020 722 111, fax 020 722 7001

VTT Technical Research Centre of Finland, Vuorimiehentie 5, P.O. Box 1000, FI-02044 VTT, Finland
phone internat. +358 20 722 111, fax +358 20 722 7001

Edita Prima Oy, Helsinki 2011

SAFIR2010. The Finnish Research Programme on Nuclear Power Plant Safety 2007–2010. Final Report. Eija Karita Puska & Vesa Suolanen (Eds.). Espoo 2011. VTT Tiedotteita – Research Notes 2571. 578 p.

Keywords nuclear safety, safety management, nuclear power plants, human factors, automation systems, operating practices, control room technology, nuclear fuels, reactor physics, thermal hydraulics, core transient analysis, steam generators, modelling, accidents, structural safety

Abstract

Major part of Finnish public research on nuclear power plant safety during the years 2007–2010 has been carried out in the SAFIR2010 programme. The steering group of SAFIR2010 consisted of representatives from Radiation and Nuclear Safety Authority (STUK), Ministry of Employment and the Economy (MEE), Technical Research Centre of Finland (VTT), Teollisuuden Voima Oyj (TVO), Fortum Power and Heat Oyj, Fortum Nuclear Services Oy (Fortum), Finnish Funding Agency for Technology and Innovation (Tekes), Aalto University School of Science and Technology (Aalto, former Helsinki University of Technology) and Lappeenranta University of Technology (LUT). In addition to representatives of these organisations, the Steering Group had permanent experts from the Swedish Radiation Safety Authority (SSM) and Fennovoima Oy (Fennovoima).

SAFIR2010 research programme was divided in eight research areas that were Organisation and human, Automation and control room, Fuel and reactor physics, Thermal hydraulics, Severe accidents, Structural safety of reactor circuit, Construction safety, and Probabilistic Safety Analysis (PSA).

Research projects of the programme were chosen on the basis of annual call for proposals. The annual volume of the SAFIR2010-programme in 2007–2010 has been 6,5–7,1 M€ and approximately 50 person years. Main funding organisations in 2007–2010 have been the State Waste Management Fund VYR with 2,7–3,0 M€ and VTT with 2,4–2,7 M€ annually. In 2010 research was carried out in 33 projects.

The research in the programme has been carried out primarily by VTT Technical Research Centre of Finland. Other research units responsible for the projects solely or in co-operation with other institutions include Lappeenranta University of Technology, Aalto University (previously Helsinki University of

Technology), Tampere University of Technology, Fortum Power and Heat Oy (previously Fortum Nuclear Services Oy), Finnish Institute of Occupational Health and Finnish Meteorological Institute. In addition, there have been a few minor subcontractors in some projects.

The programme management structure consisted of the steering group, a reference group in each of the eight research areas and a number of ad hoc groups in the various research areas.

This report gives a summary of the technical results of the SAFIR2010 programme from the entire programme with emphasis on the results achieved during the years 2009–2010. The results obtained during the years 2007–2008 have been reported in detail in the Interim Seminar Report.

Preface

SAFIR2010, The Finnish Research Programme on Nuclear Power Plant Safety 2007–2010 continued the tradition of Finnish national research programmes in nuclear energy. Organisation of public nuclear energy research in Finland as national research programmes was started in 1989 by the Ministry of Trade and Industry. Since then national programmes have been carried out first separately in the fields of operational aspects of safety and structural safety (YKÄ 1990–1994, RETU 1995–1998, RATU 1990–1994, RATU2 1995–1998), and then in combined programmes (FINNUS 1999–2002, SAFIR 2003–2006). Simultaneously research has been carried out in the national nuclear waste management programmes (JYT 1989–1993, JYT2 1994–1996, JYT2001 1997–2001, KYT 2002–2005, KYT2010 2006–2010, KYT2014 2011–2014).

SAFIR2010 research programme has been divided in eight research areas that are Organisation and human, Automation and control room, Fuel and reactor physics, Thermal hydraulics, Severe accidents, Structural safety of reactor circuit, Construction safety, and Probabilistic Safety Analysis (PSA).

The research in the programme has been carried out primarily by VTT Technical Research Centre of Finland. Other research units responsible for the projects solely or in co-operation with other institutions include Lappeenranta University of Technology, Aalto University School of Science and Technology (previously Helsinki University of Technology), Tampere University of Technology, Fortum Power and Heat Oy (previously Fortum Nuclear Services Oy), Finnish Institute of Occupational Health and Finnish Meteorological Institute. In addition, there have been a few minor subcontractors in some projects.

The programme management structure has consisted of the steering group, a reference group in each of the eight research areas and a number of ad hoc groups in the various research areas. The steering group of SAFIR2010 consisted of representatives from Radiation and Nuclear Safety Authority (STUK),

Ministry of Employment and the Economy (MEE), Technical Research Centre of Finland (VTT), Teollisuuden Voima Oyj (TVO), Fortum Power and Heat Oyj, Fortum Nuclear Services Oy (Fortum), Finnish Funding Agency for Technology and Innovation (Tekes), Aalto University (Aalto, former Helsinki University of Technology) and Lappeenranta University of Technology (LUT). In addition to representatives of these organisations, the Steering Group had permanent experts from the Swedish Radiation Safety Authority (SSM) and Fennovoima Oy (Fennovoima).

Besides the research done within SAFIR2010 and education of experts via this research, SAFIR2010 has been an important national network and forum of information exchange for all parties involved.

This report has been prepared by the programme management in cooperation with the project leaders and project staff.

More information on SAFIR2010 is found in http://www.vtt.fi/safir2010. Finnish national research on nuclear power plant safety continues in SAFIR2014 programme for the years 2011–2014. http://safir2014.vtt.fi

Contents

1. Introduction

1.1 Role of SAFIR2010 in Finnish Nuclear Safety Research

The Finnish National Research Programme on Reactor Safety for the period 2007–2010, SAFIR2010 was strongly based on the chapter 7a, "Ensuring expertise", of the Finnish Nuclear Energy Act with the objective "to ensure that, should such new factors concerning safe operation of nuclear facilities emerge that could not be foreseen, the authorities have such sufficient and comprehensive nuclear engineering expertise and other facilities at their disposal that can be used, when necessary, to analyse without delay the significance of such factors".

The objective of SAFIR2010 has been realised in the research work. Besides producing top level scientific results SAFIR2010 has been also an increasingly important platform in education of experts. SAFIR2010 has been an important network in Finland both in domestic and in international matters, too.

In the Finnish nuclear scene the period of SAFIR2010 has been very active with the renewal of the operation permit of plant units Loviisa 1 and 2 and the periodic safety review of the plant units Olkiluoto 1 and 2 as well as continuous technical updates taking place at both sites. The construction of Olkiluoto 3 unit has continued and on July 2, 2010 the Finnish Parliament accepted the applications of Fennovoima Oy and Teollisuuden Voima Oyj for a decision-in-principle on constructing new nuclear power plant units. During the period of SAFIR2010 a new player, the Fennovoima Oy, has entered the Finnish nuclear scene.

Research on nuclear safety requires profound training and commitment. The research programme has provided the backbone for this activity. During the period of SAFIR2010 the experts who have taken part in construction and use of the currently operating plants have been retiring and the speed of retirement will increase in the coming years. The licensing processes and the possibility to recruit new persons

in research projects have given an opportunity to experts from different generations to work together and thus transfer the knowledge to the younger generation.

Globalisation and networking highlight the importance of national safety research. The national research programme is an important channel for information exchange, and provides a chance to direct limited national resources to the most useful international research programmes in a more focused manner.

Figure 1. Organisations represented in the SAFIR2010 Steering Group.

The steering group of SAFIR2010 consists of representatives from Radiation and Nuclear Safety Authority (STUK), Ministry of Employment and the Economy (MEE), Technical Research Centre of Finland (VTT), Teollisuuden Voima Oyj (TVO), Fortum Power and Heat Oy, Fortum Nuclear Services Oy (Fortum), Finnish Funding Agency for Technology and Innovation (Tekes), Aalto University (Aalto) and Lappeenranta University of Technology (LUT). In addition to representatives of these organisations, the Steering Group has permanent experts from the Swedish Radiation Safety Authority (SSM) and Fennovoima Oy (Fennovoima).

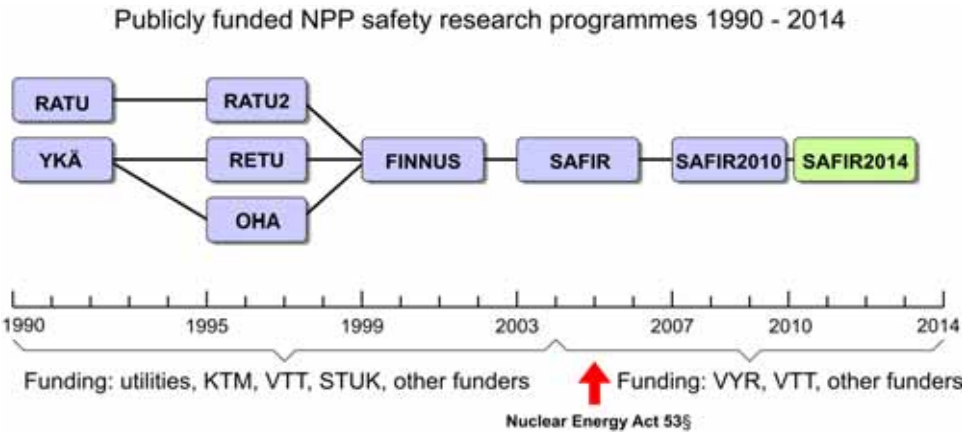

Figure 2. The history of Finnish research programmes on NPP safety.

The SAFIR2010 programme has taken advantage of the results obtained and lessons learned in the proceeding national research programmes. The programmes in the area of nuclear safety (YKÄ & RATU 1990–1994, RETU&RATU2 1995–1998, FINNUS 1999–2002, SAFIR 2003–2006 and SAFIR2010 2007–2010) have had the total volume of 102,5 M€ and 886 person years. According to the final reports of the successive programmes they have produced 3 300 publications in various categories and 33 Doctor, 18 Licentiate and 92 Master level academic degrees. The extent of the various programmes is given in Table 1. The Finnish public nuclear safety research will continue in the SAFIR2014 programme during the years 2011–2014.

Table 1. Finnish national research programmes on NPP safety in 1990–2010.

Programme	Volume, M€	Volume, person years	Total number of publications	Academic degrees		
				Dr.	Lic.	M.Sc.
YKÄ 1990–1994	15,4	168	318	6	5	10
RATU 1990–1994	8,2	76	322	1	3	3
RETU 1995–1998	9,8	107	405	3	2	2
RATU2 1995–1998	7,5	60	280	3	4	11
FINNUS 1999–2002	14,4	130	564	6	2	18
SAFIR 2003–2006	19,7	148	545	6	1	17
SAFIR2010 2007–2010	27,5	197	866	8	1	31

1.2 Research areas and projects

Research in SAFIR2010 has been conducted according to the Framework Plan [1], the Annual Plans [2–5] and decisions of the Steering and Reference Groups and additional quidance given in the management handbook [6]. The research has been to a large extent continuation of the research themes in the proceeding programme SAFIR [7, 8]. The research areas and research needs were defined in the Framework plan. SAFIR2010 research programme was divided in eight research areas, which were:

1. Organisation and human factors
2. Automation and control room
3. Fuel and reactor physics
4. Thermal hydraulics
5. Severe accidents
6. Structural safety of reactor circuit
7. Construction safety
8. Probabilistic safety analysis (PSA).

These research areas included both research projects of the named topic and interdisciplinary co-operation projects. Each research area had a Reference Group that consisted of experts from all organisations involved in the Steering Group. The Reference Groups had the responsibility on scientific guidance and supervisory in their area.

In 2010 research was carried out in 33 projects. VTT was the responsible research organisation in 26 of these projects and VTT was also the coordination unit of the programme. During the duration of the SAFIR2010 programme there have been altogether 39 separate research projects. In Table 2 the summary of the volumes of the projects in 2007–2010 is given.

The scientific results of the programme have been reported in the Annual Reports [9–12], in the Interim Seminar [13] and in the complete set of publications of the programme that have been distributed to the organisations represented in the Steering Group.

Table 2. The research projects of SAFIR2010 in 2007–2010.

			Funding (thousand Euro)				Volume (person-years)				
Group	**Project and principal research organisation**	**Acronym**	**2007**	**2008**	**2009**	**2010**	**2007**	**2008**	**2009**	**2010**	**Total**
1.						plan	y	y	y	y	
	Safety management and organisatorial learning *VTT*	MANOR	183,6	215,0	249,9	213,3	1,14	1,3	1,43	1,24	5,11
	Expert work in safety critical environment *TTL*	SAFEX	90,2	110,9	124,2	153,5	1,1	1,2	1,25	1,24	4,79
2.											
	Model-based safety evaluation of automation systems *VTT*	MODSAFE	185,6	190,6	188,0	178,0	1,48	1,63	1,7	1,48	6,29
	Certification facilities for software *VTT*	CERFAS	110,0	110,0	113,4	106,3	1,2	1,14	1,25	0,93	4,52
	Operator practices and human-system interfaces in computer-based control stations *VTT*	OPRACTICE	226,6	225,7	234,6	217,3	1,62	1,6	1,62	1,48	6,32
	Requirements engineering in nuclear power plant automation *Aalto*	VAHAYA	-	-	-	73,2	-	-	-	0,52	0,52
3.											
	Development and validation of fuel performance codes *VTT*	POKEVA	341,4	354,1	332,1	331,8	3,25	3,44	3,12	2,48	12,29
	Tridimensional core transient analysis methods *VTT*	TRICOT	305,2	283,3	322,9	319,2	2,2	1,8	2,25	2,16	8,41
	Total reactor physics analysis system *VTT*	TOPAS	285,4	307,9	307,1	303,3	2,43	2,68	2,76	2,31	10,18

4.											
	Numerical modelling of condensation pool *VTT*	NUMPOOL	98,8	100,4	105,4	101,9	0,67	0,7	0,76	0,65	2,78
	Improved thermal hydraulic analyses of nuclear reactor and containment *VTT*	THARE	296,1	321,1	339,3	321,9	2,3	2,4	2,2	1,76	8,66
	The integration of thermal-hydraulics (CFD) and structural analyses (FEA) computer codes in liquid and solid mechanics *Fortum*	MULTI-PHYSICS	82,0	-	-	-	0,51	-	-	-	0,51
	CFD modelling of NPP steam generators *VTT*	SGEN	-	127,9	106,3	121,2	-	1,02	0,84	0,83	2,69
	Improvement of PACTEL facility simulation *LUT*	PACSIM	-	80,4	108,1	83,0	-	1,05	1,4	0,96	3,41
	Participation in development of European calculation environment *LUT*	ECE	65,0	-	-	-	0,76	-	-	-	0,76
	Condensation experiments with PPOOLEX facility *LUT*	CONDEX	326,0	303,7	288,3	268,7	2,5	2,54	2,3	1,9	9,24
	Large break loss of coolant accident test study *LUT*	LABRE	54,9	-	-	-	0,48	-	-	-	0,48
	Large break loss of coolant test rig *LUT*	LABRIG	-	34,3	-	-	-	0,4	-	-	0,4
	Passive safety system simulation *LUT*	PASSIMU	-	-	31,5	43,3	-	-	0,29	0,39	0,68
	OpenFOAM CFD-solver for nuclear safety related flow simulations *Fortum*	NUFOAM	-	-	-	84,5	-	-	-	0,72	0,72

5.											
	Release of radioactive materials from a degrading core *VTT*	RADECO	85,2	85,9	85,3	115,9	0,54	0,7	0,54	0,86	2,64
	Primary circuit chemistry of fission products *VTT*	CHEMPC	316,0	208,7	275,7	281,0	3,4	1,4	1,48	1,67	7,95
	Core melt stabilization *VTT*	COMESTA	232,9	265,3	221,9	194,5	1,53	1,54	1,18	1,1	5,35
	Hydrogen risk in containments and particle bed issues *VTT*	HYRICI	153,2	153,1	-	-	0,98	0,98	-	-	1,96
	Hydrogen, debris coolability and SFP accidents *VTT*	HYBCIS	-	-	192,5	-	-	-	1,12	-	1,12
	Hydrogen combustion risk and core debris coolability *VTT*	HYBCIS2	-	-	-	175,3	-	-	-	1,05	1,05
6.											
	Risk-Informed Inspections of Piping *VTT*	PURISTA	218,2	222,8	222,4	178,6	1,56	1,35	1,2	1,08	5,19
	Fatigue endurance of critical equipment *VTT*	FATE	117,3	114,0	184,4	233,4	0,67	0,75	1,24	1,27	3,93
	Water chemistry and oxidation in the primary circuit *VTT*	WATCHEM	170,3	148,1	142,3	141,2	1,14	0,9	0,86	0,8	3,7
	Monitoring of the structural integrity of reactor circuit *VTT*	RAKEMON	214,7	206,3	230,9	226,2	1,52	1,2	1,62	1,52	5,86
	Fracture assessment of reactor circuit *VTT*	FRAS	365,0	522,2	379,0	392,1	2,9	4	2,3	2,74	11,94
	Influence of material, environment and strain rate on environmentally assisted cracking of austenitic nuclear materials *VTT*	DEFSPEED	346,6	445,1	418,1	413,7	2,7	3,3	2,95	1,8	10,75
	Renewal of active materials research infrastructure *VTT*	AKTUS	-	-	126,4	104,0	-	-	0,7	0,62	1,32

7.											
	Service life management system of concrete structures in nuclear power plants *VTT*	SERVICE-MAN	123,4	210,0	193,0	215,3	0,86	1,1	1,32	1,38	4,66
	IMPACT2010 *VTT*	IMPACT	632,2	531,8	441,1	570,0	4,5	3,9	2,5	3,52	14,42
	Structures under soft impact *VTT*	SUSI	163,7	190,2	204,1	184,1	1,14	1,38	1,3	1,14	4,96
8.											
	Challenges in risk-informed safety management *VTT*	CHARISMA	254,2	277,3	274,5	281,6	1,93	1,7	1,8	2	7,43
	Implementation of quantitative fire risk assessment in PSA *VTT*	FIRAS	164,6	180,0	177,9	158,0	1,2	1,2	1,2	0,89	4,49
	Extreme weather and nuclear power plants *FMI*	EXWE	89,2	204,9	176,9	96,2	1	1,5	1,8	1,14	5,44
9.	SAFIR2010 Administration and information (2007–2010) *VTT*	SAHA	188,3	175,0	184,2	236,7	0,9	0,9	0,86	0,95	3,61
	Total		**6485,8**	**6906,0**	**6981,7**	**7118,2**	**50,11**	**50,7**	**49,14**	**46,58**	**196,53**

1.3 Statistical information

The annual volume of the SAFIR2010-programme in 2007–2010 has been 6,5–7,1 M€ and approximately 50 person years. Main funding organisations in 2007–2010 were State Waste Management Fund VYR with 2,7–3,0 M€ and VTT with 2,4–2,7 M€ annually. The research in the programme has been carried out primarily by VTT Technical Research Centre of Finland. Other research units responsible for the projects solely or in co-operation with other institutions have include Lappeenranta University of Technology, Helsinki University of Technology / Aalto University, Tampere University of Technology, Fortum Nuclear Services Oy / Fortum Power and Heat Oy, Finnish Institute of Occupational Health and Finnish Meteorological Institute. In addition, there have been a few minor subcontractors in some projects.

Distribution of total funding in the SAFIR2010 research areas in 2007–2010 is shown in Figure 3. The corresponding distribution of the VYR-funding to the various research areas is shown in Figure 4. Distribution of funding and person years in the eight research areas of SAFIR2010 in 2010 have been illustrated in Figures 5 and 6 respectively.

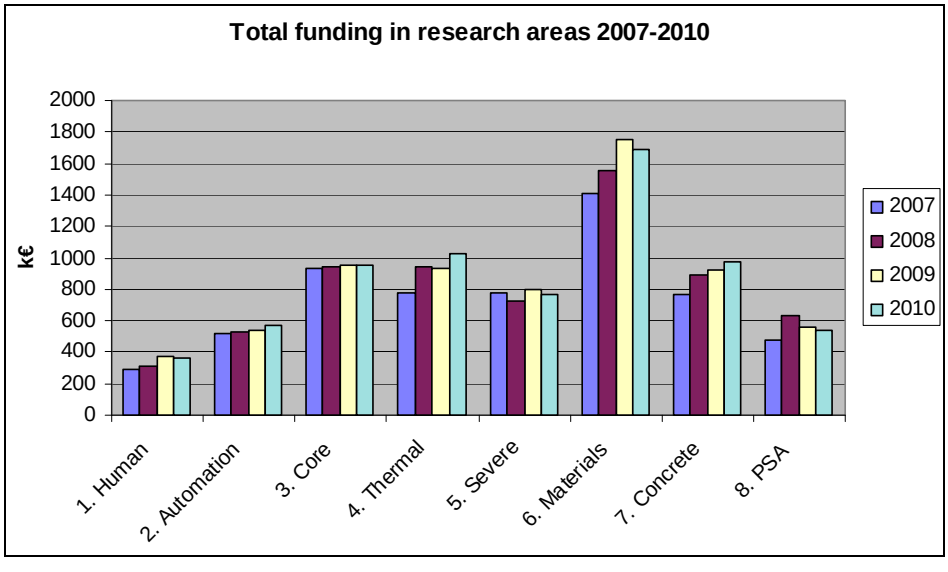

Figure 3. Distribution of total funding in the SAFIR2010 research areas in 2007–2010.

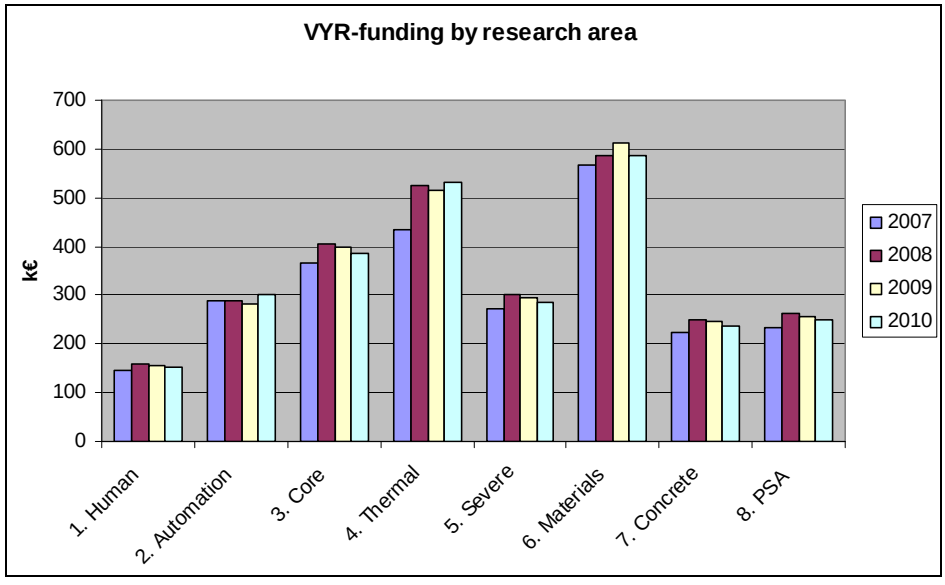

Figure 4. Distribution of VYR funding in the SAFIR2010 research areas in 2007–2010.

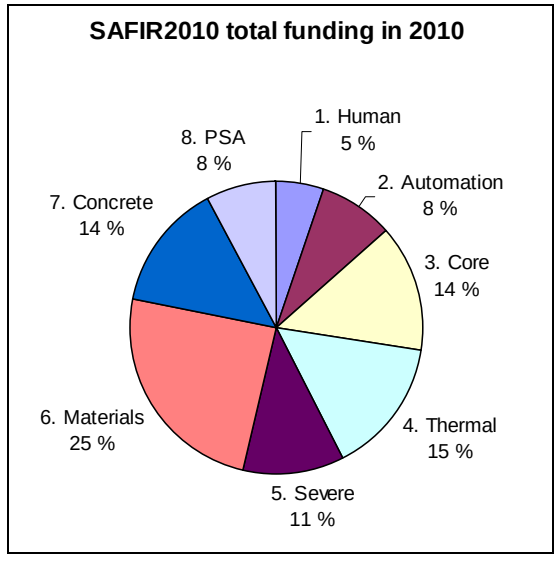

Figure 5. Distribution of funding in the SAFIR2010 research areas in 2010.

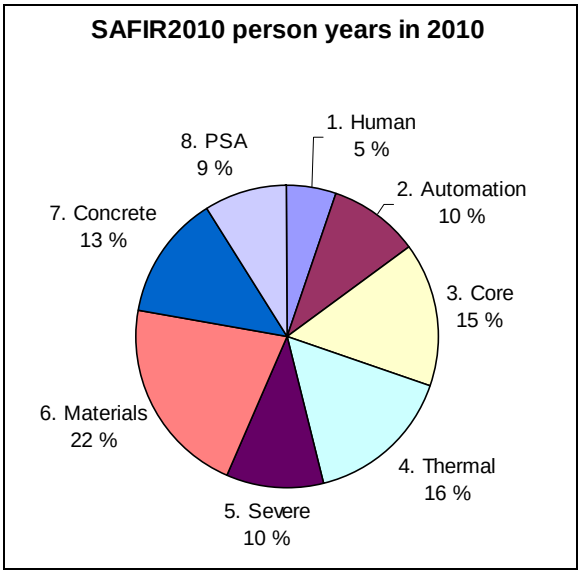

Figure 6. Distribution of person years in the SAFIR2010 research areas in 2010.

Figures 7 and 8 illustrate the funding sources and cost structure of SAFIR2010 in the year 2010.

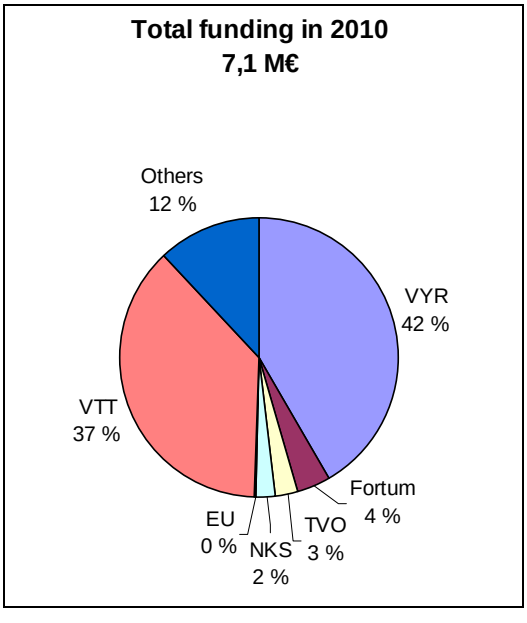

Figure 7. Funding sources in SAFIR2010 in 2010.

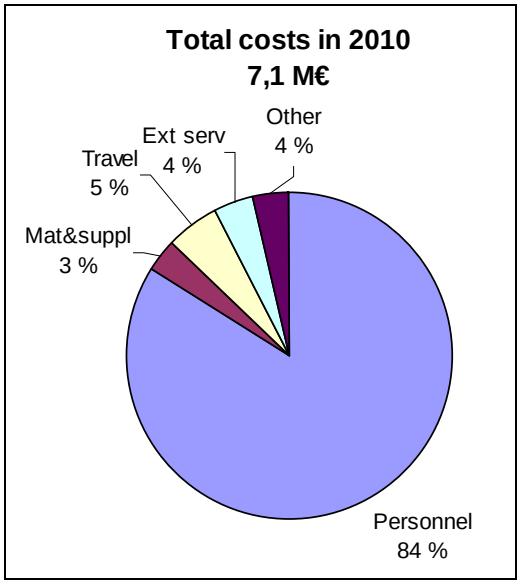

Figure 8. Cost structure in SAFIR2010 in 2010.

The programme has produced 866 publications in 2007–2010. Major part of the publications consisted of conference papers and extensive research institute reports. The number of scientific publications as well as the total number of publications varied greatly between the projects, as indicated in Table 3. The average number of publications is 4,4 per person year, and the average number of scientific publications is 0,5 per person year. Many projects have deliberately aimed at publication of the results as extensive research institute reports that are found to be more useful to the end-users than scientific publications, which has to be taken into account when judging the numbers of publications in different categories.

Table 3. Publications in the SAFIR2010 projects in 2007–2010.

Project	Scientific	Conference papers	Res. inst. reports	Others	Total	Volume pers. year
MANOR	6	13	7	7	33	5,11
SAFEX	4	14	3	7	28	4,79
MODSAFE	0	6	8	2	16	6,29
CERFAS	2	13	6	1	22	4,52
OPRACTICE	6	23	11	9	49	6,32
VAHAYA	0	0	0	1	1	0,52
POKEVA	1	6	32	0	39	12,29
TRICOT	2	10	26	2	40	8,41
TOPAS	14	12	10	4	40	10,18
NUMPOOL	0	4	4	0	8	2,78
THARE	1	3	18	17	39	8,66
MULTIPHYSICS	0	0	1	0	1	0,51
SGEN	0	2	7	2	11	2,69
PACSIM	1	2	9	2	14	3,41
ECE	0	0	0	1	1	0,76
CONDEX	2	2	13	7	24	9,24
LABRE	0	0	1	0	1	0,48
LABRIG	0	0	1	1	2	0,4
PASSIMU	0	0	2	0	2	0,68
NUFOAM	0	0	11	0	11	0,72
RADECO	0	0	7	0	7	2,64
CHEMPC	6	15	12	4	37	7,95
COMESTA	6	8	13	1	28	5,35
HYRICI	0	3	4	1	8	1,96
HYBCIS	1	3	1	0	5	1,12
HYBCIS2	1	0	2	1	4	1,05
PURISTA	8	20	13	10	51	5,19
FATE	0	4	3	1	8	3,93
WATCHEM	10	0	8	0	18	3,7
RAKEMON	0	8	10	2	20	5,86
FRAS	5	10	27	3	45	11,94
DEFSPEED	6	10	15	13	44	10,75
AKTUS	0	0	0	1	1	1,32
SERVICEMAN	1	9	11	2	23	4,66
IMPACT&SUSI	3	6	9	1	19	19,38
CHARISMA	1	24	20	22	67	7,43
FIRAS	8	12	12	6	38	4,49
EXWE	9	13	15	11	48	5,44
SAHA	0	0	11	2	13	3,61
TOTAL	**104**	**255**	**363**	**144**	**866**	**196,53**

Education of new experts has been an important task in SAFIR2010. The academic degrees obtained in the various projects have been given in Table 4. There were altogether 8 Doctoral, 1 Licentiate and 31 Master level degrees.

Table 4. Academic degrees obtained in the projects in 2007–2010.

Project	Doctor	Licentiate	Master
MANOR	1		
SAFEX		1	1
MODSAFE			1
CERFAS			1
OPRACTICE			1
POKEVA			2
TRICOT			1
TOPAS	3		2
THARE	1		
PACSIM			1
CONDEX	1		
LABRIG			1
CHEMPC			2
WATCHEM			1
FRAS			3
DEFSPEED	1		1
SERVICEMAN			1
IMPACT2010			1
CHARISMA			1
FIRAS	1		1
EXWE			9
TOTAL	**8**	**1**	**31**

1.4 Administration, seminars and international evaluation

The programme management bodies, the steering group and the eight reference groups, have met on regular basis 4–5 times annually. The ad hoc groups that have a vital role for several projects have carried out successfully their tasks.

The ad hoc groups have met upon the needs of the specific project. The number of ad hoc groups increased steadily during the period of SAFIR2010. The programme has been managed by the coordination unit VTT, the programme director, the project co-ordinator and the project managers of the individual research projects.

The information on the research performed in SAFIR2010 has been communicated formally via the quarterly progress reports, the annual plans and annual reports of the programme and the www-pages of the programme. Additional information has been given in seminars organised by various research projects. The detailed scientific results have been published as articles in scientific journals, conference papers, and separate reports.

Major events during the SAFIR2010 have been the Interim Seminar in March 2009 [13] with some 200 participants, approximately 10% from abroad, the international evaluation of the programme in January 2010 with project presentations, interviews of the steering and reference group members, exit meeting and final evaluation report [14] giving also recommendations for the next programme and Planning Seminar of SAFIR2014 in April 2010 [15] resulting in the continuation of the NPP safety research in the SAFIR2014 programme [16].

In addition to conducting the actual research according to the yearly plans, SAFIR2010 has been an efficient way of information exchange with all organisations operating in the nuclear energy sector and as an open discussion forum for participation in international projects, allocation of resources and in planning of new projects.

1.5 Structure of the report

The report contains presentation of the main scientific achievements of the projects in Chapters 2–33 both in the format of project overviews and special technical reports. For the statistical information on publications, academic degrees and project personnel as well as the list of the Steering Group, Reference Group and Ad Hoc Group members reference is made to the Annual Plans and Annual Reports at the SAFIR2010 www-pages.

1.6 Acknowledgements

The results of the SAFIR2010 programme have been produced by all those involved in the actual research projects. Their work is highly esteemed.

The contributions of project managers and project staff that form the essential contents of this report are acknowledged with gratitude.

The work of the persons in the Steering Group, Reference Groups and Ad Hoc Groups that has been carried out with the expense of their home organisations is highly appreciated.

Eija Karita Puska and Vesa Suolanen

References

1. National Nuclear Power Plant Safety Research 2007–2010. Proposal for SAFIR2010 Framework Plan. Publications of the Ministry of Employment and the Economy, 31/2006.

2. Puska, E.K. & Suolanen, V. SAFIR2010 Annual Plan 2007. VTT, Espoo, 2007. VTT Research Report VTT-R-06442-07. 36 p. + app. 177 p.

3. Puska, E.K. & Suolanen, V. SAFIR2010 Annual Plan 2008. VTT, Espoo, 2008. VTT Research Report VTT-R-02382-08. 34 p. + app. 180 p.

4. Puska, E.K. & Suolanen, V. SAFIR2010 Annual Plan 2009. VTT, Espoo, 2009. VTT Research Report VTT-R-03973-09. 34 p. + app. 186 p.

5. Puska, E.K. & Suolanen, V. SAFIR2010 Annual Plan 2010. VTT, Espoo, 2010. VTT Research Report VTT-R-03666-10. 37 p. + app. 203 p.

6. SAFIR2010 Toimintakäsikirja (SAFIR2010 Operations manual, living document at the project www-pages. In Finnish.)

7. Räty, H. & Puska, E.K. (Ed.). SAFIR. The Finnish Research Programme on Nuclear Power Plant Safety 2003–2006. Final Report. VTT, Espoo, 2006. VTT Research Notes 2363. 379 p. + app. 98 p. ISBN 951-38-6886-9; 951-38-6887-7. http://www.vtt.fi/inf/pdf/tiedotteet/2006/T2363.pdf.

8. Puska, E.K. (Ed.). SAFIR. The Finnish Research Programme on Nuclear Power Plant Safety 2003–2006. Executive Summary. VTT, Espoo, 2006. VTT Research Notes 2364. 36 p. + app. 33 p. ISBN 951-38-6888-5; 951-38-6889-3. http://www.vtt.fi/inf/pdf/tiedotteet/2006/T2364.pdf.

9. Puska, E.K. & Suolanen, V. SAFIR2010 Annual Report 2007. VTT, Espoo, 2008. VTT Research Report VTT-R-02381-08. 105 p. + app. 200 p.

10. Puska, E.K. & Suolanen, V. SAFIR2010 Annual Report 2008. VTT, Espoo, 2009. VTT Research Report VTT-R-04415-09. 102 p. + app. 184 p.

11. Puska, E.K. & Suolanen, V. SAFIR2010 Annual Report 2009. VTT, Espoo, 2010. VTT Research Report VTT-R-03922-10. 122 p. + app. 222 p.

12. Puska, E.K. & Suolanen, V. SAFIR2010 Annual Report 2010. VTT, Espoo, 20011. VTT Research Report VTT-R-01301-11. (To be published in March 2011.)

13. Puska, E.K. (Ed.). SAFIR2010. The Finnish Research Programme on Nuclear Power Plant Safety 2007–2010. Interim Report. VTT, Espoo, 2009. VTT Research Notes 2466. 535 p. ISBN 978-951-38-7266-3; 978-951-38-7267-0. http://www.vtt.fi/inf/pdf/tiedotteet/2009/T2466.pdf.

14. Bruna, G., Rastas A. & Schaefer, A. Evaluation of the Finnish Nuclear Safety Research Program SAFIR2010. Publications of the Ministry of Employment and the Economy, Energy and the climate 51/2010.

15. http://virtual.vtt.fi/virtual/safir2010/, SAFIR2014 strategy seminar.

16. National Nuclear Power Plant Safety Research 2011–2014. SAFIR2014 Framework Plan. Publications of the Ministry of Employment and the Economy, Energy and the climate 50/2010.

2. Safety Management and Organisatorial Learning (MANOR)

2.1 MANOR summary report

Pia Oedewald
VTT

Abstract

Deficiencies in organisational performance are often identified as major precursors of accidents. This is why safety-critical industries are increasingly becoming interested in understanding and managing organisational performance. Despite the significance of the organizational factors for system safety, organizational performance is not independent from the technical and economical context. Safety management should focus on the organisation as a whole. Manor-project identified a need to create a model which clarifies what is good safety performance in an organisation and how the hazards related to the technology as well as the management processes contribute to the overall safety culture. A model “Design for Integrated Safety Culture” was created as a basis for practical applications for multiple safety management practices which aim for taking the organisational behaviour into account.

Introduction

The interest towards human and organisational factors and their effect on the overall safety of nuclear power production has risen significantly during the past years in Finland. Practical steps have been taken at the power companies to utilise concepts and methods developed by behavioural and organisational

scientists. More than ten years of research on organisational culture, change management, learning of newcomers and safety culture has been carried out in the nuclear domain by VTT's researches. The research group has, for example, developed a methodology for organisational assessment and they have been active in the international safety science field [1]. This gives a good background for more focused analysis of the safety management practices, safety culture and practices of organizational learning.

The concepts of safety management, safety culture and organisational learning are defined in multiple different ways which sometimes causes confusion among practitioners. The multitude of definitions and approaches is, however, an important issue to take into consider among the managers and safety practitioners. For practitioners who aim for concrete changes in a real safety critical organisation it is of utmost importance to understand the consequences and limitations of the approach one chooses. There was a clear need to integrate the concepts and approaches used to cope with human and organisational aspects into one model and provide guidance on its utilisation.

Main objectives

The generic goal was to help the power companies and the regulator to create safety management practices that support the evaluation and management of the working practices and organizational performance based on a sound safety culture. The main objective of the research project was to study the facilitators and hindrances to organizational learning and development of safety culture in the nuclear power industry. The focus of the case studies of the project has been on the utilisation of operating experience and approaches for safety culture and human performance improvement at the plants and at the regulatory body.

Manor project was carried out as a sequence of case studies in Finland and in Sweden of which findings were combined with theoretical work.

Main results

The Manor-project found that both the power companies and the regulator found it rather difficult to systematically implement concepts and methods related to human and organisational factors as part of their safety management. For example, the statement that good safety culture is required from all organisations involved with the design, construction and operating of nuclear power plants [2] was considered as a rather vague requirement. What does good level safety

culture mean? How to prove it in practice? These questions have caused vivid discussion in Nordic nuclear communities. Furthermore, the requirement to implement lessons learned form operating experiences [3] has been interpreted as a demand for organisational learning. However, the question on how an organisation learns effectively has remained ambiguous for the power companies [4, 5].

The challenge in working with concepts such as safety culture, organisational learning and organisational evaluations stem partly from the fact that the organisations have had few behavioural and organisational science professionals. For some reason especially the power companies in Finland and largely in Sweden have tried to develop practices around these topics with their existing employees who typically have engineering background. Another reason for the challenges is that safety science, and behavioural science at the head, have clearly developed during the past ten years. There are not too many practical quidebooks for practitioners of the latests and most promising approaches. Thus, the nuclear community utilises information exchange across the companies and the international communities, such as IAEA and WANO, provide support on how to approach human errors, organisational learning, safety culture and safety management. However, the nuclear community is rather inconsistent with its safety management approaches and thus organisations utilise methods which don't have same basic assumptions and goals [6].

Management of safety is always guided by (an implicit) framework that is shared by a significant group of managers and employees working in safety critical surroundings. It contains usually assumptions about ways of evaluating, developing and maintaining safety. Thus it steers the evaluation of current challenges and strengths of the technology and the evaluation of the overall safety status of the activities. Conversely, it also defines things that are not taken into consideration, not emphasized, not evaluated and developed. People working in safety critical contexts often adopt these assumptions during their and when becoming socialized into the organization where they work. In essence, the gradual development of an approach for management of nuclear safety has been a process of development of certain type of culture in the nuclear domain [7, 8].

The nuclear industry has based its safety management on thorough risk control. Thus, it's understandable that it employs the same basic logics when it faces requirements to work with human and organisational issues. Current safety culture initiatives and event investigations, where human and organisational issues are analysed, aim to identify human errors or latent organisational weaknesses – and to find corrective actions to mitigate their effect on the technical reliability. The

nuclear organisations have gradually extended the risk control approach to cover human and organisational performance as well. An example of this is the popularity of the behavior based approaches [9], such as human performance programmes in the power companies. Although it's important that the basic risks related to certain types of human and organisational characteristics are identified, this type of safety management can provide only limited benefits on the nuclear safety in the long run. Thus safety scientists [10, 11, 12, 13] have proposed a paradigm shift towards approaches which:

- acqknowledge that humans are involved in all technical solutions (designing, building, operating, maintaining the technology) thus safety improvements and challenges cannot be divided into human and technical factors. The socio-technical system, such as certain activity in an organisation or the entire organisation, should be analysed as an entity.
- acqknowledge that human and social decision making characteristics are important for the reliability of high risk technology. The innovativeness and variability of human behaviour is more an asset than a safety problem. Thus, all the variation and flexibility of activities should not be dampened.
- acqknowledge that safety doesn't equal with absence of unwanted events. Safety is the system's ability or capability which cannot be judged solely from past outcomes.
- acqknowledge that in order to understand how safety could be increased and developed there should be a valid model of the system (the entity of humans working with certain technological solution in a certain organisational context). This requires basic knowledge on theories on human and organisational behavior.

Current safety management approaches in the nuclear field take the above mentioned premises into account partly. For example IAEA's safety culture model emphasises continuous improvement of organisational performance instead of identifying errors of individuals. Partly they work against these premises, for example operating experience practices usually differentiate events which have technical causes from those which have human causes, and these two categories may even be analysed by different organisations. This kind of inconsistency of safety management hinders the development of a sound safety culture. Furthermore the organisational learning may become inefficient because of

conflicting messages about e.g. the role of humans versus technology in the nuclear safety frustrates the employees or create confusions in communication.

Manor-project created models to describe how technical and organisational structures, management processes, individuals' psychological states and daily practices interact. The project clarified the basic premises behind the models as follows [1, 6, 13, 14, 15]:

- Safety is an emerging property of a system. Safety is not something that can be brought into the organisations along with technical solutions or management styles or new organizational structures, it emerges depending on the activities and outside conditions. It is impossible to understand safety by decomposing safety into predetermined set of factors and measuring them.
- Organisations, in turn, are systems which include the technology as well as the people using it. Organisational performance results from the interaction of humans with the object of their work and with each other in a certain environment with specified resources and technology. Organisations can also exceed the juridical boundaries of a company. Thus, a network of subcontractors in a shared work scope can be viewed an organisation as well.
- Safety management should aim at managing the organisation, not safety per se.
- To obtain an overview of safety of an organisation it is necessary to approach it from multiple viewpoints. It's important to pay attention to a) what kind of concrete and visible organisational systems and structures there exist (production technology, management systems, tools etc.), b) how people perceive and experience these systems and structures and their work in general, and c) how social interactions affect the previous.
- An organisation has good potential for safety when the following criteria are met in the organisational activity:
    1. Safety is a genuine value in the organisation which reflects to decision making and daily activities
    2. Safety is understood as a complex and systemic phenomenon
    3. Hazards and core task requirements are understood thoroughly

4. Organization is mindful in its practices
5. Responsibility for the safe functioning of the entire system is taken
6. Activities are organised in a manageable way.

– The above mentioned six criteria for good safety potential can be seen as criteria for safety culture. In other words we define organisation's safety culture as a potential for safe activities in the organisation.

– Organisational learning should promote development towards the same direction than the safety culture approach used in the organisation. Thus, the same criteria used to describe good safety culture can be utilised when trying to enhance organisational learning.

The Design for Integrated Safety Culture (DISC) -model [6, 16] was created to crystallize the characteristics of organisational safety and its organisational prerequisites. The DISC-model helps the organisations' to maintain their focus on the organisational level and management of overall safety, and not to pay unnecessary focus on the individual workers or technical failures, when they carry out activities e.g. on organisational learning, organisational safety evaluations and safety culture. The DISC-model also reminds the users that different organisational functions (such as change management, supervisory activity, competence management) should all serve the same purposes even though they are carried out by different units.

Figure 1. This figure presents the basic elements of the DISC-model; the criteria for good safety culture (inner circle) and the organisational functions (outer circle) which are necessary for developing good safety culture in the organisation.

Applications

The basic premises clarified in the Manor-project and the subseguent DISC-model provides a framework for many safety management practices. The model can be utilised in event investigations. This was tested in a study together with STUK, and the power companies. It can also be used in organisational evaluations for which the Manor group has provided a guidebook [16]. Manor has developed a safety culture survey, interview scheme and analysis criteria based on the DISC-model [16].

It has also been beneficial in evaluating the safety management and safety culture of Olkiluoto 3 construction site [17]. Further, it has served a background for discussing how to organise human factors and organisational development work in a power company [6].

Conclusions

Nuclear industry organisations are in process of utilising new safety management tools to cope with organisational phenomena and human characteristics. This requires them to critically inspect their overall safety management principles because the (quality) control type approach, which is developed for inspecting and verifying the reliability of the technology, fits poorly for organisational development. Manor-project integrated the theoretical work on system safety and human and organisational factors into the practical concepts and methods currently used in the plants in Finland and Sweden. The work resulted in e.g. the DISC-model. The Manor-project also provided multiple examples on how a shared model of the organisation and safety can help in designing interventions and communicating them to the all the stakeholders.

References

1. Reiman, T. Assessing organisational culture in complex sociotechnical systems – Methodological evidence from studies in nuclear power plant maintenance organisations. VTT, Espoo, 2007. VTT publications 627. ISBN 978-951-38-6993-9; 978-951-38-6994-6. http://www.vtt.fi/inf/pdf/publications/2007/P627.pdf.

2. Goverment Degree 733/2008, 28§ Safety culture.

3. STUK. YVL 1.11 Guide. Nuclear power plant operational experience feedback. 22 Dec. 1994.

4. Oedewald, P., Pietikäinen, E. & Haavisto, M.-L. Ydinvoima-alan organisaatioiden käyttökokemustoiminta organisaation oppimisen näkökulmasta. VTT, Espoo, 2010. Tutkimusraportti VTT-R- 01303-10.

5. Pietikäinen, E., Oedewald, P., Haavisto, M.-L., Reiman, T., Ruuhilehto, K. & Heikkilä, J. Pyrkivätkö turvallisuuskriittiset organisaatiot oppimaan kokemuksistaan? Kokemustiedon käsittelyä ohjaavat oletukset ydinvoimateollisuudessa ja terveydenhuollossa. Työelämän tutkimus – Arbetslivsforskning 2010, 8, pp. 279–290.

6. Oedewald, P., Reiman, T., Pietikäinen, E., Macchi, L. & Gotcheva, N. (Eds.) Safety management, safety culture and organisational learning in the nuclear industry. (To be published in VTT publication series 2011.)

7. Reiman, T., Pietikäinen, E., Kahlbom, U. & Rollenhagen, C. Safety Culture in the Finnish and Swedish Nuclear Industries – History and Present. NKS, Roskilde, Denmark, 2010. NKS-213.

8. Reiman, T. & Rollenhagen, C. Identifying the typical biases and their significance in the current safety management approaches. 10th International Probabilistic Safety Assessment & Management Conference, 7–11 June 2010, Seattle, USA, 2010.

9. Krause, T. The Behaviour-Based Safety Process. Van Nostrand Reinhold, New York, 1990.

10. Hollnagel, E., Woods, D. & Leveson, N. (Eds.) Resilience Engineering: Concepts and Precepts. Aldershot, UK: Ashgate, 2006.

11. Hollnagel, E. Safety management-Looking back or Looking forward. In: Hollnagel, Nemeth & Dekker (Eds.). Remaining sensitive to the possibility of failures. Ashgate, 2008.

12. SINTEF Resilience Engineering, the Sixth Perspective, 2009. A12404 ISBN 978-82-14-04834-6.

13. Reiman, T. & Oedewald, P. Turvallisuuskriittiset organisaatiot – Onnettomuudet, kulttuuri ja johtaminen. Edita, Helsinki, 2008.

14. Reiman, T., Pietikäinen, E. & Oedewald, P. Turvallisuuskulttuuri. Teoria ja arviointi. VTT, Espoo. 2008. VTT Publications 700. ISBN 978-951-38-7131-4; 978-951-38-7132-1. http://www.vtt.fi/inf/pdf/publications/2008/P700.pdf.

15. Reiman, T. & Oedewald, P. Evaluating safety critical organizations. Focus on the nuclear industry. Swedish Radiation Safety Authority, Research Report 2009:12. http://www.vtt.fi/inf/julkaisut/muut/2009/SSM-Rapport-2009-12.pdf.

16. Oedewald, P., Pietikäinen, E. & Reiman, T. A guidebook for evaluating organisation in the nuclear industry – an example of safety culture evaluation. (In press for SSM research report series.)

1. Oedewald, P., Reiman, T. & Talja, H. Safety culture: Understanding the safety significance of the job in the construction of the OL3 nuclear power plant. VTT, Espoo, 2009. Confidential research report VTT-R-01593-09.

3. Expert Work in Safety Critical Environment (SafeExpertNet)

3.1 Summary – Expertise development in nuclear power industry

Eerikki Mäki, Tanja Kuronen-Mattila, Eila Järvenpää
Aalto University

Krista Pahkin and Anneli Leppänen
Finnish Institute of Occupational Health

Abstract

The need to update and develop expertise is a never ending requirement of expert organizations (e.g. nuclear power organizations). Expertise development is a slow process. However, it can be supported in many ways. The SafeExpertNet (SAFEX) project applied interview and survey data to understand expertise and expertisedevelopment in Finnish nuclear power organizations.

The results show that expertise development is extremely dependent on the individual employees themselves. Organizations can, however, provide many methods and opportunities that support expertise development. The SafeExpertNet project produced results that can be utilized in human resource management. The results and research findings provide support for organizations in their efforts to develop expertise of their employees. The actions of closest superior of experts and the functionality of the work group were strongly connected to the development of individual expertise.

Moreover, collaboration crossing organizational boundaries offers good platform and prospects to develop expertise. Possible obstacles and facilitators of interorganizational collaboration were identified.

Introduction

Organizations operating in nuclear power industry are extremely dependent on their employees' expertise. Tasks in the industry are very demanding and require various kind of technical expertise. Nuclear power organizations must also have methods and practices that support expertise development and career development of experienced experts.

There are many definitions for expertise. Usually expertise is considered to include knowledge, skills and long experience on the specific technical or other domain. Moreover, strong motivation and independency are qualities often associated with experts and expertise. Expertise develops gradually through profound education and comprehensive work experience in an appropriate context. The development of expertise in demanding areas of work takes considerable amount of time. Studies show that becoming an expert requires several or even dozens of years of hard work [1, 2]. Expertise can not be developed only through formal education (e.g. university education) or on-site training (e.g. courses for personnel) although these provide a necessary basis for expertise development in the area of nuclear power. Fortunately, there are methods, such as a process approach for creating tacit knowledge through apprenticeship [3], that can be applied to accelerate or to improve expertise development.

This study was conducted in the context of nuclear power organizations in Finland. During the study this group of organizations was called a community or a network. In the core of this network are three nuclear power companies, regulatory bodies (Radiation and Nuclear Safety Authority (= STUK) and Finnish Ministry of Employment and the Economy) and Technical Research Centre of Finland which develops expertise in the area of nuclear energy. Additional members of this network include Finnish universities (Aalto University School of Science and Technology and Lappeenranta University of Technology), Fortum Technical Support (former Fortum Nuclear Services) and Posiva (nuclear waste management company). Finnish nuclear power community or network is difficult to define exclusively. We acknowledge that there are individuals and organizations that do have a role in Finnish nuclear power community or network, but who were not included in this study at this point. These include for example consultancy firms and subcontractors.

The SafeExpertNet project (SAFEX) utilized both qualitative (interviews) and quantitative (surveys) data. Altogether 54 experts from six Finnish nuclear power organizations were interviewed. Survey was conducted in three nuclear

power organizations in year 2008 (N = 170, response rate 59%) and in five nuclear power organizations in year 2010 (N = 279, response rate 68%).

Main objectives

The SafeExpertNet research project aimed at

- Providing new scientific knowledge and understanding about expert work in nuclear power industry
- Defining and developing practices for preserving and creating expertise in nuclear power industry
- Providing new knowledge on nuclear power expertise network and the roles of different parties (including nuclear power plants, regulators, research and educational organizations)
- Describing expertise in nuclear power network
- Defining and developing collaboration and communication in the nuclear power network.

Nuclear power expertise

Expertise in nuclear power industry is characterized by profound knowledge in specific technical domains. In addition, experts need to be able to gain understanding other disciplines as well (e.g. information management, context related knowledge, computer simulations). As important part of expertise in nuclear power industry is safety related, a survey for assessing expert work in safety critical environment was developed [4]. Organizations can utilize this survey for example as a part of their other assessments of organizational functioning or atmosphere.

Expertise development

Expertise development is extremely dependent on the individual employees themselves. In addition, organizational practices and support have a special role in expertise development as well. Table 1 summarizes practices that are applied to support expertise development, and respondents' views on how these practices support expertise development. Even though there is not much changes between years 2008 and 2010, there is positive development.

Induction to employees own work tasks and related areas of expertise were seen as an important phase of expertise development [5]. The results of the survey and interviews indicated that one of the cornerstones in developing expertise and knowledge is how to carry out efficient induction for new employees and ensure that they are assigned with meaningful and challenging projects, as this was regarded as the most effective way to learn [6]. Results from the interviews indicated that systematic career planning is an important part of expertise development and different career paths should be made visible to the employees [7]. The survey results (2008, N = 170) from three organizations showed that human recourse management practices and organizational support the respondents were most satisfied with were 1) the internal and external training, and 2) the utilization of operation events as a learning opportunity [7].

The results of the survey [6] showed that the development of individual expertise was related to the content of work, the actions of the closest superior, the functionality of the work group, and to the way a superior takes into account the safety-critical aspects of the work. Development of individual expertise was also related to the way the organization as a whole viewed safety culture.

Table 1. Applied organizational practices in supporting expertise development (scale: 1 = strongly disagree… 5 = strongly agree how the method supports expertise development). *p<.05.

	SAFEX 2008 (n = 170)	**SAFEX 2010 (n = 279)**
Internal training	3,2	3,3
External training (including conferences)	3,4	3,4
Initiation programmes	3,1	3,3
Supervision of work (e.g. mentoring)	3,1	3,2
Personal development plans	2,8	3,0
Performance appraisal	3,0	3,1
Job rotation*	2,4	2,8
Job descriptions and competence requirements specification	3,0	3,1
Analysis and development of work processes	2,7	2,8
Utilization of knowledge from other disciplines*	2,9	3,2
Evaluation of knowledge and competence risks	2,6	2,7

The personal interorganizational (expert) networks in nuclear power industry contributed to the development of individual expertise [8]. Also real hands-on collaboration (e.g. common projects) between experts from different organizations in the industry was seen as a good method for knowledge sharing and expertise development [9]. Networking and network building was also considered as an important part of expertise development by the interviewed experts. There are many structures and opportunities in the industry that support interorganizational collaboration of experts [10]. These include scientific conferences, working in other work related professional organizations (e.g. Finnish nuclear society), formal training (e.g. nuclear safety courses), and formal research and development programs (e.g. SAFIR2010).

The experts in nuclear power industry considered networks useful in developing their personal knowledge and competences as well as the industry as a whole. Experts in other organizations in the nuclear power industry provided a peer group at least on two levels. First, the experts could discuss relevant and new *technical topics* with their colleagues across organizational boundaries. This helped them to update their knowledge concerning the latest development in their own and relating expertise areas. Multidisciplinary collaboration broadens expertise and assures that different aspects are taken into account in decision making. Furthermore, collaboration with other experts provided a forum for sharing knowledge and ideas in the area on *leadership, competences and their development*. This was regarded as important opportunity, since many of the interviewed experts had a role also as a supervisor or a manager.

Interorganizational collaboration between experts

The factors affecting knowledge sharing as well as the amount and adequacy of collaboration were addressed in both surveys, 2008 and 2010. The results indicated that the need for interorganizational collaboration was slightly bigger than actual amount or quality collaboration. In the future, it is important to study what are the areas where interorganizational collaboration would benefit the experts and organizations in the Finnish nuclear power community.

Attitudes on collaboration and knowledge sharing in Finnish nuclear power community were studied with the survey. The results from five nuclear power organizations (Loviisa power plant, Fennovoima, Fortum TS, STUK, and Posiva) showed that there are four factors affecting the knowledge sharing between experts in different organizations in the nuclear power industry. These were: the

nature of knowledge, the fluency of collaboration between individual experts, opportunities for collaboration and goal orientation of collaboration (Table 2).

Table 2. Four factors influencing the success of knowledge sharing and collaboration in nuclear power industry (N = 279).

	In Finnish nuclear power community…			
	…knowledge is easily accessed and in usable form.	…fluency of collaboration in personal level is good.	…there are enough opportunities for collaboration.	…collaboration is goal oriented.
Disagree completely	**4%**	**11%**	**8%**	**1%**
Disagree somewhat	**24%**	**28%**	**22%**	**8%**
Agree somewhat	**64%**	**46%**	**48%**	**47%**
Agree completely	**7%**	**15%**	**22%**	**44%**
	100%	**100%**	**100%**	**100%**

Respondents' perception on goal orientation of collaboration is remarkably positive. 91% of the respondents agreed or completely agreed that collaboration is goal oriented. This is a clear strength characterizing interorganizational collaboration and a good basis for developmental efforts. Three other dimensions of interorganizational collaboration and knowledge sharing still have some development potential. In addition to factors affecting knowledge sharing between experts across organizational boundaries, this study also identified factors that either supported or inhibited collaboration. Respondents (N = 277) were asked to choose three main supporting and inhibiting factors of interorganizational collaboration from a list of different options (Tables 3 and 4).

Table 3. Factors supporting interorganizational collaboration between experts.

	Respondents choosing this option
Mutual trust between experts	65%
Good interpersonal relations	64%
Appreciation of expertise	44%
Shared project	40%
Positive attitudes	39%
Shared objectives in the industry	35%
Shared work practices	9%

The results of the survey indicated that trust between experts (65%), good interpersonal relations (64%) and appreciation of expertise (44%) are most significant factors supporting the interorganizational collaboration between experts in nuclear power industry. Other factors were shared project (40%), positive attitudes (39%) and shared objectives of the collaboration (35%).

Many interviewees considered that recognizing and respecting colleagues' expertise is an important part of expert work. Understanding of colleagues' expertise and own limitations regarding to that area of expertise is important when collaborating with other experts. Trust between experts, good interpersonal relations, and appreciation of others' expertise were the most significant factors supporting the interorganizational collaboration between experts in nuclear power industry [5]. This is important, since interorganizational collaboration is considered an effective method to develop expertise [11].

Table 4. Factors inhibiting interorganizational collaboration between experts.

	Respondents choosing this option
Lack of resources	58%
Lack of time	57%
Bureaucracy	35%
Negative attitudes	32%
Physical distance	28%
Competition	28%
Different procedures	26%
Mistrust	26%

The results of the survey indicated that lack of resources (58%) and lack of time (57%) are considered most significant factors inhibiting the collaboration. Other important factors were bureaucracy (35%), negative attitudes (32%), different operational approaches in the organizations (26%), distance (28%), lack of confidence (26%) and competition (28%).

Resources and time might overlap to some extent, e.g. time can be interpreted also as an important resource. Highly regulated industry can produce experiences of excessive bureaucracy and control. These experiences could affect the way employees orient themselves towards collaboration and their activeness. Employees might feel that the amount and/or methods of collaboration are too strictly defined by formal relationships between organizations and experts in the area.

Inadequate understanding of other expert areas besides one's own may hinder the collaboration in the interfaces of special technical areas. Furthermore collaboration may suffer from unclear or undefined goals and poor interpersonal chemistry between collaborating experts.

Applications

The SafeExpertNet project has aimed to produce research results that are easily applicable in all organizations in nuclear power industry. Confidential reports specified for each participating organization can serve as a benchmark or as a seed for development. They can also be utilized as part of the assessment of development efforts.

Results can be applied in planning and organizing expert collaboration across organizational boundaries in the nuclear power industry as well as supporting expertise development in intra- and interorganizational contexts. Results also provide useful guidelines on how to build expert collaboration in the interorganizational settings.

Conclusions

Supervisors do have an important role in supporting the development of expertise in organizations [12]. Being a supervisor can be a lonely position and they may lack knowledge or methods on how to support their subordinates' expertise. The help of HR personnel or other superiors (peer-to-peer support) definitely would be beneficial for them. Even some written guidelines [13] can be useful.

The SafeExpertNet project produced results that can be utilized in human resource management. The results and research findings provide support for organizations in their efforts to develop expertise of their employees. We recognize that some of the results are not easily applicable and the development efforts in nuclear power organizations may take a lot of time and work. We have summarized some development ideas in an easily accessible package [13]. The research group continues its work in SAFIR2014 programme. The research in forthcoming years is based on the findings of this project.

References

1. Cellier, J., Eyrolle, H. & Marine, C. Expertise in dynamic environments. Ergonomics 1997, Vol. 40, No.1, 28–50.

2. Hubbard Ashton, A. Experience and Error Frequency Knowledge as Potential Determinants of Audit Expertise. The Accounting Review, April 1991, pp. 218–239.

3. Säämänen, K. A Process Approach to Creating Tacit Knowledge through Apprenticeship – A Case study in Nuclear Power Plants. European Association of Work and Organizational Psychology (EAWOP) 9.–12.5.2007.

4. Pahkin, K., Leppänen, A., Mäki, E., Kuronen-Mattila, T. & Järvenpää, E. Development of a survey for expert work in safety critical environment. Presentation at the European Academy of Occupational Health Psychology (EA-OHP) 29–31 March 2010, Rome, Italy.

5. Pahkin, K., Kuronen-Mattila, T., Mäki, E., Leppänen, A. & Järvenpää, E. Asiantuntijatyö turvallisuuskriittisessä ympäristössä. Suomen Printman Oy, Hyvinkää, 2011. (In press.)

6. Pahkin, K., Leppänen, A., Mäki, E., Kuronen-Mattila, T. & Järvenpää, E. Supporting expertise in nuclear organizations. The IAEA International Conference on Human Resource Development for Introducing and Expanding Nuclear Power Programmes 14–18 March 2010, Abu Dhabi, UAE.

7. Pahkin, K., Leppänen, A., Mäki, E., Kuronen-Mattila, T. & Järvenpää, E. Improvement of expertise in nuclear industry organizations. European Association of Work and Organizational Psychology (EAWOP) – the 14th European Congress of Work and Organizational Psychology, Santiago de Compostela, Spain, May 13–16, 2009.

8. Kuronen-Mattila, T., Mäki, E., Pahkin, K., Järvenpää, E., Korhonen, K. & Leppänen, A. Verkostot asiantuntijuuden kehittymisen tukena ydinvoima-alalla. Työelämän tutkimuspäivät ”Työn ja elämän laatu”, Tampere 4.–6.11.2009. Työelämän tutkimuskeskus, Tampereen yliopisto.

9. Kuronen-Mattila, T., Mäki, E. & Järvenpää, E. Collaboration between experts – Case Finnish Nuclear Power Industry. To be submitted to International Journal of Nuclear Knowledge Management at the end of January 2011.

10. Mäki, E., Kuronen-Mattila, T. & Järvenpää, E. Knowledge sharing in interorganizational context. SAFIR2010. The Finnish Research Programme on Nuclear Plant Safety 2007–2010: interim report, 2009.

11. Mäki, E., Kuronen-Mattila, T. & Pahkin, K. Tieto kasvaa jakamalla. ATS Ydintekniikka, 2010.

12. Pahkin, K., Kuronen-Mattila, T. & Mäki, E. Avoimuus auttaa toimimaan turvallisemmin. ALARA x/2010.

13. Pahkin, K., Kuronen-Mattila, T., Mäki, E., Leppänen, A. & Järvenpää, E. Avaimia asiantuntijuuteen. Työterveyslaitos ja Aalto-yliopisto, Hyvinkää 2010.

3.2 Supervisor's role in knowledge management and expertise development

Krista Pahkin and Anneli Leppänen
Finnish Institute of Occupational Health

Eerikki Mäki, Tanja Kuronen-Mattila and Eila Järvenpää
Aalto University

Abstract

Knowledge and expertise are not only the property and intellectual capital of individuals, but also an important asset for the whole organization. Knowledge management is a challenging task; in order to be successful, one should not only understand the different practices within the company, but also know what the content of the work is like at different organizational levels and functions.

The SafeExpertNet project focused on studying the work of nuclear experts, and identifying how the organization can support the preservation and development of the expertise. One of the objectives of this project was to identify such leadership (and HR practices) that support the preservation and increase of expertise in nuclear industry. Therefore, the focus of this paper is on the role of supervisor in knowledge management and expertise development.

In this four-year project different datasets were collected: thematic interviews concerning the nature of the expertise, its development, and the organizational support for developing expertise (n = 29, in 2007) and how the safety critical aspect of their work should be taken into account in management, supervisor and team working (n = 12, in 2009) have been conducted. Surveys on the organizational practices at work in the improvement of expertise (n = 170 in 2008, n = 279 in 2010) and on initiation practices (n = 32 in 2009) have also been carried out.

All in all, the findings of the project confirmed that the role of the supervisors is demanding and significant in the knowledge management and development of expertise. The challenge of the supervisors is not only to support the development of expertise of the others, but also make sure that they can also develop their own expertise and share it with the new experts, since often the supervisors in nuclear industry organizations in Finland are also the main experts in their area.

Introduction

Knowledge and expertise are not only the property and intellectual capital of individuals, but also an important asset for the whole organization. Efficient and effective management of knowledge is relevant to all industries where knowledge and expertise are the “raw material” of the business itself and its results, products or services. Knowledge intensive organization can be defined as an organization where most work can be described as intellectual, and where well-educated, qualified employees form the major part of the workforce [1, 2]. Knowledge intensive organization should thus actively preserve the knowledge and know-how of experts, otherwise it risks losing this resource when an expert leaves his/her job.

Managing knowledge involves tools and practices for accessing, preserving, generating, utilizing and transferring individual and collective knowledge [3]. Knowledge management is not an easy task; in order to be successful, one should not only understand the content of different practices within the company, but also know what the content of the work is like at different organizational levels and functions.

Although many other industries share similar challenges in the area of knowledge management, the preservation of expertise in the nuclear industry is even more crucial due to the safety-critical nature of the industry. As a response to the risk of knowledge loss, nuclear organizations have engaged in knowledge capturing efforts. To support this task, IAEA [4] has proposed nuclear organizations to design and adopt people-centered programs that encompass themes such as workforce planning, recruitment, training, succession planning, leadership development and knowledge management. Thus, in order to address the current risks to nuclear expertise, attention should be focused on these different areas and corresponding human resource (HR) functions within the nuclear organizations

Work in knowledge intensive organizations requires a different approach and mind-set to work than before [5]. While the need to be able to use information technology at work is now a prerequisite for most jobs, knowledge work requires ability to plan and carry out work independently and make decisions. Further, social skills, communication skills, language skills, commitment to continuous learning, self-confidence and ability to take initiative are often expected from knowledge workers.

At the same time, work life has become more demanding. The problems of coping in expert positions are very real [6]. Employees are required to possess a wide range of knowledge and good networking skills. They are expected to develop their own expertise and control several simultaneous projects. In addition, they have to cope with constant change. In expert work, employees involved in a given task or a project must be able to define the problem, gather the necessary information and progressively refine and extent initial ideas to permit their successful implementation.

Management and leadership practices are important contributors to the organizational functioning and performance. Managerial practices can facilitate the development of competence of employees. Challenging tasks together with good leadership practices can also contribute to job satisfaction and job involvement. Continuous improvement practices associated with an innovative climate promote the idea of lifelong learning and the development of the personnel's competence.

Currently, work-related knowledge, organizational learning and knowledge management are regarded as prerequisites for organizational success especially in knowledge-intensive organizations. Learning can be understood as permanent or semi-permanent changes in the way individuals think and act. When individuals engage in thinking and acting, rather than merely executing a process or task, their knowledge is changed by that process [7]. The creation and sharing of work-process knowledge is related to the actual work activity. In organizations, the support of learning requires that the content of work is challenging, autonomy and participation are characteristic to the organization of work and work development, and leadership activities include features of coaching [e.g. 8, 9].

Organizations can utilize various means, organization structures, and actions to preserve expertise and to support the improvement of competences. Especially in high reliability organizations strategic management of human relations is tightly related to the reliability and efficiency of the actions in the organization [e.g. 10], and practices in HR management are related to utilization, sharing, and increase of knowledge. They can, e.g. determine management processes that allow the organization to acquire unique and valuable knowledge which is the prerequisite to innovative actions and excellent performance [11].

Supervisors in nuclear industry organizations have an important role in supporting the development of expertise in the organizations [12]. Supervisors are often experts themselves and they would like to keep their expertise in high level. At the same time, their task is to take care of the expertise of their

subordinates and other, often more administrational tasks. Supervisors may lack knowledge or methods on how to support their subordinates' expertise. The help of HR personnel or other supervisors (peer-to-peer support) would be beneficial for them.

Main objectives

The SafeExpertNet project focused on studying the work and work processes of nuclear experts and identifying how the organization can support the maintenance and development of expertise. The focus of this paper is on the role of supervisor in knowledge management and expertise development. The aim was to identify such leadership (and HR) practices that support the preservation and increase of expertise in nuclear industry.

Methods

The study comprised different phases:

1) A qualitative cross-sectional case study was conducted in two different nuclear industry organizations in 2007. A total of 18 experts, 9 managers, and 2 HR professionals participated in thematic interviews about the nature of their expertise, its development, and the organizational support they received for developing it. The interviewed experts worked mainly in safety management tasks, such as reactor monitoring, risk calculation (PSA), structural design, material technology, and radiation safety.

2) In 2008, 170 experts from three nuclear industry organizations answered a questionnaire on the organizational practices at work in the improvement of expertise. The response rate was 59%. The questionnaire included 86 questions about topics such as the way work groups work, the actions of their closest superior and management, work goals, the safety-critical aspects of work, and the level of stress. The format for answering most of the individual items was a Likert-type scale.

3) In 2009, 32 new employees (recruited less than two years ago) from one nuclear organization participating to the project answered a questionnaire which included 44 questions on initiation practices of the company. The response rate was 71%. The format for answering most of the individual items was a Likert-type scale, but there were also three open questions in

which the participants could write their experience on general initiation, on timing of the initiation and on task related initiation.

4) In 2009, 12 persons from four target organizations were interviewed on how the safety critical aspect of their work should be taken into account in upper management, supervisor level and team work. The goal was to develop a tool (a set of survey questions) with which the safety critical organizations can evaluate their actions/operations related to safety promoting behavior in different organizational levels.

5) In 2010, 279 experts from five nuclear industry organizations answered to the same questionnaire as in 2008 on the organizational practices at work in the improvement of expertise. The response rate was 68%.

Main results

The results (data 1) showed that nuclear industry experts require, in addition to domain-specific expertise in nuclear physics, also a broad set of expertise in other areas, such as information management, plant-related knowledge, computer simulation, organizations, social networks and HR management (see Figure 1). In addition to these substance areas, nuclear experts need to possess attitudes and personality traits such as commitment and enthusiasm as well as the ability to be critical and analytical, the desire to keep up high quality in their work and the willingness to openly admit shortcomings in their own knowledge base and develop these areas further. [13]

The interviews revealed that training plans and courses, cooperation with other organizations, and mentoring arrangements were useful HR practices in the development of expertise. The results also indicated that the development of expertise was easier in relatively small organizational units where experts know each other’s competence areas, in teams of persons with different backgrounds, and in work communities where self-development is encouraged. The support from leaders, well-defined organizations and systematic training were also valued. [13]

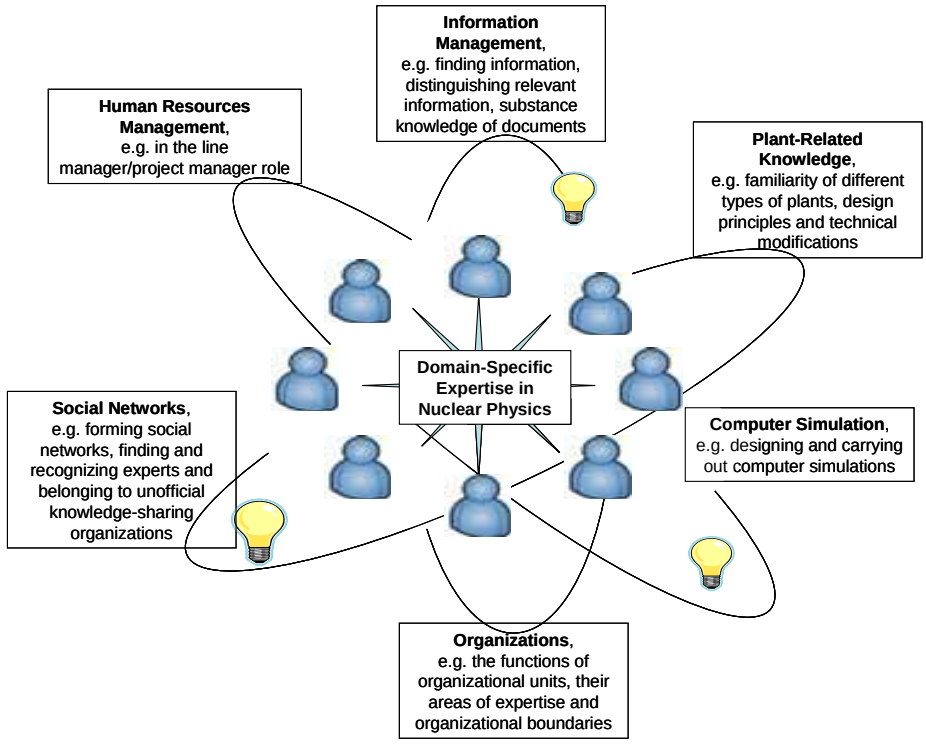

Figure 1. The Nature of Nuclear Expertise in the Studied Organizations.

All interviewees agreed that the responsibility of developing expertise is with the expert him-/herself. However, they told that it is important that the supervisor would follow and support the knowledge development. In development / feedback discussion the supervisor should discuss about the future needs of the expertise, what areas and/or in what direction the expertise should be developed, or how the expertise could be shared with the new employees. In addition to creating a formal training plan, the plan should also be followed up and modified if necessary. [14]

Based on the interviews carried out in 2007 (data 1) the way new employee is initiated to his/her work task is highly dependent on the closest supervisors. All interviewees agreed that it is the tasks of the supervisors to take care of the new employees, but the main problem is often the lack of time. [14] The results of the survey on initiation practices (data 3) supported these findings. The key issue on effective initiation practices is the effort (time and support) of the person

responsible of the initiation, mainly the closest supervisor. Also the active role of the new employee was seen as crucial for the successful initiation process.

Also the results of the survey (2008) of project confirmed that the role of the supervisors is significant in the development of expertise. The survey (data 2) showed that the development of individual expertise was related to the content of work (r = .627***), the actions of the closest superior (r = .619***), the functionality of the work group (r = .561***) and to the way a superior takes into account the safety-critical aspects of the work (r = .551***) [15]. The findings of the follow-up survey (2010, data 5) confirmed these findings [16] and showed that the development of individual expertise was also related to the way the supervisor acted on issues related to safety culture (r = .506/.535***).

The main task of the supervisors is to make sure that the tasks are carried out in their work group. At the same time, they should make sure that their subordinates maintain their motivation and willingness to develop their expertise. Supervisors are also seen as a link between the management and the work group, making sure that there is enough resources and expertise in the work group in order to reach the goals of the organization. The task of the supervisor is also to make sure that the safety aspects are taken into account in every day task performance, that decisions are based on experts' views and to give feedback. These supervisory tasks are also bases for good way of working in the safety critical organizations. Good practices in supervisor's work are highly connected to the good way of working in the safety critical organization. [16]

Applications

The SafeExpertNet project is part of the *"Organization and human factors"* research area of the SAFIR2010 programme.

The results of the project were gathered in a guide book in which tools and practices are defined to support expertise and its development in nuclear organizations. The guide book [12] is directed at supervisors and experts themselves.

The short questionnaire [16] can be used to monitor the way work groups, supervisors and the management act on issues related to the level of safety culture. Based on the results the development areas can be identified.

Conclusions

The actions of the closest superior and the functionality of the work group were strongly connected to the development of individual expertise, and for this reason, they should be considered important contributing factors. Supportive superior work, an open and incentive-building work group and meaningful work are very important for the well-being of not only individual employees, but also the whole work community, regardless of the area of expertise.

All in all, the different findings of the project confirmed that the role of the supervisors is demanding and significant in the knowledge management. The challenge of the supervisors is not only to support the development of expertise of the others, but also to make sure that they can develop their own expertise and share it with the new experts.

References

1. Alvesson, M. Knowledge work: Ambiquity, image and identity. Human relations 2001, 54:7, pp. 863–886.

2. Alvesson, M. Knowledge work and knowledge intensive firms. Oxford University Press, 2003.

3. Mäki, E. Exploring and Exploiting Knowledge. Research on Knowledge Processes in Knowledge-Intensive Organizations. Doctoral Thesis. Helsinki University of Technology, Espoo, Finland, 2008.

4. IAEA, 2006. Risk management of knowledge loss in nuclear industry organizations. Vienna.

5. Drucker, P. The Essential Drucker. Selections of the management works. Oxford, Butterworth Heineman, 2001.

6. Tuomivaara, S., Hynninen, K., Leppänen, A., Lundell, S. & Tuominen, E. Asiantuntijan luovuus koetuksella, Työterveyslaitos, Helsinki, 2005.

7. Billett, S. Learning through work. Workplace participatory practices. In: Workplace learning in context. H. Rainbird, A. Fuller & A. Munro (Eds.). Routledge, 2004. Pp. 109–125.

8. Oliveira, M.T., Oliveira Pires, A.L. & Alves, M.G. Dimensions of work process knowledge. In: Work process knowledge. N. Boreham, R. Samurcay, M. Fischer (Eds.). Routledge, London, 2002. Pp. 106–118.

9. Huys, R. & van Hootegm, G. A delayed transformation? Changes in the division of labour and their implications for learning opportunities. In: Work process knowledge. N. Boreham, R. Samurcay, M. Fischer (Eds.). Routledge, London, 2002.

10. Ericksen, J. & Dyer, L. Toward strategic human resource management model of high reliability organization performance. The Intnl. J. of Hum. Res. Mgement 2005, 16, pp. 907–928.

11. Lopez-Cabrales, A., Perez-Luno, A. & Valle Cabrera, R. Knowledge as a mediator between HRM practices and innovative activity. Human Resource Management 2009, 48:4, pp. 485–503.

12. Pahkin, K., Kuronen-Mattila, T., Mäki, E., Leppänen, A. & Järvenpää, E. Avaimia asiantuntijuuteen. Työterveyslaitos ja Aalto-yliopisto, Hyvinkää, 2010.

13. Rintala, N., Pahkin, K., Leppänen, A., Säämänen, K. & Järvenpää, E. The Nature of Expertise and HR Functions Supporting Expertise in Nuclear Industry Organizations. The IAEA International Conference 19.–22.6.2007.

14. Pahkin, K., Leppänen, A., ja Järvenpää, E. (hyväksytty) Osaamisen kehittämisen käytännöt ja haasteet ydinvoima-alan asiantuntijaorganisaatiossa. Työ ja Ihminen.

15. Pahkin, K., Leppänen, A., Mäki, E., Kuronen-Mattila, T. & Järvenpää, E. Expert work in safety critical environment: Safex summary report. SAFIR2010. The Finnish Research Programme on Nuclear Plant Safety 2007–2010: interim report. 2009.

16. Pahkin, K., Kuronen-Mattila, T., Mäki, E., Leppänen, A. & Järvenpää, E. Asiantuntija turvallisuuskriittisessä ympäristössä. SafeExpertNet 2007–2010. Työterveyslaitos, Helsinki, 2011. (Also PDF.)

4. Model-based Safety Evaluation of Automation Systems (MODSAFE)

4.1 MODSAFE summary report

Janne Valkonen, Kim Björkman, Jussi Lahtinen and Jukka Ranta
VTT
P.O. Box 1000, FI-02044 VTT, Finland
janne.valkonen@vtt.fi, kim.bjorkman@vtt.fi, jussi.lahtinen@vtt.fi,
jukka.ranta@vtt.fi

Juho Frits, Keijo Heljanko and Ilkka Niemelä
Aalto University, School of Science and Technology,
Dept. of Information and Computer Science
P.O. Box 15400, FI-00076 AALTO, Finland
jfrits@tcs.hut.fi, keijo.heljanko@aalto.fi, ilkka.niemela@aalto.fi

Abstract

The objective of the MODSAFE project was to evaluate and develop methods based on formal model checking and apply them in the safety analysis of NPP safety automation (I&C). The purpose was to develop and find a group of methods and tools that support utilities, regulators, vendors and support organizations in their practical safety evaluation efforts. The main tasks of the first two project years were to review the state of the art of employing formal methods and models for safety evaluation of industrial and nuclear safety systems, to develop basic methodology for applying model checking to safety evaluation, and to study the feasibility of the approach. The third and fourth project years concentrated on developing the approach more flexible and

suitable for analysing larger and more complex models. The research was conducted by utilizing several industrial example systems which enabled developing the methodology suitable for realistic problems and testing it with various types of systems. The results of the project show that by using model checking techniques it is possible to verify whether a design model of a moderate size safety system satisfies its key safety requirements or not, even when system failures must be taken into account.

Introduction

Modern digitalized I&C systems are employed in critical applications creating new challenges for safety evaluation. However, such work still relies heavily on subjective evaluation which covers only a limited part of the possible behaviours and therefore more rigorous formal methods are needed. Model checking [6] is a formal method that can be used for verifying the correctness of system designs. Before MODSAFE project, it had not previously been applied in the safety evaluation of nuclear power plant (NPP) automation systems (at least in Finland) but internationally it had been used in verifying the correct behaviour of, e.g., hardware and microprocessor designs, data communications protocols and operating system device drivers.

A number of efficient model checking systems are available offering analysis tools that are able to determine automatically whether a given state machine model satisfies desired safety properties. Model checking can also handle delays and other time-related operations, which are crucial in safety I&C systems and are challenging to design and verify.

Main objectives

The overall objective of the MODSAFE project was to evaluate and develop methods based on formal model checking and apply them in the safety analysis of NPP safety automation (I&C). The purpose was to develop and find a group of methods and tools that support utilities, regulators, and vendors in their practical safety evaluation efforts. The main tasks of the first two project years were to review the state of the art of employing formal methods and models for safety evaluation of industrial and nuclear safety systems [17], and to develop basic methodology for applying model checking to safety evaluation, and to study the feasibility of the approach [16, 18, 19, 20]. The objective of the third

and fourth project year was to develop the approach more flexible and suitable for analysing larger and more complex models [14, 15, 21, 22].

Model checking

Model checking [6] is a computer aided verification method developed to formally verify the correct functioning of a system design model by examining all of its possible behaviours. The models used in model checking are quite similar to those used in simulation as basically the model must describe the behaviour of the system design for all sequences of inputs. However, unlike simulation, model checkers examine the behaviour of the system design with all input sequences and compare it to the specification of the system. In model checking, at least in principle, the analysis can be made fully automatic with computer aided tools. The specification is expressed in a suitable specification language, temporal logics being a prime example, describing the allowed behaviours of a system. Given a model and a specification as input, a model checking algorithm decides whether the system violates its specification or not. If none of the behaviours of the system violate the given specification, the (model of the) system is correct. Otherwise the model checker will automatically give a counterexample execution of the system demonstrating why the property is violated. The MODSAFE project used two model checkers, NuSMV originally designed for hardware model checking and UPPAAL supporting model checking based on timed automata. These tools are introduced below.

NuSMV [5, 10] is a state-of-the-art symbolic model checker that supports state machine models where the real-time behaviour has to be modelled with discrete time steps using explicit counter variables that are incremented at a common clock frequency. NuSMV supports model checking using both the Linear Temporal Logic (LTL) [3] and Computation Tree Logic (CTL) [6] making it quite flexible in expressing design specifications. The model checking algorithms employed in this work are based on symbolically representing and exploring the state space of the system by using Binary Decision Diagrams (BDDs). In addition, SAT (propositional satisfiability) based bounded model checking is also supported by NuSMV for finding bugs in larger designs. The sophisticated model checking techniques used by NuSMV can handle non-determinism induced by free input variables well but modelling the real-time aspects can be more challenging due to the inherently discrete time nature of the synchronous state machine model employed by NuSMV.

Uppaal [11] is a model checking tool for timed systems based on modelling the system as a network of timed automata that communicate through message channels and shared variables. The timed automata have a finite control structure and real-valued clocks [1] making the modelling of timers of a system design fairly straightforward. Networks of timed automata can express the real-time behaviour of the system in continuous time and still be automatically analyzed. This is feasible because all the possible behaviours of the system can be captured using a finite graph where different clock valuations with, intuitively, the same behaviour are grouped into a finite number of equivalence classes called regions [1]. The model checking algorithms use symbolic methods to compactly represent the clock valuations associated with each state of the system in quite a memory efficient manner. The model checking algorithms employed inside Uppaal [2, 9] are able to check a subset of the temporal logic TCTL (Timed Computation Tree Logic) [2] using an explicit state model checking algorithm that explicitly traverses the finite graph induced by the behaviour of the system. The main strength of Uppaal is in analyzing complex timing behaviour of a system. However, it is not too well suited with systems with a very high amount of non-determinism as induced by, e.g., reading a large number of input variables (sensor readings) provided by the environment because each combination of inputs is explicitly explored by the employed model checking algorithms.

Main results

The results of the project show that by using model checking techniques it is possible to verify whether a design model of a moderate size safety system satisfies its key safety requirements or not, even when system failures must be taken into account. The main results and the case examples analysed during the project are shortly introduced below. The project utilised several example systems (case studies) for testing the applicability of model checking in different environments and developing approaches for efficient verification of various types of systems.

Case Emergency Cooling System

The performance of an emergency cooling system of a nuclear power plant was analyzed with model checking. The purpose of the system is to take care of the reactor core’s cooling if normal cooling systems are unavailable. A finite state NuSMV model of the system was created for testing the suitability of model

checking to verify the main safety properties of the system. The objective was to verify the correctness of the system's logical functions and test different approaches to modelling. Several properties of the system were verified with model checking and no erroneous behaviour between the system model and its specification was found. However, the purpose of the case study was to try model checking method for the first time in that type of system analysis and see how it could be used in future cases. The potential and power of the method were clearly demonstrated and the case gave a good basis for further work. For further information, see [12, 13].

Case Arc Protection System

The purpose of the analyzed electric arc protection system is to protect switchgear, electrical instrumentation and humans from highly dangerous electric arcs. The system consists of a master unit, overcurrent sensor units, and light sensor units. Sensors are installed into the protected system and connected to the master unit via optical cables. The master unit collects the alarm signals from sensors, and when necessary, launches circuit breakers that close the power feed from the protected device leading to termination of the electric arc. The master unit is based on a Programmable Logic Controller (PLC) so that the tripping logic can be freely designed for the protected system. This gives the possibility for selective tripping meaning that the protected system can be divided into several protection zones with different tripping conditions. A basic methodology for modelling safety instrumented systems was developed based on hardware model checking techniques and the NuSMV model checking tool [7]. As delays and timing-related issues turned out to be essential in such systems, alternative model checking methodology based on timed automata and the Uppaal tool was also investigated [8]. The applicability of model checking was studied with respect to verifying the correspondence of implementation of the control logic and its specification, and verifying the correctness of system design against safety properties. Also the environment of the arc protection system had to be modelled. The challenge was to find the right level of abstraction for the environment in order to guarantee the sufficient correspondence between the model and reality and to maintain the size of the model computationally feasible. The results show that the system design could be verified against its safety properties using hardware model checking techniques and the NuSMV tool as

well as using timed automata and the Uppaal tool. For further information on the verification results, see [7, 8, 12, 13].

Case Stepwise Shutdown System

The stepwise shutdown logic is used for stepwise control of the process towards the normal operating state in case of disturbances in the process to be controlled. The system is triggered if some of the process variables, for example the measurement of the temperature, deviate from the values set for normal operation. The purpose of the system is to reduce the possibility that the process enters a state where the more complicated actual shutdown function is needed. The system was modelled using NuSMV and Uppaal model checking tools and it was possible to verify basic safety properties of the system using both tools [4]. Besides model checking the design of the control logic, fulfilment of the single failure criterion was analysed with several different failure models using the NuSMV tool. It was assumed that a failure could only affect one input signal of each process variable measurement at a time and that the logical components function correctly. In the most complicated failure model, failures may remain undetected, failed input signals get a non-deterministic value, and input signals may fail or recover at any time step. The evaluation of the case system showed that it is possible to determine the fulfilment of single failure criteria with model checking. For further information, see [4].

Case UPS

Model checking was applied to the verification of the embedded control software of an Uninterruptible Power Supply (UPS). A UPS provides back-up power in case of power failure and protects connected equipment from different power disturbances. UPS devices are used in many safety critical systems to guarantee uninterrupted supply of power to the facility. A substantial part of the control software of the UPS was modelled using the Uppaal model checking tool. The Uppaal tool was chosen because the system has lots of timings of different scale and the intention was to especially investigate the different timing sequences of the system. The study focused on a set of critical failure cases for which key requirements were formalized and the behaviour of the system was analysed against the requirements using Uppaal. In two of the failure cases a timing-related misbehaviour was revealed with model checking. The results of the case study show that timed model checking can be applied to the verification

of embedded software. Model checking can be used for revealing bugs in embedded software and for verifying that the design of embedded software meets its requirements. For further information, see [23].

Case Automated Changeover Switching Unit for a Busbar

The purpose of the changeover switching unit for a busbar is to switch the power feed to an alternative power supply in case of voltage breaks. This case study complements the earlier experiences of model checking by analyzing a system that contains both analogue and digital technology and a state space explosion caused mainly by complex timing functions. To make model checking feasible with NuSMV, the lengths of the timing functions had to be scaled down. Even though some abstractions are made in the model due to complex timing properties, two hidden design errors were discovered. The analysis shows that model checking systems containing a large number of input signals and complex timing functions where the lengths of the functions differ by several orders of magnitude is challenging. The limitations of the NuSMV model checking tool are clearly demonstrated in this case study. It was discovered that one possible solution to address these problems is to develop a compositional model checking methodology, in which a larger system is split into more manageable sub-systems (see Case Emergency Diesel below).

Case Emergency Diesel

The purpose of the emergency diesel system is to provide reserve power as it is essential that electricity is always available to the maintained system. In case of a black out or a power failure in the main power supply, the diesel generators can be quickly turned on to keep the necessary devices available. The case study was utilized for developing a compositional technique for analysing large system designs with model checking. The objective of the technique is to automatically find a suitable configuration of modules that is computationally feasible but at the same time describes the system to be analysed with enough details to enable verification of the selected properties. The technique significantly reduces the manual work required in system verification but, however, only safety properties can be examined with the current methodology. It brings real added value to the model checking tool box but it is clear that additional research and development are still required. The emergency diesel system case was also utilized in the development of a modular model checking approach for modelling function

block diagrams with Uppaal. The asynchronous Uppaal models depict the system under analysis in more detail than the synchronous NuSMV models. This enables finding complex timing-related faults that cannot be found using only NuSMV. For further information on the developed techniques and the analysis of the emergency diesel system, see [24].

Conclusions

Digitalized I&C systems are able to perform increasingly complicated control tasks. They often combine real-time aspects such as timers with non-trivial control logic making their design and verification challenging. The MODSAFE project aimed at evaluating and developing methods based on formal model checking and applying them in the safety analysis of NPP safety automation.

During the project, model checking methodology was utilised in the analysis of a number of case examples through which the research group got feedback and further ideas. The methodology practically brought out its benefits by discovering several interesting behaviours of the analysed example system designs. The results of the project show that model checking is a valuable tool that can benefit utilities, regulators, and system vendors in achieving increased safety.

Despite the good results of the MODSAFE project, there still are lots of future challenges and research topics in the area. One of them is decreasing the amount of manual work when making models and analyzing the counter examples the model checker produces. The amount of work could be significantly reduced if the models could be automatically generated from the design documentation. Model checking is also currently not scalable to very large systems. New algorithms and techniques for modeling and reasoning are needed. Another challenge is the lack of confidence in the used model checking tool, the model and the checked specification. Further research is needed to find techniques to estimate and minimize these uncertainties. One more challenge is the quality of the system requirements specifications. In order to get reliable model checking results, the chain from the high level general requirements to the temporal logic formulas given to the model checking tool has to be unambiguous, traceable, and complete. Currently, the quality and the level of detail of the requirements specifications are not good enough for deriving the temporal logic statements for the model checker as such.

The methods developed and used in the MODSAFE project can be used to show that system designs contain erroneous behaviour but their correct behaviour

in all the possible cases cannot be shown. In the future, more emphasis will be put on the development of the methodology and tools for analyzing the behaviour of systems on a larger scale than before.

References

1. Alur, R. & Dill, D.L. A theory of timed automata. Theoretical Computer Science 1994, 126(2), pp. 183–235.

2. Alur, R., Courcoubetis, C. & Dill, D.L. Model-checking for real-time systems. Fifth Annual IEEE Symposium on Logic in Computer Science, Philadelphia, Pennsylvania, June 4–7 1990. IEEE Computer Society Press 1990. Pp. 414–425

3. Biere, A., Heljanko, K., Junttila, T., Latvala, T. & Schuppan, V. Linear Encodings of Bounded LTL Model Checking, Logical Methods in Computer Science 2006, 2(5:5), pp. 1–64.

4. Björkman, K., Frits, J., Valkonen, J., Lahtinen, J., Heljanko, K., Niemelä, I. & Hämäläinen, J.J. Verification of Safety Logic Designs by Model Checking, Sixth American Nuclear Society International Topical Meeting on Nuclear Plant Instrumentation, Control, and Human-Machine Interface Technologies, NPIC&HMIT 2009, Knoxville, Tennessee, April 5–9, 2009. American Nuclear Society, LaGrange Park, IL 2009. On CD-ROM.

5. Cavada, R., Cimatti, A., Jochim, C.A., Keighren, G., Olivetti, E., Pistore, M., Roveri, M. & Tchaltsev, A. NuSMV 2.4 User Manual, ITC-IRST, 2009. http://nusmv.irst.itc.it/.

6. Clarke, E.M. Jr., Grumberg, O. & Peled, D.A. Model Checking. The MIT Press, 1999.

7. Koskimies, M. Applying model checking to analysing safety instrumented systems. Research Report TKK-ICS-R5, Helsinki University of Technology, Department of Information and Computer Science, Espoo, Finland, June 2008.

8. Lahtinen, J. Model checking timed safety instrumented systems. Research Report TKK-ICS-R3, Helsinki University of Technology, Department of Information and Computer Science, Espoo, Finland, June 2008.

9. Larsen, K.G., Pettersson, P. & Yi, W. Uppaal in a nutshell. International Journal on Software Tools for Technology Transfer 1997, 1(1–2), pp. 134–152.

10. NuSMV Model Checker v.2.5.2, 2010. http://nusmv.fbk.eu/.

11. Uppaal integrated tool environment v. 4.0.6, 2009. http://www.uppaal.com/.

12. Valkonen, J., Koskimies, M., Pettersson, V., Heljanko, K., Holmberg, J.-E., Niemelä, I. & Hämäläinen, J.J. Formal verification of safety I&C system designs: Two nuclear power plant related applications, Enlarged Halden Programme Group Meeting – Proceedings of the Man-Technology-Organisation Sessions, C4.2., Institutt for Energiteknikk, Halden, Norway, 2008.

13. Valkonen, J., Pettersson, V., Björkman, K., Holmberg, J.-E., Koskimies, M., Heljanko, K. & Niemelä, I. Model-Based Analysis of an Arc Protection and an Emergency Cooling System – MODSAFE 2007 Working Report. VTT, Espoo, 2008. VTT Working Papers 93. 51 p. http://www.vtt.fi/inf/pdf/workingpapers/2008/W93.pdf.

14. Björkman, K., Frits, J., Valkonen, J., Lahtinen, J., Heljanko, K., Niemelä, I. & Hämäläinen, J.J. Verification of safety logic designs by model checking. In: Proceedings of the Sixth American Nuclear Society International Topical Meeting on Nuclear Plant Instrumentation, Control, and Human-Machine Interface Technologies NPIC&HMIT 2009, Knoxville, Tennessee, April 2009.

15. Björkman, K., Frits, J., Valkonen, J., Heljanko, K. & Niemelä, I. Model-based analysis of a stepwise shutdown logic. VTT, Espoo, 2009. VTT Working Papers 115. 36 p. + app. 4 p. http://www.vtt.fi/inf/pdf/workingpapers/2009/W115.pdf.

16. Lahtinen, J. Model checking timed safety instrumented systems. Vol. 3. Espoo: Helsinki University of Technology. TKK reports in information and computer science, 2008. ISBN 978-951-22-9445-9. http://lib.tkk.fi/Reports/2008/isbn9789512294459.pdf.

17. Valkonen, J., Karanta, I., Koskimies, M., Heljanko, K., Niemelä, I., Sheridan, D. & Bloomfield, R.E. NPP Safety Automation Systems Analysis – State of the Art. VTT, Espoo, 2008. VTT Working Papers 94. 62 p. http://www.vtt.fi/inf/pdf/ workingpapers/2008/W94.pdf.

18. Valkonen, J., Pettersson, V., Björkman, K., Holmberg, J.-E., Koskimies, M., Heljanko, K. & Niemelä, I. Model-Based Analysis of an Arc Protection and an Emergency Cooling System. VTT, Espoo, 2008. 13 p. + app. 38 p. VTT Working Papers 93. http://www.vtt.fi/inf/pdf/workingpapers/2008/W93.pdf.

19. Valkonen, J., Koskimies, M., Pettersson, V., Heljanko, K., Holmberg, J.-E., Niemelä, I. & Hämäläinen, J.J. Formal Verification of Safety I&C System Designs: Two Nuclear Power Plant Related Applications, Enlarged Halden Programme Group Meeting. Proc. Man – Technology-Organisation Session. Loen, Norway, 18–23 May, 2008.

20. Valkonen, J., Koskimies, M., Björkman, K., Heljanko, K., Niemelä, I. & Hämäläinen, J.J. Formal verification of safety automation logic designs. In: Automaatio XVIII 2009 Seminaari.

21. Valkonen, J., Björkman, K., Frits, J. & Niemelä, I. Model Checking Methodology for Verification of Safety Logics. In: Proceedings of the 6th International Conference on Safety of Industrial Automated Systems (SIAS 2010) Tampere, June 14–15, 2010.

22. Lahtinen, J., Valkonen, J., Björkman, K., Frits, J. & Niemelä, I. Model checking methodology for supporting safety critical software development and verification, European Safety and Reliability Conference, ESREL2010. Rhodes, Greece, 5–9 Sept. 2010. Reliability, Risk and Safety – Back to the Future. Ale, Papazoglou & Zio (Eds.). European Safety and Reliability Association, ESRA. London, 2010. Pp. 2056–2063.

23. Frits, J. Model Checking Embedded Control Software. Research Report TKK-ICS-R28. Aalto University School of Science and Technology, Department of Information and Computer Science. March 2010, Espoo, Finland.

24. Lahtinen, J., Björkman, K., Valkonen, J., Frits, J. & Niemelä, I. Analysis of an emergency diesel generator control system by compositional model checking – MODSAFE 2010 work report. VTT, Espoo, 2010. VTT Working Papers 156. 35 p. http://www.vtt.fi/inf/pdf/workingpapers/2010/W156.pdf.

5. Certification Facilities for Software (CERFAS)

5.1 CERFAS summary report

Hannu Harju, Jussi Lahtinen and Jukka Ranta
VTT

Risto Nevalainen
Tampere University of Technology, Pori

Abstract

As a part of the Finnish nuclear research program SAFIR2010 a project called CERFAS aimed to define necessary software certification services for nuclear industry needs. Main areas of the service development activities are process assessment and product evaluation.

Introduction

In Finland, a type acceptance certificate is required mainly in the highest safety class of instrumentation and control, I&C, equipments and systems in nuclear power plants. In the research project "Certification facilities for software (CERFAS)", the objective was to develop Software Certification Service, SCS, able to certify safety-critical software for the demands of the Finnish nuclear area.

As a part of the development of the SCS, the project produced three state-of-the-art reports [1, 2, and 3]. The first of these reports [1] examined the state-of-the-art of research and practice of software safety concentrating on software product certification. The second CERFAS-report [2] examined the state-of-the-

art of the process certification and evaluation. The third report [3] gives an overview of the Software Certification Service. The report aimed at giving basic principles in developing criteria for certification of software products.

CERFAS project created a process assessment method, based mainly on generic and nuclear specific standards, reference models and commercial process assessment approaches. Main results of the method are process specific capability ratings and conformance with nuclear specific standards. It can be applied both in safety class 2 and 3.

One of the main results of CERFAS was a guideline to producing a safety case. The guideline consists of a collection of safety case templates that includes claims, argumenting methods, set of evidence and procedures for the safety evaluation processes.

Main objectives

The main purpose of CERFAS was to develop facilities for a consortium called Software Certification Service (Figure 1). Conditions for successful operation of the consortium are the application of diverse expertise and effective evaluation tools.

Certification can be based both on generic sets of criteria and nuclear specific requirements. A goal in CERFAS has been to combine these two approaches. Most important nuclear specific requirements are standards, which include requirements for safety critical systems and software. The most relevant for software safety is IEC 60880, which can be used also as a reference for a certificate. Qualification and licensing of safety class 2 I&C systems includes a conformance statement against IEC 60880, and that is already a kind of a certificate. The other main reference is a system safety standard IEC 61513, which is based on generic IEC 61508.

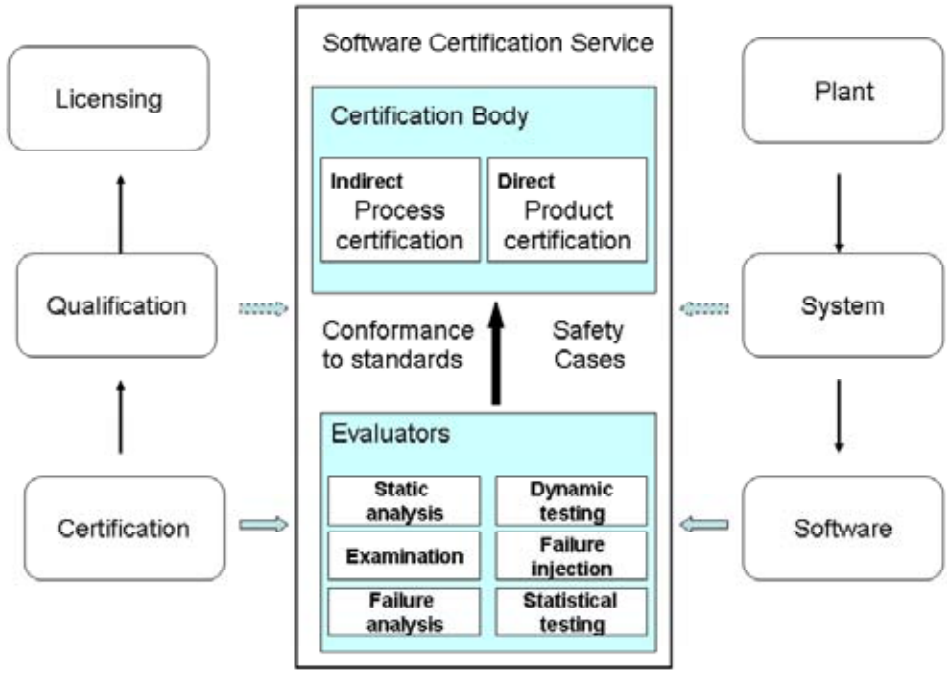

Figure 1. Main elements of Software Certification Service.

Certification can be defined as “the process of assessing whether an asset conforms to predetermined certification criteria appropriate for that class of asset” [1]. This idea of conformance with criteria is the fundamental principle of certification.

Certification requires advanced methods for evaluation of software process and the artefacts (documents, code, test plans, etc.). ISO 15504 Part 5 (known as the SPICE model) was used as the main source of process assessment. Part 5 covers all ISO 12207 processes and not all of them are relevant for certification purposes.

Many nuclear specific standards include quite similar concepts of processes as ISO/IEC 15504 Part 5, and they are also used as normative sources. A practical way to certify software processes in safety class 2 and 3 is to integrate generic approaches and nuclear specific approaches together. This was done mainly by combining process assessment indicators from ISO 15504 Part 5 and nuclear specific requirements from other standards, for example IEC 60880.

An overall description of SCS was written in 2010 as a certification handbook. The handbook covers the following issues: descriptions of product evaluation types, certification risk management, evaluation techniques and procedures, and software safety argumentation.

Main results

Specification of the software certification service

The software under certification is in most cases basic software (for example platform or COTS module), but also application software in cases where it is independent of application projects. The certification is aimed at supporting qualification of applications (software and system) that in turn supports the licensing issues.

The idea in the CERFAS project has been to integrate existing approaches together to facilitate effective and high quality certification. As a result, trust in software and the system increases and further qualification and licensing phases are easier both for the supplier and for the nuclear power plant [4].

Each certification type has its own certification elements. The framework in CERFAS (see Figure 1) assumes that a certificate is based on some reference model, norm or a set of criteria. The certificate itself is then a conformance statement against those requirements. Typically the statement consists of evidence created using a selection of methods. Some typical methods are external audits, IV&V's, reviews and inspections, code analysis and type tests. System centric certificates may include some hardware related methods, like aging tests and electromagnetic tests.

Process assessment elements of certification

A high-level and capable software development process is an essential part of software quality. Many de-jure and de-facto standards and models like ISO/IEC 15504 and CMMI are developed to assess the software process. The most rigid versions of these models are used to certify the software process. Several less disciplined approaches are also needed in process assessment, and they are defined and classified by their credibility and effort.

Many nuclear specific standards include quite similar concepts of processes as ISO 15504 Part 5, and they are also used as normative sources. IEC 61508 and IEC 60880 can be mapped with Part 5 processes quite easily and completely. So, the nuclear specific process reference model includes elements from generic and safety standards [6].

Process assessment is based on evidence, and it is quite close to the safety case approach in that sense. In ISO 15504, a piece of evidence is called an "indicator". Capability level 1 indicators are base practices and work products.

Each work product includes a set of characteristics. Capability level 2–5 indicators are generic practices and work products, and process resources. Systematic mapping of process indicators to requirements of nuclear specific standards gives quite a good coverage of evidence for certification.

Additional requirements for process assessment

Process assessment does not work in isolation and is not enough as such. It needs to be integrated with several other approaches in software certification, such as safety cases, conformance assessment and software measurement. The concept is illustrated in Figure 2, showing some typical process assessment related topics [7].

Figure 2 contains two types of topics. Some of them (clouds in Figure 2) are heavily interconnected and are always part of process assessment. For example, development process defines directly what the most important processes in the assessment scope are. Again, it defines what the essential documentation is. Process documentation points directly to product evaluation. Conformance with standards is always in the core of certification, because certification is based on some defined reference(s).

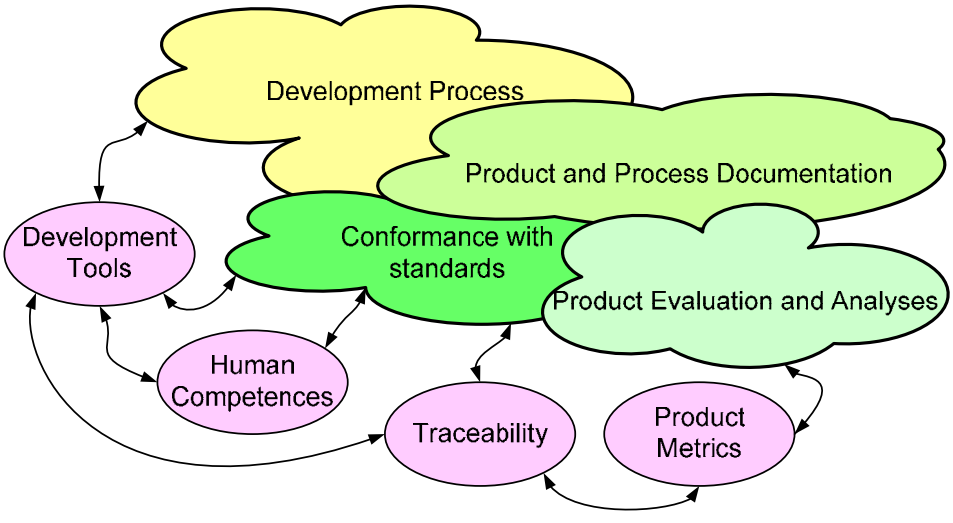

Figure 2. Some process assessment related topics in safety-critical software domain.

Some topics are more focused (some typical ones are shown as circles in Figure 2. They are sometimes mandatory elements in certification, like the proper validation

of development tools. Some others are more judgement-based, like human competences and their role in developing and validating safety-critical software. Traceability and product metrics are examples of topics that have high relevance as evidence for safety case. Note that only some of the relationships (arrows) are presented in Figure 2, which is mainly for illustration purpose.

Process assessment as a process itself is quite normal, that is, a SPICE – type process. Of course, a SPICE assessment is more formal than most improvement oriented assessments. Evidence is collected and recorded systematically, and they are a solid basis for data collection, validation and ratings. Rigour of assessment is near to Scampi-A method in strictness and formalism. Results are reported as gaps to a target level. Each gap can be classified with respect to magnitude and risk, as defined in ISO/IEC15504-4.

One additional stakeholder in process assessment is the certification body. A typical scenario is that a customer organisation orders certification from a certification body. They together decide together which references and methods are used in the certification. One basic requirement is the independent team for process assessment. Each team member has to fulfil competence requirements.

Conformance vs. capability in process certification

Conformance result is typically flat and linear, based more or less in Yes/No scale. Each non-conformance is recorded separately and the evaluation result consists mainly of those findings. So, it is a list of negative findings. This kind of evaluation is typical when an organisation is evaluated against some requirement standard. Typical example would be ISO 9001 or ISO 20000 audit.

The process assessment result is more structural. It consists of a list of processes, and each of them has a process capability profile, showing also the achieved level. Additionally, each process may have more technical results, like process attribute ratings. The rating scale is more continuous, as a minimum 4-point NPLF scale. SPICE- and CMMI-models also have an additional attribute, organisational maturity.

Safety standards, like generic IEC 61508 and nuclear IEC 60880, are conformance oriented. They may have and/or require also advanced calculations and analyses, for example requirements to evaluate the reliability of software and system. IEC 61508 is based on the concept of the safety integrity level (SIL), and SIL is 3 or 4 is typical for safety critical systems. The standard contains a set of corrective and preventive actions to achieve required reliability.

The regulatory authorities primarily need conformance results, to ensure that the system fulfils legal requirements. The Finnish nuclear safety authority STUK has its own requirements for licensing of safety-critical systems, called YVL 5.5. It has requirements for technical processes and V&V, and the requirements can be covered by conformance models. But YVL 5.5 has requirements also for the quality management system in the supplier organisation. Thus, in order to cover all YVL 5.5 requirements, some kind of combined multi-model solution must be used.

The licensee organisation is interested, in addition to conformance results, in the basic process capability results with risk analysis based on gaps. That can be done in several ways, but the capability determination mode of ISO/IEC 15504 is one specific and sophisticated model for that.

Combination of conformance and capability results is possible to achieve by classifying all evidence in both model types. Also models must be mutually mapped to cover all requirements. One problem in mapping is that generic requirements are often more abstract and then more open for various interpretations. They are often more strict, at least when taken literally.

Safety case as a documented body of evidence

Safety case is defined as “A document body of evidence that provides a convincing and valid argument that a system is adequately safe for a given application in given environment” [8]. Safety cases provide a formal argument that a system is safe, and show that any risks associated with its operation have been reduced to an acceptable level. In the safety domain, explicit safety cases are increasingly required by law, regulations, and standards. At present, several kinds of safety cases have been constructed. The following list presents some of them:

1. Goal based approach for safety case. “Increasingly, regulatory agencies are making the case for a goal-based approach, in which claims (or goals) are made about the system, and arguments and evidence support those claims”.
2. Requirements based approach for safety case. This safety case technique provides a systematic and complete way to show compliance to one or more standards.
3. Vulnerable or risk based approach for safety case. The safety case provides arguments that the risk of failures occurring due to a software malfunction is sufficiently low.

What ever the approach is, it covers the other two approaches. The safety case is defined in terms of three elements: 1) Claims about properties of the system, 2) Evidence used as the basis of the safety argument, and 3) Argument that links the evidence to the claims via a series of inference rules.

A claim is an objective which has to be achieved, for example, demonstrating that a system is safe, proving that a theorem is true, or showing that a hazard will not arise because of a given single point failure.

The following three types of arguments can be used: 1) Deterministic – relying upon axioms, logic and proof, 2) Probabilistic – relying upon probabilities and statistical analysis, and 3) Qualitative – relying upon adherence to standards, design codes etc.

Safety Case Templates, guidelines for argumentation and quality management procedures for producing of Safety Cases are given in three reports [9, 10, and 11].

The report [9] briefs the argumentation to be made by the Safety Case for the highest safety Category of I&C software of nuclear power plant. The report [9] includes guidelines for argumenting direct and credibility evidence of testing, analysing and field experience. It gives an overview of the initial point for beginning the evaluation: required artefacts, introduction to Safety Cases within safety properties and claims. Evaluation in the software certification service is based on the Safety Cases Templates given in the report [10].

The report [11] gives quality management procedures for evaluation and certification of software product safety in the highest category of I&C software in nuclear power plants. Using these procedures, we are able to ensure that the certification and evaluation process will be performed with high quality and objectively.

In general, certification is seen in CERFAS as a service to support system and software qualification and further licensing. Various areas of methods, standards and justification means are needed to support certification. Some examples are process assessment, product evaluation and use of different analyses and tests as seen in the Figure 1.

Quality management procedures

CERFAS project created a set of procedures to support certification of safety-critical software [11]. Each certification body may have their own procedure to satisfy accreditation requirements of each service. Additional guidance is needed for software certification, because such service does not exist in Finland.

Procedures are written in Finnish, to make them more usable for certification bodies. List of procedures is in Table 1.

Table 1. List of Software Certification Service procedures.

SCS01 Evaluation process model	SCS12 Accepting of current certifications
SCS02 Entering into a contract	SCS13 Rigour degrees of evaluation
SCS03 Specifying evaluation	SCS14 Supplementing and re-evaluating
SCS04 Planning evaluation	SCS15 Assessment Report Format
SCS05 Performing evaluation	SCS16 Certificate format
SCS06 Concluding evaluation	SCS17 Auditing development processes
SCS07 Mapping client's documentation	SCS18 Examining product artifacts
SCS08 Reviewing evaluation reports	SCS19 Witnessing testing and analyses
SCS09 Reporting preliminary evaluation	SCS20 Limiting liability and managing risks
SCS10 Reporting final evaluation	SCS21 Using SPICE model in product certification
SCS11 Highlighting deviations	

Conclusions

Process assessment supports directly qualification of safety-critical applications but is less relevant for certification of platforms and environments. Anyway, qualification and certification are closely related, because certification as a whole supports qualification and makes it more effective. It is possible to adapt and evolve process assessment so that it supports both qualification and certification.

A typical process assessment is done for improvement purpose. In qualification and certification, conformance and management of risks are more relevant. Process assessment, according our current knowledge, provides interesting insights in the safety aspects of a software product. For example, if there are gaps found in the relatively light-weight "ability" assessment, heavier methods like model checking can then focus on those weaknesses trying to find out if they are endangering the actual safety. The ability is also one of the industry needs, since a well documented method to get the first go/nogo decision in the purchasing process saves resources at later stages. Still, the process assessment is only a complementary method when the final validity of the product is analysed.

The Safety Case Templates of Category A [10] software product include all important safety requirements of the two software safety standards IEC 60880 and IEC 61508-3.

The templates comply with the rules of a well-known V-model of software development. There are claims for completeness and correctness of software requirements, and arguments for analysing and validating the implementation of these claims.

The Safety Case Templates of the design and implementation of the software product compose the middle section of the V-model: verification of the design and implementation phases. The design and implementation is divided into more detailed Safety Case Templates: Software structure, self-supervision, detailed design and implementation and language. In addition, there are Safety Case Templates for risk management, and pre-developed software.

The claims provided by the Safety Case Templates are mainly originated from IEC 60880 and argumenting techniques from IEC 61508-3. Claims are permanent, but more detailed criteria are needed on the case, for example making risk informed analyses to software artefacts. Guidelines for making templates are given in a CERFAS-report [9]. Results of the argumentations are written in the Safety Case Templates, summaries in the Assessment Report and individual testing reports.

References

1. Harju, H. & Pakonen, A. State of the Art of Software Certification. SAFIR2010, CERFAS. VTT, Espoo, 2007. Research report VTT-R-09699-07.

2. Nevalainen, R. & Johansson, M. Software Process and Product Quality Evaluation in Safety Critical Domains. CERFAS State of the Art Report. Tampere University of Technology. Pori. Research Report 5, 2008.

3. Harju, H. Software Certification Service: Facilities for type approval of system software product. SAFIR2010, CERFAS. VTT, Espoo, 2007. Research report VTT-R-09700-07.

4. Harju, H., Lahtinen, J., Ranta, J., Johansson, M. & Nevalainen, R. Software safety standards for the basis of certification in the nuclear domain. In: 7th International Conference on the Quality of Information and Communications Technology QUATIC 2010. Porto, Oct. 27–29, 2010.

5. Lahtinen, J., Ranta, J., Harju, H., Johansson, M. & Nevalainen, R. Comparison between IEC 60880 and IEC 61508 for Certification Purposes in the Nuclear Domain. VTT and TUCS, SAFECOMP'2010, Vienna, Sep. 14–17, 2010.

6. Nevalainen, R., Halminen, J., Harju, H. & Johansson, M. Certification of software in safety-critical I&C systems of nuclear power plants. VTT, TVO and TUCS. In: Nuclear Power. Tsvetkov, P. (Ed.). Sciyo, 2010. ISBN 978-953-307-110-7.

7. Johansson, M. & Nevalainen, R. Additional Requirements for Process Assessment in Safety-Critical Software and System Domain. Journal of Software Maintenance and Evolution: Research and Practice, incorporating Software Process: Improvement and Practice. Special Issue Paper JSME-10-0051, 14.5.2010.

8. Bishop, P.G. & Bloomfield, R.E. A methodology for safety case development. In: Safety-Critical Systems Symposium, Birmingham, UK, February 1998.

9. Harju, H. Sertifioinnin käsikirja. Kategorian A ohjelmistotuotteen turvallisuuden perusteleminen. SAFIR 2010 programme, CERFAS-project. VTT, Espoo, 2010. VTT-R-10276-10. (Handbook of Certification. Argumenting safety of a Category A software product). (In Finnish.)

10. Harju, H. & Lahtinen, J. Safety Case Templates. Category A Software. SAFIR2010 programme, SAFIR 2010 programme, CERFAS-project. VTT, Espoo, 2010. VTT-R-10277-10.

11. Harju, H., Ranta, J. & Nevalainen, R. Menettelytapaohjeet: Kategorian A ohjelmiston tuotearviointi. SAFIR 2010 programme, CERFAS-project. VTT, Espoo, 2010. VTT-R-10278-10. Procedures: Evaluation of Category A software product. (In Finnish.)

5.2 Certification facilities for software: Evaluation by Safety Case Templates

Hannu Harju, Jussi Lahtinen and Jukka Ranta
VTT

Risto Nevalainen
Tampere University of Technology, Pori

Abstract

As a part of the Finnish nuclear research program SAFIR2010 a project called Certification facilities for software (CERFAS) aimed to define necessary software certification services for nuclear industry needs. The developed service is closely based on the concept of a Safety Case which is a document and structured set of evidence that provides a convincing and valid argument that a system is adequately safe for a given application in given environment. This special report gives directions for argumentation in a Safety Case concerning I&C software of the highest safety category used in a nuclear power plant.

Introduction

Certification can be defined as “the process of assessing whether an asset conforms to predetermined certification criteria appropriate for that class of asset” [1]. This idea of conformance with criteria is the fundamental principle of certification. Certification can be based both on generic sets of criteria and nuclear specific requirements.

Conformance can be achieved only by use of several different approaches, which all provide their own evidence and support for qualification and licensing. Certification is one way to package different methods and build trust in achievement of safety. It can also be a cost-effective way for qualification, because one certificate is typically valid for all instances of the same system.

This special report gives directions for argumentation in a Safety Case concerning I&C software of the highest safety category used in a nuclear power plant. Safety Case Templates, guidelines for argumentation and procedures for producing of Safety Cases are given in three reports [2, 3, and 4].

The report [2] includes guidelines for arguing direct and credibility evidence of testing, analysing and field experience. It gives an overview of the initial point in beginning of the evaluation: required artefacts, introduction to Safety Cases with safety properties and claims, testing, analysing and field experiment evidence as part of acceptable argumentation. Evaluation in the software certification service is based on Safety Case Templates which are given in the report [3].

The report [4] gives quality management procedures for evaluation and certification of software product safety in highest category of I&C software in nuclear power plants. By these procedures, we are able to ensure that the certification and evaluation process will be performed objectively with high quality.

Certification as a service

Framework of the software certification service developed by CERFAS includes a certification body and several evaluators with dedicated methods and techniques to be used to collect evidence. Using the safety case methodology, certifiers of certification body and the evaluators are able to perform safety justification of software. Evaluators are divided into two groups: those who evaluate development processes and those who concentrate on technical aspects of the software product. Justifications must be based on conformance to technical standards valid in nuclear domain.

Safety is a feature of a system in a given context. Software of a system must be considered related to the system level requirements and these requirements must be traceable to individual software components that implement these high-level requirements. In the nuclear domain and specifically in the IEC domain, IEC 61513 gives requirements for completely bespoke development and pre-developed components such as hardware, operating systems and other software if incorporated into a design. Software safety evaluation does not only concern software. Hardware failures, design errors, erroneous inputs, human errors and mischievous attacks must also be taken into account. Unfortunately, IEC 61513 and IEC 60880 give requirements mainly for system development. They do not concern measurements that should be valuable for technical evaluation.

Evaluators make the evaluation work, which is assigned by the main certifier. In the software certification service, all evaluators justify safety of the target software by safety case methodology and the certifier collects each safety case together into a certification report. It is the certifier’s duty to become convinced of the completeness with respect to the design. The software requirements should

address all system functions allocated to software in a platform. Requirements in the system level are usually most of all related to common cause failures caused by software.

Typically, a customer organization places an order for certification to a certification body. They decide together which references and methods are to be used in the certification. An important requirement for the certification body is the satisfaction of accreditation rules, which are defined in EN 45011 and EN ISO/IEC 17020 series of standards. The evaluation process must be documented and contain an audit trail between evaluation phases and intermediate results. If the evaluation ends with a certificate, it must be publicly available for intended audience. Most relevant accreditation requirements are for product and management system certificates. Additionally, process assessment standards and models, for instance SPICE model families have their own additional guidance for conformance.

Finnish Accreditation Service, FINAS, authorizes VTT Expert Services to perform certification. This accreditation requires that EN 45011 of product certification quality program and EN ISO/IEC 17020 of audit and certification of management systems are met. VTT Expert Services has applied to FINAS for full accreditation to IEC 61508. In the full accreditation, the standards of accreditation mentioned above are substantially met.

The safety case methodology

Type testing or other kind of Independent Verification and Validation (IV&V) is typically a fundamental part of the certification. Any certification body needs a variety of services to run a certification service and to integrate different approaches as a coherent system.

Each certification type has its own assessment elements. The framework in CERFAS assumes that certification is based on some reference model, norm or a set of criteria. The certificate itself is then a conformance statement against those requirements. Typically, such statement is justified by some methods, which include external audits, IV&V's, reviews and inspections, code analysis and type tests. Safety cases provide a formal argument to justify that a system is safe.

Certification procedure

A typical assessment begins with a complete review of the plan that describes the development process by which a new software product is to be developed. The information contained should include all design steps (inputs required,

processes to be performed and outputs required), all verification activities, responsibilities and all project documentation generated.

Product requirements and design documents are reviewed next. Evidence that the required verification activities have been done shall be included. Competency records must be in place and show that those assigned to the project were competent to perform their specific tasks. When the paper review is complete, the assessment continues with detailed on-site meetings.

When all relevant documents are reviewed, interviews with the responsible personnel must take place. This is done by visiting the development and manufacturing site. One of the key interview questions is “What process was followed in the design of this project?” and “Have the safety requirements been implemented in the product”. Any discrepancies must be justified and documented by modifications to the appropriate documentation. Actors will give supplementary test cases or make analysis concerning specific safety issues. The site visit must also include witnessed validation testing and these additional testing cases.

If all documentation for both the process and the product is complete and seems fit, a safety case document is created. This step provides a systematic method to ensure that no requirements of the standards are missed. Often missing requirements are identified and the assessment must return to a previous step to correct the problem. When the safety case is judged to be accurate and complete, the certification report describing all assessment activities and their results is written.

The documentation is given to an independent auditor to verify. When the audit is complete and the independent auditor supports the certification, the certificate is issued.

Contents of the Safety Case report

Safety Case report includes the following subject matters:

- Information of the safety design and development process undertaken.
- Information of the assessment and audit processes undertaken.
- Information of the argumentations based on tests, analysis and operational experience.
- Information of the current safety status in terms of evidence obtained and unresolved hazards.
- Definition, description and configuration of the software.

- Description of the software's environment, boundaries and interfaces, including assumptions about other software, services and facilities.
- Reference to existing sub-software's assessment reports or certificates.
- Change control.
- Standards.
- Evaluation Management Report.
- Roles and Responsibilities.
- Summary of assessments findings.
- The assurance that foreseeable hazards have been identified.
- The assurance that intolerable risks have been eliminated.
- The assurance that other risks have been controlled to an acceptable level.
- The presentation that the safety analyses have taken into account the scope of the software and its normal and abnormal operation.
- A list of the assessment techniques and tools.
- Identification of the design documents referenced during the assessment work.
- Summarise the non-compliances raised in the assessment. Details of the non-compliances will be found in the Safety Case Module Reports prepared by individual assessors.

A Safety Case structure

A safety case is defined as "A document body of evidence that provides a convincing and valid argument that a system is adequately safe for a given application in given environment" [5]. Safety cases provide a formal argument that a system is safe and show that any risks associated with its operation have been reduced to an acceptable level. In the safety domain, explicit safety cases are increasingly required by law, regulations, and standards. At present, several kinds of safety cases have been constructed.

In CERFAS, a case study was performed using a safety case produced by the structure presented in Figure 1. According to the structure, certification is a judgment based on three elements: claims, evidence, and argument. The claims

recognize undesirable consequences to be taken into account and the degree of risk considered tolerable; evidence involves the results of analyses, reviews, and tests; and the argument based on the evidence makes the case, that is, the claims satisfied.

All requirements of each standard considered must be compiled and precisely documented along with the reasoning behind the requirements. Each argument is traced with evidence documents to claims showing the results of the evaluation.

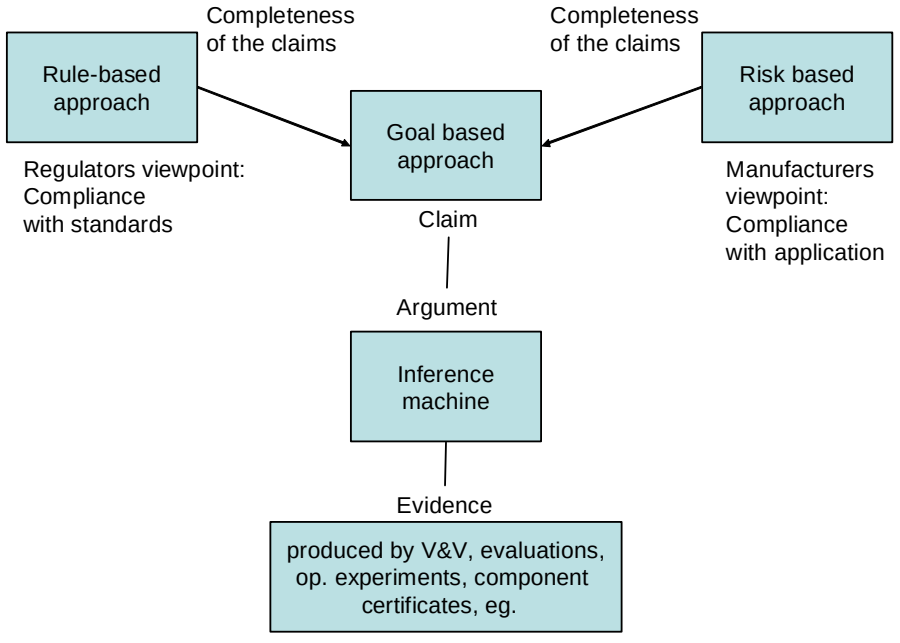

Figure 1. A safety case structure used in a certification pilot project.

A claim is an objective which has to be achieved, for example, demonstrating that a system is safe, proving that a theorem is true, or showing that a hazard will not arise because of a given single point failure.

The following three types of arguments can be used: 1) Deterministic – relying upon axioms, logic and proof, 2) Probabilistic – relying upon probabilities and statistical analysis, and 3) Qualitative – relying upon adherence to standards, design codes etc.

Good argumentation

Confidence in acceptance of safety cases is an important issue. It is affected by both information uncertainty and inadequate understanding. The quality of a

safety case is related to the concept of good and acceptable argumentation and sufficient evidence. A good argument should be refutable by appropriate evidence. For example, bad product evidence of metrics, testing or analysis can refute claims. Whereas, argumentation based on compliance with process requirements as an argument for safety, is not refutable. The argument only supports the claim for safety; it will never be able to prove that the system is safe. A good argument

- is always refutable by the evidence,
- is acceptable; it is one that is known to be true or is otherwise believable,
- is based on an unambiguous interpretation,
- provides sufficient supporting evidence,
- is relevant to the appropriate claim.

Safety Case Templates as a part of certification

Direct and credibility evidence is connected to each claim. The report [2] contents guidelines for argumenting direct and credibility evidence by testing, analysing and field experience. It gives an overview of the initial point of the evaluation: required artefacts, introduction to Safety Cases testing, and analysing and field experiment evidence as part of acceptable argumentation.

For instance, the report [2] includes requirements of direct and credibility evidence from testing. Tests should be specified for all behavioural attributes of each software safety requirement, and carried out to demonstrate that acceptance criteria for each attribute have been achieved. For evidence of testing to be credible it should include specifications, criteria, results and an analysis of discovered faults. The tests are sufficiently covered, and criteria a complete and correct interpretation of the software safety requirements.

Extracts of main claims and argumentations of Safety Case Template are presented in the following two Tables 1 and 2, respectively.

Table 1. An extract of the main claims for self-supervision design [3].

4.	**Self-supervision design meets the software requirements**
4.1	Plausibility checks are performed for minimizing potential residual faults
4.1.1	Potential residual faults are minimized by defensive programming
4.1.2	Diagnostic of potential residual faults is extensive
4.2	The system produces safe output in case of failures
4.2.1	Fail safe behaviour
4.2.2	System is in correct operation due to minor failures
4.2.3	Faults are not accumulated
4.3	Memory contents are protected or monitored
4.3.1	Potential residual faults are minimized
4.3.2	There is not any unauthorized change
4.3.3	Propagation of addressing faults or hardware faults, including intermittent faults are prevented
4.3.4	The software is maintained in its licensed form
4.4	Failure propagation is prevented by high covered error checking
4.4.1	Counters and reasonableness traps ensure that the program structure has been run through correctly
4.4.2	Any kind of parameter transfers are checked, including parameters type verification.
4.4.3	When addressing an array its bounds are checked
4.4.4	The run time of critical parts are monitored
4.4.5	Assertions are used

Table 2. An extract of the main claims and argumentation guides for the protection and monitoring of memory contents [3].

4.3	**Memory contents are protected or monitored**
	Confirm for every appropriate argument: Examination and testing are properly performed
4.3.1	Potential residual faults are minimized
	Confirm for every argument: Examination and testing processes are properly performed
	Argue by code analysis and testing that the memory contents are protected or monitored
4.3.2	There is not any unauthorized change
	Argue by examining and testing the security protection system
4.3.3	Propagation of addressing faults or hardware faults, including intermittent faults are prevented
	Argue by examining and testing that the memory space for constants and instructions are write protected or supervised against changes
	Argue by examining and testing that unauthorised reading and writing is prevented
4.3.4	The software is maintained in its licensed form
	Argue by examining and testing that the system is secure against code or unauthorised data changes by the plant operator

Conclusions

The Safety Case Templates of Category A [3] software products include all important safety requirements of the two software safety standards IEC 60880 and IEC 61508-3.

The templates comply with the rules of a well-known V-model of software development. There are claims for completeness and correctness of software requirements and arguments for analysing and validation testing the implementation of these claims.

The Safety Case Templates of the design and implementation of the software product compose the middle section of the V-model: verifications of the design and implementation phases. The design and implementation phase is divided into more detailed Safety Case Templates: Software structure, self-supervision,

detailed design and implementation and language. In addition, there are Safety Case Templates for risk management, and pre-developed software.

The claims provided by Safety Case Templates are mainly originated from IEC 60880 and argumenting techniques from IEC 61508-3. Claims are permanent, but more detailed criteria are needed depending on the case, for example making risk informed analyses to software artefacts. Guidelines for making templates are given in a CERFAS-report [2]. Results of argumentation are written in Safety Case Templates, summaries in the Assessment Report and individual testing reports.

References

1. ISO/IEC 24765 Systems and software engineering vocabulary, 2009.

2. Harju, H. Sertifioinnin käsikirja. Kategorian A ohjelmistotuotteen turvallisuuden perusteleminen. SAFIR 2010 programme, CERFAS-project. VTT, Espoo, 2010. VTT-R-10276-10. Handbook of Certification. Argumenting safety of Category A software product. (In Finnish.)

3. Harju, H. & Lahtinen, J. Safety Case Templates. Category A Software. SAFIR 2010 programme, CERFAS-project. VTT, Espoo, 2010. VTT-R-10277-10.

4. Harju, H., Ranta, J. & Nevalainen, R. Menettelytapaohjeet: Kategorian A ohjelmiston tuotearviointi. SAFIR 2010 programme, CERFAS-project. VTT, Espoo, 2010. VTT-R-10278-10. Procedures: Evaluation of Category A software product. (In Finnish.)

5. Bishop, P.G. & Bloomfield, R.E. A methodology for safety case development. In: Safety-Critical Systems Symposium, Birmingham, UK, February, 1998.

6. Operator Practices and Human-system Interfaces in Computer-based Control Stations (O'PRACTICE)

6.1 O'PRACTICE summary report

Jari Laarni, Leena Norros, Paula Savioja, Iina Aaltonen, Hannu Karvonen, Hanna Koskinen, Marja Liinasuo and Leena Salo
VTT

Abstract

In the O'PRACTICE-project the main aim has been to develop practices of Human Factors Engineering (HFE) for the design, operation, and evaluation of human-system interfaces at nuclear power plant (NPP) control rooms (CRs). This paper presents firstly a short review of the main research activities that have been carried out during the four-year period. After that, some applications and implications of the results are discussed, especially focussing on some design recommendations.

Introduction

Background

At the moment Finnish nuclear power plants are renewing their automation systems, CRs and human-system interfaces (HSIs). In control rooms there will be a change from analogue technology to digital technologies and desktop-based workstations. These changes are challenging, since they are conducted stepwise during several years, and different types of hybrid interfaces are in use during

these years. At the same time, a new plant unit is built, and its automation systems and HSIs are also based on digital technology.

Since CR modernizations and changes in plants provoke risks, there is a clear need to pay closer attention to the accomplishment of CR and HSI renewals. This need has been acknowledged among the nuclear community, and new guidelines have been developed for management, design, evaluation, and implementation of HSI renewals. There is also need to develop new tools and practices that help manage problems caused by digital technologies.

Main objectives

The O'PRACTICE-project has aimed at developing practices of Human Factors Engineering for the design, operation and evaluation of human-system interfaces at NPP CRs. We have gathered knowledge of changing operator practices and new HSI solutions in order to promote safe use of digital technologies and developed new methods and practices for the evaluation of the safety of HSIs. The aim has also been to develop expertise on user-centred design of complex industrial systems in Finland, further promote international collaboration with research and expert organizations and institutions and strengthen delivery of expertise in Finland in the field of user-centred design of technical systems.

As results of the project a Concept of operations (ConOps) for digitalized control rooms and new innovative concepts for presentation of process information have been outlined, and more reliable and valid methods for the evaluation of CRs and HSIs have been presented.

Main results

The project has been carried out by conducting a couple of empirical and case studies combined with theoretical work in the focus areas of the project (Figure 1).

Empirical studies

Two large empirical studies have been conducted at the Loviisa and Olkiluoto training simulators [1]. Based on these studies, conclusions have been drawn with regard of the integrated system validation (ISV) of the hybrid CR and HSIs, and the results have been presented in a format of an ISV document. Specifically, the aim has been to study factors that promote and inhibit the development of 1) a general operational picture of the state of the power production process and

2) the role of different sensory modalities in the development of situation awareness and communication processes among CR operators and in the development of ways of communicating with field operators.

Innovative HSI solutions

The following studies have been conducted:

– Data of Halden experiments with different HSI design solutions (ecological interface design (EID) vs. two versions of "industry-standard" user interface) has been analysed, and a final report has been prepared [2, 3].

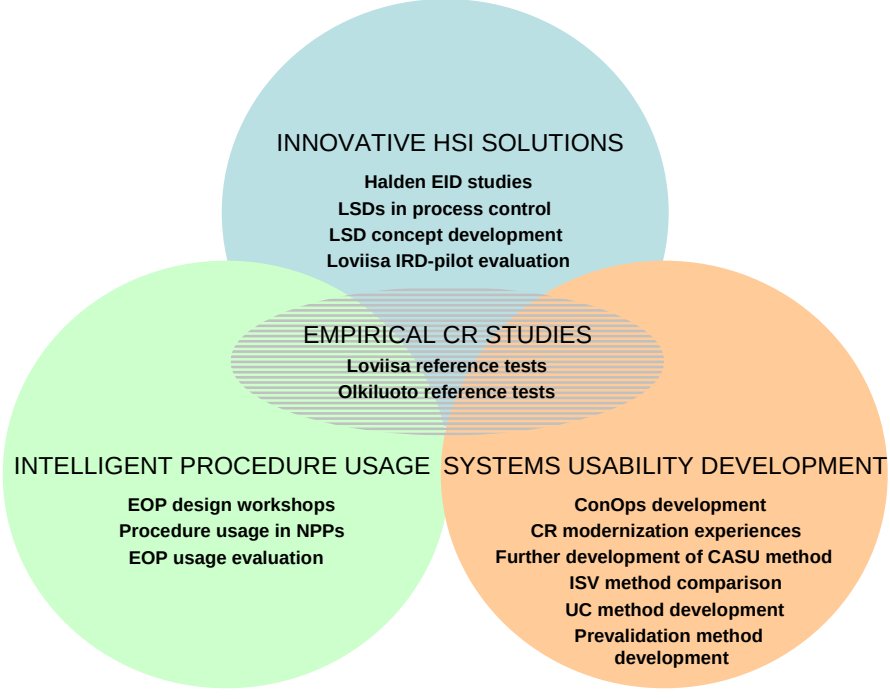

Figure 1. Main research activities in the O'PRACTICE-project during 2007–2010.

A literature review of the design and usage practices of large-screen displays (LSDs) in process industries has been prepared [3].

– Two workshops on LSD design have been organized at both Finnish NPPs. Based on them, the general framework for the LSD concept for digitalized CRs, including the description of LSDs from the point of view of their information content and usage practices, has been outlined [4].

– The design and usage practices of LSDs based on the Information Rich Design (IRD) concept have been studied in the simulator environment [5].

Intelligent procedure usage

The following studies have been conducted:

– Two workshops (one at Fortum and another on at Electricité de France) on emergency operating procedure usage have been conducted.

– Literature review on the use of computer-based emergency operating procedures has been prepared providing knowledge and insights concerning the goals, constraints and design principles in the development of new procedures and their integration with other components of the CR HSI [6].

– Based on the Loviisa reference test data, we have provided knowledge of operators' attitudes and orientations towards different types of procedures and their metaphors of procedure usage. We have also studied the role of procedures in crew communication and coordination in particular emergency situation [7].

Development of systems usability

Development of systems usability includes two subtasks: the development of the ConOps for hybrid CRs and the development of the evaluation methodologies.

ConOPs development

– Theoretical study on the role of the ConOps within the HFE design process and its links to technical design of CR and HSI systems has been carried out.

Evaluation method development

– Workshops have been arranged both at Loviisa and Olkiluoto plans concerning the modernization of CRs and HSIs in which operators' and trainers' experiences with hybrid HSIs have also been collected and analysed [8, 9].

– The earlier developed method for the contextual assessment of systems usability (CASU) has been further developed [10, 11]. We have developed new ways to model scenarios and refined our information gathering methods

and tools (e.g., an expert evaluation form, debriefing methods, and a questionnaire for the assessment of systems usability). We have also refined our methods for analyzing quantitative and qualitative data.

- Critical evaluations of the CASU method have been made, and we have compared the method to other ISV methods according to, e.g., their reference, metrics, end-user involvement and effort [12].
- The Usability Case method providing an accumulated documented body of longitudinal evidence of the degree of usability of a system has been developed [13]. The usefulness of the approach has been demonstrated by its application to the evaluation of computer systems in different application domains.
- Pre-validation test methodology has been developed. A paper has been prepared in which examples of the application of the approach are given [14].

International co-operation

- Participation in the EU/EURATOM/MMOTION-project in which a roadmap for European research on man-machine organization has been developed.
- Participation in the OECD/NEA Working Group in Human and Organizational Factors, e.g., for the identification of research issues and trends in the areas of HFE methods and tools.
- One member of the Human activity and systems usability team has worked as a secondee at Halden Reactor Project during 2009–2010 and participated in, e.g., the development of interactive display surfaces for outage control.

Applications and implications

The developed method for contextual assessment of systems usability has been used in several commission projects during 2007−2010. The research team has participated in the verification of design documents (e.g., style guide, architecture plan, verification and validation plan) and in the pre-validation and integrated system validation of CR and HSI renewals.

Ad hoc seminars and workshops on the themes (e.g., LSD design, verification and validation, and ConOps for a digitalized CR) of the O'PRACTICE-project have been regularly organized. The discussions with the stakeholders of Finnish nuclear power companies and the Finnish regulator have been useful in providing

feedback and suggestions for future studies. They have also been one of the primary means to share and disseminate the results of the project to the funding organizations and to the Finnish regulator.

At the final stage of the project the main results and implications of the studies have been presented as two PowerPoint slide sets. The PowerPoint slide presentation "Contextual Assessment of Systems Usability – Description of the method" [11] describes the methods that have been developed for the evaluation of the systems usability of CR and HSI systems. In addition to that, a slide presentation has been prepared for providing recommendations for CR and HSI design. These recommendations have been outlined based on the results of the empirical and case studies.

Some recommendations for HSE design

In the following, a short survey of some of the recommendations for HFE design based on empirical and case studies is provided. The recommendations are classified into four main groups that are related to the HFE-based design process, to the control room and HSIs, to the procedures and to the operator training.

HFE-based design process

Our interview studies suggest that it is important that CR design is based on a systematic approach. The HFE-plan must describe in a concrete manner in which way the different HFE-activities are interrelated, what kinds of input-output relations there are between them, and how the user involvement is accomplished in the design process. The plan also has to describe by which way the HFE-activities are linked to the different technical design activities during different phases of the modernization project. Furthermore, it is important that the designers and end-users collaborate to a sufficient degree within a framework of participatory user-centred design.

A systematic approach (i.e., Usability Case) is needed for the schematization of the data concerning the systems usability of HSIs. It helps to integrate the claims concerning the usability of the system to the experimental evidence.

The outlining of the Concept of Operations document is a key activity at the beginning phase of the project. Different ConOps documents should form a hierarchical system of documents, e.g., the ConOps of the main CR is a part of the ConOps of the plant. On the other hand, the ConOps of the main CR lays a

basis for several more detailed concept documents (e.g., LSD and alarm concept). We see ConOps as a "living document" the life time of which is equivalent to the plant. The ConOps should be revised and used as a design basis in every operational transformation that takes place during the plant life cycle. The ConOps serves as a communication tool in the design process, and it helps make effects of technical changes (e.g., CR modernisation) visible and thus reflectable for all relevant stakeholders.

Design guidelines should be detailed enough, and they must form a comprehensive and hierarchically structured style guide document. For the verification of the design evaluation checklists have to be prepared, which must be comprehensive and form a hierarchical system. Some recent papers provide guidance for the development of HFE checklists [15].

CR and HSI design

Results of the Loviisa and Olkiluoto reference tests suggest that the CR should support the development of an accurate mental model of the plant and the power process. Specifically, it has to support the management of the operators' primary tasks and the development of an overview of the power process. It is important that the essential process information is constantly and consistently presented, and control actions are carried out timely and without errors.

The secondary tasks (navigation, walking to panels) should be carried out efficiently, and they should not increase the operators' workload. A special emphasis must be put on visual ergonomics (e.g., visibility of the critical information from different places of the control room), physical ergonomics of the workstations (e.g., there should be enough table space) and for the sound environment of the CR (e.g., background noise should not disturb communication). All essential information should be presented in such a way that operators can detect and perceive it while sitting at the workstation (for guidance in visual job analysis, see [16]). Since the CR has to support the operating crew's collaboration, the operators' workstations should be carefully arranged with respect to one another.

Our LSD studies suggest that in the design of overview displays a good starting point is a simplified process system diagram which shows the basic process parameters, and basic trends and alarms. These displays should also support the perception of input-output relations between subsystems and provide an integrated overall view to the process.

Control elements and devices should be easy to use, and they should perform in a reliable manner. A special emphasis should be put on the usability and functionality of touch screen displays. The user interface should provide support for the selection of a control device, and sufficient feedback should indicate that a command is received.

Results of the reference tests suggest that alarm management (alarm prioritization and processing) has to be improved, since the present state is in many ways intolerable from the operator's point of view: The number of alarms should be reduced to a more suitable level, the critical alarms should be better prioritized, and the mode of alarms should be better coded. Alarms should be integrated to other displays to enable easy access to process components to which the alarm is related. The user interface should also better support the selection of the procedure that is related to the alarm.

Intelligent procedure usage

Studies on procedure usage suggest that procedure design should support the intelligent usage of procedures. By "intelligent usage of procedures" it is meant that operators have to strictly follow the requirements of a procedure if it is well suited to the operational process state, but if there are discrepancies, the operators could have a possibility to use their own initiative. In procedure design it has to be taken into account that the operator activities are typically not restricted to those listed in the procedure but include all kinds of monitoring activities that should be tackled in the training.

The procedures should be designed to support the development of an accurate picture of the state of the process and operator decision making. The target state should be that when reading the procedure text and focussing on the application of the procedure the operator's situation awareness is improved and not decreased.

Training

Operator training should support the development of active, reflective orientation, and the monitoring and controlling of the whole plant process. A special emphasis should be put on the training of communication and collaboration skills, and it is useful if the communication in accident situations follows a quite standardized communication protocol [17].

In a modernization situation training has to be seen as a multi-stage process, including enough practical training at simulators and rehearsals [18]. Training

should especially support the development of such competencies for which the procedures do not provide guidance. The operators have to understand the principles and rationale behind the new design, and the trainers should especially emphasize differences between the old and the new system and concentrate the training on these differences.

Conclusions

Several activities included in the HFE design process have been studied in the O'PRACTICE-project (for a description of the process, see [18]). The definition of the ConOps for digital CRs can be considered to be the end product of the planning and analysis phase of the framework. Research on procedure usage and HSI design is related to the design activities, and the development of evaluation methodologies is linked to the verification and validation.

The aim in the future projects is, on the one hand, to extend the focus of our research to other HFE activities, and on the other hand the aim is to delve deeper and study more thoroughly those HFE-activities that we have covered in our previous studies. To achieve these goals, we will for example develop expertise and new tools for the accomplishment of HFE activities during design process.

One of the main aims in the future projects is to study how humans and automation systems collaborate to achieve safety and production goals of NPPs. Specifically, the aim is to gather knowledge of procedure- and HSI solutions supporting accident management, and provide knowledge of the effect of the new digital automation concepts on the operator behaviour in incident and accident situations. The effect of the increased complexity of automation systems and HSIs on operators' automation awareness and on their automation skills will also be investigated.

References

1. Laarni, J., Norros, L., Savioja, P., Liinasuo, M., Aaltonen, I. & Karvonen, H. Operator practices and human-system interfaces in computer-based control stations (O'PRACTICE) – Final report, 2011. (In preparation.)

2. Salo, L. & Norros, L. The effect of display type on process control performance – Case EID. Proceedings of the Sixth American Nuclear Society International Topical Meeting on Nuclear Plant Instrumentation, Control, and Human-Machine Interface Technologies NPIC&HMIT 2009, Knoxville, Tennessee, April 5–9, 2009. American Nuclear Society, LaGrange Park, IL. (On CDROM.)

3. Koskinen, H., Salo, L. & Aaltonen, I. (Eds.). Tilannetietoisuutta tukevat näytöt prosessiteollisuuden valvomoissa. [Displays supporting situation awareness in process industry]. VTT, Espoo, 2009. VTT Tiedotteita 2495. (Partly in Finnish.) ttp://www.vtt.fi/inf/pdf/tiedotteet/2009/T2495.pdf.

4. Laarni, J., Norros, L., Koskinen, H. & Salo, L. Designing large screen displays for process monitoring and control. In: Proceedings of Enlarged Halden Project Group Meeting, May 18–23, 2008. Loen, Norway, C5.1. 8 p.

5. Laarni, J. Koskinen, H., Salo, L., Norros, L., Braseth, A. & Nurmilaukas, V. Evaluation of the Fortum IRD Pilot. Proceedings of the Sixth American Nuclear Society International Topical Meeting on Nuclear Plant Instrumentation, Control, and Human-Machine Interface Technologies NPIC&HMIT 2009, Knoxville, Tennessee, April 5–9, 2009. American Nuclear Society, LaGrange Park, IL. (On CDROM.)

6. Norros, L. & Salo, L. Operating with procedures in complex process control. Literature review. VTT, Espoo, 2009. VTT-R-04680-10.

7. Salo, L., Norros, L. & Savioja, P. Using operating procedures in NPP process control. European Conference of Cognitive Ergonomics 2009, Sept 30 – Oct 2, 2009. Helsinki, Finland.

8. Laarni, J. & Norros, L. Control room modernization at Finnish nuclear power plants – two projects compared. Proceedings of the 5th ANS International Topical Meeting on Nuclear Plant Instrumentation, Controls, and Human Machine Interface Technology, Albuquerque, Nov. 12–16, 2006.

9. Laarni, J., Salo, L. & Norros, L. A step towards more agile and adaptive management of nuclear power plant control room renewals – lessons learned from a project in Finland. The Enlarged Halden Programme Group Meeting, Gol, Norway, March 11–16, 2007.

10. Norros, L., Savioja, P. & Salo, L. Approach to Integrated System Validation of NPP control rooms. Proceedings of the Sixth American Nuclear Society International Topical Meeting on Nuclear Plant Instrumentation, Control, and Human-Machine Interface Technologies NPIC&HMIT 2009, Knoxville, Tennessee, April 5–9, 2009. American Nuclear Society, LaGrange Park, IL. (On CDROM.)

11. Norros, L., Savioja, P., Karvonen, H. & Liinasuo, M. Contextual assessment of Systems Usability – Description of the method, 2011. (In preparation.)

12. Savioja, P. Norros, L, Salo, L., Laarni, J. & Liinasuo, M. Integrated System Validation: The questions of independence and reference. Proceedings of the EHPG Enlarged Halden Programme Group Meeting, March 14–19, 2010. Storefjell, Norway.

13. Liinasuo, M. & Norros, L. Usability Case – integrating usability evaluations in design. COST294-MAUSE Workshop on Downstream Utility, 6th Nov. 2007. Toulouse, France. Pp. 11–13.

14. Laarni, J., Savioja, P., Karvonen, H. & Norros, L. Pre-validation of nuclear power plant control room design, 2011. (Accepted to HCI International 2011.)

15. Jou, Y.-T., Lin, C.J., Yenn, T.-C., Yang, C.-W., Yang, L.-C. & Tsai, R.-C. The implementation of a human factors engineering checklist for human-system interfaces uppgrade in nuclear power plant. Safety Science 2009, 47, pp. 1016–1025.

16. Anshel, J. (Ed.). Visual Ergonomics Handbook. Boca Raton: CRC Press, 2005.

17. Kim, M.C., Park, J., Jung, W., Kim, H. & Kim, Y.J. Development of a standard communication protocol for an emergency situation management in nuclear power plants. Annals of Nuclear Energy 2010, 37, pp. 888–893.

18. EPRI 1008122. Human factors guidance for control room and digital human-system interface design and modification: Guidelines for planning, specification, design, licensing, implementation, training, operation, and maintenance. Palo Alto, CA: EPRI, 2004.

6.2 Human factors in control room design: lessons learned from Fortum and TVO reference tests (O'PRACTICE)

Jari Laarni, Leena Norros, Paula Savioja, Iina Aaltonen, Hannu Karvonen, Hanna Koskinen, Marja Liinasuo and Leena Salo
VTT

Abstract

The paper focuses on the reporting of the Loviisa and Olkiluoto reference test results. Conclusions have been drawn with regard of the systems usability of the hybrid control room (CR) and human-system interfaces (HSIs). Specifically, we have evaluated the role of different information sources (e.g., conventional analogue panels, large-screen overview displays, and workstation screens) in supporting situation awareness and communication and coordination of activities between operators. We have also acquired knowledge and insights of the goals, constraints and design principles in the development of procedures and their integration with other components of the CR HSIs. At the end of the paper, some implications of the findings of the reference tests are discussed.

Introduction

The renewal of automation systems, CRs and HSIs is a current issue at Finnish nuclear power plants. In control rooms there will be a change from analogue technology to digital technologies and desktop-based workstations. These changes are challenging, since they are conducted stepwise during several years, and different types of hybrid interfaces are in use during these years. Since CR modernizations and changes in plants provoke risks, there is a clear need to pay closer attention to the accomplishment of CR and HSI renewals.

We have performed simulator tests at the Loviisa and Olkiluoto training simulator as a part of normal operator training. The tests are aimed to provide information of the effect of digitalization and of HSI changes on operator work practices. Secondly, they are aimed to function as reference tests for the forthcoming integrated system validation of the digitalized CR, and provide information of the usability and functionality of the present hybrid CR solutions.

We have coined the term "systems usability" to indicate the capability of technologies to support fulfilment of the core-task usability demands of a given work so that the objectives of the activity are met [1, 2]. Systems usability is manifested in the use of the technology through performance outcome, way of acting, and user experience.

(a) (b)

Figure 1. The (a) Loviisa and (b) Olkiluoto training simulators were used in testing Systems Usability.

Control rooms at the Loviisa and Olkiluoto plant

CRs at both plants can be considered as hybrid ones, including both analogue and digital devices (Figure 1). At the Fortum's Loviisa plant, the information streams of the plant will be completely modernized during a period of over ten years. The reference tests were carried out after the implementation of the first stage of the modernization project. The present hybrid concept includes, for example, a HSI of the new safety automation platform including Qualified Display System (QDS) touch screen displays for the reactor operator and shift supervisor to operate control rods. At the TVO's Olkiluoto plant, the automation systems of the turbine side have been renewed during the last decade. The possible renewal of the reactor automation is accomplished later in a separate project.

The main difference between the CRs of the two plants is that at the Olkiluoto plant the automation systems and HSIs of the turbine side are fully digitalized; at the Loviisa plant, the control operations are still mainly carried out by using conventional analogue systems.

Method

Three scenarios were included in the test at both the Loviisa and Olkiluoto simulators. At the Loviisa simulator two severe accident (loss of coolant accident and primary-secondary leakage) and one complicated failure (electric bus system failure) scenarios were run; at the Olkiluoto simulator, all the three scenarios were complicated failures (decay heat removal system (321) failure, ejector failure and an automation failure in a preheater line).

All the 12 CR crews (42 operators in total) participated in the reference test at the Loviisa plant; six crews (21 CR operators) participated in the test at the Olkiluoto plant. In the latter case, the participated crews were a representative sample of the Olkiluoto CR crews.

Data was collected by several methods at both simulators. Before the test sessions, all the operators were individually interviewed on their work orientation. The operator activities were observed by researchers and video recorded using several video cameras at both simulators. Some of the cameras provided an overview picture of the CR activities; head-mounted cameras provided information of the direction of operators' gaze during test runs. At both simulators a process expert evaluated the crew's performance according to five criteria by using a five-point scale. Subjective workload was measured by using the NASA-TLX self-evaluation questionnaire. After each test run, a process tracing – interview was carried out with the aim of gathering information of, e.g., the situation awareness possessed by the crews and individual operators. Finally, after all three simulator runs, each operator filled a systems usability questionnaire in which several questions of the usability of the CR HSIs were asked. In addition, at the Loviisa simulator, log files from key process parameters were collected during the test runs.

In the following, some key results of the tests at the Loviisa and Olkiluoto training simulators are presented separately. After that, some implications of the findings are discussed.

Results

Loviisa reference tests

In Loviisa reference tests, the crews' performance was overall good, and the performance differences between crews were small. In the two severe accident

situations the crews' performance was overall better than in the electric bus system failure for which there was no procedure available.

Even though there were no large performance differences between crews, some differences in the operator work practices were found. For example, the amount of communication varied quite much between crews and simulator runs. For example, some crews communicated much more frequently during the runs than other crews. Individual and team-level factors apparently do not alone explain these differences, but they may also be caused by particular features of the HSIs and procedures and the operating crews' ways of adopting them.

Some practices were noticed that are typical to hybrid control rooms: Operators had to wander a lot around the CR, since a considerable part of the information needed is displayed on the screens of the process computer system, whereas most of the control operations are carried out using hardwired panels and desks. The present hybrid control room can be thought to support collaboration between the crew members, since the panel information can be easily seen from the operators' workstations, and the operators can easily point at panel objects during discussions. In addition, operators' position in the CR already reveals to other crew members what s/he is working on.

The fact that the emergency operating procedures provided strict guidance on what the operator should do, harmonised operator performance in accident scenarios. On the negative side, it was found that the operators easily concentrated on accomplishment of the procedure, and therefore had less cognitive resources to monitor the process. Even though the procedures harmonised the operator performance to some degree, procedures were not applied in an identical fashion: For example, there were quite large differences between the crews in the exact point in time the procedure was taken into use and in how it was applied.

The procedures can be thought of as a tool for co-operation and collaboration between operators: It was found that the operators communicated quite much at the beginning phase of the run but the amount of communication decreased as the run progressed. The reason for this may be that the operators had to make some checks together at the beginning of the test run but at later stages they could work more independently.

According to the usability questionnaire, the Loviisa operators thought that the usability and functionality of the present CR HSIs is at the desired level: The HSIs support quite well the build-up of situation awareness during runs, and the process can be controlled quite efficiently with them. Overall, operators thought that digitalization is not a problem as such, and CR and HSI changes that will be

accomplished in the near future were not thought to provoke frustration and anxiety.

Some problems were, however, mentioned. Since the main part of the process information is acquired at the Loviisa CR through the process computer system, a sufficient number of display screens is required. A few of the operators thought that the current number of displays is too small, and therefore they have to change the contents of the displays quite often which increases the amount of time spent on secondary tasks. A large amount of the complaints at the Loviisa plant was related to the alarm system. Operators complained that since there are too many alarms in accident situations, they are not able to monitor and acknowledge them all. Due to this, alarms have lost their value as an important information source in accident situations.

Olkiluoto reference tests

Also in the Olkiluoto reference tests, the overall performance of the crews was good. All the crews successfully completed the tasks of the 321 system and the ejector failure. Most of the crews, however, had problems with the complicated automation failure of the turbine side (preheater line fault): only one of the six crews could find the solution to the problem by understanding and framing the logic of the starting of automatic functions. In this scenario, the operators would have to use a special feature of the new automation system, a function diagram, in order to be able to solve the problem. Even though most of the crews opened the critical display page, they could not, however, apply the diagram for the solving of the failure.

There are apparently several reasons for the latter finding. The above-mentioned crew's members, who succeeded in solving the failure, collaborated and communicated more actively than the members of other crews; the crew's turbine operator was also more familiar with the new functional diagrams of the automation system. In general, there seemed to be somewhat diverse views on whether the operators on the whole have to learn and get familiar with the new diagrams, and therefore it is possible that the training of these new functionalities has not been extensive enough.

There were some differences in work practices between the scenarios and operator roles. Overall, there were quite large differences between operators and crews in the amount of movement. On average, the operators were away from their workstations much more in the reactor-side scenario than in the turbine-

side scenarios, apparently because in the reactor-side scenario the operators had to walk to the panels and desks to carry out the required control operations. The shift supervisors were also, in general, away from their workstations for a longer period of time than the other two operators. For example, in the automation system failure, they had to go to the turbine operator's workstation to watch the new displays. In addition, some reactor operators quite actively walked away to the turbine operator's workstation, if common problem solving was required.

Overall, there were also some differences between operators and crews in the amount of communication. There seems to be a link between communication and performance: the crews that communicate and collaborate more effectively also perform somewhat better. A special problem with some of the crews was that the shift supervisor did not actively enough plan and coordinate the crew's work. Because of this, it seemed that the crew drifted from one situation to another without coordination. Even though it is the shift supervisor's task to direct and coordinate the crew's behaviour, in some of the crews the other two operators were more responsible for the coordination of activities.

Since all the scenarios were failures that have not immediate safety implications, the use of procedures was less systematic than in the accident scenarios carried out at the Loviisa simulator. The largest differences between the crews were found in the use of computerized procedures: some of the turbine operators used computer-based procedures in some of the simulator runs, whereas some of them did not use them at all. It is possible that the use of computerized procedures reduced the communication between operators: if the turbine operator is walking through a computer-based procedure without mentioning it to the shift supervisor, this may deteriorate team transparency, i.e. team members' ability to recognize and be aware of what the other members are doing and where their attention is directed at.

Some operators told that they had problems in remembering or knowing whether there is a procedure available for a specific failure scenario or not, and if they knew that the procedure exists, the problem was to identify and locate it. If the operators have to spend a lot of time on wondering about the availability of a procedure, it may have a detrimental effect on their workload.

Overall, the operators are satisfied with the usability and functionality of the HSIs at the Olkiluoto plant, even though some areas for improvement were identified. According to the usability questionnaire, the operators thought that the present HSIs are quite difficult to learn to use, and therefore quite extensive training is needed. Some operators thought that the new displays of the turbine

side are not as usable and functional as the old user interfaces. The large screen display is not actively used at the Olkiluoto plant and therefore does not provide useful overall information of the state of the process. In agreement with the Loviisa results, the management of alarms was also thought to be a problem at the Olkiluoto plant: The operators complained that too many alarms occur in failure and accident situations.

Implications of the studies

Operator performance

Both in the Loviisa and Olkiluoto simulator tests, there were some differences between operator and crew performance (e.g., in the amount of communication and movement), and some of these differences were quite large. Several factors can contribute to the observed differences (Figure 2) [1]:

- Characteristics of the scenario (e.g. severity, complexity, temporal features, familiarity)
- Characteristics of the user interface (types of informativeness, modes of interaction)
- Capabilities of the operators (operating knowledge and skills, professional orientation, ICT and automation expertise, motivation)
- Work practices of the crews (way of using information, way of using tools, communication and building shared understanding, collaboration)
- Experience of the operators (amount of training and participation in design)
- Characteristics of the organisation (organisational values and norms, goals, beliefs).

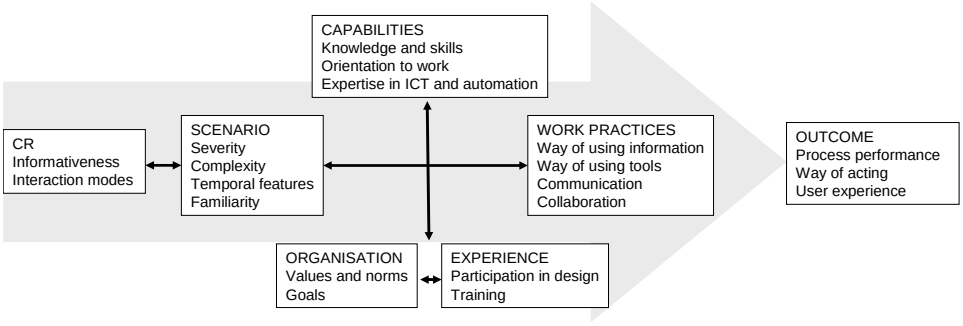

Figure 2. Mechanisms responsible for the outcome.

According to our view, all these factors are relevant, and they may interact in a complicated way. A sufficient level of difficulty of a scenario is critical in order to bring out the effect of other factors. Only when the scenario is difficult enough it is possible that the effects of other factors can be seen. For example, in the preheater line loss, one crew could solve the problem, possibly because the turbine operator was very motivated and had voluntarily acquired knowledge of new things and was therefore competent to read the functional diagram. On the other hand, the crew could also function efficiently together, and the reactor operator was able to give advice to the turbine operator at the critical moment of the run. Organisational support is also important, and the organisational demands must be clear enough: If some of the operators think that they are not required to apply a particular functional diagram during their daily work, it is possible that they do not even try to solve the problem by using them.

Operator practices

There are probably also several factors (e.g., CR HSIs, scenario, organisation, operator capabilities and experience) contributing to crews' work practices (Figure 2). For example, features of the CR HSIs affected operator movement: At the Olkiluoto simulator in which the HSIs are more extensively renewed and digitalised than at the Loviisa simulator, the shift supervisor and reactor operator were away from the workstations for a longer period of time than at the Loviisa simulator. At Olkiluoto, during the primary-side failure the operators moved more around the CR and they were away from their own workstation for a longer period of time than in the secondary-side failures. Features of the HSIs also have an impact on communication and collaboration in hybrid CRs. Overall,

it seems to be that operators communicate to a lesser degree in a digital CR than in a conventional analogue CR, since in a digital CR they may concentrate on watching the displays of their own workstation so tightly that they forget to discuss with the other operators. On the other hand, there may be a need for increased communication in a digital CR, since it is more difficult to know what the other operators are doing there than in an analogue CR. Finally, the features and attributes of procedures have an impact on operator practices. For example, in accident situations the amount of communication may decrease, if the operators have very tightly focussed their attention on reading and accomplishment of the procedure.

Systems usability

According to the usability questionnaire, the operators at both plants were quite satisfied with the present CR HSIs, and surprisingly, the overall distribution of the responses was very similar at the two plants (Figure 3). The fact that the modernization of CRs was at a different phase at the two plants did not seem to have a large impact on results.

Interestingly, there seem to be different views among operators of how the information should be presented in a fully digitalized CR and of how the operator performance should be organized there. According to one view, operators would like to have some kind of digital version of the old CR that was based on analogue technology. One of the advantages of this alternative is that a particular piece of information is always located in a particular location in the CR. What is problematic with this alternative is that the information is distributed all over the CR. On the other hand, some operators hoped that there would be available all kinds of displays, some of them large screen displays, some other smaller ones, and the operators would be able to change their content flexibly in accordance with the process state. The latter view, according to which all the critical information is available from the displays of the operator's workstation, will lead to a more flexible solution in which the possibilities of the digital technology are well utilized. One of the disadvantages of this solution is that navigation demands increase if a sufficient number of displays is not available. In addition, in this kind of CR clear practices and guidelines are needed for the management of displays that are common to all operators.

Conclusions

A hybrid CR based on both analog and digital technology does not seem to cause safety and usability concerns: Operators could carry out their tasks efficiently and in a safe manner. According to the interviews, the new digital technology does not seem to cause much frustration, and operators consider it promising. On the other hand, the new digital HSIs have some impacts on the operator practices and team performance that are not necessarily desired. These lessons should be carefully considered when planning the next steps of the modernization projects.

(a)

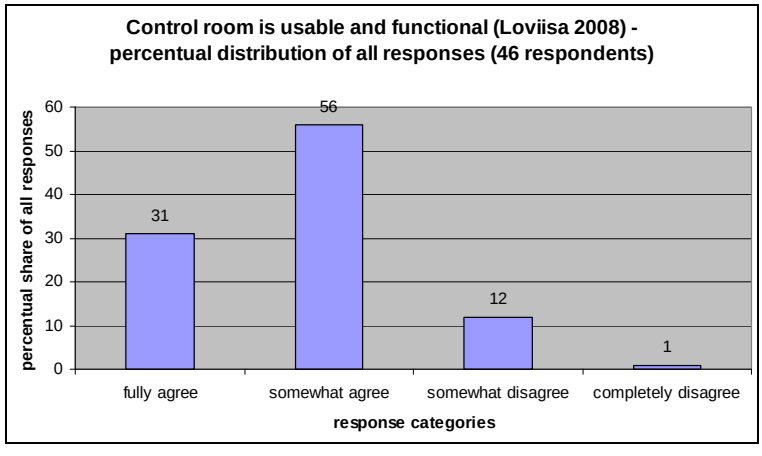

(b)

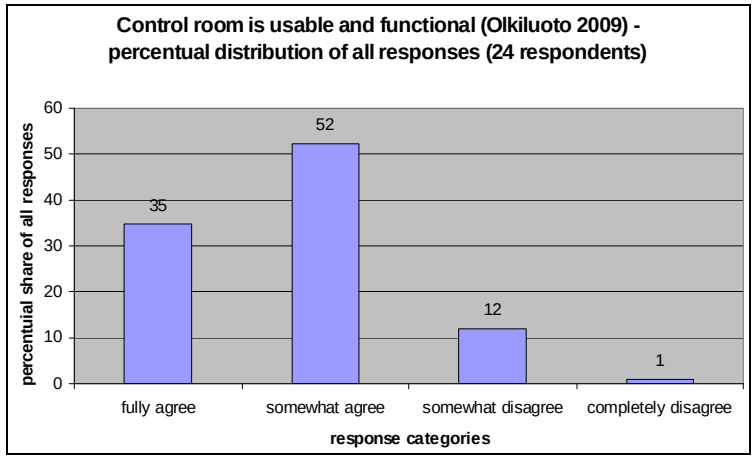

Figure 3. Usability and functionality of the (a) Loviisa and (b) Olkiluoto CRs. Relative proportion of responses to the statement "Control room is usable and functional".

Reference

1. Norros, L., Savioja, P., Karvonen, H. & Liinasuo, M. Contextual assessment of Systems Usability – Description of the method. (In preparation.)

2. Savioja, P. Norros, L, Salo, L., Laarni, J. & Liinasuo, M. Integrated System Validation: The Questions of Independence and Reference. Proceedings of the EHPG Enlarged Halden Programme Group Meeting, 14–19 March 2010, Storefjell, Norway.

7. Requirements Engineering in Nuclear Power Plant Automation (VAHAYA)

7.1 VAHAYA summary report

Mikko Raatikainen and Tomi Männistö
Aalto University, School of Science
Department of Computer Science and Engineering
P.O. Box 19210, FI-00076 AALTO, Finland
mikko.raatikainen@aalto.fi, tomi.mannisto@aalto.fi

Teemu Tommila and Janne Valkonen
VTT
P.O. Box 1000, FI-02044 VTT, Finland
teemu.tommila@vtt.fi, janne.valkonen@vtt.fi

Abstract

Requirements specify the expected characteristics of a system. Requirements engineering is an activity that defines and manages requirements in upgrades and new-builds of nuclear power plants. In the VAHAYA project, we carried out a case study on requirements engineering focusing on safety-related automation systems in nuclear power plants. The results of the study indicate that requirements engineering is becoming an increasingly important activity in the nuclear area, e.g., due to the increased complexity of the used technology. Also, other application domains can provide good practices. However, the special characteristics of the nuclear domain add special challenges to requirements engineering.

Introduction

Requirements are fundamental to specifying what a nuclear power plant (NPP) should or should not do. Among the requirements, safety and availability are the critical cornerstones of an NPP. In order to meet the safety and availability demands in a documented fashion, the engineers must apply strict procedures for change control and traceability management during the design process. However, the practices and cultures of the numerous organizations participating in power plant upgrades and new-builds vary largely. This makes requirements management a challenging task.

Requirements engineering has a long history in the different branches of technologies and industrial sectors. The practices and experiences have evolved over the years. Thus, other disciplines provide valuable insight into NPP requirements engineering. However, NPP also has unique characteristics due to extreme safety requirements, strict control by public authorities, and long construction time and operational life of NPPs.

This summary report gives an overview of the VAHAYA project that studied requirements engineering. The focus of the project was on state-of-the-practice of NPP automation, and to provide benchmarking with other domains and the state-of-the-art in general. Further details are given in the final report of the VAHAYA project [1].

VAHAYA Research Project

The VAHAYA project, as summarized in Figure 1, started with eliciting a shared understanding about the core concepts of requirements engineering. These core concepts, on the one hand, served as a basis for the project, and, on the other hand, can be used as a reference in nuclear power plant investments in the future.

Figure 1. Summary of tasks in the VAHAYA project.

Against this basis, the project conducted an empirical study of the state of the practice of requirements engineering in NPP automation in Finland. The research was carried out as a case study, a method of studying contemporary phenomenon in a real life context [2]. The data was collected by interviewing two experts representing public authority and five experts working for power companies. The interviews were semi-structured and each took roughly two hours. The pre-defined themes of the interview were requirements engineering concepts and terms; processes and practices; documentation and representation; and challenges, benefits and areas for improvement. During the interview, notes were taken by the researchers and the notes were then summarized and sent to the interviewee for review and correction. In addition, other available material was studied, such as laws and regulatory guides on nuclear safety. A summary of the results was presented and additional data was gathered in a workshop. The data analysis was carried out adhering to open and axial coding and memoing of Grounded Theory approach using the Atlas.TI qualitative analysis software tool.

In addition, requirements engineering practices were studied in selected application domains: medical technology, pharmaceutical manufacturing, aviation, railway control, and process automation. The aim was to identify areas where existing requirements engineering practices provide useful experiences to stakeholders in the Finnish nuclear industry. The applied research method was similar to the NPP domain; a difference was that each domain was interviewed only in one interview with multiple interviewees. Additionally, selected literature was reviewed.

Overview of requirements engineering

A requirement refers to an expected characteristic of a system [3]. For example, a requirement is that an NPP shall produce 1 000 MW of electricity. In addition to a system itself, a requirement can concern the development process of the system. For example, a requirement is that the development organization shall have defined change process for all design artifacts. Characteristics of a good requirement include understandability, unambiguity, verifiability, and traceability.

Requirements are written from a specific viewpoint and for specific stakeholders. A stakeholder is someone who has interests in, or concerns relative to, a system. Each requirement needs to be understood by all relevant stakeholders, but not necessarily by others. Typically, requirements are classified and different relations between the requirements are specified. For example, requirements are classified to high level business requirements and detailed technical requirements and a hierarchy between these two types of requirements is specified.

Requirements are typically written in natural language. Different structured specification methods for requirements documentation are also used such as use cases, and diagrams for visualization. In addition, formal approaches to requirements documentation have been developed.

The processes of requirements engineering are roughly divided into requirements definition and requirements management, which both have sub-processes. The former includes requirements elicitation and documentation. The latter includes change management.

Requirements engineering is one of the life cycle processes applied in system development. Other life cycle processes include configuration management, project management, and quality control. The life cycle processes interact and need to be compliant with each other. However, the details of and relations between these life cycle processes were outside the scope of this research.

Requirements engineering in NPP

In this section, the results of the case study of requirements engineering in NPP automation is presented. On the basis of the case study, we first briefly introduce the background and terminology, and then give an account of the state of the practice of requirements engineering in NPP.

Background and terminology

There are four main stakeholder groups in the NPP domain. Power companies are owners of NPPs. The power companies are responsible for operating, which includes building and maintaining, NPPs. Since the power companies have the final responsibility for plant safety, they also need to have detailed understanding about the NPP in question. However, suppliers actually supply and coordinate large construction projects within NPP, such as construction of the entire NPPs or automation renewal. Suppliers are typically large international companies. Subcontractors do smaller work items mainly for suppliers and also for other stakeholders, but are rarely responsible for a large whole. Finally, the public authority is mainly represented by Radiation and Nuclear Safety Authority (STUK). STUK has a role of discussing with operators but not defining technologies to be used, and granting operation permits for NPPs. In addition to these, there are other stakeholders such as Fingrid, as the owner of power-distribution network, and other stakeholders within the above groups, such as the environmental authorities. There are within these stakeholders various branches of technologies that need to co-operate, such as construction, automation, nuclear physics and electrical engineering.

The structure of an NPP can be divided roughly into three levels. The plant is at the highest level referring to the entire NPP. The systems are at the second level. The systems are often further divided into sub-systems. A system represents a meaningful whole. At the third level are devices such as measurement and control instruments, and physical structures of which systems consist. The devices are typically qualified off-the-shelf devices. The three levels thus represent a break down structure from the viewpoint of static structure. The breakdown structure is not necessarily a tree, e.g., a device can be part of different systems. Another viewpoint to the structure is the functions of an NPP. A function describes something that an NPP should do such as a safety shutdown. A function is, thus, a dynamic or operation time viewpoint to an NPP.

The development processes in general adhere to industry standards. Design is iterative but proceeds top-down. The supplier has had significant role and responsibility of development. The projects are long. Respectively, the life cycles are long and much of the knowledge becomes tacit among employees.

Requirements engineering

Requirements are defined for NPP for both a plant itself and for development process of the plant. The focus is on the plant requirements, whereas the development process typically adheres to industrial standards including quality control and other life cycle processes. Thus, this report also focuses on the plant requirements.

A starting point is that a plant design is based on an existing or planned plant concept; legislation and public authority regulations; and international practices and standards. The result is that a general reference architecture for the plant becomes predefined by the plant concept. However, the design solutions of a plant are rarely copied without modifications, due to power company requirements and changes in technology and legislation in different countries and over time. Therefore, construction always includes tailored design solutions.

The plant concept is used as a basis for a set of requirements that includes expected characteristics of the systems, functions, and devices of the plant. These requirements include and are compromises between the various stakeholders and branches of technologies of the plant. These requirements also include the requirements of the power company or owner, and standards applied in the plant. However, many of the power company and supplier requirements can be considered a part of and fulfilled by the plant concept and are, therefore, not included in requirements definition at least explicitly but rather in the contract with the supplier. Another major set of requirements arises from the legislation, decrees, and regulatory guides on nuclear safety (YVL). These requirements specify mainly safety requirements from the viewpoint of public authority. In addition to these general requirements applicable to any plant, STUK also makes official resolutions about the plans of the specific NPP and can include additional requirements as part of the resolution.

Requirements definition is carried out for the plant concept. The state of the practice is that most of the focus seems to be put on analysis and fulfilling requirements of public authorities and the basic functionality. Other requirements such as maintainability or ease of use are more implicit. The supplier has a significant role and responsibility in requirements definition, at least in the technical details. For example, the requirement to fulfil public authority requirements is included as a clause in the contract with the supplier. The reasons are that suppliers construct or renew the plants and thus have much control over implementation of the project.

The requirements are mostly represented as natural language sentences. The requirements are usually at a relatively detailed level. In fact, sometimes technical specifications have been proposed to be requirements. Some metadata such as identification number and classifications is used in the requirements. An issue is that requirements are often vague. For example, there can be immeasurable statements such “as well as possible,” which often originate from YVL. In recent years, additional means to visualize requirements, such as graphical representation of functions have also been piloted. During construction of the existing plants, few requirements were developed so that the requirements would be usable and available today.

Requirements are written in documents that are stored in a dedicated document management system. The documents contain meta-information typical to technical documents, such as a change log, authors, and a purpose. An exception is that STUK resolutions are put to different storages, which, however, is a task management system rather than a dedicated requirement management tool. A need for dedicated tools for requirements management has been identified and tools have been piloted. Some suppliers have already started to use dedicated requirements engineering tools.

The relationships, such as hierarchies and dependencies between requirements, are mainly captured in the requirements documents themselves in the form of references from a requirement to another requirement. Some tables and matrixes are also used to provide additional structure and organization to requirements. Nevertheless, few relationships are explicitly defined and managed. In particular, hierarchical structures are not explicit and requirements focus on the detailed level; plant level requirements are scarcely specified. The consequence is that traceability and dependencies are a challenge.

Requirements engineering in other domains

The previous section gave an account of requirements engineering in NPP, whereas in the following we highlight a few relevant observations in other domains as a comparison with the NPP domain.

In the other domain, we found out that in requirements definition, hierarchies and even classification of requirements to different types are used to some extent. A typical requirements hierarchy consisted of three levels. The highest level defined business requirements or user needs; the middle level defined requirements for functionality; and the lowest level defined technical requirements.

There were relationships between requirements at one level and between the levels. There are several benefits in organizing requirements into a hierarchy. For example, verification can be done then against all these levels of requirements. In an NPP, many of the requirements are at the technical requirements level and few hierarchies and relationships are present currently.

Dedicated requirements engineering tools are increasingly applied in industry. Many of the studied domains used tools for requirements engineering. In general, investment for tools per se in terms of time and money was not considered large, but starting to use tools required first defining processes and specifying requirements in detail. The experiences of using tools after adoption resistance were positive. However, documents were also still used. For example, an approach was to export the requirements from the dedicated requirements management tool to documents after requirements were defined. Nevertheless, even partial use of tools helped in development of requirements even if documents were also used as a means to store final versions.

An approach to licensing and control by public authority that we encountered in other domains was based largely on verification of adherence to design and construction processes rather than inspection of product details. An example of this would be a public authority review in which requirements had been written and verification had been carried out against the requirement rather than the actual content of the requirements. Another difference was that verification was not necessarily carried out by public authority itself but an external certified authority. Consequently, the technical details were not reviewed to the extent that STUK conducts reviews.

Conclusions

We have given an account of the state of the practice of NPP requirements engineering, which is anincreasingly important activity among life cycle processes, especially within automation. However, the trends, such as complexity introduced by digitalization of automation and increasingly strict safety requirements, continuously create new challenges for requirements engineering. Major challenges include representing different kinds and various levels of abstractions of requirements, management of requirements including the relationships between the requirements and traceability, and applicability of supporting tools. Requirements engineering is also a challenge in other application domains, but the challenges

are similar and good practices seem to be transferrable between application domains despite some specific characteristics of NPP domain.

References

1. Raatikainen, M., Männistö, T., Tommila, T. & Valkonen, J. Requirements Engineering in Nuclear Power Plant Automation. VAHAYA final report, 2011. (In Finnish.)

2. Yin, R.K. Case Study Research. Sage: Thousand Oaks, 2003.

3. Davis, A.M. Just Enough Requirements Management: Where Software Development Meets Marketing. Dorset House Publishing Co., Inc., 2005.

8. Development and Validation of Fuel Performance Codes (POKEVA)

8.1 POKEVA summary report

Seppo Kelppe
VTT

Abstract

Assessment, validation, and further development of the fuel behaviour codes in use at VTT have been continued topically, with attention to the most timely requirements. The main achievements include: (1) Development of a probabilistic procedure applicable for general transient conditions, or for evaluation of the number of failed rods in an accident, particularly, was completed by a suggested two-stage approach one of which features an innovative use of neural networks methodology. (2) Use of the coupled thermal-hydraulic fuel code FRAPTRAN-GENFLO was established as a versatile tool to simulate integral loss-of-coolant test arrangements and as the core tool in the probabilistic transient analyses. (3) An extensive study on the VTT-amended ENIGMA steady-state code and its several sub-models was compiled. (4) A comprehensive interpretation of the outcome of the in-pile measurements from the OECD Halden Project rod overpressure tests was issued. (5) A coupling to the ENIGMA code input from a lattice physics code was created to realistically account for the effect of gadolinium or other additives on power distribution in the pellet. (6) Recent versions of the IRSN SCANAIR code for reactivity accident analyses have been installed and applied in power reactor applications. (7) Two new versions of the USNRC FRAPCON and FRAPTRAN codes were assembled. A version of FRAPCON

3.4 consolidating previous practical amendments and cleared of intractable parts of obsolete coding was issued. (8) Part was taken in three systematic international benchmark exercises that effectively support the code validation.

Introduction

Under the auspices of the predecessors of the current project, up-to-date steady state and transient and accident fuel behaviour and performance codes have been maintained and developed. Constantly evolving fuel designs, fuel management practices and regulatory rules make it compulsory that this kind of independent research and development is upheld.

The trend in the requirements from the authority is such that in practice the applicant will increasingly need to set and verify its own well-founded limits. Requirement to estimate the number of failing rods in an accident, assessing consequences of extended operation of the fuel rods under overpressure, and the effect of burnable absorbers stem from implied regulatory practices. Fuel management issues relate to continuing demand of higher discharge burnups, to consideration of longer cycle lengths or to prospects of load-follow operation of various degrees. Fuel designs are altered geometrically and by measures for performance improvement with new materials and fuel additives.

Understanding and modelling of fuel behaviour issues can proceed no faster than experimental data are generated. A long history of development of a program and its sub-models risks the coherence of the integral code and, without careful book-keeping, leaves behind an obscure track of laboriously identifiable versions.

The main objectives below reflect intentions of keeping up with the previous needs. Further down, a few examples of the outcome are given.

Main objectives

- Maintain the main fuel modelling codes in use at VTT viz. FRAPCON and ENIGMA for steady-state, and FRAPTRAN and SCANAIR for general transients and RIA cases, respectively, in updated and validated condition.
- Completion and documentation of the probabilistic transient analysis procedure to be applicable in the estimation of the number of failed rods in an accident.

- Rectifying and finalising the coupled FRAPCON/FRAPTRAN-GENFLO code package to support independent general accident studies and serve as the core of a probabilistic accident analysis procedure.
- Reviewing the understanding of the most important fuel behaviour phenomena and the respective sub-models currently active.
- Making a comprehensive validation of the VTT-amended ENIGMA steady state code.
- Foundation of a systematic version management tool for all the programs in use.

Maintaining and developing of fuel codes

Versions of the USNRC originated fuel performance codes FRAPCON and FRAPTRAN are being received under collaboration with the Pacific Northwest National Laboratory. The versions **FRAPCON-3.4** and **FRAPTRAN-1.4** are the latest assembled and amended at VTT. FRAPCON-3.4 was adapted to the existing probabilistic procedure, and the coupling of FRAPTRAN-1.4 with the thermal hydraulic module GENFLO was secured. Another **VTT version of FRAPCON-3.4** [1] was written that consolidates a number of practical improvements taken into use at VTT. Most notably an out-of-date dynamic dimensioning that has much complicated reading the source has now been removed and replaced with standard coding. Other modifications address difficulties in compiling the code, allow power histories given as nodal values for a larger numbers of axial nodes and time steps, permit a rod or channel geometry different from standard, facilitate computing test rodlets rebuilt from power reactor rods, etc. A number of unnecessary subroutines have been deleted. These changes have simplified the code essentially.

An additional way to input a time-dependent pellet radial **power profile in ENIGMA** has been created [2]. The purpose of the enhancement is to allow a precise description of the strong early-in-life power depression in the centre of the gadolinium doped pellets and the rapid changes in the power profile during the gadolinium depletion. The model is based on combining ENIGMA with neutronics calculations. (Figures 1 and 2)

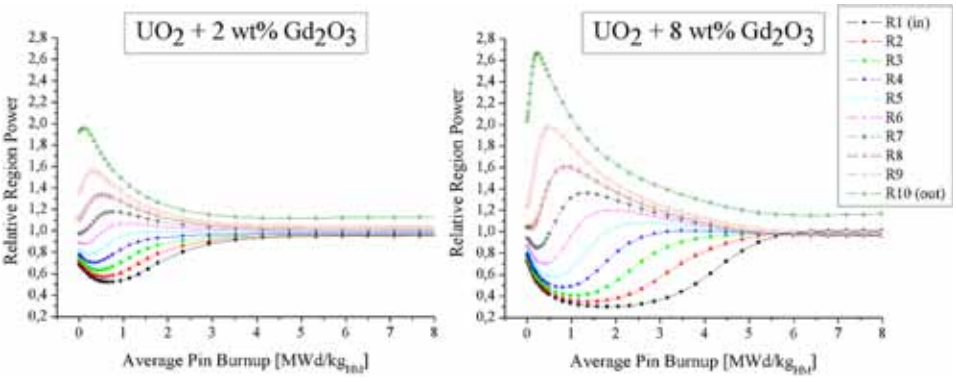

Figure 1. HELIOS-ENIGMA calculated evolution of relative power in fuel radial nodes.

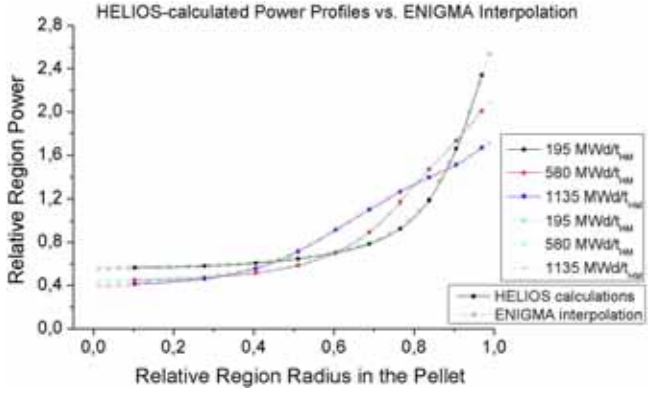

Figure 2. HELIOS-ENIGMA calculated pellet radial power profiles at various burnups.

The new model was tested against data from three Halden Reactor Project experiments. The results suggest differences between variant contents of Gd_2O_3, with better agreement for higher gadolinium amounts in the fuel. A trend of slight temperature overestimation was observed in all PWR fuels after the burnout of the absorbing gadolinium isotope. A revised thermal conductivity correlation was taken into use. The method is equally applicable to studies concerning the effect of any additive or any case that a lattice code can provide a power profile for.

Received under bilateral collaboration with the French IRSN, two versions of the, **SCANAIR code, V.7_0** being the latest, have been installed and taken into use at VTT [3, 4]. The code is particularly addressed to analyses of reactivity

initiated accidents. The newest versions provide for the first time at VTT a direct way of comparison of the results with those from a reactor dynamics code with similar level of thermal hydraulic description. Among the first applications, two types of conditions were approached that have not been actually attempted before. One concerns a reactivity transient due to a hypothetical **boron dilution incident**. With that, SCANAIR shows solid performance and a good agreement with the VTT in-house TRAB code in thermal hydraulic results, where appropriate (Figure 3).

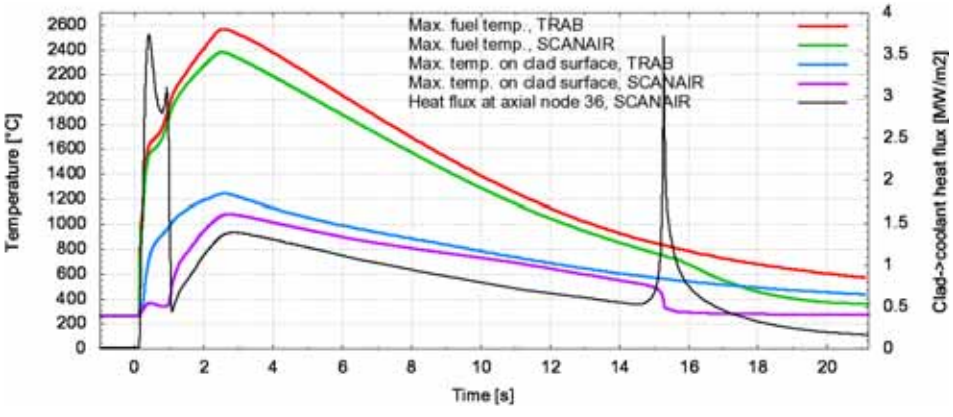

Figure 3. Temperatures and heat flux calculated with SCANAIR and TRAB codes in a hypothetic VVER boron dilution accident.

The other is simulation of behaviour of **BWR type fuel** in a reactivity accident test performed in a capsule, i.e. in pool-type cooling conditions at the NSRR reactor of JAEA of Japan. The latter included testing the fracture mechanical CLARIS module in SCANAIR. Furthermore, significance of the initialisation of the transient using various steady state codes was examined, and a strong influence can be identified.

Many of the changes made in the several codes at VTT have been focusing on a single issue at a time. Yet many phenomena are tightly interlinked, such as the fission gas release, the temperature and the heat transfer properties. In order to address these issues, a **systematic validation** should be implemented. Such a system would enable the developers to create new models and ascertain that the changes made will not adversely affect other aspects of the simulations. To facilitate the validation, the system should be able to perform stacked simulation runs for which an automated system would be warranted.

Probabilistic transient analyses

VTT's development of a statistical method for prediction of nuclear fuel failure rate in an accident is based on the fuel performance code FRAPTRAN-GENFLO. The method further utilizes the theoretical basis of nonparametric statistics (i.e. order statistics, tolerance interval theory), and Wilks' formula, in particular. Statistical parameters are identified as either global or local, the former varying over the whole core, the latter over single rods.

As an example case for the system testing, an arbitrarily dramatised large break loss-of-coolant accident in VVER-440 type reactor has been considered.

There are several ways to conduct the statistical analysis depending on the accident scenario and on which phenomena are to be included in the analysis. It is first important to decide how to take into account the propagation of modelling uncertainties throughout the calculation system. The source and form of the boundary conditions can vary and one needs to allow an amount of case-to-case flexibility to the calculation system. The distributions of the chosen parameters are defined in the next phase. The uncertainties are then combined with the tolerance interval method introduced by Wilks. With what is called Wilks' formula, one can state that when all the rods in a reactor are simulated 59 times with global variation between each of the 59 scenarios, and if the number of failed rods in the worst case is below the allowed limit, then the requirements are met with the probability of 95% and with the confidence level of 95%.

Here, two parallel ways of analyses are suggested to apply this result of "59 calculations" into practice. A large number of fuel performance code calculations with different local parameters would be conducted per each of the 59 global variations. The global variation that has the biggest number of failed rods would then be directly scaled to get the number of failed rods in the whole reactor. In the other way, the same fuel performance code calculations are used for neural network training – a novel concept in this environment – making use of the MATLAB Neural Network Toolbox™ software. If the network performs as expected, that analysis would confirm the previous result.

More detail of the procedure is given in the separate POKEVA special article.

Rod overpressure

The OECD Halden Reactor Project experiment series, IFA-610, aims at investigating fuel rod integral behaviour under overpressure and to identify cladding "lift-off" conditions. In lift-off, the pellet-cladding gap is thought to re-open by clad

creep-out due to overpressure inside the rod. A high pressure may develop at high burnup by released fission gases eventually causing the rod internal pressure to exceed the system pressure. The cladding creep-out can be partly or fully compensated by fuel swelling, depending on the pressure difference. In principle, an opening gap means increasing fuel temperature and a positive gas release feed-back.

Five of the eight IFA-610 series tests were done with UO_2 fuel of different designs (PWR, BWR, VVER), and three more with PWR MOX fuel. The fuel rod in each test is instrumented with a fuel centreline thermocouple (TC) and a cladding elongation sensor (EC). Both sensors are connected to a fast scanning system for noise and scram analyses. The overpressure inside the fuel rod is achieved by means of an external gas line.

The lift-off should manifest itself by increasing pellet centreline temperature, by increasing fuel time constant seen in noise analysis or in scram, by increasing hydraulic diameter for forced gas flow in the gap, or altered elongation behaviour.

Fuel thermocouple measurements are the most important results in the lift-off experiment series. The evolution of fuel centreline temperature normalized to power at different levels of applied overpressure provides a feedback to changes of filler gas properties and gap size. Using argon as the filler gas, the thermal feedback becomes even more pronounced in comparison with helium, because of lower thermal conductivity of the former.

A summary was prepared to qualify and review the trends in fuel behaviour from IFA-610 experiments [5]. The main focus is given to fuel temperature measurements and thermal behaviour of the fuel. Some trends are obvious, yet for definite conclusions, going into details of rod elongation data and post irradiation examination results are suggested.

No signs of cladding lift-off were observed in any of the tests below 130 bar overpressure, as the cladding creep-out is compensated by fuel swelling. Even at higher levels of overpressure, the thermal feedback appears to be weak.

With VVER fuel originated from Loviisa power plant in Finland, no sign of thermal feed-back due to lift-off could be confirmed in about 2 000 full power hours, even with levels of 250 to 300 bar overpressure in the end. VVER cladding of recrystallised E110 Zr1%Nb alloy is slightly thicker than most of the rest. Another contributor may a different relocation patter in the pellet with a central hole.

Tests were simulated with the ENIGMA code and results were compared with the measured. The ENIGMA code input was adapted, in particular to allow the user to specify a rod pressure that keeps constant so as to match the test condition.

The fuel temperature modelling with the ENIGMA code is generally in good agreement with the experimental data below the lift-off threshold, when the pellet-to-clad gap is closed. The overpressure threshold for the lift-off, seen as an accelerating increase in temperature, is suggested to occur between ~130 and ~150 bar, well in line with observations. A general trend of bigger increases of ENIGMA simulated fuel temperatures compared to in-pile measurements is apparent during the periods at high applied overpressure in every experiment, and a stronger feedback from gap opening is seen in calculations (Figure 4). This may be a sign of under-estimating the effect of pellet fragment relocation or pellet-to-clad bonding on gap conductance.

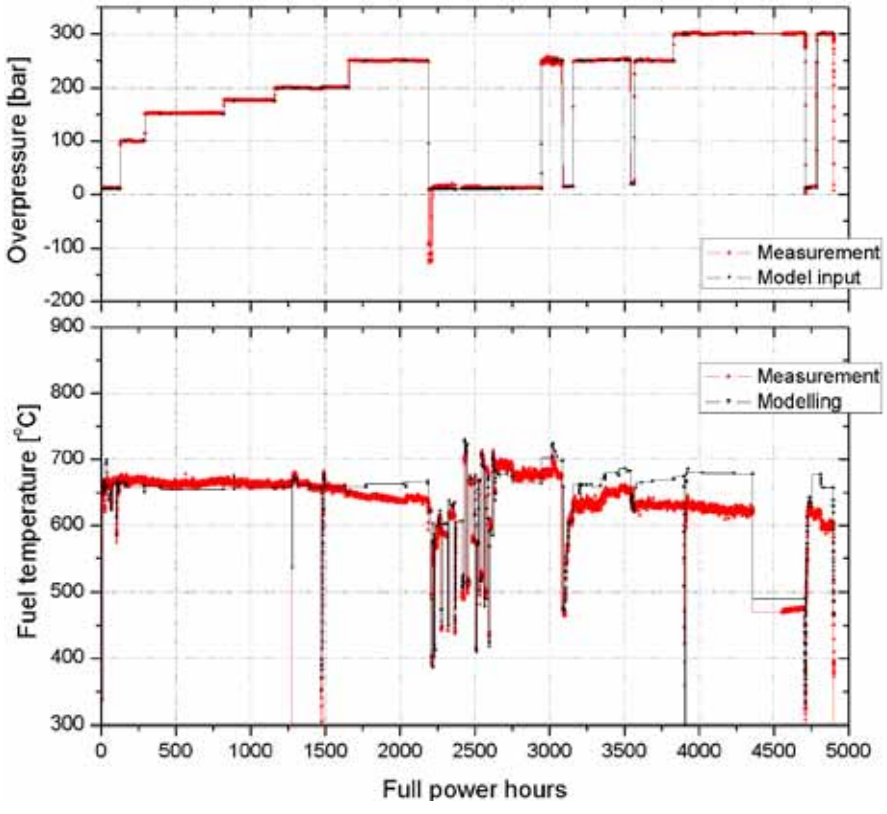

Figure 4. ENIGMA simulation of a Halden overpressure test showing over-prediction of fuel temperature at high overpressures, but no feed-back due to lift-off.

Review of ENIGMA

An extensive review of the ENIGMA code and its validation status as of the end of 2010 was compiled [6]. The report includes a description of the fuel rod and the phenomena affecting it on a theoretical level. The ENIGMA interface is described and the ENIGMA simulation models are examined. The performance of the code was assessed versus several fuel experiments.

ENIGMA is coded with an old FORTRAN 77 language, but has fortunately a modular structure that makes the implementation of new models relatively easy. However, many individual models are judged to be either old or are based on assumptions that have little experimental support. Another incentive to make this review lies in the fact that the development work at VTT extends over two decades, with a lot of information lost in between years.

In addition to a host of practical improvements and corrections, significant alterations made to ENIGMA over the years include addition of cladding material data and correlations for VVER and M5 alloys, several subroutines to control the pellet radial power distribution, several instants of re-calibration and other attempts to improve the fission gas release and thermal conductivity models, models to describe the so-called high-burnup structure, several changes to relax limitations on input parameters, attaching an automated management system to run probabilistic analyses, and a generator to produce a burnup-dependent file to initialise the SCANAIR accident code.

A number of validation calculations have been made recently, a majority of which were executed within the IAEA FUMEX III Coordinated Research Programme. These include the following (see also Table 1):

- IFPE/US-PWR-16x16-LTA Extended Burnup Demonstration Project (8 PWR rods)
- IFPE/SPC-RE-GINNA (8 PWR rods)
- IFPE/KOLA-3-MIR-RAMP Experiment (4 VVER rods) (Figure 5)
- Risø 3 Experiment II5 (one rod)
- Studsvik Inter-Ramp Experiments (20 ramps)
- GAIN case (3 wt% Gd)
- Halden Experiments
    - IFA-699 (VVER E110 creep test)
    - IFA-676 (VVEG, Gd, large grain size)
    - IFA-601.11 (VVER Loviisa, rod overpressure experiment).

On the grounds of results of the above calculations, the simulated rod dimensional changes, temperatures and fission gas release are discussed. Based on FUMEX III Studsvik Ramp Test simulations that were made with both ENIGMA and FRAPCON codes, the sub-models of the two were compared with each other. For one conclusion, the ENIGMA temperatures are higher than FRAPCON's with a closed gap and lower with the gap wide open.

Table 1. Proposed high-priority benchmark cases in the IAEA FUMEX III CRP.

Plant type	MOX	Mechanical interaction		Severe transients		FGR; Temperature etc				FUMEX 2
		PCMI	PCI	LOCA	RIA	Load follow transients	Transients	Gad/Nb	Normal operation FGR	
CANDU	CNEA 5 rods 1 undoped BU15	2 low BU from Riso 2 GE-m and II-3 *IRDMR FIO-118; FIO-119*	for parametric study – find failure threshold INTERRAMP 10G 20G SUPERRAMP PK6 and PW3 35G	FIO 131			IRDMR FIO-118; FIO-119 (7 rods in total 2+5)		Petten RO89 RO51 AECL NRU (one rod from each ring)	
LWR	IFA 629.1 PRIMO rod (BD8)	Riso3 GE7; OSIRIS - 2 rod HO9		IFA 650.2	FK1 and FK2	IFA 519.8/9 Rods DC and DK	IFA535 5 rod 9 Riso 3 rod II5 52G	GAIN Gd 701 and 301	US 16x16 PWR TSQ002 TSQ022 AREVA idealised case	
WWER							MIR Ramp rods 41 48 50 51		US 16x16 PWR TSQ022 Ginna XO3 segmented standard and annular pellets, nom gap, standard clad	
Materials										

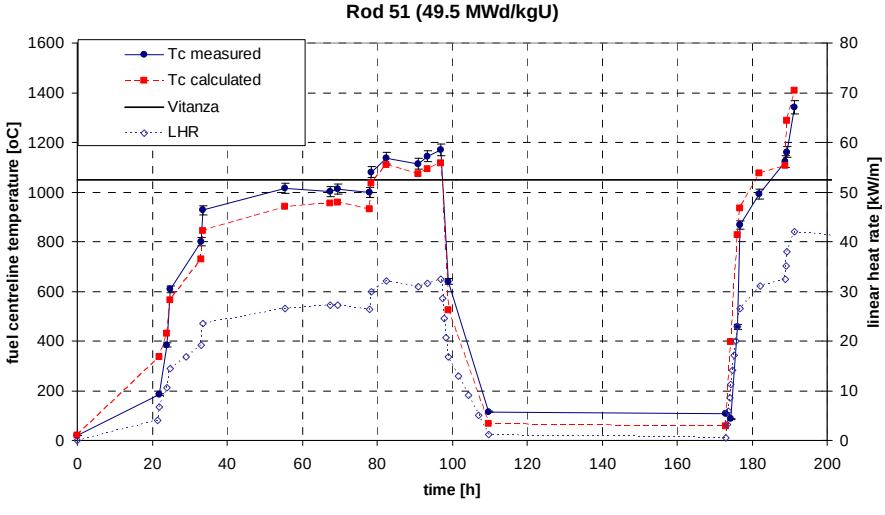

Figure 5. IAEA FUMEX III CRP: KOLA-3-MIR RAMP calculated and measured fuel temperatures in rod 51; empirical threshold for fission gas release indicated.

The study suggests that several of the basic models in ENIGMA should be improved. The **heat transfer** in its entirety should be examined with proper account of the effects of irradiation. The fuel temperature affects and is affected by **fission gas release** that is modelled after an old, probably inadequate interpretation of experiments. As there does not seem to be a coherent trend in either way in describing the **clad elongation**, effects of different manufacturing methods, dimensional interlinking and interaction with fuel pellets should be reviewed. The **creep model** for E110 alloy performs very well until the second increase of internal overpressure in a test. At the moment there are no data to judge on whether the reason of discrepancy that follows is a wrong secondary creep rate (model coefficients) or re-appearance of primary creep (insufficient model). As to fuel pellets, not only is their dimensional development linked to the fission gas release model, but evolving **fuel pellet composition** and design should be taken into account by the models. The formation and effect of the **oxidation** should be investigated especially for non-zircaloy-4 cladding and boiling water reactor environment.

Whatever changes are made to ENIGMA in the future, the documentation and knowledge transfer should be given a priority. As it is, many of the faults described in this document may not be because of a bad model but due to user error. The situation can be alleviated in the future by proper **documentation and version control procedures**.

Benchmarks

In the programme period, VTT has been the nationally nominated partner in three internationally organised benchmark-type exercises, in which performance various types of fuel performance codes have been compared with each other and in relation to experimental results where applicable.

The IAEA Coordinated Research Programme **FUMEX-III** (2008–2011) succeeds two similar efforts. VTT contribution is referred to under ENIGMA review above.

OECD NEA/CSNI Working Group on Fuel Safety has organised two code benchmark tasks around the Halden Integral loss-of-coolant tests IFA-650-3 and IFA-650.4-5 [7], respectively. In IFA-650.4, strong fuel stack axial relocation and fuel expulsion was detected. The phenomenon seems to be accentuated at very high burnups. Fuel relocation is a concern as a potential factor of impaired cooling during an accident. The FRAPTRAN-GENFLO code package was instrumental in describing the heat transfer and fuel behaviour phenomena

specific to these tests. A simplified study using calibrated FRAPTRAN-GENFLO on probable effects of fuel redistribution proves to be illustrative. A clear yet self-stabilising thermal effect is shown.

With support from the Fortum Corporation, participation in the IAEA/OECD-NEA Paks Fuel Project was realised with FRAPCON/FRAPTRAN fuel behaviour assessments accompanying VTT's parallel APROS 5.06 thermal hydraulic calculations [8].

Exchange of information and education

VTT has maintained close collaboration with the French Institut de Radioprotection et de Sûreté Nucléaire IRSN and the Pacific Northwest National Laboratory in the US by exchanging and developing fuel performance codes. With the OECD Halden Reactor Project is there is a programme of separate research undertakings agreed upon annually. Further connections with exchange of information include those with the Swedish Safety Authority Strålsäkerhetsmyndigheten (SSM) and its consultant Quantum Technology AB, the Swiss Paul Sherrer Institute (PSI), as well as the Japanese Atomic Energy Agency (JAEA) and the OECD CSNI Working Group on Fuel Safety also hosting the preparatory phase of the proposed Jules Horowitz International Programme. Moreover, the Finnish utilities' participation in commercial research projects OECE-IRSN CABRI Water Loop Project and the second OECE-NEA Studsvik Cladding Integrity Project (SCIP II) are channelled through VTT. Inside VTT, the knowledge Centre of Nuclear Energy share interests with that of Materials for Power Engineering.

A diploma thesis on the application of the SCANAIR code was completed during the project period. International conferences have been attended and younger staff members have taken part in several international short courses.

Miscellaneous

Previous deliverables of the POKEVA project have been partly reported in the SAFIR2010 Interim Report. Such items include a fairly extensive effort to diversify ENIGMA to cover unconventional thorium and inert matrix applications, development of an external high temperature oxidation model to the APROS simulator, and others.

Applications

The VTT-amended ENIGMA code has been used in BWR and VVER fuel thermal-mechanical applications with deterministic and probabilistic approaches both in power reactor and test conditions. The SCANAIR code has been applied to VVER and BWR reactivity transient simulations with realistic and hypothetic boundary conditions. VVER gadolinium-bearing fuel has been analysed with the special ENIGMA version. Codes participating in benchmark simulations were ENIGMA, FRAPCON-3.3 and FRAPTRAN-GENFLO. A reactivity accident benchmark is starting (SCANAIR V.7_0).

Conclusions

Successful measures have been taken to update and complement the fuel behaviour codes according to topical requirements. Longish development on a probabilistic rod failure estimation method in accident conditions has been essentially completed. Shortcomings in the capabilities of codes are still identified and challenges continue to exist as regards build-up of rod internal pressure – temperatures and fission gas release at high burnup – and its consequences – cladding creep and pellet relocation. Clad ballooning and axial stack relocation in a loss-of-coolant accident and clad failure estimation in reactivity transients call for more attention, too.

Education and training of young generation experts have been productive yet less than ideally effective because of high VTT staff turnover.

References

1. Stengård, J.-O. A modified version of the fuel performance code FRAPCON-3.4. VTT, Espoo, 7.10.2010. VTT Project Report VTT-R-06825-10. 15 p.

2. Klecka, L. An Enhanced Radial Power Profile Model for the ENIGMA Code. Paper presented at the Enlarged Halden Project Programme Group Meeting. Storefjell Resort Hotel, Norway 14 to 19 March 2010. OECD NEA 2010. 11 p.

3. Arffman, A. Applications of the SCANAIR code for the simulation and interpretation of reactivity initiated accidents. VTT, Espoo, 24.5.2010. VTT Project Report VTT-R-03691-10. 85 p.

4. Arffman, A. & Cazalis, B. Application of the SCANAIR Code for VVER Conditions – Boron Dilution Accident. Proceedings of the OECD-IRSN RIA Workshop held in Paris France, 9 to 11 September 2009. NEA/CSNI/R(2010)7. OECD Paris 15.12.2010.

5. Klecka, L. HRP Lift-off Experiment Summary and Modelling with ENIGMA Code Part 1. VTT, Espoo, 31.1.2011. VTT Project Report VTT-R-09939-10. 54 p.

6. Tulkki, V. ENIGMA Fuel Performance Code – 2010 Status Review. VTT, Espoo, 31.1.2011. VTT Project Report VTT-R-09938-10. 79 p.

7. Wiesenack, W. (Ed.) Benchmark calculations on Halden IFA-650 LOCA Test Results. NEA/CSNI/R(2010)6, OECD Paris 15.11.2010. 68 p.

8. Hózer, Z., Aszódi, A., Barnak, M., Boros, I., Fogel, M., Guillard, V., Györi, Cs., Hegyi, G., Horváth, G., Nagy, I., Junninen, P., Kobzar, V., Légrádi, G., Molnár, A., Pietarinen, K., Perneczky, L., Makihara, Y., Matejovic, P., Perez-Feró, E., Slonszki, E., Tóth, I., Trambauer, K., Tricot, N., Trosztel, I., Verpoorten, J., Vitanza, C., Voltchek, A., Wagner, K., Zvonarev, Y. Numerical analyses of an ex-core fuel incident: Results of the OECD-IAEA Paks Fuel Project. Nuclear Engineering and Design 240 (2010), pp. 538–549.

8.2 Statistical analysis of fuel failures in accident conditions

Asko Arffman
VTT

Abstract

A way to confine potential consequences of an accident in a nuclear reactor is to limit the number of fuel rods expected to fail in the course of the incident. Particularly, the safety regulations in Finland require that the number of failed fuel rods in the most severe accident scenario would be less than 10% of all the rods. In safety assessments, the estimation of the fraction of failing rods is conventionally based on conservative analyses, but this approach has several downsides. Sometimes it is hard to judge whether the assumptions are conservative because the phenomena in the reactor are highly nonlinear. Additionally, conservative methods often lead to excessive margins and that way to economic losses. As a result, statistical best-estimate methods have acquired an established position during the past two decades. The development started worldwide when the U.S.NRC revised its rules in 1988 to allow realistic best-estimate methods complemented with uncertainty analysis alongside with the old conservative approach. These methods are based on the selection and variation of parameters that are important in accident conditions. The accident scenario is simulated with a designated computer programme several times with different parameter values between simulations, and that way an estimation of the number of failed rods is obtained. In order to the results to be statistically reliable, enormous number of simulation runs is needed. Thus the analysis requires a lot of computer resources, and this has been a limiting factor for the breakthrough of this procedure. Different approaches have been used to reduce the number of fuel performance code calculations.

Before the current efforts in this field at VTT, there has not been a statistical or any other systematic tool in Finland for the evaluation of rod failures. Since 2006, a calculation system for statistical fuel failure analysis has been under development. The calculation procedure introduces neural networks as a new way to reduce the number of simulations. Neural networks are familiar from other applications in nuclear plant modelling but the concept is a novelty in this context. A neural network is trained with results from stacked fuel performance

code calculations, and then the network is used as a substitute for the analysis code. Further, the developed method utilizes the results of nonparametric statistics, the Wilks' formula in particular. The system has been successfully tested with a small scale analysis and it is now ready for full reactor scale applications.

Introduction

The so called CSAU (Code Scaling, Applicability and Uncertainty, 1989) methodology has been widely used as a standpoint for statistical fuel failure analysis. With the contribution of U.S.NRC, a group of experts developed this three-step method to meet the new regulations. In the first phase the accident scenario is divided to distinct segments by place and by the course of the accident, and then important phenomena are recognized for each place and time. The second phase consists of the evaluation of the fuel performance code and its ability to model the identified phenomena. Also the distributions of the related parameters are qualified. The third task is to combine the uncertainty distributions with a chosen method. Also the statistical procedure developed at VTT follows the main points of this methodology [1–6].

The new calculation system consists of small programmes that have been coded for data processing, writing inputs and steering the calculations. The primary calculation tool is the coupled fuel performance – thermal hydraulics code FRAPTRAN-GENFLO. FRAPTRAN (V1.3) is a single-rod fuel performance code developed by PNNL and it is designed to model accident conditions specifically [7]. The general thermal hydraulics code GENFLO has been exclusively developed at VTT [8]. The thermal hydraulic modelling in stand-alone FRAPTRAN has been found to be unsatisfying, and therefore the coupling with an external thermal hydraulic code has been introduced.

As an accident case for testing the calculation system, a large break loss-of coolant accident in Loviisa VVER-440 type reactor is used. However, preliminary calculations of a single representative rod showed that the cladding temperatures do not reach high enough values to result in a fuel rod failure. In order to have enough fuel failures with the stacked calculations to be used for training the neural network, the accident had to be artificially exaggerated by assuming an elevated power level during the accident and by decreasing the gas gap conductance in the source code. Because of the substantial volume of coolant in VVER-440 core during a LOCA, rod failures are generally estimated to be unlikely in this type of reactor. With the boundary conditions of a more typical

pressurized water reactor like the EPR for instance, rod failures may be more readily present during LOCAs.

Methods for statistical analyses

There are several different approaches for the statistical fuel failure analysis. The analysis methods do not exclude each other, and they can thus be used in parallel way to diminish the amount of required computer code simulations. The constant growth in computer resources has affected and will continue to affect the choice between different statistical methods. The established methods include the use of response surfaces, grouping of the rods, direct Monte Carlo sampling, and applying results of the tolerance interval theory.

Classification of the initial parameters and definition of their distributions

The initial parameters of statistical analysis can be divided by their range to two groups: local and global. Global parameters have an effect on all the rods in the reactor, whereas local parameters bring local variation. For example, the model parameters of fuel performance code are global, and fuel manufacturing parameters are local. The division of parameters to global and local should be taken someway into account in the analysis because the fuel rods have some correlation with each other. The magnitude of the correlation is unknown because it is not precisely known which parameters have the biggest influence on the integrity of the rod in an accident.

Before the actual analysis the varied parameters have to be chosen and their distributions defined. The selection can be conducted by means of a sensitivity analysis with fuel modelling codes and by searching specific variation ranges from open literature, but much of expert judgment is still needed here. Fuel manufacturing parameter ranges are usually provided by the fuel manufacturer. The choice between different statistical methods can also limit the number of parameters that can be included in the analysis. This is the case if one uses for instance response surfaces. Typically the parameter values are normally distributed, but also other distributions like uniform or triangular distributions are possible.

Response surfaces, direct Monte Carlo, grouping of the rods

Response surfaces are low-order polynomial fits between initial and result parameters. With accident simulations, one initial parameter at a time is varied and a connection to one or more result parameters is created. These connections are again gathered

as a polynomial fit. The polynomial fit can then be used to replace the actual fuel performance code calculations, as initial parameters are randomly sampled and the polynomial fit is used to predict the results. This method is useful when the relationship between initial and result parameters is simple enough, but it cannot predict for example the possible branching of the accident sequence to different directions when the safety systems are activated. With the analysis procedure developed at VTT, neural networks are used in the same way and for the same purpose as the response surfaces. The neural network approach is chosen because it is a more sophisticated tool for describing nonlinear phenomena.

Another way is to sample the values of initial parameters from their distributions using direct Monte Carlo sampling. Here the division to global and local parameters is neglected and that means loss of statistical reliability to some extent. Further, the number of simulations that are needed to reach a certain confidence level remains unknown. It is also possible to group rods with characteristics like burn-up, power level and thermal hydraulic conditions. One can then pick an arbitrary amount of rods from each group for the analysis. In any cases, the loss of statistical accuracy could be compensated by introducing some conservative assumptions.

Nonparametric statistics

The tolerance interval theory (i.e. order statistics, nonparametric statistics) gives a way to determine the number of simulations that are needed for the statistical analysis when the probability content and confidence level are predetermined. For instance, nuclear industry corporations Westinghouse [9] and Areva NP [10] both have developed their statistical methods based on the CSAU procedure with the results of nonparametric statistics chosen to be the final step to combine the uncertainty distributions.

In brief, the number of calculations can be solved using the following equation [1]:

$$\beta = 1 - \sum_{j=s-r}^{N} \binom{N}{j} \gamma^{j} (1-\gamma)^{N-j} , \tag{1}$$

where γ is the probability content inside the interval of the distribution, and β is the confidence level for which this contents is realized. The number of calculations is N. From Equation (1) one gets the relation known as the Wilks' formula:

$$\beta = 1 - \gamma^{N} . \tag{2}$$

Here the lower bound of the one sided interval is chosen to be $-\infty$ and the upper bound is the highest value of the random sample that was picked from the unknown distribution in question.

When this formula is applied to safety evaluations, the generally acceptable level is 95% probability with 95% confidence that the number of failed rods would not overstep the allowed limit. When the corresponding values are inserted to Equation (2), thus $\gamma = 0.95$ and $\beta = 0.9515$, the number of cases comes out as 59. In practice when using the Wilks' formula, one can state that when all the rods in the reactor are simulated 59 times with global variation between each of the 59 scenarios, and if the number of failed rods in the worst case is below the allowed limit, then the safety requirements are rightly met with the probability of 95% and with the confidence level of 95%. As that kind of number of simulations is out of reach with the computer resources of today, some other method is needed alongside with this result.

Developed analysis procedure and its testing

In the spirit of the CSAU methodology, the problem setting in the calculation system developed at VTT is split to distinct steps. Firstly, there are several ways to conduct the statistical analysis depending on the setup of the accident scenario, and which phenomena are included to the analysis. It is important to decide how to take into account the propagation of modelling uncertainties throughout the calculation system. Namely, the boundary conditions of a fuel performance code come from a system code and/or from a neutronics code, and those have their own uncertainties. The source and the form of boundary conditions can thus vary, and that sets an extra challenge for the first phase of the analysis. As this first step is in a sense so ambiguous, the calculation system cannot be fully solid but must be modified from analysis to analysis.

Secondly, the distributions of the chosen parameters are defined. In the third phase, the uncertainties are combined with the result introduced by Wilks. There are several ways, however, to apply this result of "59 calculations" to practice.

Alternative approaches for the analysis

There are several paths that the statistical analysis could proceed depending on the accident scenario. As an example, let us first have a look at a situation in which the course of the accident is predetermined but no boundary conditions are calculated or known beforehand. To perform the analysis with piety, one

should calculate the boundary conditions 59 times with a system code like e.g. APROS. Then there are 59 global variations of the accident and the fluctuations in boundary conditions are taken into consideration as a source of uncertainty. Naturally, also the global parameters in FRAPTRAN-GENFLO contribute to this group of 59 global variations. Next for each global case, a large number of cases with different local parameter values are calculated. The number of calculations could be for example 1 000 for each global variation. On the other hand, if the boundary conditions are considered as fixed, then that source of error can be left outside of the analysis and the problem setting simplifies.

After this, the analysis is divided to two different directions. This branching is depicted in Figure 1 where the flow chart of the calculation system is presented. In the first option designated as “Phase 1”, on the grounds of the above mentioned calculations, the worst global case is determined based on the highest number of failed rods. The number of failed rods in the worst global case can now be directly scaled to find out the number of failed rods in the whole reactor. This approach should be on the conservative side because with a smaller number of cases, deviation of rod failure numbers grows, and thus, the biggest failure number is likely higher than what it would be if all the cases had been calculated instead of extrapolation. And in the analysis, only the highest number of failed rods counts. In this case, enough cases need to be calculated to limit the deviation coming from the extrapolation of the rod failure numbers. If one would like to make a more thorough analysis, one could sample the local parameter values for all the rods in the reactor and calculate all the rods in the worst global case.

Alongside with the method presented above, the same calculation results are utilized for a neural network analysis. This is designated as “Phase 2” in the flow chart. If one has calculated for example 59 × 1 000 cases in the previous stage, one can now use these cases to train a network. This network is then used for the full analysis with both global and local parameter values sampled anew. It means that the trained network is used instead of the real fuel performance code to simulate all the rods in the reactor for 59 times.

At this point, the neural networks are considered to be used for a complementary analysis, and the analysis based on the high number of calculations (Phase 1) is the primary way. Before it can be stated that neural networks are suitable for performing these kinds of analyses, it should be made sure that they work as expected in different kinds of accident scenarios. It is not at all obvious that neural networks can be utilized in all cases and therefore there has to be also an alternative way to perform the analysis. As the experience

grows with further analyses, more can be said about how well the neural networks could be utilized to cover different scenarios.

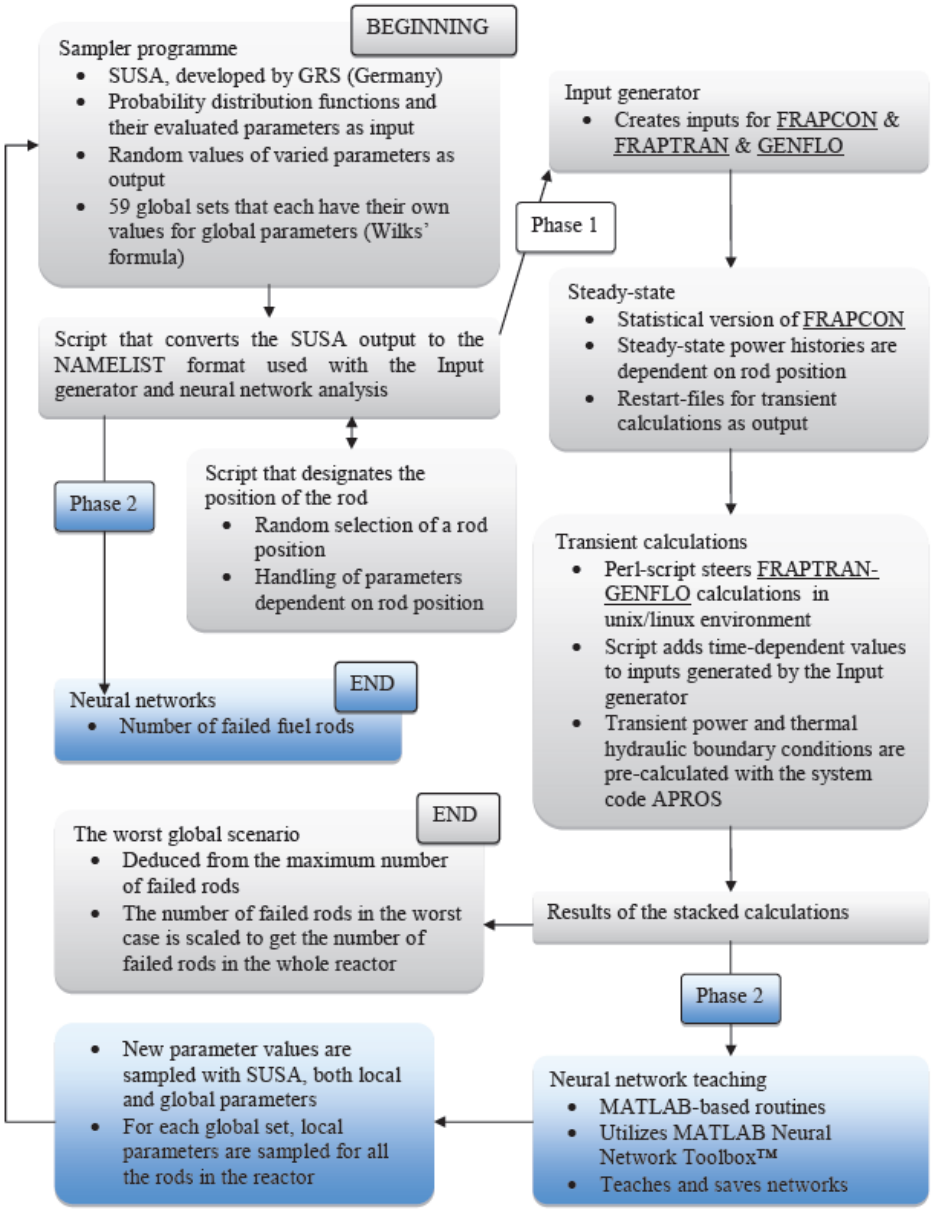

Figure 1. Flow chart of the calculation system.

Applied codes and programmes

The steady-state initializations of the stacked calculations are performed with the statistical version of the FRAPCON (V3.3) code by PNNL. The statistical version of FRAPCON is developed at VTT in 2003, and it enables the variation of selected model and fuel manufacturing parameters [11].

The actual calculation system consists of several script programmes coded for various purposes. Some external programmes are also used, like the sampler programme SUSA developed by the German Safety Authority GRS. SUSA is utilized for generating random parameter values from specified distributions. For the conversion of the sampled data into the format used in the input generating programme, two auxiliary programmes coded in Fortran 90 are made use of. Parameter values are handled in NAMELIST format which makes the input files self-documenting.

A Perl script has been written to steer the FRAPTRAN-GENFLO calculations. Major changes to the FRAPTRAN and GENFLO codes for the purpose of the statistical analysis were avoided at this point. In practice this means that model parameter values cannot be varied in FRAPTRAN because those values cannot be changed via the input file without changing the source code. If the development of statistical version of FRAPTRAN is considered, it would require a careful analysis of the utilized models and their uncertainties in the code.

The neural network analysis is conducted by using a MATLAB built-in neural network software package, the Neural Network Toolbox™. It is a general-purpose tool for neural network analyses, and its basic use is quite simple. Of course, always when operating with neural networks, one has to take extra care when interpreting the results. Network overfitting could become a problem. The same may occur if one uses insufficient amount of data to train the network in relation to the number of layers and neurons in it. Generally, one can use more complex network structures and get more complicated phenomena into view if a large data set for training is used.

Two MATLAB m-files have been written in which the neural networks are operated. The m-files have been coded in such a way that the recording and opening of the network is independent of the size and configuration of the network. The applied network is a feed-forward backpropagation network. There are several training functions included in the Neural Network Toolbox™ but here the default function is used. The function utilizes the Levenberg-Marquardt algorithm for training. Other training functions could also be tested in the future.

The default tan-sigmoid activation function has been used after each neuron and a linear function after the output layer.

Varied parameters and their distributions

The discussion about which parameters to include to statistical analyses has continued from the start of the development of the CSAU methodology. Fuel manufacturing parameters are expected to have little influence on fuel failure rate as the tolerances are quite small. Still, those parameters are included in the analysis at least for the completeness' sake.

The thermal hydraulic parameters chosen to be varied in GENFLO are at this point the three tuning factors for heat transfer and the two drift flux model parameters. In order to gain justifiable parameter ranges, previous validation reports of GENFLO were consulted. The parameter ranges were found in some cases too wide and GENFLO failed to calculate the transient through. Therefore, adequate variation ranges had to be searched by trial and error. The inaccuracy related to the hot-channel factors in APROS is taken into account by varying the overall hot-channel factor between 1 and its nominal value which is somewhat larger than unity. This way also the coolant flow- channel area in FRAPTRAN-GENFLO gets varied because it is calculated from the APROS flow-channel area divided by the hot-channel factors. All in all, the discussion about how to take into account the inaccuracies in thermal hydraulic boundary conditions continues.

Testing the neural network performance

After "dramatizing" the accident scenario, enough fuel failures were gained for the system testing as some 20% of the 100 stacked example cases that were calculated with FRAPTRAN-GENFLO ended up with a rod failure. To test the neural networks in practice, two sets of stacked FRAPTRAN-GENFLO calculations were performed. In the first set, 500 calculations were conducted. At this point it is interesting to learn how accurately the network predicts the cases that were not used for training the network. Also the effect of changing the neural network configuration by adding neurons and layers is a subject of interest.

Due to the intrinsic characteristics of neural networks, the performance of a network varies even if the training data is the same. As an example, in Table 1 the percentages of falsely predicted rods in the test set are presented. The network has two hidden layers with 5 and 3 neurons, and 425 cases (85%) of the 500 FRAPTRAN-GENFLO calculations were used for training the network and

the rest were used as a test set. Network may directly predict that the rod fails or remains intact, but the network result can as well be somewhere between these extremes. In the table, a following (arbitrary) criterion is used: if the neural network prediction deviates more than 40% from the correct result, it is considered as a misspredict ion. As one can see from Table 1, the error in predictions varies quite a lot. Still, it should be adequate that when the error is small, that particular network is recorded and used for the subsequent analysis. Thus, while a network structure with a low error fraction in its predictions is the aim, even the best structures have variation in their results.

It would be important to somehow take into account the fact that there are various power profiles during the accident in different parts of the reactor. It might be possible to cluster the positions of similar power profiles by using for example polynomial fits. In the second set of FRAPTRAN-GENFLO calculations, 900 stacked cases were calculated with different power profiles. The set consisted of three different power profiles, and each had 200 cases. The rest 300 of the 900 cases, each had one of these power profiles picked up in a random fashion. Power profiles were formed by multiplying the transient rod linear power by a fourth order time-dependent polynomial, in which the coefficients were varied from set to set. Now 67% of the cases were used for training and 33% for testing. As one can see from Table 2, network with three neurons in both hidden layers has a steadier performance compared to the network with five and three neurons. The smallest error in predictions is 2.7%, a figure that already shows quite a good accuracy.

Error in the test set appears to grow if one increases the number of neurons or layers to the network. Among the experimentations, a small network that consists of two hidden layers with three neurons in both layers is found to have the best performance. The most suitable network configuration should be sought each time an analysis is performed.

Related to the 900 stacked cases, one can state that the time of failure is significantly scattered due to the variation in local and/or global parameters. Also the axial location of the failure somewhat varies. This may indicate that more than one of the varied parameters has an effect on the cause of the failure. For the neural network testing, it is good to have this kind of variation in the training data. A weakness in the current analysis is that one cannot point out which parameter or combination of parameters caused the rod to fail. It requires additional analysis with the real fuel performance code to find out the reason(s) for rod failures.

Table 1. Percentage of falsely predicted rods in the test set of 75 cases when 425 cases were used for training the network (500 cases in total). Network has two hidden layers with 5 and 3 neurons.

5:3 –network *[%]*
12.0
13.3
34.6
8.0
4.0
5.3
5.3
9.3
5.3
5.3
5.3
4.0
1.3
13.3
8.0

Table 2. Percentage of falsely predicted rods in the test set of 297 cases when 603 cases were used for training the network (900 cases in total). Networks have two hidden layers with 5 and 3 or 3 and 3 neurons.

5:3 –network *[%]*	***3:3 -network*** *[%]*
19.5	3.0
4.7	4.7
4.3	3.0
19.2	2.7
2.7	6.7
4.0	3.7
4.0	4.0
8.1	5.1
11.4	5.4
2.7	11.1
19.2	5.7
31.6	3.7
19.2	3.0
6.7	5.1
15.5	4.7

Duration of the analysis calculations

Statistical analysis unavoidably takes a lot of time. Statistical version of FRAPCON is fast-running but the transient calculations are slower to conduct. The duration of a single FRAPTRAN-GENFLO calculation depends among other things on the time-step size and the starting and ending times of the calculation. During the critical moments of the accident, time-step size may have to be quite small in order to gain reliable results, or even for the calculation to converge. The starting time of the calculation should be some tens of seconds before the beginning of the actual transient in order to initialize the power level from low power to the steady-state power. Time-step sizes between 0.001 s and 0.01 s may be required.

If the rod does not fail and the calculation is continued for example up to 500 seconds, the calculation time of a single FRAPTRAN-GENFLO run would be about 5 minutes. If one now calculates 59 000 cases with ten calculation nodes in the linux cluster and assumes that each calculation takes 5 minutes, it would take 21 days to finish the calculations. If the time per one calculation could be reduced for instance to 2 minutes by adjusting time-step sizes and reducing the ending time of the calculation, it would take 9 days to complete the calculations. This may be an acceptable duration for this kind of analysis.

Conclusions

A calculation system for statistical fuel failure analysis has now been developed to a point that the application to full reactor scale analyses would be the next step. So far the proposed neural network approach is tested only in a small scale and therefore two parallel analyses are suggested. Fuel performance code results are thus used in two different ways: to directly scale the number of rod failures in the worst global scenario to the whole reactor scale, and to perform a neural network analysis. If the network performs as expected, that analysis would confirm the previous result. The neural network part would not require notable additional effort.

The test results of the system show quite good performance with the neural network approach. All the scripts for conducting statistical analyses are now ready to be used. Depending on the setup of the analysis, for instance on the boundary conditions and the accident scenario, the scripts will be modified accordingly. A more universal system might not be needed because the analyses are so divergent.

References

1. Rintala, J. Polttoainevaurioiden määrän tilastollinen arviointi: laskentamenetelmien selvitys. KORU2006/SAFIR2006. VTT, Espoo, 2006. Tutkimusraportti VTT-R-08163-06. (In Finnish.)

2. Rintala, J. Probabilistic Analyses for Rod Behaviour in Accident Conditions: Demonstration. POKEVA/SAFIR2010. VTT, Espoo, 2007. Research Report VTT-R-10519-07.

3. Arffman, A. Polttoainevaurioiden määrän tilastollinen arviointi: yhteenveto ja avoimet kysymykset. POKEVA/SAFIR2010. VTT, Espoo, 2008. Tutkimusraportti VTT-R-07569-08. (In Finnish.)

4. Arffman, A. Statistical Evaluation of Nuclear Fuel Failure Rate in Accident Conditions: Status Report January 2009. POKEVA/SAFIR2010. VTT, Espoo, 2009. Research Report VTT-R-00977-09.

5. Arffman, A. Statistical Evaluation of Nuclear Fuel Failure Rate in Accident Conditions: System Description. POKEVA/SAFIR2010. VTT, Espoo, 2010. Research Report VTT-R-06753-10.

6. Rintala, J. Statistical Evaluation of Nuclear Fuel Failure Rate in Accident Conditions: Users' Manual. POKEVA/SAFIR2010. VTT, Espoo, 2010. Research Report VTT-R-06817-10.

7. U.S.NRC: FRAPTRAN: A Computer Code for the Transient Analysis of Oxide Fuel Rods. NUREG/CR-6739, Vol. 1, PNNL-13576, 2001.

8. Hämäläinen, A., Stengård, J.-O. & Miettinen, J. Coupling of GENFLO Thermohydraulic Model With FRAPTRAN Code For Fuel Transients. VTT Energy, Espoo, 21.12.2000. ENE4/35/00.

9. Frepoli, C. An Overview of Westinghouse Realistic Large Break LOCA Evaluation Model. Science and Technology of Nuclear Installations, Vol. 2008, Article ID 498737. 15 p.

10. Martin, R. & O'Dell, L. Development Considerations of AREVA NP Inc.'s Realistic LBLOCA Analysis Methodology. Sci. and Tech. of Nuclear Installations, Vol. 2008, Article ID 239718. 13 p.

11. Stengård, J.-O. & Kelppe, S. Probabilistic Version of the FAPCON-3 Fuel Behaviour Code. Project Report PRO1/T7048/02, 7.2.2003.

9. Tridimensional Core Transient Analysis Methods (TRICOT)

9.1 TRICOT summary report

Elina Syrjälahti, Anitta Hämäläinen and Hanna Räty
VTT

Abstract

The objective of the project is to continue the development of the truly independent transient calculation system, which can be utilized by the safety authority and other end-users for safety analyses. Thermal hydraulics of reactor core has been the main development area in this project. 3D thermal hydraulics model based on the porous medium approach has been developed and applied in several applications. Internal coupling of TRAB-3D neutronics and SMABRE hydraulics, which offers new possibilities to model more demanding flow situations, has been developed and tested. Tools for the studying of modeling uncertainties have been developed and applied both in the plant scale and in fuel rod scale. Participation in international work groups and benchmark activities has provided crucial support for the development work.

Introduction

VTT has developed its own dynamics calculation codes for independent safety analyses since 1970's during the predecessors of the SAFIR2010 research programme. The TRAB, TRAB-3D and HEXTRAN codes have been successfully used for transient analyses of BWRs, PWRs and VVERs in Finland and elsewhere.

Besides the coupled dynamic codes, system codes as SMABRE and thermal-hydraulic solution methods have been developed.

To be state-of-the-art internationally the models of the codes must be constantly improved as the knowledge of physical phenomena and computer capabilities increase. Furthermore, new fuel and reactor designs, new loading strategies and the continuing trend towards higher fuel burnups make it necessary to further improve as well as validate the code system to be able to cope with the new challenges.

Main objectives

The objective of the project is to continue the development of reactor dynamics computer codes (TRAB-3D and HEXTRAN) at VTT, especially in the area of thermal hydraulics. The goal is to have a truly independent transient calculation system, which can be utilized by the safety authority and other end-users for safety analyses that are independent from those of power plant designers and fuel vendors. In addition to the development work itself, it is essential that the new models are validated against measurements and the results of other codes. Much of this work can be done as international co-operation in the form of calculating benchmark problems.

Internal coupling of TRAB-3D and SMABRE

The objective of the subtask was to improve the thermal hydraulics in the reactor dynamics computer code, TRAB-3D, by coupling it internally to the SMABRE code. TRAB-3D [1] is a reactor dynamics code with three-dimensional neutronics and one-dimensional thermal hydraulics in a core and in a boiling water reactors (BWR) circuit. The code can be used for transient and accident analyses of BWR and with its core model coupled to SMABRE, also for pressurized water reactors (PWR). The system code SMABRE [2] models the thermal hydraulics of light water reactors. Both codes have been entirely developed at VTT.

TRAB-3D and SMABRE have earlier been connected with parallel coupling [3]. Main advantages of internal type of coupling are possibilities to handle coolant flow reversals in core flow channels as well as modeling of cross flows in an open reactor core like EPR. Also real 3-D thermal hydraulics with the porous media modeling is planned to simulate on the basis of internal coupling realized to TRAB-3D.

In internal coupling TRAB-3D performs the neutronics calculation, SMABRE will take care of the hydraulics calculation of the whole cooling circuit including the reactor core, and the heat transfer calculation may be carried out by either code by the user's choice. On the other hand in parallel coupling TRAB-3D performs the core hydraulics and heat transfer, and the coarse SMABRE core hydraulics with fewer channels than in TRAB-3D are solved in parallel.

The basics for internal coupling were created for BWRs already in the EMERALD project as a part of the SAFIR-Programme [4, 5, 6]. In TRICOT, the work has continued for the PWR [7, 8, 9]. The internal coupling of TRAB-3D and SMABRE needed large modifications and new modules especially into SMABRE, which should still have all the old calculation capabilities with parallel coupling left in it. The unexpected death of the main developer of the code in middle 2008 forced the studies partly to new paths to make sure that finalizing of the coupling was possible.

Several extensions to internal coupling have including such calculation capabilities and features in internal coupling which already exist in separate codes, such as deviation of number of fuel assemblies and fluid channels for both codes, several initial axial power profiles or two sided heat structures for code nodes in SMABRE. The EPR and High Pressure Light Water Reactor (HPLWR) reactors have been used for the test cases because the development of the HPLWR version has been performed simultaneously with the internal coupling. Even though the HPLWR is not included in the SAFIR project, the main findings and test case calculations for HPLWR have created useful cross-checking possibilities for both code versions. Finally, the earlier BWR test cases [5] have been recalculated with the latest code version.

The main idea for the HPLWR version was to extend the capability of the code to supercritical conditions. Thus in the HPLWR project new material properties, which are created from a large international data base, have been implemented in the code and they may be used also for the general TRAB-3D/SMABRE in subcritical area. In first tests for an EPR no significant differences were found between these material properties. Further, the SMABRE point kinetics was modified in order to take into account the fluid temperature in the moderator channels [11] of HPLWR for feed backs in HPLWR. This feature is available for internal coupling and 3-D calculations, too. The application could be e.g. a water cross of BWR assembly modeled as a bypass. Updating the instructions for using the whole calculation system is just about ready but the code manuals [12] and code validation needs further effort.

The PWR test case for the coupling is in a geometry resembling the EPR reactor core with 241 hydraulic channels and 20 axial core nodes. The modeled fuel is a typical PWR fuel. The whole primary loop and the secondary loop from the feedwater tank to the turbine valves have been modeled in SMABRE. The model is not exactly identical to the model of the EPR plant. As a dynamic test case a pump seizure transient has been performed.

Already in [7, 8, 9, 10] good results were reported in comparing the core distributions for fission power, channel mass flows and fuel temperatures with stand-alone TRAB-3D and internal coupling, and also when using parallel coupling. As a final test case the capability of calculating reversed assembly-wise core flow for PWR was performed. TRAB-3D/SMABRE is not intended for LOCAs and that is why only the starting phase of blowdown was used as a demonstration. A middle size break in a cold leg was chosen to have reversed core flows early in the transient. In Figure 1 three distribution of assembly-wise core flow is depicted, about the time of flow reversal, at time with up and down flow situation and totally reversed flow in the LOCA test case for EPR. In Figure 2 void fractions at core outlet at time of flow reversal and with totally reversed flow with high steam partition. With reversed flows only part of the TRAB-3D type thermal hydraulic models included in SMABRE are usable and original SMABRE models are used instead. The result of this LOCA case has only demonstration value of internal coupling achieving reversed flows and high voiding in the core. The only general remark could be that with this kind of core model and codes the results indicates that timing of flow reversals in all core assemblies is about the same.

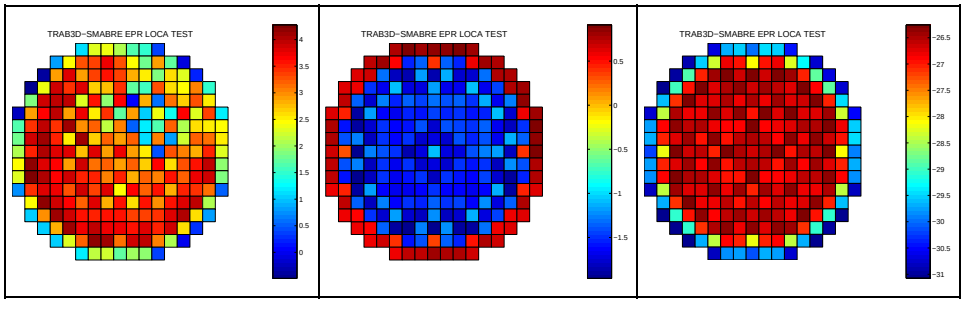

Figure 1. Assembly-wise core inlet mass flows at time of flow reversal, at time with up and down flow situation and totally reversed flow in the LOCA test case for EPR with TRAB-3D/ SMABRE.

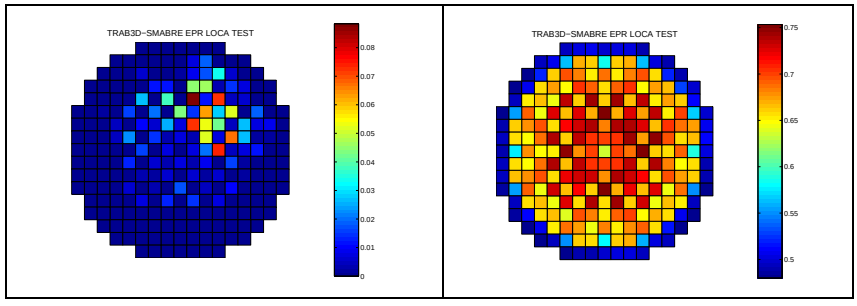

Figure 2. Assembly-wise core outlet void fraction about at time of flow reversal and with totally reversed flow in the LOCA test case for EPR with TRAB-3D/SMABRE.

The HPLWR-model for TRAB-3D/SMABRE consists of 156 fluid channels where in third of the channels flow is downwards. With two lower and upper mixing chambers the flow path is created where fluid goes three times through the core (Figure 5) and even twice before the core inlet in the moderator and gap channels. The number of fuel assemblies is 1 404, nine in each fluid channel. Figure 3 illustrates the 1 404 fuel assemblies with control rods and on the right 156 fluid channels with initial flow rates at the core inlet. The reversed initial flow rates in third of the core reflect the basic ideas and needs for internal coupling.

The CRE, control rod ejection, was analyzed with TRAB-3D/SMABRE and results with 1 404 flow channels were reported in [11]. In CRE the ejected rod set is shown in Figure 3. In Figure 4 radial and axial fission power profiles are shown at time of maximum power. The ejected rods locate in the downward flowing area, but the maximum powers are met in the evaporator, the nearest channel where also initially the highest power exists. Compared to the calculations performed in KFKI Hungary with a coupled code, the results were reasonable and the results of the two codes were close to each other. Furthermore, the SMABRE point kinetics results were compared to other system codes with good results as a part of an EU project.

As an extension to the code, the number of assemblies and the number of fluid channels were diverged. Modelling of the two-sided heat structure was also included in the code. The two sided heat structure may be used for a heavy reflector of PWR where heat input of heavy reflector is considered. Different kind of bypasses may now be modeled so that some of them contain heating while others do not. In BWR the complex fuel assemblies may be supported by assembly-wise heated bypasses or a bypass connected to four quadratic assemblies and having a shroud around as heat structure.

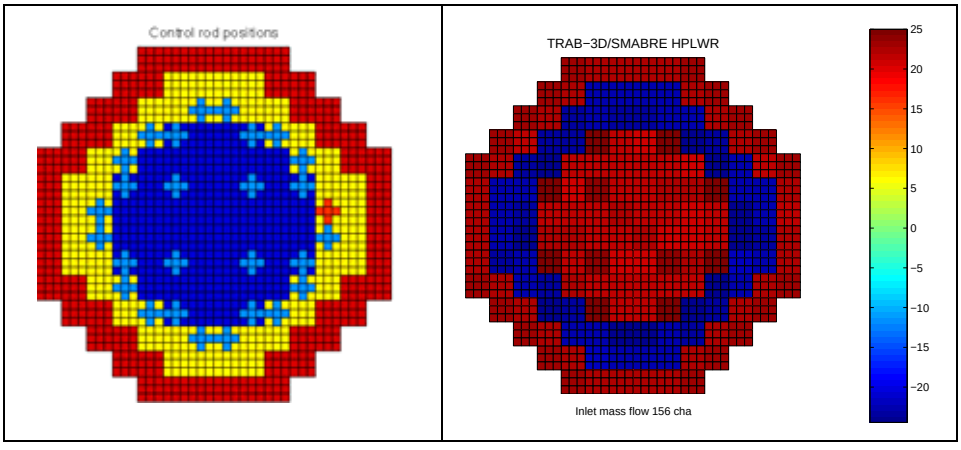

Figure 3. Cross section of HPLWR three-way core with positions of sets of five control rods among 1 404 assemblies and distribution of core inlet mass flows of 156 fluid channels with TRAB-3D / SMABRE.

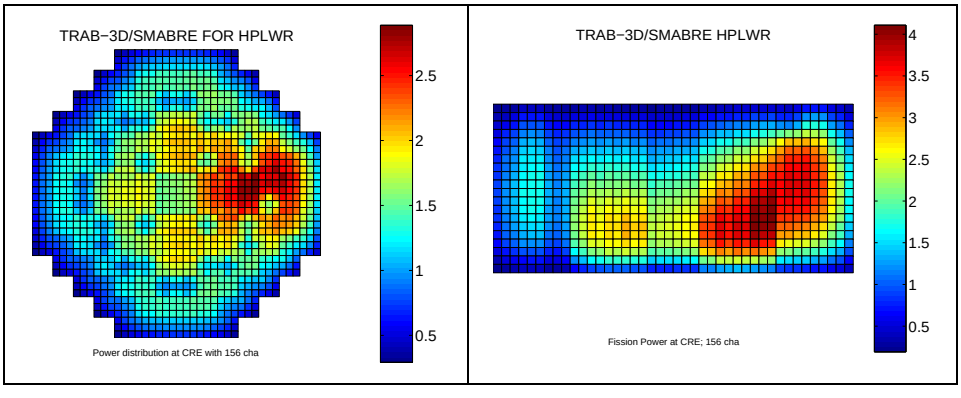

Figure 4. Assembly-wise radial and axial power profile in the ejected control rod line at time of maximum power in HPLWR with TRAB-3D / SMABRE.

Two sided heat structures are essential in modeling the HPLWR pressure vessel because about half of the vessel inlet flow falls from the upper plenum in three moderator channels, continuing upwards in three gaps. In these flow paths heat input is taken from the core channels. In Figure 6 all the flow paths at core elevation are described. The increasing of fluid temperatures in supercritical pressures as well sizes of heat structures are not fine tuned with 3-D neutronics, but the availability of this feature in internal coupling is illustrated. Here fluid temperatures in the downcomer or inside the reflector are not increased even though the same system could be used for the reflector fluid volume too.

The HPLWR cases results indicate that the multichannel and moderator channel heat transfer and feedback extensions to TRAB-3D/SMABRE work properly. In EPR cases the results with internal coupling and parallel coupling are quite close to each other, but validation is still needed to confirm several open questions encountered in this study.

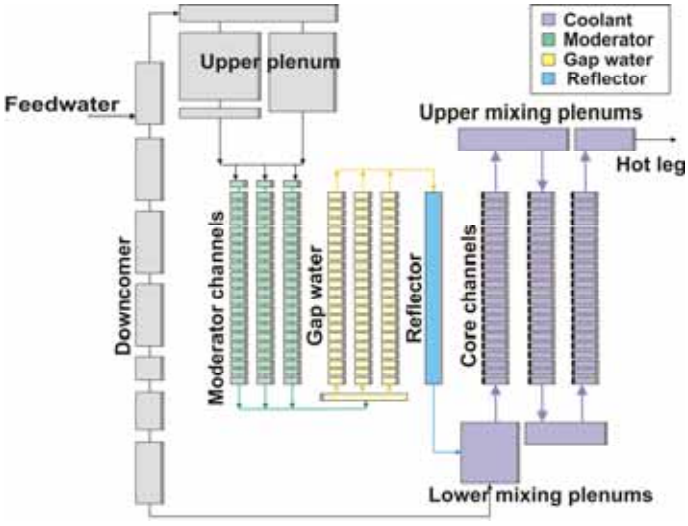

Figure 5. SMABRE nodalization for HPLWR pressure vessel and three-way core. The moderator channels and gap water is flowing between the core 156 channels, grouped here in three group.

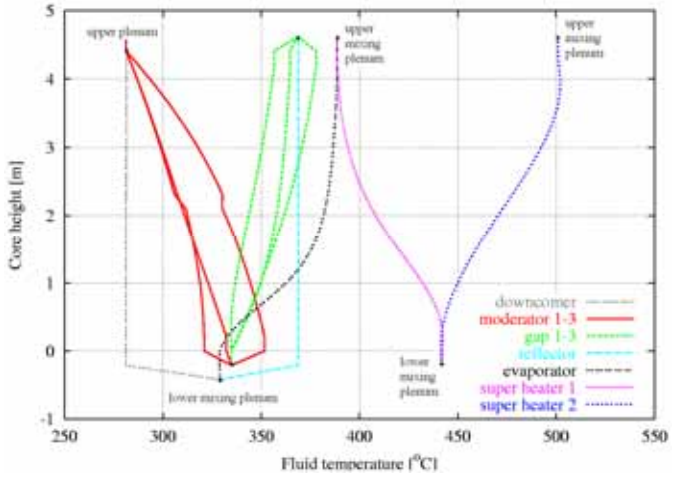

Figure 6. Axial fluid temperature profiles of flow paths in HPLWR three-way core, three moderator and gap channels, reflector and downcomer volumes before the core.

Validation of reactor dynamic codes through comparisons with TRACE/PARCS

In addition to VTT's own reactor dynamics, VTT has the possibility to use the thermal hydraulics and system simulating computer code TRACE [12], which is presently the main tool endorsed by the NRC for nuclear reactor analysis and has probably a significant role as an independent analysis tool for the regulator STUK in future. Concerning 3D neutronics calculations, TRACE includes the Purdue Advanced Reactor Core Simulator PARCS [14] as an integral part of the TRACE package. The availability of TRACE/PARCS opens new possibilities for TRAB-3D validation. Exactly the same problems can be calculated with two computer codes by a single user, and input files directly compared by the same user, in order to minimize the modelling differences.

Three cases were calculated with both TRAB-3D and TRACE/PARCS in 2007 [15]. Two were OECD NEA core transient cases (NEACRP A1 and C1), the third being the OECD NEA PWR MSLB exercise 2 separate core calculation. The overall conclusion was that the 3D nodal neutronic model is not a significant source of uncertainty in transient analysis. The uncertainties and modelling options of thermal hydraulic details cause much larger deviations. For boiling water reactors thermal hydraulics play an essential role already in the reactor core, but the real differences come largely from plant modelling.

Modeling of plant transients with the TRACE/PARCS has been started with the OECD/NEA's Kalinin-3 benchmark, in which pump trip of VVER-1000 type plant is modeled and results are compared to the measured data. A TRACE/PARCS simulation model for the Kozloduy-6 VVER-1000 plant was received from Penn State University in USA, and can be used for Kalinin-3 plant after some modifications. Due to the delays in benchmark schedule, benchmark exercise has not been completed, but useful experience on coupled TRACE/PARCS transients calculations has already been gained [16].

Sensitivity and uncertainty analysis of rector dynamic codes

In the previous research programme the first version of a new sensitivity and uncertainty analysis tool for reactor dynamics codes was developed and tested with the HEXTRAN-SMABRE [17]. In SAFIR2010 programme, the tool has been updated for use with TRAB-3D/SMABRE analysis, as well as for series of hot channel and DNB calculations with the one-dimensional TRAB-CORE code. The usability of the tool has been improved and it is now more versatile for the

management of large amount of reactor dynamics calculations [18]. The tool generates input data, performs calculations and calculates some statistical sensitivity measures, e.g. rank correlation coefficients and tolerance intervals for the output variables of reactor dynamic codes.

The tool was first tested with a control rod ejection transient of PWR with the TRAB-3D /SMABRE [18]. After that, it was applied to analyses of main steam line break accident of Loviisa power plant. Previous analysis has shown that the worst case might be reached with a smaller break size than a double-ended guillotine break. In these analyses the worst case was searched by using several break sizes. Break sizes varied from 50% to 263%, which means double-ended guillotine break, and even to damage of another steam line (in this paper break sizes over 263%). Failure of some protection systems was assumed, and analysis was repeated starting from different initial power levels. [19].

The activation of protection systems can lead propagation of accident to different paths. For that reason larger break sizes are not necessarily the worst, because with smaller break sizes the protection systems may be actuated later or even not at all, e.g. the low primary pressure causes the trip of the all RCPs in the early stage of the MSLB accident with large break sizes. Thus decrease of water temperature is stopped, as can be seen from Figure 7, and return to power is prevented. With the break sizes less than 200% the primary pressure remains slightly above the actuation limit, the RCPs remain in operation and thus decrease of water temperature is continued and the return to power is detected, Figure 8. If the actuation signal for RCP trip is lowered from 10 MPa to 8 MPa, return to power is detected also with larger break sizes. If water level measurement in steam generator of damaged loop is not damaged, trip of RCP in broken loop causes sudden increase in temperature that can be seen in Figure 7. In cases with the malfunction of water level measurement, core inlet temperature remains at lower level. Also in the cases where the RCP remains in operation, slight increase in temperature of the broken loop can be detected, because there is void in the uppermost nodes of steam generator and heat transfer is weakened. This early weakening of heat transfer even though steam generator inventory is not lost, is clearly a specific characteristic of the horizontal steam generator.

It was concluded that smaller break sizes cannot be excluded from the safety analysis, and it is important to notice also uncertainty of signals and measurements. In these analyses for the Loviisa NPP, recriticality or remarkable return to power was not detected in the MSLB accident. The developed uncertainty analysis tool has proved to be a practical system to complete the best-estimate reactor

dynamic codes HEXTRAN/SMABRE and TRAB-3D/SMABRE. With that uncertainty analysis tool it is possible to calculate a large spectrum of cases with several variations with a reasonable amount of work.

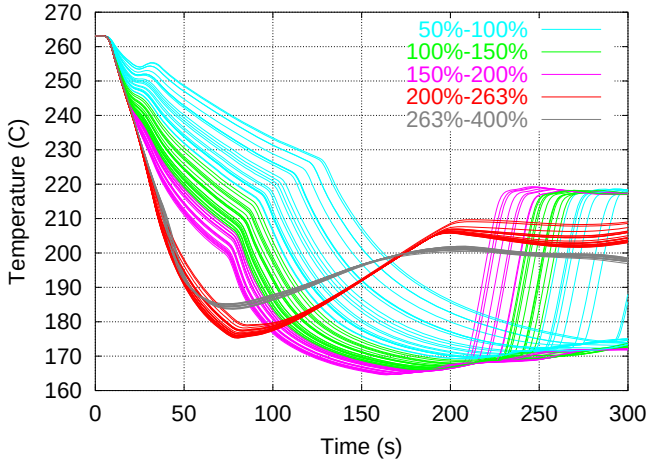

Figure 7. Water temperature at core inlet during MSLB accident, sector 2.

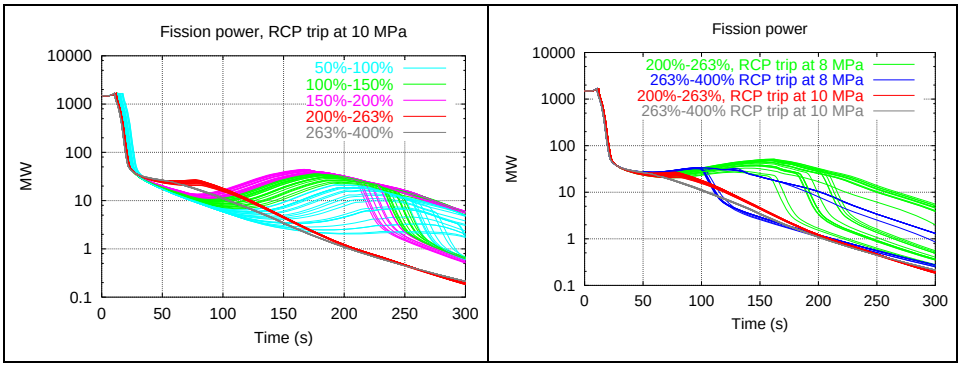

Figure 8. Fission power during the main steam line break accident. On the left actuation limit for the trip of all main coolant pumps is 10 MPa, on the right 10 MPa or 8 MPa.

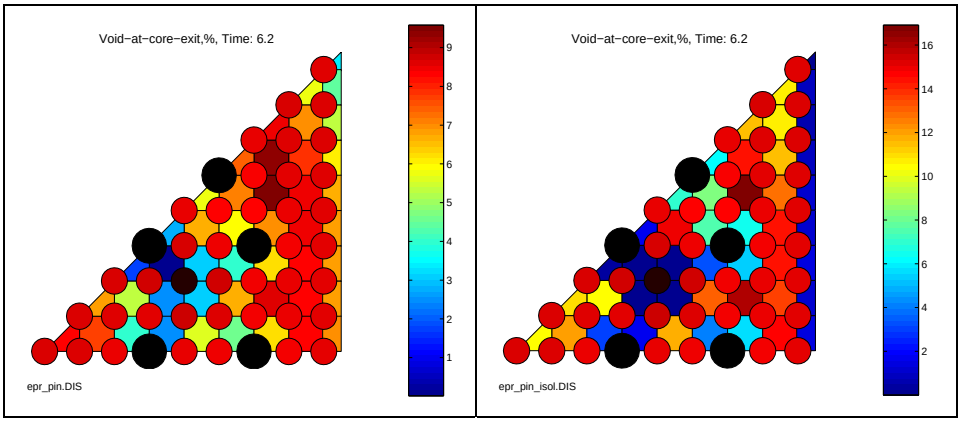

Figure 9. Void fraction at outlet of PWR fuel assembly. On the left open subchannels and on the right isolated subchannels.

Uncertainties of hot channel calculations were studied in 2010 [20]. Behaviour of the hottest fuel rods has in VTT's reactor dynamics analysis been modelled with the TRAB-CORE model. Hot channel is an isolated thermohydraulic channel with one hot fuel rod. Core neutronics and whole core thermalhydraulics is calculated either with the one-dimensional TRAB or three-dimensional TRAB-3D or HEXTRAN code, and hot channel calculation does not affect the whole core neutronics or thermalhydraulics. Hot channel conditions are defined with a hot channel factor.

One defect of the present hot channel methodology is that cross-flows and mixing inside the assembly and also between the assemblies can not be modelled with one-dimensional thermal-hydraulics models. It was assumed that the assumption of isolated channels brings additional conservatism to the calculations. Aim of the work was to study effect of mixing on the hot channel analysis with the sub-channel code COBRA that was slightly modified for the calculation of transients. Correlation selection of COBRA was also supplemented so that it is possible to use same correlations as with the TRAB code.

As an example, in Figure 9 is void fraction at core exit with same pin-wise power distribution with isolated and open sub-channels. Turbulent cross-flow between subchannels was $w_k = 0.02\ s_k G_k$, where s_k is width of the gap between subchannels and G_k average axial mass flux in those subchannels. Maximum void fraction in this hypothetical CRE case was with open sub-channels 9,6% and with isolated sub-channels 16,9%.

Especially the hot channel factor for enthalpy rise has been defined in VVER/PWR analysis very conservative way assuming that local linear power is in its maximum allowed value at normal operation. The benefit of this procedure is that the analysis covers all possible allowed core configurations not only that used in the current safety analysis. However, it was noticed that the same methodology cannot be utilized with reactor cores with bulk boiling at core exit and for fuel assemblies with more uneven positions of heated fuel rods.

Three-dimensional thermal hydraulics

The objective of the subproject was to develop methodology for 3D two-phase thermal-hydraulic modelling of the nuclear reactor core. The used porous medium approach is CFD-like, but does not use calculation mesh fitted to the structures. Instead, the fluid volumes of the mesh cells are described as porosity (volume not filled by structure). It is hoped that with this approach, it will be easier to create models, and calculation will be faster than with actual CFD.

Main applications of the PORFLO code have been the secondary side of the Loviisa steam generator, BWR fuel bundle, core debris coolability in the COOLOCE test facility and EPR pressure vessel. A more detailed description on this subtask is presented as the special report of TRICOT in this report.

International co-operation

Participation in the OECD Nuclear Energy Agency (NEA) working groups and benchmarks is one of the most important ways of validating the methods and codes used in reactor analysis. This project includes the participation in the meetings of the NEA Working Party on the Scientific Issues of Reactor Systems (WPRS), which is responsible for the organization of the reactor dynamics benchmarks among other activities. In the frame of the TRICOT project VTT has participated in the OECD/NEA Uncertainty analysis benchmark series (UAM), in the fuel bundle benchmark (BFBT) and in the Kalinin-3 benchmark.

The cooperation and information exchange on VVER safety within the AER framework together with other countries that use VVER reactors has been continued. In 2010 20th AER symposium was arranged together by VTT and Fortum. Number of participants was 54 from abroad and 26 from Finland. Altogether 71 conference papers were presented on the reactor physics, dynamics and thermal-hydraulics [21].

Conclusions

During the TRICOT project, VTT's computer code system for reactor dynamic analysis has been further developed and also validated through international benchmarks and other comparisons. Internally coupled TRAB-3D/SMABRE core is now applicable for safety analysis of PWRs with square-lattice fuel assemblies. The TRAB-3D/SMABRE code offers also possibility to model new phenomena as reversed flows in BWRs. It can be applied also to totally new reactor concepts as HPLWR.

Uncertainty and sensitivity analysis tool has been further developed during the TRICOT project and it proved to be practical system to complete the best-estimate reactor dynamic codes HEXTRAN/SMABRE and TRAB-3D/SMABRE.

The reactor core model PARCS coupled with the system code TRACE has been taken into the use at VTT in TRICOT project. Experience on calculation of TRACE/PARCS 3D transients has been gained by calculating several OECD/NEA benchmarks and comparing the results to the TRAB-3D calculations. Also the COBRA-EN code is taken into the use and is modified to be more suitable to accompany the VTT's reactor dynamics calculation system. The COBRA-EN has been used for sensitivity calculations in the modelling of hottest fuel rod of PWR reactor.

International co-operation has been continued by active participation to the work of OECD/NEA and AER.

References

1. Kaloinen, E. & Kyrki-Rajamäki, R. TRAB-3D, a New Code for Three-Dimensional Reactor Dynamics. In: 5th International Conference on Nuclear Engineering (ICONE-5). Nice, France, 26–30 May, 1997 [CD ROM]. New York: the American Society of Mechanical Engineers. Paper ICONE5-2197. ISBN 0-79181-238-3.

2. Miettinen, J. Thermohydraulic model SMABRE for light water reactor simulations. Licentiate's thesis, Helsinki University of Technology, 2000. 151 p.

3. Daavittila, A., Hämäläinen, A. & Kyrki-Rajamäki, R. Effects of secondary circuit modeling on results of PWR MSLB benchmark calculations with new coupled code TRAB-3D/SMABRE. Nuclear Technology, May 2003, Vol. 142, No. 2, pp. 116–123.

4. Miettinen, J. & Räty, H. Status of the EMERALD subtask for coupling of TRAB-3D and SMABRE. Project Report PRO1/P7037/03. VTT Processes, 31.12.2003. 6 p.

5. Miettinen, J. & Räty, H. The coupled code TRAB-3D-SMABRE for 3D transient and accident analyses. In: Räty, H. & Puska, E.-K. (Eds.). SAFIR 2003–2006, Final Report, VTT Research Notes 2363. VTT Processes. Espoo, 2006. Pp. 48–59. ISBN 951-38-6886-9. http://www.vtt.fi/inf/pdf/tiedotteet/2006/T2363.pdf.

6. Miettinen, J. & Räty, H. Status of the EMERALD subtask for coupling of TRAB-3D and SMABRE. VTT, Espoo, 1.2.2006. Project Report VTT-R-00982-06. 9 p.

7. Miettinen, J., Hämäläinen, A. & Räty, H. Status of internal coupling of TRAB-3D and SMABRE for PWR core. VTT, Espoo, 2008. VTT Research report VTT-R-00718-08.

8. Hämäläinen, A. & Räty, H. Comparison of TRAB-3D / SMABRE versions for PWR in 2008. VTT, Espoo, 2009. VTT Research report VTT-R-02411-09.

9. Hämäläinen, A., Räty, H. & Seppälä, M. Extensions to TRAB-3D / SMABRE in 2009. VTT, Espoo, 2010. VTT Research report VTT-R-0929-10.

10. Räty, H., Daavittila, A. & Hämäläinen, A. Tridimensional core transient analysis methods (TRICOT). TRICOT Summary Report. In: Suolanen, V. & Puska, E.K. (Eds.). SAFIR2010 Interim report. VTT, Espoo, 2009. VTT Research Notes 2466. Pp. 120–130. ISBN 978-951-38-7266-3. http://www.vtt.fi/inf/pdf/tiedotteet/2009/T2466.

11. Seppälä, M., Hämäläinen, A., Daavittila, A. High Performance Light Water Reactor Transient Analysis with Neutronics Feedback using TRAB-3D and SMABRE Codes. Proceedings of ICAPP ‘10, San Diego, CA, USA, June 13–17, 2010. Paper 10103.

12. Miettinen, J. (& Hämäläinen, A. in Vol. 2), Volume 1: SMABRE system models and numerical methods, Volume 2: SMABRE input, output and common description, Volume 3: SMABRE program description, Volume 4: Assessment and application of SMABRE. Volume 5: SMABRE help modules. VTT Internal Reports.

13. TRACE Theory and User’s Manuals, Division of Risk Assessment and Special Projects. Office of Nuclear Regulatory Research, U.S. Nuclear Regulatory Commission, Washington, DC.

14. Downar, T., Xu, Y., Seker, V. & Hudson, N. PARCS v3.0 U.S. NRC Core Neutronics Simulator User Manual, DRAFT (12/5/09), University of Michigan, U.S. NRC, December 2009.

15. Daavittila, A. TRAB-3D Validation through comparison calculations with TRACE/PARCS. VTT, Espoo, 2008. Research Report VTT-R-00124-08. 24 p.

16. Seppälä, M. PARCS user experiences at VTT in 2010. VTT, Espoo, 2011. VTT Research report VTT-R-00315.

17. Syrjälahti, E. New sensitivity analysis tool for the reactor dynamic codes. VTT Processes 2005. Project Report PRO1/1016/0. 15 p.

18. Syrjälahti, E. Development of sensitivity and uncertainty analysis tool for reactor dynamics codes. VTT, Espoo, 2008. VTT Research Report VTT-R-00843-08. 15 p.

19. Syrjälahti, E. & Hämäläinen, A. Sensitivity studies for the main steam line break in the Loviisa NPP with the HEXTRAN-SMABRE. PHYSOR 2010, Pittsburgh, Pennsylvania, USA, May 9–14, 2010. On CD-ROM, American Nuclear Society, LaGrange Park, IL, 2010.

20. Syrjälahti, E. Sensitivity studies for the sub-channel calculations of PWR fuel assembly. VTT, Espoo, 2010. VTT Research Report VTT-R-09072-10. 20 p.

21. Proceedings of the twentieth Symposium of AER. Hanasaari, Espoo, September 20–24, 2010. ISBN 978-963-372-643-3.

9.2 The 3D two-phase porous medium flow solver PORFLO and its applications to VVER SG and EPR RPV

Ville Hovi and Mikko Ilvonen
VTT

Abstract

Within the TRICOT project, the in-house code PORFLO is being developed for 3D thermal hydraulics, with main emphasis on modeling of two-phase flow of steam and water. Its intended main use is in reactor dynamics calculations, but several other applications are possible as well. In this paper, the main features and some specific development steps taken in 2009–2010 [1, 2] are presented on a descriptive level. The results of a few demonstrative simulations are presented in order to illustrate the potential capabilities and shortcomings of the code and the methods being used.

Introduction

Whereas computational fluid dynamics (CFD) of single-phase water is a fairly well established field of numerical science, much more remains to be done in the field of two-phase flow, which is important for nuclear applications. At the same time, the focus of thermal hydraulic simulations is gradually shifting towards 3D. Though computational resources are increasing, it is not possible in near future to use structure-fitted computational grids for complex components. Commercial codes, like Fluent, are expensive to use and do not reveal their source code even in cases where something clearly goes wrong in the simulations. This is the ‘market niche’ for PORFLO: a 3D, two-phase flow solver with complete in-house source code, in which the need for a structure fitted grid is circumvented by introducing the porous medium approach. However, the reduction in problem size comes at the cost of increasing model complexity; since the fine geometrical details are no longer simulated, the effect of those omitted details needs to be modeled. This increases the importance of the validity of the various closure laws used in the model.

Brief description of PORFLO

The most essential features of PORFLO can be listed as follows:

- 3D solution of two-phase flow of water and steam.
- Six-equation model (mass, energy and momentum conservation of water and steam).
- Cartesian staggered grid (velocities expressed at faces of pressure cells).
- Regarding the flow solution, geometry is described only as porosity (fraction of fluid volume of cell volume), but in other physical models (like heat transfer) any additional knowledge of the geometry may be utilized.
- Solution of common pressure and phase velocities is based on the PC-SIMPLE algorithm [3].
- Several preconditioned iterative methods for solution of linear systems of equations.
- First turbulence model (k-ε) is only in the testing phase; source terms for porous zones remain a subject of future work.
- Applications: isolation condenser, BWR bundle, VVER SG, COOLOCE, EPR RPV.
- Visualization of results with an easy-to-use tool, StarNode [2], based on OGRE 3D graphics library and Qt toolkit.

Latest basic development

Basic development of PORFLO, i.e. not application specific, during the latter half of Safir2010 is described here. Emphasis is on solver development, turbulence modeling and parallelization. Some more coding-oriented / practical topics, like solver code architecture or user interface, are omitted from this presentation.

Solver development

The effect of non-conservative (or primitive) formulation of the momentum equations on convergence of the solution algorithm was studied. Quite significant improvements (in some cases over 50% reductions in the number of iterations) were obtained using the non-conservative formulation instead of the conservative

one. Additionally, solution of volume fractions was improved by solving volumes of both phases, and only then expressing them as volume fractions. Furthermore, a new separate iteration was added for solving of heat transfers and temperatures.

Handling of friction terms was improved by the possibility of giving different friction correlations in three independent directions. This feature is useful e.g. with tube bundles, where the flow setting is significantly different in the direction of the tubes or in the lateral direction.

Several new discretization schemes were coded, most importantly new high order schemes. Choice of the scheme will also imply the calculation of flow area between cells based on the porosities in the cells. Even after this, some new consideration was given to the problem of expressing the free flow area at the velocity node (on the border between two pressure cells) based on porosities in the cells. Depending on the geometry, there are endless possibilities of how the flow between two pressure cells is obstructed in reality. However, the velocity should ideally always be descriptive of the total fluid volume whose velocity is to be represented. It is not self-evident in all cases how the computation should proceed.

Scalar transport

A general-purpose scheme has been created for scalar transport. This was inspired by the need to calculate transport of the turbulence kinetic energy k and dissipation rate ε in the turbulence model. The transported scalar may be e.g. the concentration of any species solved in the water. It is now easy to add new transported scalars as the user wishes. It is possible to choose between conservative and primitive form of the transport equation. Some tests of numerical diffusion are being performed.

One of the most important uses of the scalar transport scheme is the transport and spreading of boric acid concentration in PWRs, especially when calculating transients at the beginning of fuel cycle. It will be necessary to account for higher density of boron-containing water.

Turbulence modeling

Development of a turbulence model was begun in fall 2009. The most widely used of the two-equation models, the k-ε model developed by Launder and Spalding [4], was chosen. From the perspective of the entire solution process this adds two scalar fields to the list of solved variables: these are the turbulence kinetic energy per unit volume (k) and its dissipation rate (ε). As a first approach

the so called mixture model was chosen, in which the turbulence kinetic energy and turbulence dissipation rate are solved for the mixture of the two phases. The transport equations for turbulence kinetic energy and turbulence dissipation rate (k and ε), along with the corresponding production terms, are solved in a slightly different form compared to Launder and Spalding [4], for the reason that the original transport equations do not include density and were developed for finite-difference methods, the latter affecting the production terms in particular. Apart from these modifications the basic principles, model assumptions and constants of the original model still apply.

For the time being, the model has appropriate source terms at known walls only. The most difficult part will be to develop the right-hand-side source terms of the equations for the porous medium, which are highly dependent on the configuration of the material, e.g. tube / particle diameter. Once solved, the turbulence kinetic energy will affect many processes, most importantly the flow field through turbulent viscosity, but also enhancement of heat transfer, mixing of void fraction and scalar concentrations etc. Currently the predicted values of k are being initially checked, but that is difficult before their coupling to other processes, because of the feedback effect. Testing has revealed some problematic and possibly erroneous behavior when moving from walls of a test flow channel towards the centerline.

Parallelization

Some initial investigations in parallelization using Open MPI, the open source code implementation of the MPI (Message Passing Interface) standard, have been done. Domain decomposition seems to be the most suitable, and most often used, method for the parallelization of CFD codes. A key part of this method is to be able to divide the solution of linear systems of equations between parallel processes. Therefore, to asses the feasibility of this approach in general, the parallelization of the linear iterative solvers was tackled first. The coefficient and preconditioning matrices have been divided into separate blocks (one for each process) and coupling matrices have been formed that define the communications between the processes. There are currently preliminary versions of two preconditioned solution algorithms in PORFLO (CG, or Conjugate Gradient, and BiCG, or Bi-Conjugate Gradient). Parallelizability was demonstrated and good rate of convergence was achieved. Scalability may be further improved by fine tuning the communications between the processes.

Applications

Currently the most important application for which PORFLO is developed is 3D TH of a reactor pressure vessel (RPV) at various levels of detail, but the code is kept general-purpose enough to allow various other NPP applications, like steam generators and other heat exchangers, including passive safety systems, or core debris particle beds in severe accidents. The common denominator of appropriate applications is a component or subsystem in which 3D phenomena may be important, but the geometry is too complex to allow use of a structure-fitted grid.

The previous application, BFBT benchmark [5], was not actively developed further, but some new considerations were given to its computational grid: It should be continued on subchannel-scale predictions, which is more appropriate in the porous medium framework than the fine-grid 'quasi-CFD' simulations done so far.

Loviisa VVER plant horizontal steam generator

The main application on which specific development efforts were concentrated in 2009 was the VVER horizontal steam generator [6, 7]. Steady-state at full power level (approx. 250 MW per SG) was reached after a 40 second transient simulation using PORFLO. The results, gathered in Figure 1, include phase velocities, void fraction and evaporation / condensation rate on cross-section $x = 2.83$ m.

A rough comparison of PORFLO simulation results to fluent simulations, conducted in project SGEN, is presented in Figure 2. For easier comparison, a 'side view' of the void fraction distributions is plotted at the centerline of the hot collector. The same correlations were used in both codes. It can be seen that this particular result appears similar regardless of the code used.

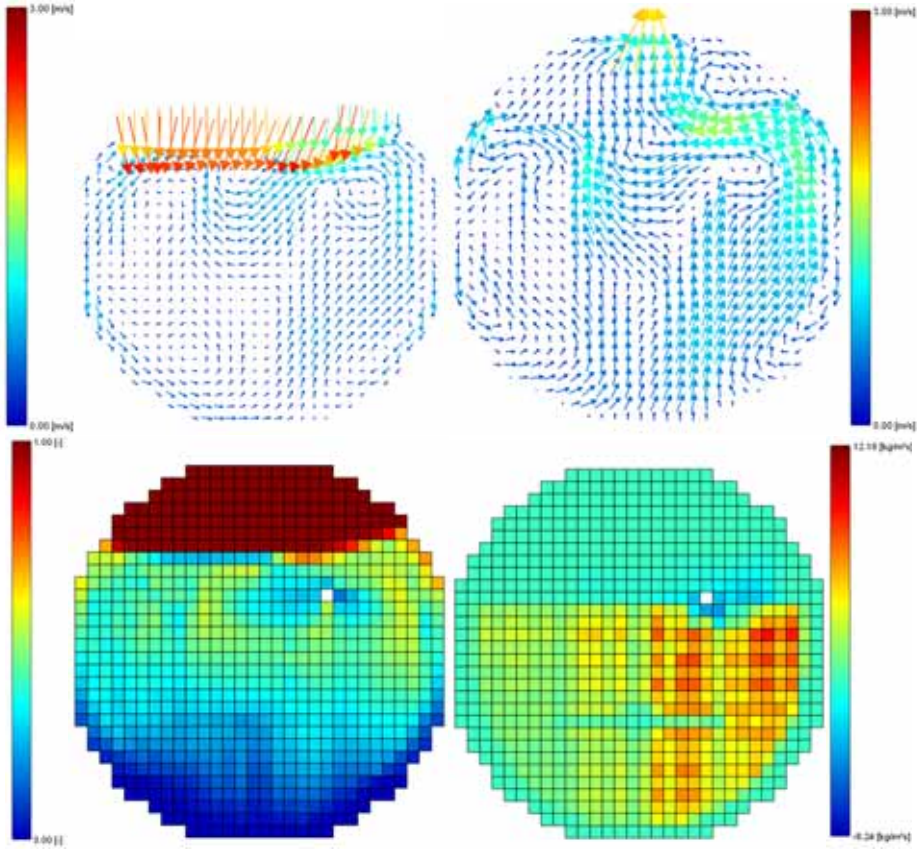

Figure 1. Liquid velocity (top left) [m/s], vapor velocity (top right) [m/s], void fraction (bottom left) [-] and evaporation / condensation rate (bottom right) [kg/m3s] on cross-section x = 2.83 m.

COOLOCE

One of the applications in 2010 was the COOLOCE test facility, which is used for studies related to coolability of corium debris particles. The first tests were performed at the COOLOCE facility of VTT, and several PORFLO simulations aiming at predicting the location of the dryout and the dryout power were run [8].

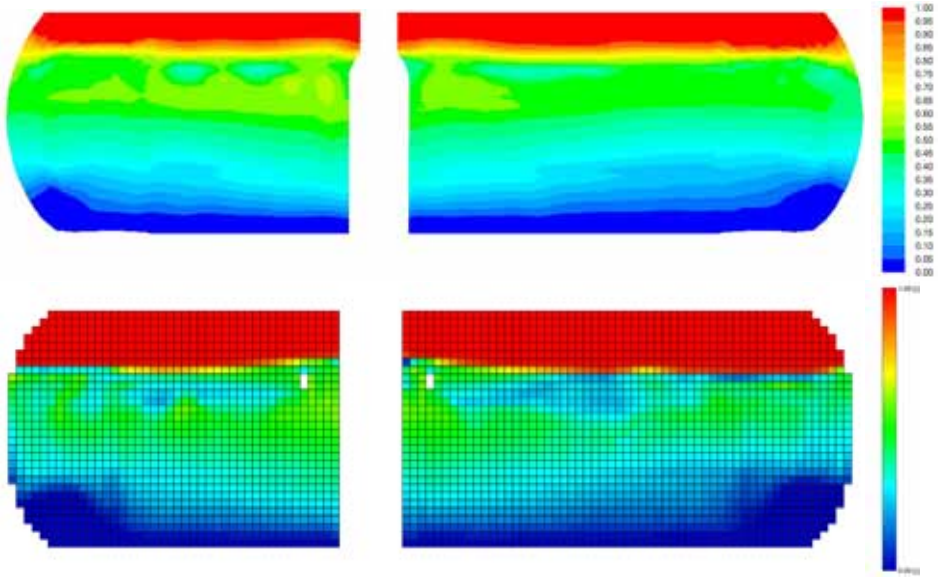

Figure 2. Comparison of Fluent (top) and PORFLO (bottom) simulation results for normal steady-state operation of the Loviisa horizontal steam generator. Shown is a side view of void fraction at the centerline of the hot collector.

EPR pressure vessel

For the first time in Finland, the Olkiluoto-3 EPR will have an open reactor core, i.e. no channel boxes enclosing the fuel elements, as is the case in Olkiluoto-1 and 2 BWRs, but also in Loviisa VVER plants. Furthermore, both the other PWR candidates for the FIN-6 plant (APR1400 and APWR) have an open core. Then, the interesting question is, to what extent the flow in each fuel element proceeds straight upwards and to what extent there is transverse mixing between the subchannels and fuels elements. More mixing will mean less probability of a local ‘hot spot’; therefore, it is very important to simulate the 3D flow field in a manner as mechanistic as possible, without resorting to artificial mixing terms. The transverse mixing is also important in such cases as ‘cold tongue’ and boron dilution. Generally, in any case where part of the reactor core (in the radial direction) is in a state other than the rest, it is important to have a proper 3D thermal-hydraulic model.

This is the background why one of the new PORFLO applications in 2010 was 3D flow in the EPR reactor pressure vessel with its 241 fuel elements and 89 control elements. PORFLO can accept geometrical information with as many details as available for this project, but as it uses the porous medium approach,

the representation during simulation is in the resolution of the grid used. In comparison to the app. 5 500 primary tubes of the VVER steam generator (previously done application of PORFLO), the EPR core has app. 64 000 fuel rods (241 fuel elements, each of which has 265 rods in a 17 × 17 geometry).

First simulations were performed with major RPV internal parts present; it is easily possible to add finer details even later. The geometry model is a computational simplification of the true physical geometry of the internals of the EPR pressure vessel, which are very complex. From the model, several computation-oriented data, like volume fractions and areas of different parts (like fuel pins) are produced in a numerical fashion. Like in other PORFLO applications, the geometry and other initial data are expressed as porosities, flow areas, power densities and heat capacities in a regular Cartesian grid. Most difficulties in PORFLO are related to the description of the Cartesian fuel assembly grid and the more or less cylindrical surroundings (including the downcomer) in a consistent manner. No special coding was done for the EPR in order to keep the code general-purpose. This resulted in the annular downcomer becoming somewhat 'tangled', but this is also the case with other curved surfaces (although softened by porosity). This may affect the simulation of mixing phenomena. With more resources for development, PORFLO could be equipped with structure-fitted grids (like usual CFD), but still use the porosity concept for fine structural details.

At the time of this writing, there is a PORFLO model of the EPR RPV that works in 'technical' sense, i.e. calculates without crashing, but not yet equipped with all realistic correlations, nor validated or coupled to other codes. Boundary conditions are given at the four inlets and four outlets. Some results of demonstration calculations are included below. The work in 2011 will be the natural continuation: more detailed application-specific development of the various closure law correlations needed, and partial validation by code-to-code comparisons or comparisons with published results of similar simulations.

Preliminary simulations of the normal nominal power thermal-hydraulic operation of the EPR RPV were performed using the six-equation PC-SIMPLE algorithm of PORFLO, as a transient simulation. System pressure was set at 15.8 MPa, total heating power at 4 291 MW, inlet mass flow rate at 23 141 kg/s and inlet temperature at 296°C. The domain was split using a nodalization of (23 × 23 × 55), which amounts to 29 095 cells. The steady state results, in Figures 3 and 4, where obtained at the end of a 100 s transient simulation. The computation time spent on a single core of a 2.992 GHz Intel Xeon quad-core processor was 15 hours. As the EPR model is developed further, the simulation results (at the moment

demonstrative only) will have to be validated on a code-to-code basis, based on published simulations.

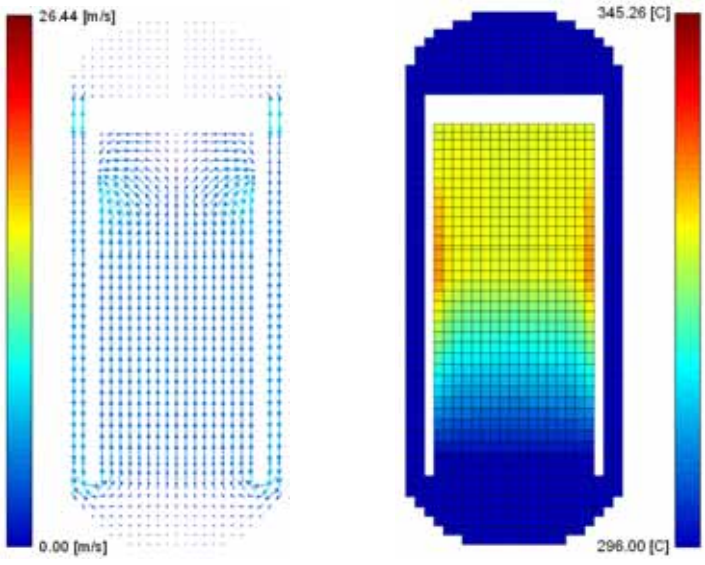

Figure 3. Side view of liquid velocity (on the left) [m/s] and temperature (on the right) [°C] from a preliminary PORFLO simulation of the EPR reactor pressure vessel. Cutting plane is located in the middle, between loop 1 and 2 outlets (left side) and loop 3 and 4 outlets (right side).

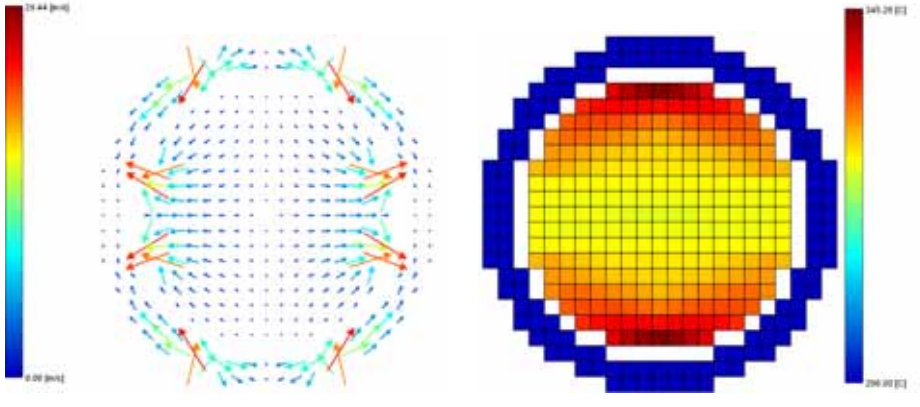

Figure 4. Top view of liquid velocity (on the left) [m/s] and temperature (on the right) [°C] from a preliminary PORFLO simulation of the EPR reactor pressure vessel. Horizontal cutting plane is located at inlet / outlet height.

PORFLO development plans

PORFLO is a 3D solver code for two-phase flow of water and steam, developed at VTT in recent years. The advantages of such in-house development include complete knowledge of and access to the source code, no license fees of code use, thorough learning of researchers doing the development and the possibility of coming up with an internationally recognized code in a field which is not yet mature.

In the period 2011–2014, the basic development of PORFLO can be divided into the following categories, which generally also apply to 2011, as it is not possible or not reasonable to perform them in a sequential time order:

1) Development of physical models (turbulence model, material properties / steam tables)
2) Numerical development (geometry, grid, boundaries, discretization schemes, solver)
3) Coding development (version management, documentation, user friendly / developer friendly source code, parallelization, user interface)
4) Application specific development (correlations etc. used for various closure laws)
5) Code coupling issues (coupling to system code / neutronics)
6) Validation (systematic validation plan; single phenomena / integral effects).

With the expected resources, it is not possible to cover all the above-mentioned areas completely. The work in 2011 will be concentrated on finalization of the turbulence model (already preliminarily developed), continuation of parallelization efforts (initial steps taken and some verifications of numerics already done) and introduction of proper steam tables (use of those in Apros agreed with the Apros team).

In parallel with PORFLO development, the international status of open-source code projects (like OpenFOAM) will be carefully monitored, and results / code tools from those forums will be utilized in cases of better cost/benefit ratio.

Conclusions

With PORFLO development and applications, we have shown that it is possible with quite restricted resources to create a computational capability for 3D, two-phase flow solution that can in many respects be compared with big, well-

established commercial codes, like Fluent. With the 'solver engine' working fine, many of the remaining problems are more application-specific (closure laws for heat transfer, frictions etc.) as in the use of any CFD code. However, the applications presented here must be regarded as 'demonstration calculations': Only with much more work would it be possible to concentrate on a single application and develop it to a reliable analysis tool. Even in the basic development, there are several big tasks (e.g. turbulence modeling, possibility of structure-fitted grids, proper steam tables, parallelization) that could well all be done, but the inevitable man-months would be needed.

References

1. Takasuo, E., Hovi, V. & Ilvonen, M. Introduction to PORFLO and user instructions 2010. VTT, Espoo, 2010. VTT Research report VTT-R-00446-11. 24 p.

2. Ilvonen, M., Hovi, V. & Inkinen, P. PORFLO development, applications and plans in 2008–2009. VTT, Espoo, 2010. VTT Research report VTT-R-01414-10. 28 p.

3. Vasquez, S.A. & Ivanov, V.A. A phase coupled method for solving multiphase problems in unstructured meshes. In: Proceedings of ASME FEDSM'00: ASME 2000 Fluids Engineering Division Summer Meeting. Boston, Massachusetts, June 11–15, 2000. Pp. 743–748.

4. Launder, B.E. & Spalding, D.B. The Numerical Computation of Turbulent Flows. Computer Methods in Applied Mechanics and Engineering, 1974. Vol. 3, pp. 269–289.

5. Ilvonen, M. & Hovi, V. The porous medium model PORFLO for 3D two-phase flow and its application to BWR fuel bundle simulations. In: SAFIR2010, The Finnish research programme on nuclear power plant safety 2007–2010, Interim report. Espoo, 2009. VTT Research Notes 2466. Pp. 131–141. http://www.vtt.fi/inf/pdf/tiedotteet/2009/T2466.pdf.

6. Hovi, V. & Ilvonen, M. PORFLO Simulations of Loviisa Horizontal Steam Generator. VTT, Espoo, 2010. VTT Research report VTT-R-01406-10. 34 p.

7. Hovi, V. & Ilvonen, M. 3D PORFLO simulations of Loviisa steam generator. AER Symposium, Hanasaari, Espoo, September 20–24, 2010.

8. Takasuo, E., Hovi, V. & Ilvonen, M. PORFLO modelling of the coolability of porous particle beds. VTT, Espoo, 2010. VTT Research report VTT-R-09376-10. 41 p.

10. Total Reactor Physics Analysis System (TOPAS)

10.1 TOPAS summary report

Petri Kotiluoto
VTT

Abstract

The purpose of the TOPAS project has been to maintain and develop stationary reactor physics code system, covering a wide range of calculation needs. Main results have been the development of a new Monte Carlo code Serpent, advanced methods for burnup calculations, and the development of sensitivity and uncertainty analysis methods. There has also been a strong interest in educating new competent people to work in field of reactor physics and nuclear safety. Several university degrees have been taken during the project, and the educational objectives have been well fulfilled. International co-operation has also been active. The results of the project will serve the needs of both the safety authorities and the power utilities.

Introduction

Together with the reactor dynamics codes, the stationary reactor physics code system has to cover the whole range of calculations, from handling of basic nuclear data, i.e. cross section libraries, over fuel and core analyses in normal operating conditions to transient and accident studies using coherent models and methods. It should be possible to follow the whole life cycle of the nuclear fuel from a reactor physics point of view until its final disposal. The same or similar models can often be used in both the static and the dynamic calculations.

Additionally, it is of utmost importance to maintain competence and train new personnel in today's situation, when the use of nuclear power is increased at the same time as the present generation of nuclear experts is gradually retiring from work. Co-operation with the technical and other universities is necessary to make new students interested in this branch of science and thus ensure that the nuclear plants in Finland will be in the hands of competent people in the future, too. The tasks of the project have provided excellent possibilities for university students to perform work for their academic degrees.

Main objectives

The objective of the project has been to further develop VTT's computer code system for reactor analysis into a unified, up-to-date and sufficiently complete entirety in order to make it possible to perform all analyses that are needed in Finland in the field of nuclear reactor physics. It should be possible to follow the whole life cycle of the nuclear fuel from a reactor physics point of view. Especially the demands of new nuclear fuel designs and the new Finnish nuclear power plant have to be taken into account. The project also includes international co-operation and the education of new experts in nuclear reactor technology.

Main results

The work has been devided into five subprojects, which deal with nuclear cross sections, development and validation of nodal methods, Monte Carlo and other radiation transport methods, criticality safety and isotopic concentrations, and development of sensitivity and uncertainty analysis methodology.

VTT has participated in OECD NEA organised JEFF project. Through this participation, knowledge about latest evaluated nuclear data files (ENDF) is maintained. The NJOY code has been used to extract cross section data for various purposes. For instance, a cross section library has been created for the new Serpent Monte Carlo code (with the earlier working title PSG) [1]. In addition, possibilities to extract covariance data with NJOY have been studied and a research report has been written on subject [2]. Also in the reactor dosimetry field, work has been done related to the dosimetry cross sections and analysing methods, such as a dosimetry library has been developed for the new NSVA-3 adjustment code. In addition, meetings of the European Working Group on Reactor Dosimetry (EWGRD) have been attended.

Related to the development and validation of nodal methods, Studsvik Scandpower's (SSP) SIMULATE-3 and CASMO-4 codes have been further tested. In addition, new persons have been trained to use CASMO and SIMULATE codes, for which purpose "Basic CMS Training Course" organised by SSP has been attended in 2007, 2008 and 2010, for instance. A survey on the status and usability of 1D data condensation methods and codes at VTT has also been performed [3] and a master's thesis has been written on subject [4]. In this work also some new modules were programmed to CROCO code, in order to enable input of SIMULATE data for the 1D condensation.

The Serpent code has been developed as a part of both the cross section and the Monte Carlo subprojects, and one of the results of the code development has been the doctoral dissertation of J. Leppänen in 2007 [5]. However, Serpent code development has not remained just as an academic exercise, but instead, Serpent has been made available worldwide during the TOPAS project and it has gained large interest and wide international user community. The main distributors of the code are the OECD/NEA Data Bank in Europe and RSICC in North America. The NEA release was issued in May 2009 (Package-ID NEA-1840, updated in January 2010) and RSICC release in March 2010 (Code Number C00757).

Serpent is especially intended for reactor physics calculations at the fuel assembly level, e.g., to calculate homogenised few-group reaction cross sections, scattering matrices, diffusion coefficients, assembly discontinuity factors, and delayed neutron parameters in an infinite-lattice geometry. During the TOPAS project also burnup calculation routines have been implemented. The first burnup calculation method was based on an external coupling to the ORIGEN2 depletion code using ABURN, a coupling code developed at VTT [6]. Thereafter, internal depletion routines have been implemented and the Serpent code has nowadays the capability to run stand-alone burnup calculation. The used burnup calculations methods are the Transmutation Trajectory Analysis (TTA) [7] and Chebyshev rational approximation method (CRAM). The latter one has been shown to be fast, robust and accurate [8], and is therefore the default option in Serpent. Recently rational approximations have been studied further in order to analyse the CRAM method in detail and to improve the accuracy [9]. The convergence of the method when applied to a large burnup system is illustrated in Figure 1. In addition, other rational approximations similar to CRAM have been studied with promising results [9]. The developed burnup calculation methods can be considered as state-of-the-art. In addition, the fast Woodcock delta-tracking method used in Serpent has been studied in more detail [10]. Also other significant code

development has been conducted and several new features have been recently added to the Serpent code, such as unionized energy grid construction methods that increase the calculation speed further [11], and probability table treatment for unresolved resonance cross sections and a built-in Doppler broadening routine [12, 13]. Some of the new capabilities have been developed in collaboration with Helsinki University of Technology. The applications of the Serpent code have been various, including also many GenIV reactor concepts, out of the scope of the SAFIR2010 programme, but relevant for the Serpent development: for instance, modelling a total of 15 000 randomly dispered TRISO fuel particles inside a PBMR type fuel pebble by the Lappeenranta University of Technology with Serpent could be mentioned as an example. Related to the more conventional LWR physics, the use of the Serpent in full-core reactor physics calculations has been tested recently in a Hoogenboom-Martin simplified full-core PWR benchmark [14, 15].The simulated reactor power distribution at core mid-plane is shown in Figure 2. More information about Serpent can be found, for instance, from the doctoral dissertation of J. Leppänen [5] and from the web site http://montecarlo.vtt.fi.

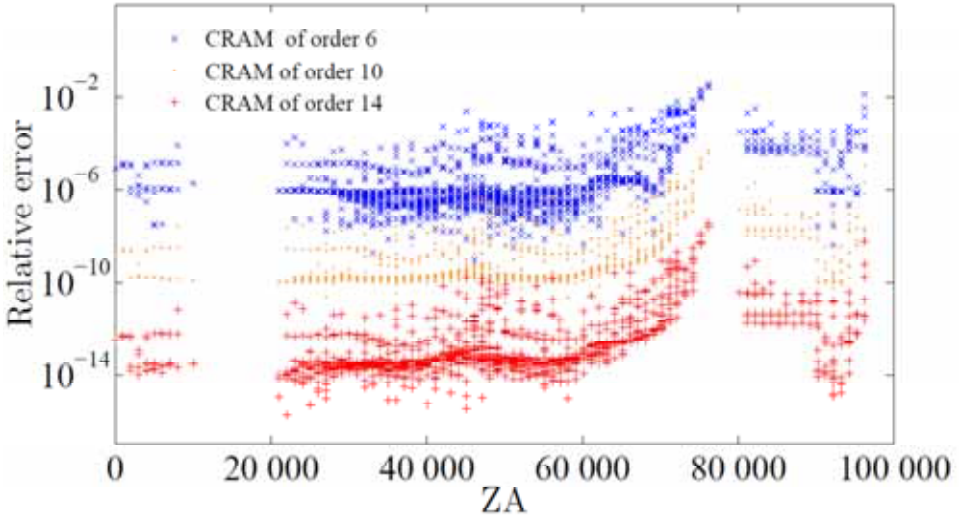

Figure 1. Relative error of CRAM applied to a burnup system with 1 532 nuclides.

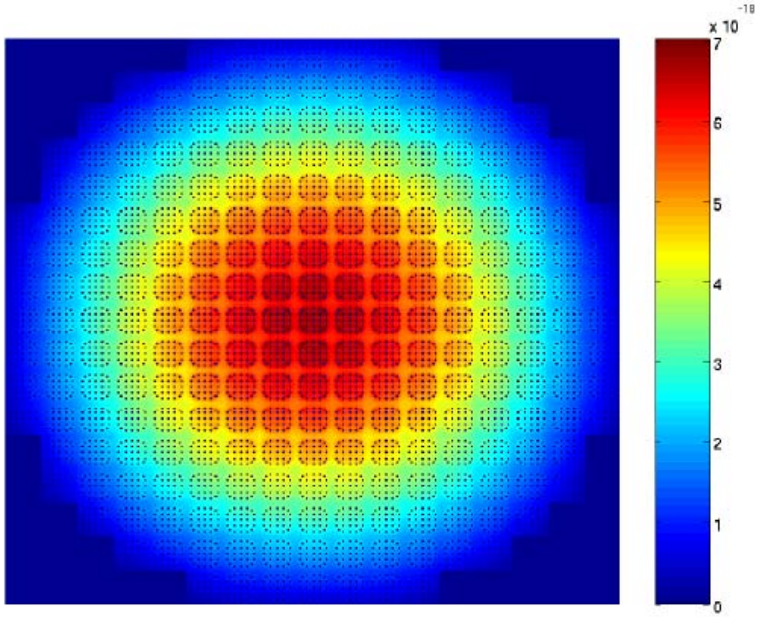

Figure 2. Reactor power distribution simulated with Serpent at core mid-plane of the Hoogenboom-Martin simplified PWR full-core benchmark [15].

During the TOPAS project also a simplified full-core reactor physics code MORA (Monte Carlo Reactor Analysis) based on the homogenized multi-group Monte Carlo method has been developed [16, 17]. For example, CROCUS reactor kinetics benchmark has been calculated with MORA [17]. The MORA code has also been used for comparison calculations in JOYO fast reactor benchmark [18] and studies of the EPR conceptual initial core. Despite some promising results, it has been seen more reasonable, however, to mainly concentrate on Serpent development.

The well-known Monte Carlo code MCNP developed in Los Alamos National Laboratory (LANL) is widely used in neutron and photon transport calculations. Latest versions of MCNP5 and MCNPX have been taken into use at VTT. F. Wasastjerna wrote a doctor's thesis in 2008 on the efficient use of MCNP in shielding calculations [19]: the performed research was related to fusion neutronics, but the studied variance reduction methods are also highly relevant in reactor physics applications. The work was performed with separate funding. In addition, several new persons have been trained to use MCNP.

In addition to the use of the Monte Carlo method also deterministic radiation transport calculation system has been maintained. This has included installation of the latest DOORS package and the BOT3P pre- and post-processing tool into VTT's linux cluster. DOORS package includes three-dimensional discrete-ordinates radiation transport code TORT developed in Oak Ridge National Laboratory (ORNL). In addition, P. Kotiluoto wrote a doctoral dissertation in 2007 on the development, validation and verification of the VTT's MultiTrans code, which uses adaptive tree multigrids and simplified spherical harmonics approximation [20]. A Linux version of the MultiTrans has also been created with some improvements to the code performance.

VTT is participating in an international consortium that will contract out radiochemical analysis of irradiated VVER-440 fuel in Dimitrovgrad. This data, when available, will be useful in verification of burnup calculation methods of isotopic concentrations [21]. For criticality safety analysis of, e.g., spent fuel storage and transportation, burnup credit (BUC) methodology has been investigated. Especially methods for coupled Monte Carlo and burnup calculations have been developed. The ABURN code [6] couples MCNP or Serpent code with isotope generation and depletion code ORIGEN2. Comparison calculations between the burnup script ABURN (coupling MCNP4C with ORIGEN2) and the two-dimensional transport theory code CASMO-4E have been made, for instance, for an EPR-type assembly [6]. Unfortunately, the developer of ABURN, Anssu Ranta-aho, resigned from VTT in 2008, and after that the ABURN development has not continued in the project.

There has been a growing interest towards uncertainty and sensitivity analysis in many fields. In reactor physics, uncertainty and sensitivity analysis is used to determine how different parameters and their associated uncertainty will affect the final computational value and its uncertainty. Traditionally, conservative models have been used, in order to ensure the nuclear safety. More realistic best estimate models could be used in the future, but this would require a reliable estimation of the associated uncertainty of the results.

In the TOPAS project, uncertainty and sensitivity analysis methods have been studied in-depth. M. Pusa has written a Master's thesis on the subject [22], and also a separate report has been written on the use of TSUNAMI code system for uncertainty and sensitivity analysis [23]. NEA has also launched an international LWR uncertainty analysis of modelling (UAM) benchmark: the benchmark has been divided into several stages. The stages concerning steady-state reactor physics uncertainty analysis have been attended. The work has included practical

realisation of the methods by making several code modifications, for instance, to the KRAM solver in CASMO, in order to allow sensitivity and uncertainty analysis based on perturbation theory. The developed methodology by M. Pusa has gained large interest from other participants of the benchmark: for instance, Paul Scherrer Institute (PSI) has requested and obtained the modified CASMO modules. In some cases, Pusa has been the only person to be able to present results in the UAM meetings, addressing not only the difficulties and challenges of the UAM benchmark, but also the high level of the work done by Pusa in this field. More profound presentation on the subject is given in a separate paper by Pusa in these proceedings.

Additional utility programmes have also been written, for instance, to transform covariance matrices of SCALE 5.1 to compatible CASMO cross section library format. Based on experience and feedback from the UAM benchmark, the developed methods represent the current state-of-the-art in reactor physics uncertainty and sensitivity analysis.

Education and international co-operation

From the educational point of view, TOPAS project has been remarkably successful. Several project members have graduated, including three doctorates [5, 19, 20] and two M.Sc. degrees [4, 22]. During 2007–2010, seven young persons (YG, ≤ 35 y) have been working for the project, including research trainees. Several training courses have been attended by the project staff, such as CMS training courses, MCNP/MCNPX workshops, Joliot&Hahn summer school, International School in Nuclear Engineering, etc. In addition, during 2009–2010 a 14 month post-doc visit of J. Leppänen to Oak Ridge National Laboratory (ORNL) in U.S.A. was arranged (partly funded from TOPAS project), related to Monte Carlo method development and offering valuable international experience.

VTT has widely participated to the OECD NEA activities, such as Nuclear Science Committee (NSC), Nuclear Development Committee (NDC), JEFF cross section project, Working Party on Nuclear Criticality Safety (WPNCS), Working Party on the Scientific Issues of Reactor Systems (WPRS), Expert Group on Uncertainty Analysis for Criticality Safety Assessment (UACSA), and LWR uncertainty analysis of modelling (UAM) benchmark and expert group. Several international conferences have been attended.

Applications

The name of the project, total reactor physics analysis system (TOPAS), is not only formulated to cohere with the research programme name, but also to reflect the need for a code system that will cover the whole range of steady-state calculations, starting from basic nuclear data, and eventually being capable to perform core analysis, criticality safety studies, activity inventory, decay heat or radiation shielding calculations, or providing starting points for transient and accident analysis. The results of the project are aimed to fulfil the present and future needs of the safety authorities and power utilities in the reactor physics in order to ensure safe and economic use of the nuclear power plants.

Conclusions

Profound knowledge related to the use of Monte Carlo method has been gained by developing an outstanding new radiation transport code Serpent which has now a wide international user community. In addition, MCNP variance reduction methods have been studied and different Monte Carlo burnup calculation methods have been developed. Especially the methods based on rational approximations to the matrix exponential in burnup calculations have been shown to be real state-of-the-art. In addition, state-of-the-art methods and tools have been developed for sensitivity and uncertainty analysis in reactor physics as well. Participation to an international LWR uncertainty analysis of modelling (UAM) benchmark has evidenced the high level of the performed work.

During the TOPAS project, three doctor's degrees and two M.Sc. degrees have been taken, and the educational objectives of the project have been well fulfilled. International co-operation has included NEA activities, such as NEA working groups and benchmark studies related to uncertainty analysis. The project personnel have had good opportunities for international networking and education by attending several international conferences, training courses, workshops, and summer schools.

References

1. Leppänen, J. PSG2 / Serpent – a Continuous-energy Monte Carlo Reactor Physics Burnup Calculation Code, User's Manual. VTT Technical Research Centre of Finland, 24 November, 2008. Available at: http://montecarlo.vtt.fi.

2. Räty, A. Covariance Data in NJOY. VTT, Espoo, 2010. VTT Research Report, VTT-R-04160-10.

3. Räty, A. On the One-Dimensional Condensation of Cross-Sections for Transient Analysis. VTT, Espoo, 2008. VTT Research Report, VTT-R-066007-08.

4. Räty, A. Homogenisation of Group Constants in Reactor Physics. Master's thesis, University of Helsinki, October 2009. 59 p.

5. Leppänen, J. Development of a New Monte Carlo Reactor Physics Code. D.Tech. Thesis, Helsinki University of Technology. VTT, Espoo, VTT Publications 640. 228 p. + app. 8 p. ISBN 978-951-38-7018-8. http://www.vtt.fi/inf/pdf/publications/2007/P640.pdf.

6. Ranta-Aho, A. Burnup calculations for an EPR-type assembly – Comparison of CASMO-4E and ABURN. In: Proceedings of the XIII Meeting on Reactor Physics Calculations in the Nordic Countries. Västerås, Sweden, 29–30 March, 2007.

7. Leppänen, J. & Pusa, M. Burnup calculation capability in the PSG2 / Serpent Monte Carlo reactor physics code. In: Proceedings of the International Conference on Mathematics, Computational Methods & Reactor Physics (M&C 2009). Saratoga Springs, New York, U.S.A., 3–7 May, 2009.

8. Pusa, M. & Leppänen, J. Computing the Matrix Exponential in Burnup Calculations. Nuclear Science and Engineering 2010, 164, pp. 140–150.

9. Pusa, M. Rational Approximations to the Matrix Exponential in Burnup Calculations. (Submitted to Nuclear Science and Engineering.)

10. Leppänen, J. Performance of Woodcock delta-tracking in lattice physics applications using the Serpent Monte Carlo reactor physics burnup calculation code. Annals of Nuclear Energy 2010, 37, pp. 715–722.

11. Leppänen, J. Two practical methods for unionized energy grid construction in continuous-energy Monte Carlo neutron transport calculation. Annals of Nuclear Energy 2009, 36, pp. 878–885.

12. Viitanen, T. & Leppänen, J. New data processing features in the Serpent Monte Carlo code. In: Proceedings of the International Conference on Nuclear Data for Science and Technology 2010. Jeju Island, Korea, 26–30 April, 2010.

13. Viitanen, T. Implementing a Doppler-Preprocessor of Cross Section Libraries in Reactor Physics Code Serpent. M.Sc.Tech. Thesis, Helsinki University of Technology. Espoo, Helsinki University of Technology, 2009.

14. Hoogenboom, J.E., Martin, W.R. & Petrovic, B. Monte Carlo Performance Benchmark for Detailed Power Density Calculation in a Full Size Reactor Core. Revision 1 (December 2009), OECD/NEA, 2009.

15. Leppänen, J. Use of the Serpent Monte Carlo Reactor Physics Code for Full-Core Calculations. In: Proceedings of the Joint International Conference on Supercomputing in Nuclear Applications and Monte Carlo 2010 (SNA + MC2010). Tokyo, Japan, 17–21 October, 2010.

16. Leppänen, J. On the feasibility of a homogenised multi-group Monte Carlo method in reactor analysis. In: Proceedings of the International Conference on the Physics of Reactors. Interlaken, Switzerland, 14–19 September, 2008.

17. Leppänen, J. On the Calculation of Reactor Time Constants Using the Monte Carlo Method. In: Proceedings of the International Youth Nuclear Congress. Interlaken, Switzerland, 20–26 September, 2008.

18. Juutilainen, P. Simulating the Behaviour of the Fast Reactor JOYO. In: Proceedings of the International Youth Nuclear Congress. Interlaken, Switzerland, 20–26 September, 2008.

19. Wasastjerna, F. Using MCNP for fusion neutronics. D.Tech. Thesis, Helsinki University of Technology. VTT, Espoo, 2008. VTT Publications 699. 68 p. + app. 136 p. ISBN 978-951-38-7129-1. http://www.vtt.fi/inf/pdf/publications/2008/P699.pdf.

20. Kotiluoto, P. Adaptive tree multigrids and simplified spherical harmonics approximation in deterministic neutral and charged particle transport. Ph.D. Thesis, University of Helsinki. VTT, Espoo, 2007. VTT Publications 639. 106 p. + app. 46 p. ISBN 978-951-38-7016-4. http://www.vtt.fi/inf/pdf/publications/2007/P639.pdf.

21. Ranta-aho, A. On the need of high quality radiochemical data. A Finnish perspective. In: ICNC 2007 – 8th international conference on nuclear criticality safety. St. Petersburg, Russia, 28 May – 5 June, 2007.

22. Pusa, M. Vaikutusalojen tarkentamiseen ja niiden epävarmuuden vaikutusten arviointiin käytetyt matemaattiset menetelmät reaktorifysiikassa. (“Mathematical methods for evaluating cross-sections and the impact of their uncertainty in reactor physics”). M.Sc.Tech. Thesis, Helsinki University of Technology. Espoo, Helsinki University of Technology, 2007. 121 p. (In Finnish.)

23. Pusa, M. Herkkyys- ja epävarmuuslaskenta TSUNAMI-ohjelmissa. VTT, Espoo, 2008. VTT Research Report VTT-R-02260-08. (In Finnish.)

10.2 Development of a sensitivity and uncertainty analysis calculation system

Maria Pusa
VTT

Abstract

This paper describes the development of a sensitivity and uncertainty (S&U) analysis calculation system for reactor physics calculations. Classical perturbation theory has been implemented within the fuel assembly code CASMO-4 to enable the computation of multiplication factor sensitivity coefficients with respect to cross-sections. In addition, a covariance library has been created and connected to the code in order to allow uncertainty analysis. The work has been carried out as a part of the international UAM benchmark.

Introduction

In recent years, the interest towards sensitivity and uncertainty S&U analysis has increased notably in nuclear engineering. In 2006, the OECD/NEA Expert Group on “Uncertainty Analysis in Modelling” decided to prepare a benchmark titled ”Uncertainty Analysis in Best-Estimate Modelling (UAM) for Design, Operation and Safety Analysis of LWRs” [1] to establish the current state and needs of S&U analysis. The idea of the benchmark is to propagate uncertainty through all stages in coupled neutronics/thermal hydraulics calculations. The inaccuracy of neutron cross-sections is one of the most significant sources of uncertainty in reactor calculations, and therefore the propagation of this uncertainty is currently the main priority. At first stage, this requires developing S&U analysis methods for reactor physics codes that are used to produce homogenized data for coupled neutronics/thermal-hydraulics calculations. The objective of the benchmark is fairly ambitious since the commonly used reactor physics codes, such as CASMO [2], HELIOS [3] and TRITON [4], do not have S&U analysis capabilities. Besides, incorporating S&U features can be quite difficult when the code is not designed from this perspective in the first place.

At VTT, the UAM benchmark was recognized as a good opportunity to get acquainted with S&U analysis. Because CASMO-4 [2] is the standard tool for lattice physics calculations at VTT, it was decided to begin developing S&U

analysis capacities to it. As a result, Classical Perturbation Theory (CPT) has now been implemented within the code to enable the computation of critical eigenvalue sensitivities with respect to cross-sections. In addition, a cross-section covariance library has been created and connected to the code to allow uncertainty analysis. This paper describes the work done in this context. Theoretical background on S&U analysis is presented and the implementation of the methods is discussed. Finally, some numerical results are presented.

Theoretical background

The purpose of sensitivity analysis is to study how sensitive a mathematical model is to perturbations in its uncertain parameters. The target of uncertainty analysis is to estimate how the uncertainty in these parameters is propagated to a response dependent on the mathematical model under consideration. In this work, the mathematical model is assumed to be the neutron transport criticality equation that can be written in operator form as:

$$\mathbf{A\Phi} = \frac{1}{k}\mathbf{B\Phi}, \tag{1}$$

where $\mathbf{\Phi} \in H_\Phi$ is the neutron flux and k is the multiplication factor. The uncertain parameters are the neutron cross-sections and they are denoted by the vector $\boldsymbol{\alpha} \in E_\alpha$ here. The response R under consideration is the eigenvalue k. Notice that it can be written in the form

$$k = \frac{\langle \mathbf{B\Phi}, \boldsymbol{\psi} \rangle}{\langle \mathbf{A\Phi}, \boldsymbol{\psi} \rangle}, \tag{2}$$

where $\boldsymbol{\psi}$ is some vector belonging to H_Φ that is not orthogonal to $\mathbf{A\Phi}$, so that $\langle \mathbf{A\Phi}, \boldsymbol{\psi} \rangle \neq 0$. The response R is hence a non-linear functional $R : H_\Phi \times E_\alpha \rightarrow \Re$.

Sensitivity analysis

In general, it is possible to define several different sensitivity measures depending on the application. When considering the criticality equation, the object is to determine the *local sensitivities*, which describe how the multiplication factor k depends on the cross-sections near the fixed point $\hat{\boldsymbol{\alpha}}$ that is their evaluated value. The natural definition for this type of sensitivity is the directional derivative in the direction of the perturbation. Since cross-sections are functions

of energy and space, the appropriate derivative is the functional derivative called the Gâteaux-variation. It follows that the sensitivity of R with respect to the perturbation $\mathbf{h} = [\mathbf{h}_\Phi, \mathbf{h}_\alpha] \in D$ at the point $\hat{\mathbf{h}} = [\hat{\mathbf{h}}_\Phi, \hat{\mathbf{h}}_\alpha] \in D$ may be defined as:

$$\delta R(\hat{\mathbf{e}}; \mathbf{h}) = \lim_{t \to 0} \frac{R(\hat{\mathbf{e}} + t\mathbf{h}) - R(\hat{\mathbf{e}})}{t} . \tag{3}$$

If sensitivity analysis is applied to the multi-group criticality equation, the Gâteaux-variations reduce to common partial derivatives with respect to the multi-group cross-sections.

When cross-sections are perturbed, the solution $\mathbf{\Phi}$ is also affected, and therefore the computation of the sensitivity $\delta R(\hat{\mathbf{e}}; \mathbf{h})$ requires that the perturbation $\mathbf{h}_\Phi$ is known. In principle, $\mathbf{h}_\Phi$ can be computed from the following *forward sensitivity system:*

$$\delta k(\hat{\mathbf{e}}; \mathbf{h})\mathbf{A}\mathbf{\Phi} + k\delta\mathbf{A}(\hat{\mathbf{e}}; \mathbf{h}) = \delta\mathbf{B}(\hat{\mathbf{e}}; \mathbf{h}) , \tag{4}$$

which can be derived by taking the Gâteaux-variation of system (1) with respect to a perturbation $\mathbf{h}$ on both sides. However, when several sensitivities are computed, this approach would require the repetitive solving of Eq. (4). Fortunately, the sensitivities can be computed more efficiently by exploiting the mathematical adjoint of Eq. (1). Classical Perturbation Theory (CPT) is an example of this kind of method.

The adjoint of Eq. (1) is defined as the system that satisfies the following relation:

$$\langle \mathbf{A}\mathbf{\Phi} + \frac{1}{k}\mathbf{B}\mathbf{\Phi}, \mathbf{\Psi} \rangle = \langle \Phi, \mathbf{A}^*\mathbf{\Psi} + \frac{1}{k}\mathbf{B}^*\mathbf{\Psi} \rangle . \tag{5}$$

The expression for the sensitivity as defined in Eq. (3) can now be written utilizing this adjoint relation. Since the operators $\mathbf{A}$ and $\mathbf{B}$ are linear with respect to $\mathbf{\Phi}$, they are also Fréchet-differentiable with respect to $\mathbf{\Phi}$, so that $\mathbf{A}'_\Phi = \mathbf{A}$ and $\mathbf{B}'_\Phi = \mathbf{B}$. Eq. (4) can thus be rewritten in the form:

$$\delta k(\hat{\mathbf{e}}; \mathbf{h})\mathbf{A}\mathbf{\Phi} + k\mathbf{A}'_\alpha(\hat{\mathbf{e}})\mathbf{h}_\alpha + k\mathbf{A}(\hat{\mathbf{e}})\mathbf{h}_\Phi = \mathbf{B}'_\alpha(\hat{\mathbf{e}})\mathbf{h}_\alpha + \mathbf{B}(\hat{\mathbf{e}})\mathbf{h}_\Phi . \tag{6}$$

For any $\mathbf{\Psi} \in H_\Phi$, not orthogonal with $\mathbf{A}\mathbf{\Phi}$ or $\mathbf{B}\mathbf{\Phi}$, it now holds:

$$\delta k(\hat{\mathbf{e}};\mathbf{h}) = \frac{\langle (k\mathbf{A}'_\alpha + \mathbf{B}'_\alpha)\mathbf{h}_\alpha, \boldsymbol{\Psi}\rangle + \langle (k\mathbf{A}+\mathbf{B})\mathbf{h}_\Phi, \boldsymbol{\Psi}\rangle}{\langle \mathbf{A}\boldsymbol{\Phi}, \boldsymbol{\Psi}\rangle}$$

$$= \frac{\langle (\mathbf{A}'_\alpha + \frac{1}{k}\mathbf{B}'_\alpha)\mathbf{h}_\alpha, \boldsymbol{\Psi}\rangle + \langle (\mathbf{A}+\frac{1}{k}\mathbf{B})\mathbf{h}_\Phi, \boldsymbol{\Psi}\rangle}{\langle \frac{1}{k^2}\mathbf{B}\boldsymbol{\Phi}, \boldsymbol{\Psi}\rangle} \tag{7}$$

$$= \frac{\langle (\mathbf{A}'_\alpha + \frac{1}{k}\mathbf{B}'_\alpha)\mathbf{h}_\alpha, \boldsymbol{\Psi}\rangle + \langle \mathbf{h}_\Phi, (\mathbf{A}^* + \frac{1}{k}\mathbf{B}^*)\boldsymbol{\Psi}\rangle}{\langle \frac{1}{k^2}\mathbf{B}\boldsymbol{\Phi}, \boldsymbol{\Psi}\rangle}.$$

If the function $\boldsymbol{\Psi}$ is chosen as the solution of the adjoint system

$$(\mathbf{A}^* + \frac{1}{k}\mathbf{B}^*)\boldsymbol{\Psi} = 0, \tag{8}$$

the response sensitivity may be computed as

$$\delta k(\hat{\mathbf{e}};\mathbf{h}) = \frac{\left\langle (\mathbf{A}'_\alpha + \frac{1}{k}\mathbf{B}'_\alpha)\mathbf{h}_\alpha, \boldsymbol{\Psi}\right\rangle}{\left\langle \frac{1}{k^2}\mathbf{B}\boldsymbol{\Phi}, \boldsymbol{\Psi}\right\rangle}. \tag{9}$$

Notice that once that adjoint solution $\boldsymbol{\Psi}$ has been obtained, the computation of the sensitivities requires only evaluating expression (9). This method is called classical perturbation theory in reactor physics.

Uncertainty analysis

The uncertainty of the cross-sections $\boldsymbol{\alpha}$ should be understood in terms of Bayesian probability interpretation. In this framework, probability is defined as a subjective measure that characterizes the plausibility of various hypotheses. When estimating parameters, all knowledge about a parameter α is assumed to be incorporated into its marginal probability distribution $p(\alpha)$. This distribution is defined so that the integral $\int_a^b p(\alpha)d\alpha$ corresponds to the Bayesian probability of the value of α belonging to the interval $[a,b]$. The distribution $p(\alpha)$ can be used to form an estimate $\hat{\alpha}$ for α. In most cases, either the mean value or mode are chosen as $\hat{\alpha}$. The spread of the distribution, on the other hand, characterizes the uncertainty related to α. Typically the

variance of the distribution is chosen to give a numerical value to this uncertainty. When several parameters are considered simultaneously, the probability distribution under consideration is their joint distribution $p(\boldsymbol{\alpha})$, and the covariance matrix of this distribution may be chosen as the descriptive statistic for the uncertainty. The uncertainty related to cross-sections is generally reported as covariance matrices.

In the Bayesian formalism, the outcome of uncertainty analysis should ideally be the posterior distribution $p(R)$ containing all the knowledge on the response R under consideration. However, since the determination of $p(R)$ is usually extremely challenging and can often only be done on a simulation basis, a common practice is to compute estimates for the mean and variance and assume the distribution $p(R)$ to be Gaussian. Usually the estimate for $\mathrm{Var}[R]$ is obtained by linearizing $R \approx \mathbf{s}\boldsymbol{\alpha}$, where $\mathbf{s} \in \mathsf{R}^{k\times 1}$, and using the identity

$$\mathrm{Var}[R] \approx \mathrm{Var}[\mathbf{s}\boldsymbol{\alpha}] = \mathbf{s}\mathrm{Cov}[\boldsymbol{\alpha}]\mathbf{s}^T \tag{10}$$

known as the *Sandwich rule*. Eq. (10) can be generalized to several responses $\mathbf{R} \in \mathsf{R}^J$ as:

$$\mathrm{Cov}[\mathbf{R}] = \mathbf{S}\mathrm{Cov}[\boldsymbol{\alpha}]\mathbf{S}^T, \tag{11}$$

where $\mathbf{S} \in \mathsf{R}^{J\times k}$. This procedure is exact, when $\mathbf{R}$ actually depends linearly on the parameters and $p(\boldsymbol{\alpha})$ is a Gaussian distribution. If $\boldsymbol{\alpha} \sim \mathrm{N}(\hat{\boldsymbol{\alpha}}, \mathrm{C}ov[\boldsymbol{\alpha}])$, it follows that $\boldsymbol{\eta} = \mathbf{c} + \mathbf{S}\boldsymbol{\alpha} \sim \mathrm{N}(\mathbf{c} + \mathbf{S}\hat{\boldsymbol{\alpha}}, \mathbf{S}\mathrm{Cov}[\boldsymbol{\alpha}]\mathbf{S}^T)$.

Implementation of sensitivity and uncertainty methods

Classical perturbation theory was implemented to CASMO-4 to enable the computation of critical eigenvalue sensitivities with respect to cross-sections. In addition, a covariance library was connected with the code to allow uncertainty analysis. The current version of the modified program (January 2011) has the capability to compute the relative nuclide-specific sensitivities and uncertainties with respect to the following parameters: total cross-section, capture cross-section, scattering cross-section, fission cross-section, fission spectrum χ, and the number of neutrons released per fission ν.

An outline of the calculation flow is shown in Figure 1. Since CASMO-4 was not originally intended for sensitivity and uncertainty analysis, the implementation of these features required modifications in several modules of the code. Outside

of the two-dimensional transport module KRAM, the cross-section routines of the code needed to be significantly modified in order to restore the nuclide-specific cross-sections with a sufficient number of energy groups for the sensitivity calculation.

The criticality equation solver in KRAM was modified to also run in adjoint mode. The multi-group criticality equation with a fixed set of directions and isotropic scattering was taken as the mathematical starting point:

$$\boldsymbol{\Omega}_m \cdot \nabla \Phi^g(\mathbf{r}, \boldsymbol{\Omega}_m) + \Sigma^g \Phi^g(\mathbf{r}, \boldsymbol{\Omega}_m)$$
$$= \frac{1}{4\pi} \sum_{h=1}^{G} \Sigma_s^{h \to g} \phi^h(\mathbf{r}) + \frac{\chi_g}{4\pi k} \sum_{h=1}^{G} \nu \Sigma_f^h \phi^h(\mathbf{r}), \; g = 1, \ldots, G. \tag{12}$$

The boundary conditions were chosen to be reflective,

$$\Phi(\mathbf{r}, \boldsymbol{\Omega}_m, E) = \Phi(\mathbf{r}, \boldsymbol{\Omega}'_m, E), \quad \mathbf{r} \in \Gamma, \; \boldsymbol{\Omega}_m \cdot \mathbf{n} < 0, \tag{13}$$

where $\boldsymbol{\Omega}_m = \boldsymbol{\Omega}_{m'} - 2(\mathbf{n} \cdot \boldsymbol{\Omega}_{m'})\mathbf{n}$ is the reflection direction. The adjoint system was formed with respect to the discretized inner product:

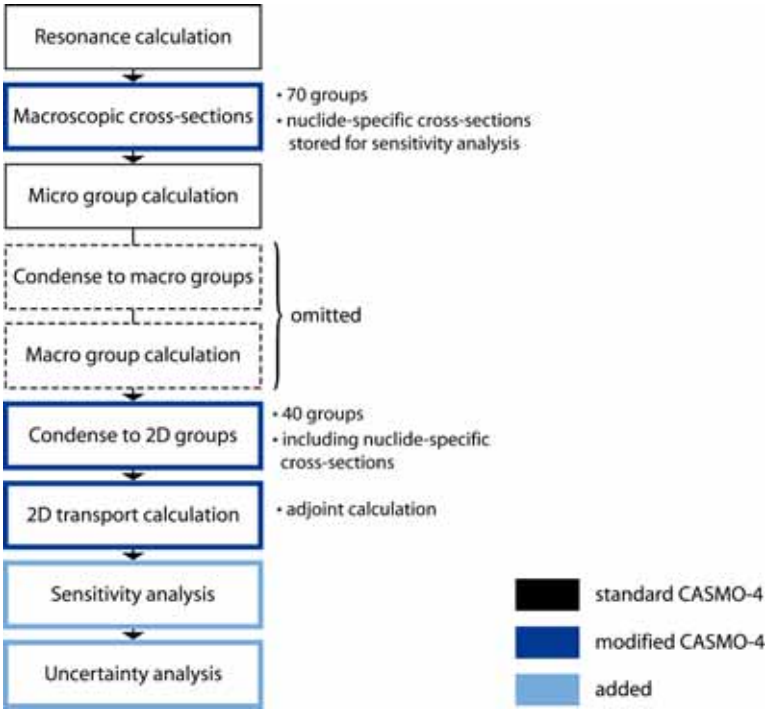

Figure 1. Outline of calculation flow.

$$\langle \mathbf{\Phi}, \mathbf{\Psi} \rangle = \sum_{g=1}^{G} \sum_{m=1}^{M} \omega_m \int_D d^3\mathbf{r} \Phi^g(\mathbf{r}, \mathbf{\Omega}_m) \Psi^g(\mathbf{r}, \mathbf{\Omega}_m) \tag{14}$$

giving the following system

$$-\mathbf{\Omega}_m \cdot \nabla \Psi^g(\mathbf{r}, \mathbf{\Omega}_m) + \Sigma^g \Psi^g(\mathbf{r}, \mathbf{\Omega}_m)$$
$$= \frac{1}{4\pi} \sum_{h=1}^{G} \Sigma_s^{g \to h} \psi^h(\mathbf{r}) + \frac{\nu \Sigma_f^g}{4\pi k} \sum_{h=1}^{G} \chi_h \psi^h(\mathbf{r}), \quad g = 1, \ldots, G \tag{15}$$

with the adjoint boundary condition:

$$\Psi(\mathbf{r}, \mathbf{\Omega}_m, E) = \Psi(\mathbf{r}, \mathbf{\Omega}_{m'}, E), \quad \mathbf{r} \in \Gamma, \mathbf{\Omega}_m \cdot \mathbf{n} > 0.$$

Because of the mathematical similarities between the forward and adjoint systems, it was possible to modify the forward solver algorithm in KRAM, so that the same module can be used to solve the forward and adjoint fluxes. Figure 2 shows an example of the two fluxes for a test case representing a PWR pin cell.

New modules were written for the computation of sensitivity and uncertainty profiles. In the sensitivity module, the sensitivity coefficients are computed according to Eq. (9) based on the systems (12) and (15) using the following discretization scheme:

$$\langle \mathbf{\Phi}, \mathbf{\Psi} \rangle \approx \sum_{i=1}^{I} \sum_{g=1}^{G} \sum_{m=1}^{M} \omega_m V_i \overline{\Phi}^{g,i,m} \overline{\Psi}^{g,i,m}, \tag{17}$$

where i denotes the mesh index. The contributions to the uncertainty in the multiplication factor k are then computed according to the Sandwich rule (10) in the uncertainty module. Examples of the sensitivity profiles for a PWR pin-cell are plotted in Figure 3.

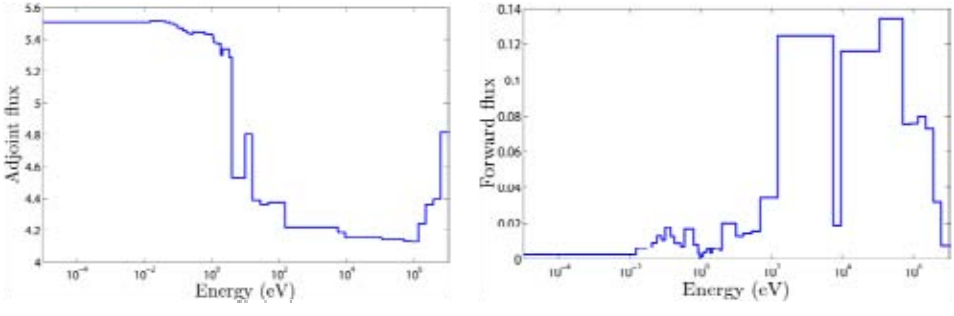

Figure 2. Forward and adjoint flux representing a PWR pin cell.

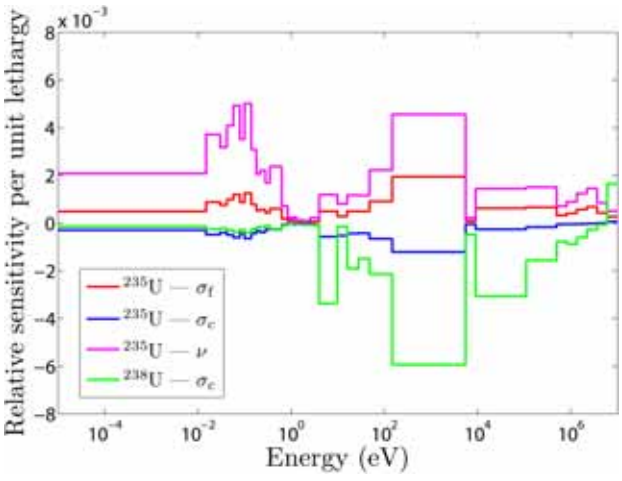

Figure 3. Sensitivity profiles for a PWR pin cell.

The sensitivity and uncertainty profiles are computed with respect to the parameters included in the cross-section model of CASMO-4. Contrary to codes intended for S&U analysis, this cross-section model contains only total capture and total scattering reactions, and the individual capture and scattering cross-section are not included in the cross-section library. It should be noted, that the sensitivities with respect to individual scattering cross-sections are not consistent with the ones computed with respect to total scattering cross-section. This is a direct consequence of the scattering source in Eq. (12) since its derivative with respect to any scattering cross-section is not generally well-defined, and can only be computed based on additional assumptions.

Processing of covariance matrices

Covariance data was taken from the SCALE-6 [4] library 44GRPCOV, which is the most comprehensive covariance library currently available. It contains relative covariance data for 401 materials and spans the full energy range of multi-group cross-section libraries. The data is given for multi-group cross-sections with 44 groups, and most of it is for individual nuclides. The library is based on true evaluations from various sources (including ENDF/B-VII, ENDF/B-VI, JENDL-3.1) and approximate covariance data. Because the covariances are given in relative terms, the library is intended to be used with all cross-section libraries, including the ones not consistent with the evaluations.

The covariance matrices were processed to become compatible with the cross-section model in CASMO-4. The main difference between the libraries is that, in CASMO, cross-sections are given for total capture and scattering reactions, whereas the covariance data is given for individual capture and scattering reactions. The cross-section model of CASMO-4 is typical for lattice physics codes that are not intended for S&U analysis, but it greatly complicates the implementation of uncertainty analysis. In this work, the covariance matrices of the various capture and scattering reactions were combined using the Sandwich rule (11). Because the relationship between the cross-sections is linear, this evokes no approximations in the Bayesian framework, if all the probability distributions are assumed to be Gaussian. This was a novel approach in this context and had not been done before.

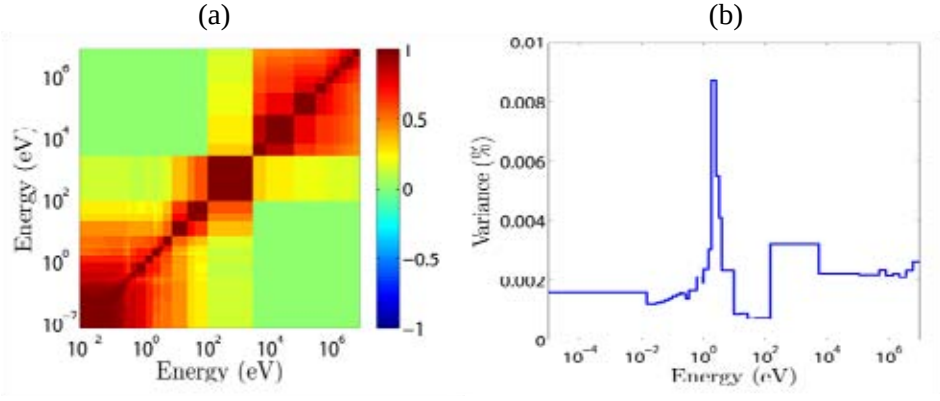

Figure 4. (a) Correlation matrix and (b) variance corresponding to fission cross-section of ^{235}U in the energy group structure of CASMO-4 fission cross-section of ^{235}U in the energy group structure of CASMO-4.

Firstly, the original COVERX-format covariance matrices were collapsed to the 40-group structure of CASMO using the code Angelo 2.3 [5] that was provided by the UAM benchmark team. The collapsing procedure in the code is based on flat flux approximation. After this, the nuclear data processing code NJOY [6] was used to transform the 40-group covariance files to BOXR format. Auxiliary FORTRAN programs were written for combining the covariance matrices. An example of the processed covariance data is shown in Figure 4, which portrays the covariance matrix of ^{235}U fission cross-section divided into components representing correlation and variance.

Numerical results

The calculation system was applied to a pin cell test problem representing TMI-1 as specified in the UAM benchmark [1]. This test problem was chosen because it can also be modeled in one dimension. Therefore the results can be compared against TSUNAMI-1D [4], which is a one-dimensional transport code intended for criticality safety analyses. With CASMO, the calculation yielded $k = 1.417$ with a relative uncertainty of $\Delta k/k = 0.512\,\%$, and using TSUNAMI-1D the values were $k = 1.415$ and $\Delta k/k = 0.489\,\%$. Table 1 shows the most significant sources of uncertainty in the computation and the corresponding sensitivity coefficients. It can be seen that the results are in very good accordance. The only notable difference in the uncertainties results from the ^{238}U scattering cross-section, which is due to the discrepancy in defining the sensitivities. Considering the notable conceptual differences between CASMO-4 and TSUNAMI-1D, the results give credence to the developed S&U analysis methodology.

Table 1. Comparison of S&U profiles for a PWR pin cell representing TMI-1.

Nuclide	Parameter pair	Sensitivity		Contribution to $\Delta k/k$ (%)	
		CASMO	TSUNAMI	CASMO	TSUNAMI
^{238}U	$\sigma_{capt} - \sigma_{capt}$	-2.603×10^{-1}	-2.215×10^{-1}	3.247×10^{-1}	2.832×10^{-1}
^{235}U	$\nu - \nu$	9.376×10^{-1}	9.390×10^{-1}	2.640×10^{-1}	2.641×10^{-1}
^{235}U	$\sigma_{capt} - \sigma_{capt}$	-1.546×10^{-1}	-1.537×10^{-1}	2.223×10^{-1}	2.095×10^{-1}
^{235}U	$\sigma_{fis} - \sigma_{capt}$	2.567×10^{-1}	2.547×10^{-1}	1.087×10^{-1}	1.040×10^{-1}
			-1.537×10^{-1}		
		-1.546×10^{-1}	-1.537×10^{-1}		
^{235}U	$\chi - \chi$	2.117×10^{-6}	7.051×10^{-9}	8.388×10^{-2}	8.839×10^{-2}
^{235}U	$\sigma_{fis} - \sigma_{fis}$	2.567×10^{-1}	2.547×10^{-1}	7.860×10^{-2}	7.674×10^{-2}
^{238}U	$\sigma_{scat} - \sigma_{scat}$	-5.893×10^{-3}	-6.220×10^{-1}	7.567×10^{-2}	1.076×10^{-1}
^{238}U	$\nu - \nu$	6.226×10^{-2}	6.093×10^{-2}	7.243×10^{-2}	7.142×10^{-2}

Summary and conclusions

Classical perturbation theory was implemented to CASMO-4 in order to enable the computation of multiplication factor sensitivity coefficients with respect to cross-sections. In addition, a covariance library was created and connected with the code to allow uncertainty analysis. Numerical results were presented and compared against TSUNAMI-1D for a pin-cell test problem representing a PWR. The results and the experience gained during the benchmark give credence to the developed methodology. If the project will be decided to be continued, the next step will be the implementation of generalized perturbation theory into the calculation system. This would allow computing S&U profiles for other quantities besides the multiplication factor.

References

1. Ivanov, K. et al. Benchmark for Uncertainty Analysis in Modeling (UAM) for Design, Operation, and Safety Analysis of LWRs. NEA/NSC/DOC(2007)23, NEA, 2007.

2. Rhodes, J. et al. CASMO-4 Users Manual. SSP-01/400, Studsvik Scandpower, 2004.

3. Helios Methods. Studsvik Scandpower, 2000.

4. Gauld, I.C. et al. SCALE: A Modular Code System for Performing Standardized Computer Analyses for Licensing Evaluations. Version 6.0, Vols. I-III, ORNL/TM-2005/39, Oak Ridge National Library, 2009.

5. Kodeli, I. Manual for ANGELO2 and LAMBDA codes. NEA-1798/03, NEA, 2010.

6. MacFarlane, R.E. et al. The NJOY Nuclear Data Processing System. Manual, Version 91, LA-12740-M, Los Alamos National Laboratory, 1994.

11. Numerical Modeling of Condensation Pool (NUMPOOL)

Timo Pättikangas, Jarto Niemi and Antti Timperi
VTT

Abstract

The behaviour of a pressure suppression containment of a BWR is studied by performing CFD and Fluid-Structure Interaction (FSI) calculations. Experiments performed at the Lappeenranta University of Technology with the PPOOLEX facility are modelled. PPOOLEX is a scaled-down two-compartment model of a pressure suppression containment of a BWR. In the experiments, vapour is blown into the drywell compartment. When the pressure increases, the mixture of air and vapour flows through the vent pipe into the water pool of the wetwell compartment. Two-phase CFD simulation of an experiment has been performed by using the FLUENT code.

Large, rapidly condensing steam bubbles may cause severe loads on the pool structures. The bubble collapse and the resulting pressure loads are first analyzed analytically and numerically by using simplified assumptions. The obtained pressure source is then used for preliminary analysis of the bubble collapse in a realistic BWR containment. Calculations of the BWR containment are performed by using an acoustic-structural FEM model with FSI coupling.

Introduction

In boiling water reactors (BWR), the major function of the containment system is to protect the environment if a loss-of-coolant accident (LOCA) should occur. The containment is designed to accommodate the loads generated in hypothetical

accidents, such as sudden rupture of a main steam line. In such an accident, a large amount of steam is suddenly released in the containment. An essential part of the pressure suppression containment is a water pool, where condensation of released steam occurs.

In a BWR, the pressure suppression containment typically consists of a drywell and a wetwell with a water pool. In a hypothetical LOCA, steam and air flow from the drywell through vent pipes to the wetwell, where the outlets of the vent pipes are submerged in the water pool. First, mainly non-condensable air or nitrogen flows through the vent pipes into the wetwell. Then, the volume fraction of vapour increases in the gas mixture. When all the non-condensable gas from the drywell has been blown into the wetwell, the blowdown consists of pure vapour. The pressure suppression pool changes this large volume of vapour to a small volume of liquid water [1].

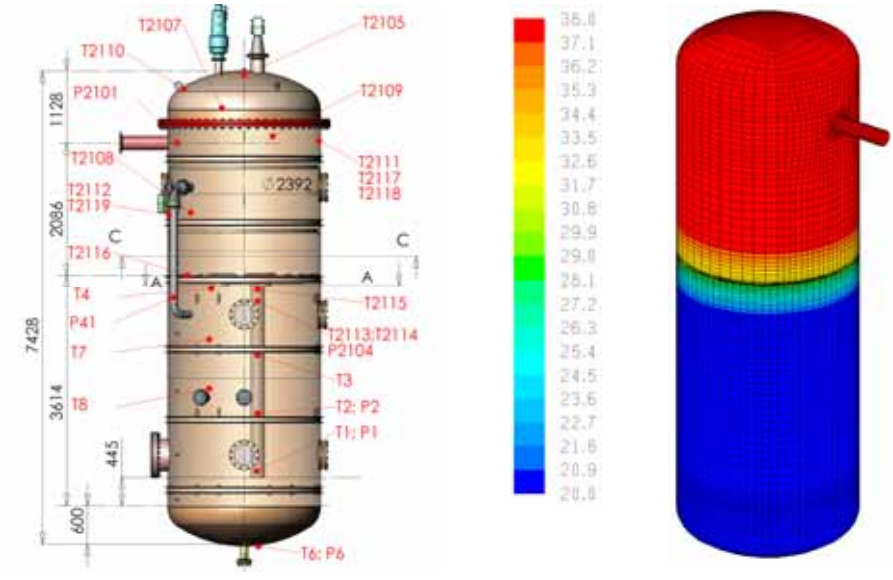

Figure 1. Pressure (Pn) and temperature (Tn) measurements in the PPOOLEX pressurized test facility at Lappeenranta University of Technology [2]. On the right, the surface mesh of the CFD model and the outer wall temperature (°C) at time t = 0 are shown.

The PPOOLEX facility [2] is a scaled-down model of a pressure suppression containment of a BWR. The pressurized PPOOLEX vessel shown in Figure 1 consists of a drywell compartment and a wetwell compartment with a water

pool. The compartments are connected with a vent pipe, whose outlet is submerged in the water pool in the wetwell.

In the PPOOLEX experiment WLL-05-02 [3], vapour was blown into the preheated drywell of the facility. The vapour jet hit the opposite wall of the drywell, where wall condensation occurred. The temperature of the walls of the drywell rose and heat was conducted through uninsulated walls to the ambient laboratory. When the pressure in the drywell increased, the mixture of air and vapour started flowing through the vent pipe into the water pool of the wetwell. In the water pool, direct-contact condensation of vapour occurred. CFD modelling of this experiment will be discussed below.

Large, rapidly condensing steam bubbles at the outlet of the vent pipe may cause severe pressure loads on the pool structures. These loads occur usually when pure or nearly pure steam is blown into the water pool at relatively low velocity [1, 5]. The first phase of the collapse induces a slight under-pressure on the walls. In the final phase, water velocity near the bubble increases to a high value and then decelerates rapidly, which creates a water-hammer propagating at the speed of sound. In this work, the bubble collapse and the resulting loads are first studied analytically and numerically. The obtained pressure source is then used for analyzing the structural effects in a realistic BWR containment by using an acoustic-structural Finite Element Method (FEM) model with two-way Fluid-Structure Interaction (FSI) coupling.

CFD modeling of vapour discharges in PPOOLEX experiments

POOLEX condensation experiments

PPOOLEX is a pressurized cylindrical vessel with a height of 7.45 meters and a diameter of 2.4 meters. The DN200 vent pipe is positioned in a non-axisymmetric location 300 mm away from the centre of the facility. The water level in the beginning of the experiments was 2.14 m from the bottom of the pool. The submergence depth of the vent pipe was 1.05 m. The PPOOLEX facility is shown in Figure 1.

In the experiments, the drywell compartment was initially filled with air at atmospheric pressure. Preheating of the wall segments was executed with vapour. After preheating, the test vessel was shortly ventilated to dry the wall surfaces and to clear the viewing windows. In the experiments, pure vapour was blown into the drywell through the horizontal DN200 pipe. For details on the experiments, see Refs [2] and [3].

Three different condensation phenomena occur in the experiments. First, some bulk condensation of vapour may occur, when vapour flows from the inlet plenum into the drywell. Second, part of the vapour is condensed on the walls of the drywell. The wall condensation is determined by the initial wall temperature in the drywell and by the heat transfer through the uninsulated walls of the drywell to the laboratory. Third, direct-contact condensation occurs in the water pool of the wetwell.

CFD modelling of the experiment WLL-05-02

The CFD mesh of the PPOOLEX facility consists of 135 000 hexahedral grid cells. The surface mesh is shown in Figure 1. The Euler-Euler two-phase model of the FLUENT version 6.3 was used, where the models for bulk, wall and direct-contact condensation were implemented as user-defined functions [3].

In the PPOOLEX experiment WLL-05-02, vapour was blown into the preheated drywell compartment of the facility. The initial temperature of the drywell was about 65°C, and the initial temperature of the water pool in the wetwell was about 20°C. The initial mole fraction of vapour in the gas phase was y_{steam} = 0.01. Temperature of the ambient laboratory was 25°C.

In the experiment, the gas jet was injected into the drywell through the inlet plenum. In the CFD calculation, the gas was assumed to be almost pure vapour containing a mass fraction of one percent of air. The maximum mass flow rate was 0.54 kg/s, and the vapour temperature in the inlet plenum was about 140°C. The mass flow rate into the drywell is shown in Figure 2.

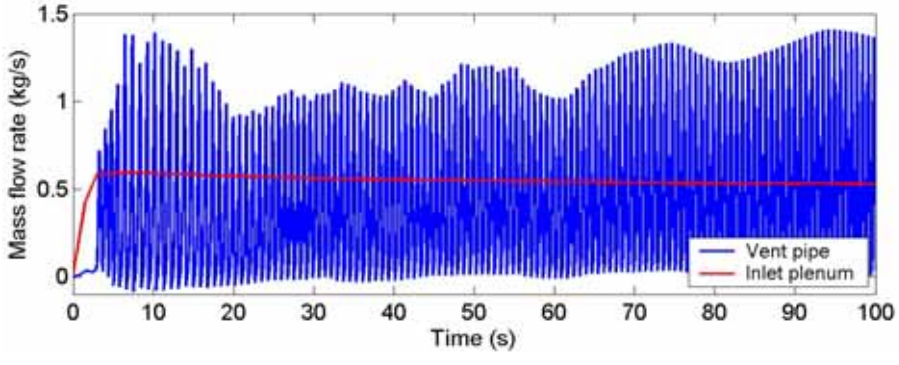

Figure 2. Mass flow rate into the drywell (red line) and through the vent pipe (blue line).

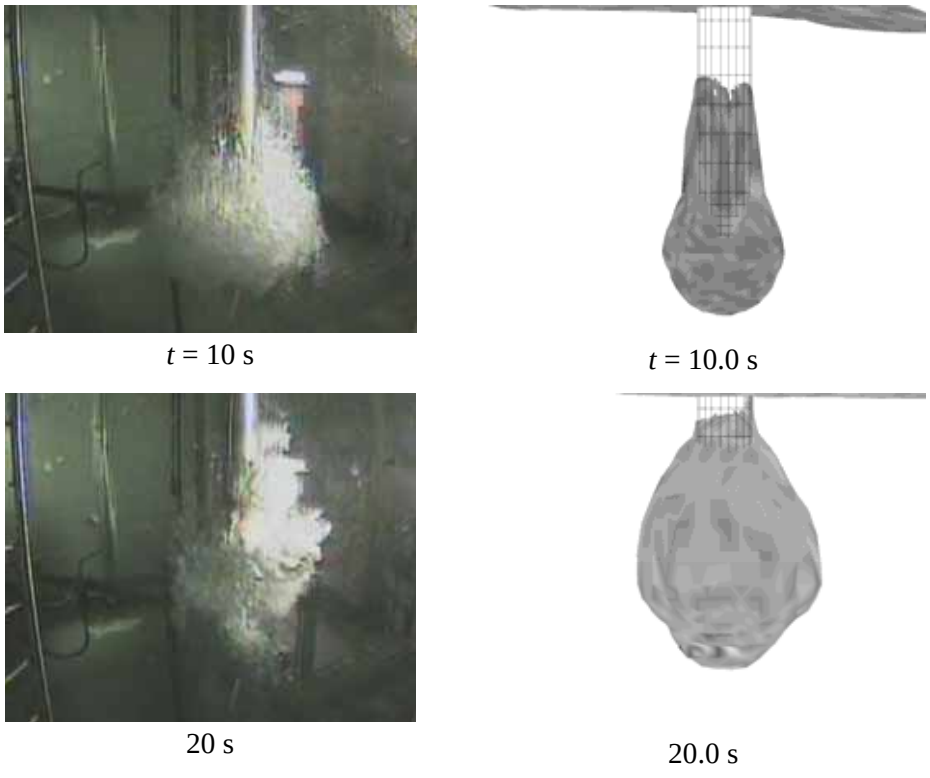

Figure 3. Photographs of gas bubbles in the water pool during the experiment WLL-05-02 [3]. On the right, iso-surfaces of void fraction in the CFD simulation are shown (α = 0.1).

When the pressure in the drywell increases, the water plug in the vent pipe starts moving downwards. The vent pipe is cleared at time t = 3 s and the first bubble is formed at the outlet of the vent pipe in the water pool. After this, new bubbles are formed with a period of about 0.72 s. The periodic formation of bubbles can be clearly seen in the sinusoidal mass flow rate through the vent pipe that is shown in Figure 2. When bubbles are detached from the vent outlet, the mass flow rate in the vent pipe becomes for awhile almost zero or is even reversed. In Figure 3, shapes of gas bubbles at the vent outlet are shown at two instants of time.

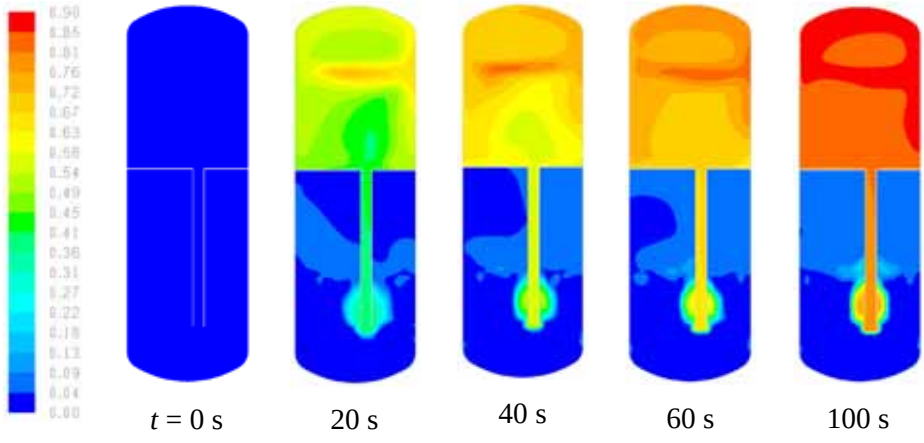

Figure 4. Mole fraction of vapour at different instants of time.

In Figure 4, the mole fraction of vapour in the gas phase is shown. The mole fraction of vapour increases rapidly from its initial value of one percent, and at time $t = 100$ s it is about 90% in the drywell. At this time, the gas flowing through the vent pipe into the water pool contains almost 80% of vapour. Strong condensation of vapour occurs on the walls of the drywell and vent pipe, which is submerged in cold water.

In the experiment, wall condensation in the drywell is studied by collecting condensate from the wall with a gutter system. The cumulative amount of condensate on the back wall, where the vapour jet hits first, is collected from a wall area of 5.25 m^2. The condensate from the front wall, where the inlet plenum is located, is also collected from a wall area of 5.25 m^2. The flow of condensate through the gutter system to the tanks causes a delay of about 25 s in the experiment.

The calculated results are compared to the measurements in Figure 5, where the cumulative amount of condensate is shown. On the back wall, the condensation is slightly overestimated by the CFD calculation. On the front wall, the condensation is clearly underestimated by the calculation. In the total amount of condensation, the errors partly cancel each other. The calculated total amount of condensation is about 10% smaller than the measured value.

In Figure 6, the calculated temperatures are compared to measurements at a few points in the wetwell. In the wetwell, the temperature of the gas space is stratified already in the beginning of the experiment. The measurements show that the stratified condition persists all the time during the experiment. In the

calculation, more mixing occurs and stratification is weaker. The calculated temperature at the top of the wetwell drops already in the beginning of the calculation and differs from the measurement.

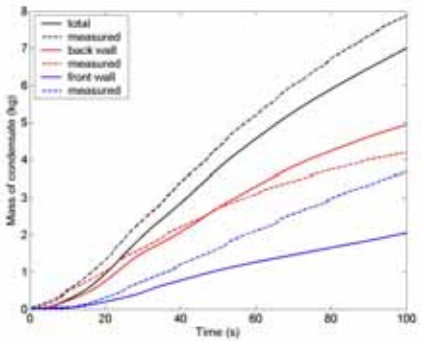

Figure 5. The cumulative mass of condensate.

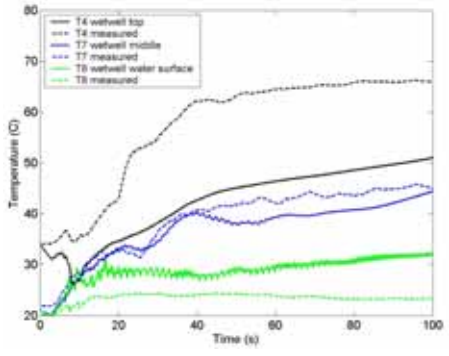

Figure 6. Calculated and measured temperatures in the wetwell.

Fluid–structure interaction

Pressure source due to a collapsing steam bubble

The collapse of a steam bubble and the resulting pressure loads were first modeled analytically by using the potential flow theory in a spherically symmetric case. For a point source in infinite region of fluid, pressure field far away from the bubble is found to be for incompressible flow

$$p(r) - p_\infty = \frac{\rho \ddot{V}}{4\pi r}$$

where p_∞ is the ambient pressure, r is the radial coordinate and ρ is the fluid density. The pressure is proportional to the volume acceleration $\ddot{V}$, i.e., the second time-derivative of the bubble volume: $\ddot{V} = 4\pi(R^2\ddot{R} + 2R\dot{R}^2)$, where R is the bubble radius. The volume acceleration consists of the "acceleration term" and of the "velocity term". The acceleration term is responsible of the pressure rise due to flow velocity deceleration at the end of the collapse. However, the largest pressure peak results from the velocity term.

For modelling the bubble collapse, the simplest case, i.e., a bubble having constant pressure in incompressible fluid [4], was first considered. From the so-called Rayleigh equation of motion for the bubble radius, the radius, surface

velocity and surface acceleration can be solved. With the simplified assumptions, the surface velocity and acceleration grow infinite as the bubble radius shrinks to zero. In reality, the fluid compressibility starts to affect the solution roughly when the Mach number becomes larger than 0.3. Also, in reality the small amount of non-condensable gas in the steam starts to limit the bubble shrinking in the late phase of the collapse.

In order to obtain more realistic results, the case where the bubble has some amount of non-condensable gas was also considered. Then, the pressure inside the bubble increases as it gets smaller. It is assumed that all steam has condensed instantaneously leaving only a small amount of non-condensable gas in the bubble. In experiments [5], even small amounts of air among the steam have suppressed the water-hammer loads. The damping of the pressure pulses was quite strong even with mass fractions of 1%. Therefore, we consider situations where the mass fraction of air is in the range of 0–1%. Assuming total pressure of 1 bar, this corresponds to partial pressures of air in the range of 0–623 Pa. Starting from an energy balance principle, the bubble radius, surface velocity and surface acceleration can be determined numerically.

The bubble collapse was also modeled with Abaqus by using stress-displacement elements and fluid equation of states for gas and water. The ideal gas law was employed for gas and the linear U_s - U_p model for water. Explicit time integration was used and the runs were geometrically non-linear with an adaptive mesh to account for the large displacements that occur near the bubble. Spherical symmetry was assumed so that the model was a narrow slice consisting of a single layer of three-dimensional elements.

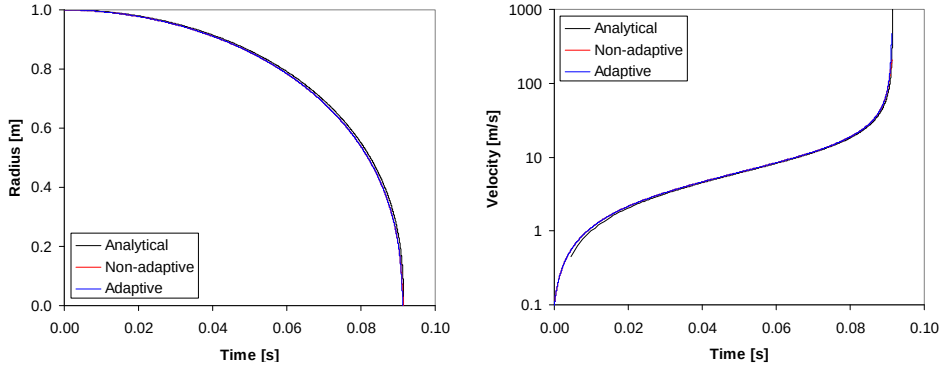

Figure 7. Bubble radius and surface velocity with constant bubble pressure. Difference between the ambient and bubble pressure is 1 bar.

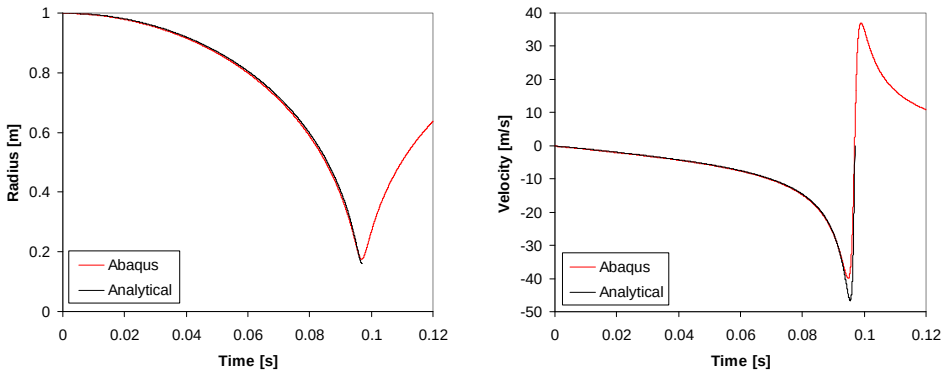

Figure 8. Bubble radius and surface velocity for an ideal gas bubble. The initial bubble pressure is 5 000 Pa and the ambient pressure is 1 bar.

The FEM solutions are first compared with the analytical one in Figure 7 for the case of constant bubble pressure. It is seen that the FEM solutions correspond quite well to the analytical one. Without mesh adaptation, the calculation is accurate except for the very late phase, where the first water element adjacent to the bubble becomes overly stretched. The finite speed of sound in the FEM solutions starts to limit the bubble surface velocity in the late phase whereas in the analytical solution the velocity grows without bounds. Results for the case where the bubble pressure is determined from the ideal gas law are shown in Figure 8.

Modeling of a sector of a BWR containment

A 22.5° sector of a realistic BWR containment including one vent pipe was modeled. For concrete, material properties $E = 39$ GPa, $\nu = 0.17$ and $\rho = 2\,400$ kg/m^3 were used for elastic modulus, Poisson's ratio and density, respectively. The damping ratio was set to 5% for the concrete [6]. The Rayleigh damping was used and this damping ratio was adjusted to be exact for frequencies 10 Hz and 150 Hz, which cover the frequency range of interest. For water, values $K = 2.224$ GPa and $\rho = 1000$ kg/m^3 were used for bulk modulus and density, respectively. For modelling the pressure load, a large bubble was considered with diameter 2.4 m and with initial pressure of 500 Pa. The resulting volume acceleration, obtained with Abaqus as described above, is shown in Figure 9.

The acoustic pressure is shown at the mid-plane of the BWR wetwell in Figure 9. The volume acceleration obtains its peak value at about $t = 17$ ms, after

which a spherical high-amplitude pressure wave starts to propagate towards the walls. The pressure wave reaches the walls in about 2 ms, after which reflections of the wave can be seen. Here also the wall motion of the containment affects the pressure field due to the FSI coupling. Deformations and stresses in the containment are shown in Figure 10. The pressure wave makes the lower part of the containment walls to bulge which causes high tensile stresses in the outer wall and high compressive stresses in the inner wall.

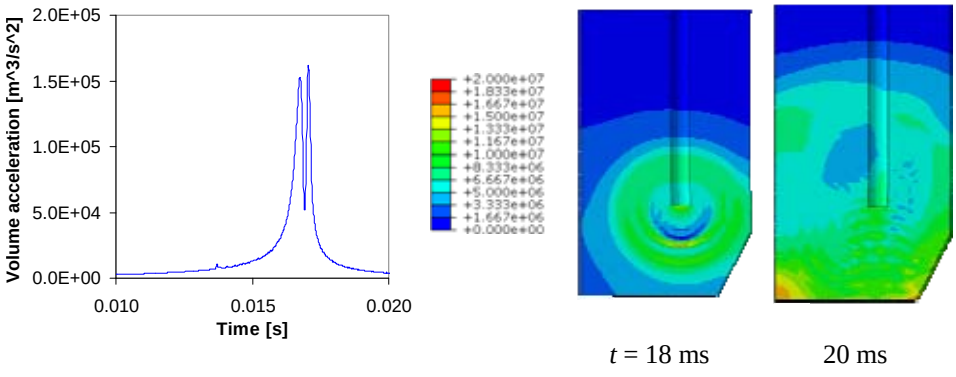

Figure 9. Volume acceleration at the pipe outlet and acoustic pressure [Pa] at the mid-plane of the BWR containment.

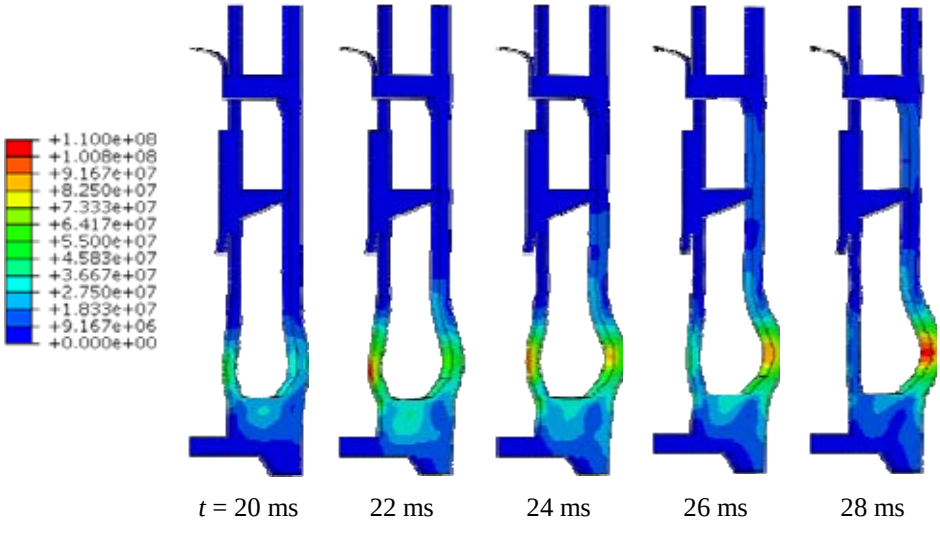

Figure 10. Deformation multiplied by 100 and von Mises stress [Pa] in the BWR containment.

Summary and discussion

CFD simulations have been performed for an experiment performed by Puustinen and Laine et al. [2, 3] with the PPOOLEX test facility, which is a scaled-down model of a BWR pressure suppression containment. Models for wall condensation and direct-contact condensation have been implemented in the FLUENT code. The models have been tested against the PPOOLEX experiment WLL-05-02.

Comparison of the wall condensation model to the experiment was complicated by the uninsulated wall of the drywell of PPOOLEX. When the wall structures have been heated by the hot vapour, the wall condensation is determined by the heat transfer from the outer wall of the drywell to the ambient laboratory. In the CFD model, the chosen heat transfer coefficient on the outer wall determines the amount of condensation. In the calculation, this also affects the pressure level inside the drywell and wetwell.

In modelling the direct-contact condensation, the challenges are in the estimation of the interfacial surface area and the heat transfer coefficient. The heat transfer and condensation in the present calculation was found to be too weak. Some vapour was able to escape from the water pool to the gas space of the wetwell. An additional challenge is presented by modelling the interfacial drag in the different regions. In the drywell, some mist is formed by the bulk condensation. In the water pool, at the outlet of the vent pipe a large bubble is formed. In addition, small air bubbles are carried away by the flow in the water pool. More work is needed in order to find suitable modelling techniques for these phenomena.

The collapse of a steam bubble results in volume acceleration, which induces pressure loads on the pool walls. As the amount of air in the bubble is decreased, the peak pressure increases. However, when the water compressibility is accounted for, the finite speed of sound becomes a limiting factor. The pressure load and stresses became high in preliminary calculations of a BWR containment, but some of the assumptions were crude and conservative. An instantaneous steam condensation was assumed, whereas in reality the condensation rate is finite. This may have a particularly large effect in the important final phase of the collapse, where the water velocity is large and the surface area of the bubble is small. Also, an infinite fluid was assumed in the calculation of the bubble collapse, but in reality the finite size of the pool hinders the collapse somewhat.

In the experiments, the bubbles have had a toroidal shape rather than spherical due to the presence of the vent pipe. It remains to be shown by detailed CFD calculations of the bubble collapse whether the torus-shaped bubble yields a smaller or larger pressure load. Although crude assumptions were needed in these calculations, they may prove useful in validating more realistic CFD calculations in future.

Acknowledgement

The authors are grateful to Mr. Markku Puustinen and Mr. Jani Laine from the CONDEX project of the SAFIR2010 Programme for providing the data from their PPOOLEX experiments.

References

1. Lahey, R.T. & Moody, F.J. The thermal hydraulics of a boiling water nuclear reactor. 2nd Edition, American Nuclear Society, 1993.

2. Puustinen, M., Laine, J., Räsänen, A. & Purhonen, H. PPOOLEX wall condensation experiments. Technical Research Centre of Finland, Espoo, 2009. VTT Research Notes 2466. Pp. 228–236.

3. Pättikangas, T.J.H., Niemi, J., Laine, J., Puustinen, M. & Purhonen, H. CFD modelling of condensation of vapour in the pressurized PPOOLEX facility. CFD for Nuclear Reactor Safety Applications (CFD4NRS-3) Workshop, Bethesda, MD, USA, 14–16 September 2010. 12 p.

4. Moody, F.J. Introduction to unsteady thermofluid mechanics. Wiley, New York, 1990.

5. Puustinen, M. Combined effects experiments with the condensation pool test facility." Lappeenranta University of Technology, Nuclear Safety Research Unit, 2006. Research report POOLEX 1/2006. 30 p. + app. 6 p.

6. U.S. Nuclear Regulatory Commission. Damping values for seismic design of nuclear power plants. Regulatory Guide 1.61, 2007.

12. Improved Thermal Hydraulic Analysis of Nuclear Reactor and Containment (THARE)

12.1 THARE summary report

Ismo Karppinen, Seppo Hillberg, Pasi Inkinen, Sampsa Lauerma, Juha Luukka, Joona Kurki, Ari Silde and Risto Huhtanen
VTT

Abstract

Calculation methods for evaluating safety of nuclear power plants has been enhanced by developing and validating both thermal hydraulic system codes APROS and TRACE and models in CFD code Fluent. Several experiments in national and international research programs have been calculated and results have compared with measured data. The validation cases has been chosen according the safety relevance of the studied phenomena and taking in account the specific features of the new plant concepts offered to Finnish utilities.

Introduction

The project is divided in three tasks, 1) validation of thermal hydraulic system analysis codes APROS and TRACE, 2) enhancements of containment thermal hydraulic analysis methods and 3) participation in the international research programs.

Main objectives

The main objectives of the project are to develop and validate calculation methods for safety evaluation of nuclear power plants. Both thermal hydraulic

system analysis codes and CFD calculations are used in the analysis and their usability is studied and enhanced. An important objective is also to train new thermal hydraulic code users and educate young experts.

Validation of system analysis codes

The thermal hydraulic system analysis codes APROS and TRACE were validated with experimental data from Lappeenranta University and OECD research programs. Thermal hydraulic system analysis codes, like APROS and TRACE, rely largely on experimental correlations. When the codes are used in conditions beyond experimental data or applied in new problems the usability of the correlations and models has to be studied. Furthermore new features in the codes and increased computer performance allow more detailed modelling. Therefore continuous validation of codes is needed. In addition code validation gives an excellent opportunity for young scientist to international co-operation.

The PWR-PACTEL research program was first supported by calculating the planned experiments with APROS reference plant model to analyze the scenario in the scale of the real power plant. The PWR-PACTEL benchmark was calculated with the model of the test facility using APROS code (Figure 1). The results of the benchmark are not yet available. The calculated PWR-PACTEL experiments are listed in Table 1.

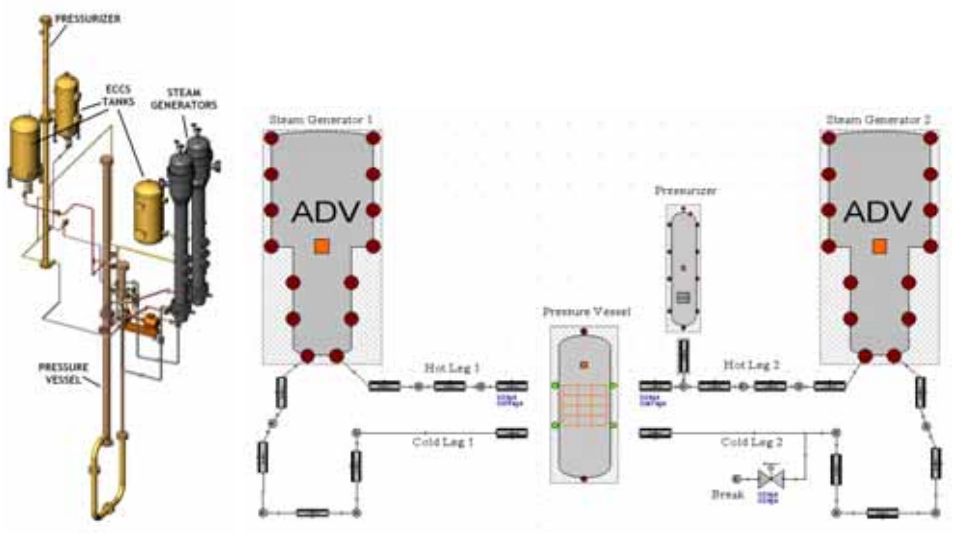

Figure 1. PWR-PACTEL test facility and APROS model.

Table 1. Calculated PWR-PACTEL experiments.

Planned experiment	**Scenario**	**Code**
PWR-PACTEL SIR	Stepped inventory reduction	APROS with reference plant model [1]
PWR-PACTEL LOF	Loss of feed water	APROS with reference plant model [2]
PWR-PACTEL SBL-50	Natural circulation in SBLOCA	APROS with reference plant model [3]
Experiment		
PWR-PACTEL benchmark	Natural circulation with inventory reduction	APROS

The ROSA/LSTF (Rig of Safety Assessment / Large Scale Testing Facility) is a full-height and 1/48 volumetrically-scaled system simulating a Westinghouse-type 3 423 MWth PWR located in Japan. The OECD/ROSA research program studied several safety significant accident scenarios [4]. Primärkreislauf-Versuchsanlage (primary coolant loop test facility) PKL is a model of German KWU 1 300 MW pressurized water reactor with 1:1 elevation scale and 1:145 volumetric scale. OECD/PKL research program studied boron dilution accidents and loss of residual heat removal in mid-loop operation (during shutdown conditions) [5]. Selected experiments of those research programs were used for APROS and TRACE validation (Table 2).

Table 2. Code validation with OECD and IVO experiments.

Experiment	**Scenario**	**Code**
PSB-VVER	Large Break LOCA	APROS [6, 7, 8]
ROSA Test 3-1	SBLOCA without scram	APROS [9]
ROSA Test 5-1	SBLOCA with SG depressurization	APROS [10] TRACE [11]
ROSA Test 6-2	0.1 % SBLOCA, pressure vessel bottom	APROS [12]
PKL Test E3.1	Failure of residual heat removal system during mid-loop operation	APROS [13]
ROCOM test 1	Simulated temperature distribution in steam line break.	APROS 3D module TRACE 3D vessel [14]
IVO CCFL test	Counter current flow in VVER-440 fuel channel	APROS [15, 16]
ISP-12	5% SBLOCA in BWR recirculation line in ROSA-III test facility	APROS [17]
ISP-50	Break of direct vessel injection line in ATLAS test facility (APR1400)	APROS [18]

International standard problems (ISP) are important code and code users benchmarking exercises were participants has to model an accident scenario without a prior information of the results (blind) or even without previous experience of modelling the test facility (double blind). The ISP-50 was organized in a new ATLAS test facility, which is a scaled model of Korean APR-1400 reactor. The ISP was for us as for most other participant a double blind exercise. The APROS model is presented in Figure 2. The test results and all calculations will be published in an OECD report.

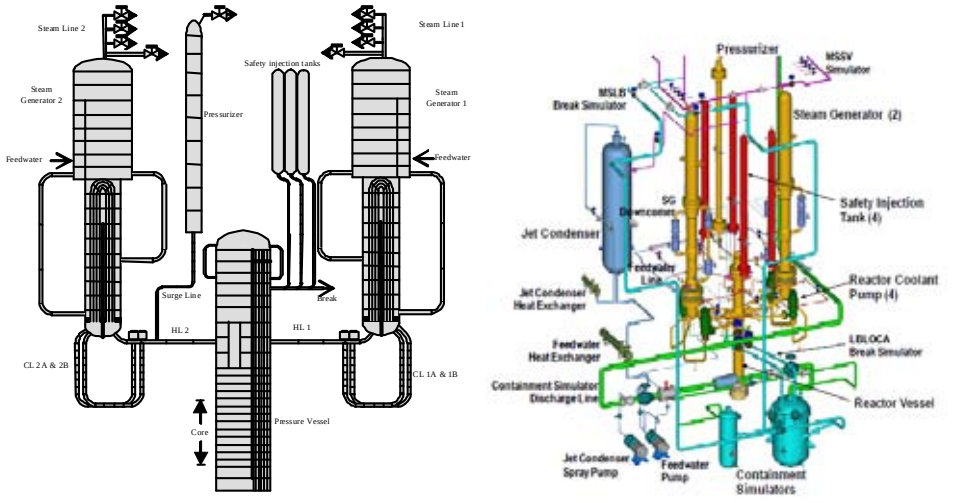

Figure 2. APROS nodalisation and ATLAS test facility.

ROCOM is a test facility simulating a KONVOI type PWR. The test 1 simulates a pseudo-steady-state of test PKL III G 3.1 at 609 s, when cold water from the loop with broken steam line flows to downcomer (minimum temperature at 609 s.). From safety point of view, the most important aspect of the test is to observe the mixing of the injected water before it enters the core region. Most of the mixing presumably occurs in the downcomer region, therefore the temperature distribution in downcomer is analyzed in more detail. Even though CFD codes are usually utilized for this kind of analysis, limited 3D simulation capabilities are included in system codes making it viable to study mixing with a full system model. However the validity of system codes for such simulations has to be assessed.

The APROS model was created using APROS 3D flow model. The model consists of homogeneous fluid model complemented with a k-epsilon turbulence model [14]. The TRACE model was created using TRACE VESSEL component. The most important difference to APROS 3D flow model is that the VESSEL component has no model for turbulence simulation.

ROCOM test 1 was calculated using both APROS and TRACE. Different nodalisation schemes were tested with both codes to obtain data on the required level of detail for simulating the downcomer temperature distribution properly. Overall, the test was adequately reproduced by both codes. Measured data and example simulation runs with both codes are presented in Figure 3. As seen in the figure, mixing was observed in the downcomer region up to almost homogeneous distribution in the lower downcomer, as in the experiment. However,

the rate of mixing was somewhat different from the experiment. More specifically, the rapid temperature homogenization in upper downcomer as observed in the experiment was not reproduced precisely. In both APROS and TRACE calculations, the mixing began higher in the downcomer and occurred more gradually than in the measured data.

Further testing should be performed to obtain more information on the suitability of both APROS and TRACE for analysing coolant mixing in the pressure vessel downcomer region. Especially a test with less mixing in the downcomer would yield more knowledge of the accuracy of APROS and TRACE 3D fluid simulation models.

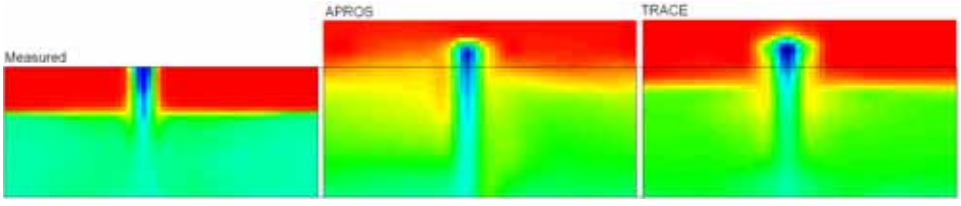

Figure 3. Experimental and measured temperature distribution in ROCOM test.

Containment thermal hydraulics

Calculation methods, with both lumped parameter and CFD codes, have been developed by calculating selected experiments. POOLEX and PPOOLEX experiments (CONDEX project) were chosen to test APROS containment capabilities to model suppression pool containment. The POOLEX STB-21, PPOOLEX STR09 and PPOOLEX STR-11 experiments studied temperature stratification and mixing in the wet well. In the experiment steam was blown to the water pool through a blowdown pipe. Small steam flowrate resulted in stratified pool and higher flow rate mixed the pool. The STB-21 experiment was modelled with a very simple nodalisation, only one node for the water pool and two for the environment. Simple user definable steam velocity criteria for stratification and mixing were added in the code to predict stratification. In some experiments this approach gave good results and it was possible to reproduce the stratification and mixing measured in the experiment. Interpretation of the latest experiments is still going on, but it looks like the steam velocity in the blowdown pipe cannot alone define stratification and mixing in all the experiments and further model development is foreseen in co-operation with KTH/Stockholm in NORTHNET framework.

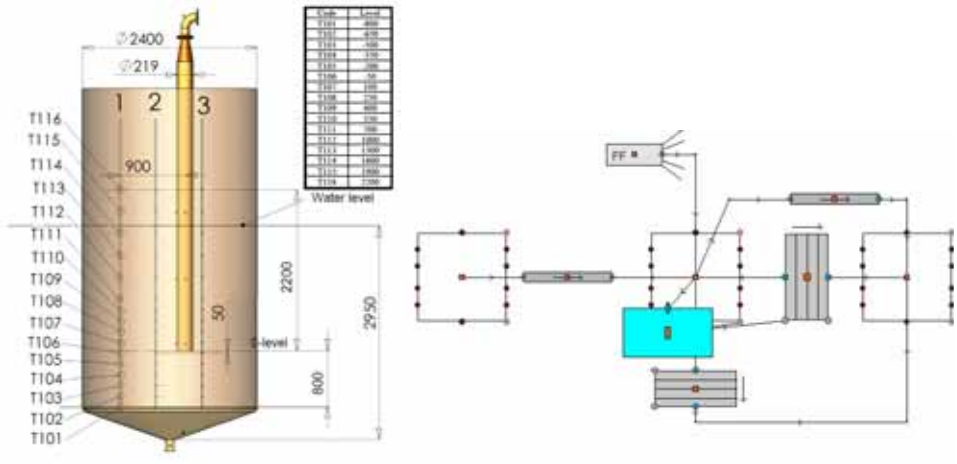

Figure 4. POOLEX suppression pool test facility and the simple APROS Containment model.

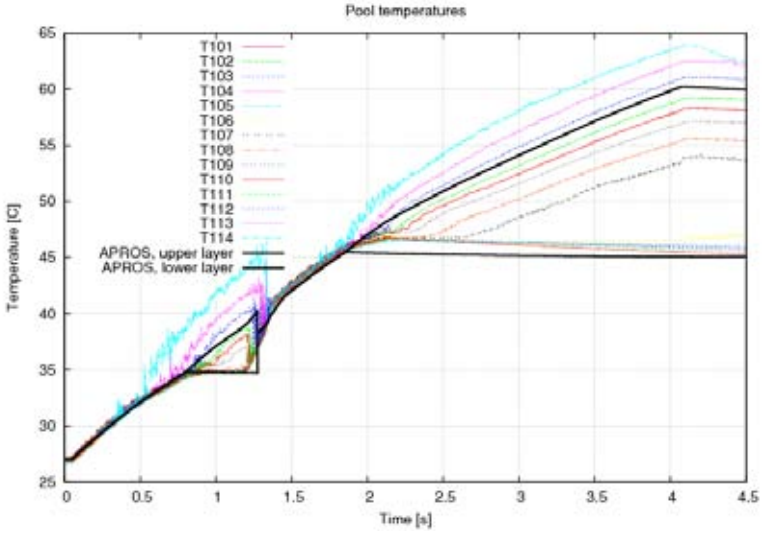

Figure 5. Measured and calculated pool water temperatures in STB-21 experiment.

A condensation benchmark in SARNET co-operation in WP 12-2 (Containment Atmosphere Mixing) was calculated with Fluent CFD code. The first test case (benchmark-0) was a condensation test on a cold wall of a rectangular flow channel. Altogether 10 organisations took part in the numerical comparison (CEA, FZJ, FZK, JRCP, JSI, NRG, UJV, UNIPI, VEIKI, VTT). The results were discussed in the WP meetings and a common report was compiled [19].

A Generic Containment code-to-code comparison was organized in the frame of SARNET-2 WP7. VTT participated in the first step of the benchmark calculation (both in blind and open phase) with the APROS Containment. A basic version of a rather simple generic containment model based on a German PWR with 1 300 MW_{el} has been developed by FZJ and delivered to participants i.e. all participant used a similar lumped parameter nodalisation in the first step of calculation. This approach facilitates verification of the codes with minimized user effects. Various ISP calculations have show that modelling choices, which the code user makes, has often a strong impact on the results. Therefore this kind of benchmark with fixed nodalisation allows "clean" code-to-code comparison. In order to provide a clear basis for comparison, a simple scenario, namely the in-vessel phase (0…12 890 s) of a SB-LOCA with loss of secondary heat sink, is considered in this initial step [20]. In order to simplify this case only the containment thermal hydraulics had to be modelled.

The rooms and compartments of the reactor and auxiliary building have been grouped into 16 control volumes (zones) including merged heat structures in order to generate a simple generic nodalisation (Figure 6).

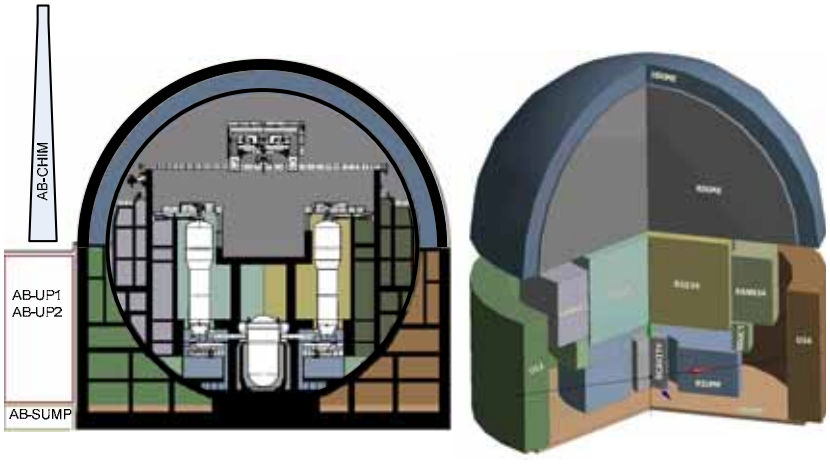

Figure 6. Control volumes within the reactor building [21].

In total, calculation results from 14 different organizations applying 9 different codes have been submitted. Because there is no experimental reference, average histories of all 22 contributions have been calculated in order to allow comparison. The deviations between the different results are demonstrated qualitatively by means of a single standard deviation band [21]. APROS calculation result on

pressure history is compared to the standard deviation band and mean value of all other calculations in Figure 7. The APROS result is well within the standard deviation band, and in general, similar trend was observed in other target variables compared.

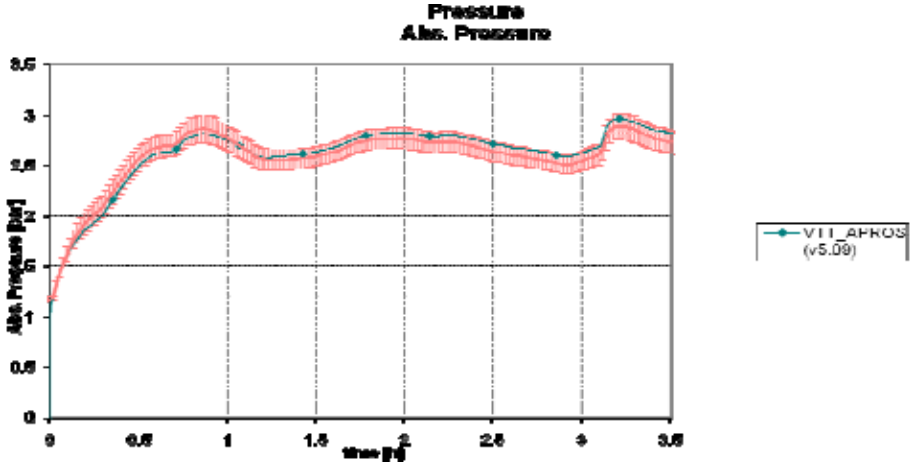

Figure 7. Calculated containment pressure compared to the mean value in SARNET Generic Containment benchmark.

Table 3. Containment code verification and validation cases.

Experiment	**Description**	**Code**
PPOOLEX STR-1, STR-4 and WLL-5	Temperature stratification in wet well and wall condensation in dry well.	APROS [22]
POOLEX STB-21, PPOOLEX STR-09 and STR-11	Temperature stratification and mixing in wet well.	APROS [23]
MISTRA MASP1 and MASP2	Containment spray efficiency	APROS [24]
SETH2/PANDA ST4-1	Containment cooler efficiency and gas stratification	Fluent [25] APROS [26]
SARNET WP12-2	Wall condensation in the CONAN test facility	Fluent [19]
SARNET2 Generic Containment benchmark	SBLOCA with loss of secondary heat sink	APROS [27]

Applications

APROS capability to simulate various transients and tested models and correlations can be used in evaluation of the safety of the new reactors to be built in Finland. Gathered experience of TRACE code will be utilized in independent safety analysis of Loviisa power plant.

The validated Fluent models to simulate wall condensation, containment coolers and convective flows can be used to analyze situations, where steam condensation influences hydrogen distribution/mixing in containment. Verified and validated APROS containment will be used in evaluating containment behaviour in postulated accidents.

Conclusions

Calculation methods for safety evaluation of nuclear power plants have been developed and validated. Both thermal hydraulic system analysis codes and CFD calculations have been used in the analysis and their usability have been studied and enhanced. An important objective has also been to train new thermal hydraulic code users and educate young experts.

References

1. Hillberg, S. PWR-PACTEL stepped inventory reduction analysis with a reference plant model. VTT, Espoo, 5.3.2008. VTT-R-02296-08.

2. Hillberg, S. Loss of Feed Water simulation with a PWR-PACTEL reference plant model. VTT, Espoo, 2009. VTT-R-00805-09.

3. Hillberg, S. & Karppinen, I. Small Break Loss of Coolant Accident simulation with a reference plant model. VTT, Espoo, 20.5.2009. VTT-R-03687-09.

4. http://www.oecd-nea.org/jointproj/rosa.html.

5. http://www.oecd-nea.org/jointproj/pkl-1.html.

6. Junninen, P. PSB-VVER Large Break LOCA pre-test analysis. VTT, Espoo, 2008. VTT-R-00194-08.

7. OECD/NEA PSB-VVER Project, http://www.oecd-nea.org/jointproj/psb-vver.html.

8. Elkin, I.V., Nikonov, S.M. & Basov, A.V. OECD PSB-VVER Project Experimental Data Report Test 5a. Electrogorsk, Russia, 2008.

9. Lauerma, S. OECD/ROSA Test 3-1 Simulation with APROS. VTT, Espoo, 28.4.2009. VTT-R-03061-09.

10. Inkinen, P. OECD/ROSA Test 5-1 Simulation with APROS. VTT, Espoo, 2009. VTT-R-00666-09.

11. Inkinen, P. OECD/ROSA Test 5-1 Simulation with TRACE. 4.5.2010. VTT, Espoo, 2010. VTT-R-02603-10.

12. Inkinen, P. OECD/ROSA-V Project Test 6-2 Simulation with APROS. VTT, Espoo, 2008. VTT-R-01629-08.

13. Hillberg, S. PKL Test E3.1 Simulated with APROS 5.09.07. VTT, Espoo, 18.6.2010. VTT-R-02556-10.

14. Inkinen, P. Modelling of ROCOM facility with APROS and TRACE. VTT, Espoo, 2011. VTT-R-00751-11.

15. Kurki, J. Validation of APROS' Upper Tie Plate CCFL Correlation in VVER 440 Geometry. VTT, Espoo, 3.2.2009. VTT-R-00730-09.

16. Kurki, J. APROS CCFL model validation. SAFIR2010 The Finnish Research Programme on Nuclear Power Plant Safety 2007–2010, Interim Report. Espoo, 2009. VTT Research Notes 2466. Pp. 182–190. ISBN 978-951-38-7266-3. http://www.vtt.fi/inf/pdf/tiedotteet/2009/T2466.pdf.

17. Lauerma, S. Validation of APROS with ISP-12, BWR SBLOCA in ROSA-III test facility. VTT, Espoo, 2011. VTT-R-00837-11.

18. Inkinen, P. Simulation of ISP-50 with APROS. VTT, Espoo, 2011. VTT-R-00749-11.

19. Ambrosini, W., Bucci, M., Forgione, N., Oriolo, F., Paci, S., Magnaud, J.-P., Studer, E., Reinecke, E., Kelm St., Jahn, W., Travis, J., Wilkening, H., Heitsch, M., Kljenak, I., Babić, M., Houkema, M., Visser, D.C., Vyskocil, L., Kostka, P. & Huhtanen, R. Comparison and Analysis of the Condensation Benchmark Results. The 3rd European Review Meeting on Severe Accident Research (ERMSAR-2008) Nesseber, Bulgaria, 23–25 September 2008. http://www.sar-net.org/upload/3-2_condensation-paper_final.pdf.

20. Kelm, St. et al. Quick-look Report on the generic Containment Code-to-Code Comparison – run0. Jülich, May 2010.

21. Kelm, St. et al. Report on the Generic Containment Code-to-Code Comparison – run0. Jülich, Dec 3rd 2010. Draft. v2.

22. Luukka, J. & Silde, A. Validation of APROS containment model against PPOOLEX experiments STR-1, STR-4 and WLL-5-2, Revision 1.0. VTT, Espoo, 15.2.2010. VTT-R-00763-10.

23. Luukka, J. Modeling of water pool stratification in POOLEX and PPOOLEX experiments with APROS containment. VTT, Espoo, 2011. VTT-R-00810-11.

24. Hänninen, M. Simulation of MISTRA containment spray experiments with APROS. VTT, Espoo, 2009. VTT-R-00654-09.

25. Huhtanen, R. Steam and helium mixture with a containment cooler, CFD simulation of Panda facility experiment ST4.1. VTT, Espoo, 2011. VTT-R-00835-11.

26. Silde, A. Simulation of experiment ST4-1 at PANDA facility with tube-bundle cooler using the APROS containment code. VTT, Espoo, 2011. VTT-R-00834-11.

27. Kelm, S., Broxtermann, P., Krajewski, S. & Allelein, H.-J. SARNET2 WP7-3 Report on the Generic Containment Code-to-Code Comparison – run0. Forschungszentrum Jülich. (To be published.)

12.2 Steam and helium mixture with a containment cooler, simulation of Panda facility experiment ST4.1 (THARE)

Risto Huhtanen and Ari Silde
VTT

Abstract

An experiment of steam and helium injection and mixing, stratification and helium enrichment due to condensation of steam in a tube bundle cooler is simulated with a CFD-code Fluent and a lumper parameter code APROS Containment. The experimental facility PANDA simulates a two part compartment connected with a corridor. The qualitative comparison with experimental results is shown.

Introduction

The work is part of OECD SETH2– research programme for studying stratification and improving and validating simulation methods of containment analysis of nuclear power plants. The project includes experimental work performed by Paul Scherrer Institute (PSI) in Villigen, Switzerland. The simulations are performed by several institutes in OECD countries. In the first phase the simulations are run as blind, i.e. only the initial and boundary conditions and the experiment profile are given. Later the simulation results are compared against the experiments. Further simulations are performed in the open phase. The APROS simulations are performed in the open phase only. The main aim of the APROS simulations is to study, whether it is possible to model satisfactory the general phenomena in a containment vessel including a tube bundler cooler, and to study different nodalization strategies suitable for lumped parameter approach.

The experiment includes mixing of steam and helium, density stratification of the gas mixture, heat transfer to a cooling device and condensation of water vapour in the cooling device. Condensation to other structures has been tried to exclude by using an elevated initial temperature of the experimental facility. This experiment is one in a larger series, described shortly in [1]. The numerical results of the experiments are open only to the participants for three years. For that reason the numerical values of the results are omitted from this paper.

Description

The experimental facility consists of two pressure vessels. The inner diameter of the vessels is about 4 m and volume of about 90 m^3. Height of the steel vessels is about 8 m. The vessels are connected with a 1 m diameter pipe. The outer surface of the structure is insulated with rock wool layer to minimize heat loss to the environment.

A cooler unit with water-cooled tube array is located in Vessel 1. The cooler works with natural convection without any active fan. Steam and helium injections are lead to Vessel 1 through an upwards-oriented pipe.

The computational grid of the Fulent model is hexahedral with some O-grid structures. The perspective view of the surface grid is shown in Figure 1a. The total number of cells is 394794. Different APROS nodalizations for both Vessel 1 and the cooler unit have been used. The most detailed 64-cell APROS nodalization is presented in Figure 2. The steel walls of the cooler unit and the outer steel walls of the facility with the rock wool layer as well as the heat losses to the environment are also modelled with APROS.

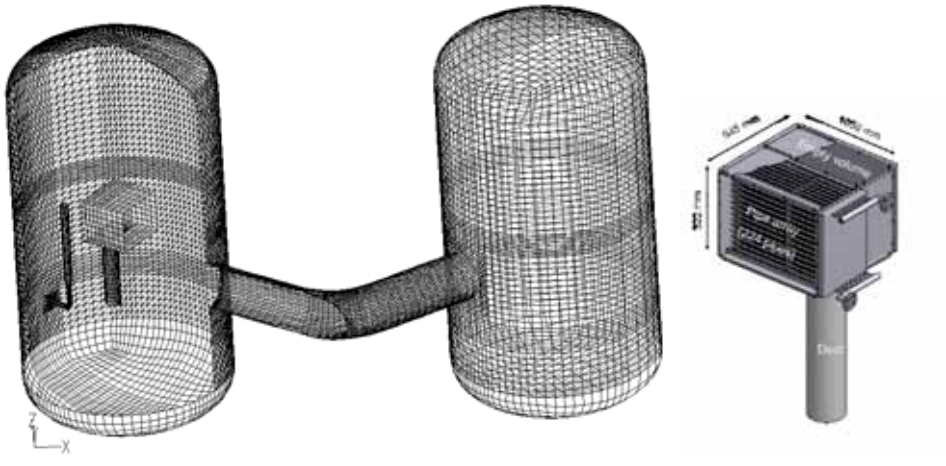

a) b)

Figure 1. a) Surface grid with some parts cut are shown. All cells are hexahedral, the triangular surface features are from post processing. b) Close view of the cooler unit.

Cooler in Vessel 1

A cooler, shown in Figure 1b, is located inside Vessel 1. The box is located in the middle of the vessel facing towards the horizontal connection pipe, thus the duct below the box is slightly offset from the axis of the vessel.

The cooler consists of a box with a duct below. The side of the box facing to the connection pipe is open for the mixture to flow in. In the box there are 224 steel pipes (external diameter 16 mm, wall thickness 1 mm) cooled with water inside. The cooling water is lead with a constant mass flow to the tube bundle from top and lead away from below. Condensed water is lead by pipes down to the bottom of Vessel 1.

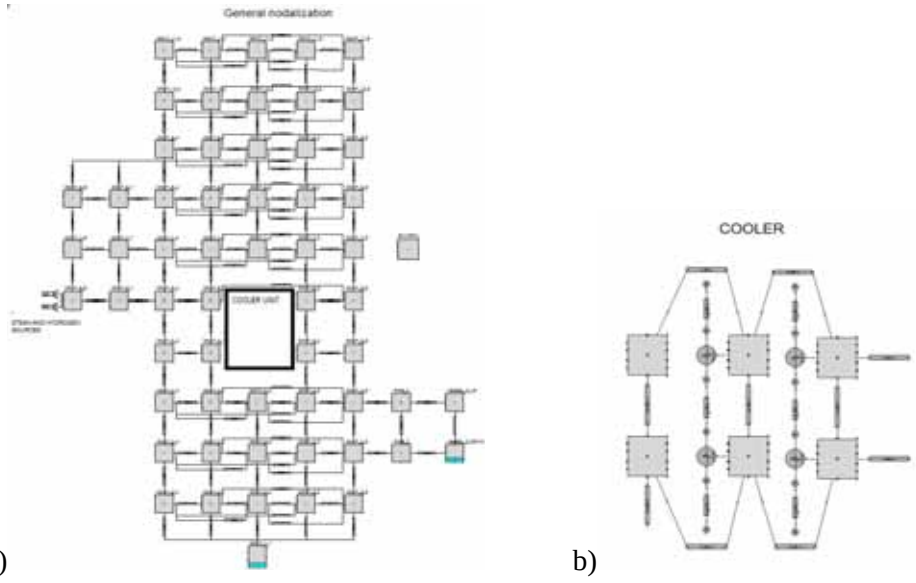

a) b)

Figure 2. a) A 64-cell APROS nodalization for vessels with a connecting pipe. b) A 6-cell nodalization for the cooler.

Both in the Fluent and APROS models the temperature rise of the cooling water is calculated from the actual heat flux to the whole cooler tube array and mass flow of coolant. As a first approximation in the Fluent simulations the temperature of the coolant is assumed to have linear dependence on height. Water pool on the base is not modelled. The cooler and the pipe array have been described as a separate, relatively fine grid attached to the other part with a non-conformal boundary (i.e. cells do not match on the boundary). The number of cells in the cooler is 202048. All pipes in the tube array are described in the grid.

In the 64-cell APROS nodalization, the cooler is modelled by 6 internal nodes. For the pipe side of the cooler the APROS thermal hydraulic model is applied.

Initial and boundary conditions

The vessels are initially filled with dry hot air. The temperature of the steel shell is the same. Pressure inside the facility is slightly elevated from atmospheric conditions. Overheated constant steam injection to Vessel 1 is about 40°C above the initial temperature. Duration of this Phase I is an hour. After that the mass flow is increased by 5% by adding helium. Inflow temperature is kept constant. Duration of the mixed release is 1 800 s (Phase II). At 5400 s the helium flow is stopped and the basic steam flow is kept for another hour (Phase III). The vessels are closed, i.e. no venting out is active. The cooling water loop is activated at the beginning of the experiment and kept constant.

Simulations and results

The first CFD-simulation was a pre-test run with the nominal initial and boundary values given. In this simulation it was assumed, that cooling water temperature distribution was linear by height inside the pipes. With this assumption the total cooling heat flux was estimated, giving the temperature rise in the tube bundle. When the simulation was compared to the selected results given in the Quick Look Report, it appeared that the estimated cooling rate is too high. That influences both pressure and flow field development. Also the nominal cooling water mass flow rate was higher and incoming water temperature lower than actually used in the experiment. Further simulations were performed with different modifications. The case matrix is shown in Table 1. The most efficient modifications of the Fluent simulations were change of cooling water mass flow rate and inlet temperature and refinement in modelling the local cooling water temperature in the tube bundle. Other modifications had only minor effects.

The pressure development in the vessel and cooling rate predicted by the Fluent and APROS codes are presented in Figure 3. Low pressure in the pre-test run of Fluent is a consequence of too high cooling rate of the cooler. The modelling refinements for Fluent mentioned above lead to better prediction of the cooling rate and the pressure. A very simple 3-cell APROS nodalization, where Vessel 1 and the cooler unit are modelled only by one uniform node, gives inaccurate results. The cooling rate is clearly overpredicted, because too much steam is able to condense on the cooler tubes. Consequently, the pressure

is underestimated. A relative detailed 64-cell APROS model simulates the pressure development very well, despite some overprediction of the cooling rate. This hints that the heat losses to the environment are slightly underpredicted.

Except the pressure level the high cooling rate influences also the flow field. In the beginning of the release the cooler fills the bottom part of Vessel 1 with colder and heavier mixture and part of that flows through the connecting pipe to the bottom of Vessel 2.

Table 1. Assumptions in the CFD-simulations performed. The mass flow is given as relative to the pre-test nominal value. Temperature shows difference to the nominal value.

Run	**Cooling water mass flow and temperature [°C]**	**Cooling water temperature**
Run 1, pre-test	1 / nominal temp	linear change from bottom to top
Run 2, post-test	0.91 / +1.1	linear change from top to bottom
Run3, post-test	0.91 / +1.1	piecewise linear change, 80% in the upper half, 20% in lower
Run 4, post-test	0.91 / +1.1	local temperature

After a while the flows inside the connecting pipe turn to other direction. In the Run 1 this turn-around takes place only after helium injection is started in Phase II. According to Run 4 this takes place after about 15 minutes, which is in line with the experiments.

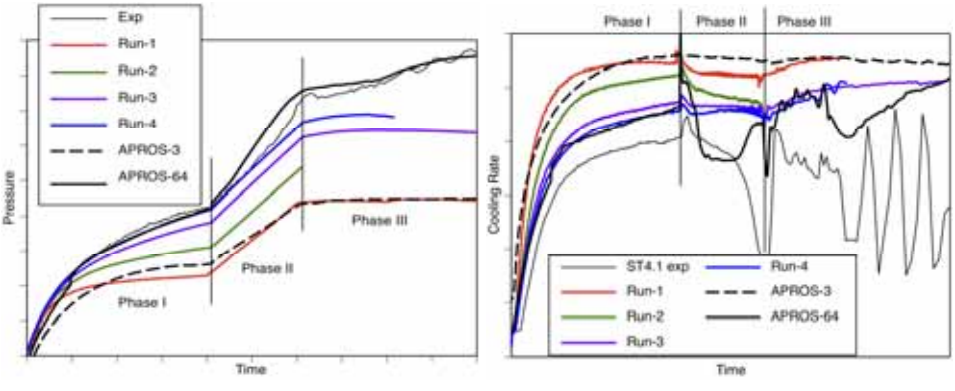

Figure 3. Pressure and cooling rate in simulation runs compared to the experimental value.

The pressure rises sharper at the end of Phase II, due to the reduction in cooler efficiency. This drop in cooling rate was not predicted in any of the CFD-simulations. Some drop of cooling rate during the helium injection phase could be seen in the APROS simulation, but the cooling rate is still over predicted.

The velocity field of the CFD-simulation at Phase I is shown in Figure 4. After the turnaround of the plume the flow field stays in principle the same, except that the duct flow is stagnated due to helium enrichment in Phase II.

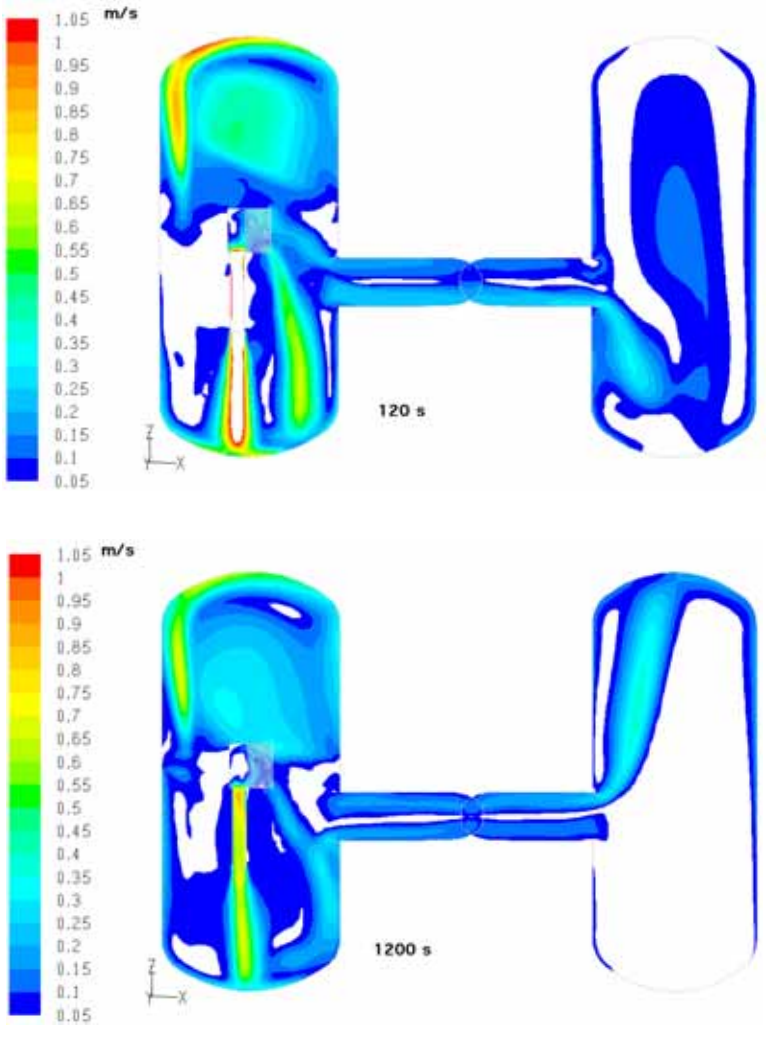

Figure 4. Flow field in Phase I with steam injection (Fluent). The mode of flow changes at about 15 minutes to the one shown at 1 200 s. Later the cooler duct flow is stagnated in Phase II due to helium enrichment.

Comparison of selected values for steam and helium concentrations is shown in Figure 5 and Figure 6. The even lines present simulation and dotted lines experiments. The general trends are fairly good. It appears that the vertical mixing in Vessel 1 is stronger in the simulation than in the experiments. Obviously the density stratification is too easily broken in the CFD simulation.

Since the APROS nodalization was relatively coarse, the lumped parameter modelling could not capture the local flow field and stratification phenomena, Generally speaking, the APROS model overestimates the mean temperature and steam concentration and underestimates the helium concentration in the upper part of Vessel 1. In the lower part of Vessel 1, the mean concentration of steam and helium is predicted quite reasonably.

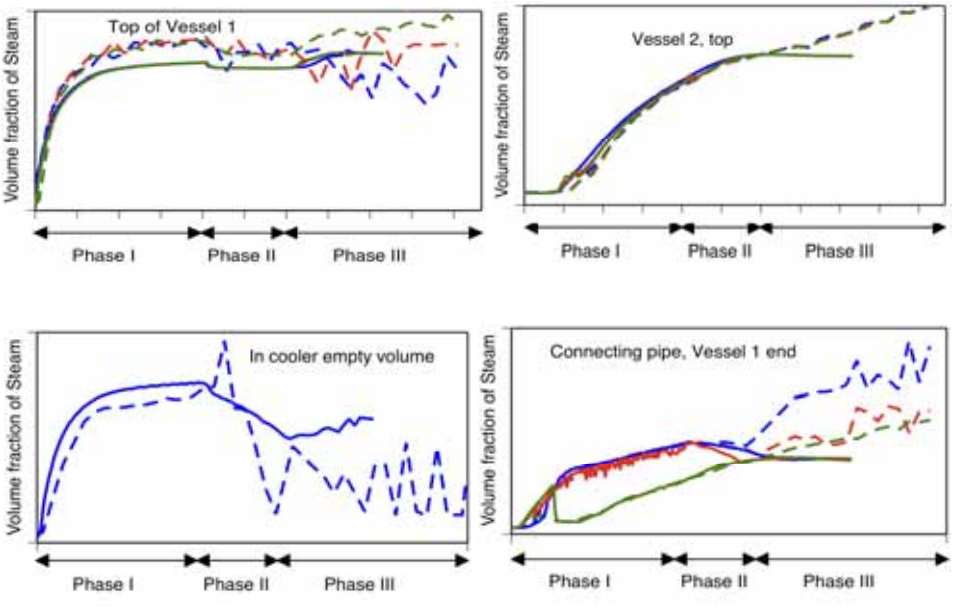

Figure 5. Comparison of steam concentrations at selected locations (Fluent). Dotted line is experiment, line is CFD-simulation.

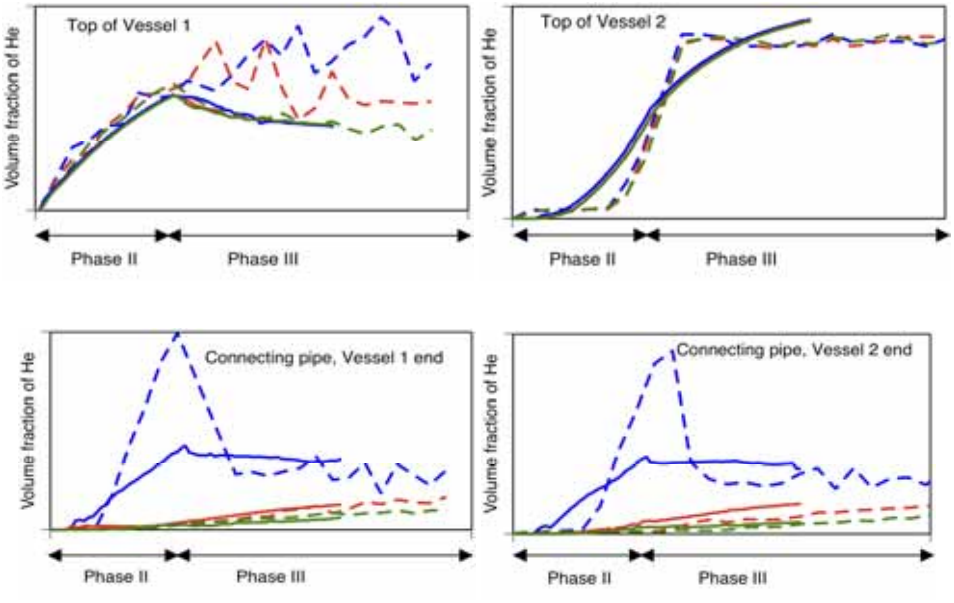

Figure 6. Comparison of helium concentration at selected locations. Dotted line is experiment, line is CFD-simulation.

Conclusions

General trend for pressure and concentrations are predicted rather well in the last CFD-simulation with refined model for the cooling water temperature distribution. In Vessel 1 the vertical mixing is slightly stronger than in the experiments. Cooling rate drop due to helium enrichment inside the cooler tube bundle is not captured. The duct flow stagnation is properly predicted, but helium concentration inside the cooler stays lower than in the experiments. This might be improved with defining the heat transfer through the cooler thin plate walls (now adiabatic). Also some grid refinement is necessary in the plume and cooler area, especially in vertical direction in order to capture stratification better.

The detailed APROS model predicts the pressure behaviour very well. Some drop in the cooling rate due to helium enrichment during the helium injection phase could be captured, but generally, the cooling rate is still overpredicted. The general conclusion of the APROS simulations is that a lumped parameter code is able to simulate the most important phenomena inside the containment including the tube bundle cooler, if the nodalization is built up properly. A very simple nodalization does not give necessarily accurate or conservative results,

and rather complicated multi-cell nodalization is needed to model satisfactory the stratification/mixing phenomena inside the cooler box and other parts of the test facility.

References

1. Kapulla, R., Mignot, G., Paladino, D., Erkan, N. & Zboray, R. Thermal hydraulic phenomena caused by the interaction of steam and steam-helium mixture wall jets with a containment cooler. Proceedings of ICAPP 2011, Nice, France, May 2–5, 2011. Paper 11093. (To be published.)

13. CFD Modelling of NPP Horizontal and Vertical Steam Generators (SGEN)

13.1 SGEN summary report

Timo Pättikangas, Ville Hovi and Jarto Niemi
VTT

Tommi Rämä and Timo Toppila
Fortum Power and Heat Oy

Abstract

A porosity model for the simulation of two-phase flow on the secondary side of both horizontal and vertical steam generators is presented. The Euler-Euler multiphase model of the Fluent CFD code is used for the simulation of the secondary side. The outer wall temperatures of the heat transfer tubes obtained by performing an APROS simulation of the steam generator are used for generating the source terms for the enthalpy equations. The model is tested by performing simulations for a horizontal steam generator of Loviisa VVER-440 nuclear power plant and a vertical steam generator of the PWR-PACTEL test facility.

Introduction

The detailed flow field of water and steam mixture on the secondary side of horizontal or vertical steam generators of nuclear power plants (NPP) is fairly unknown. This is because of the lack of large experimental devices and the difficulties related to measurements in real operating NPPs. Two-phase flow in a

complicated three-dimensional geometry is also very challenging to solve numerically. Knowledge of flow fields and temperatures would, however, be very useful in steam generator life time management and accident analysis.

Since the geometry of the secondary side of a steam generator is too complicated for detailed three-dimensional CFD simulations, some simplifications need to be made: the porous medium approach is adopted for the section of the steam generator occupied by the heat transfer tubes. As a result, detailed description of the geometry is lost within the tube filled section and the effect of the heat transfer tubes on the flow needs to be defined explicitly; the heat transfer from the primary circuit to the secondary side is described with mass and enthalpy sources and the pressure loss caused by the heat transfer tubes is described with momentum sources.

The main objective of the project is to develop a simulation methodology and tool for the modelling of horizontal and vertical steam generators of NPPs taking into account multidimensional effects and two-phase flow phenomena. In order to use the model for industrial applications, validation of the model is essential.

Three-dimensional porous media model for steam generators

The porous media approach previously used by Stosic and Stevanovic is applied [1]. The conservation equations for phase q are:

$$\begin{aligned}
&\text{mass}: && \frac{\partial}{\partial t}(\gamma\alpha_q\rho_q) + \nabla\cdot(\gamma\alpha_q\rho_q\mathbf{v}_q) = S_{\text{mass},q} \\
&\text{momentum}: && \frac{\partial}{\partial t}(\gamma\alpha_q\rho_q\mathbf{v}_q) + \nabla\cdot(\gamma\alpha_q\rho_q\mathbf{v}_q\mathbf{v}_q) = \mathbf{S}_{\text{M},q} \\
&\text{energy}: && \frac{\partial}{\partial t}(\gamma\alpha_q\rho_q h_q) + \nabla\cdot(\gamma\alpha_q\rho_q\mathbf{v}_q h_q) = S_{\text{E},q}
\end{aligned} \tag{1}$$

where γ is porosity, α_q is the volume fraction, ρ_q is the density, $\mathbf{v}_q$ is the velocity and h_q is the specific enthalpy of liquid ($q = 1$) or vapor ($q = 2$). The sum of volume fractions is $\alpha_1 + \alpha_2 = 1$. Mass transfer between the phases, i.e., evaporation and condensation, is described with the source term $S_{\text{mass},q}$ and enthalpy sources with $S_{\text{E},q}$. The drag forces caused by the primary tubes on the flow of liquid water and vapor, $\mathbf{S}_{\text{M},q}$, have been modified to apply for both quadrilateral and triangular tube arrangements [2]. All the source terms of the model are described in detail in Ref. [3].

Model for a horizontal steam generator

An APROS model of a VVER-440 horizontal steam generator is shown in Figure 1. The tubes of the primary circuit have been divided into five horizontal layers, the top most of which is shown on the left side of Figure 1. Several tubes are modeled with the same APROS component: four consecutive tubes in the horizontal direction and fifteen in the vertical direction. The portion of the secondary side occupied by the tube bundles has also been divided into five horizontal layers. Five horizontally aligned “downcomer” nodes have been added to allow some recirculation, and the area above the tube bundles (steam dome) is modeled with two nodes. The heat transferred in each of the five layers of the primary circuit is conveyed into its own node on the secondary side. The feed water flow is adjusted with a three-point control, which monitors the water level of the uppermost downcomer node.

The Fluent model for the secondary side of a VVER-440 horizontal steam generator is shown in Figure 2. The portion of the steam generator occupied by the tube bundles has been described with the porosity model, which introduces an additional pressure loss. The source terms have been implemented as User-Defined Functions of Fluent.

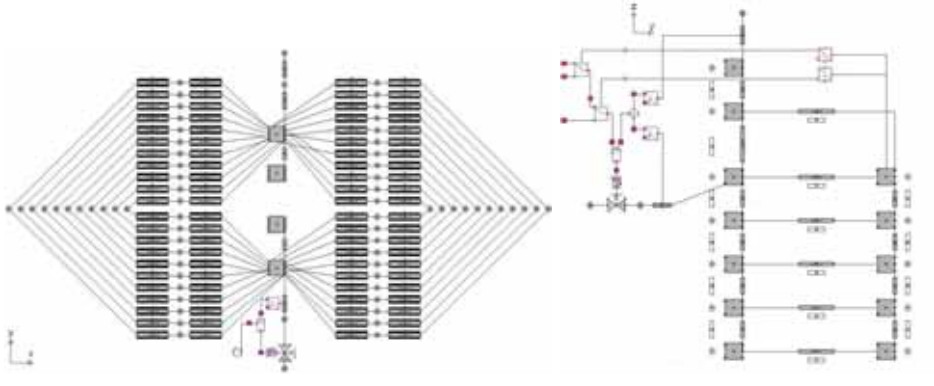

Figure 1. Primary (left) and secondary (right) sides of the APROS model of the Loviisa VVER-440 horizontal steam generator.

The model has been tested using two different meshes; a coarse mesh consisting of 87 000 grid cells and a fine mesh consisting of 930 000 grid cells. Both meshes are almost purely hexahedral, only a few thousand tetrahedral, pyramid and wedge cells have been used in the fine mesh. The free flow areas are

modeled with a finer mesh than the porous areas. The tube support plates are represented as thin walls.

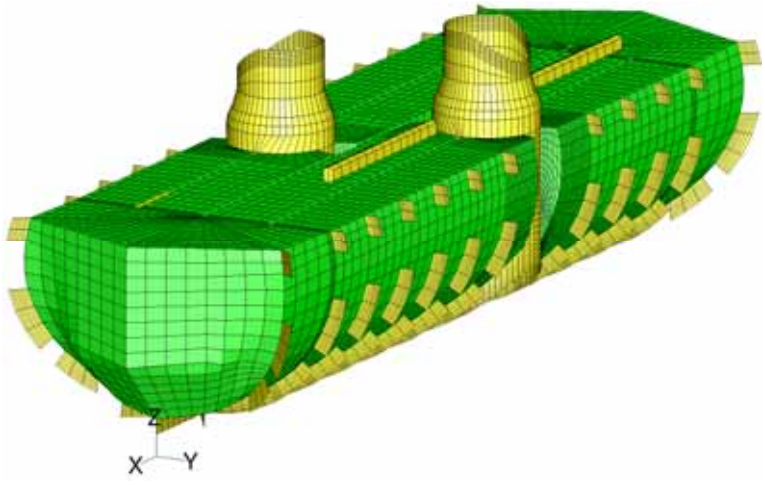

Figure 2. Fluent model for the secondary side of a VVER-440 horizontal steam generator.

Simulation of the primary circuit with APROS makes it possible to provide a realistic boundary condition for the CFD simulation of the secondary side. One-way coupling is used, in which the outer wall temperatures of the primary tubes are interpolated from the nodes of the APROS model to each grid cell of the Fluent model inside the porous region. The interpolation is based on finding the nearest APROS node for each grid cell. The outer wall temperatures are then used in the CFD simulation to determine the mass transfer between the phases and the enthalpy sources for both phases.

Validation of the horizontal steam generator model

The available measurement data on the secondary side of full size steam generators is very scarce. Only a few measurements for horizontal steam generators are known by the authors of the present report. We have chosen to compare the calculated void fractions and flow velocities to the measurements presented by Haapalehto and Bestion [4]. The four measurement points, shown in Figure 3, are located 70 cm below the top of the tube banks.

The void fraction and velocity values in the free flow area segments on certain horizontal levels are fairly constant. Thus, even if the exact horizontal coordinates of the observation points are not known to the authors of this report, the values retained are representative for the comparison against the measurements.

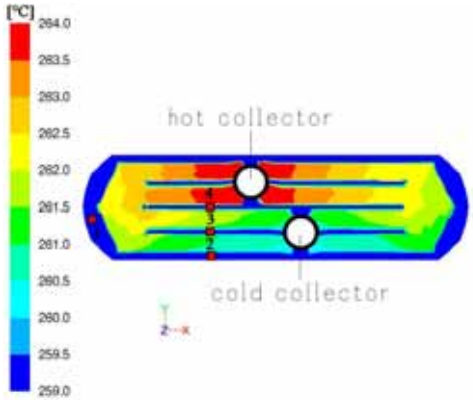

	Measurement	**Simulation**
$T_{\text{prim,in}}$	295°C	295°C
$T_{\text{prim,out}}$	265,9°C	265,7°C
$\dot{m}_{\text{prim}}$	1 560 kg/s	1 560 kg/s
P_{prim}	122,5 bar	122,5 bar
$\dot{m}_{\text{sec}}$	125,5 kg/s	130,1 kg/s
p_{sec}	46.0 bar	46,0 bar
$T_{\text{sec,in}}$	222,9°C	222,9°C

Figure 3. Outer wall temperatures of the primary tubes and the locations of the measurement points 70 cm below the top of the tube banks.

In Table 1, the calculated results are compared to measurements. The simulation results were obtained using the so-called physical velocity formulation of the porous media model of Fluent. The calculated void fractions are in very good agreement with the measured values that were in the range 0.3–0.4 at all four measurement points. The error bars of the measured velocities of liquid water were unfortunately rather large: the flow velocities were 0–0.4 m/s. The calculated values fit well within this range.

Some information is also available on the position of the water surface in VVER-440 steam generators. Dmitriev et al. present the mixture level on the hot and cold sides of the steam generator in Ref. [5]. The exact definition of the measured “mixture level” is, however, not available. In Figure 4, we have plotted the calculated 70% mixture level together with the measured result. The qualitative similarity of the calculated and measured mixture level is apparent both on the hot and on the cold side. Quantitative comparison is hampered by the difficulty in the interpretation of the measured data.

Table 1. Comparison of simulation results to measured void fractions and liquid flow velocities.

	Void1 [-]	**Void2 [-]**	**Void3 [-]**	**Void4 [-]**	**Vel1 [m/s]**	**Vel2 [m/s]**	**Vel3 [m/s]**	**Vel4 [m/s]**
Measurement	0.3–0.4	0.3–0.4	0.3–0.4	0.3–0.4	0–0.4	0–0.4	0–0.4	0–0.4
Simulation	0.31	0.42	0.31	0.30	0.31	0.30	0.07	0.26

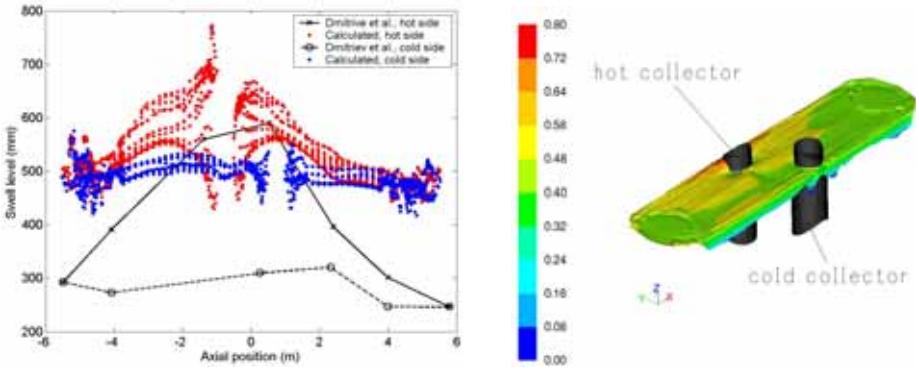

Figure 4. Vertical position of the 70% mixture level on the hot (red) and cold sides (blue), as the vertical distance from the top of the tube banks. In comparison, the swell level reported by Dmitriev et al. [5] (black).

Model for a vertical steam generator

The PWR-PACTEL test facility at Lappeenranta University of Technology is designed and constructed to be utilized in the safety studies related to EPR type pressurized water reactor thermal hydraulics [6]. The vertical steam generators of the PWR-PACTEL facility have extensive instrumentation in the primary side U-tubes. In addition, a few temperature measurements are made on the secondary side.

An APROS model of the PWR-PACTEL vertical steam generator is shown in Figure 5. The steam generator consists of 51 U-tubes which can be divided into 10 groups of different lengths. Each group is modeled with separate heat pipe components to allow for different flow rates and even flow directions between the groups.

The secondary side of the steam generator can be divided into three parts: the riser nodes in the middle, the ring space nodes (or the downcomer nodes) surrounding the riser, and the steam dome node on the top. The lower part of the riser has been divided into hot and cold sides by a divider plate. The ring space is also divided into hot and cold sides, which are connected to the hot and cold sides of the riser at the bottom. Feed water is injected to the cold side of the ring space, whereas liquid returning from the steam dome is diverted to the hot side of the ring space. Heat conduction through the steel wall separating the cold ring space from the riser is included in the model.

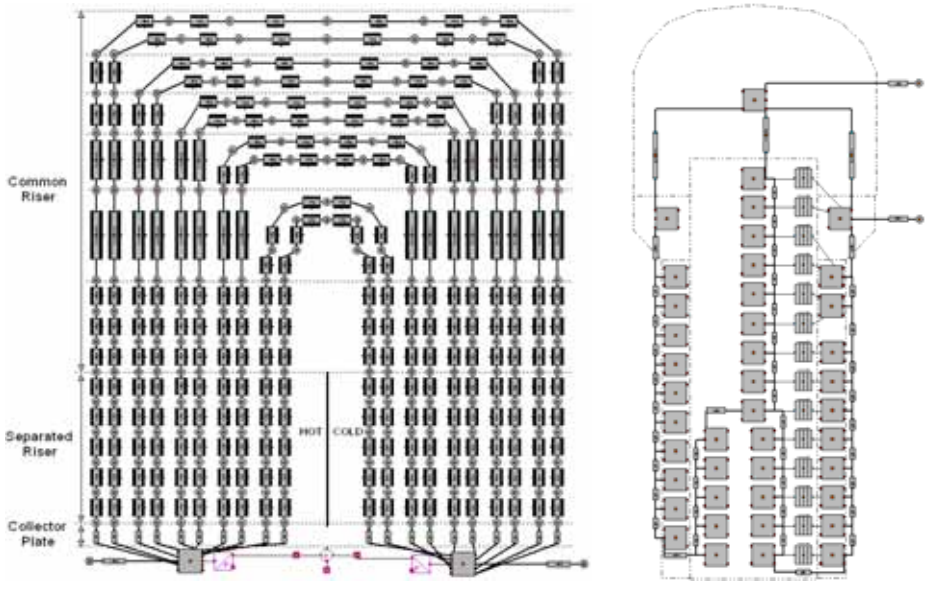

Figure 5. Primary (left) and secondary (right) sides of the APROS model of the PWR-PACTEL vertical steam generator.

The CFD mesh for the secondary side of the PWR-PACTEL vertical steam generator is illustrated in Figure 6. The surface mesh of the outer wall is shown on the left and the internal parts on the right. The porous tube regions (green), the divider plate and some wall structures (blue) are shown in the middle. The riser tube, shown in the top right corner of Figure 6, separates the riser from the ring space and contains the porous tube regions, shown in the middle. Also visible in the top right corner of Figure 6 are parts of the plates which divide the ring space into hot and cold sides. The feed water manifold is also visible on the cold side.

The purely hexahedral CFD mesh has about 200 000 grid cells. Non-conformal mesh has been used in order to refine the mesh in the region of the semicircular holes in the plate between the steam dome and the downcomer.

Simulation of experiment NC-10

The developed model was tested against a steady-state experiment, NC-10, performed by Riikonen et al. [7] with the PWR-PACTEL test facility at Lappeenranta University of Technology. The main test parameters are gathered and compared to simulation results in Table 2. The direction of the primary flow in each of the 51 U-tubes of the APROS model (on the left) and estimated flow directions based on temperature measurements in 14 U-tubes of the PWR-PACTEL facility (on the right) are presented in Figure 7. The estimation of flow directions is based on several temperature measurements along the length of each of these 14 U-tubes: a temperature decrease from the hot collector towards the cold collector indicates a flow in normal direction (in green), whereas a flat temperature distribution, close to the saturation temperature of the secondary side, indicates either a reversed flow or stagnation (in red).

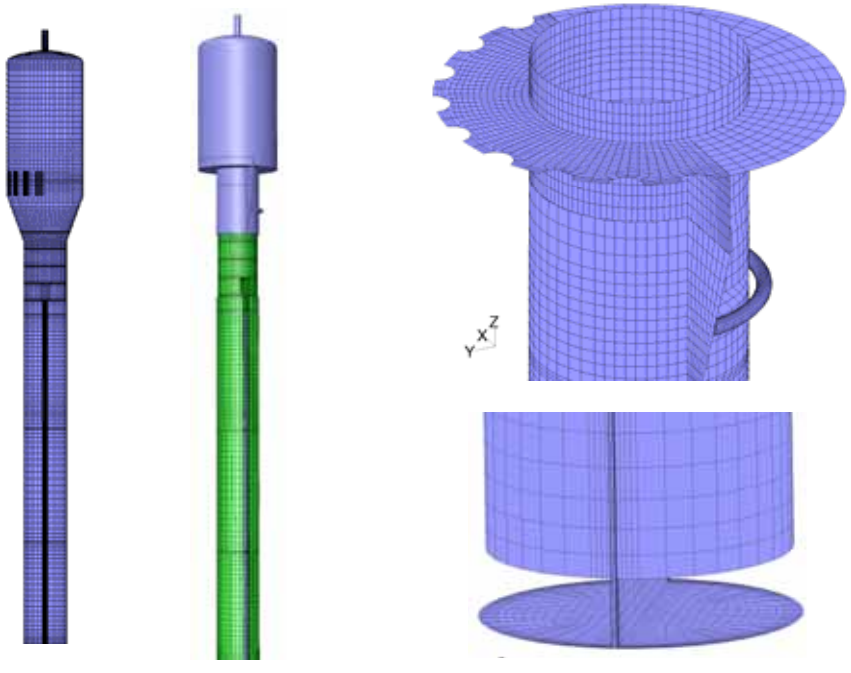

Figure 6. Surface mesh (in blue) and porous tube regions (in green) of the CFD model for the PWR-PACTEL steam generator.

The only measurements available on the secondary side of the PWR-PACTEL steam generator are thermocouple temperature measurements at seven locations. The simulated liquid temperature field and the locations of the temperature measurements are shown in Figure 8. Void fraction and liquid velocity magnitude are shown in Figure 8 on the plane that contains the axis of the steam generator and is perpendicular to the separating riser plate (*yz*-plane, $x = 0$). In addition, a comparison of simulated and measured temperatures at these seven locations is presented in Table 3.

When comparing the simulated liquid temperatures in Figure 8 and in Table 3 to the measurements in Table 3, there are two things that stand out. First, calculated liquid temperature does not reach saturation temperature (~212.4°C) anywhere within the simulation domain. Second, according to the measurements, the liquid entering the cold side of the riser tube at the bottom is significantly warmer (~8°C) than the simulation suggests. The latter could be due to leakage (in the PWR-PACTEL steam generator) from the hot side of the ring space to the cold side. In order to facilitate assembly and disassembly of the steam generator, the plates that divide the ring space in two are not completely sealed against the inner surface of the "pressure vessel". Instead the plates need to slide in and out together with the riser tube. This leakage could mix the saturated liquid on the hot side of the ring space with the relatively cold liquid on the cold side and thus increase the temperature of the liquid entering the riser tube at the bottom of the cold side.

Table 2. Main test parameters and comparison to simulations.

Parameter	**Test (NC-10)**	**APROS model**	**Fluent model**
P_{SG}	334 kW	335 kW	340 kW
p_{prim}	75 bar	75 bar	-
p_{sec}	20 bar	20 bar	20 bar
$\dot{q}_{m,\,prim}$	1.1 kg/s	1.1 kg/s	-
$\dot{q}_{m,\,feed}$	125 g/s	124 g/s	124 g/s
$\dot{q}_{m,\,vapor}$	-	124 g/s	122 g/s
$T_{prim,\,in}$	279°C	280°C	-
$T_{prim,\,out}$	216°C	216°C	-
Level	3.9 m		

Table 3. Comparison of secondary side temperature measurements to simulation results.

Point	Measurement	Simulation
1	212.6°C	211.7°C
2	213.4°C	210.3°C
3	212.7°C	211.4°C
4	212.6°C	210.9°C
5	210.8°C	202.6°C
6	212.4°C	211.5°C
7	212.3°C	211.5°C

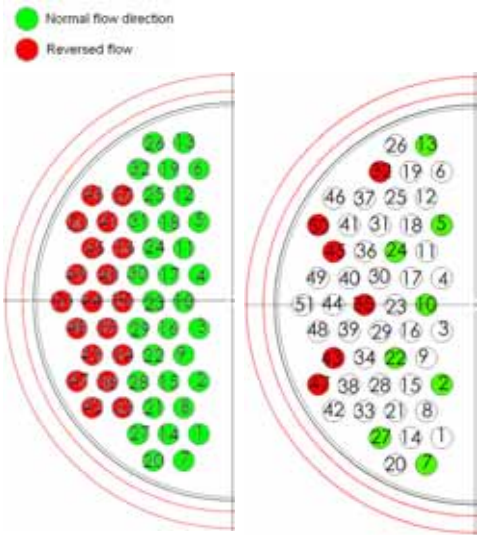

Figure 7. The directions of primary flow in the APROS model (left) and estimated flow directions based on temperature measurements of test NC-10 (right).

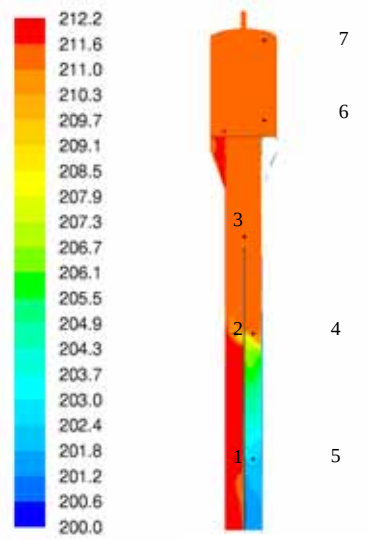

Figure 8. Liquid temperature [°C] and locations of the measurement points.

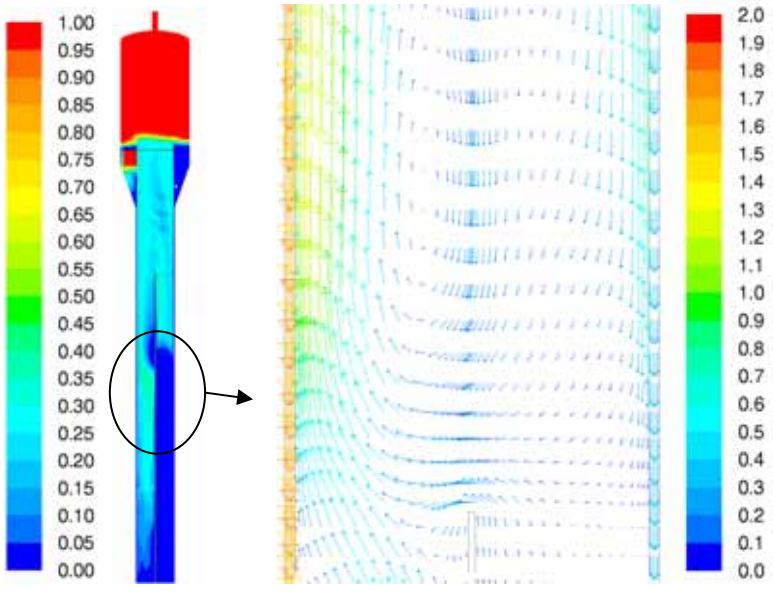

Figure 9. Void fraction [-] and liquid velocity magnitude [m/s] (yz-plane, x = 0).

Conclusions

Overall, the results obtained for the VVER horizontal steam generator come up to expectations: flow fields and void fractions behave qualitatively in a reasonable manner and distinctive features of the hot and cold sides of the steam generator are found. The main features of the flow are defined by gravitation and the density difference of the mixture between the hot and cold sides. The fine hexahedral mesh used in the simulation captures quite accurately the regions outside the tubes, such as the narrow gaps between the tube bundles.

Liquid velocities and void fractions in certain observation points agree well with the measurements found in the literature. The calculated mixture layer also has a similar shape as is observed in a real steam generator. Because the available validation data is scarce, a well instrumented experiment would be optimal for further validation studies.

With the developed model the local conditions in the steam generators can be assessed more precisely. The model can be used for comparing different operational states of a steam generator, for instance, for the examination of the behaviour of the feedwater plume with different feedwater distributions and or modifications. The distribution of the crud accumulation at the bottom of the

steam generator, which is of great interest in the life time management of the steam generator, can be modelled with the particle tracking method. In addition, if transients can be simulated successfully, the model could be used in accident analysis.

Acknowledgement

The authors are grateful to Mr. Vesa Riikonen and project PAOLA for providing the information on the PWR-PACTEL steam generator [6] and the data on experiment NC-10 [7]. The data was only made available to two of the authors (T.P. and V.H.) because an international blind benchmark calculation on the PWR-PACTEL facility was simultaneously in progress.

References

1. Stosic, Z.V. & Stevanovic, V.D. Advanced three-dimensional two-fluid porous media method for transient two-phase flow thermal-hydraulics in complex geometries. Numerical Heat Transfer 2002, Part B, Vol. 41, pp. 263–289.

2. Simovic, Z.R., Ocokoljic, S. & Stevanovic, V.D. Interfacial friction correlations for the two-phase flow across tube bundle. Int. J. Multiphase Flow 2007, 33, pp. 217–226.

3. Pättikangas, T.J.H., Niemi, J. & Hovi, V. Three-dimensional porous media model of a horizontal steam generator, CFD4NRS-3, Experimental Validation and Application of CFD and CMFD Codes to Nuclear Reactor Safety Issues, OECD/NEA & IAEA Workshop, Washington D.C., USA, 14–16 September 2010. 12 p.

4. Haapalehto, T. & Bestion, D. Horizontal steam generator modelling with CATHARE; validation of several nodalization schemes on plant data, CEN Grenoble, 2nd Int. Seminar on Horizontal Steam Generators, 1993.

5. Dmitriev, A.I., Kozlov, Yu.V., Logvinov, S.S., Tarankov, G.A. & Titov, V.F. Separation characteristics of horizontal steam generators. OKB “Gidropress” International Seminar of Horizontal Steam Generator Modelling, Vol. 1, LPR 1991.

6. Riikonen, V., Kouhia, V., Räsänen, A. & Partanen, H. General description of the PWR PACTEL test facility. Research Report, Lappeenranta University of Technology, Nuclear Safety Research Unit, YTY 1/2009. 18 p. + app. 35 p.

7. Riikonen, V. Quick look report of NC-10 experiment with PWR PACTEL facility. Technical Report, Lappeenranta University of Technology, Nuclear Safety Research Unit, YTY 4/2010. 10 p.

14. Improvement of PACTEL Facility Simulation Environment (PACSIM)

14.1 PACSIM summary report

Juhani Vihavainen and Antti Rantakaulio
LUT

Abstract

The main objective of the PACSIM project is to improve the simulation environment of PACTEL facilities with TRAC/RELAP Advanced Computational Engine (TRACE) thermal hydraulic code. TRACE code has been utilized for preparing different simulation models for the VVER and PWR PACTEL facilities. The new model of VVER PACTEL was tested against pressure and heat loss experiments. After testing the main work was concentrated on calculations of stepwise inventory reduction and small break LOCA situations including natural circulation, which clearly enlighten the VVER specific features like loop seal effect. Also, a loss-of-feedwater experiment was calculated. The calculation results agreed reasonably well with the experiments. The PWR PACTEL model with vertical steam generators was prepared and functionality was tested. Also, pressure and heat losses were defined according to experiments. The available experiments were calculated and results were found to be satisfactory.

Introduction

The Parallel Channel Test Loop (PACTEL) facility [1], constructed in the Laboratory of Nuclear Engineering at Lappeenranta University of Technology (LUT) in Finland 1990, is one of the largest facilities of its kind. It was

originally designed to model the thermal hydraulic behavior of the VVER-440 type pressurized water reactors (PWR) currently used in Finland. Recent modifications in the frame of Tekes project PAOLA have introduced a new set-up of PWR PACTEL facility, which now contains two vertical steam generators and new hot and cold loops for them.

The Finnish Radiation and Nuclear Safety Authority, STUK, has required an independent tool to support safety and licensing analysis. U.S. Nuclear Regulatory Commission (USNRC) has implemented a program called “Code Applications and Maintenance”, CAMP-program. Therefore, Finland has decided to continue participating into this CAMP-program with a new agreement. According to the agreement USNRC provides the TRACE thermal hydraulic code and Symbolic Nuclear Analysis Package (SNAP) graphical user interface to the use of the partners. Hence, TRACE code (currently version 5.0 Patch 2) has been recently implemented at LUT.

Main objectives

The main objective of the PACSIM project is to improve the simulation environment of both VVER and PWR PACTEL facilities with TRACE thermal hydraulic code. In the frame of PACSIM project on SAFIR2010 programme full model of PACTEL VVER facility has been prepared.

The use of the TRACE code enhances the preparedness to give analysis support and improves education in computational thermal hydraulics. This project aimed to develop the VVER-PACTEL model further and to prepare a complete model with three loops with necessary control modules. This gives important validation knowledge for achieving the final goal of the full-scale VVER-440 model preparation, which will be carried out outside the SAFIR2010 programme. Another objective is to prepare a new TRACE-model with vertical steam generators for the modified PWR PACTEL facility. The TRACE-code calculations will give valuable analysis and comparison support for the Apros calculations of the PWR PACTEL experiments. Figure 1 shows VVER and PWR PACTEL facilities.

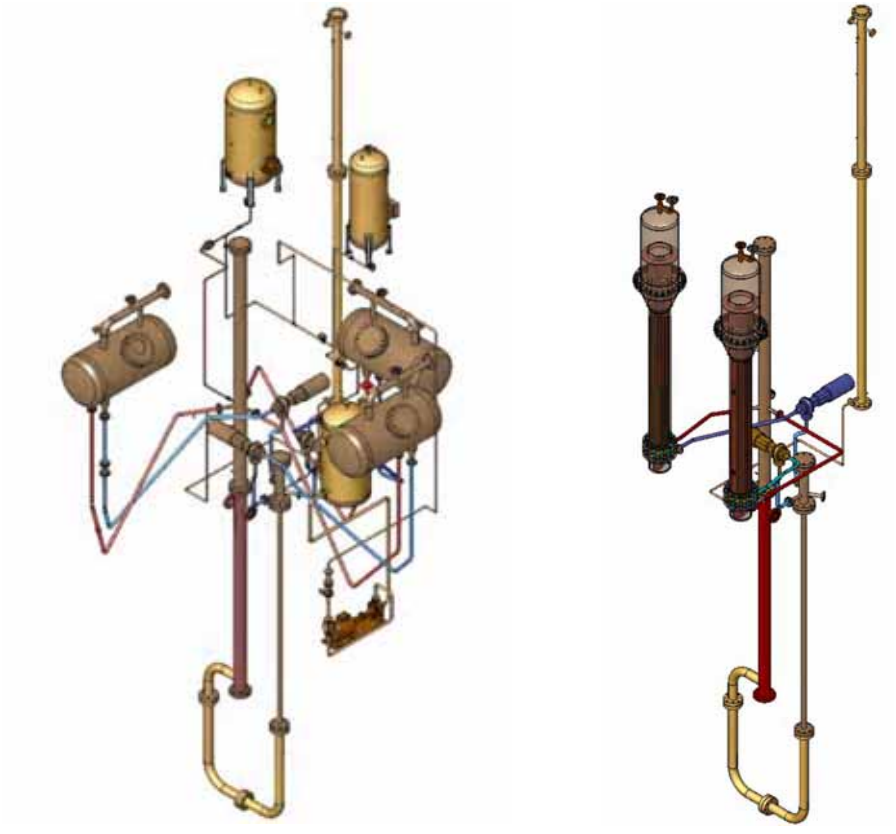

Figure 1. Views of VVER- and PWR-PACTEL facilities.

TRACE code modeling of VVER PACTEL facility

The TRACE modeling of the VVER-PACTEL is based to the guidelines on the earlier RELAP5 model. Since the RELAP5 and TRACE codes are not alike structured the transfer from RELAP5 to TRACE was not straightforward. The model geometry had to be re-evaluated and re-checked for the TRACE code configuration.

The primary side model of VVER-PACTEL consists of pressure vessel part modeled with U-shape piping and three primary loops modeled individually since they have geometry differences. Main circulation pumps and closing valves are also modeled. The upper plenum of the facility is modeled with two parallel pipes connected together with single junctions. This represents the diffusor structure, which consists of two nested concentric pipes in real facility.

Pressurizer is modeled using standard pipe component. The core section is divided in three parallel lines and the heat production in core as well as in pressurizer heaters is implemented with POWER components, which can be controlled with time dependant functions and trips. The primary tube bank in each horizontal steam generators is divided in eight rows. Three top rows represent one tube row of real PACTEL facility. Other tube rows represent two rows of real facility. Secondary side is divided in riser and downcomer sections. The top part of steam generator is modeled with separator component. The drainage outlet for the inventory reduction tests was implemented to the bottom of lower plenum. The break set-up, which was used in small break LOCA experiments was also modeled and placed to the end of cold leg 2 near downcomer. All necessary Emergency Core Cooling Systems (ECCS) were also modeled including high and low pressure injections systems (HP/LPIS) containing models of two hydro accumulators. Figure 2 presents the main view of the graphical set-up of the VVER-PACTEL created with SNAP model editor showing the loop-1 connected to the pressurizer and steam generator. Figure 3 presents the SNAP view of break set-up and the two hydro accumulators with the injection lines.

TRACE calculations of pressure and heat losses

The TRACE model of PACTEL was validated against pressure loss tests. Several PACTEL experiments have been performed to determine the pressure losses over the whole test loop both for normal and for reverse flow direction. Main parts of the facility, three primary circuits, a pressure vessel and a pressurizer surge line, were all measured separately. The model correspondence was then checked in all measured mass flow data points. The calculated results agreed well with experiment data in most cases.

Primary heat losses of the PACTEL facility were defined using the heat-up and cool-down method [4]. The model of TRACE code was modified for specific initial conditions. The secondary side of steam generators was filled with air in atmospheric pressure to minimize the heat transfer via steam generators. Only the steady state period and cooling down phases were simulated. The heat losses were adjusted by modifying the thermal conductivity of the mineral wool and the heat transfer coefficient at outer surface.

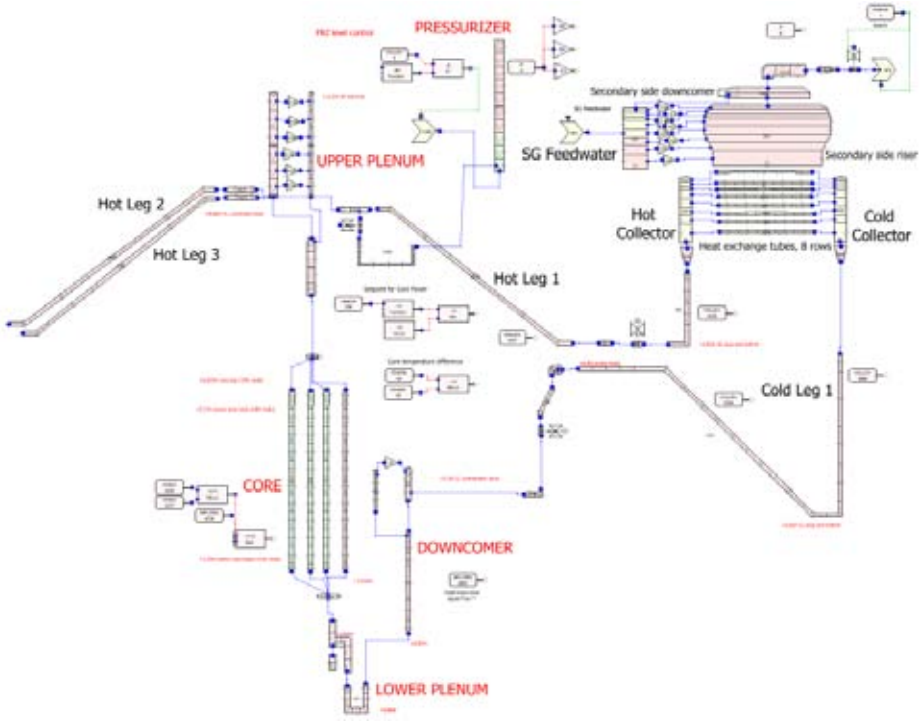

Figure 2. Main view of the VVER-PACTEL facility model by SNAP editor.

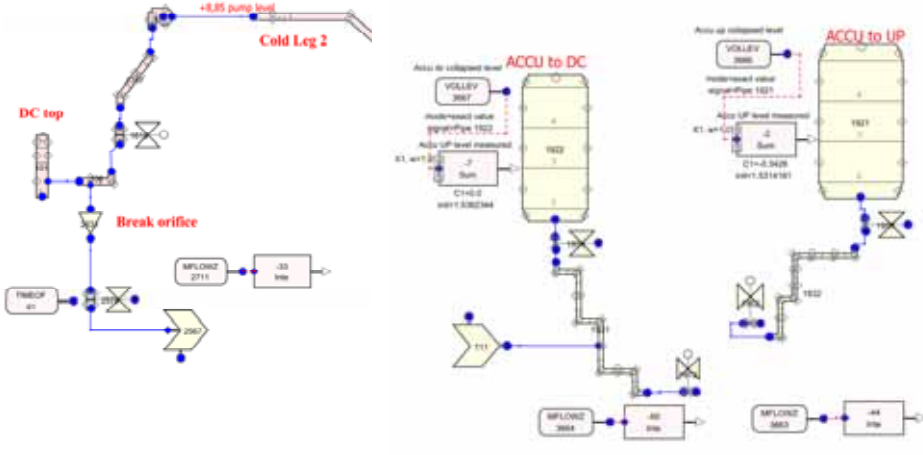

Figure 3. Break set up (left) and hydro accumulators (right) by SNAP editor.

TRACE calculations of VVER PACTEL experiments

After reaching reasonable accuracy with the heat losses calculations were continued. The next case was to calculate loss-of-feedwater experiment LOF-10 [4, 5]. This case had earlier been calculated and reported as stand-alone case [6, 7]. The objective of this calculation was to check the behavior of the steam generator model in transient case. The calculation results showed that the code is capable to model the behavior of horizontal steam generator also in natural circulation mode. Figure 4 presents the collapsed level trends with different tube bank models of the steam generator. It was found that it is necessary to model the tube bank with eight rows in order to achieve accurate result in collapsed level behavior.

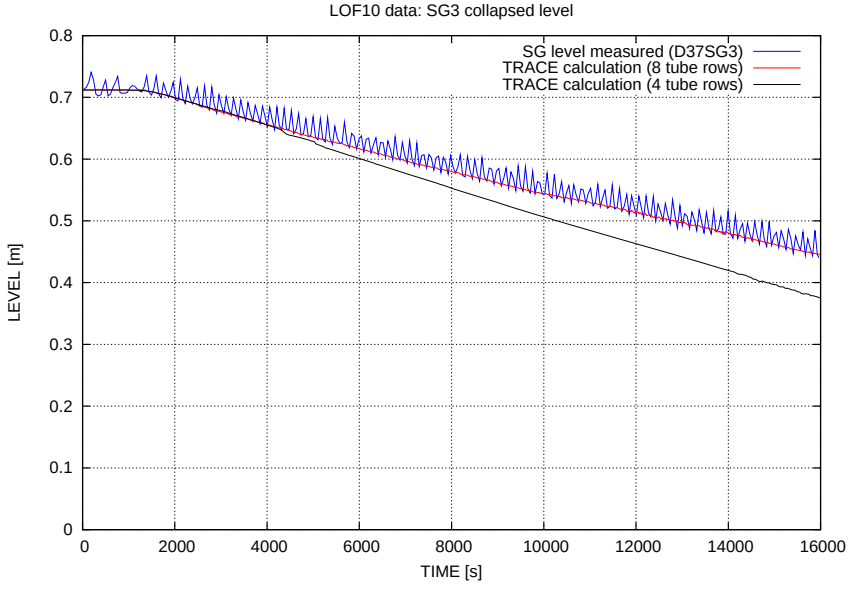

Figure 4. Measured and calculated collapsed level in steam generator. Experiment LOF-10.

The VVER PACTEL experiments chosen as validation cases were two stepwise inventory reduction (SIR) experiments and four small break LOCA (SBL) situations including natural circulation, which enlighten the VVER-specific features like loop seal effect. In small break LOCA cases the diameter of break size alternated from 1 mm to 7.8 mm. Table 1 presents the calculated VVER PACTEL experiments. In experiments SIR-21 and SIR-23 only one of the three primary-side loops of the PACTEL facility (loop 3) was used. Valves isolated other two loops. The

experiment procedure was similar in both cases. The experiment SIR-23 was carried out at nominal PACTEL pressures and experiment SIR-21 at lower pressures.

In all SBL and in IMP06 (IMPAM VVER T2.3) experiments, all three loops of the PACTEL facility were in use. The main circulation pumps were running during the steady state period except of the SBL-30 experiment, which ran in natural circulation during whole recording period. In experiments SBL-31, SBL-33 and IMP06 the accumulators were in operation. In SBL-31 and -33, the accumulators were filled with water to a predetermined level and pressurized with N_2 gas to 5.5 MPa.

Table 1. VVER-PACTEL experiments calculated with the TRACE code.

Experiment	**Break size/type**	**Objectives and conditions**
SIR-23	Stepwise primary inventory reduction	Natural circulation, 75 bar/ 42 bar , 115 kW
SIR-21	Stepwise primary inventory reduction	Natural circulation, 16 bar / 3 bar, 115 kW
SBL-30	Ø 1.0 mm, 0.04%	Behavior of steam generators, pressurizer isolated, 75 bar / 42 bar, 160 kW
SBL-31	Ø 2.5 mm, 0.22%	Testing of ACCU performance and secondary side feed and bleed
SBL-33	Ø 3.5 mm, 0.44%	Boron dilution mechanism, ACCUs, HPIS and secondary feed and bleed
IMPAM-VVER T2.3 (IMP06)	Ø 7.8 mm, 2.19%	Core power 940 kW (steady state). Decay power curve (transient). Lowered ACCU setpoint pressure and initiation of LPIS

Water in the accumulator, which injected to upper plenum, was heated up to 105°C. In experiment IMP06 both accumulators contained cold water (25°C) and pressure was reduced to 3.5 MPa. Figures 5, 6 and 7 present the pressure behavior in experiments: SBL-30, SBL-31 and IMP06 (IMPAM VVER T2.3). In SIR-calculations TRACE overestimated the primary side pressures occasionally. This discrepancy also took place in SBL-30. In calculation of IMP06 experiment the break size was the largest of the validated cases. Due to this very small value had to be set for the maximum time step. Very often, the calculations terminated before reaching the end time of experiment (2 500 s). Hence, the computing time for this calculation case was rather long.

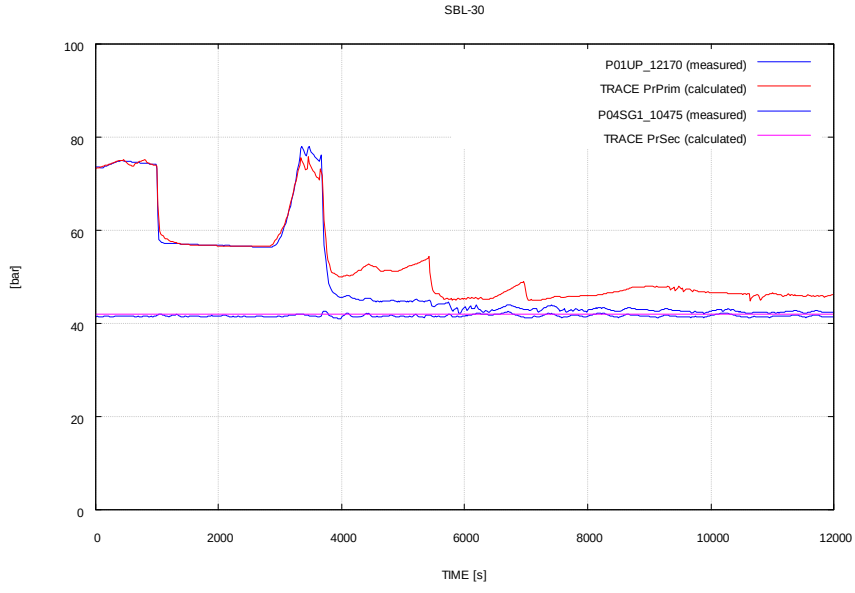

Figure 5. Measured and calculated primary side pressure in PACTEL Experiment SBL-30.

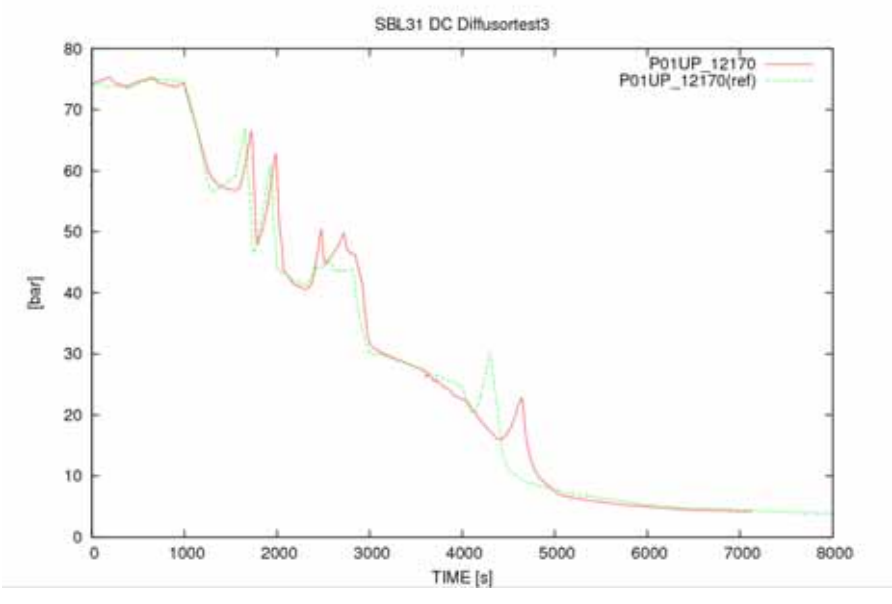

Figure 6. Measured and calculated primary side pressure in PACTEL experiment SBL-31.

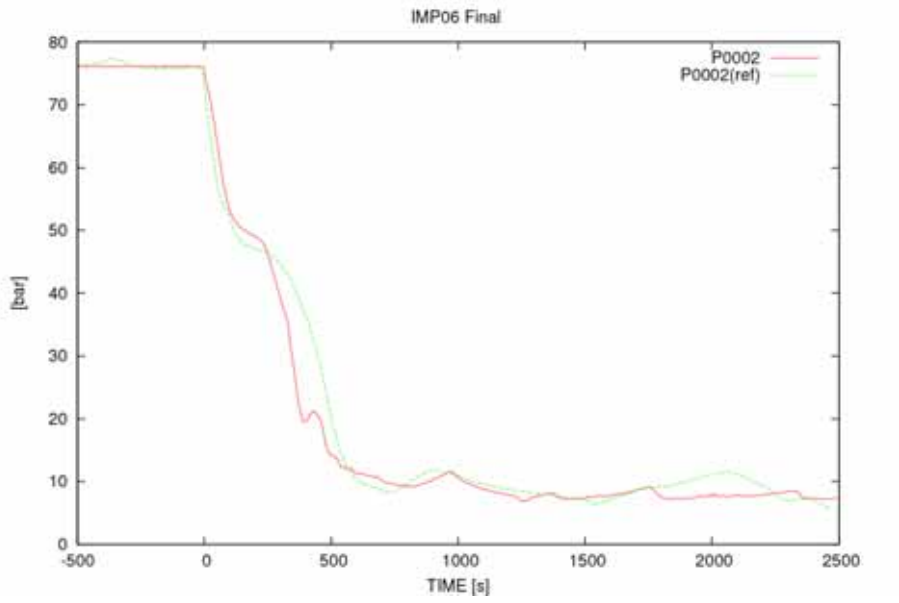

Figure 7. Measured and calculated primary side pressure in PACTEL experiment IMP06.

Modeling of PWR PACTEL facility

The main goal of this work was to create a TRACE model of PWR PACTEL with vertical steam generators and new loops. The vertical steam generators and new loops were then connected to the vessel section of the VVER PACTEL TRACE model. SNAP was used to create the model. The model consists of primary and secondary side. There is also a simple control system modeled which controls feedwater mass flow. The model is quite accurate description of the actual steam generator. Hence, the amount of the nodes is quite high deriving from high instrumentation rate in steam generator. The basic idea in modeling was to preserve the height and the volume in the model. The most used component in the model is a pipe component. Although flow channels are not always circular, pipe component can be easily used. SNAP view of the PWR PACTEL facility model is presented in Figure 8.

Primary side

Primary side consists of loops, collectors and U-shaped heat exchange tubes. Hot and cold loops were modeled with pipe components and there are no simplifications with them. The hot and cold collectors were modeled with pipe

components which have only one cell. Although collector is not a circular tube, average flow area and hydraulic diameter must be calculated. The length of the collector in the model is not exactly the same as in reality because of the elevation of connection loop. Loop is connected to the side conjunction of collector cell so then the connection elevation is the half of the length of collector. Then, the loop connection elevation is kept the same as in reality. Heat exchange tubes can be categorized to five groups by their length but if one wants to be accurate there is actually ten different groups – ten different lengths. This derives from the triangular pitch which causes small length difference. The tube bank consists of five heat exchange tube groups. Nodalization of heat exchange tubes follows locations of temperature sensors in tubes.

Secondary side

The secondary side consists of feedwater line, downcomer, riser, steam dome and steam outlet. Inlet of feedwater is modeled with a fill component, which is basically a velocity inlet. Mass flow is controlled with a level controller component. Feedwater pipe is modeled with a pipe component and it's connected to the cold side of the downcomer. Downcomer section is divided into hot and cold parts. Cold downcomer brings the feedwater flow downwards. Hot downcomer brings the condensation water from steam dome walls down through holes. Hot downcomer is connected from up to the steam dome and from down to hot riser. Cold downcomer is connected to the feedwater line and to the cold riser. Riser part consists of five pipe components: hot and cold riser, the section where U-tube's ends and the section without tubes.

TRACE calculations of PWR PACTEL experiments

The first calculations were made with stand alone steam generator with velocity inlet and pressure outlet boundaries at primary inlet and outlet. The results showed that the model is working properly. Then the steam generator model was connected to the basic PACTEL model with new primary loops. The functionality was tested and found to be satisfactory. The calculations for achieving steady state showed that model is stable.

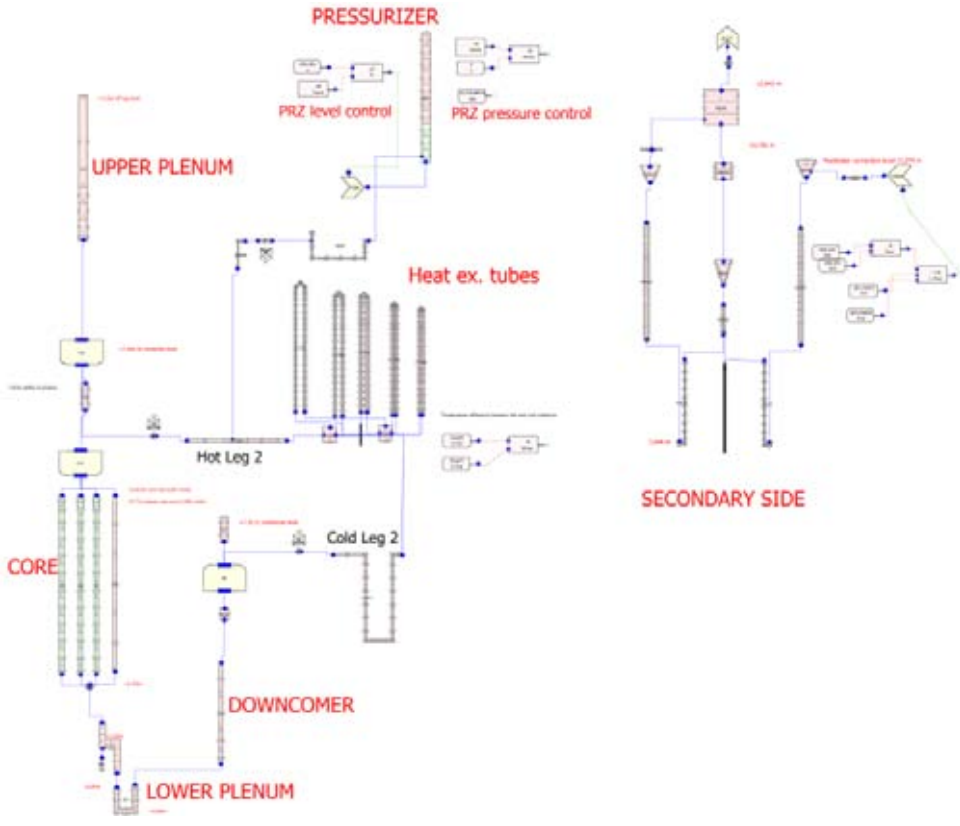

Figure 8. Main view of the PWR PACTEL facility model by SNAP editor.

The TRACE model of the PWR PACTEL test facility has been used to simulate PWR PACTEL characterizing experiments: LOF-20, SIR-31 and SBL-50 experiments. The initial conditions of the simulated experiments are presented in Table 2. All main phenomena, which took place in the experiments, were found also in the simulations. Due to ongoing benchmark on PWR PACTEL facility the information about the experiment or calculation results is restricted at the moment.

Table 2. Initial conditions in PWR PACTEL experiments.

Parameter	**Experiment**		
	LOF-20	**SBL-50**	**SIR-31**
Core power [kW]	105 ± 6	155 ± 6	115 ± 6
The primary pressure [bar]	75 ± 1	75 ± 1	75 ± 1
Secondary pressure [bar]	40.0 ± 0.6	42.0 ± 0.6	42.0 ± 0.6
Steam generator collapsed level	3.79 ± 0.12	3.9 ± 0.12	3.9 ± 0.12
Loop mass flow rate [kg/s]	0.74 ± 0.14	0.6 ± 0.14	0.75 ± 0.14
Remarks	One loop, with pressurizer	Two loops, no pressurizer	One loop, no pressurizer

Applications

The PACSIM project has produced TRACE code calculation models for VVER and PWR PACTEL facilities. The models will be used directly to the continuous research work. The models can be used for calculating the existing VVER-experiments and therefore are useful for validating the TRACE code towards full-plant VVER-model. The PWR PACTEL model is useful for calculating the experiments and can be compared to the results calculated with Apros code. This gives good basis for the PWR PACTEL to become an international project.

Conclusions

In the frame of PACSIM project at LUT new models for VVER- and PWR-PACTEL facilities have been introduced using TRACE thermal hydraulic system code with SNAP graphical tool. The VVER-PACTEL model was constructed to cover all main parts of primary and secondary sides of the facility. The functionality of the model was tested with calculations of pressure and heat loss experiments. Six experiments were chosen for validation calculations. The calculation results showed that the code is capable to model the behavior of horizontal steam generator also in natural circulation mode. The PWR-PACTEL model was also prepared. The model was tested and three experiments were calculated. The calculation results were showed rather good agreement with the experiments.

References

1. Tuunanen, J., Kouhia, J., Purhonen, H., Riikonen, V., Puustinen, M., Semken, S., Partanen, H., Saure, I. & Pylkkö, H. General description of the PACTEL test facility. VTT, Espoo, 1998. VTT Tiedotteita - Research Notes 1929. 35 p. + app. 74 p. ISBN 951-38-5338-1; 951-38-5339-X. http://www.vtt.fi/inf/pdf/tiedotteet/1998/T1929.pdf.

2. Kouhia, J. & Puustinen, M. Pressure loss tests at PACTEL test loop. Technical Report TOKE 7/99, VTT Energy, 1999.

3. Sanders, J. Methods of Heat Loss Measurement for a thermohydraulic Facility. Experimental Heat Transfer 1991, Vol. 4, pp. 127–151.

4. Kouhia, J. & Puustinen, M. Experimental Data Report on LOF-10. VTT Energy, Technical Report TEKOJA 7/98. 11.12.1998.

5. Riikonen, V. RELAP5/MOD3.1 Analysis of the PACTEL Loss of Secondary Side Feed Water Experiment, VTT Energy Technical Report, PROPA 8/94, 25.10.1994.

6. Vihavainen, J. International Agreement Report: An Assessment of TRACE V4.160 Code Against PACTEL LOF-10 Experiment, 2010. U.S. Nuclear Regulatory Commission, NUREG/IA-0237. 29 p. + app. 6 p.

7. Vihavainen, J., Riikonen, V. & Kyrki-Rajamäki, R. TRACE code modeling of the horizontal steam generator of the PACTEL facility and calculation of a loss-of-feedwater experiment. Annals of Nuclear Energy 2010, Vol. 37, No. 11, pp. 1494–1501.

8. TRACE V5.0 User's Manual. Vol. 1: Input Specification. Input Specification. 2005. USNRC, Division of System Analysis and Regulatory Effectiveness. Washington DC. 642 p.

15. Condensation Experiments with PPOOLEX Facility (CONDEX)

15.1 CONDEX summary report

Markku Puustinen, Jani Laine, Vesa Tanskanen,
Antti Räsänen and Heikki Purhonen
Lappeenranta University of Technology

Abstract

Experiments with the PPOOLEX facility in the CONDEX project focused on studying different phenomena occurring in the dry well and wet well compartments of a scaled down Boiling Water Reactor (BWR) containment volume during gas/steam discharge. In a BWR power generation system, the wet well pool serves as the major heat sink for condensation of steam in case of a primary system blowdown from a pipe break, or in case of a dedicated steam venting of the primary system. Experiments on the initial phase of a postulated steam line rupture, thermal stratification and mixing processes in the water pool, wall condensation in the dry well, dynamic loading of the pool structures, modified blowdown pipe outlet designs and the behavior of parallel blowdown pipes were carried out with a scaled down test facility designed and constructed at Lappeenranta University of Technology (LUT). Sophisticated high frequency instrumentation techniques were utilized to record measurement data from the water pool, dry well and inside the blowdown pipe(s). High-speed video cameras were used to capture the details of gas/steam bubble behavior and condensation processes at the outlet of the blowdown pipe(s).

The experiment results of the CONDEX project are of benefit mainly to the developers of simulation codes. Computational fluid dynamics (CFD) calculations at VTT in the NUMPOOL project on wall condensation, direct contact condensation (DCC) and parallel pipe behavior were compared to the PPOOLEX experiments. Furthermore, the coupling of CFD and structural analysis codes in solving fluid-structure interactions (FSI) was facilitated with the aid of load measurements during rapid condensation. Experiments on thermal stratification and mixing processes were used for the verification of the models of GOTHIC code at Kunliga Tekniska Högskolan (KTH) via co-operation in the NORTHNET and NKS frameworks. Also APROS code was used in the simulation of the stratification experiments at VTT in the THARE project.

Introduction

The common feature of current BWRs is the use of large condensation pools with a venting system for the mitigation of the immediate consequences of a conceivable Large Break Loss-of-Coolant Accident (LBLOCA) such as a main steam line break. Also, in certain advanced light water reactor concepts, during emergency cooling conditions, mixtures of steam and non-condensable gas are blown into a pool of water via an open pipe. In both cases, steam/gas bubbles form at the pipe exit, start to rise and then condense or break up to smaller bubbles. Pressure pulses generated by the collapse of steam bubbles due to rapid condensation, either at the pipe outlet or inside the pipe, may cause considerable loads or even damage when they impact upon a structure.

To achieve the CONDEX project objectives, a combined experimental/ computational program was carried out. Experimental part (LUT) of the project was responsible for the development of an experimental database on condensation pool dynamics and heat transfer at well controlled conditions and with the help of sophisticated, high frequency measurement instrumentation and high-speed video cameras [1, 2, 3, 4, 5, 6, 7, 8, 9]. Analytical/computational part (VTT, KTH) used the experimental database for the development, improvement and validation of the models and numerical simulation tools including CFD and system codes [10, 11, 12]. Also analytical support was provided for the experimental part by pre- and post-calculations of the experiments. LUT and VTT also co-operated closely in the numerical modeling of the experiments through participation in the EU/NURESIM and EU/NURISP projects, where models for

direct-contact condensation to be used in NEPTUNE_CFD and TransAT codes are being developed [13, 14, 15, 16].

Experimental work in the CONDEX project was carried out in the PPOOLEX test facility (Figure 1). It consists of a wet well compartment (condensation pool), dry well compartment, inlet plenum and air/steam line piping. The main component of the facility is the ~31 m^3 cylindrical test vessel, 7.45 m in height and 2.4 m in diameter. The facility is able to withstand considerable structural loads caused by rapid condensation of steam. The dry well and wet well volumes of the facility are scaled down according to the volumes of the corresponding compartments of the reference (Olkiluoto) plant. Steam needed during the experiments is generated with the nearby PACTEL test facility [17].

During the project the PPOOLEX facility was modified according to the needs of the individual experiment series. For example, a second parallel blowdown pipe was manufactured, the dry well compartment was thermally insulated and a collecting system for condensate was constructed. Furthermore, instrumentation and data acquisition were improved and updated on a regular basis.

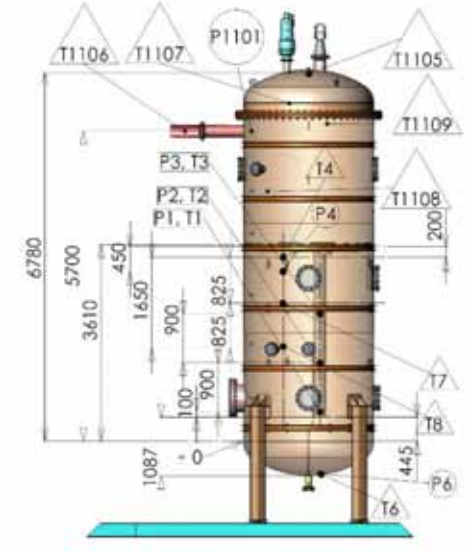

Figure 1. PPOOLEX test facility.

Main objectives

The goal of the project was to improve understanding and increase fidelity in quantification of different phenomena in BWR containment during steam discharge.

These phenomena could be connected, for example, to bubble dynamics, DCC and pressure oscillations. Thermal stratification and mixing in the pool were also of interest.

The main objective of the PPOOLEX experiments was the production of measurement data to be used for different verification purposes. Load estimation, structural analysis, fluid-structure interactions, thermal stratification and mixing processes and models of wall condensation and direct contact condensation are, for example, research areas where the data produced in the CONDEX project can be utilized. Valuable co-operation between the thermal hydraulics, numerical simulation and structural analysis branches of the SAFIR2010 research programme was created and strengthened.

Characterizing experiments

The test program with the PPOOLEX facility accompanied by numerical modeling work started in 2007 by conducting a series of characterizing experiments with gas/steam discharge through the dry well compartment into the condensation pool and by simulating the gas experiments with CFD at VTT and LUT. Figure 2 illustrates the air and steam supply system used in the experiments.

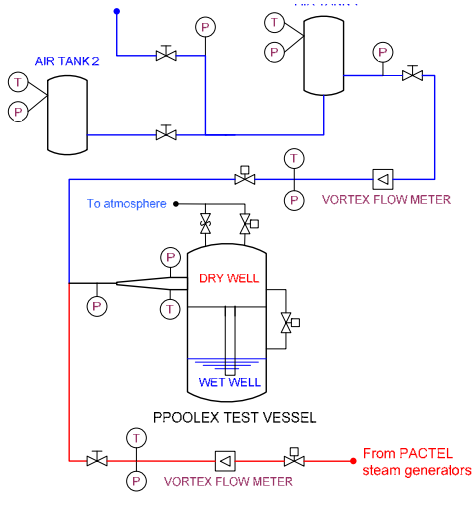

Figure 2. Arrangement of air and steam supply in the PPOOLEX facility.

Heat-up by several tens of degrees due to compression in the dry well compartment and in the gas space of the wet well compartment occurred. Temperatures also stratified strongly (Figure 3).

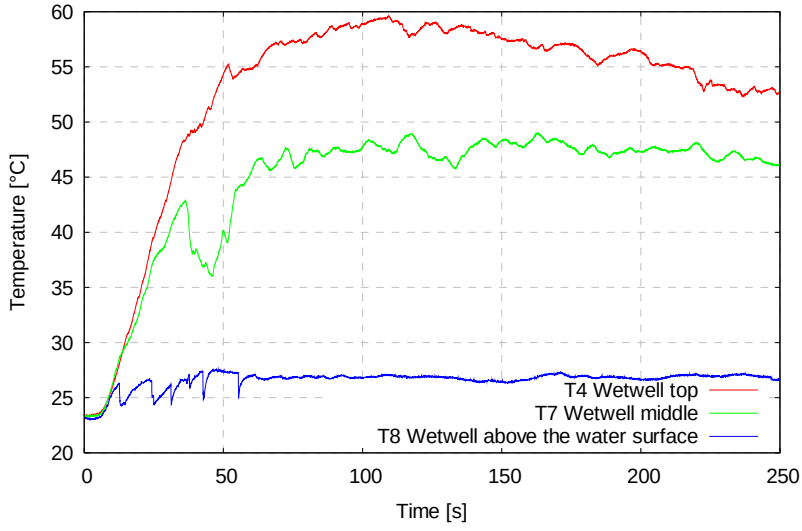

Figure 3. Stratification of temperatures in the wet well gas space during an air discharge test.

Condensation oscillations and chugging phenomenon were encountered in those tests where the fraction of non-condensables had time to decrease significantly. A radical change from smooth condensation behavior to oscillating one occurred quite abruptly when the air fraction in the blowdown pipe flow dropped close to zero (Figure 4).

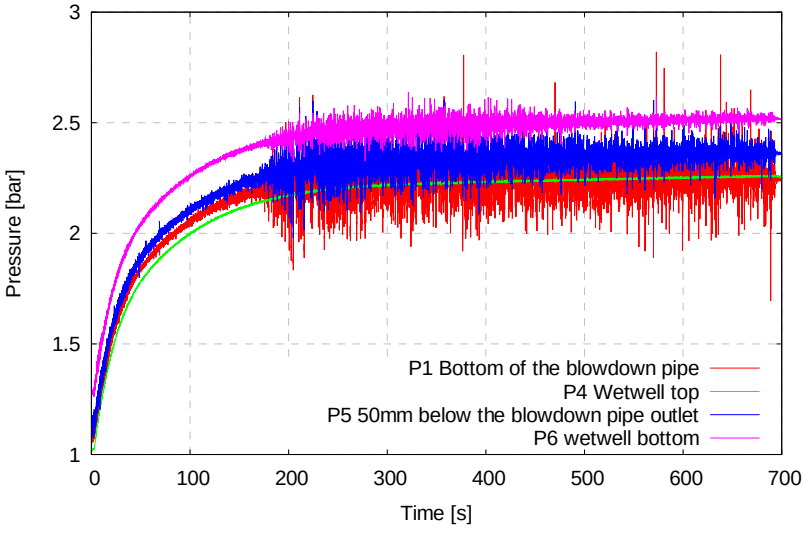

Figure 4. Radical change from smooth condensation to oscillating one as the air fraction of flow drops close to zero during discharge of steam/air mixture.

Thermal stratification and mixing

Thermal stratification and mixing were examined in two experiment series, first in 2008 and again in 2010. The objective was to study thermohydraulic loading of the wet well structures due to stratification processes as well as to produce comparison data for evaluating the capability of GOTHIC and APROS codes to predict stratification and mixing phenomena. A group of thermocouples arranged in a vertical line was added to the pool volume in order to capture the thickness of the stratification layers.

Strong thermal stratification was quite easily achieved during the first half of the experiments by using small steam flow rates (Figure 5). Total mixing of the pool volume could not be achieved in any experiment with those flow rates available in the test facility. The bottom layers heated up significantly during the increasing flow rate period but never reached the same temperature level as the topmost layers (Figure 6).

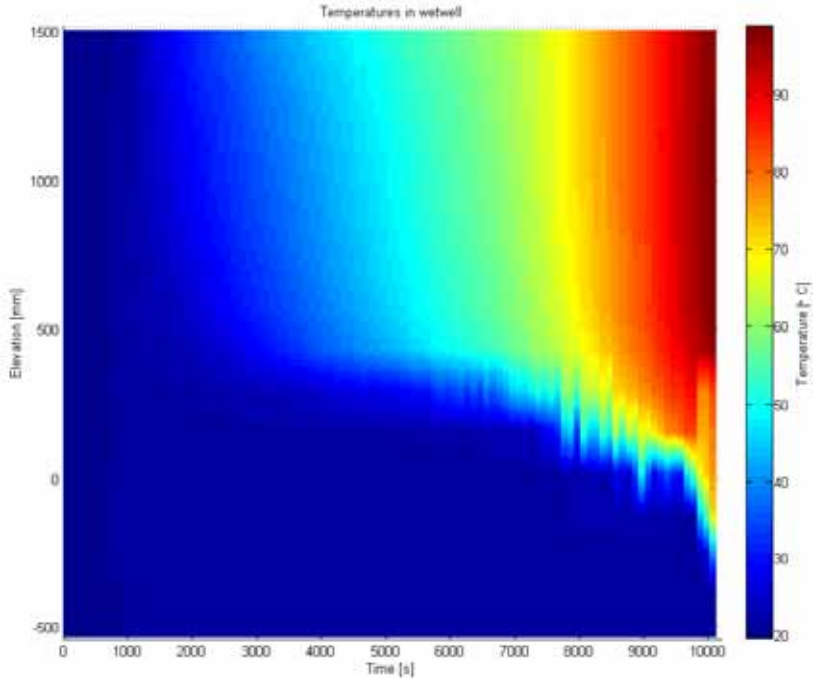

Figure 5. Development of vertical temperature distribution in the wet well pool in STR-08 test.

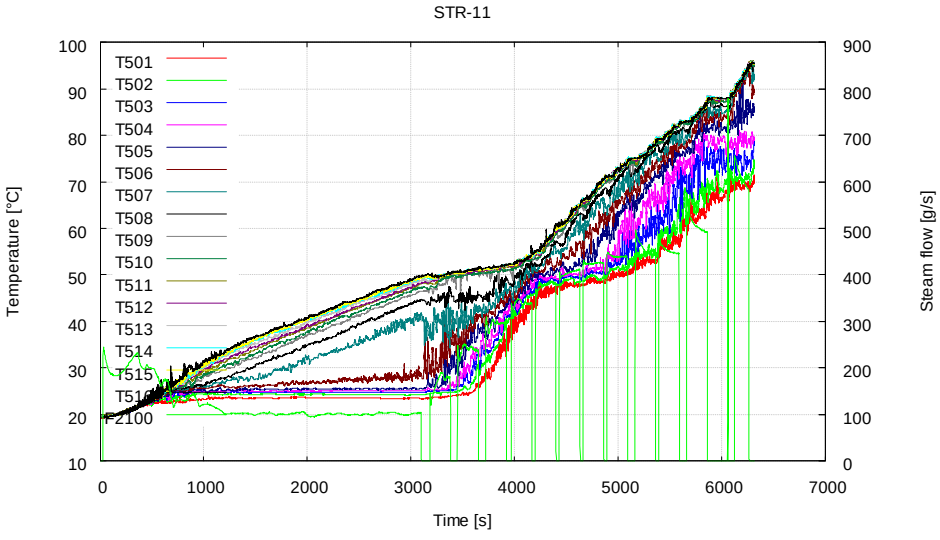

Figure 6. Temperatures in the wet well pool and steam flow in STR-11.

Wall condensation experiments

Calculation models related to steam condensation in the dry well must be improved before proceeding to the simulation of the whole containment system. For that reason, a series of wall condensation experiments was carried out. The experiments aimed at estimating the amount of condensate produced with different flow rates and pre-heating levels of the dry well structures. A system for collecting and measuring the amount of condensate from four different wall segments of the dry well compartment was installed before the experiments. In Figure 7, accumulation of condensate in the collection tanks is shown when the experiment was started without pre-heating the wall structures.

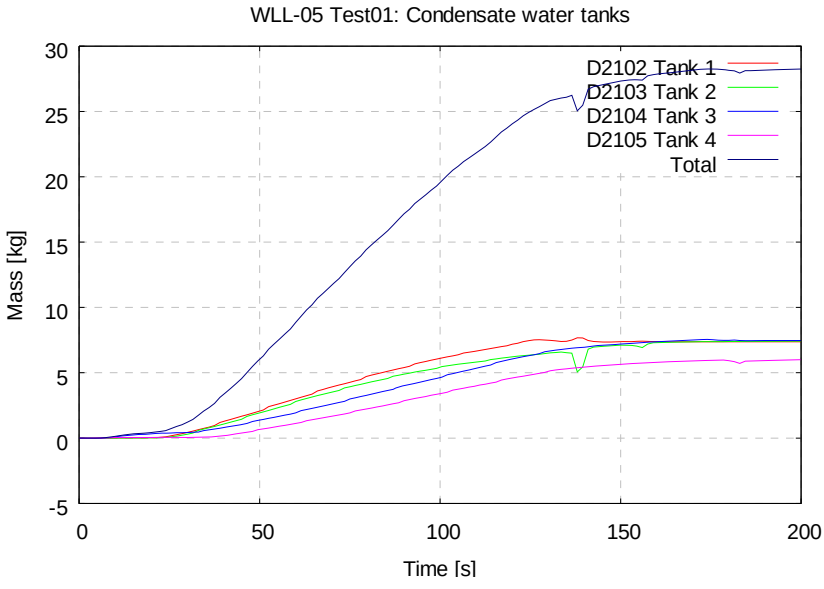

Figure 7. Accumulation of condensate in a wall condensation experiment when pre-heating of the dry well wall was not used. Steam discharge stopped at 120 seconds.

Effect of a modified blowdown pipe outlet

The effect of a blowdown pipe outlet collar design (Forsmark type) on loads caused by chugging phenomena (rapid condensation) was investigated in the COL experiments. With 20–25°C pool water up to 10 times higher pressure pulses were measured inside the blowdown pipe in the case of a straight pipe than with a collar (Figure 8). In this respect, the collar design worked as planned and removed the high pressure spikes from the blowdown pipe. Meanwhile, there seemed to be no suppressing effect on the loads due to the collar in the pool side.

Dynamic loading of pool structures

The main purpose of the DYN experiment series was to study dynamic loads caused to pool structures by different condensation modes. Steam was blown into the dry well compartment and from there through the DN200 vertical blowdown pipe to the condensation pool filled with sub-cooled water. The initial temperature of the pool water varied from 11°C to 63°C, the steam flow rate from 290 g/s to 1 220 g/s and the temperature of incoming steam from 132°C to

182°C. Non-condensables were pushed from the dry well into the gas space of the wet well with a short discharge of steam before the recorded period of the experiments.

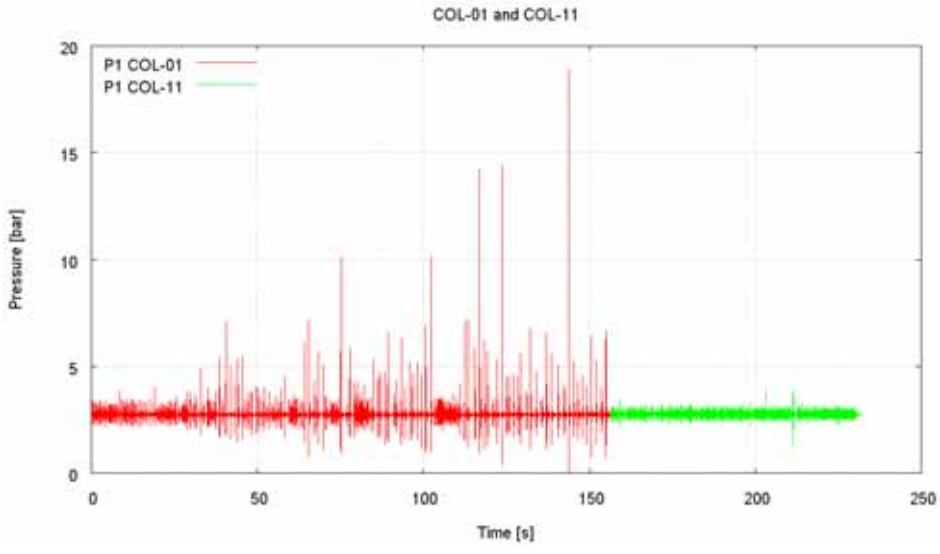

Figure 8. Pressure behavior inside the blowdown pipe with (green line) and without (red line) the collar at the pipe outlet during equal steam flow rate.

The loads experienced by the condensation pool structures depended strongly on the steam mass flow rate, pool water temperature and system pressure. The DYN experiments indicated that chugging and condensation within the blowdown pipe cause significant dynamic loads in case of strongly sub-cooled pool water (Figure 9). The level of pool water temperature is decisive. High individual pressure pulses (and loads) were missing with increased temperature and the oscillations were continuous in nature and their amplitude was almost constant.

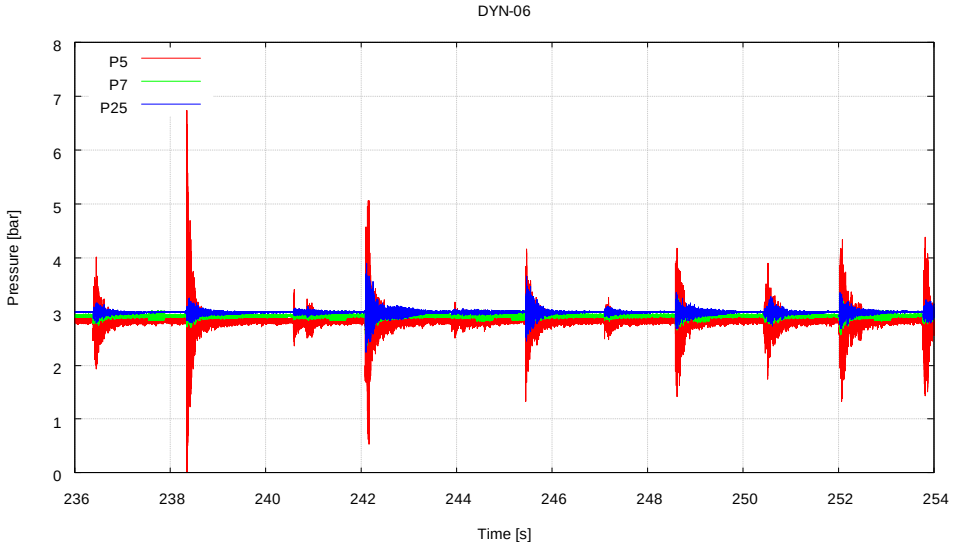

Figure 9. Pressure loads in the condensation pool during the discharge of steam into strongly sub-cooled water.

NEPTUNE_CFD simulations

The 3D simulations of the POOLEX STB-28-4 experiment with NEPTUNE_CFD_1.0.7 by using a light “merged” mesh proved better convergence than the earlier 2D-axisymmetric and 3D simulations (Figures 10 and 11). The qualitative behavior of bubble formation was promising but outstanding sensitivity to the initial location of the steam/water interface was observed. The initial turbulence level seems to be the most crucial parameter. To invoke mixing and thus developed turbulence field, few vigorous chugging cycles may be needed in the simulation. Regarding the bubble size and collapse time, e.g. the Hughes-Duffey condensation model [18] seemed to be capable to provide realistic condensation rates during the chugging mode, if the initial condition of simulation leads to mixing strong enough.

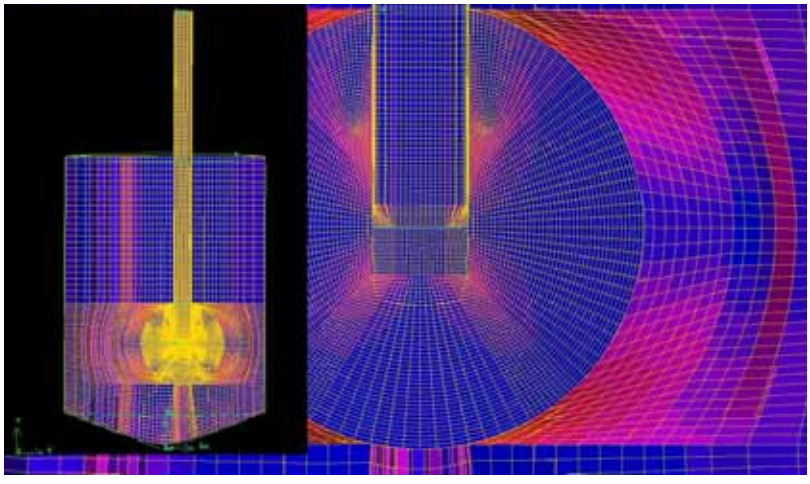

Figure 10. Merged 3D grid with spherical grid around the bubble eruption region.

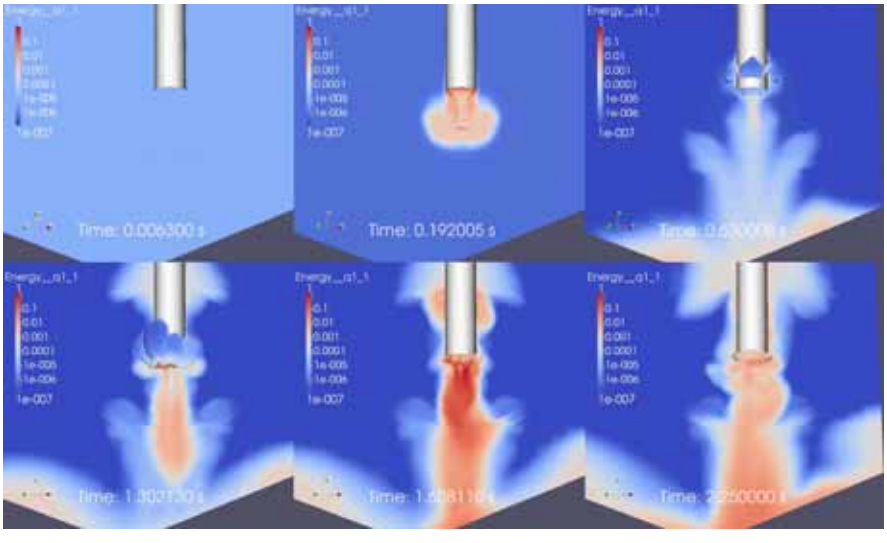

Figure 11. Turbulence kinetic energy in NEPTUNE_CFD simulation of the STB-28 experiment. Hughes-Duffey (1991) DCC model with initial surface set inside the pipe.

Applications

Using the information gained in the experiments can directly solve certain open questions of suppression pool related safety systems in existing BWRs. Additional

benefit from the project will be achieved through the use of the test results in developing and validating CFD and system codes for nuclear safety analysis. The connections of thermal hydraulics and structural loads have been studied in real conditions. The project outcome will allow the end users to analyze the safety risk of pool operation threatened by dynamic loading of DCC and quasi-static loading due to thermal stratification. More reliable prediction of condensation pool behavior based on combined CFD and structural analysis codes validated against experimental data can be directly utilized in the safety analysis of the Nordic power plants and thus improve the safety of their operation. Being part of the SAFIR2010 and NORTHNET RM3 research programs the CONDEX project has given an excellent forum for the international exchange of knowledge and experience including the Finnish and Swedish BWR operators.

Conclusions

The CONDEX project focused on studying phenomena occurring in different compartments of a scaled down BWR containment volume when steam/gas mixture was blown through dry well into a wet well water pool.

Condensation oscillations and chugging phenomenon were encountered in the tests where the fraction of non-condensables had time to decrease significantly. A radical change from smooth condensation behavior to oscillating one with pressure pulses occurred quite abruptly when the air fraction of the blowdown pipe flow dropped close to zero. The experiments demonstrated the strong diminishing effect that non-condensable gases among the flow have on dynamic unsteady loadings experienced by submerged pool structures.

In the thermal stratification and mixing experiments a large difference between the pool bottom and top layer temperatures was measured when small steam flow rates were used. No total mixing of the pool volume could be achieved in any of the experiments with those flow rates available in the PPOOLEX test facility.

A collar design at the blowdown pipe outlet removed the high pressure spikes from inside the pipe but no suppressing effect was observed in the pool side. Partly contradictory results were obtained. Further experiments on the issue are needed.

The DYN experiments indicated that chugging and condensation within the blowdown pipe cause significant dynamic loads in case of strongly sub-cooled pool water. The level of pool water temperature was decisive.

The project improved understanding and increased fidelity in quantification of the condensation pool behavior under plant's transient and accident conditions. Particularly, direct contact condensation and consequent chugging phenomena and thermal stratification and mixing were extensively studied.

A large database containing the results of the air/steam discharge experiments was generated. It can be used for testing and developing calculation methods used for nuclear safety analysis.

References

1. Puustinen, M. & Laine, J. Characterizing Experiments of the PPOOLEX Test Facility. LUT, Lappeenranta, 2008. Research Report CONDEX 1/2007.

2. Laine, J. & Puustinen, M. Steam Line Rupture Experiment with the PPOOLEX Test Facility. LUT, Lappeenranta, 2008. Research Report CONDEX 2/2007.

3. Puustinen, M., Laine, J. & Räsänen, A. PPOOLEX Experiments on Thermal Stratification and Mixing. LUT, Lappeenranta, 2009. Research Report CONDEX 1/2008.

4. Laine, J. & Puustinen, M., Räsänen, A. PPOOLEX Experiments with a Modified Blowdown Pipe Outlet. LUT, Lappeenranta, 2009. Research Report CONDEX 2/2008.

5. Laine, J. & Puustinen, M. PPOOLEX Experiments on Wall Condensation. LUT, Lappeenranta, 2009. Research Report CONDEX 3/2008.

6. Puustinen, M., Laine, J. & Räsänen, A. PPOOLEX Experiments with Two Parallel Blowdown Pipes. LUT, Lappeenranta, 2010. Research Report CONDEX 1/2009.

7. Puustinen, M., Laine, J. & Räsänen, A. PPOOLEX Experiments on Dynamic Loading with Pressure Feedback. LUT, Lappeenranta, 2010. Research Report CONDEX 2/2009.

8. Puustinen, M., Laine, J. & Räsänen, A. PPOOLEX Experiments on Stratification and Mixing in the Wetwell Pool. LUT, Lappeenranta, 2011. Research Report CONDEX 1/2010.

9. Puustinen, M., Laine, J. & Räsänen, A. Multiple Blowdown Pipe Experiments with the PPOOLEX Facility. LUT, Lappeenranta, 2011. Research Report CONDEX 2/2010.

10. Pättikangas, T., Timperi, A., Niemi, J. & Kuutti, J. Modelling of Blowdown of Air in the Pressurized PPOOLEX Facility. VTT, Espoo, 2008. Research Report VTT-R-02233-08.

11. Timperi, A. Fluid-Structure Interaction Calculation Using a Linear Perturbation Method. 20th International Conference on Structural Mechanics in Reactor Technology (SMiRT 20), Espoo, Finland, August 9–14, 2009. Paper 1898.

12. Li, H., Kudinov, P. & Villanueva, W. Condensation, Stratification and Mixing in a BWR Suppression Pool. Stockholm: KTH. 2010. Research Report, NORTHNET Roadmap 3.

13. Tanskanen, V. & Puustinen, M. CFD Simulation of Air Discharge Tests in the PPOOLEX Facility. LUT, Lappeenranta, 2008. Research Report CONDEX 3/2007.

14. Tanskanen, V. & Jordan, A. CFD Simulation of STB-31 Experiment by Using Neptune-CFD and TransAT Codes. LUT, Lappeenranta, 2010. Research Report CONDEX 3/2009.

15. Tanskanen, V. & Jordan, A. 3D CFD Simulation of STB-28 Steam Discharge Experiment. LUT, Lappeenranta, 2011. Research Report CONDEX 3/2010.

16. Tanskanen, V., Lakehal, D. & Puustinen, M. Validation of Direct Contact Condensation CFD Models Against Condensation Pool Experiment. Poster, XCFD4NRS Workshop, Grenoble, France, September 10.–12. 2008.

17. Tuunanen, J., Kouhia, J., Purhonen, H., Riikonen, V., Puustinen, M., Semken, R.S., Partanen, H., Saure, I. & Pylkkö, H. General Description of the PACTEL Test Facility. VTT, Espoo, 1998. VTT Research Notes 1929. 35 p. + app. 74 p. ISBN 951-38-5338-1. http://www.vtt.fi/inf/pdf/tiedotteet/1998/T1929.pdf.

18. Hughes, E.D. & Duffey, R.B. Direct Contact Condensation and Momentum Transfer in Turbulent Separated Flows. International Journal of Multiphase Flow 1991, 17(5), pp. 559–619.

15.2 PPOOLEX tests with two blowdown pipes (CONDEX)

Markku Puustinen, Jani Laine, Antti Räsänen and Heikki Purhonen
Lappeenranta University of Technology

Abstract

An experimental study was performed in the PPOOLEX test facility designed and constructed at Lappeenranta University of Technology (LUT) to investigate chugging phenomena (rapid condensation) while steam is discharged through two parallel blowdown pipes into the condensation pool filled with sub-cooled water. The main objective was to examine if the blowdown pipes behave synchronously or not and to evaluate structural loads due to pressure oscillations and to compare the loads to those in a single blowdown pipe situation. Furthermore, it was studied if the pipe material, polycarbonate, used in the earlier experiment series with two blowdown pipes has had an effect on the general chugging behavior and measured loads. The experiments produced also relevant comparison data for computational fluid dynamics (CFD) calculations at VTT.

The initial temperature of the condensation pool water was 20°C. The steam flow rate ranged from 220 g/s to 2 350 g/s and the temperature of incoming steam from 148°C to 207°C. High pressure loads were measured inside the blowdown pipes due to rapid condensation of the steam volumes in the pipes and resulting water hammer. The formation and collapse of steam bubbles and the movement of the steam/water interface inside the pipes was slightly non-synchronous. The high speed video recordings and high frequency pressure measurements revealed, that at maximum there can be a 70 ms time difference between the occurrence of steam bubble collapses at the outlets of the two pipes. There was no clear pattern in which pipe the steam bubble first started to collapse. Several successive bubbles could collapse first, for example, in pipe 1 but then the order changed for a single or several cycles.

Introduction

During a possible steam line break accident inside the containment a large amount of non-condensable (nitrogen) and condensable (steam) gas is blown

from the upper dry well to the condensation pool through the blowdown pipes in a typical containment design of a Boiling Water Reactor (BWR). The wet well pool serves as the major heat sink for condensation of steam.

Condensation pool issues have been investigated experimentally at LUT within the national Finnish research programs on nuclear power plant safety [1, 2, 3, 4, 5, 6, 7, 8, 9]. Most of the experiments have been conducted with a single blowdown pipe. However, in power plants several parallel blowdown pipes connect the dry well compartment to the wet well pool. These pipes can have an effect on each other which makes the blowdown situation more complicated. For this reason, an experiment series on steam discharge via two parallel blowdown pipes from the dry well into the condensation pool was carried out in the PPOOLEX test facility at LUT.

PPOOLEX test facility

The PPOOLEX facility consists of a wet well compartment (condensation pool), dry well compartment, inlet plenum and air/steam line piping. The main component of the facility is the ~31 m^3 cylindrical test vessel, 7.45 m in height and 2.4 m in diameter. The facility is able to withstand considerable structural loads caused by rapid condensation of steam. The dry well and wet well volumes of the facility are scaled down according to the volumes of the corresponding compartments of the reference (Olkiluoto) plant. Steam needed during the experiments is generated with the nearby PACTEL facility [10]. Sophisticated high frequency measurement techniques and high speed video equipment are used. Table 1 lists the main design features of the PPOOLEX facility.

Table 1. Main design features of the PPOOLEX test facility.

Volume	Total	31.1 m^3
	Dry well compartment	13.3 m^3
	Wet well compartment	17.8 m^3
Test vessel outer diameter		2.4 m
Height	Total	7.45 m
	Dry well compartment	3.18 m
	Wet well compartment	4.27 m
Max. overpressure		0.4 MPa
Max. underpressure		0.05 MPa
Max pressure difference across the intermediate floor		0.2 MPa
Max operating temperature		190°C
Wall thickness	Vessel head	10 mm
	Bottom end	10 mm
	Lowest wall segment	10 mm
	Other wall segments	8 mm
Construction material		Stainless steel (EN1.4301)

The dry well compartment is separated from the condensation pool with a removable floor. Horizontal piping (inlet plenum) for the injection of gas and steam penetrates through the side wall of the dry well compartment. The length of the inlet plenum (DN200) is 2.0 m. A remote-controlled valve in the steam line is used for initiating steam discharge. Six windows allow visual observation of the internals. The dry well compartment is thermally insulated. A sketch of the test vessel is shown in Figure 1.

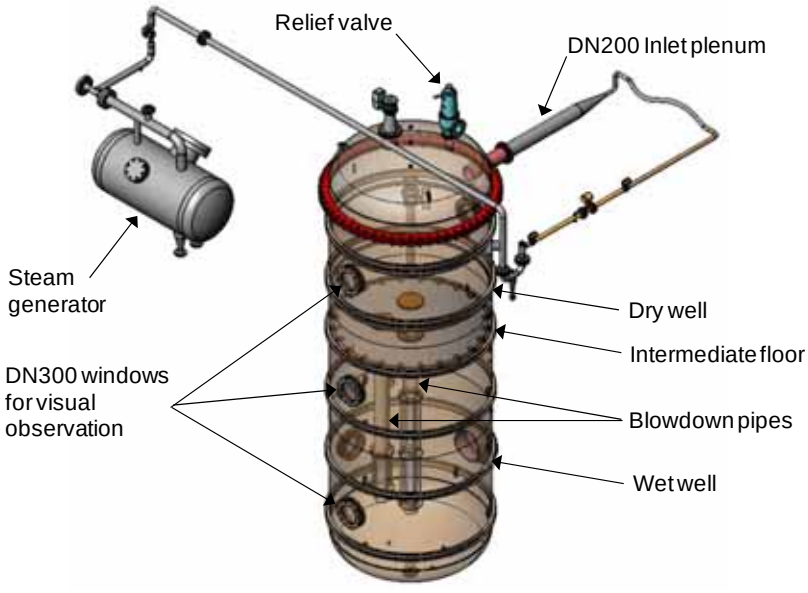

Figure 1. PPOOLEX test vessel.

For the parallel blowdown pipe experiments in 2010 a second blowdown pipe was manufactured and installed to the PPOOLEX facility (Figure 2). The DN200 (Ø219.1 x 2.5) blowdown pipes are positioned inside the condensation pool in a non-axisymmetric location, i.e. pipe 1 is 300 mm and pipe 2 500 mm away from the centre of the pool. The total length of both pipes is 3 209 mm. The pipes are made from austenitic stainless steel AISI 304L. In the 2009 experiment series with two blowdown pipes, the lower ends of the pipes were made of transparent polycarbonate. There is a huge difference between the two materials, for example, in thermal conductivity.

The test facility is equipped with several thermocouples for measuring steam and pool water temperatures and with pressure transducers for observing pressure behaviour in the dry well, inside the blowdown pipes, at the condensation pool bottom and in the gas phase of the wet well. Steam flow rate is measured with a vortex flow meter in the steam line. Additional instrumentation includes, for example, strain gauges on the pool outer wall and valve position sensors. A data acquisition system enabling high-speed multi-channel measurements is used. For an accurate observation of air/steam bubbles at the blowdown pipe outlet a high-speed digital camera is available. Figure 2 shows a monitoring view of the measurements.

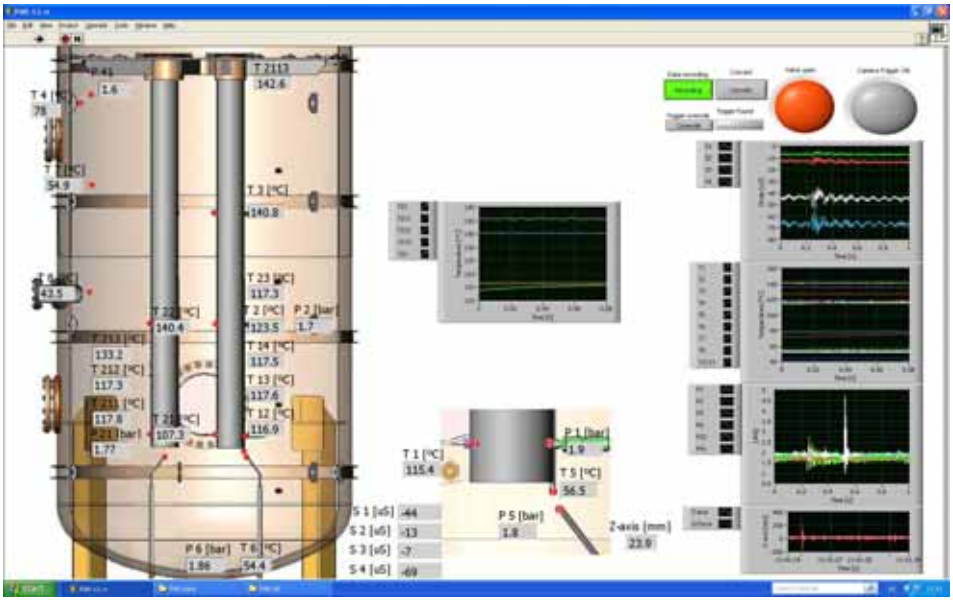

Figure 2. Monitoring of measurements in the two blowdown pipe experiments.

Experiment program

The test program in November–December 2010 consisted of seven experiments (labeled from PAR-07 to PAR-13) with two steel blowdown pipes. Before the experiments the condensation pool was filled with isothermal water at 20°C to the level of ~ 2.14 m i.e. the blowdown pipe outlets were submerged by 1.05 m. The initial pressure of the steam source, PACTEL steam generators, varied from 0.6 MPa to 2.5 MPa. Considerably high pressure levels were used in order to utilize the heat stored in the structures for the production of extra steam. The steam flow rate ranged from 220 g/s to 2 350 g/s and the temperature of incoming steam from 148°C to 207°C. Control of the steam flow rate was done remotely from the control room of the laboratory.

Initially, the dry well compartment was filled with air at atmospheric pressure. After the correct initial pressure level in the steam generators had been reached the remote-controlled shut-off valve in the steam line was opened. As a result, the dry well compartment was filled with steam that mixed there with the initial air content. Pressure build-up in the dry well then pushed water in the two blowdown pipes downwards and after a while the pipes cleared and flow into the wet well compartment began. First, the flow was almost pure air and condensation

at the pipe outlet was very weak. As the fraction of steam among the flow increased the condensation phenomenon intensified. Typically somewhere between 100 and 200 seconds into the experiments the steam fraction in the dry well reached 98–99%. Chugging region of the condensation mode map was reached when the flow had decreased enough to let the steam/water interface periodically enter the blowdown pipe. Most of the experiments also stretched to the overlapping "transition" region as the pool water temperature exceeded 45–50°C. Figure 3 presents the PAR-07–PAR-13 experiments placed on the condensation mode map of Lahey and Moody [11] on the basis of the steam mass flux in each pipe and the pool bulk temperature.

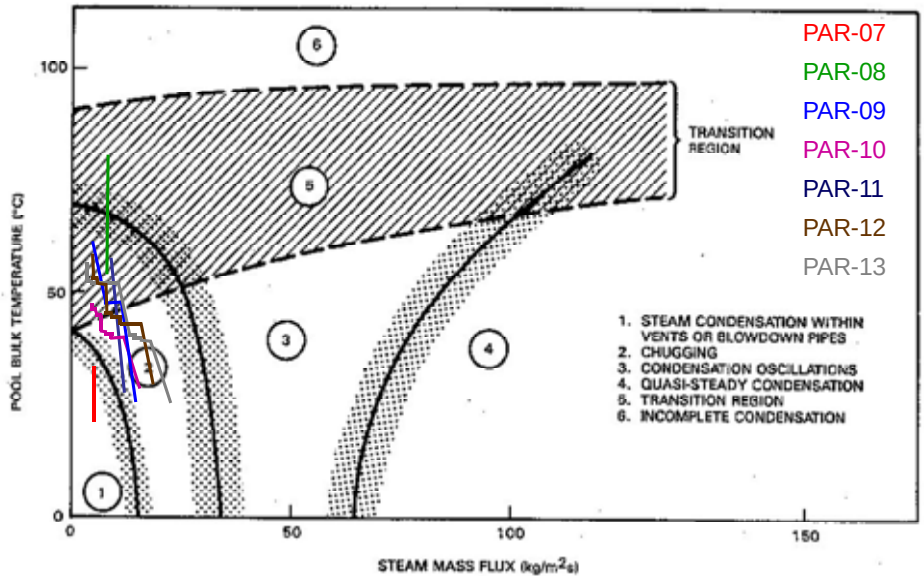

Figure 3. Two pipe experiments placed on the condensation mode map of Lahey and Moody.

Experiment results

During the most intensified chugging periods of the experiments underpressure sucked water high into the pipes after the collapse of large steam bubbles at the outlets of the pipes. From Figure 4 it can be seen that water ingress back into the blowdown pipes occasionally reached even the thermocouple on the elevation of 1 180 mm above the pipe outlet.

Chugging caused dynamic loads to the pool structures in the PAR experiment series. High pressure pulses were measured inside and below the blowdown

pipes during the most intensified chugging period. When the pressure waves reached the pool bottom their amplitude had damped considerably. The highest pressure spikes on the bottom were almost an order of magnitude lower than those measured below blowdown pipe 1.

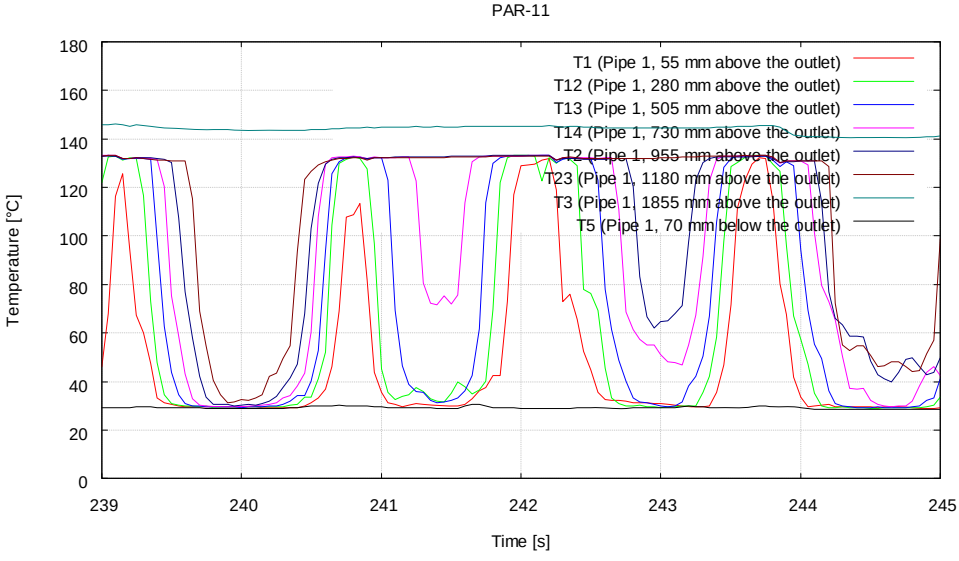

Figure 4. Temperatures inside and at the outlet of blowdown pipe 1 during the most intensified chugging period.

By examining the high speed video recordings from the outlet elevation of the pipes in detail one can see that the formation, and particularly the collapse, of the parallel bubbles did not always happen synchronously, Figure 5. This is verified with the help of the recorded pressure measurements close to the lower ends of the pipes. By plotting the curves in a millisecond scale one can first see the development of an underpressure due to rapid condensation and then the individual pressure pulses (and their periodic oscillations) associated with the collapse of the parallel steam bubbles, Figure 6.

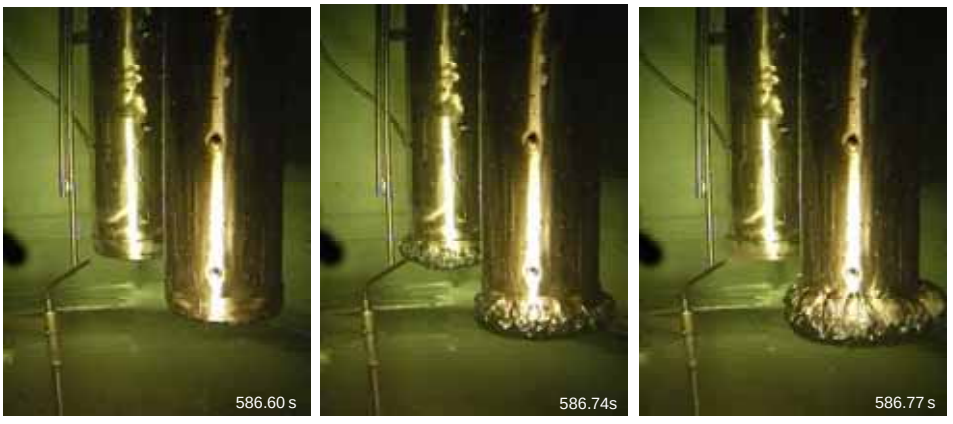

Figure 5. Non-synchronous collapse of steam bubbles at the outlets of the two blowdown pipes.

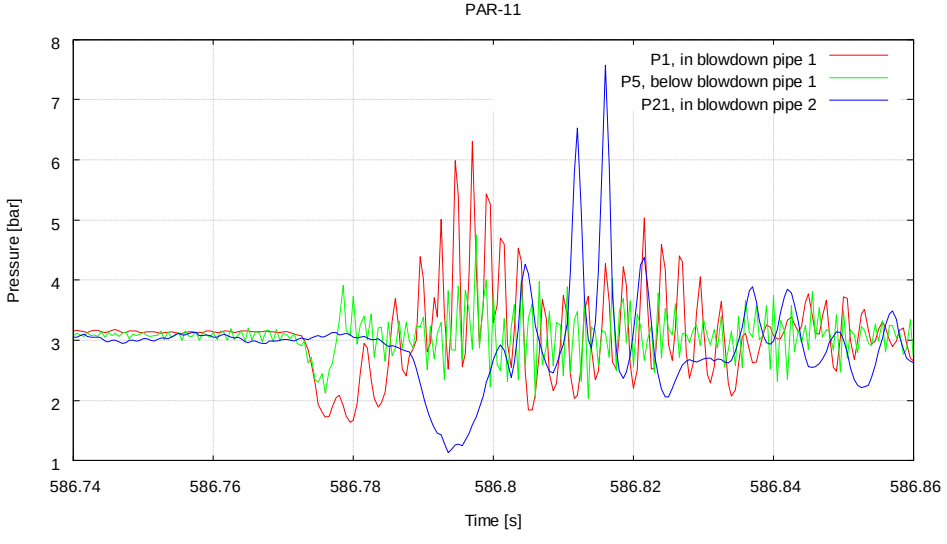

Figure 6. Pressure pulses caused by the non-synchronous collapse of parallel steam bubbles at the outlets of the two blowdown pipes.

There was no clear pattern in which pipe the steam bubble first started to collapse. Several successive bubbles could collapse first, for example, in pipe 1 but then the order can changed for a single or several cycles. The time difference between the first pressure spikes caused by the parallel collapsing bubbles can range from 10 to 70 milliseconds.

Figures 7 and 8 show some measured pressure curves from a single blowdown pipe and from a two blowdown pipe experiment, respectively. The steam mass flux per one pipe (assuming equal division between the pipes in the two pipe experiment) is about 16.5 kg/m^{2}s during the examined period in both experiments.

The curves reveal that the amplitudes of the highest pressure pulses inside the pipes were in the range of 0.4–0.5 MPa in both experiments. The behavior of pressure below the blowdown pipe outlet was, however, somewhat different. It looks like the formation of bubbles happened quite continuously in the one pipe case while the bubbles formed more periodically and grew bigger before collapsing in the two pipe case. As a result, the transducer below the pipe registered higher pressure loads in the two pipe experiment. The high speed video recordings show almost a continuous pulsating steam bubble at the single pipe outlet but only now and then appearing larger bubbles and water ingress into the pipes in the two pipe experiment. This kind of result would indicate that a two blowdown pipe system tends to change the flow behavior compared to a single pipe system although the used steam mass flux per pipe was the same.

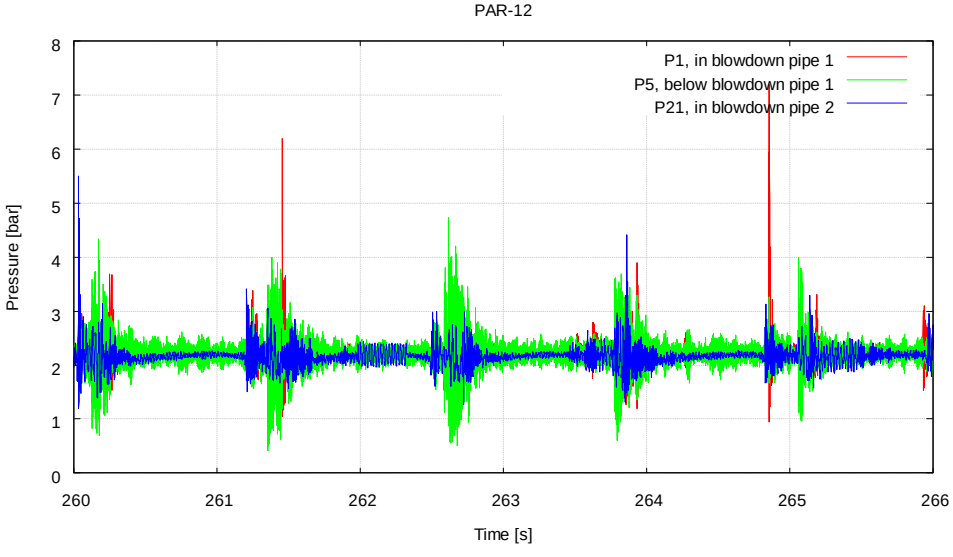

Figure 7. Pressure inside and at the outlet of the blowdown pipe with a 16.5 kg/m2s mass flux in a single pipe experiment.

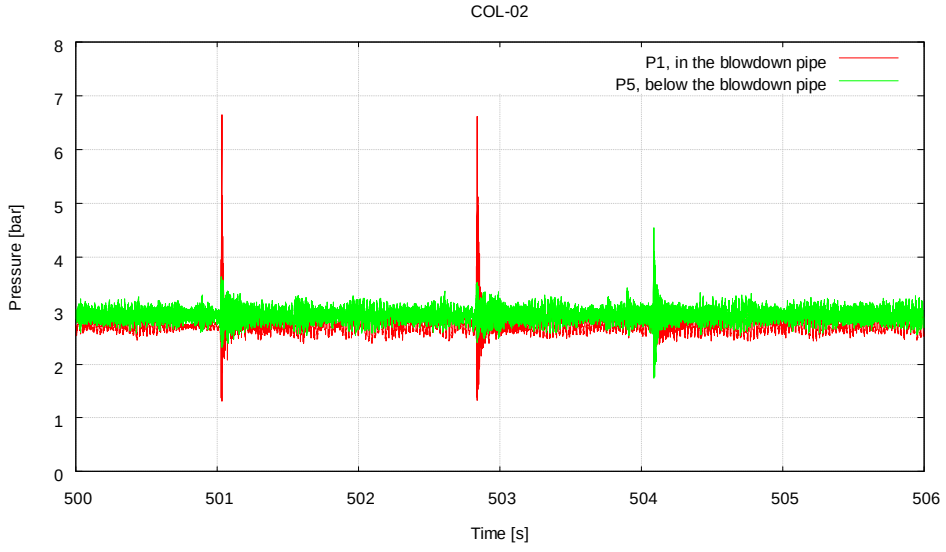

Figure 8. Pressure inside the two blowdown pipes and at the outlet of pipe 1 with a 16.5 kg/m^{2}s mass flux in a two pipe experiment.

The pipe material has an effect on the condensation phenomena inside the blowdown pipes. When the experiments done in 2009 with the polycarbonate blowdown pipes were compared with the steel pipe experiments in 2010 a huge difference between the measured pressure curves inside the pipes could be observed. With the same test conditions the amplitude of the pressure pulses caused by water hammer was considerably larger in the steel pipe experiments. It seems like the flow mode was different with the polycarbonate pipes from that with the steel pipes. Due to minimal heat conduction through the polycarbonate pipe wall condensation tended to happen at the pipe outlet and therefore no high pressure loads due to water hammer were experienced inside the pipe.

Conclusions

An experimental study was performed in the PPOOLEX test facility designed and constructed at LUT to investigate chugging phenomena while steam is discharged through two parallel blowdown pipes into the condensation pool filled with sub-cooled water. The main objective was to study if the blowdown pipes behave synchronously or not and to evaluate structural loads due to pressure oscillations and to compare the loads to those in a single blowdown

pipe situation. The experiments produced also relevant comparison data for CFD calculations at VTT.

High pressure loads were measured inside the blowdown pipes due to rapid condensation of the steam volumes in the pipes and resulting water hammer. The formation and collapse of steam bubbles and the movement of the steam/water interface inside the pipes was non-synchronous if the examination is extended to a millisecond scale. Up to a 70 ms time difference between the occurrences of steam bubble collapses at the outlets of the two pipes was possible. There was no clear pattern in which pipe the steam bubble first started to collapse. Several successive bubbles could collapse first, for example, in pipe 1 but then the order changed for a single or several cycles. The results indicated also that a two blowdown pipe system tended to change the flow behavior compared to a single pipe system although the used steam mass flux per pipe was the same. Blowdown pipes made of steel experienced larger pressure loads than pipes made of polycarbonate. Due to the lower heat conductivity of polycarbonate no rapid condensation of large steam volumes happened inside the pipe.

References

1. Laine, J. & Puustinen, M. Steam Blowdown Experiments on Chugging. LUT, Lappeenranta, 2005. Research Report POOLEX 2/2005.

2. Puustinen, M. Combined Effects Experiments with the Condensation Pool Test Facility. LUT, Lappeenranta, 2006. Research Report POOLEX 1/2006.

3. Puustinen, M. & Laine, J. Characterizing Experiments of the PPOOLEX Test Facility. LUT, Lappeenranta, 2008. Research Report CONDEX 1/2007.

4. Puustinen, M., Laine, J. & Räsänen, A. PPOOLEX Experiments on Thermal Stratification and Mixing. LUT, Lappeenranta, 2009. Research Report CONDEX 1/2008.

5. Laine, J., Puustinen, M. & Räsänen, A. PPOOLEX Experiments with a Modified Blowdown Pipe Outlet. LUT, Lappeenranta, 2009. Research Report CONDEX 2/2008.

6. Laine, J. & Puustinen, M. PPOOLEX Experiments on Wall Condensation. LUT, Lappeenranta, 2009. Research Report CONDEX 3/2008.

7. Puustinen, M., Laine, J. & Räsänen, A. PPOOLEX Experiments with Two Parallel Blowdown Pipes. LUT, Lappeenranta, 2010. Research Report CONDEX 1/2009.

8. Puustinen, M., Laine, J. & Räsänen, A. PPOOLEX Experiments on Dynamic Loading with Pressure Feedback. LUT, Lappeenranta, 2010. Research Report CONDEX 2/2009.

9. Puustinen, M., Laine, J. & Räsänen, A. PPOOLEX Experiments on Stratification and Mixing in the Wetwell Pool. LUT, Lappeenranta, 2011. Research Report CONDEX 1/2010.

10. Tuunanen, J., Kouhia, J., Purhonen, H., Riikonen, V., Puustinen, M., Semken, R.S., Partanen, H., Saure, I. & Pylkkö, H. General Description of the PACTEL Test Facility. VTT, Espoo, 1998. VTT Research Notes 1929. 35 p. + app. 74 p. ISBN 951-38-5338-1. http://www.vtt.fi/inf/pdf/tiedotteet/1998/T1929.pdf.

11. Lahey, R.T. & Moody, F.J. The Thermal-Hydraulics of a Boiling Water Reactor. American Nuclear Society, Illinois. 2nd edition, 1993.

16. Passive Safety System Simulation (PASSIMU)

16.1 PASSIMU summary report

Virpi Kouhia
Lappeenranta University of Technology

Abstract

The PASSIMU project was set to review and study passive safety system features utilized in chosen nuclear power plant concepts. The focus was on seven Generation III nuclear power plant concepts, which were options for the next nuclear power plant units in Finland. The aim was to review situation in modelling passive safety systems, in respect of computational preparedness and the possible needs for new experiments.

The first goal of the project was to prepare a state-of-art review on the passive safety system concepts [1–4]. The task was fulfilled with preparation of a report, based on purely publicly available information [5]. The review introduced the plant concepts, passive safety systems, phenomena related as well as some code validation and experimental research aspects. The second sub-task focussed on system code testing in conditions typical for passive safety system operation. Two PACTEL experiments on VVER-640 studies were chosen for simulation test cases [6, 7], and utilization of the latest APROS version in simulations resulted to be fairly satisfactory [8]. The last task was to study the applicability of experimental facilities, resources and already gained experiences in passive safety system related experimental studies. Lappeenranta University of Technology has a wide experience on thermal-hydraulic experimental research, planning, constructing and operating test facilities, and this know-how and available hardware could be utilized in future studies on passive features [7, 9]. Additional laboratory premises, modern measurement equipments and data acquisition systems provide also new sophisticated possibilities.

Introduction

The evaluation and validation of the passive safety systems are mainly based on the experiments and computer code analyses. The operational conditions where passive features are present, such as low driving force, pressure and flow rate, are typically beyond the original design conditions of the codes. The computer codes and experimental facilities should be reviewed in order to ensure the availability of analytical tools in the specific conditions.

The PASSIMU project was divided into three sub-tasks. The first task was to prepare a report to review state-of-art situation on particular passive safety system concepts [1]. The project included also a code calculation case on specified conditions to provide a short insight on potentials of available analytical tools. In addition, the task was set to provide a background review on possibilities of the available experimental resources at Lappeenranta University of Technology. Hence, PASSIMU contributes to preparedness for the future needs, prior to the construction licence stage of the new plants. The project orients to activate ideas for experimental and analytical modelling.

Main objectives

The objective of the PASSIMU project was set to study passive safety system in particular nuclear power plant concepts [1]. The focus was on seven Generation III nuclear power plant concepts and the passive features in those. These nuclear power plant concepts were proposed as options for the next nuclear power plant units in Finland [2–4].

The first assignment within PASSIMU was to gather information on the chosen nuclear power plant concepts and specifically on designed passive safety systems in those. This task was fulfilled in a form of a review, a state-of-art report on the subject [5]. Another aim of the project was set to review the availability of analytical tools also in low pressure, driving force and flow conditions, beyond the normal design conditions of the system codes. As an example, a computer code was tested in chosen matching and challenging example cases, presented in the research report [8]. As the code validation depends on the available experimental data, the experimental evaluation situation needed also to be reviewed. Hence, the third PASSIMU task focused on experimental research resources at Lappeenranta University of Technology in respect of passive safety system evaluation, i.e. the possible availability of facilities and other experimental resources for passive safety system evaluation processes were to be reviewed [7, 9].

Review on passive safety systems

The first goal of the PASSIMU project was set as writing a state-of-the-art report to review validation status on modelling passive safety systems. The background material for the review was retrieved on purely publicly available publications on the last decade and. the review is more of a directional than an unambiguously consummate type [5].

In the chosen seven nuclear power plant designs including four pressurized and three boiling water reactor designs, the passivity features are utilized in some part(s) of a safety system function, or within the whole safety system(s) (Table 1) [1–5]. These concepts involve large amount of phenomena and characteristics connected to passivity features [1]. Hence, the scope of the review information retrieval was set mainly to chosen nuclear power plant design specific publications. The review included short descriptions of the nuclear power plants, passive safety system functions in them and some reviews on research activities. The report includes tables on passive systems verification, phenomena and characterization, operational situations and experimental and computational related research activities. The review was developed as background information for the project purposes including large reference list to be utilized [5].

Table 1. Passive safety systems utilized in nuclear power plant concepts [5].

PASSIVE SYSTEM (PWR)	AES2006	APR1400	APWR	EPR
Gravity driven drop of control rods	X	X	X	X
Double containment structure (structural integrity)	X	X	X	X
ECC accumulators	X*)	X	X	X
Steam generator passive heat removal	X			
Passive containment cooling	X		X**)	
Molten core in/ex-vessel cooling		X*)	X*)	
Core catcher	X	X*)	*)	X
Passive catalytic recombiners	X	X	X	X
ASSIVE SYSTEM (BWR)	**ABWR**	**ESBWR**	**KERENA**	
Hydraulic insertion of control rods	X	X	X	
Emergency boron injection		X	X	
Containment / reactor building structure (structural integrity)	X	X**)	X	
Containment pressure suppression pool	X	X	X	
Isolation / emergency condenser system	X	X	X	
Passive containment cooling	X	X		
Core flooding		X	X	
Molten core treatment (in/ex-vessel cooling)				
Core catcher & cooling systems	X	X		
Passive catalytic recombiners	X*)		X*)	

*) *unclear status, **) partially passive*

Test calculations

Another sub-task of PASSIMU was to test thermal-hydraulic system code(s) in a low pressure, flow and driving force situation, typical conditions for passive safety systems. Finally, two older PACTEL experiments were chosen to be the test cases in this sub-task, as these experiments were set to study features of the passive safety systems in suitable matching conditions, and the measurement data was readily available. At late 1990s, PACTEL was used in a modified set-up to fit in studies of VVER-640 type NPP concept focussing on the operation of designed passive safety system (Figure 1). The PACTEL set-up included original pressure vessel parts connected to additional two large tanks with connecting pipelines simulating the reference passive pool system. In addition, earlier performed code calculations with four thermal-hydraulic system codes provided a suitable comparison for the present calculations. [6, 7]

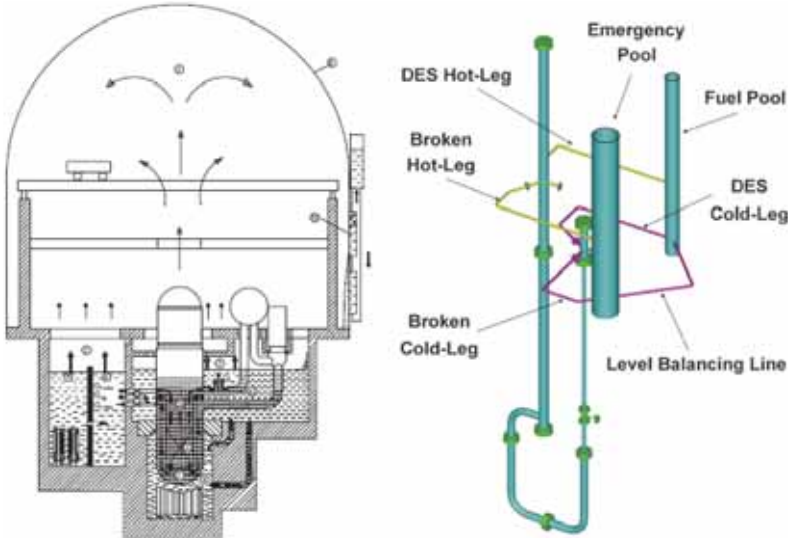

Figure 1. VVER-640 hot leg break (left [6]) and modified PACTEL set-up (right [8]).

The latest APROS code 5.09 -version was utilized to re-produce the post-test calculations on the chosen two tests. These calculations were performed with two simulation models, simple and modified models of the facility set-up. The simulation calculations were able to reproduce the main three events of the transients, i.e. first one-phase heating period, second oscillating transition period, and third steady two-phase natural circulation period (Figure 2). The

simulation model behaviour improved after modifications to the nodalization scheme of the pools, as the more complex pool nodalization improved circulation in the pools. The predictions of the simulations approached the measured results (Figures 2 and 3). These calculation cases produced satisfactory quantitative and qualitative results compared with the measured data [8].

Experimental experiences and possibilities

The third sub-task was focussed on studying the applicability of experimental facilities, other resources and gained experiences in passive safety system related experimental studies. Lappeenranta University of Technology has quite a wide experience on thermal-hydraulic experimental research, including database of about 900 experiments. The facilities include separate effect as well as large integral test facilities, such as PACTEL (PWR PACTEL) and PPOOLEX. These facilities could be available for future studies, either as side facility such as steam or other convenient environment provider, or as part of a modified set-up system with additional passive features attached to them, such as elevated tanks, pools or condensers. The operative unit at the university in this field of research, i.e. the Nuclear Safety Research Unit, has well established preparedness to plan and construct also new separate effect test facilities and rigs. The new additional laboratory premises could provide surroundings for example systems simulating operation of passive systems utilizing gravity forces. Also, modern measurement equipments and data acquisition systems would provide more sophisticated possibilities, as the enhancement of the infrastructure is on-going. [7, 9]

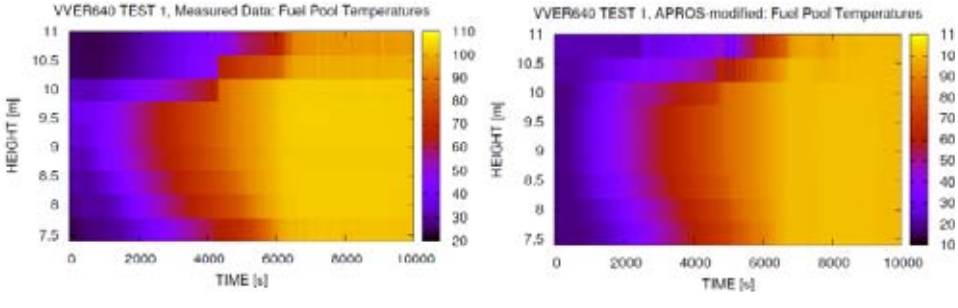

Figure 2. PACTEL pressure vessel collapsed level: present APROS simulations (left [8]) and earlier code calculations (right [6]).

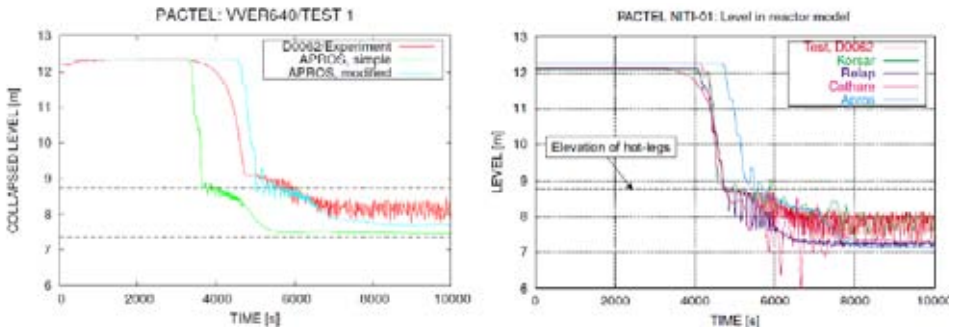

Figure 3. Temperature profiles in fuel pool generated from measured data (left) and APROS simulation (right) [8].

Conclusions

The project was set to contribute to preparedness for the future needs, prior to the construction licence stage of the new plants. The project deliverables, the three reports, provide some background material for further planning in future projects. The project orients to activate ideas for experimental and analytical modelling.

References

1. IAEA, Passive Safety Systems and Natural Circulation in Water Cooled Nuclear Power Plants, IAEA, Vienna, 2009. IAEA-TECHDOC-1624. ISBN 978-92-0-111309-–2. November 2009, Austria.

2. Säteilyturvakeskus (STUK), Alustava turvallisuusarvio Olkiluoto 4 -ydinvoimalaitos-hankkeesta, Liite 1: Laitosvaihtoehtojen soveltuvuuden arviointi. 4.5.2009, STUK. 80 p.

3. Säteilyturvakeskus (STUK), Alustava turvallisuusarvio Loviisa 3 -ydinvoimalaitos-hankkeesta, Liite 1: Laitosvaihtoehtojen soveltuvuuden arviointi. 30.9.2009, STUK. 80 p.

4. Säteilyturvakeskus (STUK), Alustava turvallisuusarvio Fennovoiman ydinvoimalaitos-hankkeesta, Liite 1: Laitosvaihtoehtojen soveltuvuuden arviointi. 19.10.2009, STUK. 80 p.

5. Kouhia, V. Review of Designs and Validation Aspects of Passive Safety System in Advanced Nuclear Power Plant Concepts. Research Report, PASSIMU 1/2009, 10.5.2010.

6. Bánáti, J., Virtanen, E., Purhonen, H., Alexandrine, S. & Volkova, S. Experimental and Numerical Study of Long term Cooling of VVER-640 Reactor in the PACTEL Facility Using Thermal Hydraulic Codes. Ninth International Conference on Nuclear Engineering (ICONE-9), Nice, France, 2001.

7. Purhonen, H. Experimental Thermal Hydraulic Studies on the Enhancement of Safety of LWRs. Acta Universitatis Lappeenrantaensis 293. Lappeenrannan teknillinen yliopisto, Digipaino, 2007. ISBN 978-952-214-500-0.

8. Kouhia, V. Simulation of Experiments on Start of Natural Circulation and Long Term Cooling. Research Report, PASSIMU 1/2010, 28.1.2011.

9. Kouhia, V. Possibilities in Experimental Research on Evaluation of Passive Safety Systems. Research Report, PASSIMU 2/2010, 31.1.2011.

17. OpenFOAM® CFD-solver for Nuclear Safety Related Flow Simulations (NuFoam)

17.1 NuFoam summary report

Juho Peltola (Ed.) and Timo Pättikangas
VTT

Thomas Brockmann and Timo Siikonen
Aalto University

Timo Toppila and Tellervo Brandt
Fortum Power and Heat Oy

Abstract

A validation plan for utilization of an open source OpenFOAM® CFD-library in nuclear safety application has been created. The single phase solvers have been tested by taking part in a blind OECD/NEA benchmark. Near-wall treatment of selected turbulence models and wall heat transfer were validated in turbulent pipe flow with coupled heat transfer. Available two-phase solvers have been evaluated, enhanced for simulation of bubbly flows and tested.

Introduction

In the field of nuclear safety analysis, Computational Fluid Dynamics (CFD) has become an increasingly popular tool for thermo-hydraulic investigations. There are several suitable, commercial and open-source, CFD-codes available, but in recent years an open-source CFD-library called OpenFOAM® released by OpenCFD Ltd. (UK, www.openfoam.com) has been gaining popularity worldwide.

The code has originated in Imperial College London during the early 1990's and was published as open-source in 2004.

Compared to commercial solvers, the benefits of an open source CFD code are transparency, infinite customizability and lack of licensing fees, which brings the cost structure of massively parallel computation down to a feasible level. Compared to other open source CFD codes, the benefits of OpenFOAM® are a large, active and growing user base, modern approach to mesh handling with unstructured and polyhedral meshes, parallelization and an object oriented code structure that makes it fast and easy to implement new models and solvers in the top level code.

Distinct drawbacks of OpenFOAM® are the lack of public, formal documentation and – partially because of the previous point – a very steep learning curve. Generally it can also be said that many of the features of OpenFOAM® represent the state-of-the-art, but often lack the polish to directly apply them to practical engineering problems. In this project we try to alleviate these drawbacks from the perspective of nuclear safety analysis to make OpenFOAM® a practical tool for these applications.

OpenFOAM® and OpenCFD® are registered trademarks of OpenCFD Ltd. and this project has not been endorsed or approved by OpenCFD Ltd.

Main objectives

The main aim of the project is to validate OpenFOAM® as a tool for nuclear safety related simulations. An application oriented approach for validation is used. The first goal is to be able to simulate transient single-phase flows and heat transfer in a complex geometry, especially in the fuel assembly and its head parts, more accurately using efficient parallel computing. As a result, we expect to have more detailed understanding of the coolant mixing and the results can be used e.g. in verifying safety issues when increasing the burn up of the fuel.

Another branch of the project is to adapt and extend OpenFOAM® two-phase flow capabilities for nuclear safety analysis applications, specifically to two-fluid turbulent gas-fluid flow simulations with heat transfer, boiling and condensation. The validation results and lessons learned in the single-phase tasks are applied in two-phase solver development.

An important goal of the project is also to strengthen the Finnish CFD community in the field of nuclear safety and to participate in Northnet and other international cooperation.

Validation plan

When a new simulation method for real (nuclear safety) applications is taken into use, a validation process is required. Considering the intended use of the method, the validation process helps to establish best practices for its usage and to determine how accurately the model represents the real world. In order to harmonize and guide the validation work during the many years of the project in various organizations, the project practices are written down as a validation plan. The validation plan aims to be a living document, updated constantly during the project while the code and the models improve and new applications are taken under the validation work.

The validation work is focused on a few nuclear safety related applications at a time. The applications are chosen based on which application would benefit most from CFD simulation with OpenFOAM®, which models are available in the code and what kind of validation data can be found. The first application chosen is the modelling of single and two-phase flow inside a PWR fuel assembly, as presented above.

The validation is essentially based on the use of relevant experiments and on the comparison of simulations to experimental data. The practical approach is to first use separate effect experiments to find the accuracy of basic models of the code, and then integral type of experiments to find the accuracy of all models together, relevant for the application in mind. In the validation plan it is stressed that only the relevant and reliable experiments with error estimations should be used.

The code and model verification as well as solution verification must be made before the model is validated against experiments. Practically this means that it is first ensured that there are no relevant errors in the code, that the simulation is made based on the best practices and that the simulation error is determined. Systematic code verification is out of the scope of this project, and the OpenFOAM community with thousands of users is relied on to find the relevant code errors. However it was found out during the first year of the project that the simulation of the separate effect tests can bring out also code errors, which can be corrected easily as the code is open source. The solution verification must be ensured by using the best practices of CFD and also by detailed reporting of simulation work and error estimations of simulation.

The validation project is planned to continue for many years and to rely on work of many organizations and persons. To ensure the continuing work with no

loss of data or overlapping, common procedures for documentation and archiving are also presented in the validation plan.

Simulation of single-phase flows

Two separate single-phase flow tasks have been completed in the project. Firstly, Aalto University took part in a blind OECD/NEA benchmark and secondly, the near-wall treatment of selected turbulence models and wall heat transfer was validated by VTT.

OECD/NEA T-junction benchmark

Damage may be triggered in water line systems by the internal flow itself, which is an engineering problem that has interest also in the nuclear industry for safety reasons. In this task, the attention was on the turbulent mixing of warm and cold flows in a T-junction. Repeated surface temperature changes create stresses on the pipes and material fatigue may lead to fractures and leaks. If the transient large-scale turbulence behaviour could be modeled accurately, it would give new ways of noticing the risks and avoiding them. OECD/NEA arranged a blind benchmark exercise to model the turbulent mixing. This task is based on the case specified in the exercise.

The T-junction geometry consists of the main duct and a perpendicularly attaching branch duct with diameters D_M = 0.14 m and D_B = 0.10 m respectively. The flow temperatures were T_M = 19 C and T_B = 36 C. The Reynolds numbers are Re_{DM} = 80 000 and Re_{DB} = 109 000 respectively. The wall heat transfer was assumed to be negligible. The main flow is fully turbulent and the branch flow is a developing turbulent flow. The fluid was assumed incompressible, but a simple thermo physical model was added to include temperature dependency of the viscous and buoyancy forces.

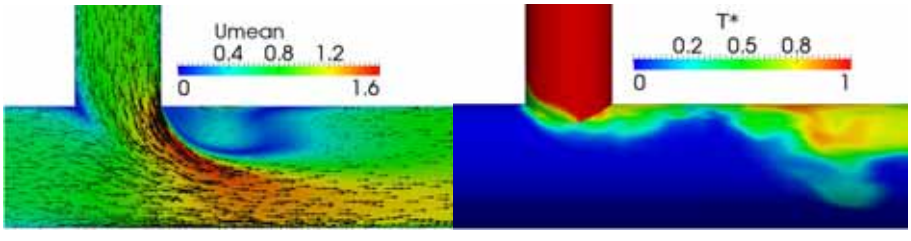

Figure 1. Detached-eddy simulation. i) Time-averaged velocity field on plane intersection. ii) Instantaneous temperature on the surface.

The OpenFOAM 1.5 and 1.6 codes were used in the simulation, applying the PISO pressure-velocity coupling algorithm. Numerics were second-order accurate with backward-method time integration and central differencing schemes with optional filtering and flux limiters were used for the spatial discretizations.

Different turbulence modelling approaches were applied, but most time was spent with the large-eddy simulation method (LES). The subgrid-scale turbulence effects were included with the dynamic Smagorinsky model proposed by Piomelli and Liu [1]. The flow was solved accurately to the wall and no special wall treatments are used. A dimensionless first cell height was $y^+ < 1$. Total number of cells was $3.8 \cdot 10^6$, which includes a 20 D_M long downstream pipe to follow the mixing. Fully turbulent inflow conditions were created by circulating the inflow. The LES simulation was repeated with axially refined grid ($9.8 \cdot 10^6$ cells), but the coarse grid was used otherwise.

Traditional Reynolds-averaged Navier-Stokes (RANS) simulation method was also tested, applying the popular two-equation SST k-ω model. The last turbulence modelling approach was the more recent detached-eddy simulation (DES). The near-wall turbulence is completely modelled as with RANS, but the large space flow is simulated in LES-mode. The delayed version of the Spalart-Allmaras turbulence model is applied, which allows using grids designed for LES [2].

The LES results are quite reasonable in comparison with the PIV-measurements made by Vattenfall, but erronous inflow conditions are a possible source for some inaccuracy. The branch flow was assumed fully turbulent in the simulations against the specifications. However, the inflow conditions may have only a limited influence on the results. Another problem is that accurate near-wall velocity profiles were not achieved with LES. Because of the thin velocity profile at high Reynolds numbers, it is likely that a finer grid would be required also in the wall parallel directions. At the bottom, the velocity profile also becomes very thin due the impingement and the level of turbulence is reduced. On the top, there is a large separated flow domain. Figure 2 shows the velocity profiles at one axial location.

The RANS model did not perform properly in this case and produced incorrect results, although the velocity profile is accurate near the junction. Still, the reasons require investigation. Accurate fully turbulent inflow conditions were achieved with DES, but the results disappoint a little in the mixing flow region: the velocity decreased near the walls and increased in the middle. It could be that it is difficult for the model to handle the transition between RANS- and LES-modes in complex flow situations.

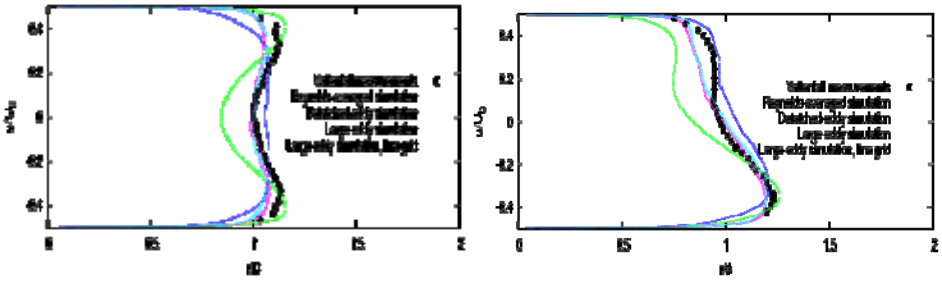

Figure 2. Time-averaged axial velocity field at a distance of 3.6 D_M from the junction. i) On a horizontal line. ii) On a vertical line.

The main goal of this work was to model transient behavior of the surface temperatures accurately. However, the error is significant with the time-averaged results. Depending on the model and place, the order of error varies between 5–20% of the total range. The most accurate results were produced with the DES approach, although the results are weak on the sides of the duct at early axial distances. Heat fluctuation timescales and magnitudes are likewise more accurate with the DES than the LES.

Validation of turbulence near-wall treatment and wall heat transfer

This section is based on the OpenFOAM 1.7.x (17.11.2010) release. The near-wall treatment of selected turbulence models was validated by simulating a relatively high Reynolds number (Re_D = 45 000, 80 000 and 169 000) fully developed pipe flow with different turbulence models and near-wall mesh resolutions. The dimensionless wall distances, y^+, to first cell centre on the meshes used were 1, 5, 10, 30, 100 and 250.

Two commonly used turbulence models were tested: the standard *k-ε* model and SST *k-ω* model using their respective wall functions. The *k-ε* model wall functions are valid in the logarithmic region of the boundary layer, where y^+ is from 30 to 300. The ω wall function of the SST *k-ω* model uses a blended approach, which should work reasonably well even with very dense near-wall meshes. Two different turbulent viscosity wall functions were tested: the standard logarithmic law-of-the-wall and the Spalding continuous function that should give better results if the first cell is in the buffer layer (y^+ = 5...30). For turbulent wall heat transfer, a Jayatilleke wall function was used.

Figure 3 shows a comparison of near-wall axial velocity profiles from all the simulations. As expected, the *k-ε* model over predicts the first cell velocity when

first cell y^+ is 5 and 10. The Spalding wall function improves the results, but the difference is relatively small. The SST *k-ω* model also over predicts the velocity at $y^+ = 5$ and 10, but the error is much less. With the $y^+ = 1$ mesh the results follow the laminar $u/u_\tau = y^+$ relation. It is not shown here, but with the exception of *k-ε* model at mesh $y^+ = 5$ and 10, the simulated turbulent kinetic energy and dissipation results compare quite well with experimental results of Lawn [3].

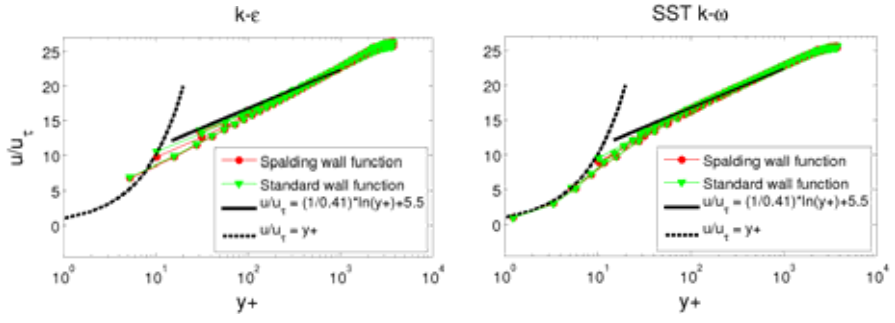

Figure 3. Simulated near-wall velocity profiles with kEpsilon and kOmegaSST turbulence models. Normalized with friction velocity from the Colebrook equation.

Figure 4 compares the simulated results to experimental correlations. The friction coefficient is compared to the Colebrook correlation and the Nusselt number to the classic Dittus-Boelter and Gnielinski correlations. With the exception of the *k-ε* model with mesh $y^+ < 30$, the simulations capture the general trends and are within 10% of the correlations.

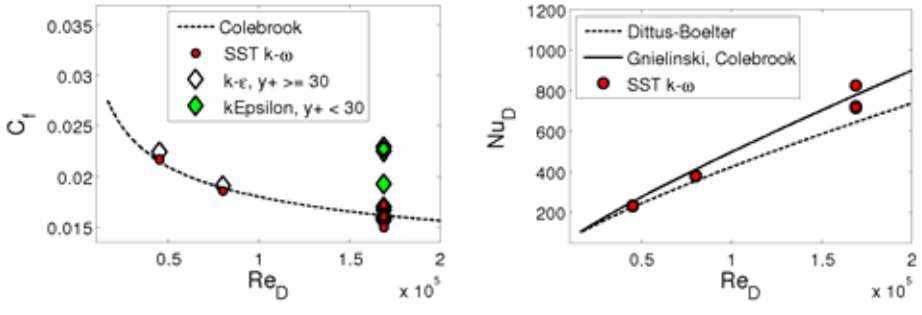

Figure 4. Comparison of buoyantPimpleFoam simulated friction coefficient (left) and Nusselt numbers with experimental correlations.

The conjugated heat transfer solver, chtMultiRegionFoam, was first tested by simulating the above fully developed turbulent pipe flow with temperature-coupled copper pipe and a fixed outside temperature. The chtMultiRegionFoam flow solution was identical to the buoyantPimpleFoam result and the temperature of the fluid-solid interface was well predicted. For the second test, the same pipe was placed horizontally in air and two cases were simulated: a free convection at Rayleigh number, $Ra_D = 10^5$ and a forced convection at Reynolds number, ReD = 120. Figure 5 shows an excellent match with results presented in literature. The local simulated Nusselt number in the free convection case is compared to benchmark simulation of Saitoh et al. [4] and in the forced convection case to experimental results of Eckert and Soehngen [5].

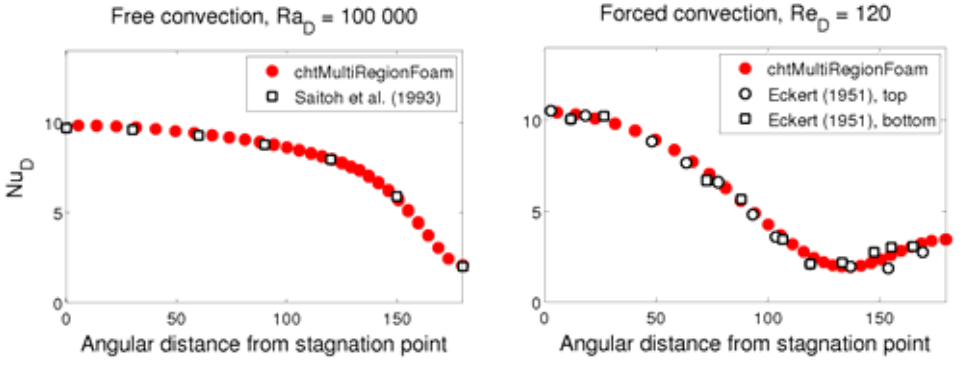

Figure 5. Comparison of simulated local Nusselt numbers of with results presented in literature for a horizontal cylinder and a cylinder in crossflow.

Simulation of two-phase flows

While the OpenFOAM® single-phase solvers are relatively mature and well tested, the two-phase solvers are much less so, particularly in the Euler-Euler approach. A solver called “twoPhaseEulerFoam” was selected as the basis for further development.

Generally, twoPhaseEulerFoam provides all the basic functionality of an Euler-Euler two-phase solver, but the emphasis of the sub models implemented is on granular flows and fluidization. For simulation of bubbly flows in nuclear safety applications, several sub models are found lacking: No drag models that are suitable for bubbles are included and only a constant value is available for lift and virtual mass coefficients. The turbulent dispersion and wall lubrication force models are completely absent. Not to mention the complete lack of heat transfer.

To enhance the capabilities, a new solver based on twoPhaseEulerFoam was created. Several models used in recent publications by Frank et al. [6], Hosokawa and Tomiyama [7] and Krepper et al. [8] were implemented in the new solver. All-in all, several bubble aspect ratio models, bubble drag models, bubble lift models, wall lubrication force models, turbulent dispersion models and models for the bubble induced turbulence were implemented.

To test the solver and the newly implemented models, three experimental vertical bubbly flows by Hosokawa and Tomiyama [7] and FZD MT-Loop 074 [6, 8] were simulated. From the experiments in a pipe with a diameter of 25 mm, Cases 1 and 3 with superficial flow velocity of water was 0.5 and 1.0 m/s were selected. Different wall lubrication force models and bubble induced turbulence modulation models were tested in five variations for each flow case.

The Antall et al. wall lubrication force model failed to prevent gas collecting on the walls in the Hosokawa and Tomiyama Case 1. However, the Antal model correctly predicted the volume fraction peak location in Case 3, as seen in Figure 6. The Frank wall lubrication model tended to overestimate the wall lubrication force. The Sato bubble induced turbulence predicted best the effective fluid phase viscosity and thus the turbulent dispersion. On the other hand, the turbulent kinetic energy was significantly under predicted and the results of the Sato model were furthest from the experimental values.

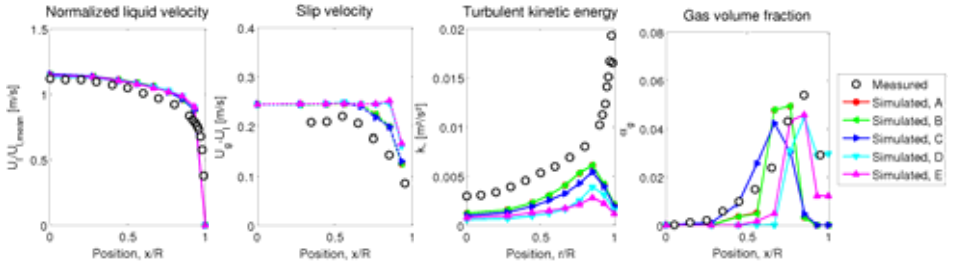

Figure 6. Comparison of experimental and simulated axial velocities, turbulent kinetic energy and gas volume fraction in Hosokawa and Tomiyama Case 3.

From the FZ-Dresden MT-Loop experiment 074, two different sections were simulated and compared to studies of a fully developed flow by Frank et al. [6] and the developing flow after the gas injection point by Krepper et al. [8] The MT-Loop 074 experiment is a 4 m long vertical bubbly air-water pipe flow with inner diameter of 51.2 mm. The Reynolds number of the fluid flow is 55 000 and

the gas phase is injected at the bottom of the pipe from 19 capillary tubes. Measurement results are only available for gas volume fraction and bubble size.

For the simulations a periodic test case was used. Three simulations were performed with different bubble induced turbulence modelling approaches. The simulation with the Sato bubble induced turbulence model used also by Frank et al. [6] predicted results similar to their k-ε simulation. The only difference is a slightly higher wall peak that is located slightly more inwards. Both the present and Frank et al. k-ε simulations underestimate the turbulent dispersion, and only the SST k-ω simulation of Frank et al. is able to predict the wall peak correctly.

Krepper et al. [8] studied the development of the gas distribution right after the gas injection and published experimental and simulated results at four different heights. Initially, the experiment was simulated with different bubble induced turbulence models and the general behaviour was found to be similar to that published by Krepper et al. However, there were distinct differences in the development of the gas distribution in the intermediate measurement height. Further investigation revealed sensitivity to the inlet boundary conditions and a mismatch between the single- and two-phase turbulence models. The two-phase model predicted significantly lower level of turbulence, which is an indication that there is a problem in the two-phase turbulence model.

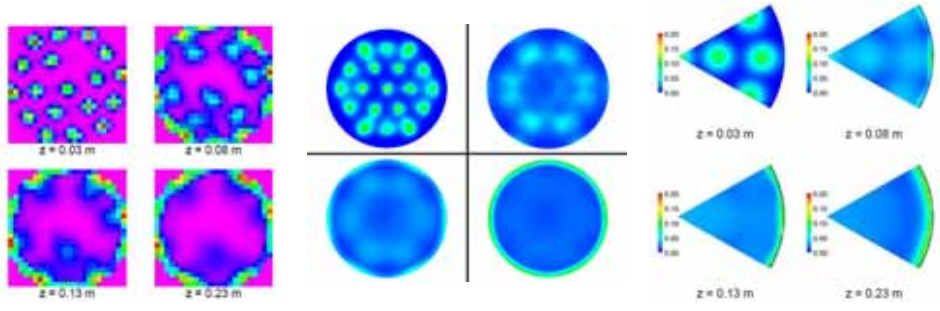

Figure 7. Comparison of experimental (left) and simulated gas volume fractions with twoPhaseNuFoam (middle), and by Krepper et al. [8] (right). Left and right pictures are from Krepper et al [8].

At this stage of the solver development, the best results were obtained with the Sato bubble induced turbulence model. It is a widely used model, but in this case its success may hinge on its independence of the general turbulence model, as it tends to under predict the level of turbulence. Different wall lubrication force models gave the best results in different cases, but the Frank model gave reasonable

results in all the cases. However, these cannot by any means be considered as final conclusions, because the radial volume fraction profile is a result of balancing the lift, wall lubrication force and turbulent dispersion and it is apparent that the turbulence modelling in the two-phase solver requires an overhaul.

Conclusions

From the T-junction work it can be concluded that the state of the accuracy is not yet satisfying. In the blind benchmark exercise our LES submission ranked high in the velocity data comparisons with other participants, but below average in the heat transfer accuracy. During this project some new issues have been found, which could be done to improve the velocity as well as the temperature results further. Certain aspects of the grid were found to cause trouble. There is still room to improve the numerical accuracy of the heat transfer equation treatment.

The tested turbulence models and near-wall treatments proved satisfactory and comparable with other codes, but more general and advanced wall functions would be beneficial. In the laminar horizontal cylinder test case excellent results were achieved, which validate the basic flow and heat transfer solutions without the uncertainties of turbulence modelling. The coupled heat transfer solver was confirmed to be capable of multiple gas, liquid and solid regions with different turbulence models and equations-of-state. The flow solutions of the single-region and coupled heat transfer solvers matched each other and the heat conduction in the pipe wall matched analytical results. On coarse meshes the k-ε model gave more accurate results, but the SST k-ω model gave reasonably good results on all the meshes. The next step for validation of the single-phase flow solvers is more complex flows and geometries that are closer to practical applications.

The existing OpenFOAM® two-phase solvers were found to lack important sub models for bubbly flows. The required models were implemented in a new solver, which was tested against experimental and simulated results from the literature. Qualitatively the results match, but it was found out that the turbulence model of the two-phase solver under predicts the level of turbulence compared to the literature results and results of the single-phase OpenFOAM® solvers.

Since the end of the two-phase portion of this project, weaknesses in the two-phase turbulence modelling that affect the results have been identified and corrected in an internal development version of the solver, and partially in the official 1.7.x release. The two-phase solver still requires development for nuclear safety applications.

References

1. Piomelli, U. & Liu, J. Large-eddy simulation of rotating channel flows using a localized dynamic model. Physics of Fluids, April 1995, Vol. 7, pp. 839–848.

2. Spalart, P.R., Deck, S., Shur, M.L., Squires, K.D., Strelets, M.K. & Travin, A. A New Version of Detached-eddy Simulation, Resistant to Ambiguous Grid Densities. Theor. Comput. Fluid Dyn. 2006, Vol. 20, pp. 181–195.

3. Lawn, C.J. The determination of the rate of dissipation in turbulent pipe flow. J. Fluid Mech. 1971, Vol. 48, part 3, pp. 477–505.

4. Saitoh, T., Sajiki, T. & Maruhara, K. Benchmark solutions to natural convection heat transfer problem around a horizontal circular cylinder. Int. J. Heat Mass Trans. 1993, 36, pp. 1251–1259.

5. Eckert, E.R.G. & Soehngen, E. Distribution of heat-transfer coefficients around circular cylinders in crossflow at Reynolds numbers from 20 to 500. ASME, Heat Transfer Div. 1951. Paper No. 51-F9.

6. Frank, T., Zwart, P.J., Krepper, E., Prasser, H.-M. & Lucas, D. Validation of CFD models for mono- and polydisperse air-water two-phase flows in pipes. Nuclear Engineering and Design 2008, 238, pp. 647–659.

7. Hosokawa, S. & Tomiyama, A. Multi-fluid simulations of turbulent bubbly pipe flows. Chemical Engineering Science 2009, 64, pp. 5308–5318.

8. Krepper, E., Schmidtke, M. & Lucas, D. Modelling of Turbulence in Bubbly Flows. 7th International Conference on Multiphase Flow, Tampa, FL, USA, May 30 – June 4, 2010. 7 p.

18. Release of Radioactive Materials from a Degrading Core (RADECO)

18.1 RADECO summary report

Tommi Kekki, Riitta Zilliacus and Maija Lipponen
VTT

Abstract

The deposition of IO_x particles on painted concrete samples and the study on iodine desorption from IO_x particle deposition was a joint effort between RADECO and CHEMPC projects. The experiments with iodine oxide deposition on painted concrete, showed some release of gaseous iodine. The desorption of iodine was enhanced on newly painted surface. According to these experiments the formation of the organic iodine is very limited. However, some migration of iodine on the surfaces may be possible by sequential revolatilization and re-trapping. Further experiments would be needed at higher temperature, at high humidity and with different representative surfaces such as metals, paints and cable jacket materials.

Nitric acid is a principal radiolytic compound produced in large, and its production is another important problem concerning pH of solutions, owing to its chemical properties of being a strong acid and a strong oxidizing agent. The G value was determined for nitric acid formed from air and for the nitric acid formed from the water. G-value calculated of these moist air results is 2.42 parallel experiments gave G-value 2.32. The determination of G-value for NO3 formation of water in radiation gave G-value 0.024. A preliminary experiment to study the influence of painted surface in the nitrate concentration was made by irradiating water with and without painted concrete block. The preliminary results with the 2.6 kGy dose gave 4 times more nitrate into the water than in blank case.

Introduction

The iodine released from the damaged fuel can be volatile and come into contact with painted surface in gas phase. The formation of volatile organic iodides is possible. The trapping of elemental iodine is relatively easy but volatile organic iodides are difficult to trap and therefore may increase the iodine releases to the environment significantly. The painted surface can also trap iodine in the gas phase.

The second subtask in the RADECO project was the investigation of production of nitric acid during high gamma field. Nitric acid is a principal radiolytic compound produced in large, and its production is another important problem concerning pH of solutions, owing to its chemical properties of being a strong acid and a strong oxidizing agent.

Main objectives

The iodine work continues with studies to measure the rate of organic iodide formation from iodine (as I_2) adsorbed from the gas phase on dry painted surfaces and then irradiated (in the water phase) to measure organic iodide formation. Together with CHEMPC project the behaviour of IO_x particles compared to I_2 in gas phase was studied [1]. Comparison of experimental studies of organic iodide formation on painted surfaces from international programs (PHEBUS-FP, EPICUR, OECD/BIP) was done [2]. VTT participate in OECD/BIP project (1.7.2007–31.3.2011). The information from that project was useful to compare with our own experimental results.

The formation of nitric acid during high dose rates was tested. It is known that gamma irradiation of air/water will lower the pH. The high dose is achievable using Gammacell 220 device in Otaniemi. Using the $FeSO_4$ dosimeters the dose was measured [3].

Formation of organic iodine on painted surface

The paints used in these experiments were those used in Finnish NPPs. Samples of the different paint ages (TEKNOPOX old and new) were exposed to iodine in the gas phase to achieve a pre-determined surface loading (mg/m^2) of iodine, and then irradiated in the gas phase to measure organic iodide formation.

The scope of work was to establish the rate constants for adsorption of iodine on painted surfaces for a given set of conditions in the gas phase using ^{131}I as radioactive tracer. Together with CHEMPC project of SAFIR2010 research

Programme the behavior of IO_x particles compared to I_2 in gas phase was studied. Measurements of the amount of organic iodides generated by irradiation of pre-loaded samples were measured by using selective adsorbent [1].

The mass of iodine, measured with the help of ^{131}I tracer, on painted concrete samples after impactor sampling and after iodine desorption is presented in Figure 1.

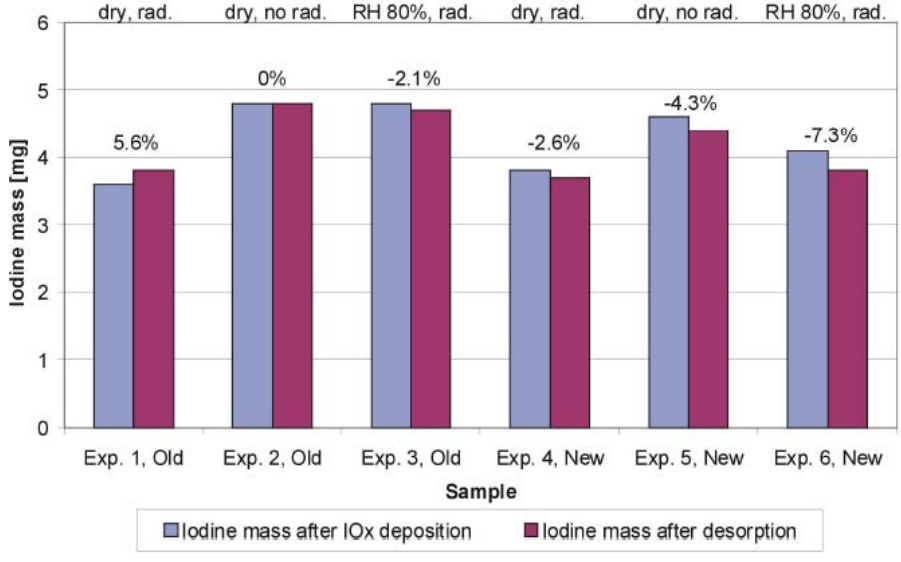

Figure 1. The mass of iodine on samples after IOx deposition, after desorption and the change in iodine mass [%] after desorption.

Although the accuracy of iodine mass determination was poor; according to the trend of results it seems that iodine is capable to be desorbed from iodine oxide deposition. The desorption is even more enhanced on newly painted surface. Anyway, these results showed the potential of deposited iodine oxide particles to release gaseous iodine. This would most likely happen in containment during a severe accident. These experiments were conducted as a scoping study.

The flooding of the wells as part of accident management can cause some changes in iodine behaviour. The effect of high pH water on the release of iodine from the painted surfaces still needs to be studied. The rate of organic iodide formation was studied by first producing the preloaded samples with iodine on the painted surface by adsorbtion of iodine (as I_2) from the gas phase on dry painted surfaces. Then the preloaded samples were irradiated with gamma rays

in the water phase and the release of organic iodide liquid traps and facility surfaces was measured

The results of iodine release into aqueous phase are presented together with the results from previous experiments performed in gas phase in Table 1.

Table 1. Release of iodine from painted concrete surface. Iodine adsorbed on the surface as gas.

Experiment *in gas phase **in water	Total I in the experiment, [mg/cm^2]	Radiation dose [kGy]	I released from the surface, % of total I	Iodine found in water phase, % of total I	Trapped I_2, % of total I	Trapped organic I, % of total I
*1	0.06	47 -	5.3 1.5		< 0.5 < 0.5	< 0.2 < 0.2
*2	0.13	12 -	0.93 0.99		< 0.2 < 0.2	<0.2 < 0.2
*3	0.015	43 -	4.6 1.5		< 0.2 < 0.2	< 0.2 < 0.2
**4	0.032	3.6	3.0 2.9	2.3 2.8	0.13 <0.1	<0.2 <0.1

Some of the I in all of the experiments in gas phase was released from the surface, but it was immediately adsorbed on the other surfaces, reaction vessel, and gas lines. The amount of organic or elemental iodine trapped in the filters was negligible. The experiments in the water phase show faster release of iodine from the surface into the water. Some iodine was found in the trap collecting elemental iodine. Organic iodide formation was not detected.

Formation of nitric acid during high gamma dose

The formation of nitric acid in water/air system was measured by irradiating the known mixture with a gamma source and determining the amount of nitric ions formed in the irradiation after chemical treatment by spectrophotometry. When nitric acid is formed during the irradiation in a closed system with water present it is totally absorbed into the water phase. The sample of this water is treated with sodium hydroxide, heated to dryness and the residue is dissolved to a dilute perchloric acid. The amount of nitrate is measured quantitatively by spectrophotometry (λ = 210 nm). When experiments are performed using various gamma doses, the G-value for the formation of nitric acid can be calculated by using the slope of the absorbance/ dose graph.

First series of tests were done with a small amount of distilled water and air irradiated in a closed vessel, so called moist air test. In addition some tests only

with pure water phase were done. These test give more information on the formation of nitric acid in the water phase where the concentration of nitrogen is very low compared to the gas phase (air). The last preliminary tests were done using moisture air and painted concrete block to see what effect painted surfaces is. All tests were done in temperature (c.a. 25°C, 1 atm). The results of experiments can be seen in Table 2.

Table 2. G-values of different cases.

Measurement case	G-value
moist air in closed system	2.42
moist air in closed system	2.32
water in closed system	0.024
moist air and painted block in closed system	preliminary results about 4 times higher than moist air in closed system

Conclusions

The experiments with IO_x particle deposition on painted concrete, showed some release of gaseous iodine. The desorption of iodine was enhanced on newly painted surface. In the experiments in the air iodine released from the paint was adsorbed on the surfaces, reaction vessel, and gas lines. The reaction with the surface was so rapid that it was impossible to determine the chemical form of iodine. The amount of organic or elemental iodine trapped in the filters was negligible. The experiments in the water phase show faster release of iodine from the surface into the water. Some iodine was found in the trap collecting elemental iodine. Organic iodide formation was not detected.

There is a large scatter in the results from all of the programmes (PHEBUS-FP, EPICUR, OECD/BIP), so it is difficult to make comparisons between the different studies. The behaviour of iodine in water is dependent on the pH. High pH prevents the formation of elemental iodine and decreases the formation of volatile organic iodides. Chemical and radiolytic interactions with surfaces lead to evolution of gaseous iodine in the form of molecular iodine (I_2) and volatile organic iodides such as methyl iodide (CH_3I). These gaseous species are susceptible to radiolytic and chemical destruction in the atmosphere or deposition on surfaces. The absorption of molecular iodine on painted surfaces depends on the

ambient humidity or the amount of water absorbed by the paint. Only a small portion of the total amount of the iodine released is detected in the gas phase at the end of the irradiation tests. The results from RADECO project was the same level, mostly under detection limits. The balance between removal mechanisms and the mechanisms for gaseous iodine production leads to the observed steady-state concentration of gaseous iodine.

The G-value was determined for nitric acid formed from air and for the nitric acid formed from the water. G-value calculated of these moist air results is 2.42 parallel experiments gave G-value 2.32. The G-values found in literature for nitric acid formation from air range $G_{(HNO3)}$ = 2.3–2.7 molecules/100 eV [4, 5]. Compared to literature values measurement results were exact the same level. The determination of G-value for NO_3 formation of water in radiation gave G-value 0.024. This is three times that given in literature. The G-values found in literature for nitric acid formation from water is $G_{(HNO3)}$ = 0.007 molecules/100 eV [6]. Our experiment was made in room temperature. Increasing the temperature decreases the amount of nitrogen dissolved in water and decreases the G-value for nitric acid formation in water. A preliminary experiment to study the influence of painted surface in the nitrate concentration was made by irradiating water with and without painted concrete block. The preliminary results with the 2.6 kGy dose gave 4 times more nitrate into the water than in blank case.

References

1. Zilliacus, R., Kärkelä, T. & Kekki, T. Formation of organic iodide on painted surface with IO_x particles. VTT, Espoo, June 2010. VTT-R-02161-10.

2. Lipponen, M., Kekki, T. & Zilliacus, R. Comparison of experimental studies of organic iodide formation on painted surfaces. VTT, Espoo, January 2011. VTT-R-00775-11.

3. Zilliacus, R. & Kekki, T. Formation of nitric acid during high gamma dose. VTT, Espoo, January 2011. VTT-R-00774-11.

4. Farhat, A. & Rodgers, M.A.J. Radiation Chemistry, Principles and Applications. New York, VCH Publishers, 1987.

5. Spinks, J.W.T. & Woods, R.J. An Introduction to Radiation Chemistry. John Wiley & Sons, Third ed. 1990.

6. Beahm, E.C., Lorenz, R.A. & Weber, C.F. Iodine evolution and pH control. NUREG/CR-5950.

19. Primary Circuit Chemistry of Fission Products (CHEMPC)

19.1 CHEMPC summary report

Teemu Kärkelä, Ari Auvinen, Jarmo Kalilainen, Jussi Lyyränen, Tuula Kajolinna, Jouni Pyykönen, Tapani Raunio, Leif Kåll, Riitta Zilliacus, Unto Tapper, Tommi Kekki, Raoul Järvinen and Jorma Jokiniemi
VTT

Abstract

In this report is summarized the work performed in CHEMPC project. The aim in the project was to study the transport and chemistry of fission products in primary circuit and in containment during a hypothetical severe accident. The fission product chemistry in primary circuit was experimentally studied at VTT and at IRSN. The reactions on surfaces were also investigated. Experimental studies on fission product transport in SGTR sequences were conducted in international ARTIST and ARTIST-2 programs at PSI. The radiolytical oxidation of iodine in containment conditions was studied in co-operation with Chalmers University of Technology. Experiments were conducted both at VTT and at Chalmers. Based on previous experiments, modelling studies on the behaviour of ruthenium oxides in air-ingress accident were conducted. As a part of international co-operation, CHEMPC project included also follow-up of Phebus FP and ISTP programs as well as ISTC program project EVAN.

CHEMPC project is funded by Finnish Research Programme on Nuclear Power Plant Safety 2007–2010 (SAFIR 2010), VTT, Nordic Nuclear Safety Research (NKS), Institut de Radioprotection et de Sûreté Nucléaire (IRSN) and Fortum Nuclear Services Ltd.

Introduction

The focus in CHEMPC project was on studying the transport and chemistry of fission products during a hypothetical severe accident. The fission products studied in experiments were ruthenium and iodine. Both of these species are very volatile and their radiotoxicity is high [1, 2]. Therefore, the aim was to find out the gaseous and aerosol species which transports through the primary circuit and to study also the reactions of fission products on the surfaces of primary circuit. Another aim was to investigate the behaviour of fission products in containment.

The project included international co-operation in the field of severe accident studies. It involved participation in the interpretation of results from release and transport experiments with real spent fuel. VTT has also provided instrumentation and experimental expertise to international research programs.

Another important topic in CHEMPC project has been the transport of FPs in possible steam generator tube rupture scenarios. Despite their fairly low probability such containment by-pass scenarios have been considered risk dominant because of their estimated large source term to the environment. Currently, retention to the circuit is not taken into account in risk analysis due to lack of crucial aerosol models and experimental data. VTT participated in international ARTIST program carried out at PSI, in which retention of particles to various structures of a vertical steam generator was experimentally studied. In addition, separate effect experiments were carried out at VTT to quantify resuspension of particles from broken steam generator tube. As a result, a unique database on particle retention in steam generator to be utilized in safety assessments was gathered. It was found out that retention of particles especially in flooded bundle was much more efficient than estimated by pool scrubbing models. Particle deposition into the upper structures of the steam generator was fairly modest.

Fission products behaviour in primary circuit

In order to gather more information on the high temperature chemistry of ruthenium, the transport of ruthenium through reactor cooling system in severe accident conditions has previously been studied at VTT. The experimental data was interpreted in this project and the behaviour of volatile ruthenium oxides in decreasing temperature gradient (1 700–300 K) could be explained by detailed CFD modelling of the facility [3]. The results have been shared through the international Severe Accident Research NETwork (SARNET).

As iodine is keen to react with other materials, the chemistry of iodine is complex. It causes difficulties in modelling the behaviour of iodine with severe accident analysis codes. IRSN has started an ISTP program project CHIP to study gas phase chemistry of iodine to enhance the current severe accident models. Sampling system for high and low temperature sections of the CHIP facility were designed and constructed at VTT [4].

In addition to CHIP, a similar EXSI facility aimed at studying iodine chemistry at primary circuit surfaces at VTT was built as well. Its computer controlled properties are advanced and it can be used to collect several samples during one experiment. EXSI has already been used in experiments. As a result, e.g. high fraction of gaseous iodine was found to be transported through primary circuit when boron oxide was reacting with caesium iodide on oxidised stainless steel surface at 650°C. Similar high fraction of gaseous iodine was also found in Phébus FPT-3 experiment where control rods were made of boron carbide B_4C.

Diffusion denuder

The analysis of collected aerosol sample on a filter is not simple. There is usually an artefact of gaseous species reacting with particles on filter when transporting through the filter. That causes an error in analysis of both gaseous and aerosol samples. Diffusion denuder technique was studied in the project to solve this problem concerning fission product iodine.

Gas or vapor molecules diffuse rapidly to the wall of a diffusion sampler and adsorb onto the wall coated with material suitable for collecting the gas. Diffusion tubes have been used to measure diffusion coefficients of several gases in the air. Since 1980, diffusion denuders followed by a filter pack have been developed to sample atmospheric vapors and particulate aerosols. Using this sampling technique one can separate gaseous species from particles and thus minimize sampling artefacts due to the presence of these gases [5].

Pui et al. [6] designed a compact coil denuder consisting of a 1.0 cm inner diameter and 95 cm long glass tube bent into a three-turn helical coil with a 10 cm diameter (Figure 1). The heat and mass transfer rates to the tube wall in a curved tube are much higher than those in a straight tube operated at the same conditions [5].

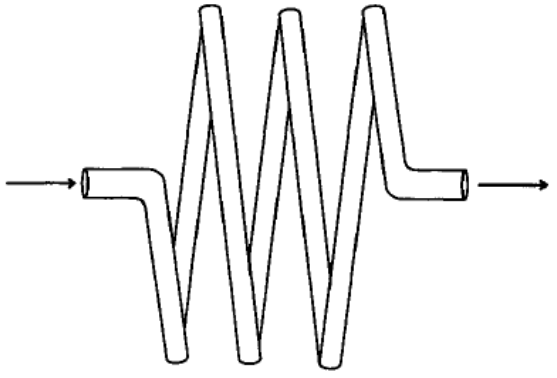

Figure 1. In this figure is presented a sketch of diffusion denuder tested in the project. It will be used to separate gaseous iodine from aerosol iodine and thus minimize sampling artefacts. [5, 6]

In this study the denuder was used to trap gaseous iodine. It was made of copper, which is known to trap elemental iodine effectively [7]. It was tested with radioactive tracer ^{131}I. As a result, the retention of iodine oxide aerosol was only less than 2% of aerosol fed in. The collection efficiency of gaseous iodine was more than 99%. These results will be verified with another test in future.

Follow-up of international programs

CHEMPC project has included follow-up of international Phebus FP and ISTP programs as well as ISTC program project EVAN.

The major undertakings in Phebus FP follow-up were the reviews of FPT-2 and FPT-3 final reports regarding fission product transport in the primary circuit of the facility. The experiments were highly interesting as in FPT-2 test the revaporisation of all volatile fission products in the circuit was directly measured for the first time in realistic conditions. The results from that experiment indicated also significant change in the FP transport close to the end of the fuel degradation phase. Furthermore, the changes in iodine concentration in the containment seemed to be almost exactly the opposite to the predictions of severe accident codes [8]. FPT-3 was the first experiment conducted with B4C control rods instead of AIC control rods. In that experiment the fraction of gaseous iodine released to the containment was 85%. However, in the containment the gaseous iodine fraction decreased very rapidly [9].

ISTP program includes the aforementioned CHIP experiments, in which VTT has participated. In addition, iodine and ruthenium chemistry in containment has

been studied in EPICUR project, B_4C degradation in BECARRE project and cladding degradation in MOZART project. The construction of the VERDON facility for HBU and MOX fuel degradation experiments has also been followed-up in ISTP program.

ISTC program project EVAN included several subprojects of which fission product release from molten pool and resuspension experiments were reviewed by VTT.

Radiolytical oxidation of iodine

One hypothesis in modelling iodine behaviour in the containment has been that radiolytic processes destroy gas phase molecular iodine to form iodine oxide or iodine nitrogen oxide particles. The objective of this study was to verify the possible formation of iodine containing aerosol when gaseous iodine is exposed to radiation. EXSI facility was also applied in the study of radiolytic oxidation of gaseous iodine in containment conditions conducted together with Chalmers University of Technology. It was found out that UV-radiation (c-type) alone was not able to oxidise elemental iodine in gas phase. However, UV-radiation produced significant amount of ozone even with fairly low oxygen concentration (2%-vol). Ozone reacted with gaseous elemental iodine causing almost instant nucleation of iodine oxide aerosol particles. The particle growth took place by agglomeration and by surface reaction to final mobility diameter of 60–120 nm depending on the initial iodine concentration. It seemed that ozone increased the retention of iodine, probably by surface reaction, in the facility. The observed formation of iodine oxide particles would largely explain the particularly peculiar behaviour of gaseous iodine in Phebus FP experiments.

In case of a hypothetical severe accident it is very likely that iodine at least partly deposits on painted walls of a reactor containment building. Iodine may react with painted surfaces to form organic iodine species. These organic species are a possible source of volatile iodine, which may increase the fraction of releasable iodine. Therefore, it is important to study the transport of organic iodine in containment conditions. Another question is, in which form are the organic iodides transported as gaseous molecules or as aerosol particles resulting from organic iodides reacting with radiolysis products. To answer this last question methyl iodide was fed into the EXSI facility in an air mixture. UV-light (c-type) was used as a source of radiation to produce ozone from oxygen. A separate generator was also applied to reach higher ozone concentrations.

It was found that the formation of aerosol particles was very fast when ozone and methyl iodide were present in the facility. Even a very low concentration of ozone produced high number concentration of particles. The measured aerosol mass concentration increased with increasing temperature and ozone concentration. Because the particle diameter was quite small (< 180 nm), their settling velocity is low. Therefore, iodine containing aerosols may exist in containment atmosphere for a long period of time. Part of methyl iodide was always transported through the facility regardless of experimental conditions. The transported fractions for both methyl iodide and ozone decreased with increasing reaction temperature. The main gaseous reaction products were methanol and formaldehyde. Especially at elevated temperature other reaction products, such as formic acid and methyl formate, became important as well (Figure 2).

During a hypothetical severe accident the containment atmosphere contains several types of radiation (e.g. alpha, beta and gamma). The effect of different radiation types on iodine is not well known. In this project was also studied the effect of gamma radiation in air on the decomposition of gaseous methyl iodide and the formation of gaseous and aerosol reaction products. Another aim was to study the formation of ozone by gamma radiation. As a result, the formation of ozone in air by gamma radiation was very low compared to the formation by UV (c-type) radiation. The formation of higher ozone concentration requires longer residence time of flow in gamma radiation.

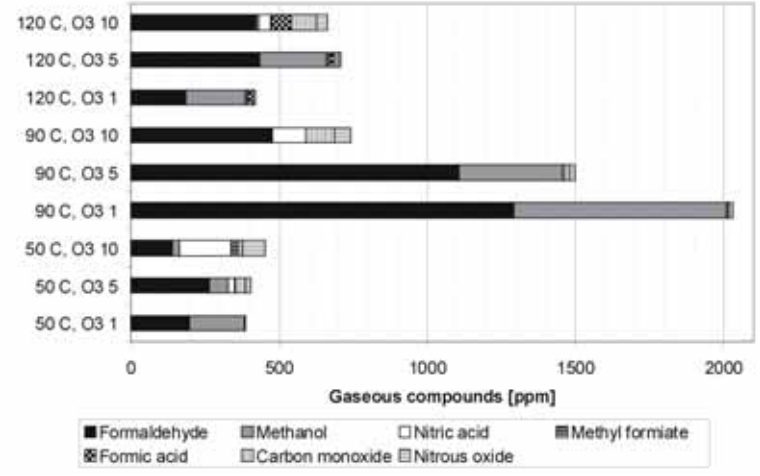

Figure 2. In figure are shown the measured gaseous reaction products (as ppm) from oxidation of methyl iodide with ozone. The temperature of the facility and the power setting of ozone generator are presented on vertical axis.

The amount of measured gaseous reaction product species in experiments with gamma radiation was low compared to previous experiments with UV (c-type) radiation. The main gaseous reaction products were formaldehyde and iodoform (CHI_3). The formation of iodoform has not been detected in experiments with UV radiation. Carbon monoxide seemed also to be a reaction product. The formation of aerosol particles was very low. This is also due to low production of ozone in gamma radiation. Therefore the oxidation of iodine into iodine oxide aerosol was prevented.

SGTR scenarios

Particle resuspension experiments

Particularly in containment by-pass sequences retention of FPs in the circuit would significantly decrease the source term. In this work particle deposition and resuspension experiments were measured with online instrumentation [10]. The experiments were unique as the amount of deposited material was monitored simultaneously at several locations within a tube. The deposition mechanism, deposition velocity and flow velocity could also be adjusted independently. Particle size, shape and density were well characterised in the experiments.

According to the results, the most important parameter affecting resuspension seemed to be particle size. Flow rate during the deposition phase seemed to also influence on adhesion force distribution. Deposition mechanism did not directly influence resuspension. However, it affected on the size of deposited particles. Particles that had resuspended from the walls seemed to fell to the floor of the tube. This would indicate that the resuspension must have taken place as fairly large agglomerates. Also simultaneous deposition and resuspension seemed to be significant in laminar as well as in turbulent flow.

ARTIST program

Aim of the ARTIST program has been to provide an international forum to create and share information on SGTR scenarios. High quality experimental data for development of both fundamental and application oriented models have been produced during the program. Data have also facilitated evaluation of effectiveness of severe accident management guidelines. During the project methodology for SGTR risk assessment using ARTIST experimental data have been further developed. The objective is to produce international consensus on

re-assessment of SGTR induced environmental risk during DBA and SA. Preliminary results from the re-assessment have been published.

ARTIST program consist of seven phases, in which various mechanisms related to FP retention during SGTR sequence have been experimentally studied. These include aerosol retention in broken SG tubes, retention in bundle at break stage and at far-field, aerosol and droplet retention in separator and dryer, retention in flooded bundle as well as integral experiments with complete vertical steam generator.

In broken SG tubes the retention was dynamic depending on particle size and concentration. Steam condensation increased decontamination factor significantly [11]. Largest retention in dry conditions was found to take place however in the break stage depending primarily on particle size and concentration [12]. Retention in the far-field of the bundle as well as in the separator and dryer section was rather limited [13]. The most effective retention took place in flooded bundle with submersion of the break between at least 3.2 and 3.8 meters. In such case the decontamination factor was found to vary between 300 and 2000 [14]. VTT participated in ARTIST integral experiments, which yielded results consistent with the separate effect experiments. In the integral tests the highest retention was observed at the break stage of the SG [15].

Applications

In this project was developed an automatic sampling system, which is able to collect gaseous and aerosol samples from high and low temperature. The sampling system is applied at IRSN to study the gas phase high temperature chemistry of FP compounds at CHIP facility. At VTT similar sampling system is used in EXSI facility dedicated to measure reactions of FP compounds at the surfaces of primary circuit.

In order to enhance the analysis accuracy of automatic sampling system, the diffusion denuder technique was developed to separate gaseous species from particles and thus minimize sampling artifacts due to the presence of gases. This technique will be used in future experiments with EXSI facility.

The chemistry of ruthenium and iodine has been studied in primary circuit and containment conditions. The results have been shared in the frame of SARNET network and the wide database will be utilized in the development of severe accident codes.

Conclusions

The CHEMPC project (2007–2010) focused on the transport and chemistry of fission products in primary circuit and in containment. As a part of severe accident phenomena, the reactions of fission products on the primary circuit surfaces and the resuspension of FP aerosol in circuit were studied as well. The data on the behaviour of fission products can be utilized in safety assessment and plant analysis codes.

During the project a fully automated system, capable of extracting gaseous samples from high temperature (700–1 000°C) and cooling them down to 150°C with only negligible losses, was constructed. The sampling system is applied at IRSN to study the gas phase high temperature chemistry of FP compounds at CHIP facility. At VTT similar sampling system is used in EXSI facility dedicated to measure reactions of FP compounds at the surfaces of the primary circuit.

EXSI facility was also applied in the study of radiolytic oxidation of iodine in containment conditions conducted together with Chalmers University of Technology. It was found out that UV radiation produced significant amount of ozone even with fairly low oxygen concentration (2%-vol). Ozone reacted with gaseous elemental iodine causing almost instant nucleation of iodine oxide aerosol particles. In the case of organic iodine, it was also found that the formation of aerosol particles was very fast when ozone and methyl iodide were present in the facility. The main gaseous reaction products were methanol and formaldehyde. Especially at elevated temperature other reaction products, such as formic acid and methyl formate, became important as well. Because the measured aerosol particle diameter in the experiments was quite small (< 180 nm), their settling velocity is low. Therefore, iodine containing aerosols may exist in containment atmosphere for a long period of time.

The experiments on the radiolytical oxidation of gaseous methyl iodide by gamma radiation were conducted at Chalmers University of Technology. As a result, the formation of ozone in air by gamma radiation was very low compared to the formation by UV radiation. The main gaseous reaction products were formaldehyde and iodoform. Carbon monoxide seemed also to be a reaction product. The formation of aerosol particles was very low.

Very important information especially on the behaviour of fission products was received from Phebus FP and ISTP follow-up programs. International co-operation have helped greatly in the design and interpretation of also the separate effect experiments carried out at VTT.

References

1. Mun, C., Contrel, L. & Madic, C. Review of literature on ruthenium behaviour in nuclear power plant severe accidents. Nuclear Technology 2006, Vol. 156, No. 3, pp. 332–346.

2. Girault, N., Dickinson, S., Funke, F., Auvinen, A., Herranz, L. & Krausmann, E. Iodine behaviour under LWR accident conditions: Lessons learnt from analyses of the first two Phebus FP tests. Nuclear Engineering and Design 2006, Vol. 236, No. 12, pp. 1293–1308.

3. Kärkelä, T., Backman, U., Auvinen, A., Zilliacus, R., Lipponen, M., Kekki, T., Tapper, U. & Jokiniemi, J. Experiments on the behaviour of ruthenium in air ingress accidents – Final Report. VTT, Espoo, 2007. VTT-R-01252-07.

4. Auvinen, A., Lyyränen, J., Kärkelä, T., Kåll, L., Järvinen, R., Roine, J. & Vänttinen, S. Qualification of the sampling systems for CHIP test facility – Final report. VTT, Espoo, 2007. VTT-R-11382-07.

5. Baron, P.A. & Willeke, K. Aerosol measurement: principles, techniques and applications. John Wiley and Sons, Inc., 2001. P. 582,

6. Pui, D.Y.H., Lewis, C.W., Tsai, C.J. & Liu, B.Y.H. A compact coiled high-performance denuder for the sampling of atmospheric pollutants. Atmos. Environ. 1990, 17, pp. 2605–2610.

7. Chamberlain, A.C., Eggleton, A.E.J., Megaw, W.J. & Morris, J.B. Physical chemistry of iodine and removal of iodine from gas streams. J. Nucl. Energy, Parts A and B 1963, Vol. 17, pp. 519–550.

8. Gregoire, A., March, P., Payot, F., Ritter, G., Zabiego, M., de Bremaecker, A., Biard, B., Gregoire, G., Schlutig, S. & Phebus, P.F. FPT2 Final Report, IRSN DPAM/DIR-2008-272, Document Phébus PF IP/08/579, 2008.

9. Payot, F., Haste, T., Biard, B., Bot-Robin, F., Devoy, J., Garnier, Y., Guillot, J., Manenc, C., March, P. & Phebus, P.F. FPT3 Final Report. IRSN DPAM/DIR-2010-148, Document Phébus PF IP/10/587, 2010.

10. Raunio, T. Experimental Study on Fine Particle Resuspension in Nuclear Reactor Safety. Masters Thesis, Helsinki University of Technology, Faculty of Information and Natural Sciences, 2008.

11. Lind, T., Suckow, A. & Dehbi, A. Summary report on ARTIST Phase I tests for in-tube retention. Paul Scherrer Institut, TM-42-08-03, ARTIST-71-08, 2008.

12. Lind, T., Suckow, A. & Dehbi, A. Summary report on ARTIST Phase II tests for retention in the break stage. Paul Scherrer Institut, TM-42-08-04, ARTIST-72-08, 2008.

13. Lind, T., Suckow, A. & Dehbi, A. Summary report on ARTIST Phase III tests for retention in the far field. Paul Scherrer Institut, TM-42-08-05, ARTIST-73-08, 2008.

14. Dehbi, A., Suckow, A. & Lind, T. Summary report on ARTIST Phase V tests for retention in the flooded bundle. Paul Scherrer Institut, TM-42-08-18, ARTIST-75-08, 2008.

15. Lind, T., Suckow, A. & Dehbi, A. Summary report on ARTIST Phase VII tests for retention in the integral mock-up facility. Paul Scherrer Institut, TM-42-08-08, ARTIST-77-08, 2008.

19.2 Primary circuit chemistry of iodine

Jarmo Kalilainen, Teemu Kärkelä, Pekka Rantanen, Johanna Forsman,
Ari Auvinen, Unto Tapper and Jorma Jokiniemi
VTT

Abstract

In this study, improvements were made to experimental facility which was constructed in order to study the effect of primary circuit surface on the transport of fission products. The improvements included new primary diluter, new automated sampling system, and new sampling program, able to collect more online temperature, pressure and flow rate data. Also, two experiments were conducted in order to test the updated facility and gain new knowledge of the formation of gaseous iodine in different temperatures.

The experimental work showed that the results obtained with the updated experimental facility were comparable with the previous experimental work. Further, it was showed that gaseous iodine can be formed in reaction between caesium iodide and molybdenum oxide at 400°C temperature.

Introduction

In a severe nuclear accident, reactor core is largely damaged. Cooling system is unable to remove all the heat from the reactor core and the core materials start to melt. Core materials contain fission products which can form aerosol and drift to the primary circuit [1]. Iodine is considered to be an important fission product in the safety analysis because several very volatile gaseous iodine compounds are formed in containment building conditions [2]. Specific activity of iodine is high and it is accumulated in human body.

After the TMI-2 (Three Mile Island Unit 2) accident in the year 1979, severe accident research has played a significant role in international reactor safety analysis [3]. International Phebus Fission Product programme is the largest research program in the world focusing on severe accident phenomena in light water reactors [2]. Phebus experiments provided lots of experimental data on iodine release from the fuel. Some of the iodine results where not at all expected, which showed the need to carry out more detailed separable effect experiments.

One of the phenomena that needed closer investigation was iodine compounds release due to reactions on primary circuit surfaces.

The initial conditions of Phebus FPT3 experiment differs the most from the other Phebus experiments since the material of the control rods used was boron carbide B_4C. The overall behaviour of iodine also differed significantly from previous Phebus tests [2]. In FTP3, only a very small fraction of iodine was transported as aerosol in the circuit. Approximately 85% of the iodine released in the containment was in gaseous form [4]. Clearly, boron was at least partly responsible for the change in the iodine behaviour.

None of the calculations made in advance had predicted such high gaseous iodine fraction in conditions described above. This indicated that iodine chemistry codes did not include all the phenomena that could be important in a severe nuclear accident. The results also showed that more precise experiments on iodine behaviour in primary circuit during severe accident conditions were needed.

Goal

The aim in this study was to improve the instrumentation of the EXSI facility [5]. As a result, even more accurate measurements on the transport of iodine in severe accident conditions could be conducted. Also, two preliminary studies were carried out in order to verify, whether the updated facility would work properly.

Updated experimental facility

The modifications to the old experimental facility [5] were made in order to improve the sampling system and gather more data of the changes in pressure and temperature during the experimental work. Also, changes in the primary diluter were made to further reduce the particles depositions on its walls. In the process of designing the new primary diluter, the material of the reaction furnace tube was also changed from alumina to stainless steel. Figure 1 shows a schematic picture of the new experimental facility. No changes were made in the online aerosol measurement line, located after the ejector diluter D2, or the interior of the sampling furnace.

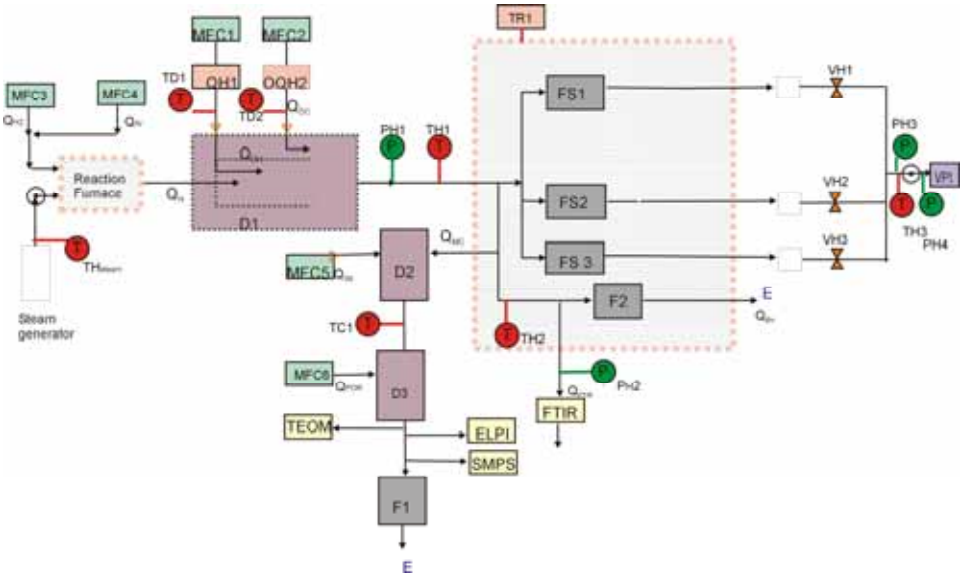

Figure 1. Schematic picture of the upgraded EXSI facility.

Primary diluter and reaction furnace

In order to reduce the depositions by condensation and thermophoresis at the beginning of the facility, the structure of primary diluter hot dilution part and reaction furnace tube were modified. Figure 2 shows a schematic picture of the new furnace tube and primary diluter design.

The new furnace tube is made of stainless steel instead of alumina. The furnace tube has a narrowing from 24 mm tube to 10 mm in diameter. The narrow side of the tube has a screw thread where the primary diluter can be fasten, thus preventing the leakage from the tube diluter assembly. The outer diameter of the diluter has been designed so that during the experiment, the hot dilution part of the diluter is situated inside the reaction furnace all the way to the hot gas inlet tube, seen in Figure 2. This further enhances heating of the hot dilution gas, before it is mixed with the flow from the reaction furnace and with the cold dilution flow.

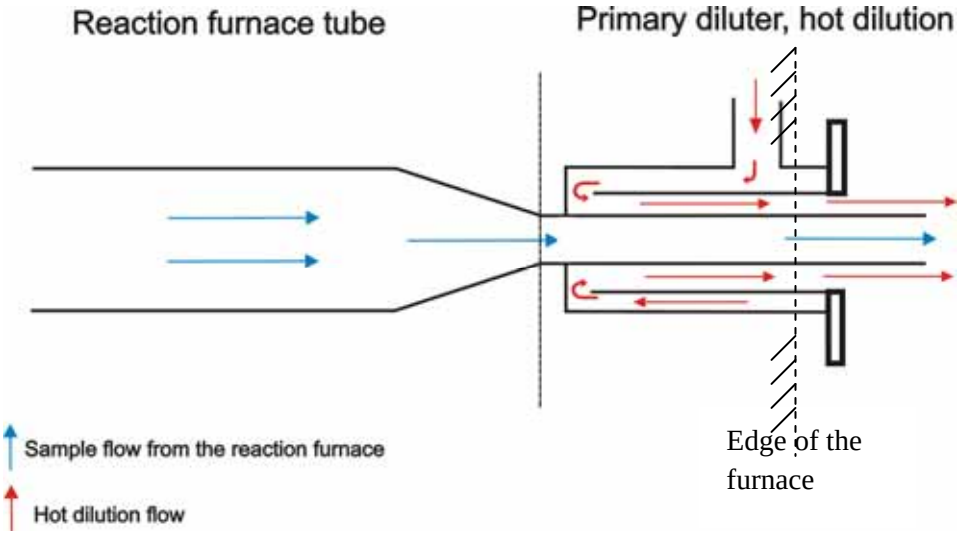

Figure 2. Schematic picture of the new primary diluter hot dilution part and reaction furnace tube.

Another improvement was also made on the set-up responsible of heating the hot dilution gas. In the new facility, both hot and cold dilution gas can be heated with Mayer-vastus 930 W flow heaters. Flow heaters are operated by using the controlling computer. Argon is used as both hot and cold dilution gas. Mass flow controllers MFC1 and MFC2 are used to control the hot and cold dilution gas flows, respectively. Thermocouples TD1 and TD2 measure the temperature of the hot and cold dilution gas, respectively. TD1 and TD2 are located right before the primary diluter. TH1 and PH1 are used measuring the temperature and pressure of the main line after the primary diluter, respectively. H_2 and argon flows to reaction furnace are controlled with mass flow controller MFC3 and MFC4. All the mass flow controllers on the facility are controlled with the controlling computer.

Water vapour concentration is controlled with critical orifice. Thermocouple TH_{STEAM} is used to measure the temperature of steam generated on the steam generator.

Sampling system

The sampling system of the new facility has been entirely automated. The filter sampling is started by imputing the desired sampling time to the controlling computer and choosing the desired sampling line. As the sampling switch has

been activated on the program, the controlling computer automatically opens the valve (FS1, 2 and 3 on Figure 1) on a right sampling line, and again closes it after the sampling time has expired. Valves used on the sampling lines are Swagelok type SS-42GS6MM-A15C3AN01-R02K.

Thermocouple TH3 measures the temperature of the flow just before the critical orifice, used in the sample collection. Pressure sensors PH3 and 4 are used measuring the pressure both sides of the critical orifice. Gas flow to sampling lines during samplings is calculated and logged online by the controlling computer. For the calculations of the sampling flow, the program uses an equation:

$$Q_{sampling} = (1.875 - 4.259 \cdot 10^{-3} T + 4.332 \cdot 10^{-6} T^2) \cdot (1.607P - 0.141) \qquad (1)$$

In Eq. (1), T = TH3 and P = PH3.

The sample to online aerosol measurement devices is drawn with ejector diluter by using nitrogen as a dilution gas. Dilution flow to the ejector is controlled with mass flow controller MFC5. After this, the sample is diluted with again with N_2 on porous tube diluter controlled with the mass flow controller MFC6. On FTIR line, PH2 is used to measure the pressure before FTIR.

Experimental work

Two experiments were conducted for the testing of the new facility. The first experiment with CsI as a precursor in an alumina crucible was done in order to see, if the new results were comparable to the results obtained from the experiments with the old facility [5]. The second experiment featured CsI and molybdenum oxide (MoO_3) as a precursor in an alumina crucible. Also, the temperature of the reaction furnace and hot dilution gas was reduced to 400°C. In the previous experiments, CsI particles seemed to react with Mo depositions at the part of the facility in which temperature was clearly below 650°C. Lower temperature in the second experiment was used in order to study if such reaction produce significant amount of gaseous iodine.

Like in previous work, three different carrier gas mixtures were used during both experiments. Different gas compositions are shown in Table 1. The water vapour flow, used in the experiments corresponds to flow rate 0.5 l/min at normal pressure and 0°C.

Table 1. Gas flow rates and volume percentages during each sampling.

		Sampling		
		A	**B**	**C**
Argon	Flow rate [l/min] (NTP)	3.3	3.2	2.9
	Gas vol-%	86.8	84.2	76.3
Steam	Flow rate [l/min]	0.5	0.5	0.5
	Gas vol-%	13.2	13.2	13.2
Hydrogen	Flow rate [l/min] (NTP)	0	0.1	0.4
	Gas vol-%	0	2.6	10.5

Results and discussion

Figure 3 shows the aerosol and gaseous reaction product mass concentrations in first experiment, calculated from the filter and bubbling bottle ICP-MS data. These data shows that as the concentration of H2 in atmosphere is increased, the amount of gaseous iodine in the reaction products was decreased. This coincides with the results observed in the previous experiments with the older facility [5]. The main difference is that the amount of gaseous iodine released in steam-argon flow is significantly higher than before. All the other gaseous and aerosol I and Cs concentrations are lower than in the corresponding experiment with the old facility. Increased gaseous iodine release was most likely caused by the change of reaction furnace tube material from alumina to stainless steel. Caesium can now react also with the furnace tube, thus causing release of gaseous iodine.

The mass concentrations of depositions in different parts of the facility are shown in Figure 4. Compared to results obtained from the measurements with previous facility [5], the particle depositions to primary diluter have increased, whereas the depositions to furnace tube and main line have decreased. This would indicate that the new primary diluter did not perform optimally. Deposition into the diluter was likely the primary reason for the decreased release of CsI aerosol. Fortunately, deposition can be substantially decreased by making a minor change into the structure of the diluter.

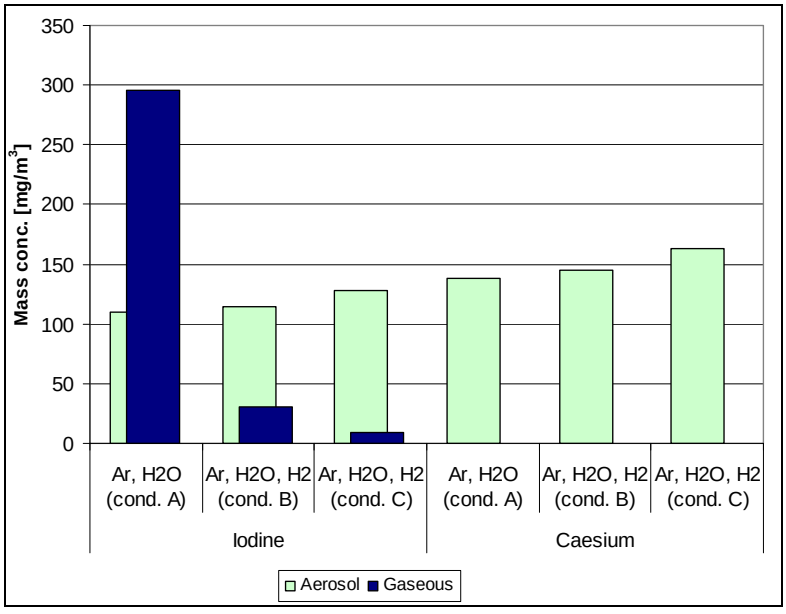

Figure 3. Iodine and caesium mass concentrations in the first experiment, calculated from aerosol filter and bubbling bottle ICP-MS data.

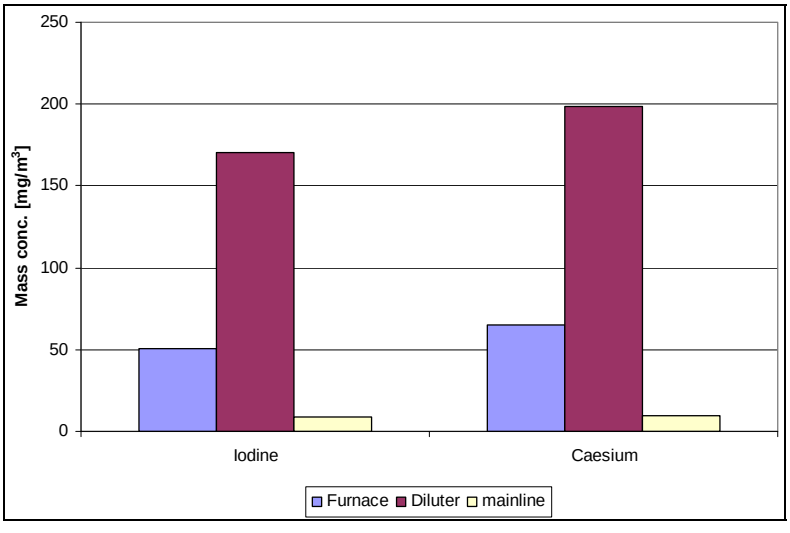

Figure 4. Mass concentrations of I and Cs depositions in different parts of the facility, obtained from ICP-MS analysis of the deposition samples.

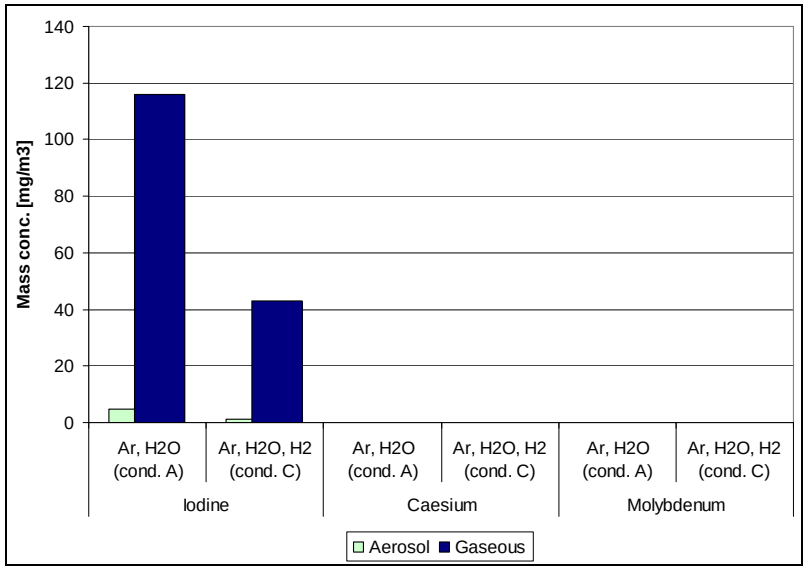

Figure 5. Iodine, caesium and molybdenum mass concentrations in the second experiment, calculated from aerosol filter and bubbling bottle ICP-MS data.

The mass concentrations measured in second experiment with CsI and MoO_3 as precursors in alumina crucible are shown in Figure 5. Data from the sampling B showed unreasonably low mass values compared to samplings A and C, and is thus removed from the results. No indications why sampling B had failed could be found from the logged pressure or flow rate data. This means it was probably caused by a leakage in the sampling line.

Results from the second experiment show clearly that gaseous iodine was formed when CsI and MoO_3 precursor materials reacted at 400°C. Figure 5 also shows that very little aerosol particles were formed during this experiment. This was also verified by the online aerosol measurement devices such as TEOM and SMPS, which measured very low particle mass and number concentrations, respectively. This result gives a very strong confirmation to the assumption made after the previous experiments [5], that the gaseous iodine can be formed with the reactions between CsI and Mo depositions at the parts of the experimental facility where the temperature is much lower than 650°C.

Conclusions

As an outcome of the work, a unique experimental facility in the field of nuclear safety was developed and built. Updates of the facility include new automated

sampling system, new primary diluter and improved data logging capability. The properties of the facility are focused on the study of the behaviour of iodine in primary circuit during a hypothetical severe accident. It gives new information e.g. about the effect of reactions on primary circuit surfaces on the release and transport of iodine.

The improved facility has been tested and a few preliminary experiments have already been conducted. These experiments showed that as CsI precursor was used in alumina evaporation crucible, the results coincided mostly with the old experimental data. The main difference was the lower overall mass concentration of reaction products, which was probably caused by deposition into the primary diluter. It was also seen that when CsI and MoO_3 were used as precursor materials, gaseous iodine was released at 400°C temperature, which was already predicted in the light of previous experiments conducted with the old facility. To improve the performance of the facility, a slight change into the structure of the diluter has to be made. Also, the surface of the reaction furnace tube will be pre-oxidized in the coming experiments. An extensive experimental study of fission product transport within the primary circuit will be conducted in SAFIR2014 program.

References

1. U.S. Nuclear Regulatory Commission, Primary System Fission Product Release and Transport. NUREG/CR-6193, June 1994.

2. Girault, N., Dickinson, S., Funke, F., Auvinen, A., Herranz, L. & Krausmann, E. Iodine behaviour under LWR accident Condition: Lessons learnt from analyses of the two Phebus FP tests. Nuclear Engineering and Design 2006, 236(12), pp.1293–1208.

3. Jokiniemi, J., Kilpi, K., Lindholm, I., Mykkänen, J., Pekkarinen, E., Sairanen, R. & Silde, A. Vakavien reaktorionnettomuuksien ilmiöt. VTT, Espoo, 1995. VTT Tiedotteita 1628. 103 s.

4. Haste, T., Payot, F., Bosland, L., Clement, B. & Girault, N. Main outcomes of fission product behaviour in the Phebus FPT3 test. 4th European Review Meeting on Severe Accident Research (ERMSAR-2010), May 11–12, 2010. Bologna, Italy.

5. Kalilainen, J., Kärkelä, T., Zilliacus, R., Tapper, U., Auvinen, A. & Jokiniemi, J. Chemical reactions on primary circuit surfaces and their effect on fission product transport in a severe nuclear accident. (To be submitted.)

20. Core Melt Stabilization (COMESTA)

20.1 COMESTA summary report

Tuomo Sevón and Ilona Lindholm
VTT

Abstract

COMESTA project has investigated core melt behavior in a severe accident. Experiments have been conducted in international cooperation on the subjects of molten core – concrete interactions, melt pool coolability and steam explosions. Competence for computational modeling of severe accidents has been developed.

Introduction

In the very unlikely event of a severe accident, the core of a reactor melts. The target of severe accident management is to keep the containment intact and to prevent the release of radioactive materials to the environment. To reach this target, the molten corium must be cooled down. COMESTA (Core Melt Stabilization) project was set up to investigate the behavior of molten corium in the containment. In particular, the phenomena of molten core – concrete interactions (MCCI), coolability of core melt and steam explosions were investigated, and competence for computational modeling of severe accidents was developed.

Main objectives

The project consisted of several separate tasks. An experiment on the interaction between oxidic corium and hematite-containing concrete was performed in the

VULCANO facility in Cadarache, France. The experiment is described in a separate article in this publication.

The project involved participation in several international research programs. International cooperation allows expensive experiments to be conducted in an affordable way for the participating countries. In the OECD MCCI-2 project, the objective is to experimentally investigate interactions between molten corium and concrete and coolability of core melt. In the OECD SERENA-2 project, experiments on steam explosions are conducted. Both of these international projects employ real nuclear reactor materials, which makes the experiments very challenging. In addition, Finland's membership in the U.S. NRC's CSARP (Cooperative Severe Accident Research Program) is part of the COMESTA project. Through CSARP, licenses for using the integral severe accident simulation program MELCOR are obtained for all Finnish nuclear energy organizations.

Expertise in computational modeling of severe accidents was developed with two codes. The MC3D code was utilized in reactor-scale steam explosion simulations. Abilities of the MELCOR code for simulating two-phase counter-current flows were tested.

HECLA experiments

In the previous years of the project, HECLA experiments investigated interactions between metallic melt and concrete. They involved pouring of 50 kg of stainless steel at almost 1 800°C into cylindrical concrete crucibles that were made of hematite-containing concrete, which is used in the EPR reactor pit. In the last two years, a final report of the experiment series was written and the results were published in the Nuclear Engineering and Design journal [1].

OECD MCCI-2 (Melt coolability and concrete interactions)

MCCI-2 was an international project for investigating core melt coolability and its interactions with concrete. There were 13 participating countries in the project, and it was managed by OECD NEA. The project started in 2006 and ended in 2010. Ten challenging experiments were conducted at Argonne National Laboratory in the United States. All of them were operationally successful, thanks to the experienced team working at Argonne.

WCB-1 (Water-Cooled Basemat) experiment was proposed by Finland. Its objective was to test the operation of a core catcher where a corium melt pool is cooled by cooling channels at the bottom. The configuration resembles the core

catcher of the EPR, even though it is not identical. 400 kg of corium melt, including UO_2 and ZrO_2, was generated with a chemical thermite reaction. Decay heat was simulated by heating the melt with electricity at 80 kW power. At the bottom of the melt pool there was a water-cooled steel panel. Water was also poured to the top of the melt pool. The main result of the experiment was that the water-cooled basemat was able to stabilize the melt and the heat flux downwards was smaller than VTT's expectations.

SSWICS-12 and -13 experiments tested the possibility to cool down a corium melt pool by injecting water to the melt from the bottom. The results support the earlier findings that bottom water injection, so-called COMET concept, is a very efficient method of cooling a melt pool, at least in the small scale experiments. Implementing the system to a full-sized reactor pit may be challenging.

CCI-6 experiment investigated cooling of a corium melt pool with early top flooding. 900 kg of oxidic corium melt was generated in a concrete crucible and then heated at 210 kW power. Water was poured on the top of the melt pool at the beginning of the test. It was known beforehand that early flooding is more efficient than late flooding because the concrete content of the melt is smaller. However, the early flooding was even more efficient than expected. The water on the top of the melt pool was able to completely quench the melt and stop its interaction with concrete.

Earlier, a detailed heat transfer analysis of the CCI experiments 1, 2 and 3 was conducted at VTT [2]. Now this analysis was extended to two new experiments, CCI-4 and -5. It was found out that the new experiment data fits well to the same heat transfer correlations that were derived from the first three experiments. Only small changes to the statistical correlations were caused by the increased amount of data.

A previously developed Excel macro for testing the CCI heat transfer correlations was now updated with the new versions of the correlations. To facilitate speaking about the macro, the name FinCCI was given for the code. The main new feature, compared to other similar codes, is that FinCCI solves the heat conduction equation in the concrete, while most other codes ignore the conduction. On the other hand, some important phenomena, like heat loss through the melt pool surface, are simulated with very simplified methods in FinCCI.

All the available two-dimensional experiments with oxidic corium were simulated with FinCCI. In order to test the predictive capabilities of the code, the same set of parameters was used for all the experiments, instead of tuning the parameters for each experiment separately. Quite good results were obtained for experiments with LCS concrete type (Figure 1). On the other hand, siliceous

concrete experiments (Figure 2) have turned out to be difficult to model, and their simulations involve large uncertainties.

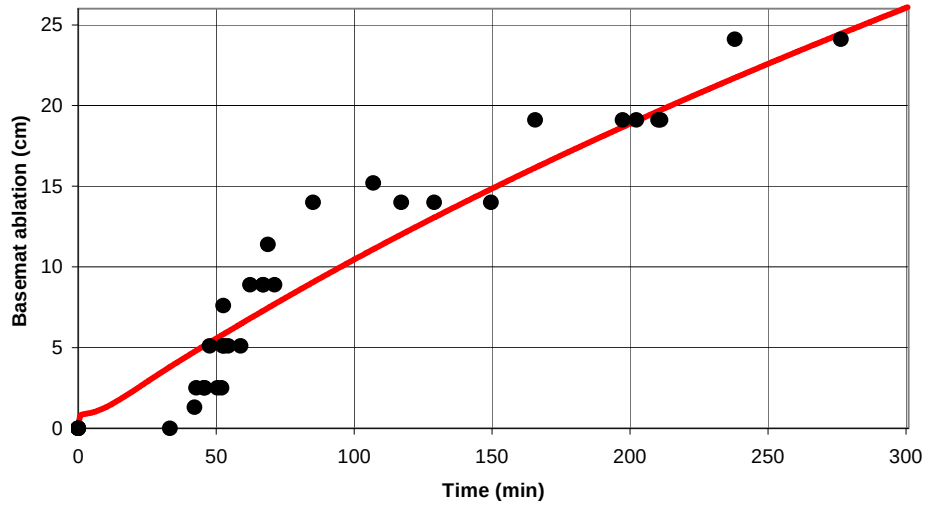

Figure 1. Basemat ablation in CCI-2 experiment with LCS concrete type. The dots show the measured ablation, and the line is the simulation with the FinCCI code.

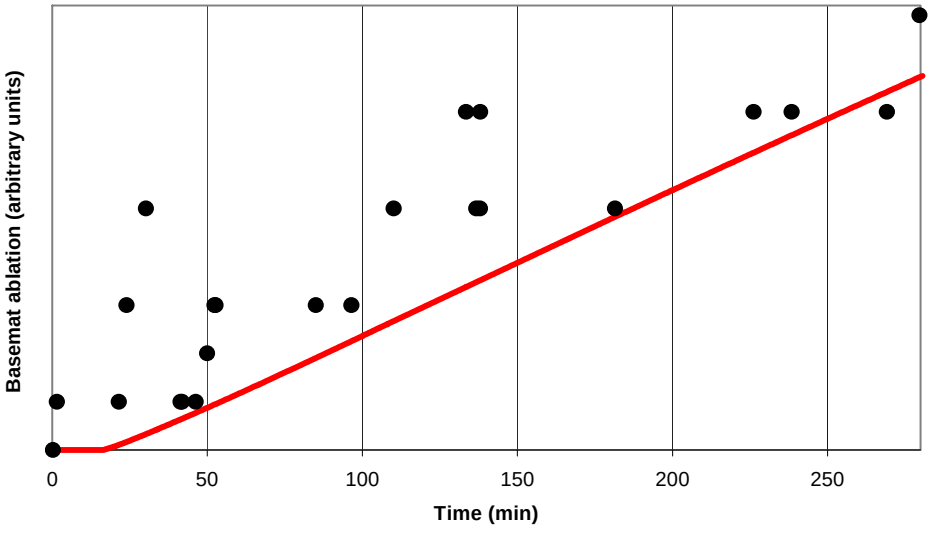

Figure 2. Basemat ablation in CCI-5 experiment with siliceous concrete type. The dots show the measured ablation, and the line is the simulation with the FinCCI code. The ablation scale is hidden because the publicity of the results is restricted until the end of 2012.

OECD SERENA-2 (Steam explosion resolution for nuclear applications)

The main current international research activity in the area of steam explosions is the OECD SERENA-2 project, in which Finland participates along with ten other countries. SERENA-2 project involves conducting steam explosion experiments and performing simulations of the experiments by the participating organizations as a supporting activity during the period of 2008–2012.

The technical objective of the SERENA-2 experimental program is threefold: Firstly, to provide experimental data to clarify the explosion behavior of prototypic corium melts. Secondly, to provide more refined experimental data for validation of explosion models for prototypic materials. This includes spatial distribution of fuel and void during the premixing and at the time of explosion, and explosion dynamics. And thirdly, to provide experimental data for the steam explosion in more reactor-like situations to verify the geometrical extrapolation capabilities of the codes.

These targets are pursued with performance of parallel experiments with two test facilities: KROTOS located in France and TROI located in Korea. A total of 12 experiments are planned, out of which 9 have been carried out by the end of 2010. KROTOS and TROI tests employ a maximum of 5 and 20 kg, respectively, of real core melt material heated up to 100–200°C above the liquidus temperature of the mixture. The larger scale in TROI allows investigation of 3-D behavior of the premixing and explosion phases, which are the prevailing conditions in the reactor case. The water pool, into which the core melt is released as a jet, is subcooled. Subcooled water has been observed to promote energetic fuel–coolant interaction. The applied compositions of the melt address the effects of different mass fractions of UO_2 and ZrO_2 (70:30 and 80:20, respectively), the effect Zr metal (8.5 wt-%) in the oxidic mixture and the effect of steel (Fe, Cr) and fission products (Ba, La, Sr) on fuel–coolant interaction.

The developed advanced X-ray tomography technique and image processing have produced data on local void conditions in the water pool during premixing. This was identified as a critical deficiency in experimental data for model development in the preceding SERENA-1 project. Another important outcome of the SERENA-2 project is that no spontaneous steam explosions have taken place in any of the carried out experiments. An external trigger at the bottom of the test section has produced energetic fuel–coolant interactions. The experiments will yield a practical range of explosion efficiency for different core

melt compositions. Furthermore, it seems prudent to assume that the issue of higher explosion potential of UO_2/ZrO_2 mixture in proportion 70/30 wt-% will be resolved by the end of the project. The data of post-test debris particle size distribution and morphology for each test will be included in the test reports.

The analytical activities in the SERENA-2 project have included pre- and post-test calculations of the tests with a number of computer codes, e.g. TEXAS-V and MC3D, which are in use in Finland. The comparisons of the calculated results and the measurements have shown that the 3-D models predict the pressures and wall impulses better than a 1-D code. Plant benchmark calculations will be carried out for sample PWR and BWR cases during 2011. This exercise will supplement the analysis results obtained in the SERENA-1 project.

Two-phase counter-current flow simulations with MELCOR

In a counter-current flow, liquid and gas flow through the same channel in opposite directions. Vertical air–water counter-current flow experiments were simulated with MELCOR 2.1, an integral code for simulating severe accidents. The simulated experiments (Figure 3) involved water outflow and air inflow through a hole in the bottom of a single-outlet vessel [3]. It was concluded that MELCOR significantly underestimates vertical counter-current flow rates. [4]

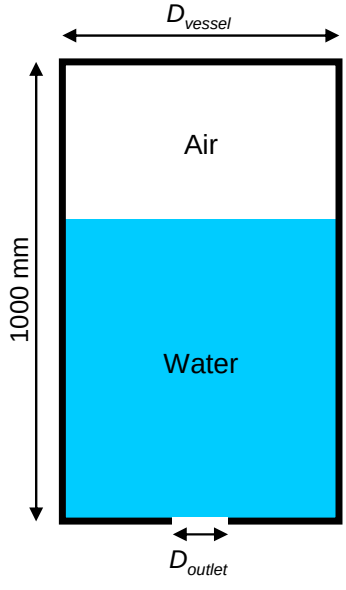

Figure 3. The cylindrical single-outlet vessel that was used in the counter-current flow experiments by J. Kubie [3].

In discussions with the code developers, it was found out that MELCOR's counter-current flow models have been validated using form loss coefficient zero. This setting gives the correct counter-current flow rates, but it would grossly overestimate single-phase flow rate through the same flow path. Two possibilities for fixing the problem were found: modifying the void fraction equation for counter-current flow, or using form loss and frictional pressure drop equations that are different in counter-current flow than in co-current flow. Both of these would require modifying the MELCOR source code, so it is up to the code developers to work with this issue. While waiting for the code developers' action, MELCOR users are recommended to use zero momentum exchange length parameter for all vertical flow paths. This brings the counter-current flow results slightly closer to the correct values without affecting single-phase flow rates.

Applications

The results from the OECD MCCI and SERENA projects have been employed in Olkiluoto safety analyses for STUK. The MELCOR code, the license of which is acquired through the COMESTA project, is constantly being used for safety analyses of nuclear power plants by VTT, Fortum and TVO.

Conclusions

The HECLA and VULCANO experiments have given new information about the behavior of the special sacrificial concrete used in the EPR reactor pit. The OECD MCCI-2 program has increased the state of knowledge of two-dimensional melt–concrete interactions and coolability of melt pool, with real nuclear reactor materials. Similarly, the OECD SERENA-2 program generates new information on steam explosions with prototypic materials. The international research programs are also good opportunities for networking and sharing of knowledge. Through Finland's membership in the CSARP program, the COMESTA project provides all Finnish nuclear energy organizations with a license to use the MELCOR severe accident analysis computer code. Expertise on the use of the MC3D and MELCOR codes was developed in the project.

References

1. Sevón, T., Kinnunen, T., Virta, J., Holmström, S., Kekki, T. & Lindholm, I. HECLA experiments on interaction between metallic melt and hematite-containing concrete. Nuclear Engineering and Design 2010, Vol. 240, pp. 3586–3593.

2. Sevón, T. A Heat Transfer Analysis of the CCI Experiments 1–3. Nuclear Engineering and Design 2008, Vol. 238, pp. 2377–2386.

3. Kubie, J. A model of liquid outflow from single-outlet vessels. Proceedings of the Institution of Mechanical Engineers Part C – Journal of Mechanical Engineering Science 1999, Vol. 213, pp. 833–847.

4. Sevón, T. Modeling Steam Condensation and Counter-current Flow with MELCOR. CSARP Meeting, September 14–16, 2010. Bethesda, Maryland, USA.

20.2 VULCANO VB-U7 experiment on interaction between oxidic corium and hematite-containing concrete (COMESTA)

Tuomo Sevón
VTT

Lionel Ferry and Christophe Journeau
CEA

Abstract

In the reactor pit of the European Pressurized Water Reactor (EPR), a special kind of sacrificial concrete type is used. The concrete is made of both siliceous (SiO_2) and hematite (Fe_2O_3) aggregates. There was very scarce public experimental data about the behavior of this special concrete type in a severe accident. In co-operation with CEA, an experiment was conducted at the VULCANO facility in Cadarache, France. This VB-U7 experiment involved interaction between oxidic corium, containing UO_2 and ZrO_2, and the hematite-containing concrete. It was found out that the special concrete type behaves in the same way as ordinary siliceous concrete but differently from limestone-common-sand (LCS) concrete.

Introduction

In a severe accident, the core of a reactor melts and forms corium, a mixture that includes molten UO2 and ZrO2. When the reactor pressure vessel fails, the molten corium is discharged to the reactor pit. The EPR severe accident management strategy [1] is based on temporary melt retention in the reactor pit and then spreading the molten mixture of corium and concrete as a thin layer over a large area (170 m^2) in the core catcher (Figure 1). There is no water in the pit, which prevents steam explosions. The pit floor and walls are coated with 50 cm thick layer of sacrificial material, which is made of a special concrete type that contains hematite (Fe_2O_3). Due to the high temperature and decay heat of the corium, the sacrificial concrete melts. Eventually the melt plug at the bottom of the pit fails, and the melt flows through the discharge channel to the core catcher, which is dry at that moment in order to prevent steam explosions. Arrival of the melt triggers passive flooding of the core catcher. The large heat transfer area makes it possible to cool the melt by water from top and bottom.

Because the core catcher is separated from the reactor pit, mechanical loads due to the pressure vessel failure do not damage the core catcher.

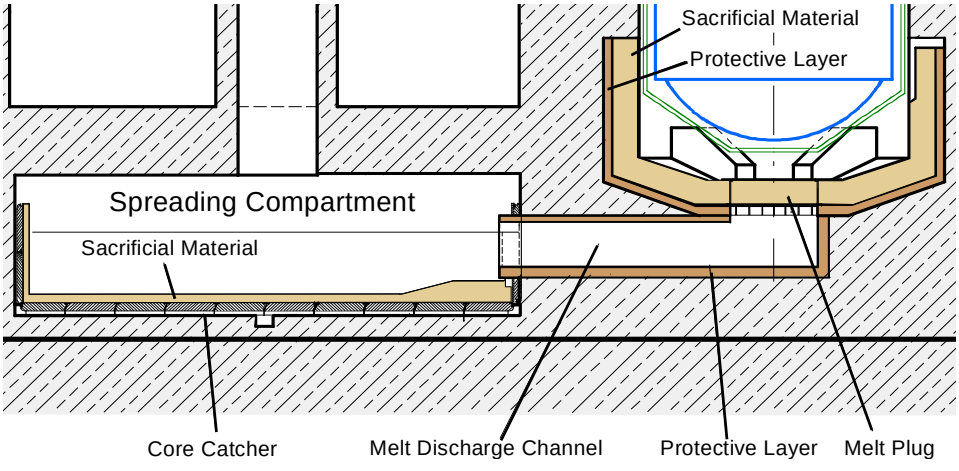

Figure 1. EPR reactor pit and core catcher. Figure by Areva NP.

Ablation (i.e. melting) of the sacrificial concrete in the floor of the reactor pit should last sufficiently long time so that practically all corium has discharged from the reactor before the failure of the melt plug. Too early failure of the melt plug could cause some late-coming melt to flow to the core catcher when it is already flooded with water. This, in turn, could cause a steam explosion or hamper the spreading of the corium to a coolable configuration. Predicting the failure time of the melt plug requires knowledge of the interaction between molten corium and hematite-containing sacrificial concrete.

Earlier, the interaction between molten stainless steel and hematite-containing concrete has been investigated in the HECLA experiments at VTT [2]. However, Finland does not have facilities for handling large amounts of molten radioactive materials, and therefore we are not able to perform experiments with real corium. This deficiency was solved by cooperating with CEA. In the VULCANO VB-U7 experiment in Cadarache, France, interaction between the hematite-containing concrete and molten oxidic corium, including UO_2 and ZrO_2, was investigated. The experiment was funded by the European Atomic Energy Community Sixth Framework Programme under contract n° 036403 (PLINIUS FP6). The work of VTT's personnel was funded from the SAFIR2010 program.

Experiment Facility

The corium melt is generated in a plasma arc furnace (Figure 2). The length of the furnace is 50 cm and diameter 40 cm. The material is loaded to the furnace as a powder. Then a plasma arc is formed between two electrodes that are made of graphite. The maximum heating power is about 200 kW. The heat generated by the plasma arc causes the powders to melt. The external surface of the furnace is cooled by water. Before melting the UO_2 + ZrO_2 corium in two stages, ZrO_2 powder is partially melted and works as a thermal insulator at the periphery of the furnace. This so-called self-crucible protects the furnace walls from the melt temperature that exceeds 2 000°C. The furnace is rotating, in order to keep the materials pressed against the furnace wall by centrifugation. After reaching the target temperature, the furnace is tilted and the corium is poured into the test section.

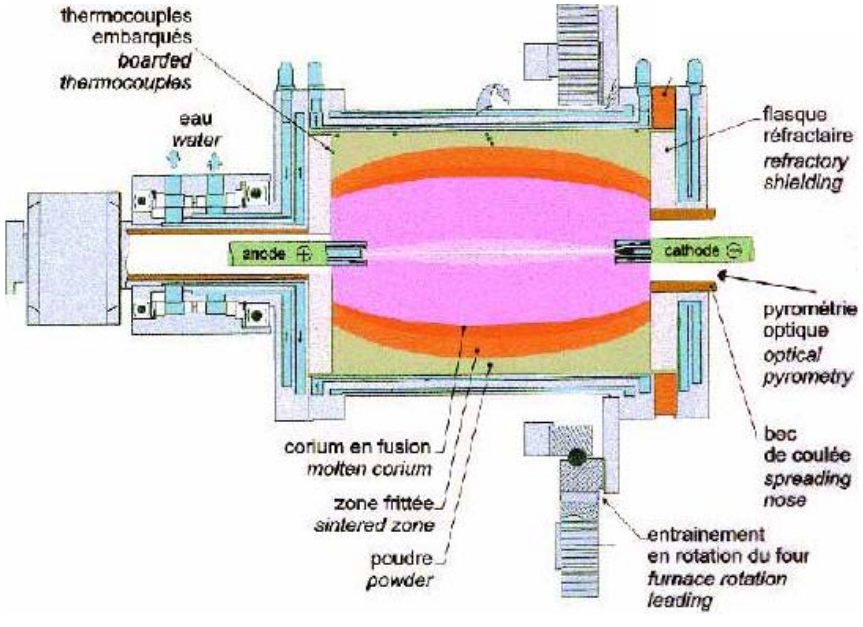

Figure 2. Plasma arc furnace in the VULCANO facility for melting corium.

The test section was a half-cylindrical concrete crucible with inner diameter of 30 cm (Figure 3). The concrete is red due to the included hematite (iron oxide, Fe_2O_3). The symmetry surface of the half cylinder was covered with a ZrO_2 plate, which acted as a nearly adiabatic surface. 129 thermocouples were embedded in the concrete for measuring the ablation depth evolution. In order to simulate

decay heat, the crucible is surrounded by induction coils that are able to heat the melt. A limitation in the induction heating technique is that the power is absorbed only in liquid corium. Possible solid crusts at the interfaces cannot be heated, even though in a real reactor accident decay heat would be generated also in solid corium. The test operations are controlled remotely from a control room, which is located in a separate building (Figure 4).

Figure 3. VULCANO VB-U7 concrete crucible before the experiment.

Figure 4. Control room of the VULCANO facility.

Results

The VB-U7 experiment was performed on the 15th of October, 2009. 53.8 kg of oxidic corium at about 2 250°C was poured into the concrete crucible. The melt was heated with induction at the average net power of 21.2 kW. At 1 h 20 min a failure in the cooling system of the power source stopped the induction heating. The failure was fixed in 21 min, after which the heating power was restarted. At 2 h 38 min the concrete crucible broke and some corium flowed out of the test section, which ended the experiment.

The concrete ablation in the experiment is plotted in Figure 5. The chart shows the maximum sidewall and basemat ablation depths as a function of time, and it is based on the ablation temperature of 1 160°C. This corresponds to the arbitrary value of 50% liquid mass fraction of the concrete in thermo-chemical GEMINI calculations. The sidewall ablates about six times faster than the basemat until the power outage at 80 min. It is probable that the phenomena after the power outage are not prototypical due to the thick crusts that developed during the outage. The faster sidewall ablation is also clearly visible from Figure 6, which shows sketches of the ablation profiles every 1 000 seconds. The exact shape and curvature of the ablation front is of course an approximation due to the limited number of thermocouples in the concrete.

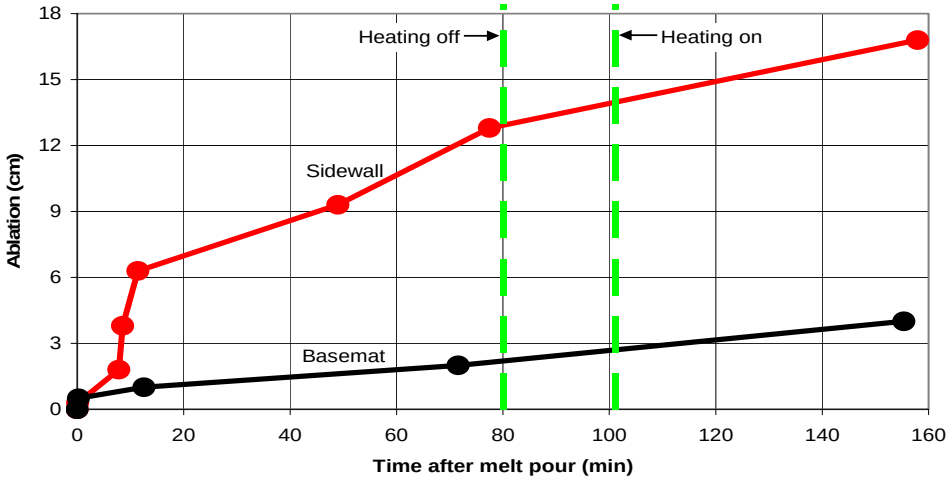

Figure 5. Concrete ablation in the VULCANO VB-U7 experiment, based on the ablation temperature of 1 160°C.

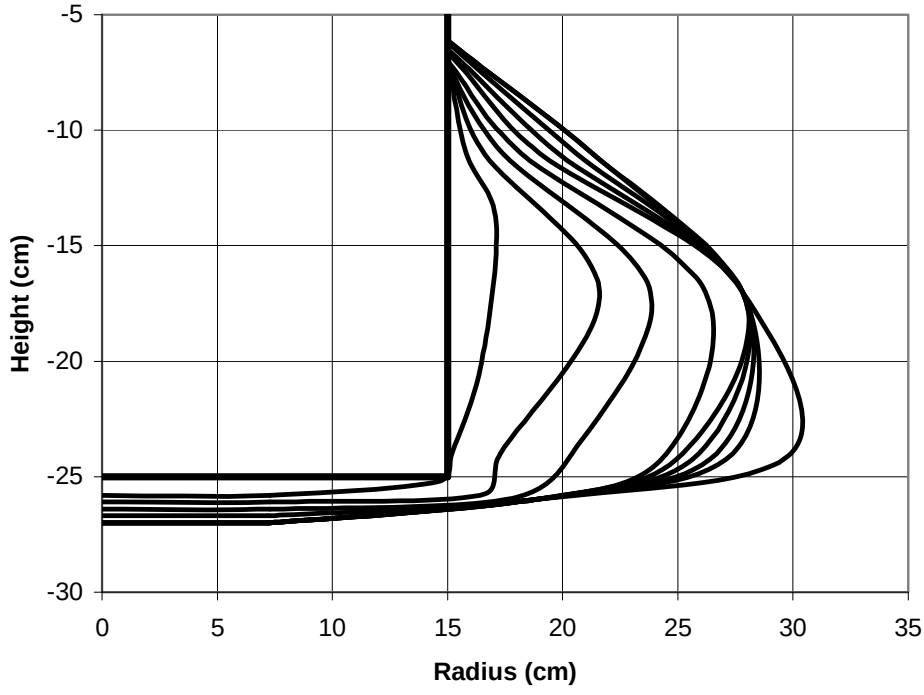

Figure 6. Ablation profile at 1 000 s intervals at 135° angular position in the VULCANO VB-U7 experiment, based on the ablation temperature of 1 160°C.

Conclusions

An experiment on the interaction between oxidic corium and hematite-containing concrete was performed at the VULCANO facility in Cadarache, France, in cooperation with CEA. The special concrete type is the same that is used in the reactor pit of Olkiluoto 3 EPR.

It was found out that the ablation of the sidewall was significantly faster than the ablation of the basemat. This is similar behavior as has been observed with ordinary siliceous concrete type. On the contrary, for another common concrete type, LCS (limestone-common-sand) concrete, the sidewall and basemat ablation rates are about equal. The physical reason for the difference is not yet known. Based on the experiment findings, we can apply the same calculation models for the hematite-containing concrete as are used for siliceous concrete. This reduces uncertainties in simulating EPR severe accident scenarios.

References

1. Fischer, M. The Severe Accident Mitigation Concept and the Design Measures for Core Melt Retention of the European Pressurized Reactor (EPR). Nuclear Engineering and Design 2004, Vol. 230, pp. 169–180.

2. Sevón, T., Kinnunen, T., Virta, J., Holmström, S., Kekki, T. & Lindholm, I. HECLA experiments on interaction between metallic melt and hematite-containing concrete. Nuclear Engineering and Design 2010, Vol. 240, pp. 3586–3593.

21. Hydrogen Combustion Risk and Core Debris Coolability (HYBCIS)

21.1 HYBCIS summary report

Eveliina Takasuo, Stefan Holmström, Ville Hovi and Risto Huhtanen
VTT

Abstract

The HYBCIS project has focused on two different topics in the area of severe accident research: the coolability of porous core debris beds and the risk of hydrogen combustion in containments. A new test facility, COOLOCE has been designed and built for experimental investigations of coolability of porous particle beds with a flexible geometry. The main objective of the experiments is to compare the coolability of a heap-like (conical) particle bed configuration to that of an evenly-distributed cylindrical particle bed. The first experiments with a conical particle bed have been performed. Along with the experimental work, simulation tools are applied to model the phenomenon. The assessment of hydrogen risk in containments consists of computational analysis addressing hydrogen distribution, mitigation and combustion. In the present project, simulations of slow hydrogen deflagrations have been performed using the FLUENT CFD software. The simulation work is closely connected to the OECD THAI research project whose follow-up has been done within the HYBCIS project.

Introduction

At the Finnish BWRs in Olkiluoto, the flooding of the lower drywell of the containment is a key part of the severe accident management strategy. As a

result of the reactor pressure vessel failure, molten core material is discharged into a deep water pool into the flooded lower drywell of the containment. The corium is fragmented and it is expected to form a porous particle bed from which decay heat must be removed in order to prevent dryout and re-melting of the material. The coolability of porous particle beds has been investigated at VTT within the STYX test series [1, 2]. In these experiments, the effects of pressure, particle size stratification, particle bed depth and downcomers in cylindrical beds consisting of irregular particles were examined.

In realistic accident scenarios, the particle bed may not be evenly distributed in the containment. Instead, heap-like geometries which allow multi-dimensional flows into the particle bed are possible (e.g. [3]). Multi-dimensional flooding tends to increase the dryout heat flux and improve coolability. On the other hand, a heap-like particle bed is higher than a cylindrical bed of the same volume. This implies that, in order to exit the particle bed, steam has to travel a longer distance within the bed interior which might reduce the local dryout heat flux. In order to evaluate the effects of the bed geometry on dryout heat flux, the design of a new laboratory scale test facility named COOLOCE (Coolability of Cone) was initiated in the beginning of 2009. The components of the old STYX test facility were utilized where possible. However, a new test pressure vessel was acquired, and the particle bed section including the electrical heating system was completely reconstructed. The first experiments aiming for dryout were performed in the fall of 2010.

Methods to model the dryout process and predict the dryout power for different kinds of particle beds range from simple one- or zero-dimensional correlations to 3D fluid dynamics models. In recent years and in the preceding projects, effort has been focused on validating different analytical and numerical models that could be applied to the assessment of power plant scenarios [1, 2]. The simulation tools currently in use at VTT are the MEWA 2D and PORFLO 3D codes which provide the capability to model multi-dimensional flow configurations.

The rather comprehensively validated MEWA code has been developed by the IKE institute at Stuttgart University specifically for particle bed analysis [4], and it has been taken into use at VTT through the EU network project SARNET-2. PORFLO is an in-house code that has been applied to model different flow problems encountered in thermal hydraulics related to nuclear power plant safety. The application of the code to particle bed coolability was started in 2010. The motivation to this was to examine the possibilities for a full 3D model of the particle bed geometry and to train a new PORFLO user. The code has been

under continuous development at VTT, mainly within the SAFIR2010/TRICOT project. Both MEWA and PORFLO treat the particle bed as porous medium.

The interest in numerical modeling of hydrogen behavior derives from the need to validate the computational tools applied in the severe accident management of Finnish nuclear power plants. The issue is of importance e.g. for the EPR unit of Olkiluoto 3 and the Loviisa PWRs. Gas mixtures containing hydrogen may be formed in the containment as a result of the oxidation of zircaloy of the fuel rod cladding during a core melt accident. The possibility of hydrogen combustion that would threaten containment integrity has to be ruled out by mitigation measures such as passive autocatalytic recombiners (PARs) and effective atmospheric mixing. The codes used to model hydrogen distribution and combustion in recent years include the French TONUS code and the commercial FLUENT code [5, 6].

During the present project, FLUENT has been used to model hydrogen deflagration experiments conducted at the THAI facility within the frame of the OECD/NEA THAI programme (Thermal-hydraulics, Hydrogen, Aerosols, Iodine). This work can be seen as continuation for the modeling of the THAI hydrogen distribution experiments which was done in 2008 [6]. The follow-up of the THAI programme between 2007 and 2009 has also been done within the HYBCIS project and its predecessor HYRICI. The international research programme has addressed a variety of issues related to hydrogen and fission product behavior.

Main objectives

The main objectives of the project included the design and construction of a new test facility used for experiments investigating the coolability of porous particle beds, and to model hydrogen behavior within the nuclear power plant containment for code validation purposes. The new test facility, COOLOCE, is used to measure dryout power within particle beds of different geometries. The main objective of this work that will be complemented within the frame of SAFIR2014 is to compare dryout power and coolability of a conical bed to that of a cylindrical bed. This is done in order to estimate the difference in coolability between an evenly distributed top-flooded particle bed (cylindrical bed) and a heap-like (conical) particle configuration, and to obtain new data for code validation and development. The goal of the modeling of hydrogen mixing and combustion was to continue and complement the validation work of CFD tools such as FLUENT for predictions of hydrogen behavior in containments. Large-scale experimental data of hydrogen

and recombiner issues as well as fission product behavior was obtained by participation to the international OECD project THAI.

Particle bed coolability experiments

The COOLOCE test facility consists of a pressure vessel which contains the particle bed section with its heating arrangement, the feed water system and the steam removal system [7]. During the experiments, the test particle bed is submerged in water pre-heated close to saturation conditions and boiling occurs in the bed interior. The decay heat is simulated by resistance heaters that are installed in a vertical configuration aiming for a volumetrically uniform power distribution within the particle bed.

Dryout is searched by stepwise increases of heating power until one or more temperature sensors inside the particle bed indicate a steady increase from saturation temperature. This indicates loss of coolant (dryout) in this part of the particle bed and the configuration is not in a coolable state. An overview of the test facility is presented in Figure 1. The heating arrangement and the particle bed section filled with the particle material are illustrated in Figure 2.

Figure 1. An overview of the COOLOCE test facility. The components are 1) feed water pre-heater, 2) feed water control valve, 3) connection box for the electrical heaters 4), pressure vessel, 5) condenser and scale for measuring condensate mass flow, 6) video monitoring and 7) pressure gauges.

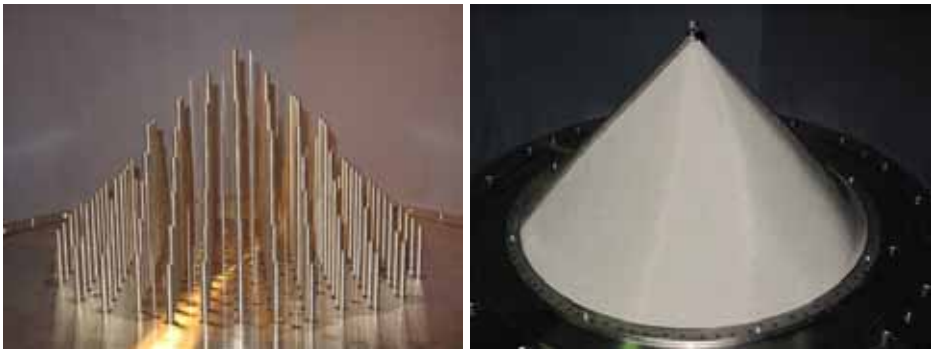

Figure 2. The heating arrangement of the conical particle bed (left) and the ready particle bed with the particle material held in place by a wire net (right).

The experiments conducted using a conical particle bed showed relatively high dryout power: 40 kW at 1.9 bar pressure and 38 kW for 1.6 bar pressure. The dryout power is calculated based on the mass flow of the condensing steam. Dryout occurred in the upper central part of the conical configuration which is in accordance with theoretical expectations and the MEWA and PORFLO simulations. Typically to multi-dimensional coolant flow configurations, the dryout zone did not spread from the initial location according to the temperature sensors.

Particle bed coolability simulations

The MEWA 2D severe accident code includes a porous media model that solves the momentum and mass conservation equations for the fluid phases and the energy equation for the liquid, gas and solid phases. A rather similar approach is used in the in-house code PORFLO with the main exception that a fully 3D solution of the equations is done. This facilitates a detailed solution of the flows in compex geometries. The application of PORFLO to model the coolability of porous particle beds has been started along with the assembly of the COOLOCE test facility. Friction and heat transfer models suitable for porous beds have been incorporated into the code and test simulations with the new code version have been run.

MEWA has been used to model the STYX experiments with a range of parameters variations. A comprehensive set of post-test simulations has been performed of the STYX downcomer experiments [2]. Following the completion of the STYX analysis in 2009, design calculations of the COOLOCE experiments were done as well as the first post-test simulations of the first COOLOCE

experiments. The PORFLO modeling work as a new branch of the code development is more directly aimed at reproducing the conditions present in the conical particle bed experiments (i.e. the three-dimensional flow configuration in compex geometries) [8]. Examples of PORFLO predictions of saturation (liquid fraction in the pores) and liquid velocity in the conical particle bed in dryout conditions are shown in Figure 3.

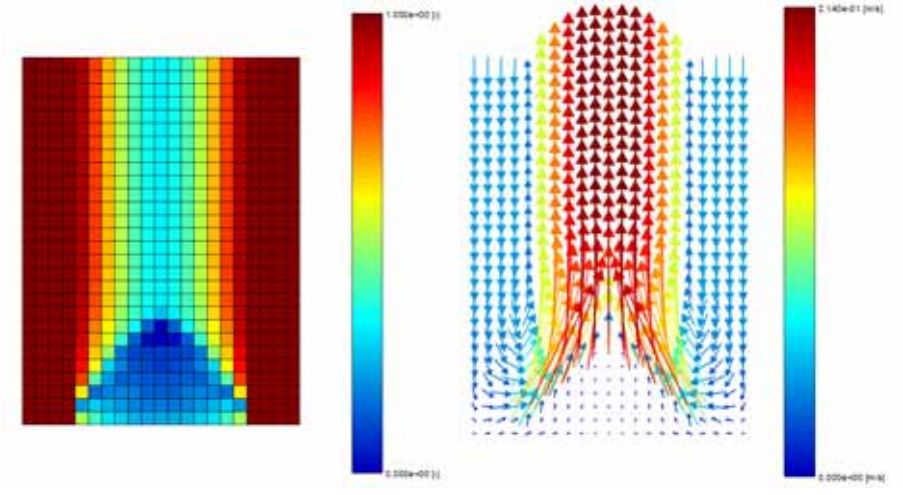

Figure 3. Saturation (left) and the vectors of liquid velocity (right) in the central vertical cross-section of the 3D PORFLO model of the conical particle bed. Dryout has occurred in the cells near the top of the cone.

It has been observed that both codes are capable of reproducing the dryout process qualitatively well. Dryout occurs consistently in the bottom of the geometry for top-flooded cylindrical particle beds, or near the top of the cone for conical particle beds. This can be illustrated by the saturation profiles within the particle beds. The saturation profiles at different power levels in the centre of the conical particle bed are shown in Figure 4.

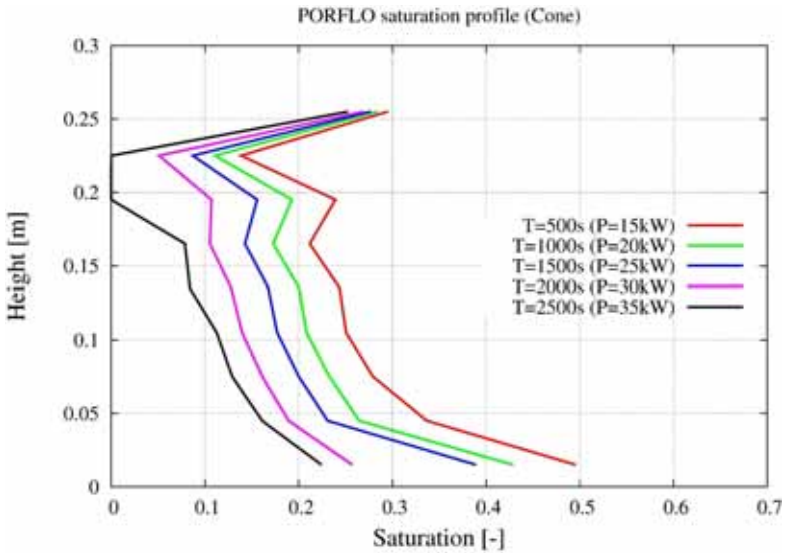

Figure 4. Liquid saturation as a function of the particle bed height in the centre of the conical bed at different power levels during a PORFLO simulation. Zero saturation (dryout) has been reached in the topmost part of the configuration at T = 2 500 s (corresponds to conditions presented in Figure 3).

Comparisons of the measured and predicted values of dryout power show some discrepancies between the codes and the experimental results. In general, the models underestimate the coolability of the conical test set-up. The post-test calculations thus far have been conducted assuming that the heat generation in the modeled particle bed is uniform which is not the case in the experimental set-up. The reason for the discrepancies and the role of the heating arrangement are expected to be clarified when more experimental data becomes available and more post-test simulations will be run.

Modeling of hydrogen combustion

The THAI hydrogen deflagration simulations were conducted as part of the ISP-49 standard problem calculations. The experiments addressed slow deflagrations with variable hydrogen and steam concentrations, initial temperatures and combustion direction [9]. The ISP consisted of a blind and an open phase which included experiments conducted at the THAI and ENACCEF facilities. The open and blind phase THAI experiments, namely HD-2R and HD-22, were modeled using FLUENT 6.3. Turbulent mixing in the simulations was modeled by the

standard k-ε model and the combustion rate by the eddy break-up (EBU) approach. Both experiments investigated upwards combustion with a lean initial hydrogen mixture. In the blind phase experiment (HD-22), the initial mixture contained steam.

The results revealed that the overall combustion process (i.e. the maximum pressure and temperature) is well predicted by the model. However, there is no treatment for laminar flame propagation in the model. Since the test vessel is rather large and there are no internal structures in the vessel during the deflagration experiments to increase turbulence, it may be expected that laminar combustion is significant at least in the early stages of the deflagration. Thus, the present model is not capable of simulating the spreading of the flame front in detail. Comparison to previous simulations which yielded realistic results suggests that the model is more suitable for cases with strong turbulent flame acceleration caused by obstacles [10].

In the modeling of the blind phase (HD-22) the following model variations were added to the "basic" combination of the k-ε model and the EBU combustion model: a limitation based on the Arrhenius reaction rate which prevents the reaction from spreading into unburned cold areas, and a limiter which prevents combustion in the cells next to the vessel walls. Separate test runs using the variations were performed. It was observed that the Arrhenius-limited reaction produces a flame front that has a different shape than without the limiter. In the HD-2R and HD-22 simulations without this limiter, the flame front in the beginning of the deflagration is very similar. Comparison of the flame fronts in the simulations of HD-2R (no limiter) and HD-22 (including limiter) is illustrated in Figure 5.

The aim of ruling out combustion in the wall cells was to prevent the increased near-wall reaction rates that cause the reaction to propagate first along the walls. The combustion that "climbs" up the wall is typical to the k-ε model with the standard wall functions because the model predicts increased turbulent mixing in the wall shear layer. In reality the matter is rather complex, e.g. the heat losses that affect reaction rate might prevent this fast combustion at the walls. The results showed that the limiter reduces the flame velocity at the wall. However, the significance of this to the overall combustion would require further studies.

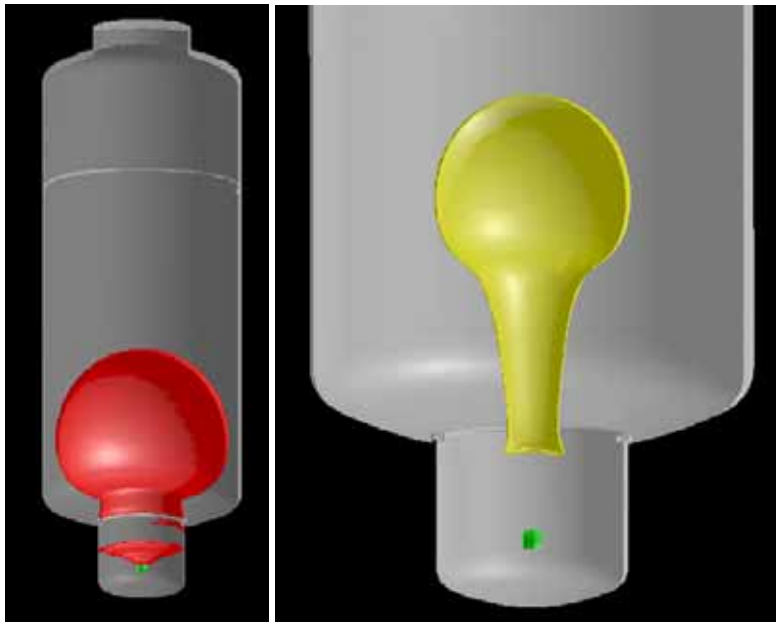

Figure 5. The flame front in the THAI HD-2R (left) and HD-22 (right) simulations in the initial phase of the simulation. The difference in the shape of the flame fronts is due to model differences.

Conclusions

A new experimental facility has been designed and constructed for investigations of particle bed coolability in different geometries. The first test series with a conical particle bed has been performed. In the future, the test series will be complemented by cylindrical particle bed experiments. The MEWA and PORFLO simulation codes have been used in modeling of the particle bed dryout behavior. PORFLO is an in-house code that utilizes the porous medium approach for solving flow problems encountered in nuclear power plant thermal hydraulics. Both codes appear to be capable of simulating the overall process of particle bed dryout realistically but further studies are needed in order to assess their capabilities to predict the values of dryout power correctly. The work conducted within this research topic gives an opportunity to combine our own experimental research to in-house code development activities, and focus on the issues of interest for the Finnish nuclear power plants.

The modeling of the THAI experiments, performed within the second topic of the project, suggests that relatively good predictions of hydrogen combustion in

the containment can be obtained by FLUENT simulations. However, the simulations indicate that a more detailed model for the flame front propagation is necessary in case laminar combustion plays a significant role. Appropriate user-defined models and an in-depth understanding of the application are required in order to make the correct selections of physical models and numerical parameters for the simulations. The OECD THAI research project has focused on hydrogen distribution, combustion and mitigation issues. Project participation and follow-up has made the new experimental data produced by the international programme quickly available to the Finnish nuclear energy partners.

References

1. Lindholm, I., Holmström, S., Miettinen, J., Lestinen, V., Hyvärinen, J., Pankakoski, P. & Sjövall, H. Dryout Heat Flux Experiments with Deep Heterogeneous Particle Bed. Nuclear Engineering and Design 2006, 236, pp. 2060–2074.

2. Takasuo, E., Holmström, S., Kinnunen, T., Pankakoski, P.H., Hosio, E. & Lindholm, I. The effect of lateral flooding on the coolability of irregular core debris beds. Nuclear Engineering and Design 2010. doi:10.1016/j.nucengdes.2010.04.033.

3. Karbojian, A., Ma, W.M., Kudinov, P. & Dinh, T.N. A scoping study of debris bed formation in the DEFOR test facility. Nuclear Engineering and Design 2009, 239, pp. 1653–1659.

4. Bürger, M., Buck, M., Schmidt, W. & Widmann, W. Validation and application of the WABE code: Investigations of constitutive laws and 2D effects on debris coolability. Nuclear Engineering and Design 2006, 236, pp. 2164–2188.

5. Takasuo, E. Modeling of Hydrogen-Air Detonations in the TONUS CFD Code and its Application to the FLAME F-19 Test. Proceedings of the 16th International Conference on Nuclear Engineering (ICONE-16). May 11–15, 2008. Orlando, Florida, USA.

6. Visser, D.C., Komen, E.M.J., Houkema, M., Siccama, N.B., Kyttälä, J., Huhtanen, R. & Takasuo, E. FLUENT Calculations of the Hydrogen Distribution in a Containment during the OECD-NEA THAI HM-2 Experiment. The 13th International Topical Meeting on Nuclear Reactor Thermal Hydraulics (NURETH-13). Kanazawa, Japan, September 27 – October 2, 2009.

7. Takasuo, E., Kinnunen, T., Pankakoski, P.H. & Holmström, S. Description of the COOLOCE test facility – Conical particle bed. VTT, Espoo, 2010. VTT Research Report VTT-R-08956-10.

8. Takasuo, E., Hovi, V. & Ilvonen, M. PORFLO modelling of the coolability of porous particle beds. VTT, Espoo, 2011. VTT-R-09376-10.

9. Kanzleiter, T., Gupta, S., Fischer, K., Ahrens, G., Langer, G., Kühnel, A., Poss, G., Langrock, G. & Funke, F. OECD-NEA THAI Project (Reactor Safety Research Project 150 1326). Final Report. Hydrogen and Fission Product Issues Relevant for Containment Safety Assessment under Severe Accident Conditions. Becker Technologies GmbH, Eschborn, Germany. March 2010. Report No. 1501326–FR 2.

10. Bentaib, A., Bleyer, A., Wilkening, H., Baraldi, D., Takasuo, E. & Huhtanen, R. Hydrogen combustion with concentration gradients in experiments and simulations: preliminary results of ENACCEF benchmark. ERMSAR-2007, Karlsruhe, Germany, 12–14 June, 2007.

21.2 The COOLOCE test facility

Eveliina Takasuo, Stefan Holmström, Tuomo Kinnunen, Pekka H. Pankakoski, Ville Hovi and Mikko Ilvonen
VTT

Abstract

A new test facility, COOLOCE has been designed and built for experimental investigations of coolability of porous particle beds with a flexible geometry. The main objective of the experiments is to compare the coolability of a heap-like (conical) particle bed configuration to that of an evenly-distributed cylindrical particle bed. The first experiments with a conical particle bed have been performed. The results suggest that the dryout power is relatively high in the conical particle bed. In addition to the experimental work, analytical work on the issue, including code development, is performed.

Introduction

At the Finnish BWRs in Olkiluoto, the flooding of the lower drywell of the containment is an important part of the severe accident management strategy. In the course of a core melt accident, corium is discharged from the reactor pressure vessel into a deep water pool in the lower drywell of the containment. Corium is fragmented and it is expected to form a porous particle bed from which decay heat must be removed in order to prevent re-melting of the material. Boiling and water infiltration into the particle bed interior play key roles in the heat removal. The objective of the coolability experiments conducted at VTT is to measure the heat fluxes which result in local dryout within the porous bed and thus verify the coolability of the debris for severe accident scenarios.

The effects of pressure, particle size stratification, particle bed depth and downcomers for cylindrical beds consisting of irregular particles have been examined in the STYX experiments, the first of which were conducted in 2001 and the latest in 2008 [1, 2]. The depth and the pressure ranges in the experiments characterized the conditions expected at the Olkiluoto containments during a core melt accident. In realistic accident scenarios, the particle bed may not be evenly distributed in the containment. Instead, highly irregular geometries which allow multi-dimensional flows into the particle bed are possible (e.g. [3]). Multi-

dimensional flooding tends to increase the dryout heat flux and improve coolability. For instance, increases of about 45% in the overall coolability have been predicted by calculations of multi-dimensional flows in homogenous configurations [4]. This is because in a cylindrical top-flooding configuration, the counter-current flow limitation restricts the water flow into the bed interior at a point when high enough vapor flux is reached. The critical vapor flux is higher for bottom or lateral flooding cases where co-current flows of steam and water are possible. An example of the difference in the flow principles between top and multi-dimensional flooding is illustrated in Figure 1.

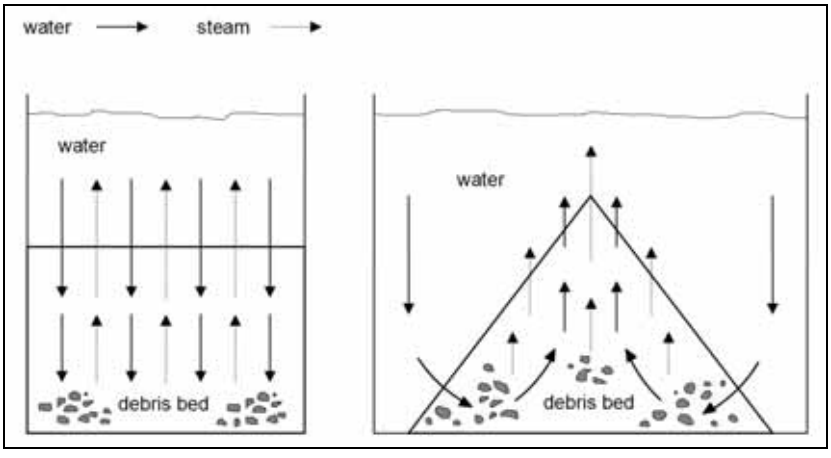

Figure 1. The conceptual difference in the flow configuration between an evenly-distributed cylindrical particle bed (left) and a heap-like particle bed (right) submerged in water. Solid and dashed lines indicate the directions of liquid and vapor flow, respectively.

On the other hand, a heap-like particle bed which allows multi-dimensional flooding is higher than a cylindrical bed of the same volume. This implies that, in order to exit the particle bed, steam has to travel a longer distance within the bed interior which may reduce the local dryout heat flux. In order to evaluate the effects of the bed geometry on dryout heat flux, the design of a new laboratory scale test facility named COOLOCE (Coolability of Cone) was initiated in the beginning of 2009. The components of the old STYX test facility were utilized where possible. However, a new test pressure vessel was acquired, and the particle bed section including the electrical heating system was completely reconstructed. The first experiments aiming for dryout were performed in the fall of 2010.

The main computational tools used for analyzing the particle bed coolability are the MEWA 2D code (developed by the IKE Institute of Stuttgart University

[5]) and the in-house 3D code PORFLO. The application of PORFLO to the modeling of debris beds was started in 2010 [6]. Several friction and heat transfer models verified for porous media modeling are included in the codes.

The experimental facility

The main components of the COOLOCE test facility are the pressure vessel which contains the particle bed section with its heating arrangement, the feed water system and the steam removal system [7]. An overview of the test facility is presented in Figure 2. The test vessel has a volume of 270 dm^3 with the outer diameter of 613 mm and a design pressure of 7 bar. The decay heat is simulated by electrical resistance heaters arranged in a vertical configuration which aims for a volumetrically uniform power distribution within the test bed. The total maximum power of the heaters is approximately 55 kW. The pressure vessel is equipped with sightglasses that can be used for visual observations of boiling in the fluid volume (by a video recorder).

Figure 2. An overview of the COOLOCE test facility. The components are 1) feed water pre-heater, 2) feed water control valve, 3) connection box for the electrical heaters 4), pressure vessel, 5) condenser and scale for measuring condensate mass flow, 6) video monitoring and 7) pressure gauges.

The particle bed section

The heating arrangement of the conical particle bed consists of 137 heaters of different lengths. There are 69 thermocouples installed between the heaters which are used to detect dryout. The particle bed itself (ø 500 mm) is composed of highly corrosion-resistant ceramic beads with the diameter of 0.8–1.0 mm. The height of the particle bed is 270 mm and it is held in conical shape by a wire net. The heating arrangement and the packing of the conical particle bed with the spherical beads are shown in Figure 3. Spherical particles are used for an easy determination of the hydrodynamic losses for the porous material without the need for separate evaluations of effective particle diameter.

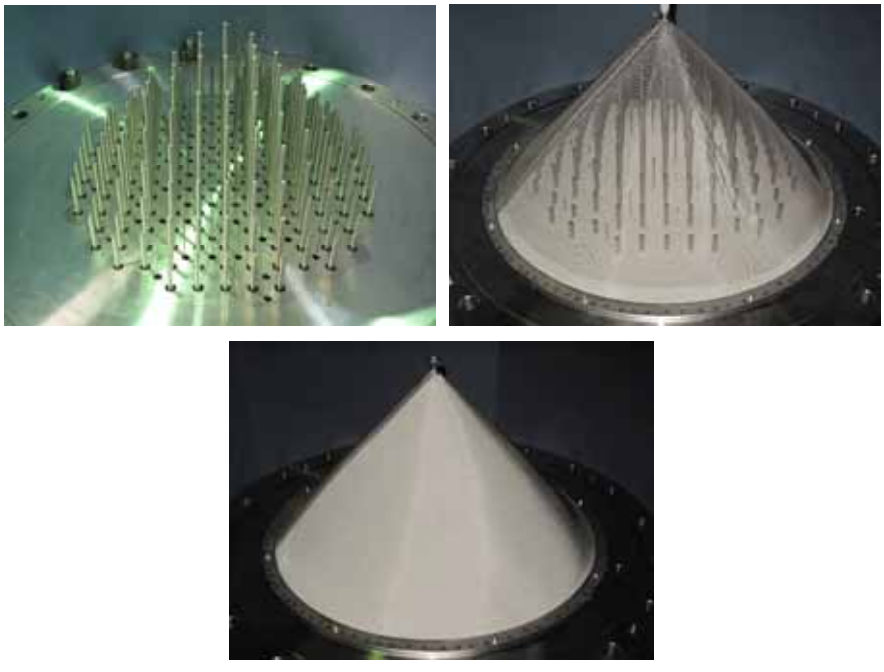

Figure 3. The heating arrangement of the conical particle bed (top left), the filling of the bed with particles (top right) and the ready conical bed. The thin rods between the larger heaters are temperature sensors.

The COOLOCE-1 and -2 experiments

During the experiments, dryout is searched by stepwise increases of heating power until one or more temperature sensors inside the particle bed indicate a steady increase from saturation temperature. This indicates loss of coolant (dryout)

in the sensor location. A holding time of 20 to 30 minutes is applied between the power increases in order to see whether a dryout is developed, or a coolable steady-state is reached. A warm-up sequence during which the volume of water is heated up to saturation temperature precedes the test runs. Preliminary testing of the facility and a start-up experiment were conducted before proceeding to the experiments aiming for dryout.

The COOLOCE-1 experiment was performed at nominal 2 bar absolute pressure with 2 kW power steps. Dryout was indicated by a sensor near the centre of the cone at the height of 170 mm from the bottom of the cone at the control power level of 46 kW. The boiling rate was estimated based on mass flow rate of the condensing steam which yielded a power value of about 40 kW. Since the heat generated by the heaters is transferred from the particle bed effectively by boiling, the calculated value may be assumed to be a good estimate of the actual dryout power. The difference between the control and calculated power values is explained by heat losses e.g. through the pressure vessel walls. The power density corresponding to the 40 kW total power is 2 286 kW/m^3. The temperature and power histories during the experiment are presented in Figure 4.

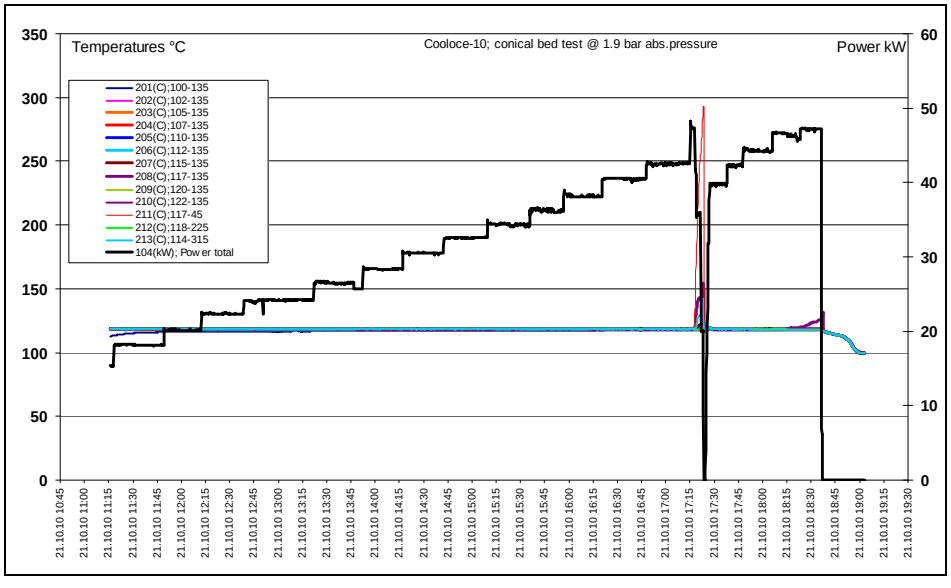

Figure 4. Temperature and control power histories in the COOLOCE-1 experiment. Two temperature excursions are seen, at 47 kW and at 46 kW (the latter is the more accurate value seen after a longer holding time).

The COOLOCE-2 experiment was planned to be conducted at atmospheric pressure by fully opening the steam line valve during the experimental run. However, it was seen that it was not possible to maintain such a low pressure even though the pressure control had worked well in the previous experiment. This was because of the contraction of flow in the steam line that had been designed for lower flow rates for the STYX experiments. At the time of dryout, the pressure had increased up to 1.6 bar and the measured dryout power was 44 kW. Taking into account the heat losses, this corresponds to 38 kW. The corresponding power density is 2 171 kW/m^3. The power increase scheme was similar to the COOLOCE-1 experiment. Compared to the previous experiments the measured power values were high. The maximum dryout power seen in the STYX tests was 37 kW observed at 7 bar absolute pressure [2] and prior to the new tests, this was also the highest level of output power that the facility had been run with.

It was found that some of the central heaters had malfunctioned during the experiments. Removal of the particle material for repairs and/or the installation of a cylindrical particle bed for the comparison experiments revealed surface damage on the heaters in the locations where the heaters had been exposed to steam, giving a rather clear indication on the location of the dryout zone. Nevertheless, it was verified that dryouts are achievable and can be measured in the entirely novel particle bed geometry and heating arrangement of the COOLOCE set-up. Future work includes the comparison test series with a cylindrical particle bed and possibly the installation of more resistant heaters for further experiments with the conical bed.

Analysis of the experimental results

The analytical part of the work included the design calculations of the test facility by the MEWA code, incorporating the debris bed models into the PORFLO code and testing of the new models. The first post-test calculations of the experiments described above have been done. The simulation codes solve the momentum, mass and energy conservation equations for the fluid and solid phases. Several options of closure models for particle bed friction and the different, rather complex heat transfer mechanisms are incorporated into the codes [5, 6].

The water infiltration into the conical particle bed occurs laterally (through the surface of the cone) as was illustrated in Figure 1. To simplify the case, it is assumed that the heat generation is uniform throughout the particle bed similarly

to a realistic core debris bed (comparison experiments with a cylindrical bed will shed more light on the effect of the non-prototypic heating arrangement). In pre-dryout steady-state conditions, the heating power is consumed by the phase change of water to steam, and the evaporated liquid is replaced by infiltration from the surrounding pool. Steam exits the particle bed through the surface of the cone. Co-current circulation of the two-phase mixture, in which water is entrained with the steam flow due to interfacial drag, is formed into the system of particle bed and pool. In the experiments, vigorous boiling was observed in the pool near the cone. An example of boiling during the COOLOCE start-up experiment is presented in Figure 5.

Figure 5. Boiling in the water pool near the surface of the conical particle bed in the COOLOCE start-up experiment.

In order to reach dryout in co-current flow conditions, the mass flux of steam has to be high enough to replace liquid in an entire cross-section of the particle bed [8]. The cross-sectional area of the conical particle bed is reduced with height. Since the steam generation is homogenous within the particle bed (due to the uniform heating), the thermal loading, or the steam flux per unit of area is higher near the top of the cone. Thus, dryout is expected to occur in the topmost part of the conical bed. In the conical configuration, no drastic change in the void fraction distribution occurs between the coolable and dryout conditions. The void fraction is highest near the top at all pre-dryout power levels. Dryout can be identified of the void fraction gradually reaching unity and the increase of solid temperature in the dried-out zone.

The main features of the development towards dryout are captured by the numerical models. An example of void fraction in a PORFLO simulation just after dryout has been reached is seen in Figure 6. The void fraction in the simulation is 1.0 in the topmost cells. In the experiments, dryout was also seen in the central top part of the particle bed. On its part, this suggests that the experimental flow conditions are similar or close to the simulated ones. The temperature sensors indicated a dryout location slightly lower than the one in the simulations. This might be explained by the heaters not reaching the bed surface and the positions of the temperature sensors which (obviously) have an effect on the accuracy of the determination of the dryout location.

Some discrepancies exist in the predictions of the MEWA and PORFLO codes and the measured dryout power. Generally, the models tend to underestimate the coolability compared to the experimental results. The measured dryout power was 50% greater than some of the predictions. A possible explanation is the channeling effect caused by the heating arrangement which may result from the locally increased porosity near the surfaces of the heaters. A more comprehensive analysis is provided when more experimental data becomes available.

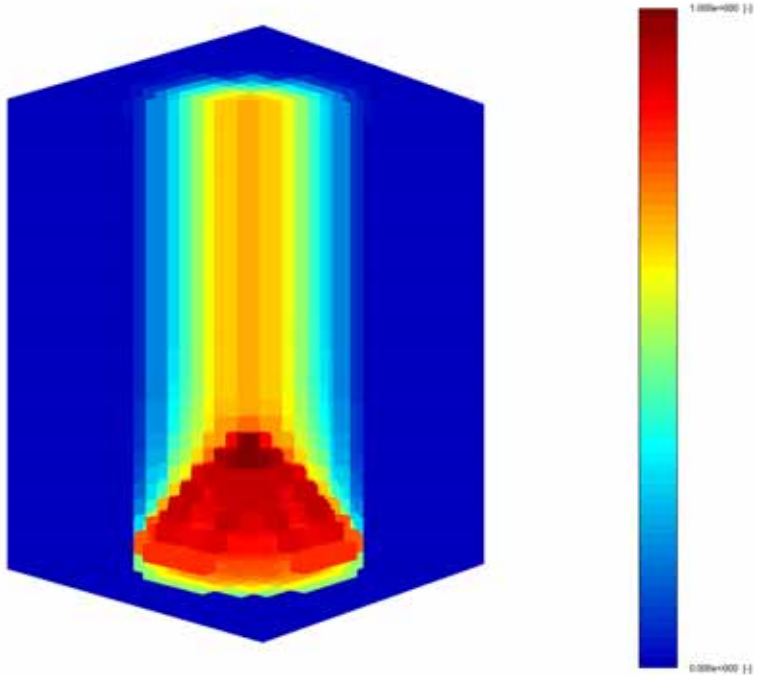

Figure 6. A PORFLO prediction of void fraction within the conical particle bed at the dryout power level of 35 kW.

Conclusions

A new test facility, COOLOCE has been designed and built for experimental investigations of coolability of porous particle beds with a flexible geometry. The first experiments have been run with a conical (heap-like) particle bed, and the test arrangement has been found suitable for measuring dryouts in the novel experimental set-up. However, the power required to achieve dryout in the experimental set-up was observed to be rather high compared to the previous STYX experiments. This represents a technical challenge to the test facility because of the limitations of the power output, and the heat resistance of the heaters, but might be a promising result considering the extension of the studies to power plant scenarios.

Pre-test and the first post-test simulations aiming to evaluate the dryout power have been performed. The location of the measured dryout in the upper central region of the conical debris bed was found to be in accordance with the predictions given by MEWA and PORFLO simulations. In the future, the experimental results can be used for analysis of the codes' capabilitites to predict dryout power (heat flux) and for assessing the effect of particle bed geometry in large-scale power plant applications.

References

1. Lindholm, I., Holmström, S., Miettinen, J., Lestinen, V., Hyvärinen, J., Pankakoski, P. & Sjövall, H. Dryout Heat Flux Experiments with Deep Heterogeneous Particle Bed. Nuclear Engineering and Design 2006, 236, pp. 2060–2074.

2. Takasuo, E., Holmström, S., Kinnunen, T., Pankakoski, P.H., Hosio, E. & Lindholm, I. The effect of lateral flooding on the coolability of irregular core debris beds. Nuclear Engineering and Design 2010. doi:10.1016/j.nucengdes.2010.04.033.

3. Karbojian, A., Ma, W.M., Kudinov, P., Davydov, M. & Dinh, T.N. A Scoping Study of Debris Formation in DEFOR Experimental Facility. 15th International Conference on Nuclear Engineering (ICONE-15), Nagoya, Japan, April 22–26, 2007.

4. Ma, W.M., Dinh, T.N., Buck, M. & Bürger, M. Analysis of the Effect of Bed Inhomogeneity on Debris Coolability. 15th International Conference on Nuclear Engineering (ICONE-15), Nagoya, Japan, April 22–26, 2007.

5. Bürger, M., Buck, M., Schmidt, W. & Widmann, W. Validation and application of the WABE code: Investigations of constitutive laws and 2D effects on debris coolability. Nuclear Engineering and Design 2006, 236, pp. 2164–2188.

6. Takasuo, E., Hovi, V. & Ilvonen, M. PORFLO modelling of the coolability of porous particle beds. VTT, Espoo, 2011. VTT-R-09376-10. 41 p.

7. Takasuo, E., Kinnunen, T., Pankakoski, P.H. & Holmström, S. Description of the COOLOCE test facility – Conical particle bed. VTT, Espoo, 2010. VTT Research Report VTT-R-08956-10. 18 p.

8. Schmidt, W. Influence of Multidimensionality and Interfacial Friction on the Coolability of Fragmented Corium. Doctoral Thesis. Institut für Kernenergetik und Energiesysteme, Universität Stuttgart, May 2004. Pp. 16–18. ISSN 0173-6892.

22. Risk-informed Inspections of Piping (PURISTA)

22.1 PURISTA summary report

Kaisa Simola, Otso Cronvall, Ilkka Männistö, Matti Sarkimo and Ari Vepsä
VTT

Abstract

The overall objective of the PURISTA project was to support the implementation of risk-informed in-service inspection (RI-ISI) at Finnish nuclear power plants by studying relevant issues related to RI-ISI. Main objectives were the development of structural reliability methods for quantification of piping leak and break probabilities, the development of methods for evaluating inspection capability and the link between inspection qualification, detection probability and RI-ISI, and studying issues related to risk-ranking, selection of inspection sites and acceptance criteria of a RI-ISI programme. The project has contributed to several international activities, including the participation in the work of the Task Group on Risk (TGR) of the European Network for inspection and Qualification (ENIQ).

Introduction

The purpose of risk-informed in-service inspections (RI-ISI) is to achieve a coherent in-service inspection management by taking into account the results of plant-specific risk analyses in defining the inspection programme and focusing the inspections efforts to the most risk-significant locations. Ideally the optimisation of ISI can lead to improved safety and availability, reduced radiation doses and reduced inspection costs.

From a technical perspective, a typical RI-ISI process consists of the following main steps:

- Definition of RI-ISI scope, collection and analysis of the required input data
- Identification and evaluation of piping failure consequences
- Identification and evaluation of piping failure potential
- Risk ranking
- Definition of the new inspection programme.

Typically, before implementing the RI-ISI programme, the results of the RI-ISI analysis are required to be submitted to the national regulatory body for approval.

Even if RI-ISI has been widely applied in the US, European utilities and safety authorities have identified need for further research in several RI-ISI related issues. Furthermore, the US RI-ISI approaches cannot always be adopted as such since they have been originally developed to the US regulatory environment, and do not comply as such with national regulations and different standards in many European countries.

The overall objective of the PURISTA project has been to support the implementation of RI-ISI at Finnish nuclear power plants by studying relevant issues related to it. In Finland, the use of risk-informed methodology in planning new ISI programmes is a regulatory requirement, and both domestic utilities are developing RI-ISI programmes for the existing plants. Also the ISI programme for the new EPR unit will consider risk insights.

Main objectives of the PURISTA project were the following:

- To develop structural reliability methods for quantification of piping leak and break probabilities
- To develop methods for evaluating inspection capability and the link between inspection qualification, detection probability and RI-ISI
- To study issues related to risk-ranking, selection of inspection sites and acceptance criteria of a RI-ISI programme.

The main research activities and results of the PURISTA project are described in the following.

Assessment of piping failure potential

In quantitative assessment of piping degradation potential, failure probabilities are obtained computationally based on associated physical characteristics and

susceptibility to various degradation mechanisms. For the assessment of the most common degradation mechanisms, structural reliability models (SRM) have been developed. However, the acceptance of thus obtained assessment results as representing some form of true or absolute value varies, e.g. because for the time being there are no standardised or commonly accepted SRM procedures or analysis tools. Quantitative values can however serve at least in quantifying relative differences in the probability of failure through taking into account piping component geometry, material properties, loads and inspection strategies. One promising way to improve the accuracy of the SRMs is to use statistical estimates based on both plant specific and global databases in order to provide anchoring/calibrating points for single SRM estimates, in relation to which they could be improved in other locations as well. Quantitative approaches can also be used to conduct sensitivity studies, for instance to assess the impact of inspection capability and interval on the failure probability.

Probabilistic fracture mechanics modelling

Research work on structural reliability analysis methods at VTT has resulted in further development of a probabilistic fracture mechanics (PFM) tool VTTBESIT. This tool is an extended modification of a deterministic fracture mechanics analysis code originally developed by the Fraunhofer-Institut für Werkstoffmechanik (IWM), Germany. With the VTTBESIT code it is possible to quickly compute the stress intensity factor values along the crack front and, based on this, simulate the crack growth.

VTTBESIT was extended and enhanced with the addition of certain probabilistic capabilities. Firstly, probabilistic distributions for depth and length of existing fabrication cracks have been added to the code. Provided developments include assessment of initiation probability of low-cycle fatigue induced cracks as well as probabilistic treatment of cyclic loads in PFM analyses concerning low-cycle fatigue induced cracking. These new features were tested in a pilot analysis of the auxiliary feedwater system in a Finnish BWR unit [1]. Also, probabilistic distributions for depth and length of stress corrosion induced cracks were developed and added to VTTBESIT. These new input data distributions were tested in a pilot analysis of the shutdown cooling system in a Finnish BWR unit [2, 3]. In the same connection Latin Hypercube Sampling (LHS) simulation capability was added to VTTBESIT.

A joint Nordic research project called PODRIS to benchmark the VTT PFM analysis tool against PRoSACC and NURBIT tools used in Sweden as well as

JRC approach developed in Netherlands was completed during 2009 [4]. Its scope included application of these analysis tools to selected structural reliability cases and comparison of the results. The analysis results matched mostly at least quite well, thus providing added confidence on the use of the benchmarked approaches. The project also investigated the use of simplified probability of detection (POD) curves, and the results indicated that the approximation of the POD with a simple step function could be justifiable in RI-ISI applications.

A licentiate thesis on structural lifetime, reliability and risk analysis approaches for power plant components and systems [5] was also completed within the project.

Vibration induced high cycle fatigue

Vibration in operational conditions is a potential source of high cycle fatigue in piping systems. In addition to inducing fatigue, vibration tends to tear existing cracks rapidly through the pipe wall once they have been nucleated. In this case, cracks are unlikely to be detected in NDT inspections in time before a leak occurs. For these reasons, it is clear that severity of vibration should be assessed somehow. Traditionally, control of piping vibration has been carried out by measuring velocity or acceleration of vibration and comparing the measured values against recommendations and guidelines that can be found in codes, standards and other type of literature.

Potentiality of fatigue is partly determined by magnitude and frequency of occurrence of stress variation in piping material. These factors can be assessed by strain gauge measurements. However, this method has also its own disadvantages. A study within PURISTA concentrated on investigation and quantitative validation of a method with which vibration induced stress variation can be estimated without performing strain gauge measurements [6]. In the investigated method, operational displacements shapes, ODS, as actually measured at the system, are used as an input in the forced vibration analysis which is performed with a finite element model of the system. As a result of the analysis, estimate for the vibration induced stress variation can be obtained at every location of the system that is included into the model.

Test subject of the study was a pipeline of the secondary feed water system at Loviisa 1 WWER plant for which measured ODS were readily available. In order to verify the investigated method, strain gage measurements were carried out at the system. The results of these measurements were then processed with a computer code which was developed to support the evaluation of the method.

The code performs first rainflow cycle counting for the strain data. After that it computes statistical distribution for the resulting strain amplitudes.

The same procedure can be applied also for the simulated strains resulting from the forced vibration analysis. Finally, obtained two sets of statistical distributions for the strain amplitudes can be compared against each other yielding information about validity of the method.

Reliability of in-service inspections

The impact of ISI on plant safety depends on the capability of the inspection system to detect flaws. The reliability of inspections is an important input for RI-ISI analysis. If a quantitative RI-ISI analysis is to be performed, then a quantitative measure of inspection effectiveness is needed in order to calculate the reduction in risk associated with the inspections.

PURISTA project has addressed the ISI reliability from two directions. On one hand, the reliability of inspections has been investigated through NDT simulations. On the other hand, the importance of inspection capability assumptions in risk-informed ISI has been studied, and the relationship between inspection qualification and flaw detection probability has been addressed.

NDT simulations

The capability of a NDT inspection is a sum of many parameters that are contributing to the final outcome. Examples of the factors that have influence on the inspection result in the case of ultrasonic inspection are component properties (geometry, material), inspection technique (probe, setting values, contact stability, scanning path), and flaw parameters (geometry, size, location, orientation). The study of the influence of different parameters and their variations using real experimental tests is often laborious task because large number of test blocks and inspection runs are needed. Also the assessment of the probability of detection (POD) requires considerable amount of experimental test results to be statistically reliable. To reduce the costs of practical test samples and real inspection tests computer modelling and simulations can be considered. Modern simulation programs provide different possibilities to replace at least a portion of the practical tests with computed results.

Using a simulation program it is possible to create a very realistic ultrasonic inspection case and produce “inspection” data files that are similar with files originating from real practical inspections. The material property settings include

structural noise and attenuation adjustments and those can be set to imitate the reality. Thus the defect indication appearance is not necessarily obvious and the analysis of the result files is more realistic and challenging. Such virtual inspection result files could be applied for training and verification of the inspection techniques but also to produce data for POD assessment.

Some results of virtual ultrasonic inspections performed using a planar specimen including several defects (notches) on its back surface are shown in Figure 1. When simulations are run using different inspection parameters (different probe specifications) there is clear variation in the defect detection. Some simulation results show clearly visible indications from all 13 defects set in the simulated test sample while in some results nearly all indications are buried in the noise and are thus not visible.

Currently the NDT simulation programs are developed to include tools to produce POD assessments. Different parameter e.g. defect property values can be defined as exactly set values or distributions for computation of indication amplitude. Thus studies with selected parameter variations can be made efficiently. Some programs (for example Civa version 10) include tools to present the results directly as POD curves. Such curve can be computed usually as function of defect size. One or several other parameters (for example defect orientation angles) can be defined as uncertain parameters and given using distributions. The computation is then performed using a simple Monte Carlo approach applying the given parameter variation. The final result is presented in form of POD-curves.

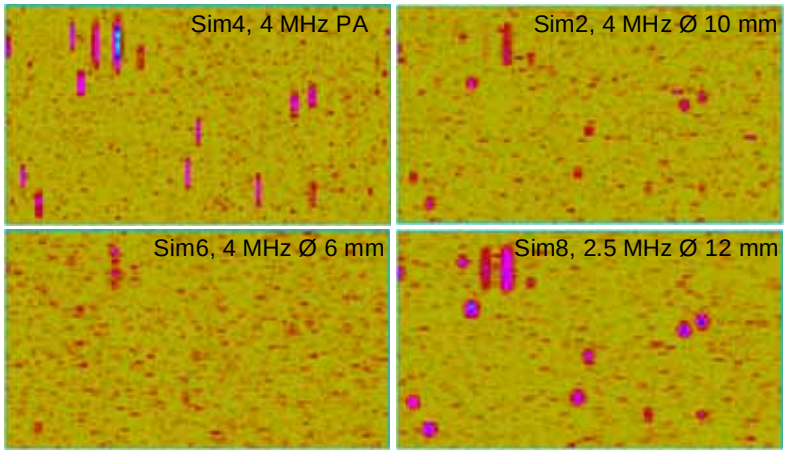

Figure 1. Top views (C-scans) of four simulated inspection runs of plate with several defects (total 13 defects). Different ultrasonic techniques (probe characteristics) are applied and the result plots show clear differences in visible indications (large red and red/blue spots) [7].

Relationship between inspection qualification and probability of detection

A POD curve could provide ideal data for evaluating ISI reliability, but there can be significant problems associated with generating realistic POD curves by practical trials. The ENIQ inspection qualification methodology [8], based on a combination of a qualitative technical justification and practical trials, is used to provide high confidence that an inspection system will achieve its objectives. However, it is not designed to provide a quantitative measure of the type that can be used in RI-ISI analysis.

Approaches to quantify the confidence which comes from inspection qualification according to the ENIQ procedure were investigated in a joint European project [9, 10]. Two pilot qualification studies were performed to demonstrate the application of the quantification methods in practice, and to identify needs of further work and issues to be addressed in the guidelines. The most structured quantification approach is based on weighting and scoring the elements of the technical justification, and using a Bayesian approach to combine the information from a quantified technical justification with the results of practical trials. The pilot studies highlighted a number of issues that require further work or that should at least be drawn to the attention of those who intend to apply the methodology. Guidelines were developed for the application of the structured quantification approach. Consideration should also be given to how to construct a technical justification to facilitate the quantification of the NDT capability.

Benchmarking RI-ISI methodologies

VTT participated in the international RI-ISI benchmarking project RISMET [11]. RISMET was initiated by ENIQ TGR and coordinated by the JRC and OECD/NEA, and it was conducted in 2006–2009. More than twenty organizations from Europe, U.S., Canada and Japan participated in the project.

In the RISMET project, various RI-ISI methodologies and the deterministic ASME XI approach were applied to the same case, consisting of four selected piping systems of Ringhals 4 PWR unit (see Figure 2). Several criteria were identified for selecting these systems:

- All safety classes should be covered
- A variety of degradation mechanisms should be covered
- Good coverage of risk categories should be achieved

- Systems with significant increase or decrease in number of inspections (before /after applying RI-ISI) should be included
- Balance between initiating and mitigating systems should be ensured.

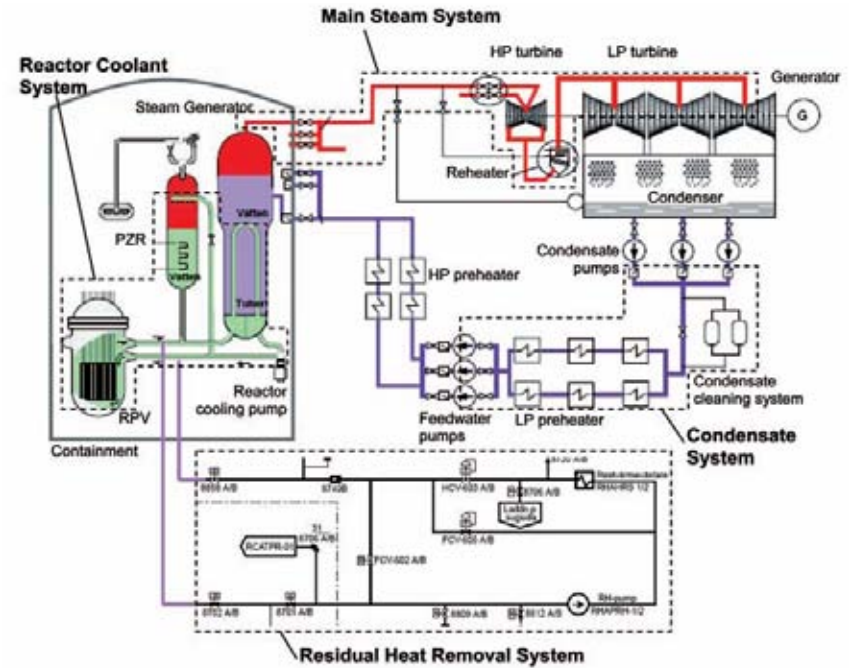

Figure 2. Scope of the RISMET benchmark project [11].

The results of the applications were analysed and compared by evaluation groups, who addressed following issues: (1) scope of the application; (2) failure probability analyses; (3) consequence analyses; (4) risk ranking, classification and selection of segments/ sites, and definition of inspection programs; and (5) regulatory aspects.

Even if the scope of the benchmark was limited to 4 systems, the variety regarding safety class, potential degradation mechanisms and pipe break consequences ensured a good coverage of issues for a comparative study. The risk-informed methodologies showed some significant differences and resulted in slightly different risk ranking and selection of inspection sites. However, the results of the benchmark indicated that the risk impact of these differences is small, and the RI-ISI approaches identify safety important piping segments that are ignored by approaches not using the probabilistic safety assessment (PSA). The results of the benchmark exercise RISMET improve the knowledge on

differences in approaches and their impact on plant safety, and promote the use of risk-informed ISI.

International co-operation

International co-operation has been an essential part of the PURISTA project. A large part of the research work was done in co-operation with European organisations and in international networks. Besides the contributions to the previously referred projects PODRIS, "Relationship between inspection qualification and probability of detection" and RISMET, VTT has actively participated in the work of the Task Group Risk of the European Network for Inspection and Qualification, ENIQ TGR [12]. The TGR works towards developing European best practices for RI-ISI methodologies. VTT led the work on writing recommendations for the use of expert panels in RI-ISI, and RI-ISI updating. VTT also contributed to the development of a recommended practice on verification and validation of structural reliability models used in RI-ISI.

VTT participated in IAEA consultant group to develop a technical document on RI-ISI [13]. The publication describes the general process of developing and implementing risk-informed in-service inspection (RI-ISI) methodologies, the technological issues which lie behind the methodologies, application status, and the current development activities.

Conclusions

The applications of risk-informed approaches to redefine in-service inspection programmes are increasing all over the world, and RI-ISI projects are going on at Finnish nuclear utilities. The PURISTA project has aimed at supporting the RI-ISI implementation in Finland.

The results of the international RI-ISI benchmark study showed that RI-ISI approaches that base the consequence assessment on a plant specific PSA model have the capability to identify risk important inspection locations that might otherwise be ignored. It also pointed out that a RI-ISI process itself is a valuable exercise, since it forces the project team to review the piping degradation potential and to identify direct and indirect consequences of piping failures.

Many results of the PURISTA project are not restricted to RI-ISI application, but can be used more widely in the safety management of structural components. Probabilistic structural integrity assessment tools may be applied in structural safety analyses, and in updating PSA initiating event frequencies. Sufficiently

reliable estimates of stresses and their fluctuations allow better evaluation of low-cycle fatigue risks. Inspection reliability studies support the development of the link between inspection qualification and quantification of inspection capability. The results of inspection simulation studies can be used in connection to the inspection qualification. Studies of RI-ISI implementation can also be utilised in other risk-informed applications, such as testing and maintenance planning.

References

1. Cronvall, O., Simola, K., Vepsä, A. & Alhainen, J. RI-ISI pilot study of the auxiliary feed water system of the Olkiluoto OL1 NPP unit. VTT, Espoo, 2008. VTT Research Report VTT-R-01414-08. 47 p. + app. 12 p.

2. Cronvall, O., Männistö, I. & Alhainen, J. Development of Risk Informed In-Service Inspection Analysis Procedures and Application to Finnish BWR Unit Piping Components. VTT, Espoo, 2009. VTT Research Report VTT-R-00650-09. 48 p.

3. Cronvall, O. & Alhainen, J. On assessment of initial cracks for RI-ISI analysis purposes. Proceedings of the 20th International Conference on Structural Mechanics in Reactor Technology (SMiRT 20), Paper 1797. Espoo, Finland, August 2009. 10 p.

4. Simola, K., Cronvall, O., Männistö, I., Gunnars, J., Alverlind, L., Dillström, P. & Gandossi, L. Studies on the effect of flaw detection probability assumptions on risk reduction at non-destructive inspection. In: Ale, B., Papazoglou, I. & Zio, E. (Eds.) Reliability, Risk and Safety – Back to the Future. Proceedings of the European Safety and Reliability Conference ESREL2010, CRC Press. Pp. 1513–1518.

5. Cronvall, O. Structural lifetime, reliability and risk analysis approaches for power plant components and systems. Licentiate Thesis, Aalto University School of Science and Technology, School of Engineering, Department of Structural Engineering and Building Technology, Espoo, Finland, 2011. (Draft, left for approval in November 2010, to be published during early 2011.)

6. Vepsä, A. Operational Displacement Shape Based Estimation of Vibration Borne Stress Variation in a Pipeline. Proceedings of the IMAC XXVI A Conference and Exposition on Structural Dynamics, 4–7 February 2008, Orlando, USA. 14 p.

7. Sarkimo, M. Flaw detection trial using virtual ultrasonic testing. In: Proceedings of Baltica VIII Conference on Life Management and Maintenance for Power Plants, 18–20 May, 2010. Helsinki–Stockholm–Helsinki. VTT Symposium 264. Pp. 204–220.

8. ENIQ. European methodology for qualification of non-destructive testing: third issue. European Commission, 2007. EUR 22906 EN. 40 p.

9. Gandossi, L., Simola, K & Shepherd, B. The link between risk-informed in-service inspection and inspection qualification. Insight: Non-Destructive Testing and Condition Monitoring 2009, Vol. 51, No. 1, pp. 16–20.

10. Gandossi, L., Simola, K & Shepherd, B. Application of a Bayesian model for the quantification of the European methodology for qualification of non-destructive testing. International Journal of Pressure Vessels and Piping 2010, Vol. 87, No. 2–3, pp. 111–116.

11. Gandossi, L., Simola, K., Stevenson, P., O'Regan, P., Lydell, B., Hultqvist, G., Leijon, A. & Enger, K. A benchmark study on risk-informed in-service inspection methodologies (RISMET). ATW International Journal for Nuclear Power 2010, Vol. 55, No. 7, pp. 450–457.

12. Simola, K. & Gandossi, L. Risk Informed In-Service Inspection Activities within the European Network for Inspection and Qualification. In: Proc. of PSAM 10 – 10th International Probabilistic Safety Assessment & Management Conference, 7–11 June 2010, Seattle, Washington, USA, Paper 45, IAPSAM – International Association of Probabilistic Safety Assessment and Management, Seattle, Washington, 2010.

13. Risk-informed in-service inspection of piping systems of nuclear power plants: process, status, issues and development. IAEA Nuclear Energy Series No. NP-T-3.1. IAEA, Vienna, 2010.

23. Fatigue of Primary Circuit Components (FATE)

23.1 FATE summary report: FABELLO for valid fatigue tests in LWR coolant water

Jussi Solin, Jouni Alhainen, Esko Arilahti, Jukka Väinölä, Pieti Marjavaara,
Erkki Järvinen, Matti Halonen, Mikko Patalainen, Kalle Kaunisto,
Pekka Moilanen et al.
VTT

Abstract

FABELLO is assumed to be the first and only fatigue facility in Europe capable to perform valid LCF tests in LWR coolant waters for determination of design curves similar to ASME III design curve. The FABELLO facility is applicable to verification of new designs, to research on parametric influences in the environmental effects and to develop mechanism informed fatigue model for ageing of NPP primary circuits.

Introduction

Fatigue is often claimed as the most important ageing mechanism in NPP primary circuit pressure boundaries. Major thermal transients occur always, when a plant is started or shut down. Smaller or larger temperature gradients across the piping walls are also created, when the steady state operation is disturbed by power adjustment, valve operation or other action causing a change of local water temperatures. Periodically used spray lines and the surge line, which

connects the main circulation loop and pressurizer in a PWR are typical locations for such time-dependent temperature changes.

Figure 1 gives an example of a typical thermal transient in the surge line of a PWR. The shape of the strain transient is of interest, because a change in flow causes an abrupt reaction with high strain rate. A low strain rate towards the steady state condition develops during the stabile flow phase. Obviously, this results in a lower environmental effect than measured in a laboratory test with constant strain rate and what the currently available models predict [1, 2]. A similar shape of transient has been utilised also for the EPR fatigue evaluation [3].

The Radiation and Nuclear Safety Authority (STUK) issues YVL guides, which set requirements for licence holders or applicants in Finland. Requirements on strength and structural integrity assessment of primary circuits are given in the YVL-guide 3.5 Ensuring the strength of nuclear power plant pressure devices [4]. Since 2002 this guide has stated that influence of environment (coolant water) shall be accounted for in fatigue assessment.

The Safir-FATE project aimed in understanding the mechanisms of material ageing caused by cyclic stressors during plant operation and their application to practical fatigue assessment of primary loop pressure boundaries.

Development of reliable capabilities to perform critical experiments and modelling work plays an important role in this work. It should be noted that generation of a material data base for design purposes goes beyond the scope of the Safir programme, but critical tests need to be performed for development of quantitative mechanism based and risk informed fatigue models and to check validity of (sometimes hidden) assumptions in component assessment.

This presentation will briefly summarise the research challenges and results concerning the project as a whole in 2007–2010. However, the focus of this paper is in introduction of the FABELLO facility for fatigue experiments in simulated LWR hot water environment. FABELLO was designed, manufactured and tested in the project, which also provided the main challenge of the project.

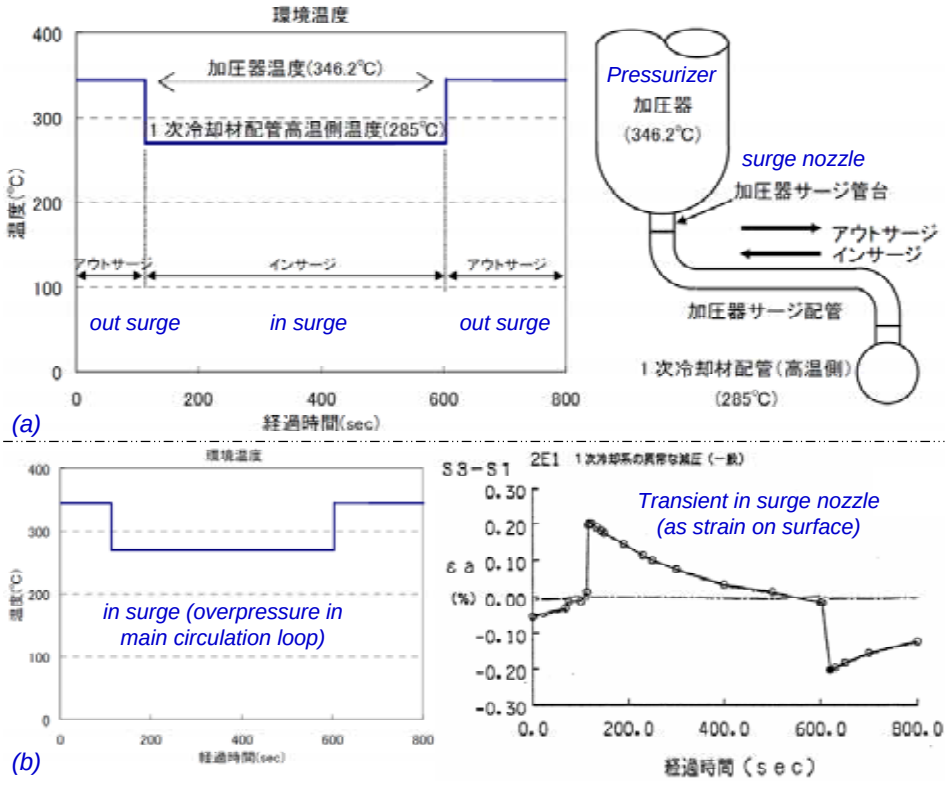

Figure 1. Typical thermal transient in a PWR (a), the same as a strain cycle (b). Graphs from [5].

Main objectives and their evolution during the project

The mission for this project was given by the 2002 update of YVL 3.5 guide [4]. According to YVL 3.5 chapter 3.2.6, fatigue assessment shall be based on S-N-curves applicable to each material and conditions. Furthermore, YVL 3.5 specifically states that justification is required, if ASME III fatigue curves are used for assessing environment assisted fatigue. It was assumed that the YVL requirements can be fulfilled in different ways, but an option for experimental verification of the design curve in relevant environments should be available, in particular for the pressure boundary materials in new designs. Experimental work would also be needed to develop proper understanding of the related ageing mechanisms and to assess controversial claims on applicability of the new requirement issued shortly before planning of this project by YVL 3.5 in Finland and TENPES guidelines in Japan [4, 6].

Taking into account the limited scope and funding base of the programme, the original aim was to approach the challenge with two co-ordinated projects. Safir-FATE was to focus on mechanisms of fatigue in primary water and an industry-driven R&D project was to provide application oriented experimental work in substantial volume and with Tekes support. However, the idea of parallel projects was soon withdrawn but this project was continued and the objectives were focused to:

- Developing the first in Europe ASTM E-606 (and ASME III) compatible fatigue facility for LWR environments. The old small scale LCF bellows equipment had been modified to other purpose and a new design allowing standard size specimens was still considered a necessity.
- Experimental work including metallography (TEM) began in air environment to enhance understanding and expertise on the complex cyclic behaviour of austenitic stainless steels and to learn for the coming work in PWR environment.
- Meanwhile, publication of the U.S. NRC Regulatory Guide 1.207 in 2007 [1, 7] and revision of the ASME III design curves for stainless steels in 2009 [8] brought also the air curve (without environmental effects) to spotlight of the international debate and reading of the YVL 3.5 guide. This gave reason to study the endurance in air as well.

Main results and conclusions in the project

The development of the new equipment turned out to be an oversized challenge for the funding, personnel resources and management available to the project. It continued for three years, but during the fourth year, the FABELLO equipment was finally ready for demonstration and fulfilled the expected performance criteria.

Cyclic response of the available stainless test materials was found to be even more complex than anticipated. This can actually be interpreted in terms of irreversible changes of microstructure. For certain laboratory test conditions we could say even more provocatively: “before cracking, the test material is not any more the same as in beginning of the test”.

The complex cyclic response is supported by observations in transmission electron microscopy (TEM) of fatigued samples [9–11]. In particular, a notable amount of martensite was found in samples fatigued for long life at low strain amplitude. Martensite formation is not a new finding, but previous studies have

considered higher strain amplitudes. We do not yet know for sure, what triggers the pronounced secondary hardening at a very accurately predictable number of cycles, but we can see a notable amount of martensite generated during the hardening [11].

The cyclic deformation has a tendency to become localised both macroscopically and microscopically. The heterogeneity observed and difficulties to definitely interpret the local dislocation microstructures is well in line with this. However some clear trends were found and, no doubt, the objective of gaining expertise and experience in analysing the cyclic deformed stainless steels was achieved.

Concerning the issue of modified design curves, our endurance results obtained for different stainless steel grades – including 100% relevant NPP piping material – do not support the updates by U.S. NRC and ASME [7, 8]. Determination of valid design curves would go beyond the scope of Safir2010 programme, but the tentative results indicate no need for updating the curve for the material grades used in the current Finnish NPP's. The old Langer curve [12] works as accurately as the new one [1], or even more accurately. This issue was discussed already in the mid term seminar [13, 14].

Test facility for LCF in primary coolant

To be able to accurately measure specific environmental effects and perform parametric studies, a novel experimental facility was developed by VTT [15-18]. A specimen diameter (4mm) less than the minimum recommended by the ASTM procedure was used, but this was not considered crucial, as long as the data was not aimed for verifying design data of reactor components. However, the small scale facility was not any more directly available and a new facility for standard tests was considered necessary.

Transient simulation

The importance of real loading sequence has been pointed out in a wide range of experimental research and also in the YVL 3.5 guide [4]. Looking at the available data as a whole, it seems that the sequence effects are highly depending on the plant transient type and material cyclic response at the particular strain ranges. If accuracy of fatigue assessment is to be improved by considering sequence effects, alloy sub-class specific effects may need to be evaluated. In other words, austenitic stainless steels cannot be considered as a uniform material group.

Further research to clarify transferability of existing laboratory data to relevant materials and real plant conditions is recommended.

For that purpose we built a new control and measuring system suitable for effective and flexible simulation of complex plant transients. The new capability has been verified in tests conducted in air and in pressurised hot water. Different wave forms were used, including the "EPR transient" as shown in Figure 2.

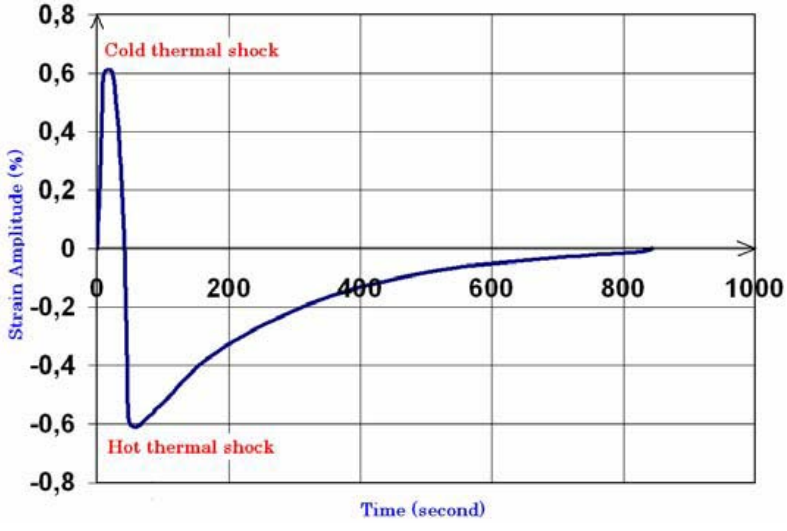

Figure 2. Typical strain history of cold and hot thermal shocks corresponding to a safety injection transient in a PWR. [3]. The real transient is symmetric with slow return of strain to 0 after the peak (see Figure 1), but the down-ramp has been shortened to save laboratory time.

Direct strain control

Strain measurement within the gage section is not easy to arrange and some laboratories (not VTT) utilise indirect strain control based on a "companion specimen" strategy for calibration of the measurements in the environment [19]. Applicability of indirect strain measurement was investigated and found unacceptable for stainless steels. The remote strain response is not linearly correlated to the true strain, not even during a single cycle or transient and the complex cyclic hardening-softening-hardening response makes it impossible to accurately control the true strain through remote measurements for stainless steel, Figure 3. Switching to indirect strain control would have simplified the experimental work in hot water, but it cannot be recommended [13].

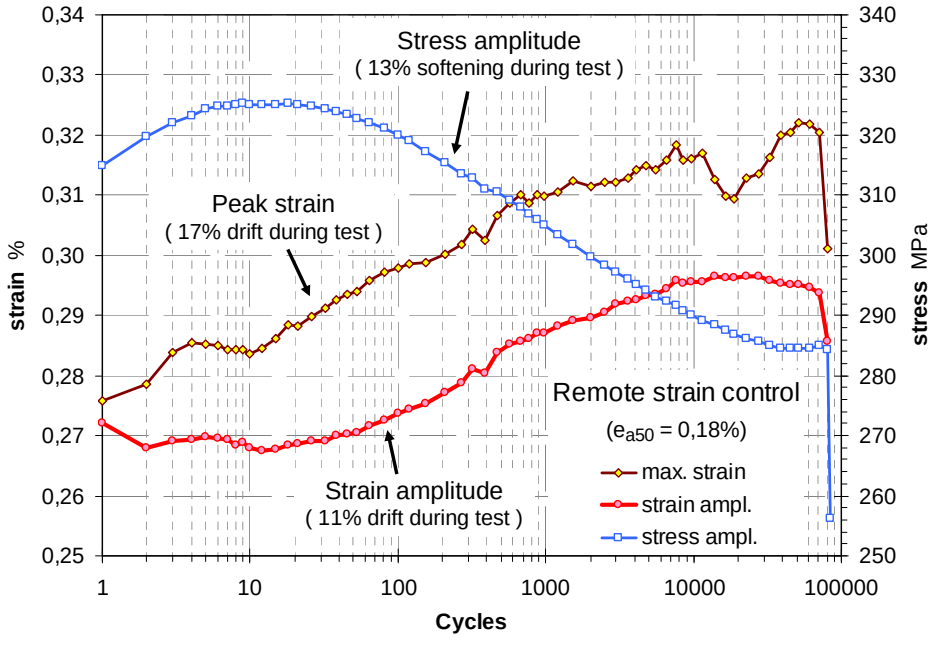

Figure 3. Drift in the true strain during a remote strain controlled test for alloy 316 [13].

Design of the FABELLO

The new FABELLO equipment is powered by servo-controlled pneumatic system. It generates a pressure difference between the bellows and pressurised water inside the pressure vessel, where simulated PWR or BWR coolant water is circulated. This arrangement eliminates the need for moving load train through the pressure boundary of the test chamber. The load acting in the specimen is accurately deduced from the pressure difference.

Four existing pressure vessels and a water circulation loop were taken as a starting point. The limited space in the vessels actually caused major challenges for the FABELLO design, Figure 4. Relatively large bellows were needed to get sufficient load capacity with a reasonable pressure difference. In theory, a maximum capacity would be obtained, if the pressure in bellows would range from zero to double of the water pressure. However, so large range is not used. In any case, the resulting load capacity is sufficient for LCF tests with 8 mm specimens of austenitic stainless steels.

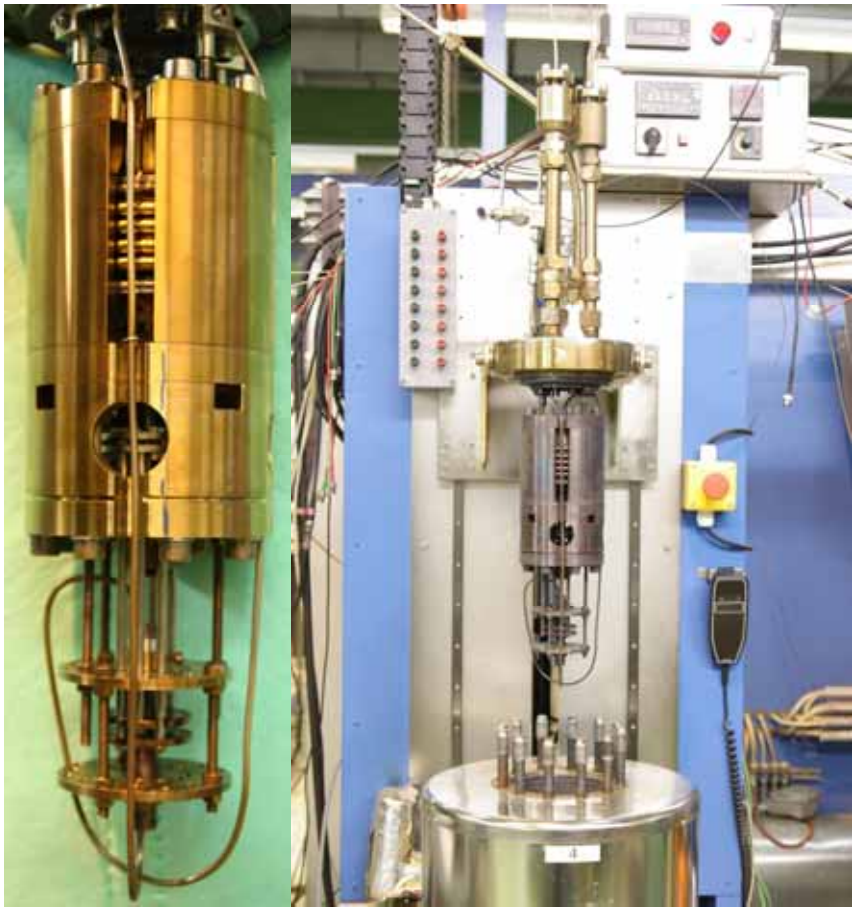

Figure 4. FABELLO unit before and after three months in 300°C pressurised water.

The specimen, Figure 5, is inside the rigid load frame of FABELLO. The strain measuring device is carefully mounted to the polished mid section of the specimen after closing the frame. This is a very critical phase because the mounting must be secured without scratching the specimen. Furthermore, sharp knife edges or high pressing forces would introduce a notch and potential crack initiator in the specimen.

Performance of FABELLO

The specimen design for FABELLO was tested in room temperature air at strain amplitudes 0,3–0,6% with constant amplitude and transient (Figure 2) straining. The obtained data was identical to tests with standard specimens.

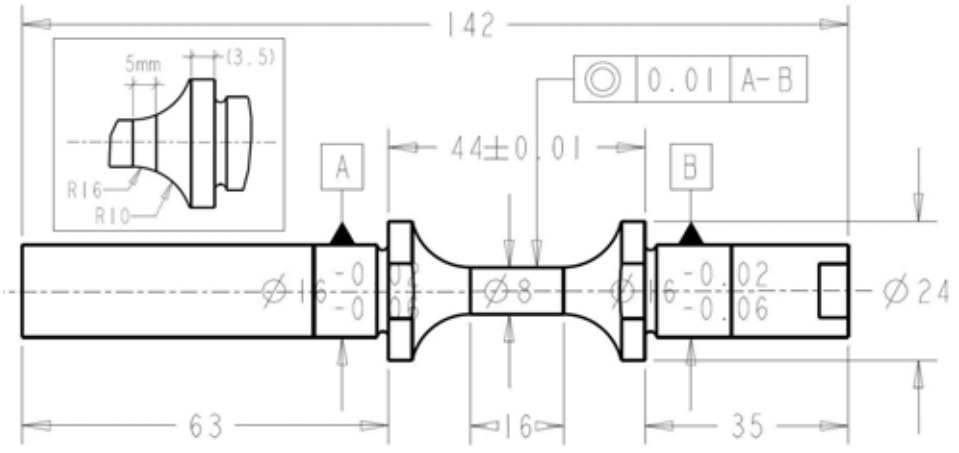

Figure 5. LCF specimen for the FABELLO.

Next a FABELLO unit was immersed in 300°C pressurised water for three months. Strain controlled cyclic testing was performed for a titanium stabilised alloy 321 with numerous control and straining parameters. The introduced strain sequences included transients similar to the “EPR transient” in Figure 2. The measured hysteresis loops shown in Figure 6 were measured almost three months after beginning of the testing.

Also hold periods were included and in cases where the same strain amplitude was used before and after the hold, clear indications of strain ageing were observed, Figure 7. Strain ageing was seen as a pronounced yield point and in many cases also as instability of loading. The pneumatic loading device acts as a flexible gas spring with low damping. The oscillation during the first pull after strain ageing was repeatable. It was consistently measured several times for the first pull, but disappeared after it.

The instability and oscillation is assumed to depend on the low slope of strain hardening curve after yielding. It is possibly triggered by some abrupt (serrated) flow in macroscopic slip bands having been developed during the previous straining. If the hypothesis on serrated flow is correct, this should also occur in pulling of pre-strained materials with bellows loaded equipment and would provide a sensitive measurement of material tendency to serrated flow. Servo-hydraulic and mechanical testing machines would not oscillate as much as the gas loaded bellows.

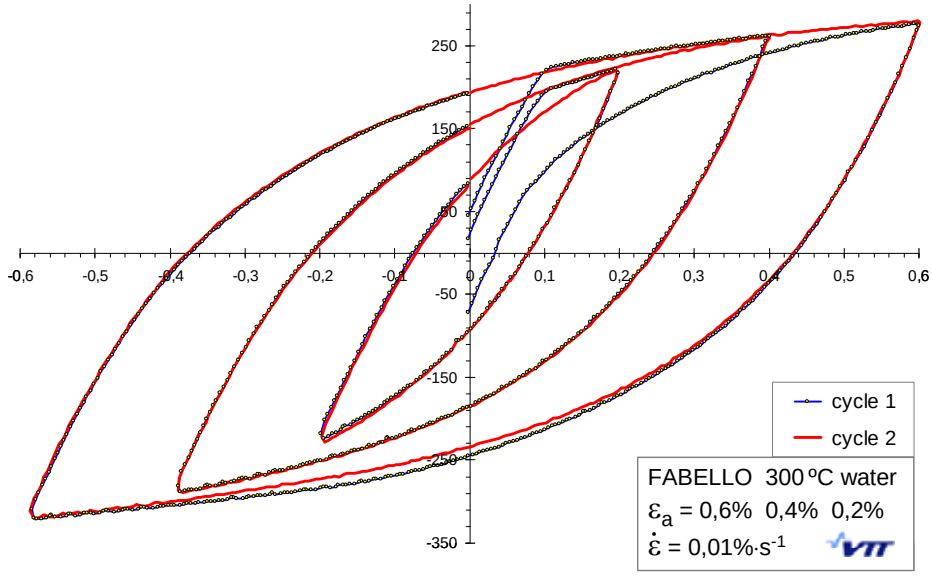

Figure 6. Hysteresis loops measured in 300°C pressurised water by the FABELLO. Two first cycles after each change of strain amplitude are shown.

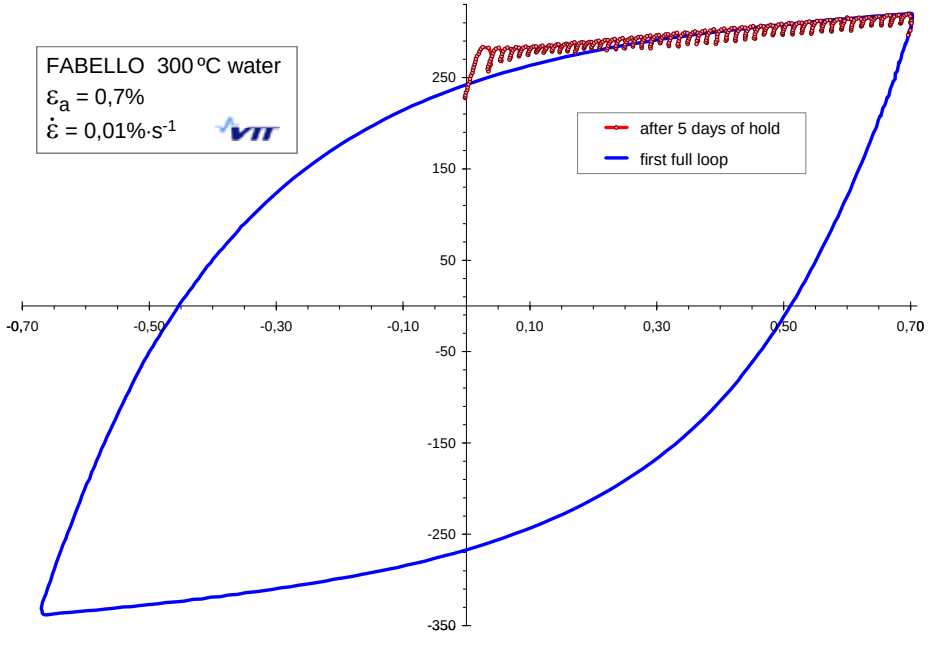

Figure 7. Hysteresis loops showing strain ageing and loading instability for the first ¼ cycle after 5 days of hold in 300°C.

Conclusions

The FABELLO facility meets the basic requirements (ASTM E-606, ASTM E-1012) for determination of qualified ASME design curve data. Four units are available for verifying the design curve for the relevant LWR environments and loading sequences.

Further tuning of the pneumatic system will be needed, if high strain rates are to be used in tests. However, excellent hysteresis loops were measured at low and medium strain rates in 300°C pressurised water. This indicates that the equipment is suitable also for scientific research to clarify the mechanisms involved in fatigue of primary loop pressure boundaries.

References

1. Chopra, O. & Shack, W. Effect of LWR Coolant Environments on the Fatigue Life of Reactor Materials. Final Report. NUREG/CR-6909, ANL-06/08, Argonne Nat. Lab., 2007. 118 p.

2. JSME, 2009. Codes for Nuclear Power Generation Facilities, “Environmental Fatigue Evaluation Method for Nuclear Power Plants,” JSME S NF1-2009. The Japan Society of Mechanical Engineers, Tokyo, Japan, 2009. (Comprehensive revision of the 2006 issue.)

3. Le Duff, J.-A., Lefrançois, A. & Vernot, J.P. Effects of surface finish and loading conditions on the low cycle fatigue behavior of austenitic stainless steel in PWR environment – Comparison of LCF test results with NUREG/CR-6909 life estimations. Proceedings of PVP 2008-ICPVT11 2008 ASME Pressure Vessel and Piping Division Conference, July 27–31, 2008. Chicago, USA. Paper PVP2008-61894. 10 p.

4. STUK, YVL-guide 3.5, Ensuring the strength of nuclear power plant pressure devices, issue 5.4.2002. (Original in Finnish, translations exist.)

5. Japan Nuclear Energy Safety Organization, 2005. Fatigue reliability of nuclear facilities and materials performance in the environment. Annual report on Demonstration Project in 2004. 303 p. (In Japanese.)

6. Nishimura, M., Nakamura, T. & Asada, Y. TENPES Guidelines for environmental fatigue evaluation in LWR nuclear power plant in Japan. Proceedings of 2nd International Conference on Fatigue of Reactor Components 29–31 July, 2002. Snowbird, Utah. 11 p.

7. U.S. Nuclear Regulatory Commission Regulatory Guide 1.207, 2007. “Guidelines for evaluating fatigue analyses incorporating the life reduction of metal components due to the effects of the light-water reactor environment for new reactors”. 7 p.

8. ASME, 2009. ASME Code, Section III, Division 1, Appendices, Mandatory Appendix 1 Design Fatigue Curves. Addendum 2009b.

9. Karlsen, W., Solin, J. TEM examination of low-cycle fatigue deformation microstructures in 316 stainless steel. VTT, Espoo, 2007. VTT Research Report VTT-R-07810-07. 15 p.

10. Karlsen, W. Deformation microstructures of 316L stainless steel after interrupted low-cycle fatigue tests. VTT, Espoo, 2008. VTT Research Report VTT-R-07909-08. 16 p.

11. Karlsen, W. Deformation microstructures of fatigued and annealed Ti-stabilized austenitic stainless steel. VTT, Espoo, 2011. VTT Research Report VTT-R-09487-10. 28 p.

12. Criteria of the ASME Boiler and Pressure Vessel Code for design by analysis in sections III and VIII division 2. Pressure Vessels and Piping: Design and Analysis, A Decade of Progress, Vol. 1. ASME 1972. Pp. 61–83.

13. Solin, J., Alhainen, J. & Karlsen, W. Fatigue of primary circuit components (Fate-Safir) – cyclic behaviour and fatigue design criteria for stainless steel. SAFIR2010 – The Finnish Research Programme on Nuclear Power Plant Safety 2007–2010, Interim Seminar, 12.–13.3.2009. 13 p.

14. Solin, J. Low cycle fatigue of stainless steel. Baltica VIII. Life Management and Maintenance for Power Plants. Vol. 1. Auerkari, Pertti & Veivo, Juha (Eds.). VTT, Espoo, 2010. VTT Symposium 264. Pp. 77–94.

15. Solin, J., Karjalainen-Roikonen, P., Moilanen, P. & Marquis, G. Fatigue testing in reactor environments for quantitative plant life management. 2nd Int. Conf. on Fatigue of Reactor Components, 29–31 July, 2002. Snowbird, Utah, EPRI. 16 p.

16. Solin, J., Karjalainen-Roikonen, P., Arilahti, E. & Moilanen, P. Low cycle fatigue behaviour of 316 NG alloy in PWR environment. 3rd Int. Conf. on Fatigue of Reactor Components, 3.–6.10.2004, Seville, EPRI/OECD. 19 p.

17. Solin, J. Fatigue of stabilized SS and 316 NG alloy in PWR environment. Proceedings of PVP 2006-ICPVT11 2006 ASME Pressure Vessel and Piping Division Conference, July 23–27, 2006. Vancouver, BC, Canada. Paper PVP2006-ICPVT11-93833.

18. Solin, J. Fatigue behaviour of 316 NG alloy and plant aged titanium stabilised stainless steel in PWR environments. Proceedings of Fontevraud 6, SFEN International symposium 18–22.9.2006, Fontevraud, France. Vol. 2. Pp. 1121–1132.

19. Majumdar, S., Chopra, O.K. & Shack, W.J. Interim fatigue design curves for carbon, low-alloy, and austenitic stainless steels in LWR environments, NUREG/CR-5999 (ANL-93/3) for U.S. Nuclear Regulatory Commission, Washington DC, 1993. 48 p.

24. Water Chemistry and Oxidation in the Primary Circuit (WATCHEM)

24.1 WATCHEM summary report

Petri Kinnunen and Timo Saario
VTT

Introduction

Boron (^{10}B) in the form of boric acid (H_3BO_3) is commonly used as a neutron poison in PWRs and WWERs. To minimise corrosion of primary circuit structural materials the acidicity of boric acid is compensated by adding lithium hydroxide (LiOH) in PWRs or potassium hydorxide (KOH) in VVERs. Fuel vendors and authorities have set upper limits to Li^+ and K^+ levels (as well as to some impurities), as both alkali are suspected to increase the oxidation rate of fuel cladding materials. Longer fuel cycles and higher burn-up of fuel require higher ^{10}B concentration and thus higher Li^+ or K^+ levels in the beginning of cycle. There is a need for better understanding of the oxidation process and the mechanism by which the alkali and impurities affect the rate of the process.

Main objectives

The main objectives of the work carried out within the WATCHEM project were to develop an in situ technique for monitoring of the fuel cladding oxidation process, to determine experimentally the effects that modified water chemistries may have on the oxidation rate of typical fuel cladding materials and to develop a theoretical model for the oxidation process.

Experimental

All experiments were performed at 310°C in a laboratory pressure vessel connected to a re-circulation loop. Two fuel cladding materials, Zircaloy-4 (Westinghouse, USA, nominal alloy composition, wt.%: Sn 1.50, Fe 0.20, Cr 0.10, Ni < 0.007, balance Zr) and E110 (Zr-1%Nb, Chapetsky Mechanical Plant, Russia, nominal alloy composition, wt.%: Nb 1.00, Sn <0.01, Fe 0.014, Cr < 0.003, Ni < 0.004, C < 40–70 wppm, Si 46–90 wppm, N < 30–40 wppm, Hf 300–400 wppm, balance Zr) were investigated.

Experiments were carried out in four different environments:

1) normal PWR conditions –2.2 ppm Li as LiOH, 1150 ppm B as H_3BO_3, 2.35 ppm of dissolved H_2 (~26 cm^3 kg^{-1} STP), inlet oxygen content < 5 ppb, pH_{300} ~ 6.9
2) PWR with elevated Li concentrations –5.4 and 10 ppm Li as LiOH, other parameters similar to those in environment 1, pH_{300} ~ 7.3–7.6
3) beginning-of-cycle WWER water chemistry –11, 28 and 56 ppm K as KOH, 1150 ppm B as H_3BO_3, 2.35 ppm of dissolved H_2 (~26 cm^3 kg^{-1} STP), inlet oxygen content < 5 ppb, pH_{300} ~ 6.9–7.6
4) Similar environment as in test 3 with 11 ppm K as KOH but with 120 and 1 000 ppb of fluoride as NaF.

The main experimental technique used was electrochemical impedance spectroscopy (EIS) in a semicontinuous fashion during the 1–5 days of exposure to the simulated primary water. After the exposure the specimens were removed from the pressure vessel to estimate the total thickness of the oxides by SEM. For the simulation and fitting of impedance spectra to the transfer function derived from the kinetic model, Microcal Origin-based in-house software was employed.

Main results

Figure 1 summarises the effect of Li^+ and K^+ content on the thicknesses of oxide films formed on E110 in simulated PWR and WWER coolant conditions for 140 h at 310°C. There is a noticeable increase in film thickness with increasing alkali concentration, the trend of this increase being supralinear.

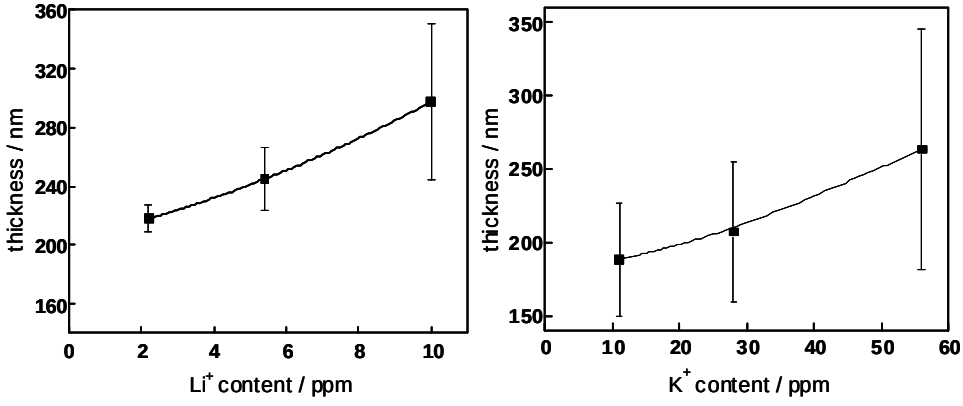

Figure 1. Microscopic estimates of the oxide film thickness on E110 after 140 h of exposure to simulated coolant as depending on the Li+ content (left), K+ content (right).

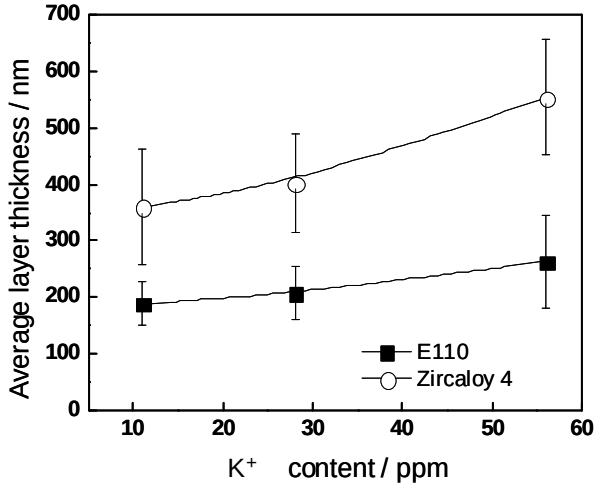

Figure 2. Microscopic estimates of the oxide film thickness on E110 and Zircaloy 4 after 120 h of exposure to simulated WWER water as depending on the K+ content.

Figure 2 shows the difference in oxide thickness between the two studied alloys. The thicknesses increase with K+ content for both alloys, this increase being more pronounced when the concentration is changed from 28 to 56 ppm. Another important fact is that the thickness of the oxides on the Zircaloy 4 samples is significantly higher than that on E110 electrodes, the difference between the oxides on the two alloys becoming the larger, the higher K+ content in the electrolyte.

Impedance Z is resistance of a system to alternating current, analogous to the electric resistance of a material. According to Ohm's law voltage (U) is resistance (R) times the current (I), U = R*I ≈ Z*I. Simplifying, in the case of a PWR or WWER environment, one may take that the voltage is the redox-potential (~constant), resistance is equal to impedance at low frequencies and current is the oxidation (corrosion) current which is directly proportional to the oxidation rate. Thus, the value of impedance at low frequencies becomes inversely proportional to the oxidation rate. In general, the higher is the value of impedance at low frequency end of the spectrum, the lower is the oxidation rate.

Increasing K^+ concentration results in a decrease in impedance, as shown in Figure 3 for E110 fuel cladding. Thus, increase of K^+ concentration increases the oxidation rate of E110 as well as the thickness of the resulting oxide film at a given exposure time. This result is in line with the microscopic data shown in Figures 1 and 2.

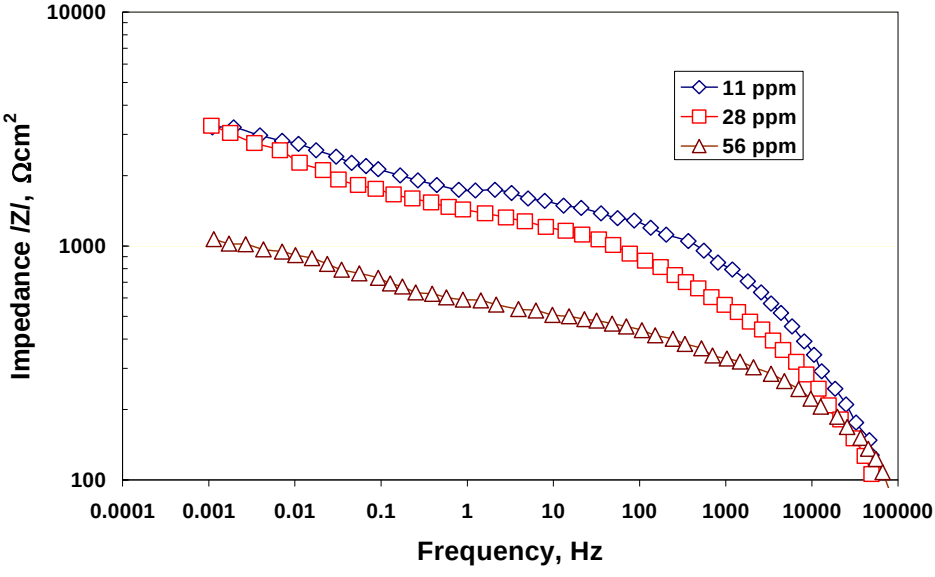

Figure 3. Effect of K+ concentration on the impedance magnitude of E110 fuel cladding. WWER primary water, T = 310°C, exposure time 120 hrs.

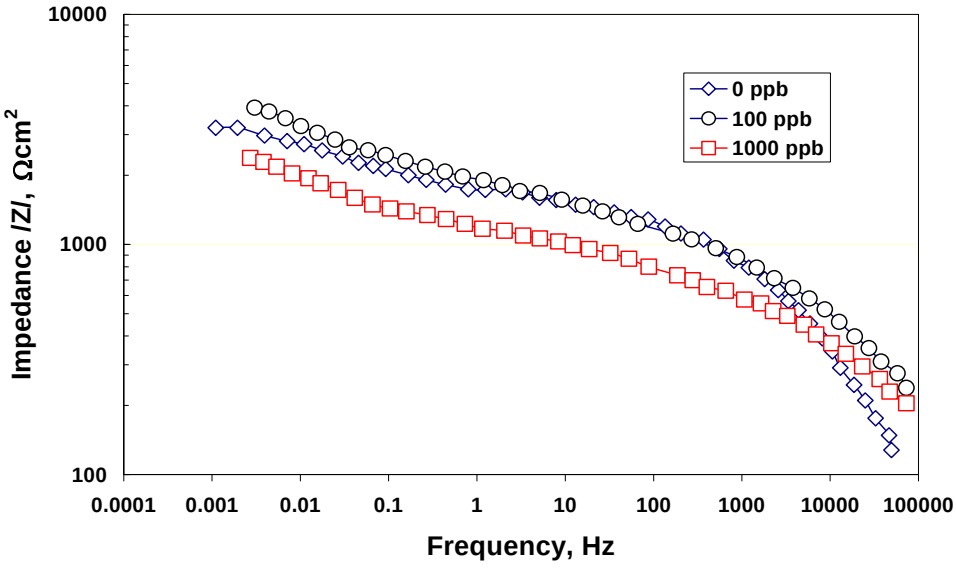

Figure 4. Effect of fluoride (F-) concentration on the impedance magnitude of E110 fuel cladding. WWER primary water, T = 310°C, exposure time 120 hrs.

An example of the effect of impurities on impedance magnitude is shown in Figure 4. Fuel vendor has set a maximum limit at the beginning of cycle for fluoride ions at $[F^-] \leq 100$ ppb. By comparing Figures 3 and 4 it is clear that while the impedance magnitude is almost unaffected by $[F^-] = 100$ ppb, there is a clear decrease of impedance at the level of $[F^-] = 1\,000$ ppb. As explained above in case of K^+ and Li^+, a decreasing impedance indicates an increasing oxidation rate.

In order to help to understand the observed features in the results, the oxide film modelling using the Mixed Conduction Model (MCM) [1] was employed. A scheme of the reactions considered in the proposed model for the initial stages of oxidation of a fuel cladding alloy is shown in Figure 5.

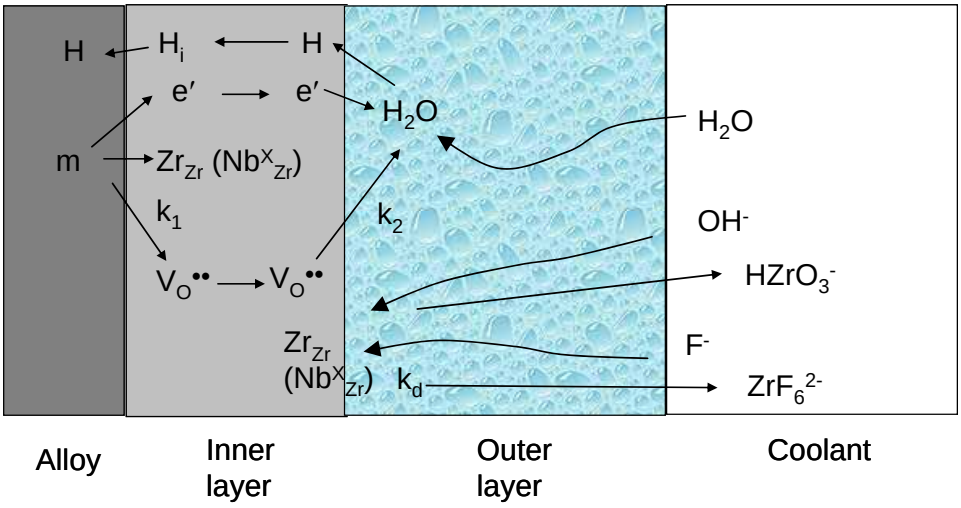

Figure 5. A scheme of the proposed model for the corrosion of a fuel cladding material in a PWR/WWER coolant.

At the alloy/barrier layer interface oxidation of Zr (and also of Nb and other alloying elements in the Zr-matrix) proceeds. The oxidation reaction is considered to be irreversible since the corrosion potential of zirconium alloys in simulated PWR and WWER coolants (determined in this case by the dissolved hydrogen content) is much higher than the equilibrium potential of Zr oxidation.

The barrier layer is considered to be a mixed conductor in which both electrons and oxygen vacancies are transported under the influence of both concentration and potential gradients. Since moving oxygen vacancies can act as effective traps for electrons, it can be assumed that the diffusivities of ionic and electronic defects are comparable.

At the barrier layer/outer layer interface, oxygen vacancies can react with water incorporated in the outer layer via pores and cracks to achieve barrier layer growth. This process is accompanied with atomic hydrogen incorporation in the barrier layer and its further transport within this layer to reach the underlying alloy.

At the barrier layer/water interface, restructuring of that layer occurs resulting in the formation of an outer layer. This restructuring could proceed via dissolution, the rate of which is influenced by the concentration of alkali and fluoride by e.g. the following reactions

$$ZrO_2 + OH^- \xrightarrow{k_d} HZrO_3^-$$

$$ZrO_2 + 2F^- \xrightarrow{k_d} ZrO_2F_2^{2-}$$

The transport of matter and charge through the defective outer layer is assumed to take place via short circuit paths like imperfections and cracks, or interconnected porosity. Thus no concentration gradient of oxygen vacancies is thought to be present in this layer and the transport mode through it is presumed to be pure migration.

Following the line of reasoning above and in [2], the overall impedance of the cladding / oxide / coolant system can be written as being a sum of the resistance of the electrolyte, R_{el}, and the impedances of the barrier layer and the outer deposited layer, Z_b and Z_{out}, respectively,

$$Z = R_{el} + Z_b + Z_{out} \tag{1}$$

For the impedance of the outer layer, trials of different distributed functions demonstrated that the so-called Havriliak-Negami impedance [3] gave the best fit to the experimental data

$$Z_{out} = \frac{R_{out}}{\left[1+\left(j\omega R_{out} C_{out}\right)^{u}\right]^{n}} \tag{2}$$

Here C_{out} and R_{out} are the capacitance of the outer layer and the apparent resistance of defect migration through that layer, whereas *u* and *n* are fractional exponents. The Havriliak-Negami response represents a generalisation of the Constant Phase Element (CPE) to account for asymmetric capacitive loops. The Havriliak-Negami element has been proposed originally for polymer dispersions and can be regarded according to the original authors as the impedance of a two phase mixture, which seems to be a good approximation for the outer layer of oxide.

The impedance of the barrier layer is given by the sum of the impedances characterising its electric properties and ionic transport through it in parallel

$$Z_b = \left(Z_e^{-1} + Z_{ion}^{-1}\right)^{-1} \tag{3}$$

The electronic contribution to the impedance, Z_e, is related to the spatial variation of the steady-state concentration of oxygen vacancies in the oxide, which creates a positive ionic space charge that requires electronic compensation to achieve electroneutrality. The following expression for Z_e has been derived earlier [3]

$$Z_e = \frac{RT}{2j\omega F\vec{E}\varepsilon\varepsilon_0}\ln\left[\frac{1+j\omega\rho_d\varepsilon\varepsilon_0 e^{\frac{RT}{2F\vec{E}L_b}}}{1+j\omega\rho_d\varepsilon\varepsilon_0}\right] \quad (4)$$

Here $\rho_d = \frac{RTk_1}{F^2 D_e k_2}$, ε is the dielectric constant of zirconium oxide, assumed to be equal to 22, ε_0 is the dielectric permittivity of free space, ω is the angular frequency and D_e is the diffusion coefficient of the electronic current carriers.

On the other hand, the impedance due to the motion of oxygen vacancies, Z_{ion}, has been shown [3] to be well approximated by

$$Z_{ion} = R_t + \frac{RT}{4F^2 k_1\left[1+\sqrt{1+\frac{j\omega(RT)^2}{(F\vec{E})^2 D_O}}\right]} \quad (5)$$

The above described model for the transport of electronic and ionic charge carriers through the oxide film is known as the Mixed Conduction Model (MCM). The kinetic and transport parameters, namely, the rate constant of oxidation at the alloy/barrier layer interface, k_1, the diffusion coefficient of oxygen vacancies, D_O, the field strength in the barrier layer, $\vec{E}$, the charge transfer resistance at the alloy/oxide interface, R_t, the $\rho_d\varepsilon$ parameter defined in eqn. (5), as well as the parameters characterizing the outer layer (C_{out} and R_{out}) were estimated using non-linear least square fitting of the experimental spectra to the transfer function derived in the previous paragraph.

An example of the set of parameters extracted from the measured impedance spectra is shown in Figure 6. The thickness of the inner (barrier) layer decreases dramatically when Li^+ concentration increases from 5.4 ppm to 10 ppm. Simultaneously, the diffusion coefficient of oxygen vacancies, D_O, through the barrier layer increases by roughly a decade. More detailed information on the modelling results is given in references [3] and [4].

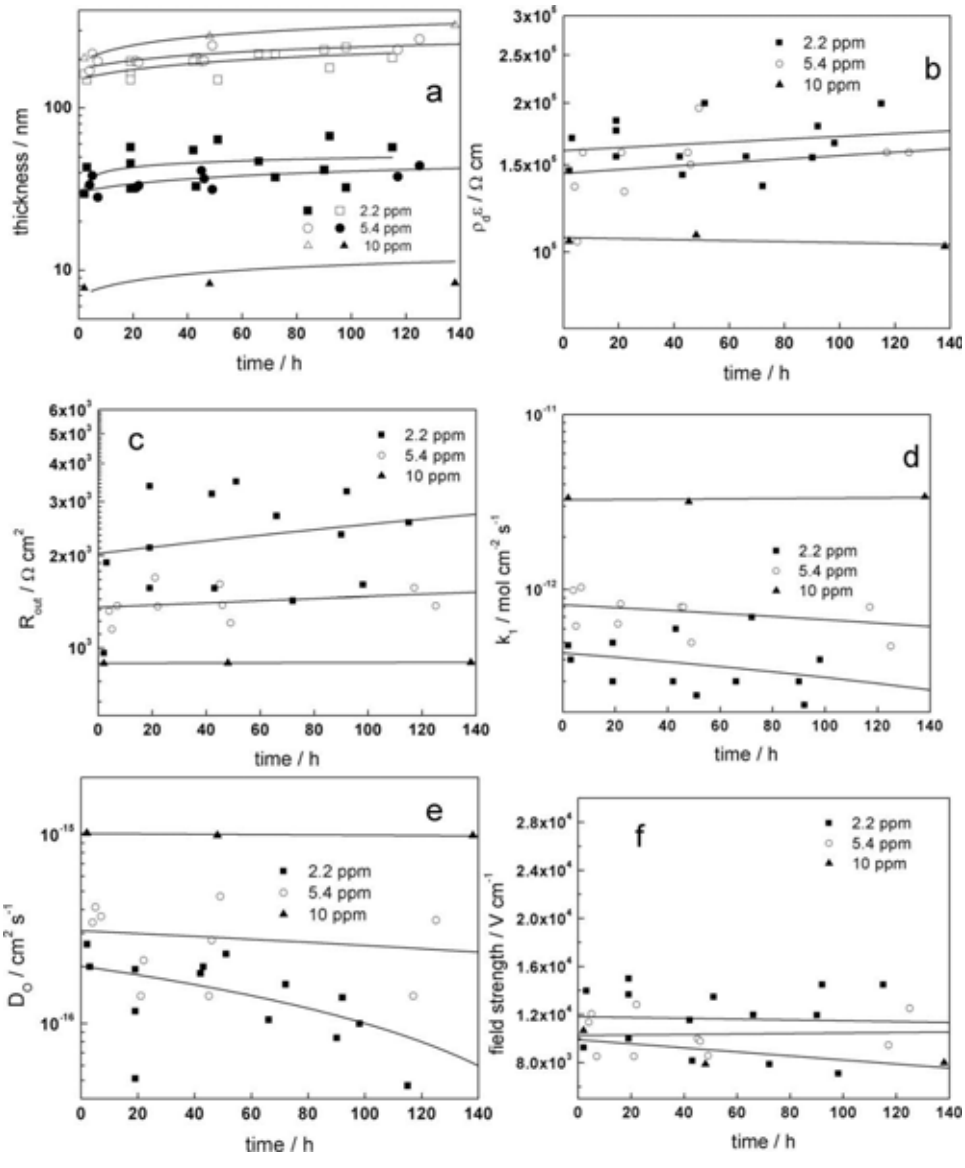

Figure 6. Dependences of the (a) inner (full symbols) and outer (open symbols) layer thickness, (b) the parameter ρdε, (c) the resistance of the outer layer Rout, (d) the rate constant of zirconium oxidation at the alloy/oxide interface k1, (e) the diffusion coefficient of oxygen vacancies DO and (f) the field strength in the inner layer on the time of exposure of alloy E110 to the simulated PWR coolants with different Li+ content.

Applications

The in situ measurement technique and model developed for the oxidation of zirconium-based fuel cladding alloys has been verified. The technique is sensitive for changes in the alkali concentration and impurities in the PWR/WWER primary water. Ranking of PWR/WWER fuel cladding alloys can be performed in a fraction of the time needed when using conventional methods. Similar conclusions have earlier been made regarding BWR fuel cladding alloys [2]. The effect of transient chemistry, like that during beginning of cycle, can also be verified using the tools developed within this work. The modelling tools enable arriving at a more detailed understanding of the rate limiting steps in the fuel cladding oxidation process, which again is useful in development of new alloys and in better understanding of the risks involved in water chemistry changes.

Conclusions

The following main conclusions can be drawn from the work performed:

- The in situ technique developed is sensitive for changes in PWR/WWER primary chemistry and can be used to generate a ranking order for potential fuel cladding alloys.
- The model developed has been shown to result in a very detailed understanding of the fuel cladding oxidation process. The calculated estimates of the thickness of the whole oxide film after 120 h of exposure agree very well with the microscopic estimates of the total oxide thickness, indicating the validity of the proposed model for the zirconium oxide film. The thickness of the inner layer is several times smaller than that of the outer layer, which indicates that the corrosion properties of the zirconium alloys in the initial stage of oxidation are controlled by a thin (barrier) layer close to the alloy/oxide interface. The thickness of the outer layer increases with the concentration of $Li^+/K^+/F^-$ in the electrolyte.
- The rate constant of zirconium oxidation at the inner interface increases with the concentration of $Li^+/K^+/F^-$. The order of this reaction vs. Li^+ is close to 2, whereas the estimated order vs. K^+ was of the order of 1. This difference indicates that the effect of increased Li^+ content is due not only to the increase in alkali concentration, but there is an additional effect of Li^+ itself. This could be in principle related to the incorporation of Li^+ in the oxide film on zirconium alloys.

- The resistivity of the outer layer, which can be regarded as an inverse of the transport rate in this layer by easy path migration, decreases with increasing alkali and fluoride content, indicating that this layer becomes more defective and thus indirectly supporting the hypothesis that the restructuring process that leads to the formation of that layer is dependent on the solution composition, i.e. water chemistry. The resistance of the outer layer Rout does not depend on the type of alloy.

References

1. Bojinov, M., Fabricius, G., Kinnunen, P., Laitinen, T., Mäkelä, K., Saario, T. & Sundholm, G. Electrochemical study of the passive behaviour of Ni-Cr alloys in a borate solution – a mixed-conduction model approach. J. Electroanal. Chem. 2001, 504, pp. 29–44.

2. Bojinov, M., Hansson-Lyyra, L., Kinnunen, P., Saario, T. & Sirkiä, P. In-situ studies of the oxide film properties on BWR fuel cladding materials. Journal of ASTM International 2005, Vol. 2, No. 4, 183–198.

3. Bojinov, M., Cai, W., Kinnunen, P. & Saario, T. Kinetic parameters of the oxidation of zirconium alloys in simulated WWER water – effect of KOH content. Journal of Nuclear Materials 2008, Vol. 378, No. 1, pp. 45–54.

4. Bojinov, M., Karastoyanov, V., Kinnunen, P. & Saario, T. Influence of water chemistry on the corrosion mechanism of a zirconium–niobium alloy in simulated light water reactor coolant conditions. Corrosion Science 2010, Vol. 52, No. 1, pp. 54–67.

25. Monitoring of the Structural Integrity of Reactor Circuit (RAKEMON)

25.1 RAKEMON summary report

Ari Koskinen, Stefan Sandlin, Tarja Jäppinen, Matti Sarkimo,
Mikko Vepsäläinen and Esa Leskelä
VTT

Abstract

Developing techniques and monitoring systems that can be used to monitor the structural integrity of the primary circuit components is quite essential. Basic pilot monitoring system was developed and constructed during 2007 and 2008. In 2009 and 2010 pilot monitoring system was further developed and monitoring tests were performed with austenitic stainless steel (316LN) pipe. The final aim was to develop measurement systems both for detection and analysis of macroscopic flaws and microscopic changes in the material that are often preceding the macroscopic failure.

It is also necessary to develop inspection techniques that can be applied to reactor circuit components where the access is restricted and decreasing the reliability of inspection. The geometry and the material properties of the component to be inspected must always be considered when an ultrasonic test is planned. Ultrasonic inspection simulations for difficult geometries (nozzles) and anisotropic weld metals were done with simulation program CIVA (versions 8, 9 and 10).

Fibre optical monitoring methods have been developing rapidly in recent years and nowadays there are already fibres that can resist radiation. Also methods for

correcting measurement errors arising from radiation induced attenuation have been developed. The potential of using fibre optical monitoring technology in nuclear environments was evaluated in 2008. It was noticed that metal embedded fibres are in strong compression and polymer coating is eliminated. Therefore it could be possible that drift in Bragg wavelength due to volumetric changes and radiation induced hydrogen evolution from the polymer coating on the fibre could be eliminated with metal embedded fibres.

Closed cracks are very dangerous because they can stay undetected for many inspection cycles due to inspection restrictions related to closed cracks. A new ultrasonic method has been developed for these closed cracks. The subharmonic ultrasonic inspection is developed at Tohoku University Japan and it seems to be very promising for these dangerous closed cracks.

Steam generators are one part in the PWR type nuclear power plant that can be restricting the lifetime of the plant. Inside the steam generators there is known to be magnetite deposition on tubing and between tubes. The inspection data of steam generators contain also additional information than flaw indications. Recently eddy current data has been applied to show locations of magnetite deposition on tubing. Improvement of eddy current analysis, e.g., concerning magnetite deposition on tubing and between tubes, and flaw sizing was started in 2009 by performing literature review. Also an experimental study on detecting magnetite deposition between tubes was made in 2010.

Understanding the variations in the local environmental condition facilitating iron deposition in steam generators should be improved. Pertinence of water chemistry based predictions, NDE monitoring results concerning iron deposition and plant observations and experience were studied and documented as literature reviews during 2009 and 2010.

Introduction

Non-destructive testing techniques are used to monitor the condition of the structures of reactor circuit during the operation of nuclear power plants. The in-service inspections (ISI) are normally performed during the shutdown period but there is also increasing need to monitor the condition of components during service by on-line methods. The tendency worldwide and also in Finnish nuclear power plants is to improve the efficiency of in-service inspections by applying risk-informed methods to the selection of inspection items, methods and timing of in-service inspections. This kind of ISI-programme is supported by on-line

monitoring techniques that are used to focus the inspections to areas where failures are most probable and/or consequences are most severe.

There is a specific need to improve the reliability of NDE-techniques used for the ISI of bimetallic welds and inspection items where access is limited. Ultrasonic simulation can be used to optimize the inspection techniques for these problematic inspection areas.

The aim of RAKEMON project was to develop techniques and monitoring systems that can be used to monitor the structural integrity of the primary circuit components. The aim was to develop measurement systems both for detection and analysis of macroscopic flaws and microscopic changes in the material that are often preceding the macroscopic failure.

It is also necessary to develop inspection techniques that can be applied to reactor circuit components where the access is restricted and decreasing the reliability of inspection. This kind of inspection items are e.g. welds with coarse grain size and nozzle welds where the difficult geometry is restricting the performance of inspection.

International atomic energy agency (IAEA) launched a coordinated research programme (CRP) on advanced, surveillance, diagnostics and prognostics techniques used for health monitoring of systems, structures and components in nuclear power plants. RAKEMON project took part of this international project which started in 2008 and will be finalized in early 2011. Two-piece IAEA publication will be published during 2011.

Monitoring of the structural integrity of reactor circuit

On-line monitoring is defined as an automated method of monitoring instrument output signals and assessing instrument calibration while the plant is operating, without disturbing the monitored channels. In the simplest implementation, redundant channels are monitored by comparing each individual channel's indicated measurement to a calculated best estimate of the actual process value. This best estimate of the actual process value is referred to as the process variable estimate or estimate. By monitoring each channel's deviation from the process variable estimate, an assessment of each channel's calibration status can be made. An on-line monitoring system can also be referred to as a signal validation system or data validation system [1].

Pilot monitoring system and monitoring tests

Pilot monitoring system was designed for monitoring the structural integrity of a component in nuclear power plant's primary circuit. In 2007 the basics for the design of monitoring system was studied and the components were outlined. In 2008 construction of pilot monitoring system for ultrasonic online monitoring was done and preliminary tests made. With conventional methods coupling between transducer and inspection item was found out to be extremely difficult. Nevertheless advanced versions of the monitoring system were constructed during 2009 and 2010.

The system itself included the inspection item, ultrasonic and heating equipment and adjustable frame. The inspection item was austenitic stainless steel pipe (316LN). Dimensions of the pipe were:

- Length is 300 mm
- Outer diameter is 168.7 mm
- Wall thickness is 14.1 mm.

The basic idea of this system was to monitor flaws in this pipe for longer periods. Typically flaws appear in the welding zone but in this case they were produced in the base material. The actual cracks were produced by thermal fatigue and their dimensions and locations were precisely documented. There were also Electrical Discharge Machining (EDM) notches for comparing the indications from cracks and notches.

The cracks were produced in-situ to the inspection item with controlled thermal fatigue loading. With this method the cracks grow with natural thermal fatigue damage mechanism. The crack location in the inspection item is affected by the local material properties. Especially if the sample contains stress risers or marked homogeneities the cracks grow in to the natural weakest location. There are no artificial initiators used in the process and the microstructure of the inspection item has not been changed. The true crack depth is known through Trueflaw destructive validation [2].

Many different types of transducers with angles varying between 30°–70° were used in inspections. The inspection item was heated up to 300°C (Figure 1) and insulation was removed from the area of inspection. Because of the high temperature, water was not applicable for coupling. Therefore high temperature paste was used as couplant. The flash point, which is the lowest temperature at which it can vaporize to form an ignitable mixture in air, with this paste was only 300°C. The

paste also dried up on the inspection surface and made the next inspection interval even more difficult. Therefore paste removal process after each inspection should be developed before the system can be used in industrial applications.

Figure 1. Inspection item and heating element inside insulation.

The differences in indications between thermal fatigue cracks and similar size EDM notches were also studied and one example can be seen in Figure 2. This phenomenon will be studied in MAKOMON project during SAFIR 2014 program. CIVA is an ultrasonic simulation program and in this task it was used for simulation of different types of indications. Those simulations showed clearly the difference in indications between EDM notch and crack like indication. CIVA is not particularly designed for this kind of indication simulation but was still very useful and promising in the simulations made.

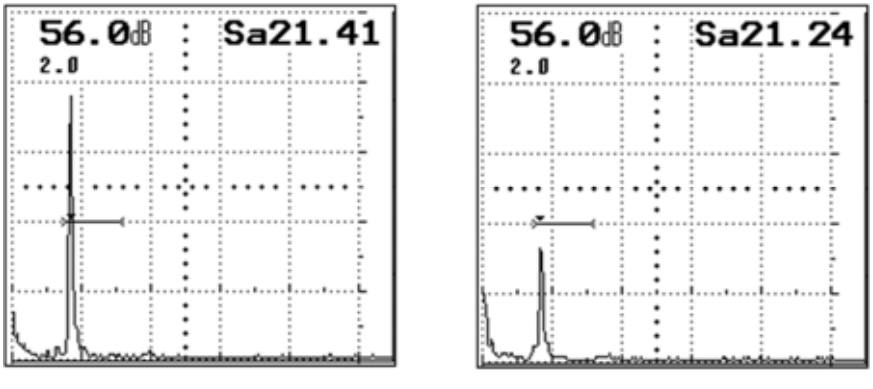

Figure 2. Indication from EDM notch on the left hand side and from similar size thermal fatigue crack on the right hand side.

Inspection of items with limited access, difficult geometry or unfavourable grain structure

The geometry and the material properties of the component to be inspected must always be considered when an ultrasonic test is planned. In many cases these factors can be challenging and careful examination of the case is needed to ensure reliability of the inspection. Simulation of the ultrasonic inspection using computer program (CIVA) can be one part of necessary work providing tools to study how the ultrasonic beam is propagating in structure and what kind of signals can be expected to be received from the reflectors in the inspection area. The difficult inspection geometries (nozzles) and anisotropic weld metals were modelled in 2007 and 2008 with simulation program CIVA version 8.

Recently promising results have been achieved by applying Phased Array-technique to in-service inspection of piping and components of nuclear power plant. One challenging task is to detect and determine defects locating below or inside the austenitic cladding of reactor pressure vessel. By applying phased array technique in data acquisition and SAFT-algorithm for data analysis the reliability of the inspection can most probably be remarkably improved. In 2008 the application of phased array technique to anisotropic weld metal was experimentally tested by using test blocks containing defects. Inspections were done with Omniscan phased array system and with two 32 channel probes (transmitter-receiver). The data collected with Omniscan phased array system was transferred to Ultravision for data analyse. The same test block was also simulated with CIVA program and the results were compared to original measured results (Figure 3). Simulations were run using different inspection techniques including conventional probe construction as well as phased array probe applying different focal laws. Some studies of the beam shape in the inspection area were presented. The defect responses of the reflectors inserted in the real test block were computed and analysed. The results of the simulation using different techniques were then compared with each other and also with available experimental measurement results.

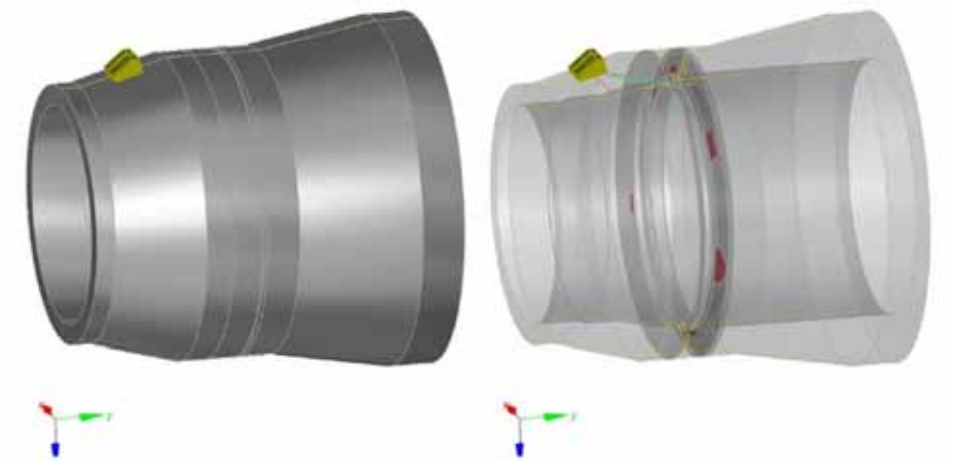

Figure 3. Simulation of real test block with CIVA [3].

In 2009 and 2010 simulation were focused on comparing real measurements and simulations. Sampling Phased Array (SPA) also known as Full Matrix Capture method is very promising and relatively new ultrasonic inspection method. Two different types of test pieces were inspected using SPA method and then simulated with the latest version of CIVA program. Afterwards these results and simulations were compared with each other.

Choice of fibre optical monitoring methods

It has generally been assumed that fibre optical sensors cannot be used in high radiation environment due to radiation induced light attenuation in the fibre. This is not completely true anymore because radiation resistant fibres have been developed as well as methods for correcting measurement errors arising from radiation induced attenuation. Raman distributed temperature sensing has been demonstrated for example with fibres wound along the primary loop of the experimental fast reactor JOYO in Japan. In this experiment the fibre got a total gamma dose of more than 7.7 × 103 C/kg (0.26 MGy in air). For a fibre placed on the primary loop of a commercial light water reactor this dose would correspond to more than 35 years of use [4].

Fibre Bragg gratings (FBGs) can be used to measure for example temperature and/or strain. For FBGs the strain and/or temperature information in wavelength coded, so a variation in intensity is not critical as long as the Bragg peaks can be detected well above the noise level. SCK-CEN has tested a special type of Bragg

gratings (so called Chemical Composition Gratings, CCGs) in the core of their BR2 reactor to a total gamma dose in excess of 1.5 GGy and to a neutron fluence of 7.5 × 1 019 n cm-2 [4]. The CCGs remained fully functional but a drift in Bragg wavelength was observed. This shows that all problems are not solved, but that the FBGs have potential even for incore monitoring.

It has been assumed that radiation induced hydrogen evolution from the polymer coating on the fibre degrade the FBGs. Further, radiation induced volumetric changes of the fibre may be responsible for the drift in Bragg wavelength. Metal embedded fibres are in strong compression and the volumetric changes may therefore be minimal; the polymer coating is also eliminated. It would be essential to repeat the irradiation tests with metal embedded high temperature stable FBGs.

The potential of using fibre optical monitoring technology in nuclear environments was evaluated in 2008. Also international research networks have been utilized in the evaluation process. The focus has been on monitoring needs where traditional electrical sensors do not work well and on monitoring issues where an electrical sensing solution does not exist.

Subharmonic ultrasonic inspection

Traditional ultrasonic systems operate in linear mode; i.e. the received scattered ultrasound from defects lies in the same frequency range as the insonifying ultrasound. The amplitudes of waves diffracted or reflected at a crack tip or a crack surface are determined by the acoustic impedance mismatch between the material and the air gap. For tight cracks the acoustic impedance mismatch may be negligible. In nonlinear testing, defects behave as active radiation sources of new frequency components rather than as passive scatterers as in conventional ultrasonic inspection [5].

The new ultrasonic method for imaging closed cracks based on subharmonic ultrasound has been developed at Tohoku University in Japan (SPACE). Performance, reliability and applicability to inspection of real NPP components with this method were studied in 2009 by means of literature review and by being in close contact with international colleagues. Reliable inspection would be an important progress in the detection of dangerous closed cracks.

The latest studies show that there are some resent improvements done by the Japanese. The single crystal lithium niobate transmitter has been replaced by an 8-channel lithium niobate array transmitter to facilitate steering of the insonifying ultrasound. Further, both the transmitter array and the receiver array have been

integrated into a shoe to facilitate scanning. It seems that closed parts of the crack, which are not observed at fundamental frequency, can be observed at subharmonic frequency. Also recent results obtained in Sweden (Royal Institute of Technology) on the linear and nonlinear ultrasonic response of dry and water confining rough interfaces in partial contact are reported. An important result of the work in Sweden is that a thin layer of water in the crack has a much more pronounced influence on the linear and nonlinear ultrasonic response than previously assumed. This fact may also have consequences for the performance of the SPACE method. More research is needed on these issues and work will be continued in MAKOMON project in SAFIR 2014 program.

Steam Generator lifetime monitoring

In 2009 there was a new area of research concerning steam generator lifetime monitoring attached to RAKEMON project. Steam generators are one part in the PWR type nuclear power plant that can be restricting the lifetime of the plant. In those steam generators there is known to be magnetite deposition on tubing and between tubes. The inspection data of steam generators contain also additional information than flaw indications. Recently eddy current data has been applied to show locations of magnetite deposition on tubing. Improvement of eddy current analysis, e.g., concerning magnetite deposition on tubing or between tubes and flaw sizing was started in 2009 by performing literature review. Also an experimental study on detecting magnetite deposition between tubes was made in 2010.

Understanding the variations in the local environmental condition facilitating magnetite deposition in steam generators should be improved. A literature review on secondary water chemistry was made in 2009 and another literature review on deposit formation in PWR steam generators was made during 2010. In these reviews the deposit formation in secondary water chemistry is thoroughly studied.

Conclusions

Developing techniques and monitoring systems that can be used to monitor the structural integrity of the primary circuit components is quite essential. The aim is to develop measurement systems both for detection and analysis of macroscopic flaws and microscopic changes in the material that are often preceding the macroscopic failure.

It is also necessary to develop inspection techniques that can be applied to reactor circuit components where the access is restricted and decreasing the

reliability of inspection. This kind of inspection items are e.g. welds with coarse grain size and nozzle welds where the difficult geometry is restricting the performance of inspection.

Fibre optical monitoring methods have been developing rapidly in recent years and nowadays there are already fibres that can resist radiation. Also methods for correcting measurement errors arising from radiation induced attenuation have been developed.

Closed cracks are very dangerous because they can stay undetected for many inspection cycles due to inspection restrictions. There has been new ultrasonic method developed for these closed cracks. The subharmonic ultrasonic inspection is developed at Tohoku University, Japan and it seems to be very promising for these dangerous closed cracks.

References

1. On-line Monitoring for Improving Performance of Nuclear Power Plants. Part 1: Instrument Channel Monitoring, IAEA-NE-D-NP-T-1, IAEA, Vienna, 2007. 137 p.

2. Kemppainen, M. Realistic Artificial Flaws for NDE Qualification – A Novel Manufacturing Method Based on Thermal Fatigue. Doctoral dissertation, TKK Dissertations 35, Espoo, 2006. 93 p.

3. Sarkimo, M. Simulation of ultrasonic inspections on the test block YP 001. VTT, Espoo, 2009. VTT Research Report VTT-R-00634-09. 19 p.

4. Sandlin, S. Applicability of Distributed Fibre Optical Temperature Sensing and Fibre Bragg Gratings in Nuclear Radiation Environments. VTT, Espoo, 2007. VTT Research Report VTT-R-13509-07. 16 p.

5. Solodov, I. & Busse, G. Elastic wave nonlinearity for monitoring of localized damage in engineering materials. 19th International Congress on Acoustics, Madrid, 2–7 September 2007. 6 p.

25.2 Linear and nonlinear ultrasonic techniques for evaluation of partially closed cracks

Stefan Sandlin and Ari Koskinen
VTT

Abstract

Cracks are usually initiated by fatigue, but when water enters the cracks, growth will mainly be controlled by corrosion and such cracks are called stress corrosion cracks (SCC). SCCs constitute a major threat to the structural integrity of nuclear power plant components. Unfortunately closure stresses and/or water containment may render the cracks more or less transparent to ultrasound used in traditional testing. Due to the transparency the crack size may be underestimated in an ultrasonic examination, or the crack may even not be observed at all. Different nonlinear ultrasonic techniques have recently been studied in order to enhance sizing and detectability of partially closed and possibly water confining cracks. Nonlinear NDE utilizes new frequency components that are generated at the crack. These new frequency components may be higher harmonics or subharmonics. In this article we concentrate on work done at Tohoku University in Japan and at Royal Institute of Technology in Sweden. Tohoku University has developed a technique called “Subharmonic Phased Array for Crack Evaluation” (SPACE) and some recent progresses in this field will be reviewed. The Royal Institute of Technology has done both experimental and theoretical work on the linear and nonlinear ultrasonic response of dry and water confining rough surfaces in partial contact. Selected experimental results will be presented. The Swedish work has the nature of fundamental research while the Japanese work is more practically oriented.

Introduction

Traditional ultrasonic systems operate in linear mode; i.e. the received scattered ultrasound from defects lies in the same frequency range as the insonifying ultrasound. The amplitudes of waves diffracted or reflected at a crack tip or a crack surface are determined by the acoustic impedance mismatch between the material and the air gap. For tight cracks the acoustic impedance mismatch may be negligible. In nonlinear testing, defects behave as active radiation sources of

new frequency components rather than as passive scatterers as in conventional ultrasonic inspection [1]. The nonlinear techniques are therefore sensitive to closed fatigue or stress corrosion cracks. In non nonlinear ultrasonics cracks may be observed by acoustically activated contact clapping in cracks. The nonlinear modulation frequencies caused by clapping of the crack interfaces often unveil flaws with higher contrast and more reliably than higher harmonics [2]. A minimum amplitude of the insonifying ultrasound is needed for generation of subharmonics; this is illustrated by Yamanaka et al. [3] by saying “if we find subharmonic waves when increasing the input wave amplitude, there is a partly closed crack, hidden in the object”.

Tohoku University in Japan has developed a method in which cracks are monitored both at the insonifying (or fundamental) frequency f and at the subharmonic frequency f/2 using a phased array for focused reception of ultrasound and a $LiNbO_3$ single-crystal transmitter for generation of intense ultrasound. The method therefore combines normal phased array testing with phased array testing at subharmonic frequency [4]. This imaging method is called subharmonic phased array for crack evaluation (SPACE). Different nonlinear ultrasonic methods for evaluation of closed cracks have been proposed for decades (based on superharmonics), but SPACE seems to include several new innovative ideas. Subharmonics have a better signal-to-noise ratio than superharmonics because subharmonics are generated only at closed cracks while superharmonics are generated also in transducers, liquid couplers and electronics. Further, the attenuation of the subharmonic waves is lower than that of the fundamental wave and the superharmonic waves. As will be seen, the combination of subharmonic wave detection and phased array technique seems to lead to substantial improvement beyond the present state-of-the-art in sizing and detection of closed cracks. On the application side, localization and sizing of closed or partially closed fatigue and stress corrosion cracks in nuclear power plant components was already mentioned. Another important application could be detection of flaws in dissimilar metal joints. These joints can be made by for example diffusion bonding, explosion welding, clad welding, brazing etc. A flaw at the interface between two different metals may be difficult to observe using ultrasonic techniques as there is a strong reflection also from a perfect interface. In nonlinear ultrasonic technique this kind of flaws become active radiation sources of subharmonic ultrasound and the SPACE method is therefore expected to be effective in quality evaluation of these kinds of joints. The SPACE method has

already been described in an earlier report [5], so we will now restrict ourselves to the latest developments.

The work done at the Royal Institute of Technology in Sweden presents an ultrasonic technique designed to discern partially closed cracks that are subsurface (dry) from those that are surface-breaking and water confining. The technique exploits the effect of water confinement within a partially closed, surface-breaking crack on the acoustic response of the defect. Experimental results illustrate the characteristic dependence of the stiffness on the load applied to dry and water filled interfaces and it is shown that current models cannot account for the liquid mediated forces between tight solid surfaces [6]. It is nearly certain that all cracks which open to the internal surface of a component will be water filled (even during shut down) and therefore these new findings may have important consequences for practical inspections. This is because the thin water layer in a tight crack seems to behave different than for example the relative thick layer of water used as coupling medium between an ultrasonic transducer and the component.

Subharmonic phased array

A schematic view of the SPACE equipment developed at Tohoku University can be seen in Figure 1. Intense ultrasound is transmitted to the crack using a lithium niobate crystal. The scattered signals from the crack at fundamental (f) and subharmonic frequencies (f/2) are received by a phased array. The results are presented as a sectorial scan.

In a later development the transmitter was replaced by an 8-channel lithium niobate array for steering of the incident ultrasound. Further, both the transmitting and receiving arrays were integrated in a shoe as shown in Figure 2 to facilitate scanning. The right part of Figure 2 shows an arrangement used to test the steering of the transmitted ultrasound. The ultrasonic displacement amplitude was measured by a laser interferometer. The displacement amplitudes varied from a few nm up to about 30 nm.

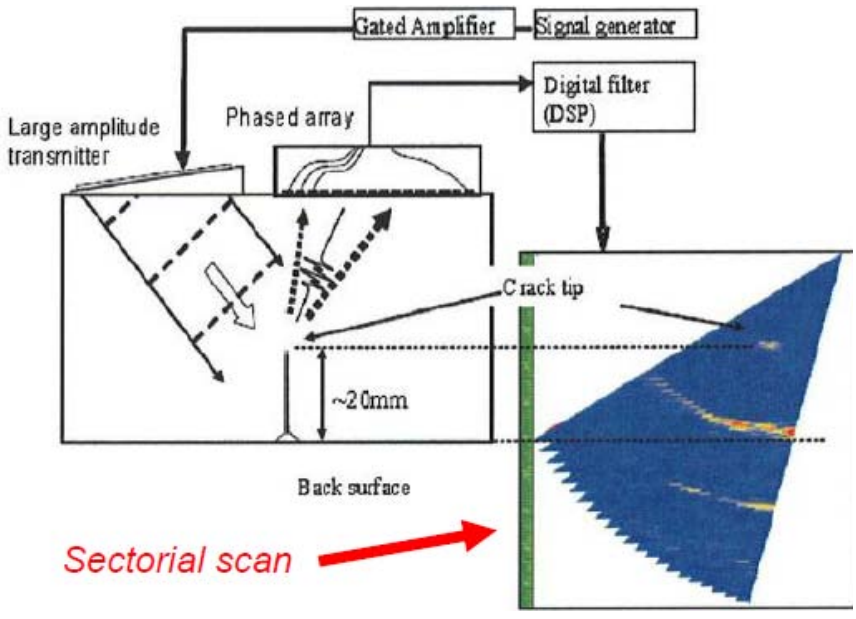

Figure 1. The principle of SPACE. A lithium niobate crystal transmits intense ultrasound onto the crack and scattered signals of fundamental (f) and subharmonic frequencies (f/2) are received by the phased array to the right [7].

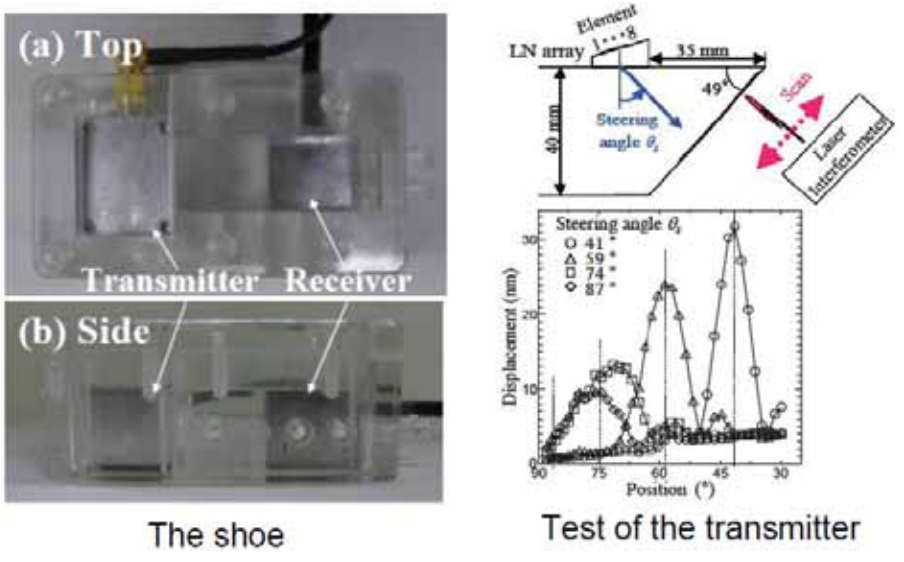

Figure 2. Both the transmitting and receiving arrays are integrated in a shoe to facilitate scanning [8]. A laser interferometric test of the transmitting array is shown to the right [9].

Crack detection and sizing results

The aluminium (A7075) compact tension (CT) specimen shown in Figure 3 was used to demonstrate the performance of the SPACE method [8]. The crack length was measured at positions a, b, c, d, and e after 48 000 and 87 000 fatigue cycles and the imaging results are shown in Figure 4. The distribution of crack depths is shown in Figure 5. Subharmonic frequency always gives a larger crack depth indicating that the closed crack can be observed at subharmonic frequency but not at fundamental frequency. As seen from Figure 5 the difference in crack depth measured at fundamental and subharmonic frequency is larger near the sides of the specimen. This indicates that the crack tip was closed with a higher closure stress near the sides. The Japanese researchers have also demonstrated the use of the SPACE method to size and detect fatigue and stress corrosion cracks in stainless steel [5].

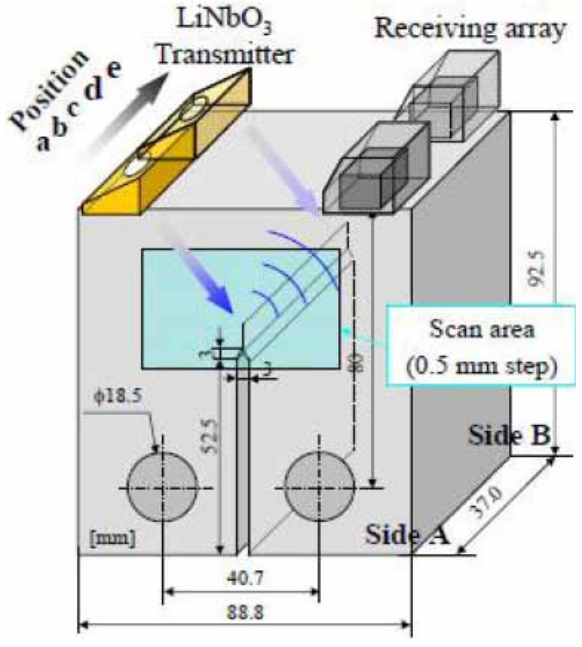

Figure 3. A CT specimen used to test the SPACE method. Ultrasonic phased array images were taken at positions a, b, c, d and e [8].

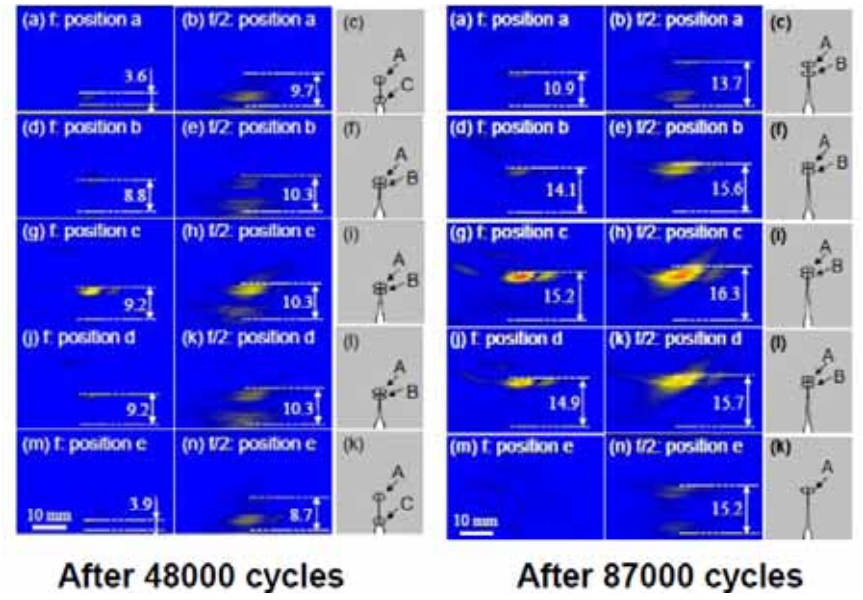

Figure 4. The imaging results at fundamental and subharmonic frequency after 48 000 and 87 000 fatigue cycles. The different imaging positions are shown in Figure 3 [8].

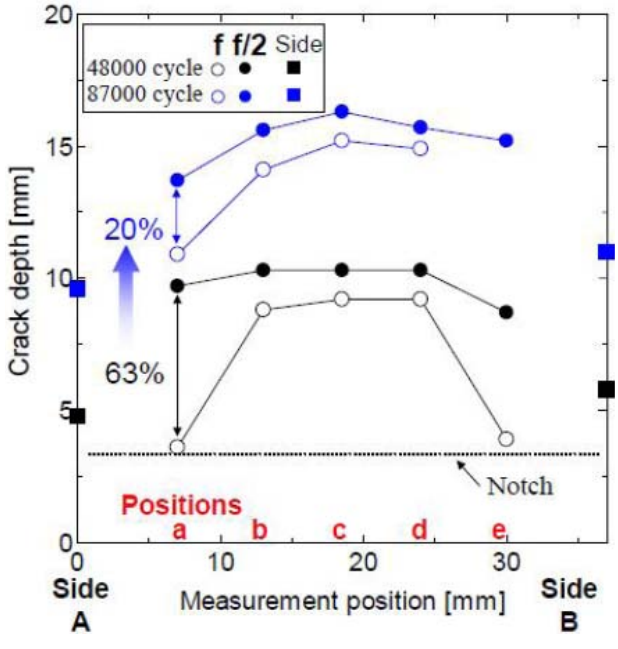

Figure 5. The distribution of crack depths at different position after 48 000 and 87 000 fatigue cycles. The crack is more closed near the sides of the specimen [8].

Linear and nonlinear ultrasonics at the Royal Institute of Technology

At the Royal Institute of Technology in Sweden the ultrasonic response of dry and water confining rough surfaces were investigated as function of the load pressing the surfaces against each other. The linear and nonlinear behaviour of the interfaces were compared. All measurements were carried out in reflection mode, i.e. the same transducer acted both as transmitter and receiver. The frequency of the transducer was 5 MHz and the wave train consisted of 24 sinusoidal cycles. Four different steel samples were used (S1, S2, S3 and S4) to build three different interfaces, S1-S2, S1-S3 and S1-S4 with different roughness. S1 was used in all measurements as a medium for propagating the incident and returning waves. A block diagram of the experimental setup is shown in Figure 6.

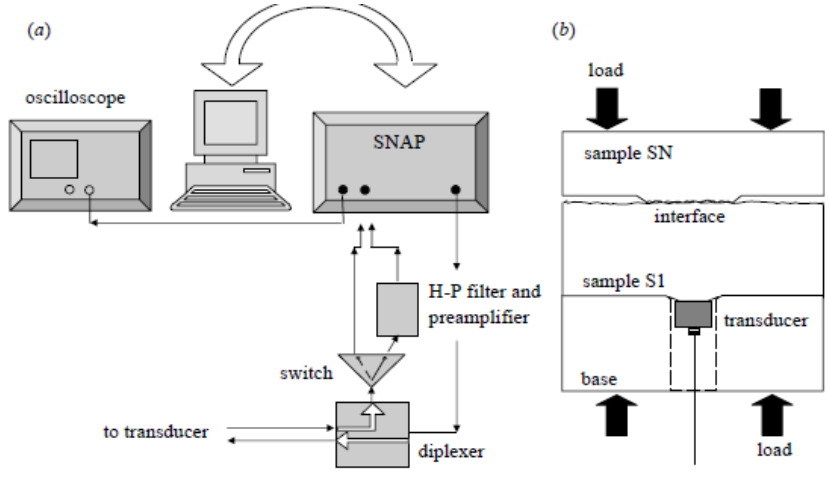

Figure 6. The experimental setup for comparing the ultrasonic linear and nonlinear response of dry and water confining interfaces at different loads. The instrumentation is shown to the left and the transducer and the interface-forming specimens to the right. SN stands for S2, S3 and S4 [6].

Linear and nonlinear ultrasonic response of dry interfaces

Figure 7 illustrates the behaviour of the reflected fundamental frequency signal during a complete loading cycle. The reflection decreases for increasing loads (closure). The effect is largest for the smoothest interface S1-S2 as expected. Figure 8 illustrates the behaviour of the amplitude of the nonlinear signal (second harmonic) during a complete loading cycle for the same three interfaces.

The behaviour of the nonlinear signal is quite different compared to the linear signal; it grows steeply when the loading starts, reaches a maximum and, in some cases, starts to decrease slightly. The growth rate is largest for the smoothest interface S1-S2. This illustrates the fact that nonlinear ultrasonic signals are not generated at completely open dry interfaces (cracks). The threshold of noise was approximatively at -80 dB, so the dynamic range of the nonlinear signals was a bit over 20 dB and it increases with decreasing roughness. Further, Figure 8 illustrates that nonlinear signals are generated more effectively during the unloading part of the cycle. Pecorari & Poznic [10] also give the following estimate of the relative strength on the linear and nonlinear signals: "Considering that the time-domain signal, which is examined for its content at twice the frequency of the incident wave, undergoes a pre-amplification of 40 dB with respect to the linear signal, the results […] illustrate that the nonlinear response is 70–80 dB below the fundamental component". Pecorari & Poznic, however, state that the transducer sensitivity is about 25 dB lower at second harmonic frequency (2f) compared to the sensitivity at fundamental frequency (f).

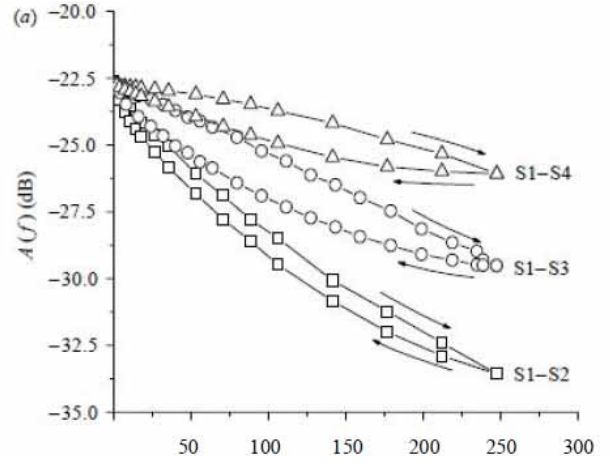

Figure 7. Amplitude of the linearly reflected ultrasound as function of interfacial load (MPa) for three dry interfaces: S1-S2, S1-S3 and S1-S4. The amplitude decreases with increasing closure load [10].

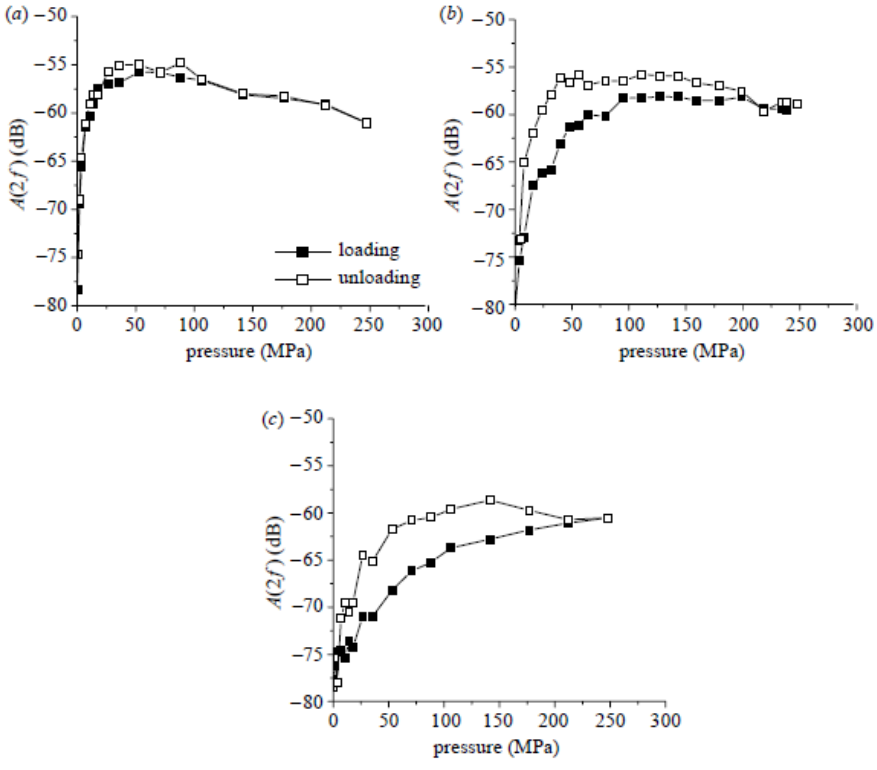

Figure 8. Amplitude of the nonlinear (second harmonic) response as function of interfacial load for three dry interfaces, (a) S1-S2, (b) S1-S3 and (c) S1-S4. Note the initial increase in amplitude [10].

Linear and nonlinear ultrasonic response of water confining interfaces

Linear and nonlinear ultrasonic response of water confining rough interfaces subjected to a varying load was measured with de-ionized water between the two interfaces. Figure 9 shows the linear response of the two interfaces S1-S3 and S1-S4 when the load is increased from 0 to about 25 MPa. There is an initial dramatic reduction in response of the smoother interface S1-S3. The behaviour of the rougher interface S1-S4 is similar, but the initial reduction in amplitude is less pronounced. A comparison of Figure 7 (dry) and Figure 9 (water confining) indicates that some dramatic qualitative change occurs to the interface mechanics when the interface is filled with water. A similar conclusion can be drawn from the nonlinear signals by comparing Figure 8 (dry) and Figure 10 (water confining). Note the smaller scale on the pressure axis in Figure 9 and Figure 10 i.e. the initial effect starts at much smaller loads.

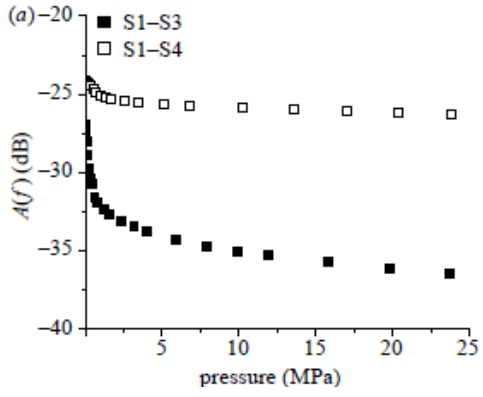

Figure 9. Amplitude of the linear response as function of interfacial load for two water confining interfaces S1-S3 and S1-S4 [10].

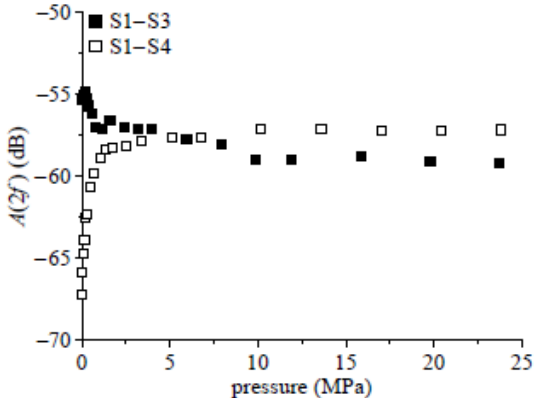

Figure 10. Amplitude of the nonlinear (second harmonic) response as function of interfacial load for two water confining interfaces S1-S3 and S1-S4 [10].

Comparison of response from dry and water confining interfaces

From the measurements of linear and nonlinear ultrasonic signals from dry and water confining interfaces subjected to varying closure loads Pecorari & Poznic [10] make the following summarizing conclusions:

1. The dependence of the amplitude of the wave reflected by a water confining interface on the applied closure load is qualitatively rather different from that of a dry interface between the same surfaces.
2. The dependence of the nonlinear response on applied closure load varies dramatically with the surface topology.

3. The maximum nonlinear response seems to be weakly dependent on the roughness of the interface.
4. The bulk nonlinearity of water is not entirely responsible for that of the water confining interfaces. The dynamic range of the nonlinear signals was more than 20 dB over the noise level (≈ -80 dB) and the nonlinear signal from bulk water was estimated to -73 dB.

Conclusions

The SPACE technique was originally developed by Japanese researchers (Tohoku University) to detect and size partially closed fatigue and stress corrosion cracks. The performance was examined in an earlier review article [5]. In the present article we presented some resent improvements done by the Japanese. The single crystal lithium niobate transmitter has been replaced by an 8-channel lithium niobate array transmitter to facilitate steering of the insonifying ultrasound. Further, both the transmitter array and the receiver array have been integrated into a shoe to facilitate scanning. This is a first step to make field tests possible. From the presented results it seems that closed parts of the crack, which are not observed at fundamental frequency, can be observed at subharmonic frequency.

In the second part of this article we present some recent results obtained in Sweden (Royal Institute of Technology) on the linear and nonlinear ultrasonic response of dry and water confining rough interfaces in partial contact. An important result of the work in Sweden is that a thin layer of water in the crack has a much more pronounced influence on the linear and nonlinear ultrasonic response than previously assumed. This fact may also have consequences for the performance of the SPACE method when applied to water confining cracks. More research is needed on these issues.

References

1. Solodov, I. & Busse, G. Elastic wave nonlinearity for monitoring of localized damage in engineering materials. 19th International Congress on Acoustics, Madrid, 2–7 September 2007. 6 p.

2. Pfleiderer, K. Frequenzkonversion aufgrund nichtlinearer akustischer Phänomene: Grundlagen und Anwendung zur defektselektiven zerstörungsfreien Prüfung. Institut für Kunststoffprüfung und Kunststoffkunde der Universität Stuttgart, 2006. 120 p.

3. Yamanaka, K., Mihara, T. & Tsuij, T. Evaluation of closed cracks by analysis of subharmonic ultrasound. Insight 2004, Vol. 46, No. 11, pp. 666–670.

4. Ohara, Y., Mihara, T., Sasaki, R., Ogata, T., Yamamoto, S., Kishimoto, Y. & Yamanaka, K. Imaging of closed cracks using nonlinear response of elastic waves at subharmonic frequency. Appl. Phys. Lett. 2007, 90, Issue 1, pp. 011902-1–011902-3.

5. Sandlin, S. A breakthrough in ultrasonic detection and sizing of partially closed cracks? VTT, Espoo, 2009. Research Report VTT-R-08989-09. 20 p.

6. Poznic, M. & Pecorari, C. So… is this a surface-breaking crack? Journal of Mechanics and Structures 2006, Vol. 1, No. 4, pp. 743–762.

7. Yamanaka, K., Sasaki, R., Ogata, T., Ohara, Y. & Mihara, T. Time domain analysis of subharmonic ultrasound for practical crack sizing. Review of Quantitative non-destructive Evaluation 2006, Vol. 25, pp. 283–290.

8. Ohara, Y., Hashimoto, M, Shintaku, Y. & Yamanaka, K. Monitoring growth of closed fatigue crack using subharmonic phased array. Review of Quantitative Non-destructive Evaluation 2010, Vol. 29, pp. 903–909.

9. Shintaku, Y., Ohara, Y., Endo, H., Hashimoto, M. & Yamanaka, K. Observation of closed crack discrimination by steering intense ultrasound and with shoe to house transmitter and receiver. Proceedings of Symposium of Ultrasonic Electronics 2009, Vol. 30, pp. 251–252.

10. Pecorari, C. & Poznic, M. On the linear and nonlinear acoustic properties of dry and water-confining elasto-plastic interfaces. Proceedings of the Royal Society A, 2006. Pp. 768–788.

26. Fracture Assessment of Reactor Circuit (FRAS)

26.1 FRAS summary report

Päivi Karjalainen-Roikonen, Kim Calonius, Antti Timperi, Otso Cronvall, Heikki Keinänen, Juha Kuutti, Kalle Kaunisto, Anssi Laukkanen, Lauri Elers, Matti Valo, Petteri Lappalainen and Tapio Planman and Pekka Nevasmaa
VTT

Abstract

The FRAS project (Fracture assessment of reactor circuit) project aims at (i) calculation of design and unforeseeable loads and their effects on a structure by applying numerical modelling; (ii) development of advanced fracture mechanics assessment tools and analysis methods based on material characterisation, damage mechanisms models and structural performance, in order to control structural failure both in cases of postulated initial flaw and environmentally assisted (internal) material damage; (iii) determination of degradation in material properties during service. This report summarises the results of the four year FRAS project (2007–2010).

Introduction

During recent years several structural analysis assessment methods have been established. Nonetheless, need for more accurate methods in load definition, true 3D flaw assessment, as well as irradiation embrittlement evolution assessment, still remains. Generally, numerical simulation of loads has treated different components as separate, even though they belong to the same aggregate, thereby

disregarding the interaction of support loads on the entire system. Concerning loads, also local manufacturing process induced and often relatively high residual stresses, especially in load carrying welds, need to be researched further, including both the physical phenomenology as well as more realistic 3D numerical simulations. Applicability and limits of sub-modelling techniques in numerical simulation of crack growth need to be investigated further. Feasible 'engineering assessment tools' cannot be reliably applied, unless they have been tailored and verified for the particular plant and component in question. Traditionally, material's fracture toughness has been determined applying deep-notched 'high-constraint' specimens enabling conservative estimates to be derived. Sophisticated constraint corrections are required for shallow surface cracks with lower constraint, particularly in the case of asymmetric crack fronts during crack growth and to acquire representative assessment fracture properties. Present limitations for specimen's measuring capacity in fracture resistance testing and under ductile crack growth are presumably unrealistic and hence need revision. Unified model for irradiation embrittlement is still lacking, despite of intensive previous research. Recently, advanced multi-scale modelling techniques of material damage micromechanism have allowed micro-scale investigation of relevant damage mechanisms, without a necessity to postulate a pre-existing flaw and extent the usability of traditional fracture mechanics. This provides means for realistic material damage assessment for environmentally assisted failure, such as stress corrosion cracking, irradiation embrittlement, ageing embrittlement and hydrogen embrittlement that do not require the existence of pre-existing flaw. In conjunction with modern FEM structural analysis methods, the application of advanced modelling techniques enables realistic structural integrity assessment of a component, or structure, over an entire 'chain' from micro- to macro-scale.

Main objectives

The objectives for fracture risk assessment comprise (i) calculation of design and unforeseeable loads and their effects on a structure by applying numerical modelling; (ii) development of advanced fracture mechanics assessment tools and analysis methods based on material characterisation, damage mechanisms models and structural performance, in order to control structural failure both in cases of postulated initial flaw and environmentally assisted (internal) material damage; (iii) determination of degradation in material properties during service.

Main results – Definition of loads

The greatest uncertainties in the assessment of structural integrity of a component are often associated with accurate determination of loads. The subproject aims at calculating of design and unforeseeable loads & welding stresses and their structural effects by applying numerical modelling and analyses methods. These calculations contribute to crack growth analyses for reactor circuit components and, finally, the assessment of component's defect sensitivity. The study was concentrated in three specific areas.

Loads transferred by supports

The objective was to define the external loads transferred by supports to the reactor circuit components or internal loads from the reactor circuit to the surrounding structures. During 2007–2008, finite element modelling methods provided by commercial Abaqus code for pipes and different types of supports and restraints were delineated. Stiffness propertises of pipes and supports were calculated with separate and combined models. A guillotine pipe break was chosen as a dynamic test case that was simulated with different kind ofs of three dimensional models. Larger models consisted of shell and solid elements. In smaller models they were substituted with special purpose elements. Simple and typical pipeline geometry and materials were chosen. The results were compared with each other and their reliabilities were evaluated.

Initially, material properties were linear and everything was considered to be in room temperature, but during the last two years of the project, nonlinear material properties with strain rate dependency were used. It was seen that in respect to the eigenmodes the pipe element model was adequate and almost as accurate as a shell element model with a fine mesh, especially when the pipe bend was modelled with elbow elements. Nonlinear spring elements were found to act realistically and seemed very suitable for modelling restraints in this kind of dynamic problems. The dynamic analysis results of the pipe element model corresponded well to the ones of the much larger shell element model. [1]

Later, an earthquake assessment according to the EU codes has been conducted with that model of a short pipe section. [2] In order to study a longer section of a pipeline, a finite element model of boiler feedwater pipe fitted with modern supports has been built using the knowledge gathered earlier within this project. Some preliminary analyses have been conducted with that model and the results

have been compared with some test results and corresponding results of more simplified models found in literature. [3]

Fluid-structure interaction

Thermal loads are among the most important loadings in the structural integrity assessment of NPPs. Computational Fluid Dynamics (CFD) has potential for describing these loads much more accurately than traditional simplified methods, although for many applications further validation work is needed.

CFD calculations of buoyancy-driven flows were performed for two simplified validation cases and for the more realistic HDR (Heißdampfreaktor) experiment [4, 5]. Later, CFD calculations of the Vattenfall thermal mixing experiment were carried out. Various Reynolds-Averaged Navier-Stokes (RANS) turbulence models were tested: eddy viscosity models with linear and non-linear stress-strain relation and Reynolds stress models. The profiles of temperature, velocity and turbulence quantities were predicted qualitatively quite correctly. Thermal mixing was, however, clearly too low with all turbulence models which is a common feature of RANS calculations in the complex three-dimensional mixing point.

In order to predict the time dependent thermal fluctuations due to turbulent mixing, Large-Eddy Simulation (LES) or similar models are usually required which is computationally very expensive. Development of a more feasible approach was started, in which the spectrum of the fluctuations is estimated from a formula obtained from turbulence theory and the total power of the fluctuations is obtained from an inexpensive RANS calculation. From the spectrum, a realistic temperature load is generated by superposition of harmonic components with random phase-differences. Lifetime calculations for the Vattenfall case showed clearly more realistic results when compared with the traditional sinusoidal method [6].

Weld residual stresses

The welds of the reactor circuit components are the most likely locations for cracks to initiate and propagate. One notable factor causing this are the locally confined and often remarkably high weld residual stresses (WRSs). They have a central role especially concerning stress corrosion cracking (SCC). The WRS distributions are caused by the welding process history and the elastic-plastic properties of the involved materials. The computational modelling of WRSs and their behaviour during long-term plant operation is challenging. Within this sub-

project both FEM based numerical methods and analytical procedures were applied.

A review and comparison of commonly used WRS assumption procedures was carried out [7]. WRS assumption procedures (ASME, BS 7910: 1999, R6 Rev. 4, SSM handbook, SINTAP, API 579 and FITNET) were applied to a representative set of NPP pipe component welds with base material of both austenitic stainless steel and ferritic steel. Remarkable deviations in the WRSs computed for the same case were often observed. Moreover, the WRS procedures were found to be notably conservative. As compared to the underlying data, they indicated tensile side upper bound profiles and were not self-equilibrating, which is unrealistic.

Relaxation of WRSs due to various typical/anticipated load transients during the plant operation of a BWR type safe-end welded to a nozzle and a pipe was simulated using FEM based code Abaqus [9]. The initial WRSs were assumed acc. to the SINTAP procedure. History of 28 typical load transients, analysed with an axisymmetric model, was included in a single analysis run in a realistic chronological order. Thus, the effect of structural memory, i.e. the effect to each present elastic-plastic stress/strain state of all earlier loads, was fully included. Analysis showed that the maximum transverse-to-weld-WRSs in the weld centre line had decreased approximately 50 MPa. Also, a set of computational crack growth analyses including the WRSs and their decrease due to load transients were performed for the considered weld using the VTTBESIT. The considered degradation mechanism was SCC.

Numerical simulations of WRS distributions in the safe-end/pipe joint weld region under constant cyclic loading were carried out [8, 10]. An advanced elastic-plastic material model covering stress/strain hardening behaviour caused by both cyclic mechanical and thermal loads were applied in the analysis. The model has been developed by the Oak Ridge National Laboratory (ORNL) especially for stainless steels. Several load cycle sequences with different load amplitudes covering loading condition ranges from moderate to relatively severe were covered. Based on the obtained FEM simulation results analytical expressions for the assessment of WRS relaxation were formed.

VTTBESIT crack growth analysis code was further developed to take account the alteration aspect ratio, i.e. crack depth divided by its length, during crack growth as well as the growth increment based all SIF values over the crack front. A set of computational SCC growth analyses including WRSs were carried out with VTTBESIT [11]. According to the results most of the WRS decrease occurs

during the first five to ten load transients/cycles. Whereas according to the SCC computation results in the cases including the decrease in WRSs also the crack growth rates were to varying extent slower as compared to the cases with WRSs remaining in their initial values.

Main results – Advanced fracture mechanical assessment methods

The sub-project aims at developing advanced finite element method assessment tools and fracture mechanics analysis methods based on material characterisation, damage mechanisms models and structural performance, in order to control structural failure both in cases of postulated initial flaw (surface-flaw) and environment assisted (internal) material damage, such as in case of irradiation embrittlement, ageing embrittlement and stress-corrosion cracking. Coupled with Subproject 1, this finally enables the assessment of component's defect sensitivity.

Engineering assessment tools and submodelling technique

Application of various engineering analysis tools in the framework of structural integrity and fracture assessment of reactor circuit were considered. First numerical studies for various components were performed. Afterwards a part of the focus of the task purpose of this study was to test and utilizes the Zencrack fracture mechanics code that works together with commercial finite element software such as Abaqus or Ansys.

The Zencrack code [12] utilises un-cracked mesh of the component and can be used to generate finite element (FE) meshes containing multiple cracks for computation of fracture mechanics parameters (J – integrals, stress intensity factors) and computation of crack growth. By automatically substituting specialist elements or 'crack blocks' into standard meshes the code enables the user model various crack configurations. An example of Zencrack generated model is shown in Figure 1. Zencrack utilizes the Paris law for fatigue crack growth modelling. Zencrack is an extension to commercial software and thus normal analysis features such as thermal loading and 3-D crack analyses can be applied.

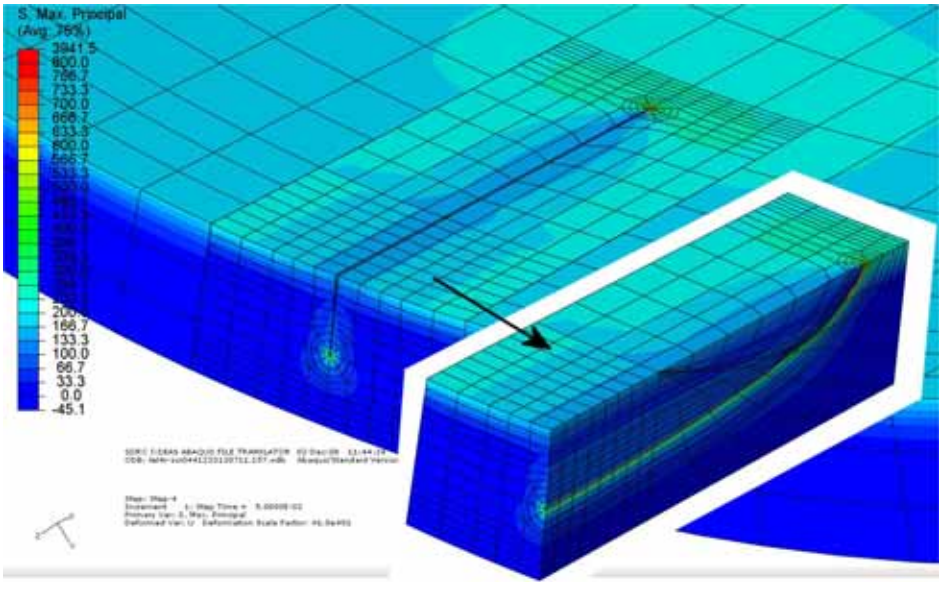

Figure 1. Example of Zencrack crack definition [13].

Concerning numerical analyses nozzle corner crack was first studied [13]. The results of the simplified solution were conservative in comparison to numerical (finite element) results.

The engineering assessment computer code VTTBESIT2.1 for fracture assessment was shortly presented. Unfortunately the further development of the solver part of the code is not possible. Thus in the continuation specific components (e.g. T-joints) was be studied using finite element method as presented afterwards.

The NESC-6 project, which deals with the benchmark analysis of a set of 3 tests on beam specimens with simulated embedded flaws in the scope of a PHARE project (EUROPAID/116529/D/SV/CZ), was participated [14].

Various fracture mechanics analyses were carried out to evaluate the applicability of the Zencrack code [15, 16]. Studied applications included several simple handbook case fracture analysis, a benchmark analysis from NULIFE project, thick-walled cylinder fracture analysis, a fast fracture benchmark analysis, a T-joint crack criticality analysis and a combined Zencrack submodelling analysis. The effects of thermal loading, corrosive environment, residual stress and non-zero mean stress and 3-D geometries and constraints were studied in the analyses. Very good agreement with the reference results was observed. Also a procedure to automatically perform Zencrack analyses for structural models generated from a database was developed.

The power of sub-modelling in the numerical finite element simulations was demonstrated.

The present experience shows that the Zencrack code is suitable for engineering crack growth applications utilising the Paris law. It is useful for developing cracked finite element models of complex 3D shapes. The concept of crack blocks, which allow the user to control mesh density and distribution, makes this program applicable to any cracked structure in principle.

In general Zencrack provides easy means to carry out fracture mechanics analyses such that no laborious manual crack front meshing is needed. This feature is valuable if the analyst has to perform many crack growth analyses for different type of cracks and loads but in case of small number of analysis Zencrack does not provide any functionality not achieved manually. The automated crack generating and analysis procedure that has been developed in the project makes it possible to combine Zencrack.

Assessment of 3D flaws

Transferability of fracture mechanics material data associated with different levels of specimen constraint has been investigated by performing numerical work to assess the fracture toughness transition between standard CT and SENB-type specimens and 3D cracks of various geometries and crack shapes for cleavage initiation and propagation using the WST model (EUROCURVE, VOCALIST and PERFECT data from Areva). The work assesses how fracture toughness is affected by different crack types as well as “realistic“ crack features (such as asymmetric crack fronts). The results have been coupled to the constraint formalism build within the Master curve methodology and fracture mechanical constraint assessment methods of Fitnet, Sintap and R6. The results provide complete means for assessing the effects of constraint on fracture mechanical material properties, both with respect to reduction of analysis conservatism and enabling optimized material usage, as well as presenting methods for handling situations where otherwise unconservative assessment results would result using traditional methods. These methods are as such suited for assessment of “real” structural material properties.

The international round robin on fracture resistance determination for low constraint cracks was launched in 2010. In the round robin a method to measure the J-integral fracture toughness and the extent of crack growth in a single-edge-cracked tension SE(T) specimen will be used. The specimen geometry and

loading mode is designed to produce a level of crack-tip constraint in the test that is similar to the constraint experienced in service for a surface circumferential flaw in a pipe under tension or bending load. The test is intended to be used for structural steels.

Micromechanical modelling

The WST model has been developed to act as a predictive tool for ductile-to-brittle transition region response. The WST model was further fitted with crystal plasticity results to improve upon the cleavage initiation failure criterion [17]. In addition to development of the WST model, an MSc thesis was completed where the so called ”Bordet” model was implemented and applied for brittle fracture assessment [18]. An example of application of the WST model to predict effects of irradiation is presented in Figure 2, where reference temperature trend curves obtained on an experimental basis and evaluated using local approach are compared to those computed by using the WST model.

Multiscale methods have been introduced as means applicable for researching the effects of irradiation. Discrete dislocation dynamics simulation was applied to investigate the mechanisms of deformation in a material containing irradiation damage.

The WST model has been shown to possess the abilities to treat fracture in cases where a state of lowered constraint prevails, and with the aid of parallel work carried out in PERFECT and PERFORM60 projects, has been introduced with features enabling the assessment of effects of irradiation. Further improvements can be expected as more results incorporating intra grain crystal plasticity effects become available and are integrated into the model.

Additionally, several multiscale methods, ranging from atomistic to mesoscopic, have been taken into use and are being actively utilized in study of cleavage fracture, crack growth [19] and response of material to the effects of irradiation as well as aging.

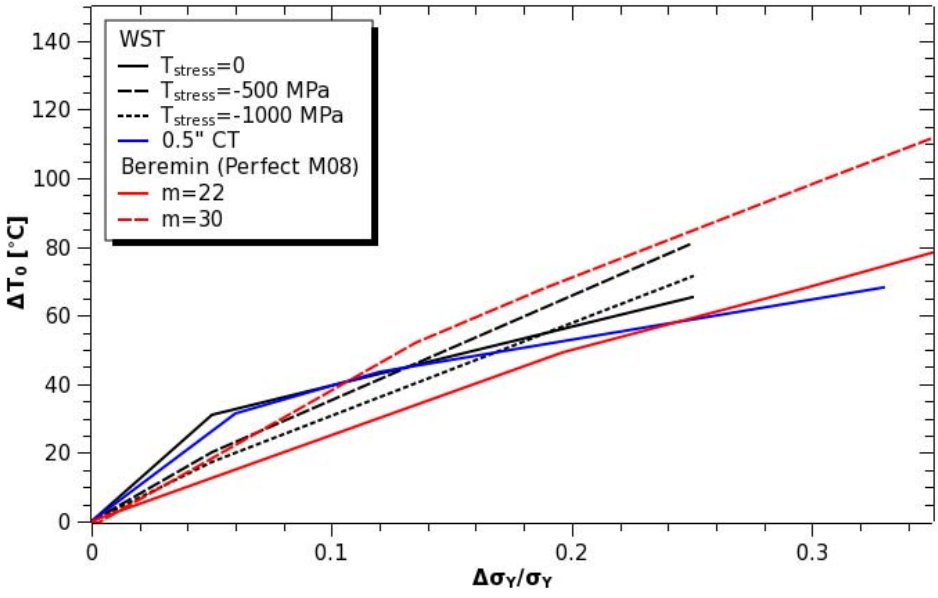

Figure 2. Comparison of WST and Beremin model results for reference temperature shift resulting from irradiation induced hardening. [18]

Main results – Advanced surveillance techniques

Irradiation embrittlement covers wide range of physical and technical phenomena starting from changes in steel microstructure due to collision of neutrons with iron atoms and ending with the technical description of the brittle-ductile transition temperature shift as a function of neutron fluence and steel impurity contents. Material toughness can be measured with Charpy-V test or with fracture mechanical test. It is essential that the measured toughness is material property, i.e. the dependence of the measured toughness on specimen size, type or geometry is known. The above aspects were included to some extent into the subtask.

Ductile crack growth measuring capacity

Fracture mechanical test specimen size validity limits and overall measuring capacity in ductile tearing were assessed [20]. Fracture resistance curves were determined for four steels using both small SEN(B) and 25 mm C(T) specimens. In Figure 3, a typical result of fracture resistance characterization is presented. Four different materials were tested. The SE500HR, X80 and super duplex steels were tested at room temperature and DQT HT80 steel at 100°C. Results

indicates that $J_{\max}$ is the limiting factor for these steels rather than crack growth limit, $\Delta a_{\max}$.

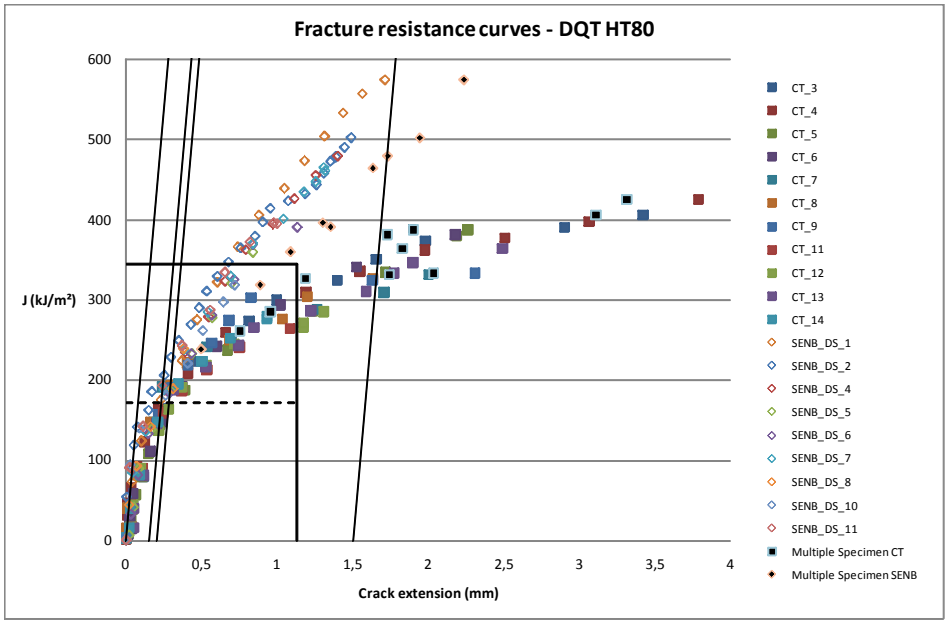

Figure 3. Fracture resistance curves – DQT HT80 steel.

Also cohesive modelling for the material tearing process was applied and the results were compared with experimental results. Cohesive modelling is represented by a traction-separation law (TSL). The cohesive parameters consisting of fracture strength and fracture energy were calibrated such that calculated load-load line displacement (LLD) relation matched the experimental results using both SEN(B) and C(T) specimens. Linear, exponential and plastic softening behaviour was studied and linear TSL shape was found to produce results closest to the experimental results. Although the load-LLD relation was calculated with accuracy the simulated J-R curve was not in good agreement with the experimental results.

Irradiation embrittlement

The limitations of the Master Curve and the correct way of its application were studied and further developed within an IAEA CRP-8 “Master Curve Approach to Monitor Fracture Toughness of Reactor Pressure Vessels in NPPs”. Fracture

toughness data on various reactor pressure vessel (RPV) steels were analysed for quantifying the toughness issues associated with RPV surveillance testing and integrity analyses, using the Master Curve approach. The work covered three topic areas: constraint/ geometry effects, fracture toughness vs. temperature and dynamic loading conditions. [21, 22, 23]

Ten laboratories contributed to a round robin in the framework of the consolidation of analytical tools needed to support loss of constraint issues in the application of the Master Curve. It was found that the ANSYS code produces systematically higher forces. Remaining differences for the other finite element codes were very small. The outcome of the CRP Phase 8 provided reference data for the ASTM E 1921-05 loading rate estimation and a revised adjustment data for fracture toughness testing could be proposed from the results. No influence of the loading mode (monotonous loading vs. partial unloading) on the Master Curve reference temperature T_0 was detected. The results confirm that the Master Curve shape is far insensitive to neutron fluence for typical RPV steels, as also previous experience has shown. This result is significant, because it supports the use of standard ASTM E 1921 as such also for most irradiated ferritic steels which fulfil the application limits specified in the standard. For the varying crack depth data, the results exhibited T_0 differences from about 40 to 70°C between a/W = 0.1 and 0.5, with the shallow crack showing the lower T_0.

The results obtained in CRP Phase 8 provide supplementary data for measuring fracture toughness directly using small surveillance size specimens and applying the Master Curve approach for RPV structural integrity assessment in nuclear power plants. The IAEA coordinated research projects (CRPs) have been sponsored by the IAEA.

Small angle neutron scattering (SANS) was used for characterising the size distribution of small defects in irradiated and reference steels. Its sensitivity to chemistry of the defects is, however, limited. Figure 4 shows the measured size distributions of Loviisa irradiated 501 steel in various irradiation-annealing conditions.

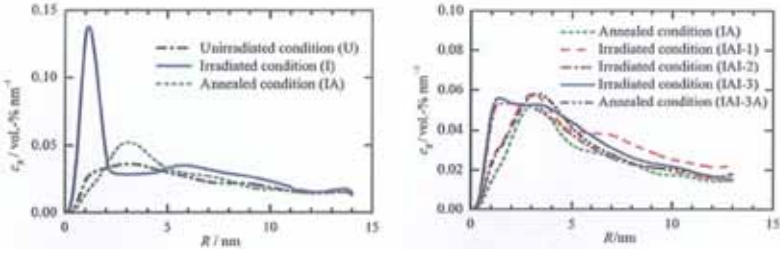

Figure 4. Volume percentage of the defect is given on the y-axes and defect size on the x-axes. The left side figure indicates that the number of approximately 1.5 micrometer defects is large in the irradiated condition but low in the un-irradiated as well as in the IA-condition. The right side figure indicates that the defects do not appear again during re-irradiation after annealing. One can speculate that copper precipitates appear after irradiation but they do not dissolve back to the matrix in annealing or they grow larger during annealing and hence they are no more pronounced during re-irradiation.

The conventional trend curve development is based on pre-determined functions, which include copper and phosphorus contents, neutron fluence and fluence rate and which may be also nonlinear. In the nonlinear neural network type analysis part or all dependences will be determined freely. The IAEA VVER-440 database, which includes 121 weld and 100 base metal Charpy-V shift data points, was analyzed using the new technique. In Figure 5 results from two trial functions are shown. The new fits also suggest a small flux effect. The description is shown in Figure 6. The new analyzing technique is more flexible than conventional fitting techniques but it is not possible with the limited and old data base to make conclusive statements on the reliability of the derived descriptions.

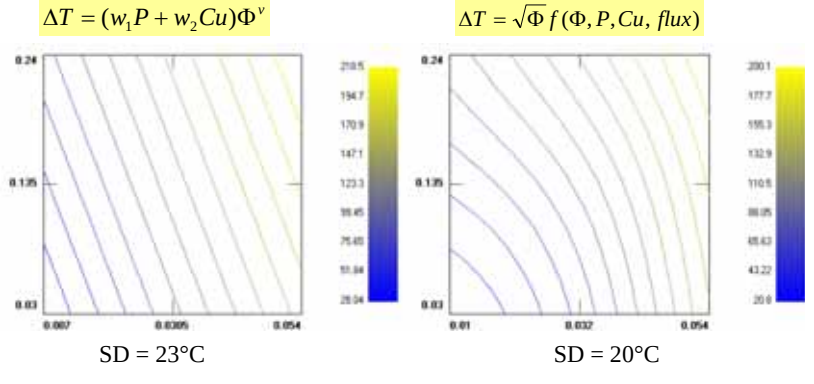

Figure 5. Constant ΔT-shift contours (at constant ΔT steps) of two trial functions. The left side function has the form of the Russian norm and the right side function a SQRT(Φt) term, which guarantees zero shift at zero fluence, times a freely determined function f(Φ,P,Cu,flux). Φt = 50, flux = 1.

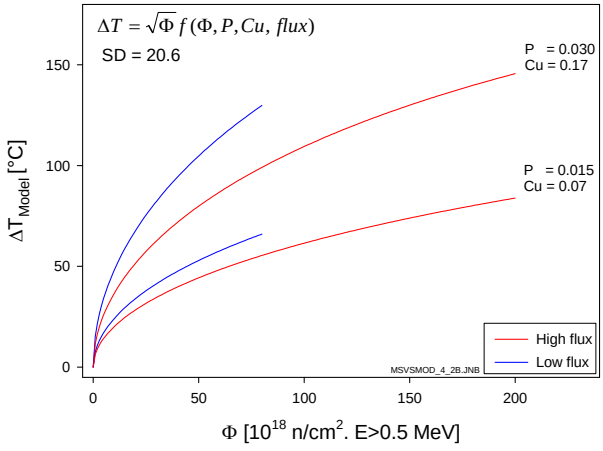

Figure 6. Prediction of a flux effect based on the IAEA data base.

Resistivity measurements of the Loviisa irradiated 501 steel were initiated, the equipment was acquired and the experimental capability was achieved. Specific resistivity is sensitive to irradiation damage even if it is not a defect selective method. The main objective of the measurements is to characterize in detail annealing response to the resistivity, i.e. to use isochronal annealing as a spectroscopy. Phosphorus and copper based defects are assumed to have different annealing response, which is aimed to be identified with the measurements.

Applications and conclusions

The results will be applied to assess structural safety of nuclear reactor components, as well as to evaluate their remaining lifetime during service, by coupling between advanced numerical modelling tools and material's characterisation data, in order to cover the entire chain of structural safety related aspects coupling the interaction of effects of loads, existing flaws, material's relevant damage mechanisms and degradation of properties during service.

References

1. Calonius, K. Numerical Studies on Dynamic Behaviour of Pipelines. VTT, Espoo, 2009. VTT Research Report VTT-R-01025-09.

2. Calonius, K. Numerical Studies on Dynamic Behaviour of Pipelines, Part 2. VTT, Espoo, 2010. VTT Research Report VTT-R-01214-10.

3. Calonius, K. Numerical Studies on Dynamic Behaviour of Pipelines, Part 3. VTT, Espoo, 2011. VTT Research Report VTT-R-00739-11.

4. Timperi, A. Numerical simulations of turbulent buoyancy-driven flows. VTT, Espoo, 2008. VTT Research Report VTT-R-11339-07, Espoo. 49 p.

5. Timperi, A. Simulation of thermal striping in a HDR experiment. In: SAFIR2010. The Finnish Research Programme on Nuclear Power Plant Safety 2007–2010, Interim Report. Puska, E.K. (Ed.). VTT, Espoo, 2009. VTT Research Notes 2466. http://www.vtt.fi/inf/pdf/tiedotteet/2009/T2466.pdf.

6. Hannink, M.H.C. & Timperi, A. Simplified methods to assess thermal fatigue due to turbulent mixing. In: Proc. of ICONE19 Conference, Chiba, Japan, 2011.

7. Cronvall, O. Review and Comparison of Welding Residual Stress Definitions. VTT, Espoo, 2008. VTT Research report VTT-R-01415-08. 102 p.

8. Cronvall, O. Practical inclusion and behaviour of welding residual stresses in structural integrity analyses of NPP primary circuit components. VTT, Espoo, 2009. VTT Research report VTT-R-00962-09. 53 p.

9. Cronvall, O. Welding Residual Stress Relaxation in NPP Components Under Operation – A Literature Study. VTT, Espoo, 2010. VTT Research report VTT-R-02200-10. 82 p.

10. Cronvall, O. Simulated Behaviour of Welding Residual Stresses in NPP Primary Circuit Components Subject to Cyclic Loading. VTT, Espoo, 2010. VTT Research report VTT-R-02199-10. 53 p.

11. Chauhan, M. & Cronvall, O. Computational Study On Weld Residual Stress Relaxation and Crack Growth In NPP Primary Circuit Components. VTT, Espoo, 2011. VTT Research report VTT-R-09790-10.

12. Zencrack 7.5. Zentech International Ltd. 2007.

13. Keinänen, H. Engineering tools for fracture assessment and development of sub-modelling technique. VTT, Espoo, 2008. Research Report VTT-R-04305-08. 18 p.

14. Keinänen, H. Benchmark analyses for fracture mechanics methods for assessing of sub-clad flaws. Computation of “abnormal” large scale specimen “1E7”. VTT, Espoo, 2007. Report VTT-R-09462-07.

15. Keinänen, H., Kaunisto, K. & Kuutti, J. Application of Zencrack code for crack initiation and growth cases. VTT, Espoo, 2009. Research Report VTT-R-00513-09. 36 p.

16. Kuutti, J., Keinänen, H. & Kaunisto, K. Developments in utilizing Zencrack code in fracture mechanics analyses. VTT, Espoo, 2011. Report VTT-R-XXXXXXX. 42 p.

17. Wallin, K. & Laukkanen, A. New developments of the Wallin, Saario, Torronen cleavage fracture model. Engineering Fracture Mechanics 2008, Vol. 75 (11), pp. 3367–3377.

18. Lindroth, P. Master's Thesis, Aalto University, Department of Applied Mechanics, 2009. 76 p.

19. Andersson, T. Analysis of discontinuities in metallic materials with the extended finite element method, Master's Thesis, Aalto University, Department of Applied Mechanics, 2010. 80 p.

20. Elers, L. The validity of fracture resistance curve characterization methods for extended ductile crack growth. VTT, Espoo, 2008. VTT Research Report VTT-R-10197-08. 58 p.

21. Lidbury, D., Diard, O., Marini, B., Bugat, S., Keim, E., Wallin, K. & Planman, T. Prediction of irradiation damage effects in reactor components: update of progress in RPV mechanics subproject. Proc. Conf. ASME PVP 2007/ CREEP 8:2007. ASME Pressure Vessels and Piping Conference, San Antonio, Texas, July 22–26, 2007. ASME. Pp. PVP2007–26076.

22. Planman, T., Onizawa, K., Server, W. & Rosinski, S. IAEA coordinated research project on Master Curve approach to monitor fracture toughness of RPV steels: applicability for highly embrittled materials. Proc. Conf. ASME PVP 2007/CREEP 8:2007. ASME Pressure Vessels and Piping Conference, San Antonio, Texas, July 22–26, 2007. ASME. Pp. PVP2007–26097.

23. Planman, T., Server, W., Wallin, K., Rosinski, S. Application of the Master Curve approach for abnormal material conditions. Proc. Conf. ASME PVP 2007/CREEP 8:2007. ASME Pressure Vessels and Piping Conference, San Antonio, Texas, July 22–26, 2007. ASME. Pp. PVP2007–26257.

24. Valo, M. & Bulsari, A. Non-linear analyses of VVER-440 surveillance data. VTT, Espoo, 2008. VTT Research Reporti VTT-R-03047-08. 55 p.

25. Ulbricht, A., Bergner, F., Böhmert, J., Valo, M., Mathon, M.-H. & Heinemann, A. SANS response of VVER440-type weld material after neutron irradiation, post-irradiation annealing and reirradiation. Philosophical Magazine 2007, Vol. 87, No. 12, pp. 1855–1870.

26.2 Advanced numerical fracture assessment methods

Anssi Laukkanen, Juha Kuutti, Tom Andersson and Päivi Karjalainen-Roikonen
VTT

Abstract

The increase in computational capacity has made numerical analyses an indispensable tool in fracture mechanics. Many commercial structure analysis codes have implemented fracture mechanics routines easily available to the end-user. Traditional fracture mechanics analyses can now be carried out with relative ease and research in this field is focused on crack growth simulation methods and more detailed numerical material fracture mechanism modelling. Various numerical fracture assessment methods have been researched and applied during the course of the FRAS project. The cohesive zone modelling approach and crack tip remeshing approach are presented with numerical examples. The abilities of the extended finite element method for assessment of non-rectilinear crack propagation are demonstrated for a mixed-mode type of a crack analysis. Progress in modelling of effects of irradiation to ductile to brittle transition fracture toughness is presented. Research carried out in the project shows that the methods can be applied to model failure in nuclear applications but determining model parameters is essential in obtaining reliable results.

Introduction

Analytical solutions are available only for a limited number of fracture mechanical problems and numerical approximations are a necessity. Numerically determined stress intensity factor solutions have been published for a wide range of applications. The most popular generally applied numerical method in fracture mechanics is finite element method on which many of the advanced methods presented here are based. Many commercial structure analysis codes have implemented fracture mechanics routines easily available to the end-user.

In traditional mechanics problems using finite element method the structure is divided to discrete areas or volumes called elements connected to each other with nodes. Approximative solution is then sought for the elements and nodes using the discretized forms of mechanical equilibrium equations. In finite element modelling of fracture mechanics problems the crack can be represented

using mesh topology and modified elements that yield to produce crack tip singularity. Stress intensity factors and J-integrals can then be estimated from the discrete crack front stresses and strain state. Material plasticity can also be taken into account to model crack tip blunting.

Numerical analysis of stationary cracks has developed to a mature state. Sometimes it is desirable to analyze crack growth. In a finite element model growing cracks often require a special technique to propagate cracks and the analysis must include a growth criterion. Much research on the applicability of these techniques has been carried out some of which is presented in this paper. The family of methods which at present appears to be the most successful one is the extended finite element method (XFEM).

The study of fracture toughness in the ductile-to-brittle transition region employs methods such as local approach models and micromechanical models like the WST model. These methods when applied as a part of a multiscale framework of methods enable the modelling of effects of irradiation to fracture properties, initiating from a structure of a damaged material and ending up with the irradiation induced shift in the fracture toughness reference temperature.

Crack growth simulations

Numerical simulation of fracture and crack propagation has become an important aspect of structural reliability analysis. In the field of traditional finite element method smeared crack approach, discrete crack and element erosion approach combined with local remeshing are known methods for modelling material fracture. In these numerical crack growth strategies the increment of crack advance is related to the element size in the mesh making the crack growth simulation mesh-dependent. All of the presented methods include mathematical parameters with little correspondence to any physical property of the material. Therefore the parameters in crack growth simulations often need to be adjusted such that simulated results match the experimental data.

Traditional crack growth methods

The smeared crack concept can be considered as a representation of series of microcracks where the cracks are smeared over an entire element. In the smeared crack approach, the direction of crack formation is usually defined by the maximum tensile principal stress. The crack is formed along the plane normal to the stress. When the crack is formed, a local coordinate system is fixed to the

crack such that one of the coordinates points in the direction normal to the crack surface. Smeared crack approach method is not suited for distinct sharp cracks because it is unable to capture the stress field around the crack tip. One discrete cracking approach is the node release technique. This can be modelled using direct node-to-node ties or element surface-to-surface ties using cohesive elements. In the technique initially crack surfaces are separated by progressively releasing the ties that bind the nodes together when a specified failure criterion is met. The free crack surface propagates along the predefined element boundaries. Due to the simplicity of the method it is been widely used and known to produce accurate results if the crack path is known a-priori. An extension of this method is modelling all interelement surfaces as possible separation paths e.g. using cohesive elements.

Element erosion technique is also applied. In this technique the failed elements are removed from the model creating free surfaces. This violates the balance and conservation laws of mechanics and is thus very approximative way of modelling crack propagation. The popularity of this technique is due to its simplicity to implement. For ductile crack growth the Gurson–Tvergaard plasticity [1] model can be applied to simulate crack growth by element erosion technique.

Discrete crack propagation by local remeshing makes possible to propagate arbitrary cracks through the mesh by removing the local mesh around the crack path and creating new elements to accommodate the crack so that crack faces are represented explicitly by element edges or faces. This requires that the model is regenerated during the analysis. In 2-D cases remeshing is straightforward and can be done with relative effort. Three dimensional remeshing is much more complex. Some research has been carried out in implementing these crack growth routines into commercial FE-codes and some FE-packages support this directly (WARP3D [2]) and there are third-party software to carry out this type of analysis together with FE-software (e.g. Zencrack presented as an example later). Most of these methods have in common that they are developed for metallic materials and utilize well known fracture mechanics parameters to assess crack criticality and growth path.

Crack growth by crack tip remeshing

The Zencrack code [3] utilises un-cracked mesh of the component and can be used to generate finite element (FE) meshes containing multiple cracks for computation of fracture mechanics parameters (J – integrals, stress intensity factors)

and computation of crack growth. By automatically substituting specialist elements or ‘crack blocks’ into standard meshes the code enables the user model various crack configurations. An example of Zencrack generated model is shown in Figure 1. Zencrack utilizes the Paris law for fatigue crack growth modelling. Zencrack is an extension to commercial software and thus normal analysis features such as thermal loading and 3-D crack analyses can be applied.

Submodelling technique can be applied to simplify crack tip remeshing simulations. When applying submodelling, the region of interest, crack tip and front in this case, is modelled in more detail using a submodel that is tied to the global model far from the crack. Only the submodel is then updated to accommodate crack growth making the remeshing process much simpler. As the results of the global model do not have do be updated every time the computational effort is also greatly reduced.

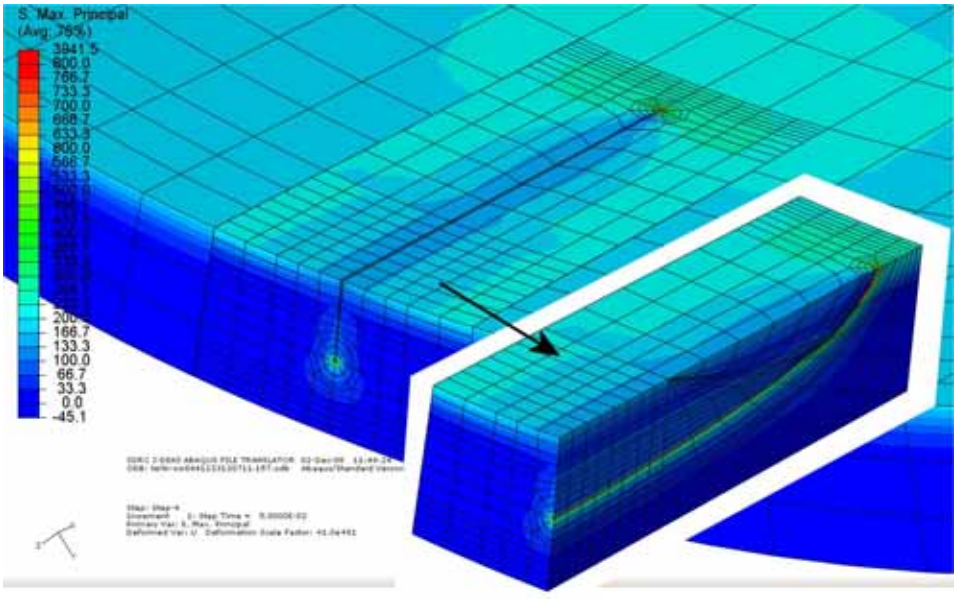

Figure 1. Example of Zencrack crack block methodology.

Cohesive Zone modelling

In cohesive modelling [4] the tearing process consisting of void initiation, growth and coalescence is represented by a mathematical traction-separation law (TSL) in the cohesive zone. In numerical analyses the crack path often needs to be modelled a-priori using cohesive ties. The difficult part is selecting the shape

of the TSL. At some point the stresses are high enough to cause void growth so that force over the crack starts to decrease. As the loading is continued the voids still grow and combine decreasing the force exerted across the crack faces. If the material still intact between the voids undergoes plastic hardening the effective force decrease can be small. In brittle crack growth the load decrease is much more instant. However at some point the voids have combined fully and crack can be considered to have increased the length of the cohesive tie. Cohesive ties can be cohesive elements, cohesive surfaces or nodal ties that follow the cohesive law. This process is depicted in Figure 2.

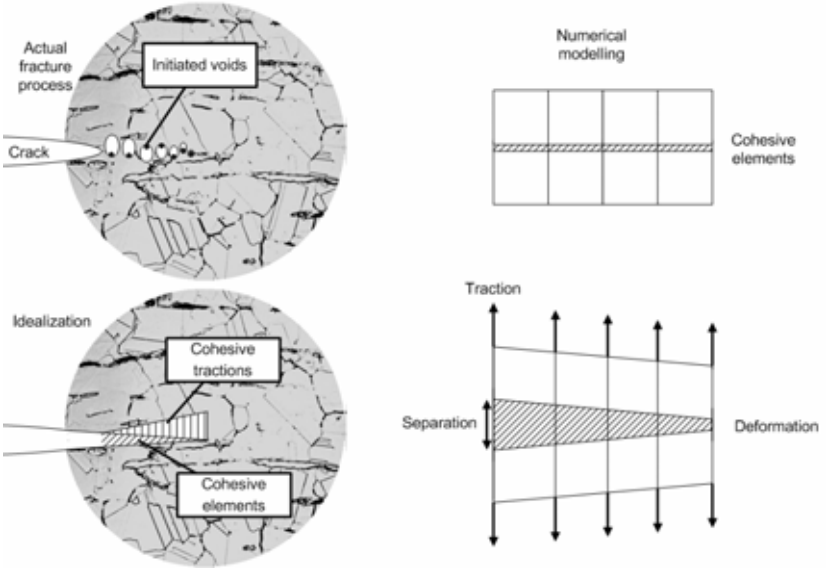

Figure 2. Principle of cohesive zone modelling of fracture.

In the current project cohesive modelling technique was applied to simulate crack propagation in material toughness tests using C(T) and SEN(B) specimens are simulated. Aim was to determine the cohesive parameters for this material such that the simulated load – load line displacement curve and J-R curve match the experimental results. The cohesive parameters consisting of fracture strength and fracture energy were calibrated such that calculated load-load line displacement relation matched the experimental results using both SEN(B) and C(T) specimens. Linear, exponential and plastic softening behaviour was studied and linear TSL shape was found to produce results closest to the experimental results. Figure 3 shows an example of the crack growth process in C(T) specimen using cohesive elements.

Although the load-LLD relation was calculated with accuracy the simulated J-R curve was not in good agreement with the experimental results. The reason for this is that the obtained parameters produced a too wide fracture process zone. Cohesive zone modelling has been successfully applied in literature to produce good agreement in both load-LLD curve and J-R curve after the cohesive parameters were determined using appropriate experiments. It was found that increasing cohesive strength to obtain more localized fracture would cause significant plasticity in the crack front disturbing the cohesive behaviour as strain energy dissipated plastically instead of cohesively.

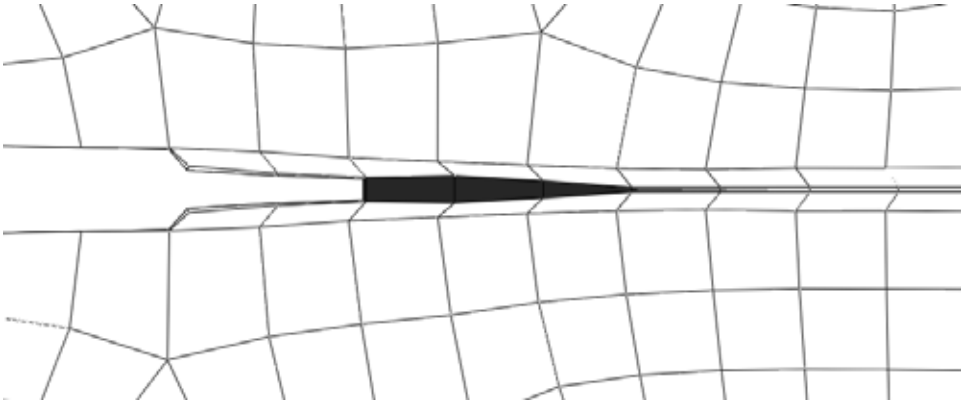

Figure 3. Crack growth modelling in C(T) specimen using cohesive elements. Element darkness indicates magnitude of damage. First two elements have completely failed and are removed from the analysis.

Overall the analyses indicated that while cohesive zone modelling can be applied to simulate ductile crack growth special attention must be paid to numerical modelling of the structure starting from mesh design. When post-calculating experimental tests the effects of numerical issues on results can be studied and avoided such that correspondence between calculated and measured results is achieved but the situation is much more complex when applying the numerical procedures without reference results.

Advanced mathematical representation of material discontinuities

Novel techniques such as the extended finite element method (XFEM) [5] provide attractive method for arbitrary crack propagation analyses. This kind of technique considers the crack to be a strong discontinuity in the displacement

field such that the crack faces are not represented by free element surfaces. Crack initiation is still often governed by cohesive zone models or crack is extended in specified segments in direction obtained from fracture mechanics parameters.

Within FRAS, a XFEM code was developed using general purpose C++ based finite element libraries. Overall the code was found to be effective in relatively simple crack propagation cases. In the future other more complex and thus more realistic material models are to be introduced as well as interfacing to other available tools and codes. This would allow the analysis far more realistic fracture mechanical problems. Also a better mesher will be incorporated and analyses of three dimensional, a step more realistic, models are planned with geometric detail of structural component nature. Rewrites in C++-language are considered for some parts to extend the abilities and link to existing codes for multiscale analysis. Examples of crack propagation analyses under mixed-mode conditions are presented in Figure 4.

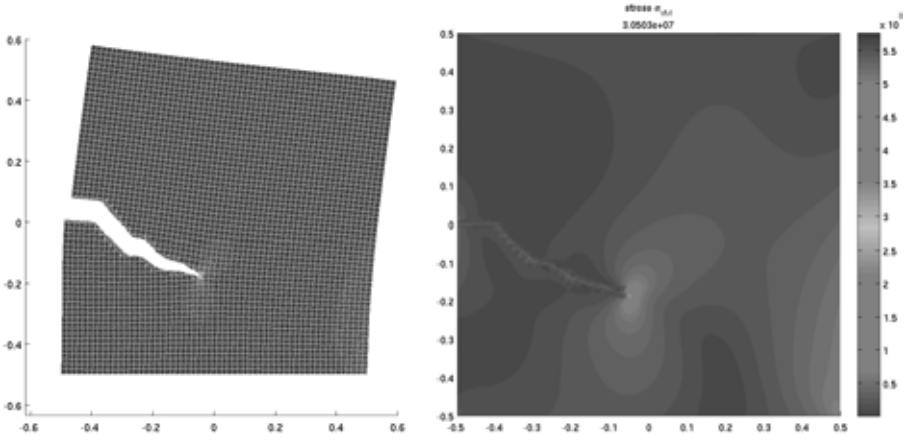

Figure 4. Crack trajectory and contour plot of equivalent stress in a XFEM analysis.

Multiscale and micromechanical modelling for irradiation embrittlement

The most accurate means of assessing the probability of cleavage initiation and propagation are the so called ”local approach” models for fracture, which are often referred to as micromechanical models for cleavage fracture. These models enable the accurate assessment of risk for cleavage failure of material in a

specific service affected state, undergoing for example an operational stress state or transient conditions. Latest developments in this field of research have focused on introduction of the effects of irradiation in material behavior, thus enabling the computational evaluation of aged component integrity.

The WST model [7] has been developed to act as a predictive tool for ductile-to-brittle transition region response, example of application for a pressure vessel steel is presented in Figure 5.

As a part of work integrating the effects of irradiation to cleavage fracture toughness models, thus enabling the computational assessment of embrittlement, various multiscale tools have been coupled to micromechanical models. An as example, one of the prime avenues of research in understanding the link between degradation of fracture toughness and irradiation is the link between mechanisms of plastic flow in a damaged material and the effects this has on cleavage fracture initiation and propagation. A method applied in this study is discrete dislocation dynamics (DDD), an example of such analysis is presented in Figure 6.

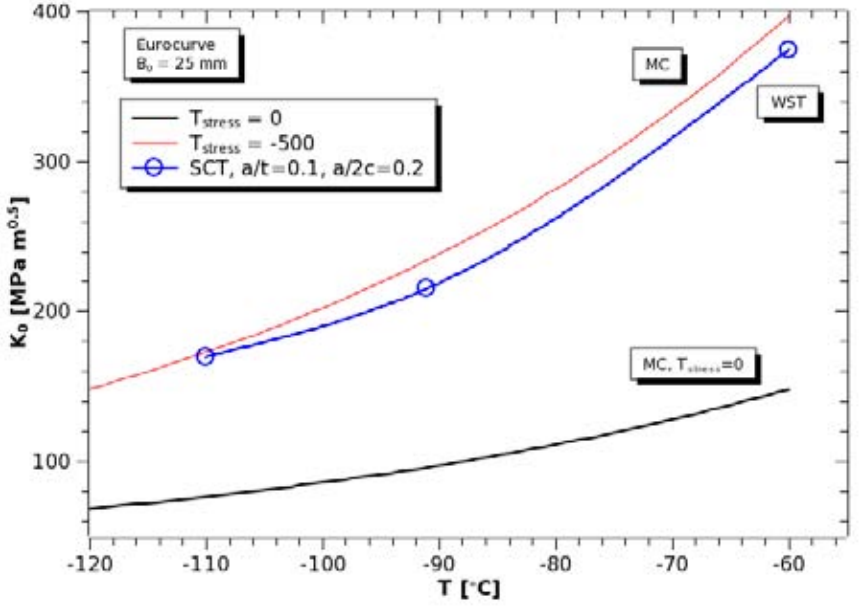

Figure 5. Comparison of WST model and Master Curve predictions for low constraint fracture toughness in the ductile to brittle transition region.

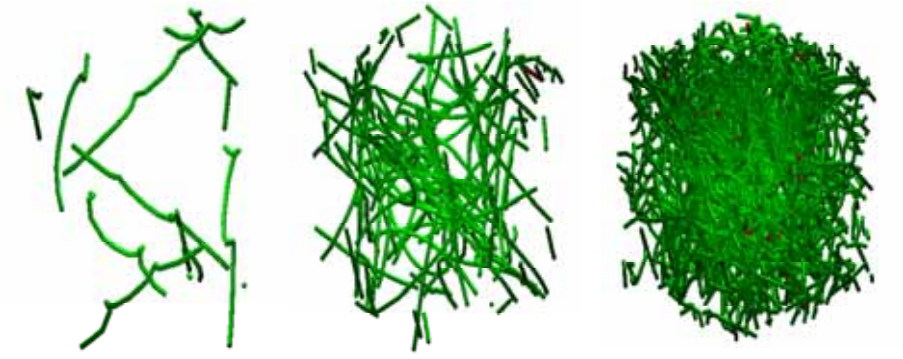

Figure 6. Evolution of dislocation structure for constant applied strain rate in a DDD analysis to study the mechanisms of plastic deformation in a damaged material.

Conclusions

The increase in computational capacity has made numerical analyses indispensable tool in fracture mechanics. Many commercial structure analysis codes have implemented fracture mechanics routines easily available to the end-user. Traditional fracture mechanics analyses can now be carried out with relative ease and research in this field is focused on crack growth simulation methods and more detailed numerical material fracture mechanism modelling. Of numerical crack growth methods the cohesive zone modelling approach and crack tip remeshing approach were presented with numerical examples. Research carried out in the project shows that the methods can be applied to model failure in nuclear applications but determining crack growth related material parameters is essential in obtaining reliable results.

When the methods can be applied to simulate experiments reliably focus of the research must be aimed at transferability, i.e. determining whether the methods and parameters are directly applicable in simulating fracture in nuclear applications.

Other developing aspects of numerical fracture mechanics assessment methods are mathematical representation of cracks to reduce mesh dependency and local approaches and damage mechanics to model the fracture process in detail. The extended finite element method has been introduced as a promising numerical method and its more widespread use will be pursued.

Within FRAS, the revised WST cleavage fracture model was implemented, tested, and tried for computation of material cleavage fracture behavior in the ductile-to-brittle transition region. The WST model has been shown to possess

the abilities to treat fracture in cases where a state of lowered constraint prevails, and with the aid of parallel work carried out in PERFECT and PERFORM60 projects, has been introduced with features enabling the assessment of effects of irradiation. Further improvements can be expected as more results incorporating intra grain crystal plasticity effects become available and are integrated into the model. Several multiscale methods, ranging from atomistic to mesoscopic, have been taken into use and are being actively utilized in study of cleavage fracture and response of material to the effects of irradiation as well as aging.

In future works, tighter integration between experimental tasks, mechanistic approaches and structural integrity evaluation will be pursued to further even better exploitation of results.

References

1. Tvergaard, V. On localization in ductile materials containing spherical voids International Journal of Fracture 1982, 18(4), pp. 237–252.

2. WARP3D. 3-D Dynamic Nonlinear Fracture Analyses of Solids Using Parallel Computers, Release 13.16, Department of Civil Engineering, University of Illinois at Urbana-Champaign (UIUC), 2010.

3. Zencrack 7.6. Zentech International Ltd. 2009.

4. Cornec, A., Scheider, I. & Schwalbe, K. On the practical application of the cohesive model. Engineering Fracture Mechanics 2003, Vol. 70, No. 14, pp. 1963–1987.

5. Zi, G. & Belytschko, T. New crack-tip elements for XFEM and applications to cohesive cracks. International Journal for Numerical Methods in Engineering 2003, 57(15), pp. 2221–2240.

6. Andersson, T. Analysis of discontinuities in metallic materials with the extended finite element method. Master's Thesis, Aalto University, Department of Applied Mechanics, 2010. 80 p.

7. Wallin, K. & Laukkanen, A. New developments of the Wallin, Saario, Torronen cleavage fracture model. Engineering Fracture Mechanics 2008, Vol. 75(11), pp. 3367–3377.

27. Influence of Material, Environment and Strain Rate on Environmentally Assisted Cracking of Austenitic Nuclear Materials (DEFSPEED)

27.1 DEFSPEED summary report

Ulla Ehrnstén, Wade Karlsen and Janne Pakarinen,
Matias Ahonen and Pasi Kuivalainen
VTT

Mykola Ivanchenko, Tapio Saukkonen and Hannu Hänninen
Aalto University, Engineering Materials

Abstract

The DEFSPEED project (Influence of material, environment and strain rate on environmentally assisted cracking on austenitic nuclear materials) focussed on increasing the understanding of environmentally assisted cracking (EAC) and irradiation assisted stress corrosion cracking (IASCC) mechanisms in austenitic nuclear materials. Several sub-tasks were performed to achieve the set objectives during the four year project. The Super Slow Strain Rate Testing technique (SSSRT) was developed and employed for initiation studies on austenitic nuclear materials in LWR environments followed by in-depth investigations on deformation distribution. Austenitic nuclear materials show dynamic strain ageing behaviour, as described in a thesis work. The effect of environment on fracture toughness properties in nickel-based welds at slow strain rate in hydrogenated water was determined both for materials from dissimilar metal welds as well as on pure weld metal

specimens. Irradiated austenitic stainless steels from plant internals were characterized using transmission electron microscopy (TEM) to increase the knowledge of radiation induced segregation and defect structures, which both play a role in IASCC. The latest international knowledge, applied for customer work, was brought to Finland by participating in international co-operation within the fields of EAC and IASCC. Education of new experts in the field of nuclear materials is an important objective for all SAFIR 2010 projects. In addition to participation of young experts in the project, a digital report archive was built, containing reports on nuclear materials written by VTT.

Introduction

Environmentally assisted cracking in sensitised stainless steels plagued the BWR fleet in the 80's, and led to several successful mitigation actions. Later EAC has been observed in non-sensitised stainless steels, where deformation is one of the key issues. A relatively new phenomenon is EAC in austenitic stainless steels in PWR's, connected mainly, but not only, to out-of-specification water chemistry conditions. Further, EAC in nickel-based alloys has today a major influence on the usability of both PWR's and BWR's. The major life time restrictive phenomenon for core components is cracking due to neutron radiation, irradiation assisted stress corrosion cracking, IASCC. Investigations on the influence of neutron radiation on the microstructure and microchemistry increase the overall understanding of IASCC.

Localisation of plastic deformation and the interaction between strain localisation and oxide film formation are considered to play a key role in EAC and IASCC. Several phenomena, such as dynamic strain ageing, recovery, environmentally enhanced creep, relaxation and dislocation channel formation (especially in internals) can affect localisation of deformation [1]. Understanding of these phenomena is important, e.g., in order to be able to predict and quantify the risk for environmentally assisted cracking in austenitic nuclear materials. These predictions can be used e.g. for selection of reliable criteria for NDE programs. Better mechanistic understanding of EAC and IASCC mechanisms is particularly important in the context of the ageing fleet of existing NPP's and of long lifetimes planned for new NPP's.

Main objectives

The main objectives of the DEFSPEED project were to increase the mechanistic understanding of environmentally and irradiation assisted stress corrosion cracking

(EAC and IASCC) in austenitic nuclear materials, and to educate new experts within this field by performing the tasks described in the following.

Strain localisation in austenitic stainless steels

Super slow strain rate tests, SSSRT's, were employed to investigate crack initiation and especially strain localisation, which is a precursor for crack initiation, of austenitic materials in LWR conditions. The technique was first evaluated using two strain rates ($1 \cdot 10^{-7}$ s^{-1} and $1 \cdot 10^{-8}$ s^{-1}) and two material conditions, i.e., sensitised Type 304 stainless steel with or without 10% cold work by tension. The evaluation work [2–3] showed an increased sensitivity of the test with decreasing strain rate, manifested by a higher amount of intergranular cracking and smaller strain to fracture with decreasing strain rate. Further SSSRT's were performed on pre-deformed non-sensitised stainless steel type AISI 316L in BWR environment. A new test device was also designed and taken into operation during the project.

Of totally 16 specimens made of non-sensitised AISI 316L material, pre-deformed to four different levels of cold work by tension, i.e., 8, 15, 20 and 28%, and further strained to a maximum of 9% in simulated BWR environment, macroscopic cracking was observed in four specimens. Of these, intergranular cracking was observed in one specimen while the cracking mode was transgranular in the other three specimens. The intergranular cracking occurred in a specimen with 15% pre-deformation that was further strained 5.6% at super slow strain rate in BWR simulated environment. The intergranular crack had occurred at the location of strain gage, Figure 1, where the local degree of deformation was obviously high. Once initiated, the crack continued to grow intergranularly in the less deformed material. All the other specimens with cracking had been pre-deformed to a higher degree of cold work, i.e., 20 or 28% and further strained at a super slow strain rate for at least another 5%. This finding further emphasises the role of local deformation and strain gradient on intergranular crack initiation susceptibility [4]. This behaviour has been observed frequently also in field failures.

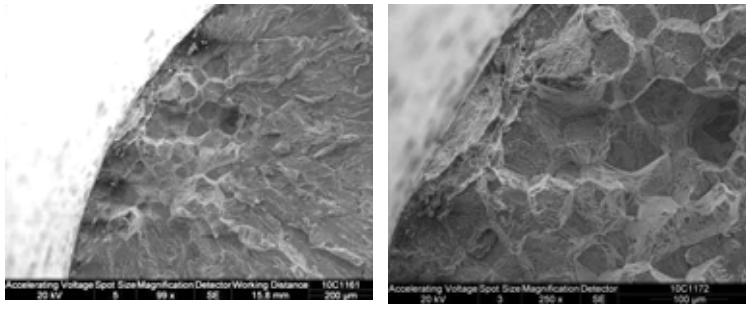

a) b)

Figure 1. SEM-pictures of the fracture surface at the location of crack initiation (a and b) in a 15% pre-deformed AISI 316L SSSRT-specimen strained 5.6% in simulated BWR environment. Intergranular cracking had initiated at the strain gage, where the local degree of deformation was obviously high, resulting in a strain gradient at the surface.

The calibrated [5] electron back-scattered diffraction, EBSD, intra-grain mis-orientation maps from sensitised and non-sensitised stainless steel specimens as well as from a welded pipe section showed a non-uniform distribution of plastic strain. The plastic strains are higher in the vicinity of grain boundaries than inside the grains, Figure 2 and Figure 3, and the distribution is locally non-uniform at the surfaces [6–7]. The non-uniform distribution of plastic strains is affected e.g. by δ-ferrite and by local changes in the grain size. The latter was observed to also influence crack initiation. TEM-investigations [8, 9] showed strain localisation on a sub-micron scale to shear bands, which at low strain rate impinge on grain boundaries, resulting in a bloom of strain in the adjacent grain.

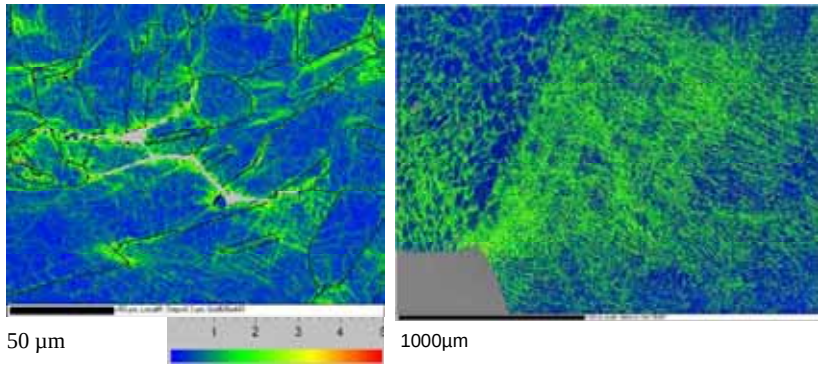

a) b)

Figure 2. EBSD map (a) of a crack tip area in a solution annealed and sensitised Type 304 stainless steel after SSSR-testing in simulated BWR environment and in pipe weld section (b). Localisation of deformation at the grain boundaries and at the fusion line can be observed.

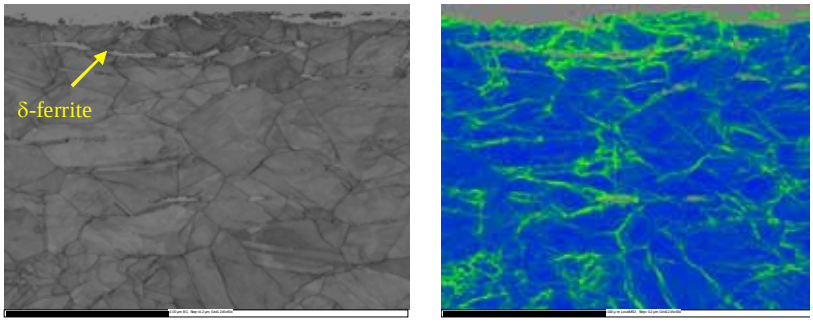

a) b)

Figure 3. Grey scale (a) and EBSD map (b) of the surface of a non-sensitised AISI 316L SSSRT specimen, pre-deformed 20% and further strained 5% in simulated BWR environment. A higher degree of plastic strain is observed in the austenite at the location with a δ-ferrite stringer just below the surface.

Dynamic strain ageing of austenitic nuclear materials

Dynamic strain aging (DSA) is a material phenomenon most commonly associated with the appearance of serrations in tensile stress-strain curves at particular test temperatures. DSA is important for structural stainless steels because it has also been associated with the anomalous evolution of strength and ductility with temperature, both for tensile and fatigue tests. Further, the DSA phenomenon may be important to the overall deformation behaviour of stainless steels as a contributor to strain localisation.

Based on the tensile tests using different strain rates, DSA-maps have been constructed for austenitic stainless steels of Type 304 and 316 and for nickel-based materials Alloy 600 and 690, Figure 4 [10–16]. Serrated yielding starts at a lower temperature in Alloys 600 and 690 (observed between 150 and 600°C) compared to Type 316NG austenitic stainless steel (observed above ~200°C.) Dynamic strain ageing behaviour as manifested by serrated yielding is, thus, observed at LWR-relevant temperatures in all of the above mentioned materials at strain rates below 10^{-4} s^{-1}. The activation enthalpies for DSA onset (120 kJ/mol for the stainless steels and 159 kJ/mol for the Ni-base materials) correspond to the diffusion of interstitials, i.e., nitrogen (in AISI 316NG) and carbon (in Alloy 600), determined using internal friction measurements. From the TEM-studies [17] it was concluded that the diffusive redistribution of interstitial atoms in the DSA regime most likely affected the deformation behaviour of the material by promoting planar slip, which in turn promotes strain localisation [18].

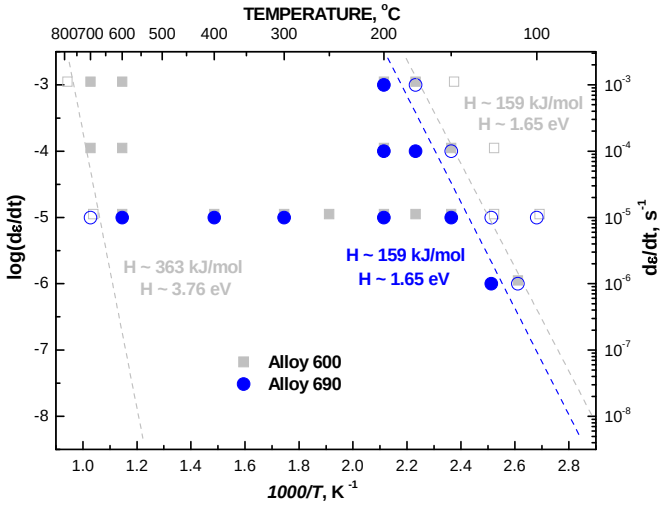

Figure 4. DSA-map for Alloys 600 and 690, where serrated yielding is observed at temperature between 150 and 600°C at strain rates $<10^{-4}$ s^{-1}.

Characterisation of irradiated stainless steels

As the world's fleet of light-water reactor nuclear power plants age, cracks have emerged in core structures which have been exposed to neutron irradiation. An ability to predict the instances and extent of such cracking can enable better assessment of the performance and integrity of reactor core components for safe and economic extension of the operating lifetime of power plants. Conducting transmission electron microscope (TEM) examinations of materials that have been removed from service in real reactors makes an important contribution towards understanding the phenomenon better.

During the course of the DEFSPEED project, analytical TEM examinations have been conducted on a number of different irradiated materials from the Halden project. These included a Type 304 austenitic stainless steel centre filler assembly plate exposed to neutron irradiation in the French Chooz A PWR, from a Type 304L control rod blade from the Barsebäck 1 BWR, and from three cold deformed and irradiated Type 316 stainless steels in irradiated and non-irradiated conditions [19–24]. The dose levels extend from ~1.6 dpa to 30 dpa.

The presence of a high density of dislocation loops was confirmed in all of the materials, a consequence of the fact that the density rapidly saturates at about 1 dpa. However, the median loop diameter ranged from about 3–4 nm at 1.5 dpa, up to 6.7 nm at 30 dpa. Small voids or bubbles were also found within the matrix of

the high dose material, having about 3–4 nm in diameter in the control rod blade material, but 1–2 nm in diameter in the centre filler assembly plate material. The low dose materials had no evidence of such void features. Compositional analyses indicated the expected depletion of chromium at the grain boundaries in the high dose materials, while at 1.5 dpa the difference between Cr composition in the matrix and at the grain boundary was less apparent, Figure 5. There was also a strong tendency for co-segregation of nickel and silicon at the grain boundaries, and in the higher dose materials, also as precipitates in the matrix. Figure 6 shows the silicon segregation.

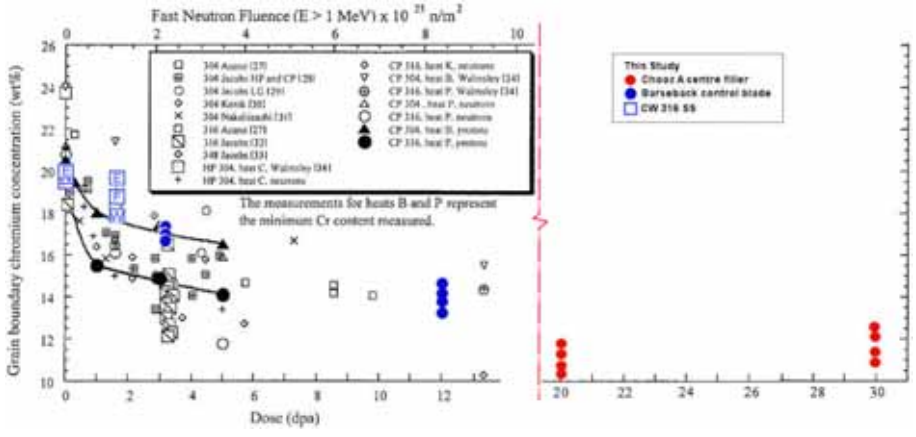

Figure 5. Radiation induced depletion of Cr at the grain boundaries of the irradiated materials of this project, compared to literature data.

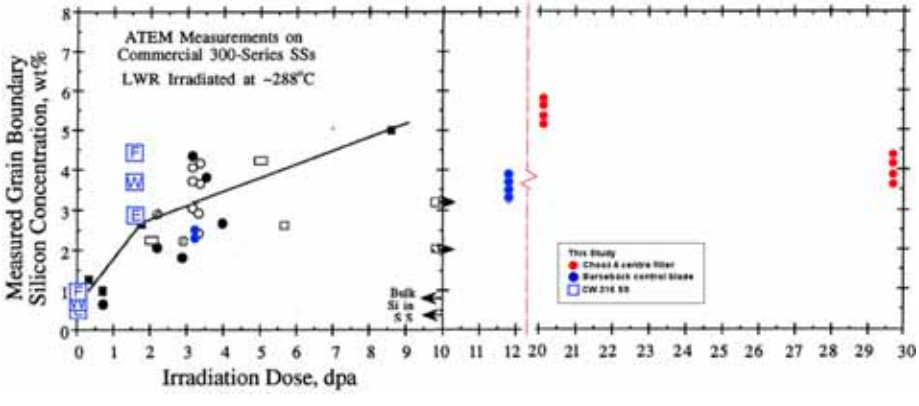

Figure 6. Radiation induced segregation of Si at the grain boundaries of the irradiated materials of this project, compared to literature data.

Influence of the strain rate and environment on fracture toughness properties of austenitic materials

Low Temperature Crack Propagation (LTCP) is a hydrogen-induced degradation mechanism that has been observed in laboratory conditions in nickel-based weld metals of Alloy 182/82 and Alloy 152/52 and in high strength Alloy X-750. LTCP may occur in hydrogenated water, at low temperature, with slow loading rate and high stress in pre-cracked nickel-based materials. The phenomenon occurs especially in the temperature range of 50 to 150°C. LTCP presently has got high interest internationally, and several projects are ongoing on this topic in the USA, Japan and Europe. The work within the DEFSPEED-project was started as a Master of Science work [25] and continued with a broader test matrix. A structural integrity evaluation was also performed using the toughness values obtained.

The influence of environment and strain rate was measured using sub-size specimens prepared from dissimilar metal welds (DMW), where the weld materials were Inconel 52 and 182 and the pure weld metals were made of Inconel 52, 152, 82 and 182. The results reveal a decrease in the fracture toughness of Ni-based weld materials in hydrogenated water at 55°C at low strain rate (0.1 mm/h) [26–28]. The decrease is more remarkable in specimens from pure weld metals than in specimens cut from dissimilar metal welds, Figure 7.

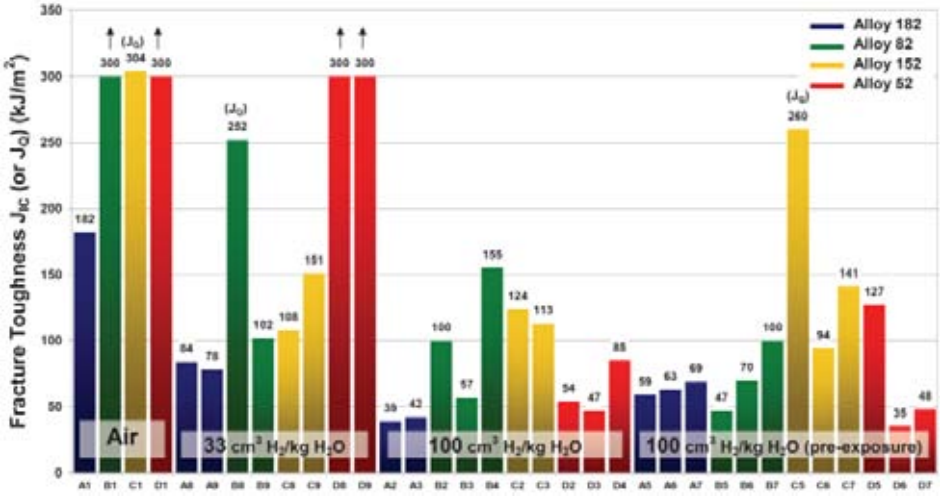

Figure 7. A summary of the J_{IC} (and J_Q) values of all the tested pure weld metal specimens.

A structural integrity analysis in connection with LTCP was performed. The calculation was performed for a nozzle/safe-end joint made of Alloy 182 with a postulated axial half-elliptic crack on the inner surface. Two cases were considered, i.e., shut-down and emergency cool-down situations. The transient heat transfer and stress/strain distributions through the DMW wall were calculated, also taking into account the weld residual stress distributions. Then the crack sensitivity analyses were performed using both analytical equations and a fracture mechanics based analysis code VTTBESIT. The considered limiting criterion was the crack tip value of mode I J-integral, J_I, reaching the corresponding fracture toughness, J_{IC}. For all studied analysis cases, the critical crack sizes are relatively large, e.g. in the depth direction from 52 to 98% of the wall thickness, which was assumed as 40 mm [29].

International co-operation and education

Education of new experts in the field of nuclear materials is an important objective for all SAFIR2010 projects, so also for the DEFSPEED project. Young persons, as students, researchers and technicians, worked within the DEFSPEED-project. Through active participation in international expert working groups and conferences, the latest international knowledge was brought to Finland, where it is then utilised in research projects as well as in conducting failure analyses and other customer work. The international meetings also have an important educational aspect.

As a tool for knowledge transfer, a digital report archive was built containing all VTT reports written on nuclear materials over the years. New reports are added to this archive as they become available.

Applications and conclusions

Non-homogeneous microstructures always occur in welded structures and materials fabricated by different methods and subjected to complex strain paths. Investigations on strain localisation are important e.g. for old plants with respect to life extension and increased power outputs, but also for new components utilized in modernisations and new builds. Materials having non-homogeneous microstructures do not deform uniformly, even though engineering design often assumes uniform deformation. Mechanistic understanding and data on different phenomena are important for enabling prediction and quantification of the risk for environmentally assisted cracking in austenitic materials in BWR’s and PWR’s.

Such predictions can be used for guiding the selection of reliable criteria for NDE programs. It is also needed when trying to understand and predict the very long incubation times for crack initiation, as observed e.g. for Ni-based materials in operating power plants. The increased knowledge on EAC is particularly useful when conducting failure analyses on plant components. The influence on non-homogeneous microstructures on localisation of deformation on a macroscopic and microscopic level was shown in the performed investigations. The non-homogeneous localisation of deformation was also observed to affect EAC crack initiation.

Conducting transmission electron microscope (TEM) examinations of materials that have been removed from service in real reactors makes an important contribution towards better understanding the role of irradiation in promoting EAC and IASCC. This information could possibly also be used for evaluation of a need for adjustments of chemical composition requirements for materials for new internals. The performed investigations have added novel data on defect structures and radiation induced grain boundary segregation in stainless steels subjected to neutron irradiation.

Knowledge and data on the influence of environment on the behaviour of nuclear materials is important for the structural integrity assessment of nuclear components. In this project, the behaviour of nickel-based materials in hydrogenated environments was investigated and the level of the degradation of fracture toughness properties in hydrogenated environment was measured. An example of the influence of the degraded fracture toughness properties on the structural integrity of a safe-end structure was evaluated. Such results are also important for optimisation of water chemistry, especially during shut-down, in order to avoid situations where the risk for LTCP may occur.

The report data base created in this project will ease knowledge transfer and assist in avoidance of reinventing problems, increase plant life management and safety of power plants.

References

1. Ehrnstén, U. & Hänninen, H. Environmentally Assisted Cracking of Non-sensitised Stainless Steels – Possible Affecting Phenomena. Fontevraud 6, Contribution of Materials Investigations to Improve the Safety and Performance of LWRs. Fontevraud Royal Abbey, France, 18–22 Sept. 2006. French Nuclear Energy Society, SFEN, 2006. Pp. 1–10.

2. Taivalaho, L. Nanoprobe work on sensitized AISI 304 material used in the DEFSPEED project. VTT, Espoo, 2008. VTT Research Report VTT-R-01544-08. 22 p.

3. Ehrnstén, U. Interim report on Super Slow Strain Rate Tests of Austenitic Materials in Nuclear Environments – Report on Work Performed in 2007. VTT, Espoo, 2008. Research Report VTT-R-00795-08. 25 p.

4. Ehrnstén, U., Karlsen, W., Saukkonen, T. & Hänninen, H. Deformation localisation and crack initiation in austenitic stainless steels. This seminar.

5. Saukkonen, T. & Hänninen, H. Determination of Calibration Curves for Measuring Plastic Strain by EBSD in AISI 316 and AISI 304 Stainless Steel Power Plant Materials. Work Report for the DEFSPEED project. 12 p.

6. Ehrnstén, U., Saukkonen, T., Karlsen, W. & Hänninen, H. Deformation localisation and EAC in inhomogeneous microstructures of austenitic stainless steels. 14th Symposium on Environmental Degradation of Materials in Nuclear Power Systems – Water Reactors. Virginia Beach, Virginia, USA, 23–27 August, 2009. 10 p.

7. Saukkonen, T., Ehrnstén, U. & Hänninen, H. Microstructure and Plastic Strain Distribution in an AISI 304 Stainless Steel Power Plant Pipe Weld Studied by EBSD. Royal Microscopical Society, 15th Electron Backscatter Diffraction Meeting, 31 March – 1 April 2008, University of Sheffield, England. 16 p.

8. Karlsen, W. Deformation microstructures of super-slow strain rate tested austenitic stainless steel. VTT, Espoo, 12.06.2009. Report VTT-R-04205-09. 15 p.

9. Pakarinen, J. TEM study of the effect of prior cold work on the deformation microstructures of SSSRT tested AISI 316 stainless steel. VTT, Espoo, 2011. Report VTT-R-00321-11.

10. Ehrnstén, U., Ivanchenko, M., Nevadacha, V., Yagodzinskyy, Y., Toivonen, A. & Hänninen, H. Dynamic Strain Ageing of Nitrogen-alloyed AISI 316L Stainless Steel. Proc. of Eurocorr 2004, Nice, France, 13.–16.9.2004, Event No. 226. 10 p.

11. Ehrnstén, U., Ivanchenko, M., Nevdacha, V., Yagodzinskyy, Y., Toivonen, A. & Hänninen, H. Dynamic Strain Ageing and EAC of Deformed Nitrogen-Alloyed AISI 316 Stainless Steels. 12th Symposium on Environmental Degradation of Materials in Nuclear Power Systems – Water Reactors, TMS, 2005. Pp. 1475–1482.

12. Hänninen, H., Ivanchenko, M., Yagodzinskyy, Y., Nevdacha, V., Ehrnstén, U. & Aaltonen, P. Dynamic Strain Ageing of Ni-base Alloys Inconel 600 and 690. 12th Symposium on Environmental Degradation of Materials in Nuclear Power Systems – Water Reactors, TMS, 2005. Pp. 1423–1430.

13. Ivanchenko, M., Yagodzinskyy, Y. & Hänninen, H. Effect of Plastic Deformation on Anelastic Mechanical Losses in Multicomponent Substitutional Austenitic Alloys. Materials Science and Engineering A 2006, 442, pp. 458–461.

14. Ivanchenko, M., Yagodzinskyy, Y. & Hänninen, H. Effect of DSA on Interstitial Redistribution in AISI 316NG steel and Inconel 600 Alloy. Proceedings of Third Nordic Symposium for Young Scientists in Metallurgy, TKK, Espoo, Finland, May 14–15, 2008. HUT, Faculty of Chemistry and Material Science, Department of Material Science and Engineering, Multiprint Oy, Espoo, 2008. Pp. 68–71.

15. Ivanchenko, M., Yagodzinskyy, Y., Ehrnstén, U., Karlsen, W. & Hänninen, H. Manifestations of DSA in Austenitic Stainless Steels and Inconel Alloys. 20th International Conference on Structural Mechanics in Reactor Technology (SMiRT 20), Espoo, Finland, August 9–14, 2009.

16. Ivanchenko, M., Yagodzinskyy, Y., Hänninen, H. & Ehrnstén, U. Dynamic Strain Ageing of Ni-base Alloy Weld Metals in Comparison to Alloy 600 and 690. 14th Symposium on Environmental Degradation of Materials in Nuclear Power Systems – Water Reactors. Virginia Beach, Virginia, USA, 23–27 August, 2009.

17. Karlsen, W., Ivanchenko, M., Ehrnstén, U. Yagodzinskyy, Y. & Hänninen, H. Microstructural Manifestation of Dynamic Strain Ageing in AISI 316 Stainless Steel. Journal of Nuclear Materials 2009, Vol. 395, pp. 156–161.

18. Ivanchenko, M. Dynamic Strain Aging of Austenitic Stainless Steels and Ni-Base Alloys. TKK Dissertations 248. Engineering and Architecture, November 2010. 90 p. + app. 38 p. URL:http://lib.tkk.fi/Diss/2010/isbn9789526034454/.

19. Karlsen, W., Dohi, K. & Onchi, T. Observation of channel deformation in mildly-deformed, low-dose 304L austenitic stainless steel. Proceedings of 13th Symposium on Environmentally Degradation on Materials in Nuclear Power Systems-Water Reactors. Whistler, B.C., Canada, August 19–23, 2007. Canadian Nuclear Society, CNS, 2007.

20. Karlsen, W. Examination of Dynamic Strain Ageing Microstructures in 316 Stainless Steel by TEM. VTT, Espoo, 2007. Research Report VTT-R-10235-07. 10 p.

21. Karlsen, W. & Aaltonen, P. FEGSTEM Study of 12 dpa Barsebäck 304L and 20 dpa and 30 dpa Chooz A 304 SS. VTT, Espoo, 2007. VTT Research Report VTT-R-01215-07. 14 p.

22. Karlsen, W. Characterisation of LWR Irradiated Stainless Steel Internal Components by FEG-STEM. VTT, Espoo, 2007. VTT Research Report No VTT R-07773-07. 14 p.

23. Karlsen, W. Grain Boundary Analyses of 30 dpa Chooz A 304 SS Centre Filler Assembly. VTT, Espoo, 2008. VTT Research Report VTT-R-01344-08. 13 p.

24. Karlsen, W. TEM characterization of three non-irradiated CW316 stainless steels. VTT, Espoo, 1.6.2010. Research Report VTT-R-03736-10. 18 p.

25. Ahonen, M. Ympäristön ja muodonmuutosnopeuden vaikutus austeniittisten materiaalien murtumisvastuskäyttäytymiseen. VTT, Espoo, 2008. Tutkimusraportti VTT-R-06172-08. 64 p. (In Finnish.)

26. Ahonen, M. Effect of Hydrogenated Low Temperature Water on Fracture Toughness of Nickel Based Weld Metals. VTT, Espoo, 2007. 29.01.2010. VTT Research report VTT-R-00474-10. 45 p.

27. Ahonen, M., Ehrnstén, U. & Hänninen, H. Effect of hydrogenated low temperature water on fracture toughness of nickel-based weld metals. Baltica VIII. Life Management and Maintenance for Power Plants. Vol. 1. Auerkari, Pertti & Veivo, Juha (Eds.). VTT, Espoo, 2010. VTT Symposium 264. Pp. 372–383.

28. Ahonen, M., Ehrnstén, U. & Hänninen, H. Low temperature crack propagation of nickel-based weld metals in hydrogenated PWR primary water. Fontevraud 7, Contribution of materials investigations to improve the safety and performance of LWRs, 26–30 September, 2010. Avignon, France. Fontevraud, 2010. 11 p.

29. Cornvall, O. Structural Integrity Study Concerning LTCP Phenomenon. VTT, Espoo, 17.01.2011. VTT Research report VTT-R-00055-11.

27.2 Deformation localisation and EAC in inhomogeneous microstructures of austenitic stainless steels

Ulla Ehrnstén, Wade Karlsen and Janne Pakarinen,
VTT

Tapio Saukkonen and Hannu Hänninen
Aalto University School of Engineering

Abstract

Inhomogeneous microstructures, e.g. grain size, dislocation density etc., always occur in welded structures. Varying manufacturing methods leading to complex strain paths result in highly varying cold work and consequent residual strains. The role of strain localisation is probably playing a key role as a precursor for crack initiation but its mechanisms are still not fully known. If strain localisation occurs by a creep mechanism, the incubation time for crack initiation can be very long, as frequently observed in NPPs.

EBSD employed to measure strain distributions in a Type 304 austenitic stainless steel weld shows a high variation in residual strain distribution, which was verified by hardness measurements as well as with residual stress measurements. Strain localisation investigations were also performed on specimens from Super Slow Strain Rate Test (SSSRT) using a very slow strain rate of $1 \cdot 10^{-8}$ s^{-1}. This is in the creep strain rate range, where diffusion along dislocation cores and grain boundaries occur together with grain boundary sliding. SSSRT's were performed in simulated BWR environment on sensitized Type 304 and non-sensitised Type 316L austenitic stainless steel either with or without cold deformation. Local variation in the amount of surface cold-work affects crack initiation. Local variations of grain size also affect strain localisation. During crack growth, strain localisation occurs at grain boundaries ahead of the crack tips.

Introduction

Intergranular stress corrosion cracking (IGSCC) of sensitized stainless steels in oxidising boiling water reactor (BWR) environments caused major capacity factor losses in the 1970 and 1980's. Large research programs to solve the problem were launched, major factors contributing to the problem were identified

and quantified, and remedial actions were taken. Consequently, the amount of IGSCC in sensitised stainless steels decreased remarkably. The remedial actions included development and employment of low-carbon stainless steels, new welding techniques decreasing the residual stresses and eliminating sensitisation, as well as improvement of the water chemistry with different measures. More recently, the role of cold-work in promoting IGSCC has gained more broad attention. This is due to the observation that non-sensitised, low carbon stainless steels can also suffer from IGSCC, and that this type of cracking is connected to cold working. Also, the observed risk for IGSCC in PWR conditions has added to the importance of understanding EAC initiation better.

Localisation of plastic deformation and the interactions between oxidation and strain localisation are most probably playing a key role in the cracking of sensitised as well as non-sensitised, cold-worked stainless steels. Localisation of deformation can be affected by several phenomena, such as dynamic strain ageing, environmentally enhanced creep, dynamic recovery and relaxation. All these can also be influenced by cold deformation. Cold deformation, i.e., deformation below the recrystallisation temperature, occurs due to welding, grinding, machining, forging etc. Some degree of cold deformation is unavoidable in, e.g., HAZ's, as manifested by increased hardness and dislocation density as well as residual stresses and strains. The influence of cold deformation is, on the other hand, dependent on factors such as the degree of deformation, the deformation temperature, strain rate, strain path, alloy composition, etc. The particular deformation temperature is important because it dictates the means of transmitting strain, and thereby the predominant deformation mechanism during dynamic loading. Low temperatures typically promote displacive transformation, but higher temperatures clearly promote slip, since dislocation motion is a thermally activated process. Higher temperatures also increase the vacancy concentration and diffusion rates of vacancies, and, thus vacancy-accelerated dislocation climb is more prominent with increasing temperature. Likewise, dislocation movement leads to dynamic recovery in the material by the annihilation of dislocations of opposite sign. That has an effect of reducing the number of dislocations, which counteracts strain hardening. Time also affects the kinetics of dislocation-related deformation mechanisms. For that reason, the rate of loading can have a significant effect on the consequent mode of strain transmission, and/or on the stress at which straining occurs.

Of particular interest to crack initiation is the heterogeneity of deformation within a material. As a consequence of processes such as post-weld material

shrinkage or surface machining or grinding, local cold work alters the local material condition. This can lead to a non-uniform deformation response on a local scale. On a still finer scale, heterogeneous deformation can occur in a multi-grain material due to the randomness of the lattice orientation with respect to the critical resolved shear stress. As some grains are more suitably oriented for deformation, they undergo more deformation than their neighbouring grains, resulting in a heterogeneous distribution of local strain. Strain may also be localised within a single grain, as a consequence of the formation of shear bands.

A mechanistic understanding of the effects of plastic deformation on IGSCC is important, especially as the trend in NDE inspection strategy is towards risk-informed inspection. A mechanistic understanding is also important in order to increase the understanding of the possible risk for IGSCC in PWR-plants, and for increased understanding of the reasons of the typically very long incubation times for crack initiation.

Material and experimental methods

The investigations focused on studies of localisation of deformation was comprised of characterisation of residual strains using electron back-scattered diffraction, EBSD, of specimens made of sensitised Type 304 and non-sensitised Type 316L stainless steels after super-slow strain rate testing in simulated BWR environment. The results were compared to the results from residual strain and stress measurements on a nuclear weld. The deformation structures were also investigated using transmission electron microscopy, TEM.

Super-slow strain rate tests in simulated BWR environment

The chemical composition of the two stainless steel materials used for SSSRT's is presented in Table 1. The tests used round tensile type specimens with a ∅4 mm gauge region 12 mm in length.

Table 1. Chemical composition of the stainless steels.

Material	C [%]	Si [%]	Mn [%]	P [%]	S [%]	Cr [%]	Mo [%]	Ni [%]	N [%]
Type 304	0.048	0.45	0.75	0.030	0.011	18.4	0.22	11.1	0.037
Type 316L	0.03	0.48	1.75	0.031	0.029	16.72	2.00	10.16	0.055

The sensitised material was from the same high carbon material as used for the residual strain and stress measurements. It was tested with and without pre-deformation, at two strain rates, i.e., $1 \cdot 10^{-7}$ s^{-1} and $1 \cdot 10^{-8}$ s^{-1}. The non-sensitised Type 316L material was pre-deformed to four different levels, i.e., 5, 15, 20 and 28%, and was strained in simulated BWR environment at the slower strain rate only. All the specimens made from sensitised stainless steel were strained to fracture, while the non-sensitised SSSRT specimens were mainly strained to ~5% in BWR environment. One set of specimens was tested in two phases, first 5% and if no macroscopic cracking was observed, additional straining of < 4%, was applied. The non-sensitised specimens were tested in either as-machined or in polished condition. Pre-deformation was made by tension at room temperature.

Experimental results

Results from measurements of local strain distribution in a Type 304 nuclear weld

The EBSD-measurements across a whole weld revealed that the highest degrees of plastic strain (10–20%) were found in the heat affected zone (HAZ), close to the root area of the weld, Figure 1a. This highly deformed zone extended 5–7 mm from the fusion line to the base material. In the HAZ, localisation of strain at the grain boundaries was also observed. In the weld, strain localisation at the weld bead and dendrite boundaries was observed. The amount of plastic strain in the base material decreased towards the outer surface of the pipe. The strain values obtained by hardness measurements, which are easy to perform on e.g. field failure components, were in fairly good agreement with the EBSD results.

The residual strain measurements correlate well with results of residual stress measurements made using the Contour method, Figure 1b. The residual stress decreases towards the outer surface of the pipe, where it is mainly compressive.

Super-slow strain rate test results

Intergranular cracking (IG) was obtained in all SSSRT specimens made of sensitised type 304 SS. The results showed an increased sensitivity of the slow strain rate test with decreasing strain rate, manifested by a higher amount of intergranular cracking (46% vs. 36% for sensitised material) and smaller strain to fracture (3% vs. 7% for sensitised material) with decreasing strain rate. The

results also showed the detrimental influence of deformation manifested by a higher amount of intergranular cracking in specimens that had been cold deformed 10% before the SSSR-testing (90% IG in cold deformed specimen and 46% IG in non-cold-deformed specimen). Both crack initiation and growth was intergranular, and small steps were typically observed at the crack mouths, indicating a shear strain component, Figure 2.

Of a total of 16 specimens made of non-sensitised Type 316L material, macroscopic cracking was observed in four specimens. Of those, intergranular cracking was observed in one specimen, while in the other three specimens the cracking mode was transgranular environmentally assisted cracking. The macroscopic intergranular cracking occurred in a specimen having 15% pre-deformation that was further strained 5.6% at the super-slow strain rate in simulated BWR environment. The intergranular crack had occurred at the location of strain gauge contact, Figure 2b, where the local degree of deformation was obviously high, as was the strain gradient at the surface. Once initiated, the crack continued to grow intergranularly in the less deformed material. All the other specimens with macroscopic cracking had been pre-deformed to a higher degree of cold work, i.e., 20 or 28% and further strained at least 5% at the super-slow strain rate. This finding further emphasises the roles that local deformation and a strain gradient have on intergranular crack initiation susceptibility. This behaviour has also been frequently observed in field failures.

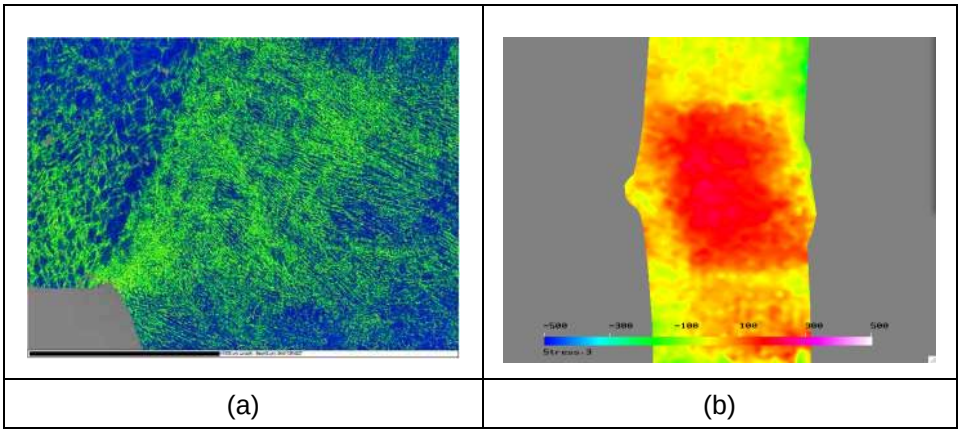

Figure 1. Local lattice mis-orientation map from the fusion line area of the weld root in a nuclear weld made of Type 304 austenitic stainless steel (a) and the residual stresses in the same weld (b).

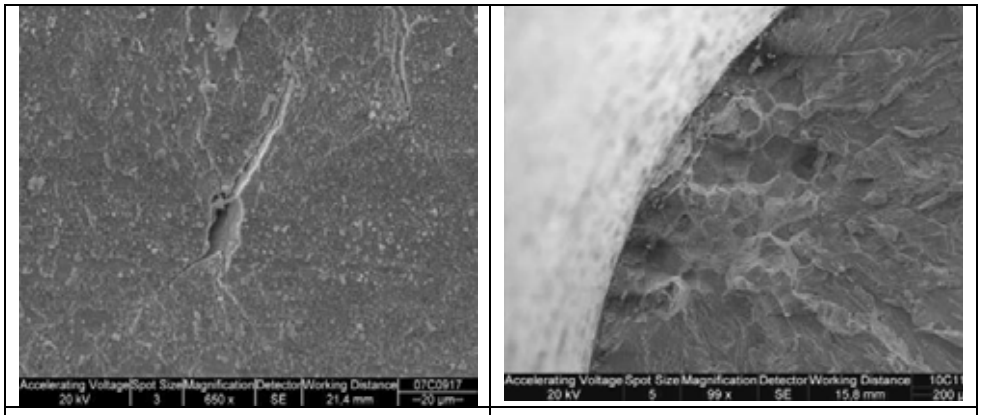

(a) (b)

Figure 2. Intergranular crack initiation was observed in sensitised Type 304 SS, with indications of a shear strain component (a). Intergranular cracking was also observed in non-sensitised Type 316L SS (b). The local deformation from the strain gauge has obviously affected initiation.

Oxide layer cracking is considered to be a prerequisite for crack initiation. Surface cracking was found in all the investigated SSSRT specimens when examined by SEM. Such small features are challenging to investigate further by SEM, but additional information can be gained by utilizing focussed ion beam, FIB, to make a micro-section of the crack. As seen in Figure 3, the cracks can be restricted only to the oxide layer, and not necessarily result in EAC crack initiation in the substrate (alloy) below.

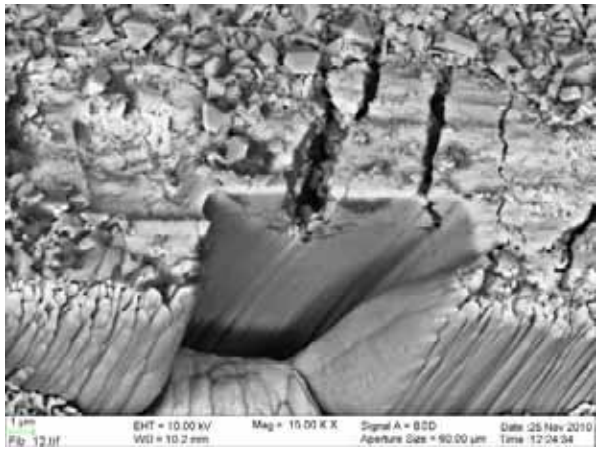

Figure 3. FIB milled micro cross section imaged by using FEG-SEM. The surface crack in the oxide seems to stop at the oxide-metal interface.

Results from electron backscattered diffraction, EBSD, investigations

The results from the EBSD investigations show non-uniform distribution of plastic strains in specimens made from sensitised and non-sensitised stainless steel, with higher plastic strains in the vicinity of grain boundaries than inside the grains, Figure 4. Non-uniform distribution of the plastic strains was also observed at the surface of the specimens, indicating local strain gradients. The local strain distributions at the surface seem to affect the location of crack initiation, which would occur at the location with the smallest degree of local strain. Also the local differences in grain sizes in the sensitised stainless steel affected the strain distribution, being higher in the region with smaller grain size compared to a neighbouring area with larger grain size, Figure 5. Intergranular cracks with a length on the order of one grain, without further crack growth, were seen in some specimens, Figure 4b. Thus, very short crack formation, although being a prerequisite for cracking, does not necessarily lead to crack growth in all cases.

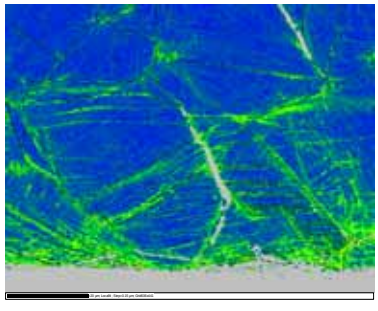

20 µm
(a)

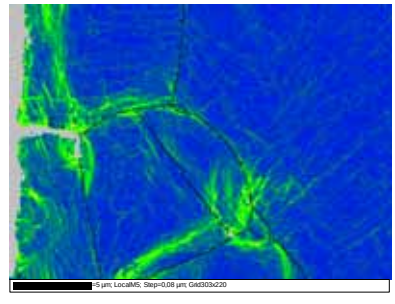

20 µm
(b)

Figure 4. Mis-orientation maps close to the surface of SSSRT specimens showing less strain at the location of the crack initiation site compared to the immediate surrounding, and preferential strain at the grain boundaries in both sensitised (a) and non-sensitised stainless steel (b).

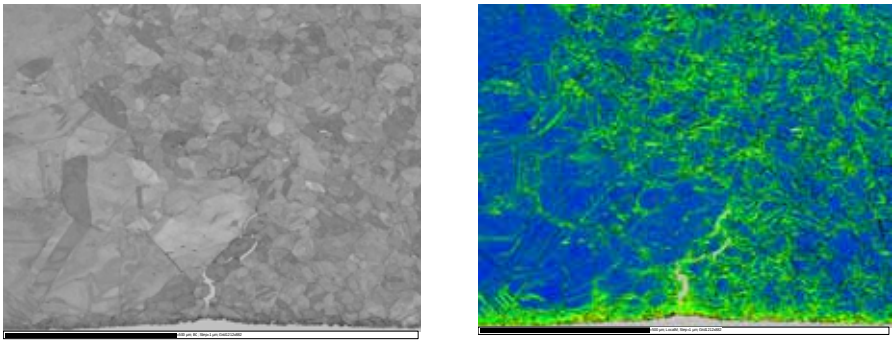

Figure 5. Pattern quality map (a) and local mis-orientation map (b) close to the surface of a non-cold-worked SSSRT specimen, showing more strain in the area with smaller grain size compared to that with larger. The strain is localised at the grain boundaries.

Transmission electron microscopy results

The TEM results revealed several differences between the materials, depending upon the prior cold-work, strain rate and proximity to the fracture surface. The most obvious differences were evident between the specimens which had been cold-worked and those which were not. The cold-worked material had a much higher density of dislocations, arranged in a cellular structure, while the lower density of dislocations in the non-cold-worked material was arranged in a planar structure, Figure 6. The materials strained at $1 \cdot 10^{-7}$ s^{-1} differed in a similar way. The uniformly-elongated region of the materials did not exhibit much difference as a function of strain rate. Close to the fracture surface, the accumulation of further strain had promoted cell size reduction in the cold-worked material. Of particular interest was that, at the lower strain rate, strain was localised to shear bands, and when those shear bands impinged on a grain boundary, a bloom of strain was formed in the adjacent grain, Figure 7.

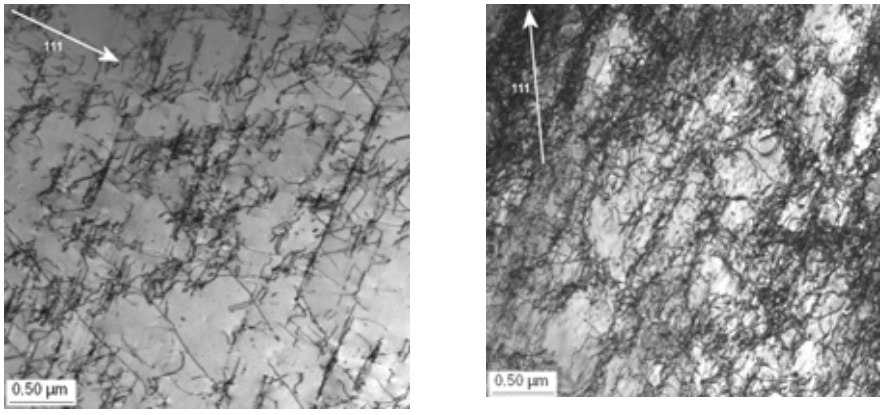

(a) (b)

Figure 6. The microstructures of the non-cold-worked (a) and cold-worked (b) Type 304 stainless steel after straining at $1 \cdot 10^{-8}$ s^{-1} show clear differences. The dislocations in the cold-worked material are arranged in a cellular structure, while the lower density of dislocations in the non-cold-worked material is arranged in a planar structure.

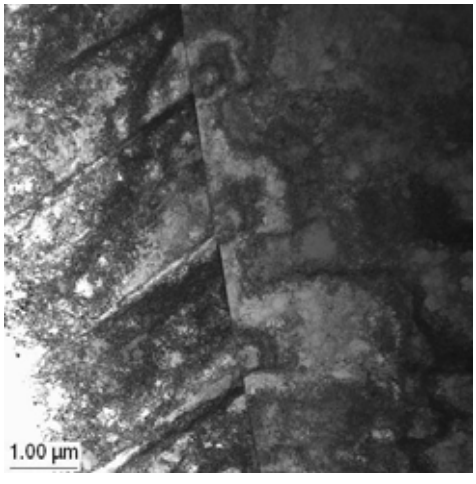

Figure 7. TEM-picture showing shear bands impinging on a grain boundary, producing a bloom of strain in the adjacent grain. The specimen is sensitized and 10% cold-worked Type 304 stainless steel and strained at $1 \cdot 10^{-8}$ s^{-1} in simulated BWR environment.

Discussion

The results from the super-slow strain rate tests on deformed and non-deformed sensitised Type 304 austenitic stainless steel showed an increased sensitivity of the test with decreasing strain rate, manifested by a higher amount of intergranular

cracking and smaller strain to fracture with decreasing strain rate. It also revealed a detrimental influence of prior deformation. Crack initiation is affected by local inhomogenities in the material, e.g. differences in grain size and surface deformation resulting in residual strain gradients. This was also observed in non-sensitised and pre-deformed Type 316L stainless steel, where macroscopic intergranular cracking was observed in a specimen where the strain gauge had resulted in heavy local deformation at the location of initiation. The detrimental effect of cold-work is well known. What is less known is the influence of strain gradients and its influence on crack initiation through localisation of deformation. Further investigations are needed e.g. to understand the importance of absolute levels of deformation compared to gradients, e.g., the influence of a scratch in a polished surface compared to one in a moderately machined surface.

The investigations of a typical nuclear power plant weld showed inhomogeneous distribution of residual strains and stresses both at a macroscopic and microscopic level. On a macroscopic level, higher residual stresses and strains were measured in one of the two HAZ's. The evolution of residual stresses and strains during welding is a result of several parameters, including the position of the welding torch, the stiffness of the component (which changes with the amount of weld passes), the interpass temperature, etc. A non-homogeneous distribution of the residual stresses and strains in the HAZ's on each side of a weld is typical. On a microscopic level strain localisation at grain boundaries was observed. Residual strains were also observed in the weld metal, indicating that a driving force for crack growth exists in the weld, although weld cracking is not typically observed in NPPs. The EBSD-measurements on sensitized Type 304 stainless steel SSSRT specimens revealed non-uniform deformation, with higher plastic strains in the vicinity of grain boundaries than inside the grains and non-homogeneous strain distribution both next to the surface of the specimens and inside the material.

The TEM results showed differences between the materials, depending on prior cold-work, strain rate and proximity to the fracture surface. Localisation of deformation was observed through observations of shear bands. When shear bands terminate at a grain boundary, and the orientation of the neighbouring grain restricts effective strain transmission, an increase in the local stress occurs, as indicated by the strain blooms observed in the adjacent grain in a specimen tested in simulated BWR environment at the super slow strain rate of $1 \cdot 10^{-8}$ s^{-1}. This can also be the reason for the EBSD observations showing higher strains in one of two neighbouring grains.

Considering a material comprised of grains of random orientation, there is always a level of heterogeneity imposed by the differences in the local critical resolved shear stress superimposed on the macroscopic strain distribution within the material. The combination of strain heterogeneity both at the multi-grain level, and via shear bands within the grains, would most likely enhance the local residual stresses. Thus, the residual stresses arising locally from pre-straining of the materials of real components can be expected to be an important precursor to crack initiation.

In the presence of an aqueous environment there is additionally the possibility for corrosion processes to take place. From a deformation standpoint, of particular interest is the possibility that corrosion processes at the material surface can result in the injection of additional vacancies into the material locally. These corrosion-produced vacancies interact with dislocations, enhance dislocation mobility and can produce increased creep rates locally and, thus, further enhance localisation of deformation.

Non-homogeneous microstructures always occur in welded structures and materials fabricated by different methods and subjected to complex strain path. This non-homogeneity results in inhomogeneous strain and stress distribution, which obviously affect both crack initiation and growth.

Acknowledgments

The DEFSPEED project was financed by VYR (State Waste Management Fund), VTT and the Swedish Radiation Safety Authority. The Contour measurements were performed in PULU project financed by Tekes and TVO.

References

1. Ehrnstén, U., Saukkonen, T., Karlsen, W. & Hänninen, H. Deformation localisation and EAC in inhomogeneous microstructures of austenitic stainless steels. 14th International Conference on Environmental Degradation of Materials in Nuclear Power Systems – Water Reactors, Virginia Beach, Virginia, USA, August 23–27, 2009.American Nuclear Society 2009,Vol. 2. Pp. 910–919.

2. Pakarinen, J. TEM study of the effect of prior cold work on the deformation microstructures of SSSRT tested AISI 316 stainless steel. VTT, Espoo, 2011. Report VTT-R-00321-11.

28. Renewal of Active Materials Research Infrastructure (AKTUS)

28.1 AKTUS summary report

Seppo Tähtinen
VTT

Abstract

The objectives of this study is to carry out a survey on present and future technical needs of active materials research and testing facilities at VTT. This survey will be the basis for the engineering design for the infrastructure and technical testing facilities.

Introduction

The study is urgent due to the renovation work and needs in the present location at VTT. The present infrastructure and main part of the facilities have been built in the 1970's and are, thus not technically up to date and the infrastructure is not fully serving all the requirements needed to enable fulfilment of today's tasks. Further the needs of operating nuclear power plants today have changed from the start of the nuclear technology in Finland and the construction of new plants will also generate new needs to assure long term demand for nuclear specific infrastructure.

The nuclear specific infrastructure is essential in the nuclear safety research and in providing support for the nuclear power plants and for the authority as well. The possibility to handle activated materials, mainly structural materials, will also promote efficiently education and training of new experts in the field.

Main results

The survey on the present infrastructure and research facilities at VTT identified following basic functions and research topics.

- Mechanical, microstructural and fracture mechanical characterisation of active structural materials (e.g., hot cells)
- Radiochemistry
- Nuclear waste deposition
- Dosimetry and other experimental work linked to nuclear technology (e.g. development of γ-scanning technology for the JHR MTR programme of CEA and European consortium)
- First wall material research for Fusion technology programmes
- Iodide filter measurements
- Support functions for FiR1 test reactor.

Additionally there are a substantial number of people carrying out modelling work on reactor physics, fuel performance, nuclear waste, fusion technology both at VTT and Aalto University. The number of persons working in the nuclear field at VTT is about 130–140 persons and the estimated turnover is about 18 M€ per year.

It is foreseen that in the near future the demand for national nuclear research services will increase or at least remain at the present level. This assumption is based on the following points, e.g., aging of present nuclear power plants, construction of OL3 plant, decisions on new nuclear power plants, building of nuclear waste repository plant, implementation of EU SET plan, participation in Jules Horowitch Reactor project and in several international R&D programmes, i.e., OECD Halden project, Gen4 and fusion projects.

Survey on European hot cell capabilities

During past decades several hot cell facilities in EU have been closed, renovated or completely rebuild. These rearrangements have often been connected with shutdowns of the nuclear research reactors as in the case of CEA Grenoble, Forschungszentrum Julich (FZJ), Karlsruhe Technology Institute (KIT) and Risø National Laboratory. These major rearrangements of nuclear research activities

particularly in France and Germany have also resulted in more focused responsibilities between different laboratories particularly when it concerns material or fuel research. In France new hot cell facilities at CEA Saclay and EdF Chinon concentrates only on material research and research on fuel is concentrated in CEA Cadarache and Marcoule. Fuel and waste research in Germany concentrates in Joint Research Centre Institute for Transuranium Elements (JRC ITU) whereas safety related material research is carried out at Forscshungzentrum Rossendorf (FZR) and fusion material research at renovated hot cells at FZJ and KIT. It is also noted that in United Kingdom all nuclear services has been concentrated into the National Nuclear Laboratory (NNL) which have build a new nuclear research facility at Sellafield where also existing material hot cells have been renovated.

The FP6 HOTLAB project in 2006 has made an inventory of the present research capabilities of several European hot laboratories available within Europe. Following an agreement with the IAEA, the HOTLAB PIE and transport casks catalogue, were integrated in the IAEA PIE Database in 2008. The merged data are kept at the iNFCIS website http://www-nfcis.iaea.org and are jointly managed by the IAEA and the HOTLAB working group.

Conceptual engineering design for new infrastructure

VTT have subcontracted conceptual engineering design for new building where all nuclear research activities at VTT are concentrated. The boundary value for conceptual engineering design was chosen as the large concept, i.e., 9 hot cells with 150 persons, which was based on the results of the previous survey on requirements. Special emphasis was taken on radiation safety, e.g., material handling, waste disposal and laboratory design and constructions. The result of the conceptual engineering design is a new building where office, laboratory and hot cells facilities form separate sections. The builder and owner of the new building will be Senaatti-kiinteistöt Oy and VTT will rent the facilities.

The present status of the project of the renewal of the nuclear infrastructure at VTT is in the decision making process concerning all parties in question.

29. Service Life Management System of Concrete Structures in Nuclear Power Plants (SERVICEMAN)

29.1 SERVICEMAN summary report

Erkki Vesikari, Liisa Salparanta and Kim Calonius
VTT

Esa Turunen
ÅF-Consult Oy

Abstract

The main objective of the project was to develop a service life management system for concrete structures in nuclear power plants. The service life management system consists of a service life management tool for the design of maintenance, repair and renovation (MR&R) of structures over the design period and supplementing risk and structural analyses to consider especially the safety aspects. By the service life management system the safety, performance and serviceability are secured during the operational life of the plant.

Introduction

The service life management system for concrete structures in nuclear power plants (ServiceMan) was developed in VTT together with the Finnish power companies, TVO and Fortum. By the management system it is possible to conduct systematic maintenance policy and to plan, organize and optimize the maintenance strategy of concrete structures in NPPs.

The actual service life management system includes:

- Database and tool for service life management. The service life management tool includes prediction of degradation in structures, guarding of safety limits, timing of condition assessments, timing and specification of MR&R actions, and evaluation of life cycle costs and environmental impacts.
- In-service operations of the service life management system are:
    - Implementation of condition assessments for structures,
    - Implementation of maintenance and repair actions, and,
    - Updating the degradation models.

The supplementary analyses to guarantee the structural safety the containment building:

- Material and component level failure analyses,
- Structural failure analyses, and,
- Cracking analyses.

Actual service life management system

Service life management tool ServiceMan

Together with a designer the service life management tool, ServiceMan, is capable of:

- Timing condition assessments,
- Timing and specification maintenance, repair and rehabilitation (MR&R) actions,
- Time and planning MR&R projects (project planning) and
- Balancing MR&R costs with budget (annual resources planning).

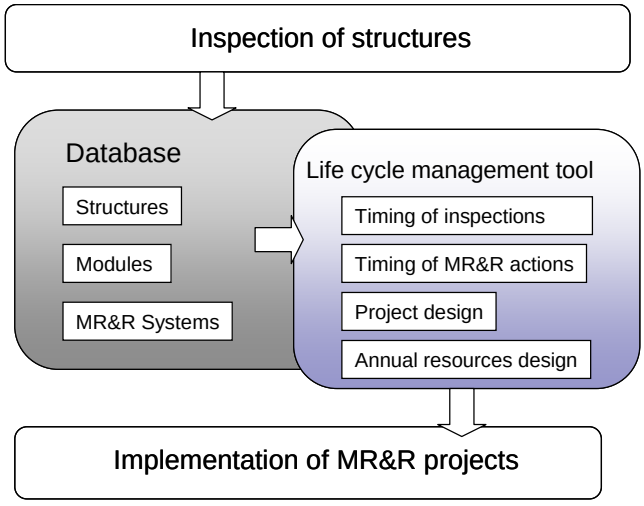

Figure 1. Service life management system. Database and service life management tool.

The methodological background for the management system was developed during the EC FP5 project LIFECON (2001–2003). A scheme of the planning process is presented in Figure 1 [7]. The process starts from the inspection of structures and ends in the implementation of MR&R projects. The LC management tool uses the data of the system database and makes preliminary plans for the MR&R actions. The system database contains data on structures, modules and MR&R systems.

ServiceMan is an MS Excel based tool which contains the necessary databases and calculation procedures in the same program file. The plant units are shared into structures, which are the main building parts such as the containment, sea water channelling etc. The structures are further devided into modules. The breakdown of the structures into modules is made based on the principle that the modules are approximately uniform with respect to materials, structural features and exposure. Modules are the basic units in service life evaluation, life cycle analyses and life cycle planning processes.

The service life management tool can be used for systematic and proactive maintenance of concrete structures in nuclear power plans. The core process of the system is the combined condition, cost and environmental impact analysis. The condition analysis is based on degradation models and the Markov Chain method.

The management system is described in more detail in other reports [1, 11, 12].

Degradation models of the Service life management system

The so called DuraCrete-models (named according to a European project with the same name) were selected for predicting the service life with reference to carbonation, chloride penetration and corrosion of reinforcement. These models were supplemented by a study that made it possible to apply the Duracrete models also to corrosion at cracks of concrete [9].

One possible degradation problem in concrete NPP structures is the deterioration of concrete and reinforcing steel as a result of irradiation in the vicinity of the reactor pressure vessel. A high fluence of neutron radiation affects adversely the mechanical properties of both concrete and reinforcement. However, based on the available reports it seems that the fluence of neutron radiation during the planned service life of the existing Finnish power plants does not reach to the level that would be deleterious for the structural integrity or safety of structures. More research is required in this area, however [9].

The development of degradation models calls for continuous research and international cooperation. That is why a part of the financing of the project was directed to national and international cooperation. The national cooperation included participation in concrete technological research cooperation with other owners of infrastructure (BTS). Partners in the BTS-research cooperation were The Finnish Transport Agency (the Finnish Transport Agency was formed on 1 January 2010 of the Finnish Maritime Administration, the Finnish Rail Administration and the central administration of the Finnish Road Administration), Radiation and Nuclear Safety Authority, City of Helsinki, City of Tampere, City of Espoo, City of Turku. The research in BTS has been focused around durability and aging management of concrete structures. DURAINT was a special project sprouted from this cooperation. It included extensive field tests together with laboratory tests and theoretical modelling. The results obtained from the DURAINT project were utilised in the development of degradation models [2].

The international cooperation included participation in OECD/NEA/CSNI/IAGE (Integrity and Aging) work group and participation in COST C25 network on “Sustainability of Constructions: Integrated Approach to Life-time Structural Engineering”.

Condition assessment of cooling water systems

During the service life of a nuclear power plant condition assessments based on material samples and laboratory analyses will be carried out. The objective of the

condition assessments is to determine the real carbonation rate and the real rate of chloride penetration and to validate the degradation models with these data.

A condition assessment was performed for the cooling water channels of Olkiluoto and Loviisa power plants. This condition assessment was meant to be a model for later condition assessments during the service life of a plant. The condition assessment was based on concrete samples taken from structures and laboratory tests. The samples were taken from (a) above the water level, (b) tidal zone, and (c) below the water level.

The concrete samples were subject to the following laboratory tests and analyses:

1. Determination of the carbonation depth.
2. Determination of the chloride profile.
3. Microstructure analysis based on thin sections.

Based on the results the remaining depassivation time of corrosion was evaluated. The results of this condition assessment were reported in a special report [10].

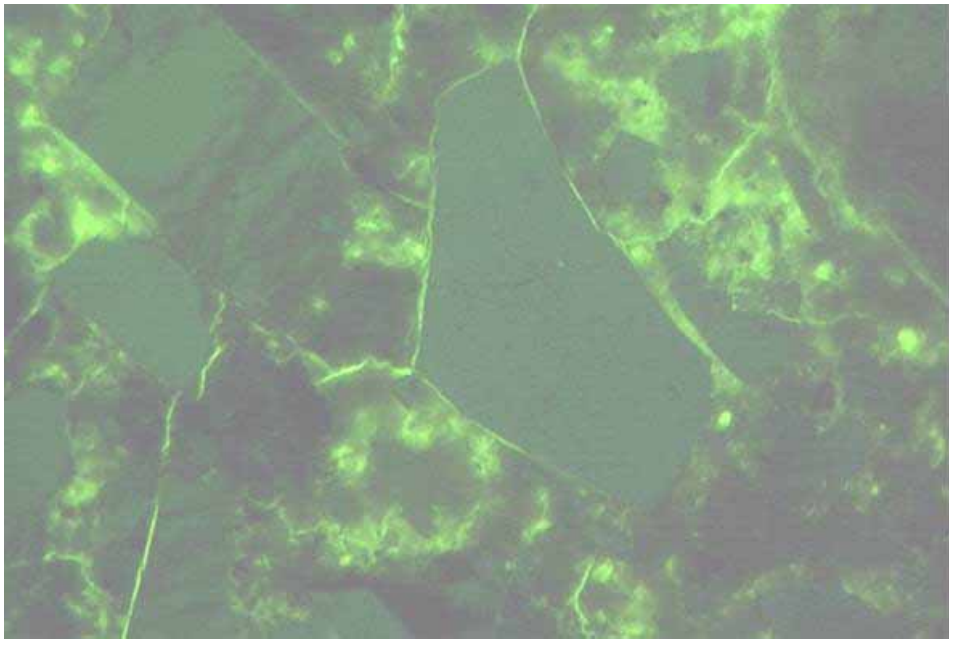

Figure 2. Cracking in concrete. Thin section, fluorescence light.

Supplementary analyses

Time variant failure analyses on structural steel components of NPP containment structures

The failure analyses were conducted for prestressing tendons, fastening bolts and steel liners in containment buildings of Finnish nuclear power plants.

The failure analyses were divided into four phases: (1) Failure Mode and Effect Analyses (FMEA) for identifying the degradation mechanisms of object components (tendons, bolts and steel liners) and the possible effects of them on the structural behaviour and safety of the containment, (2) Fault Tree Analyses (FTA) for evaluating the probability of corrosion to start in the object components within a defined time after construction of the containment, (3) Time variant Reliability Analyses (TRA) for evaluating the probability of component failure to occur with time after corrosion has started, and, (4) Final Estimation for evaluating the failure probability of component failure to occur with time after construction of the containment. The final estimation was done based on the results of FTA and TRA.

Two special workshops were arranged in 2009 for practical evaluation of the corrosion probabilities. The participants of the workshops were TVO and Fortum Power and Heat (Finnish power companies), STUK (Radiation and Nuclear Safety Authority), VTT (Technical Research Centre of Finland) and TKK (Helsinki University of Technology).

The probability of corrosion failure in prestressing tendons, fastening bolts and steel liners were evaluated to be small within the probable lifetime of the plants. With this general conclusion some conditions are noticeable, however. The methods and results of the analyses have been presented in detail in a special report [8].

Figure 3 shows an example of the fault tree analyses.

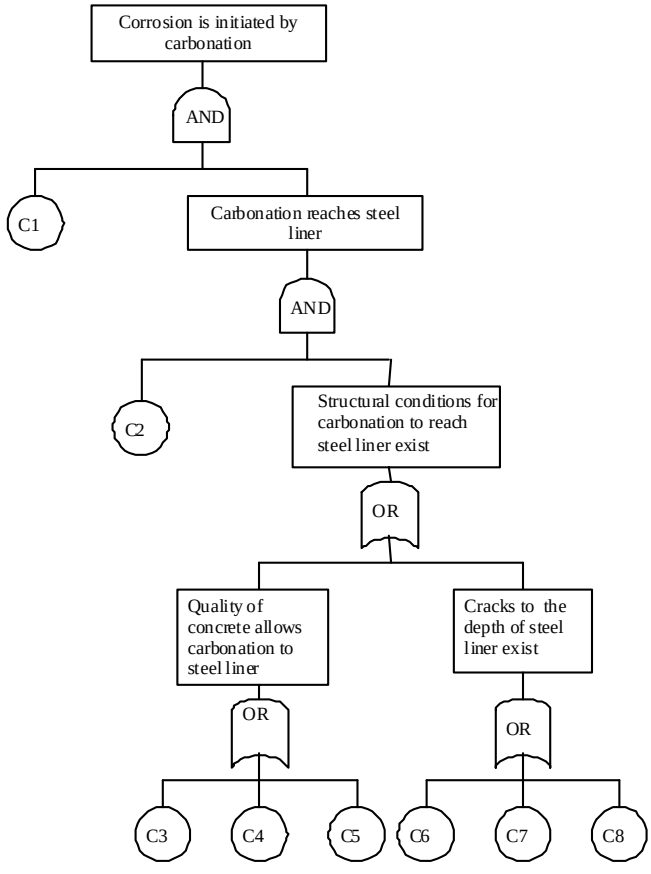

Figure 3. FTA for carbonation initiated corrosion of steel liner.

C1 General conditions of corrosion (moisture, oxygen) exist.
C2 CO2 is in the surrounding air.
C3 Errors in concreting allow carbonation up to the steel liner in 40 years.
C4 Defective curing (plastic cracking etc.) allow carbonation up to the steel liner in 40 years.
C5 Fires and other later effects allow carbonation up to the steel liner in 40 years.
C6 Cracking caused by local tensile stresses (e.g. around penetrations).
C7 Cracking caused by pressure and leaking tests.
C8 Cracking caused by forced deformations (e.g. sinking of foundations etc.).

Structural analyses

The containment building of Olkiluoto 2 nuclear power plant was modelled with finite element method (FEM). The main goal was to evaluate the structural integrity of the post-tensioned cylindrical containment wall in case some of the

tendons are broken. A secondary goal was to study the structural integrity of the liner which is post-cast alongside the inner surface of the containment wall.

Two quite distinctively different models were built. In the first one, concrete structures are represented geometrically in a precise manner using solid elements. Besides the cylinder, also the base slab, some of the internal structures and the pools resting on the cylinder were included in the model. The second model contains only the cylinder which is modelled with shell elements that represent the geometry in a more simplified manner.

Both models incorporate exactly the same post-tensioning tendons modelled with truss elements which are either rigidly embedded inside the solid elements or tied with the shell elements without any bond slipping behaviour. This is an acceptable assumption for the grouted tendons. The calculated tensile stress values for the end of designed lifetime are applied to the tendons by using thermal expansion analogy. The soft bending reinforcement is modelled as smeared rebar layers.

For the cracking analyses, element forces and moments were calculated with the shell element model and transferred into IVODIM system which is explained in a more detail below. The breaking of a tendon is modelled either by removing the whole tendon or by removing the contact with concrete within an anchoring distance. Forces calculated in the former case are used in the cracking analyses. Figure 4. shows the solid model on the left and the shell model on the right.

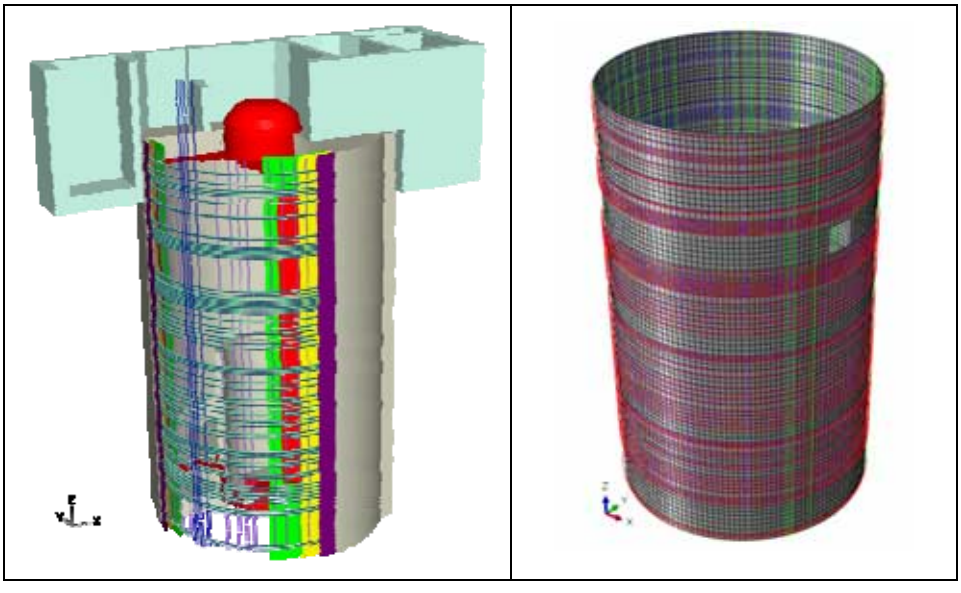

Figure 4. Solid model and shell model.

According to these linear stress analyses, the stress increase in concrete due to breaking of a tendon is of minor degree. The stress increase in the nearest tendons is relatively almost negligible. Based on that, it can be concluded, that a statically induced damage to tendons does not affect significantly the other tendons. The chain reaction, where the damage propagates mechanically to the other tendons, is very unlikely to take place in normal operating and testing conditions. [1].

Cracking analyses

The development of serviceability limit state design for reinforced concrete structures was started in 2007 and continued until the end of year 2008. The design system is utilising the results of FEM analyses and dimensioning is done through the IVODIM design tool according to the selected standard (National building code of Finland B4, DIN 1045, SNiP-84). The system is applicable within structural analysis and limit state design especially in reinforced concrete structures of nuclear power plants.

During the year 2007 the design algorithm of serviceability limit state design accordance with Eurocode 2 was developed. In 2008 the developed design algorithm was programmed into the IVODIM design tool developed for structural design and analysis of reinforced concrete structures. Also the Eurocode 2 design algorithm for ultimate limit state was developed and programmed and necessary verification tests were conducted. Reliability of the program was ensured by simple hand calculations for limited number of shell and beam elements and loading conditions. [4, 5]

During the year 2010 the crack width analysis was made for the containment building of Olkiluoto 2 nuclear power plant. The analysed containment is a prestressed concrete shell structure. The analysis was made according to Finnish design code B4 using the IVODIM design tool. [3]

Modelling of the containment building was carried out using quadrilateral 4-noded shell elements for the concrete structures and truss elements for the tendons. Only the cylindrical, prestressed concrete wall with the thickness of 800 mm was considered. Dead load of structures and loads due to the prestressing were included in all six cases studied. Cases 1 and 2 were without tendon damage, Cases 3 and 4 had one broken tendon (tendon 160 in Figure 5), and Cases 5 and 6 had three broken tendons (16, 159, 160). A test pressure of 0.3 MPa

was included in cases 2, 4 and 6. The break of a tendon was modelled by removing the broken tendon(s) from the calculation model. [3]

The crack widths were calculated for the whole containment and the results of a control area were analysed more precisely. The control area and its cross-section are shown in Figure 5. The control area is fully compressed in both surfaces of vertical direction in all studied loading cases but also in both surfaces of horizontal direction in loading cases without test pressure. The tensile stresses existed only in both surfaces of horizontal direction in loading cases with test pressure. [3]

The maximum crack widths of the undamaged Case 2 were 0.020 mm and 0.119 mm in inner and outer surface, respectively. The corresponding values were 0.037 mm and 0.188 mm in Case 4, and 0.053 mm and 0.269 mm in Case 6. The orientations of these cracks are nearly perpendicular to the horizontal reinforcement. [3]

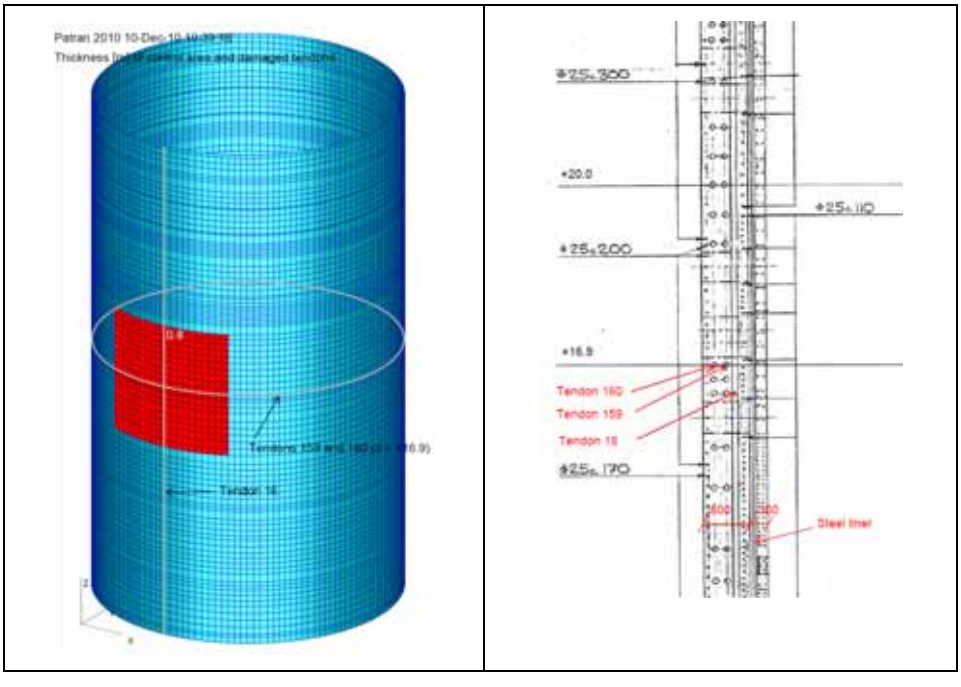

Figure 5. Control area coloured in red (left) and cross-section of containment (right).

The results indicate that the break of a horizontal tendon is more critical than the break of a vertical tendon. The massive dead load of structures has a favourable effect on stresses in the vertical direction. [3]

This cracking analysis showed that cracks penetrating the whole concrete cross-section can appear during the containment pressure test. If one or more tendons are broken the cracks will be much bigger.

Conclusions

The Service life management system for concrete structures of the Finnish nuclear power plants (Olkiluoto 1 & 2, Loviisa 1 & 2) was developed in VTT together with the power companies. The actual service life management system includes the databases and tools for conducting systematic maintenance policy and for planning, organizing and optimizing the maintenance strategy of concrete structures in NPPs. For addressing the safety aspects of degredation supplementary analyses were conducted for the containment buildings. These included material and component level failure analyses and structural level failure and cracking analyses.

References

1. Calonius, K. Structural failure analyses of post-tensioned containment building of Olkiluoto 2 nuclear power plant. Technical Research Centre of Finland. Research Report. VTT, Espoo, 2010. VTT-R-00327-11. 50 p.

2. Kuosa, H., Vesikari, E., Holt, E. & Leivo, M. Field and Laboratory Testing and Service Life Modelling in Finland. Nordic Miniseminar on Nordic Exposure Sites, 12–14 Nov. 2008. 18 p.

3. Turunen, E. & Iivonen, P. Crack Width Analysis for Containment Building of Olkiluoto 2 Nuclear Power Plant. The Finnish Programme on Nuclear Power Plant Safety 2007–2010. Research report, 2010. 18 p.

4. Turunen, E. Halkeilevan teräsbetonirakenteen jäykkyyden redusointi ja mitoitus-algoritmi toteuttaen Eurokoodin määräykset (Stiffness reduction and a design algorithm of cracking concrete structures in compliance with Eurocode regulations). Helsinki University of Technology, Master's Thesis, 17 December 2007. 119 p.

5. Turunen, E. & Iivonen, P. Serviceability limit state and crack width analysis of concrete structures according to Eurocode 2. The Finnish Programme on Nuclear Power Plant Safety 2007–2010. Research report, 2009. 31 p.

6. Vesikari, E. & Rissanen, T. Risk Assessment Methods with Special Reference to Aging Effects in Containment Buildings of Nuclear Power Plants. The Finnish Programme on Nuclear Power Plant Safety 2007–2010. VTT, Espoo, 2009. Research Report. VTT-R-10610-08. 51 p.

7. Vesikari, E. Service life management system of concrete structures in nuclear power plants. VTT, Espoo, 2007. VTT Publications 648. 82 p. http://www.vtt.fi/inf/pdf/publications/2007/P648.pdf.

8. Vesikari, E. Corrosion of Structural Steel Components in Containment Buildings of Nuclear Power Plants – Time Variant Failure Analysis. The Finnish Programme on Nuclear Power Plant Safety 2007–2010. VTT, Espoo, 2008. Research Report. VTT-R-06470-09. 90 p.

9. Vesikari, E. Degradation and service life of concrete structures in nuclear power plants. The Finnish Research Programme on Nuclear Power Plant Safety 2007–2010. VTT, Espoo, 2008. Research Report VTT-R-02323-08. 40 p.

10. Vesikari, E. Condition Assessment of Cooling Water Channels in Finnish Nuclear Power Plants. The Finnish Programme on Nuclear Power Plant Safety 2007–2010. VTT, Espoo, 2010. Research Report VTT-R-10. 56 p.

11. Vesikari, E. Life Cycle management Tools using LIFECON Procedures and Calculation Methods. COST C 25. Sustainability of Constructions. Integrated approach to Lifetime Structural Engineering. Proc. Int. Seminar. Dresden 6–7 Oct. 2008. 10 p.

12. Vesikari, E., Hiltunen, V. & Mattila, A. Service Life Management System of Concrete Structures in Nuclear Power Plants. Proc. Int. Conf. Aging Management of Nuclear Power Plants and Waste Disposal Structures (AMP 2010). Toronto 7–10 Aug. 2010. 8 p.

29.2 Description of the service life management system ServiceMan

Erkki Vesikari
VTT

Vesa Hiltunen
Teollisuuden Voima Oy

Aki Mattila
Fortum Power and Heat Oy

Abstract

A service life management system, ServiceMan, for concrete structures in Finnish nuclear power plants was developed in cooperation with the Finnish nuclear power companies. The system is predictive, probabilistic and life-cycle based. It takes into account several aspects of structural lifetime quality, such as performance, condition, financial costs and environmental impacts. By the service life management system the accepted structural performance and uninterrupted service of concrete structures can be ensured during the planned operating lifetime of the Finnish nuclear power plants.

Introduction

A service life management system, ServiceMan, for concrete structures in Finnish nuclear power plants was developed in cooperation with the Finnish nuclear power companies. The work was done under the auspices of the SAFIR 2010, the Finnish research program for nuclear safety. The system is predictive and life-cycle based and works with probabilistic degradation models. It determines the condition of structural parts and gives optimised timings of intervention actions and calculates the financial costs and environmental impacts. By the service life management system the accepted structural performance and uninterrupted service of concrete structures can be ensured during the planned operating lifetime of the Finnish nuclear power plants.

The methodological ground of the service life management system was developed during the EC FP5 project LIFECON (2001–2003) [1]. According to this methodology the structures are divided into smaller parts which can be treated as homogenous with respect to materials, structural features and

environmental conditions. The structural parts are called “modules” and they serve as basic structural units in the analysis and planning processes of the system. The structural and modular databases which serve as initial data sources in the calculation processes are consistent with the modular breakdown of structures.

The core of the management system consists of a combined condition, cost and environmental impact analysis. The condition analysis is based on degradation models, predefined limit states of condition and the Markov Chain method. The condition analysis is capable of predicting the probability of the modules to be at any condition state at any year during the design period. The analysis contains also an automatic condition guarding system which is able to trigger maintenance, repair and rehabilitation (MR&R) actions whenever the predefined limit state of condition is exceeded with a maximum allowable probability. [2, 3, 4]

Procedure

Figure 1 shows the calculation process of the life cycle management tool. The structural and modular databases and the database of MR&R systems are seen on top. The database of MR&R systems contains data on protection systems (such as coatings), repair systems and rehabilitation systems including data on unit costs, environmental impacts and reference service life. The structural database contains some data on the structure such as the year of manufacture etc. The module database is larger containing data on materials, structural dimensions, inspection data, history data on repairs and data on planned MR&R actions.

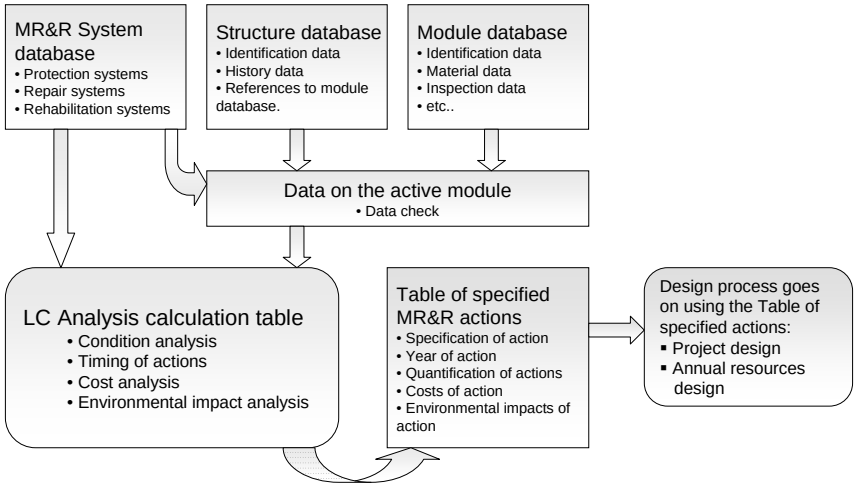

Figure 1. Calculation process of the service life management tool.

Each module in turn is subject to the analysis and planning process. The data pertaining to the active module is gathered from the databases and they are checked by a special routine. Then the data are inserted in the LC analysis table (Figure 1). As a result of the combined condition, cost and environmental impact analysis MR&R actions for the active module are automatically specified and timed. The timing of actions is optimally determined based on the condition. The MR&R action specifications with evaluated costs and environmental impacts are transported from the LC analysis table to a special table of specified MR&R actions. All modules are treated in the same way. The analysis routine is systemised so that the same procedure is applicable to all modules irrespective of their appearance or use. From the data table of specified MR&R actions the process goes on with project design and annual resources design.

Combined life cycle analysis

The core of the management system consists of a combined condition, cost and environmental impact analysis. The condition analysis is conducted automatically based on degradation models and predefined limit states of condition. The condition analysis is probabilistic and based on the Markov Chain method. It is capable of predicting the probability of the structure to be at any of the condition states in any year during the design period. The analysis is done based on several degradation modes such as physical degradation of concrete, carbonation and corrosion, chloride penetration and corrosion, carbonation and corrosion at cracks and chloride penetration and corrosion at cracks. Furthermore the degradation of the possible protection system is analysed in the same way. The retarding effect of the protection method on the degradation rate of the structure has been modelled. The analysis is extended over the whole design period (Figure 2).

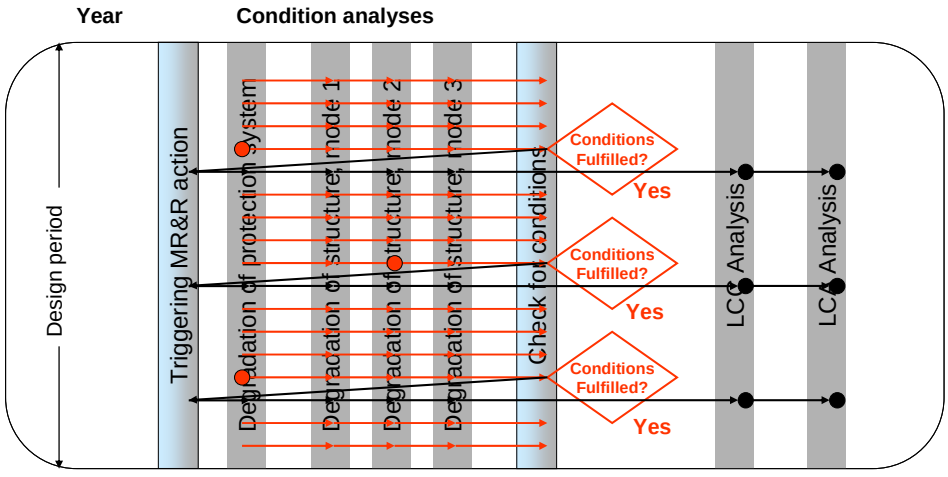

Figure 2. Combined LC analysis and the automatic triggering of MR&R actions.

Each year a check is made if the conditions of triggering MR&R actions with regard to any of the degradation modes are fulfilled. If that is not the case evaluation of the degradation continues in the next year etc. When finally the conditions for a MR&R action are fulfilled the action is executed in the next year. Then the condition of the structure is re-evaluated with special repair models. At the same time the costs of the action are added in the cost calculator and the environmental impacts are added in the respective LCA calculator.

After the repair the process continues and the fulfilment of conditions is again checked every year. The conditions which are checked are the following:

- is the action defined (the designer may or may not want to have a protection or repair action used)?
- is the maximum allowable probability of exceeding the limit state exceeded?
- is the maxim number of re-applications of protection or repair exceeded?

If the action is defined and the maximum allowable probability of exceeding the limit state is exceeded the action is triggered next year provided the maximum number of re-applications is not exceeded. Otherwise no action is triggered and only degradation proceeds.

By this means the life cycle action profile for the design period is automatically produced. When the life cycle action profile is defined the life cycle costs and the environmental impacts from the MR&R actions performed during the whole

design period are calculated automatically by the side of the condition analysis. The total costs are calculated as real costs and as present value costs.

Input data and start of planning

Most of the input data for the design procedure are given in the databases. Only the design period and the discount rate are inserted by the designer (Figure 4). In the module database the following data of past and future actions are given:

- Past MR&R actions (Figure 3, Phase -1)
- Predefined actions with optimal automatic timing
- Predefined actions with predefined timing.

The past MR&R actions are stored in the database by giving the code and the year of the action. The action may be either protection or repair action. The condition analysis is capable of taking into account also the past actions when evaluating continuously the condition of the structure.

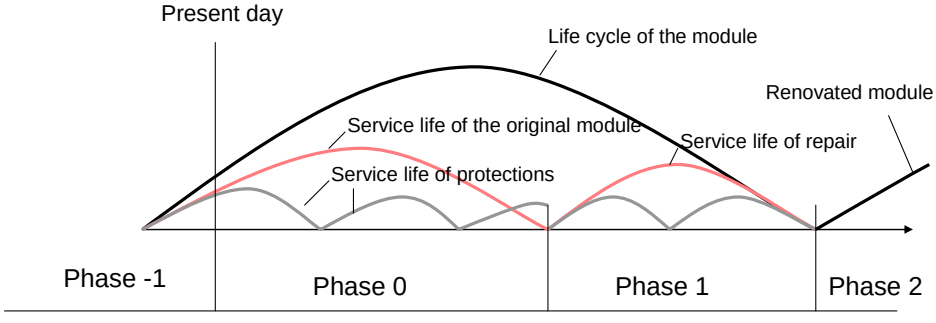

Figure 3. Rules for specification of future actions.

In the case of predefined actions with predefined timing the code of the action (either protection or repair action) is given together with the defined year of the action. The effect on the condition of the structure is taken into account in the same way as in the case of the past MR&R actions.

In the case of automatic timing of predefined actions the following data are given concerning both the protective actions and the repair actions of the structure:

- Is the action defined?
- If defined what is the code of the action?

- For timing of the action what is the maximum probability of exceeding the limit state?
- What is the maximum number of reapplications?

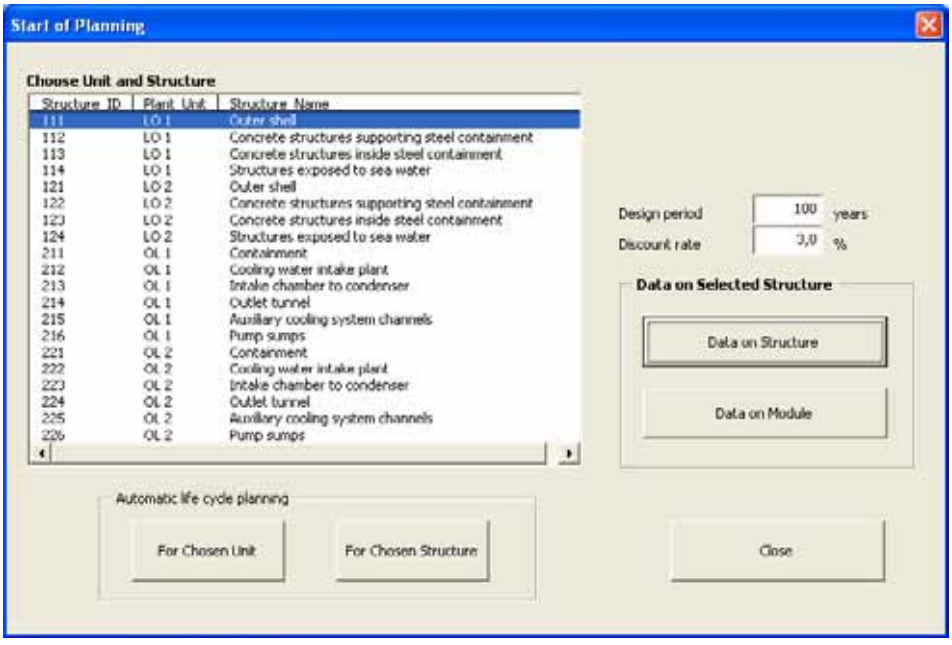

Figure 4. Start of planning.

In case of protection actions the above definitions are given both for the period before the first repair (Phase 0, Figure 3) and after the first repair (Phase 1, Figure 3).

In Figure 4 the Start of planning form of the ServiceMan tool is presented. In the list window the plant units and the structures of the units are displayed. The designer chooses one of the structures. Pressing the buttons on the right hand side he/she can see the data of that structure or the data of the modules pertaining to that structure consistent with the database. From the buttons at the bottom of the form the designer can start the automatic life cycle planning.

Main results

After a few seconds from the start of the automatic planning the Action profile display opens (Figure 5). As a result of the planning process the following results are obtained:

- MR&R action profiles (with timings) for each module
- Data on costs and environmental impacts
- Condition analyses based on various degradation types
- Timing of special inspections
- LCC and LCA summary data.

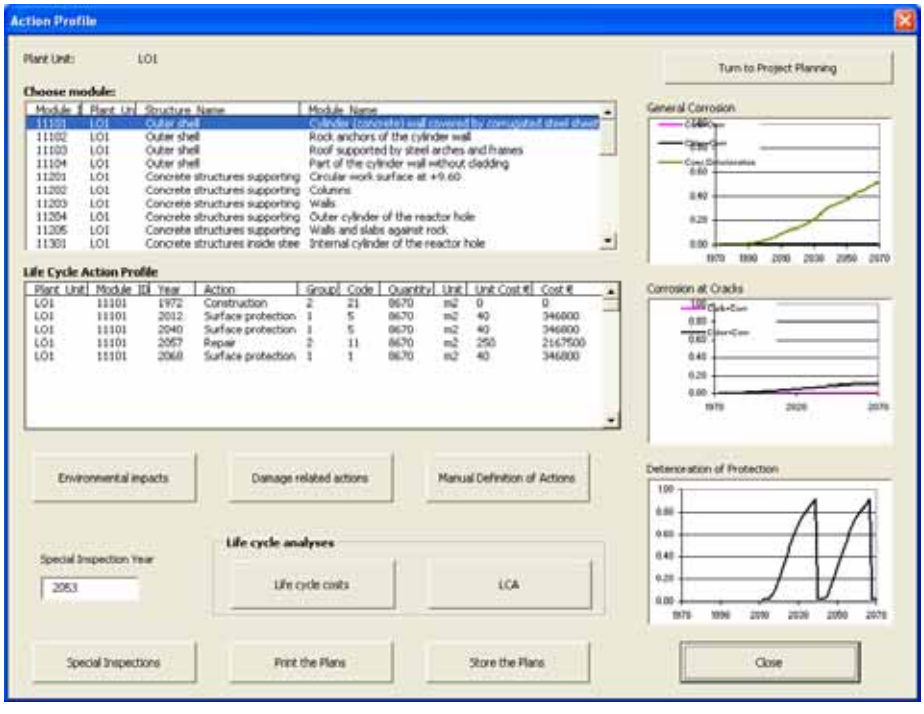

Figure 5. Action profile display.

In the upper list window the modules of the selected structure or optionally the modules of the whole unit are shown. When the user selects by clicking one of the modules the action profile of the module is appeared in the lower list window. The following data is presented in the list of actions:

- Plant unit
- Module ID
- Year
- Action
- Action group
- Code of action
- Quantity of action
- Unit of the quantity
- Unit cost and
- Total costs.

By pressing the button below the action list window full data of the environmental impacts are displayed.

Also the degradation curves in the figures are updated immediately when the module is selected from the upper list window. In the uppermost figure the probability of exceeding the limit state is presented for corrosion at uncracked concrete surface. In the middle figure the corresponding probability is presented for corrosion at cracks. In the lower figure the degradation of the protection is presented.

In the same display the year of next special inspection for the module is given. The special inspection is done for taking samples from the structure. From the samples the carbonation depth and the chloride penetration depth are measured and this data is inserted in the database. Using this data the degradation models are automatically calibrated and the timings of MR&R actions are re-evaluated.

Summary data from the whole design period (including all the MR&R actions from the selected design period) can be obtained by pressing the buttons in the frame “Life cycle analysis”. By pressing the button “Life cycle costs” a form with cost data is opened (Figure 6). The cumulative real costs, cumulative present value costs, average annual costs and equalised annual costs from the MR&R actions of the selected module are presented. By pressing the option button “For chosen structure” the respective LC cost data of the structure are obtained and by pressing the “For whole plant unit” the LC costs of the whole plant unit are obtained. By pressing “LCA” in the Life cycle analysis frame the LCA display will open and the data on environmental impacts are obtained in the same way as the LC costs.

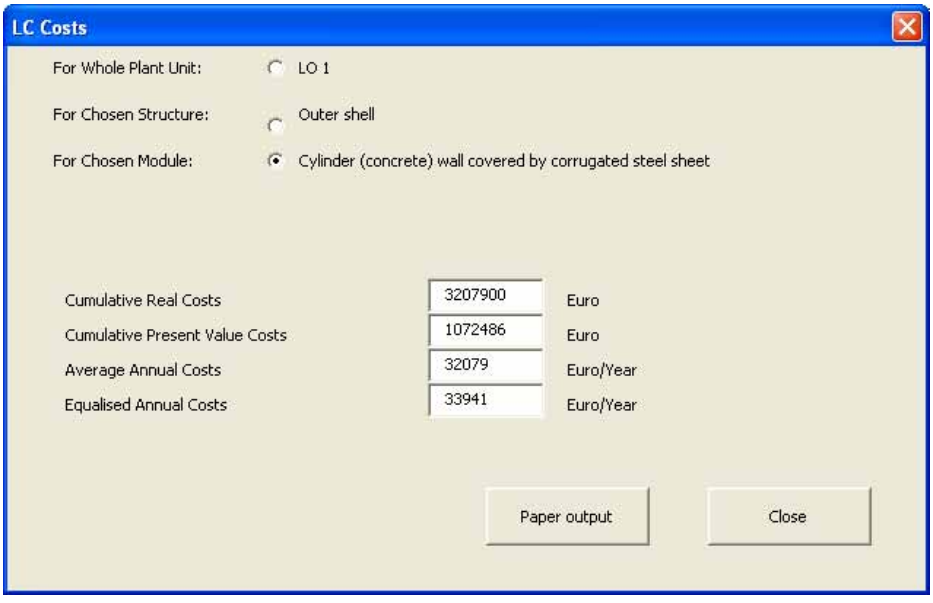

Figure 6. LC costs display.

If the designer is not satisfied with the automatically prepared life cycle profile he/she can alter it by manual definition (see the "Manual definition of actions" button in Figure 5). This is done simply by defining the MR&R action (code) and the year of action. By this means the designer can completely change the automatically made life cycle action profile. However, the automatic triggering of actions may be kept in force in spite of the manual definitions. By this means the system guarantees that the maximum allowable condition limits are never exceeded.

Other aids

Other aids are provided for the designer:

- Possibility to combine MR&R actions into projects (project design)
- Annual resources design taking into account the budget constraints
- Cost scenario over time.

After the action profiles have been specified the user can start project planning. Project planning means grouping of the actions into projects. Tentatively ServiceMan tool allocates the MR&R actions timed for the same year to the same project irrespective of the module to which the action will be done.

However, the designer can manually arrange the actions into different projects and even make small changes in the timings of actions. The grouping of actions is beneficial because of the synergy profit that can be gained by concurrent implementation of actions.

The annual resources design means balancing the annual MR&R costs with the budget over time. Accordingly, the budget can be planned beforehand. On the other hand, if the budget is constrained, the MR&R costs may be adjusted according to the budget by making changes in the annual project plan.

The cost scenario is given as a cumulative curve of total annual real costs and total annual present value costs over time (Figure 7).

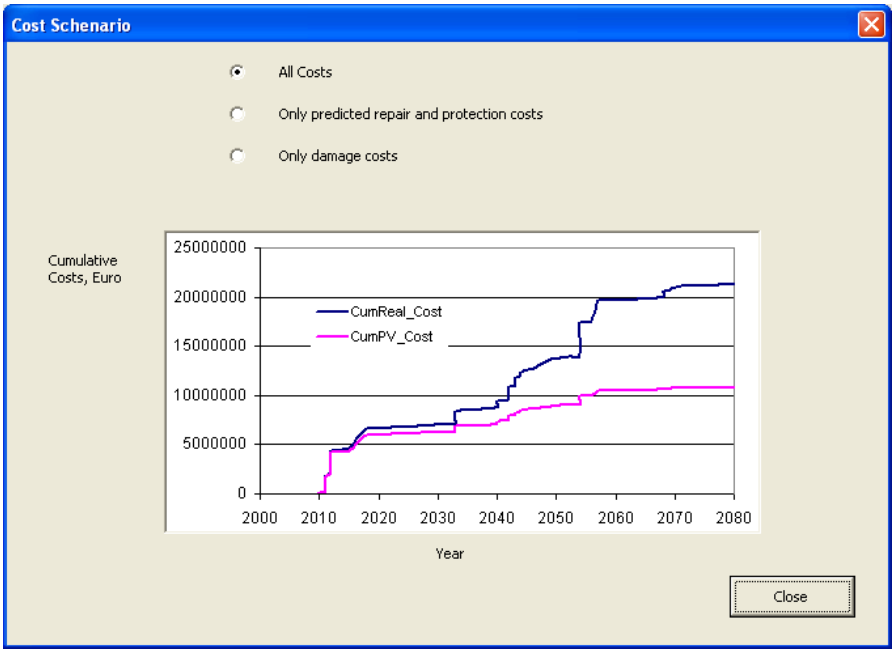

Figure 7. Cost scenario.

Conclusions

The project “Service life management system in nuclear power plants” (ServiceMan) under the auspices of the research programme SAFIR 2010, that started in 2007, aims at developing a service life management system for concrete structures in nuclear power plants in Finland. The service life management system is capable of predicting degradation in structures with respect to different degradation types

and is able of timing special inspections and MR&R actions for the remaining operating life of the plant.

The Service life management tool can be used for systematic and proactive maintenance of concrete structures in nuclear power plans. The core process of the system is the combined condition, cost and environmental impact analysis which can automatically produce optimised LC action profiles. The system provides also a possibility for project design and annual resources design.

References

1. Söderqvist, M.-K. & Vesikari, E. Generic technical handbook for a predictive life-cycle management system of concrete structures (LMS). Lifecon GIRD-CT-2000-00378 Lifecon Deliverable D1.1, final report, 2003. 170 p. http://lifecon.vtt.fi/.

2. Vesikari, E. Service life management system of concrete structures in nuclear power plants. Espoo, VTT, 2007. VTT Publications 648. 82 p. http://www.vtt.fi/inf/pdf/publications/2007/P648.pdf.

3. Vesikari, E., Puttonen, J., Hiltunen, V. & Mattila, A. Service Life Management System of Concrete Structures in Nuclear Power Plants. Proc. Int. Conf. Structural Mechanics in Reactor Technology (SMiRT 20). Helsinki 10–14 Aug. 2009. 7 p.

4. Vesikari, E., Hiltunen, V. & Mattila, A. Service Life Management System of Concrete Structures in Nuclear Power Plants. Proc. Int. Conf. Aging Management of Nuclear Power Plants and Waste Disposal Structures (AMP 2010). Toronto 7–10 Aug. 2010. 8 p.

30. IMPACT2010 (IMPACT) and Structures under Soft Impact (SUSI)

30.1 IMPACT and SUSI joint report

Kim Calonius, Ilkka Hakola, Simo Hostikka, Arja Saarenheimo,
Ari Silde and Ari Vepsä
VTT

Markku Tuomala
TUT

Abstract

An impact test apparatus has been built in autumn 2004 to test especially soft missile impacts against reinforced concrete walls. The apparatus has been designed to be suitable also for investigating fuel spreading, e.g. measuring droplet size and velocity. At the beginning of the project, one of the main purposes was to measure the force time function during the impact. It was enabled by a thick force plate with force transducers installed in front of the supporting frame. The main aim of the project is to produce data for verifying and developing numerical models and methods. This work has been carried out within the SUSI project.

The spread of liquid fuel as a result of an aircraft crash may cause a sudden fire with hazardous effects on the safety of the NPP. The spread phenomena have been studied at VTT in the IMPACT tests both experimentally and numerically. The goals of the study were to increase a general understanding of the liquid dispersion phenomena under impact conditions, to measure some of

the input parameters needed for numerical simulations, and to take in use and to validate simulation methods for the determination of fuel spread and fires. The Fire Dynamics Simulator (FDS) program was used to estimate the fraction of the aircraft fuel that accumulates into pools burning on the ground and to examine the heat exposures resulting from a 10 ton kerosene release.

Introduction

In order to obtain reliable numerical results the methods and models should be verified against experimental data. The accuracy and capability of numerical methods in analysing reinforced concrete structures under soft missile impacts are studied. Test results used in this study are recorded within the IMPACT project. All the calculation work presented is performed within the SUSI project.

The main aim of the SUSI project is to develop and take in use numerical methods for predicting response of reinforced concrete structures to impacts of deformable projectiles that may contain combustible liquid (“fuel”). Structural behaviour, in terms of collapse mechanism type and the damage grade, will be predicted both by simple analytical methods and by more involved non-linear FE-models.

An other essential objective is the development and calibration of suitable analytical and numerical methods, which can be applied in real scale analyses of fuel spreading and fire risk. Primarily, the suitability of Fire Dynamics Simulator code (FDS) for the current issue will be further studied, and the testing and validation of the sub-models will be continued. New aim is the full-scale simulation of fuel spread and combustion following an aircraft crash by utilizing the data gained from the VTT IMPACT tests and from GRS.

IMPACT Phase 2, tests and measurement

During the IMPACT Phase 2 project, concrete walls with thicknesses of 150 mm and 250 mm have been used as targets. The walls have included bending reinforcement, occasionally shear reinforcement and in some tests post-tensioning bars for producing a designed compression in the concrete.

New features of Impact apparatus

At the beginning of IMPACT project (Phase 1), the missile was shot from inside the acceleration tube and thus acted also as a piston. It was made of carbon steel

and the maximum diameter and weight were 500 mm and 100 kg, respectively. The missile had to withstand as high air pressure as 20 bars and its shape was also limited to a round pipe without any protruding parts such as wings. Therefore, quite soon the set-up was changed and the missiles were shot using a steel rails installed at the top of the acceleration tube. The missile was accelerated using thin steel plate fixed to the piston and coming out of a gap in the top of the acceleration tube wall, see Figure 2. Presently, more complicated geometries can be used and wings are possible to be attached on the sides of the missile. On the other hand, the missile has to have some type of carriage or sledge fixed to its bottom. In some basic tests with high impact velocities the heavy carriage had a significant effect on the perforation. The carriage was made of carbon steel and may have had a cutting effect on the reinforcement while perforating the wall.

Figure 1. Modified impact apparatus in 2011.

In IMPACT 2 project, the apparatus was modified by installing a steel corner profile above the acceleration tube, see Figures 1 and 2. The height of this cover is adjustable by threaded rods for many sizes of missiles. The missile moves now freely between the rails and the corner profile and therefore no carriage is

needed. The new system has the advantage that the missile pipe does not include any additional rigid parts and the crushing force contribution to the load function is the folding force of the missile.

Figure 2. The corner profile installed above the acceleration tube.

Also an aluminium plate has been installed between the acceleration tube and the piston catcher. The plate prevents particles, moisture and pressure waves to interfere with the laser sensors and video cameras, see Figure 2.

During impact tests, the back part of acceleration tube has to withstand the highest air pressures and therefore it is strengthened by longitudinal stiffeners at the bottom of the pipe. The rearmost part of the tube is also replaced by an 8 mm thick steel plate. The maximum pressure is now 20 bars. The strengthened back part is shown in Figure 3 on the left.

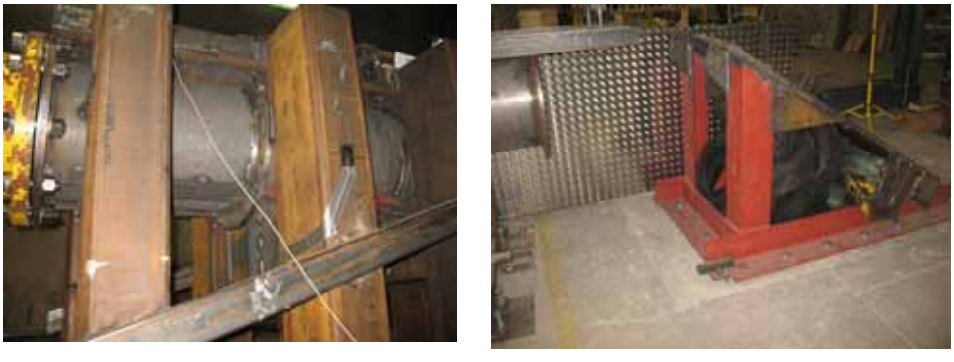

Figure 3. The backpart of the acceleration tube (left). The aluminium shelter plate (right).

The impact apparatus has now been used for about 6 years and more than 100 tests have been performed. The main dimensions and capabilities of the testing facility are described below in Table 1.

Table 1. Main dimensions and capabilities of the testing facility.

Length of the accumulator	13.5 m
Length of acceleration tube	12.0 m
Maximum weight of the missile	50 kg
Maximum speed of the missile	190 m/s
Dimensions of the target	2 m by 2 m
Maximum pressure	20 bars

Dynamic properties of the supporting frame

While the supporting structure is not totally rigid, its dynamic properties have to be investigated. The natural frequencies of the system have been researched in M. Sc. Thesis by K. Kaunisto by modelling the system and also by performing impact tests using a heavy impact hammer with a mass of 124.2 kg, a length of 0.55 m, a diameter of 0.19 m and a shaft length of 2.8 m. The test arrangement is shown in Figure 4.

Figure 4. Schematic drawing of the heavy impact hammer and picture of a test performance.

Measurements

The measurements in impact tests are done using 32 channels and sampling frequency of 200 kHz. The used sensors include high frequency laser sensors, shown in Figure 6, for measuring the actual speed of the missile, force transducers to measure the force-time function of impact, deflection transducers, see Figure 6, to measure the deflection of the concrete wall and strain gauges to measure strains in different locations, shown in Figure 5. Strain gauges have been installed on rebars or stirrups located inside the concrete slab, glued and protected before casting the concrete. Electrical wires have been protected also by plastic pipes, which are connected to reinforcement, and finally pulled to surface of the concrete far from hitting point, see Figure 5. The strain gauges have also been fixed on the back supporting pipes in order to be able to measure the supporting forces, shown in Figure 5. The strains on concrete surface have been measured by long strain gauges.

Figure 5. Strain gauges fixed on reinforcement (left) and on back pipes (right).

Figure 6. Strain gauges glued on the front surface (left) and laser sensors (right).

In some tests with high impact velocity and hard missile, the missile perforated the wall. The residual velocity of the missile is difficult to measure due to concrete particles and dust that fly around the missile, as shown in Figure 7. In front of the wall, the impact velocity is measured using laser sensors, shown in Figure 6, but at the back, due to the dust, neither these sensors nor any video cameras could be used. Instead, the residual velocity can be defined using high speed camera still frames from the front of the wall. After perforation the tail of the missile, shown in Figure 7, can be seen and the velocity can be defined when the shutter speed of camera is known. Some still frames during an impact are shown in Figure 8.

The other method to measure the post velocity is shown in Figure 9. Two plywood plates have been installed behind the wall. The plywood thickness has been selected to resist the concrete particles but not the heavy missile itself. While the missile perforates the plywood plate, it is recognized by strain gauges glued on the surface of the plywood, shown in Figure 9.

Figure 7. Hard missile with a tail (left). Concrete wall and dust after perforation (right).

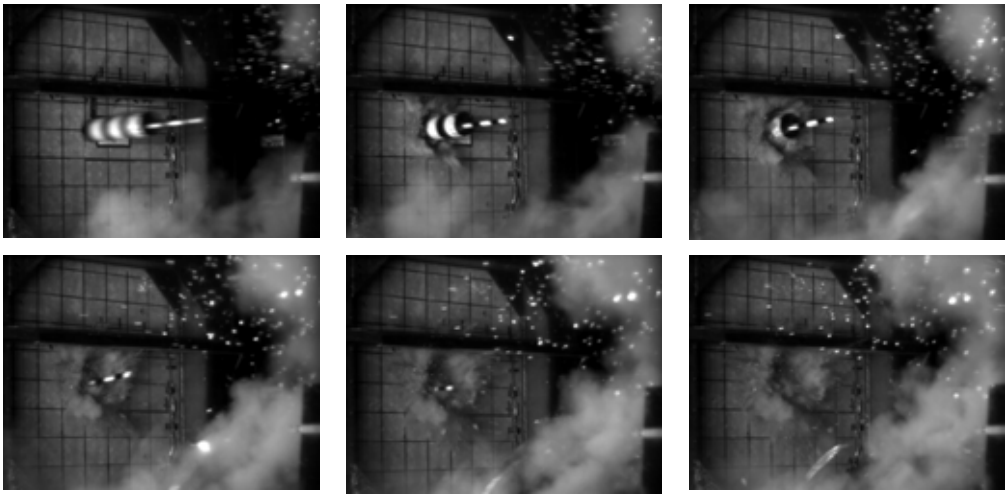

Figure 8. An example of still frames of missile with tail during perforation.

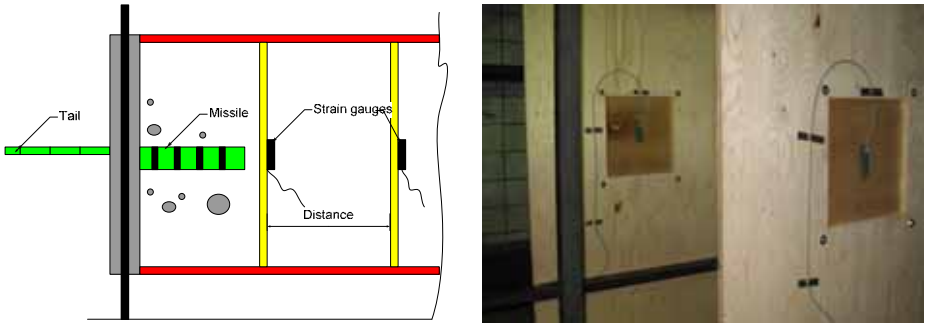

Figure 9. Measuring system for the residual velocity (left) and strain gauges glued on plywood surfaces (right).

Stainless steel missile

Many kinds of missiles have been used to study the impact phenomena and to achieve the desired force-time function. The missiles have been made of carbon steel, stainless steel and aluminium. The latest soft missile tests have been performed with thin walled stainless steel missiles, which induce desired and reproducible load functions, because the material is mainly folding without tearing or breaking. The stainless steel missile has a diameter of 254 mm, a thickness of 2 mm, a length of 2.1 m and a weight of 50 kg, shown in Figure 10 on top left. The water filled stainless steel missile is shown in Figure 10 on top

right. The mass of water has been 25 kg and the water tank can be located in middle or front part of the missile. The so-called hard missile is made of steel pipe with diameter of 168 mm. Its total length is 640 mm and total weight is 50 kg and it is filled with light concrete, see Figure 10, bottom.

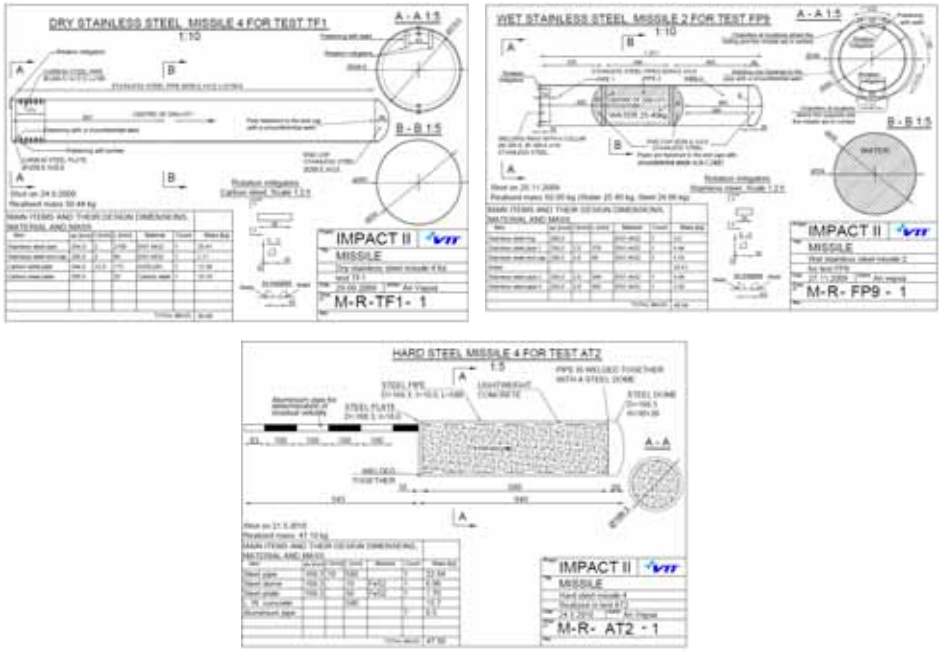

Figure 10. Various types of missiles. Dry stainless steel missile (top left), water filled stainless steel missile (top right), hard carbon steel missile (bottom left).

Material tests

The materials used for missile, target and its reinforcement are tested to find out the actual properties. Missile aluminium and steel are tested using tensile tests. At least 3 tests have been made for every ordering batch to define yield point, 0.2 proof strength and tensile strength. The strength of concrete is tested either by a cubic or a cylindrical specimen. Compression strength, splitting tensile strength, Young's modulus and density have been defined. The reinforcement has been tested also by compression test.

In some cases, also tri-axial tests have been conducted in order to have more information about the tri-axial properties of concrete. These tests have been conducted in Aalto university either using constant radial pressure or by increasing it. The apparatus and sensors used in the tests are shown in Figure 11.

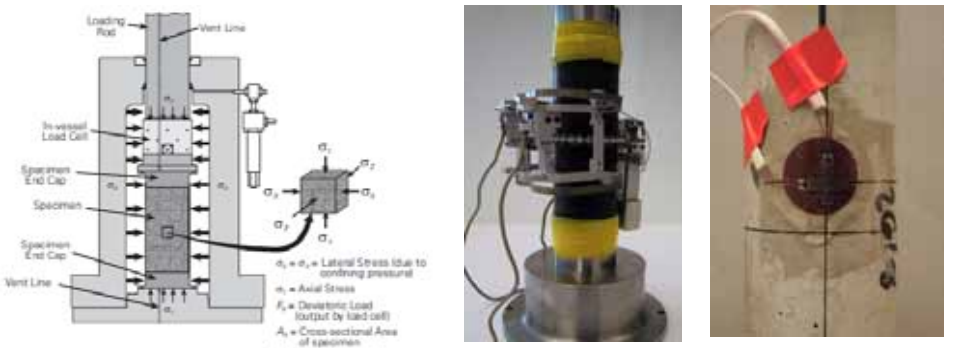

Figure 11. Tri-axial apparatus (left), axial and circumferential extensometer (middle) and strain gauges glued on specimen (right).

Numerical studies on impact loaded reinforced concrete walls

Deformable stainless steel missile

The main aim of the impact tests with deformable stainless steel missiles was to find out a new, reliably predictable missile type, Figure 10. The desired crushing mechanism was folding, since there have been problems with the previous aluminium missiles which were mainly crushing by an unstable tearing mechanism.

First, the stainless steel missiles were shot to a force plate. The force measurements were mainly successful. The tests were simulated with finite element method using Abaqus/Explicit version 6.9-2 [1] and shell elements in three dimensional space. The simulations concentrate on the missile behaviour and the impact force. Calculations with Riera method [2] were also done. The deformed shapes were very similar in the tests and corresponding FE simulations, see Figure 12. The deformation mode was folding in both cases. According to these studies the impact load and the crushing behaviour of the chosen missile type are well predictable. This is of major importance when planning tests on reinforced concrete slabs. Force plate test FP8 was carried out using a stainless steel missile with a mass of 50.12 kg and a velocity of 102 m/s. Measured and calculated force-time functions are presented in Figure 13.

Figure 12. The deformed missile of test FP8 in the FE simulation and in the real test.

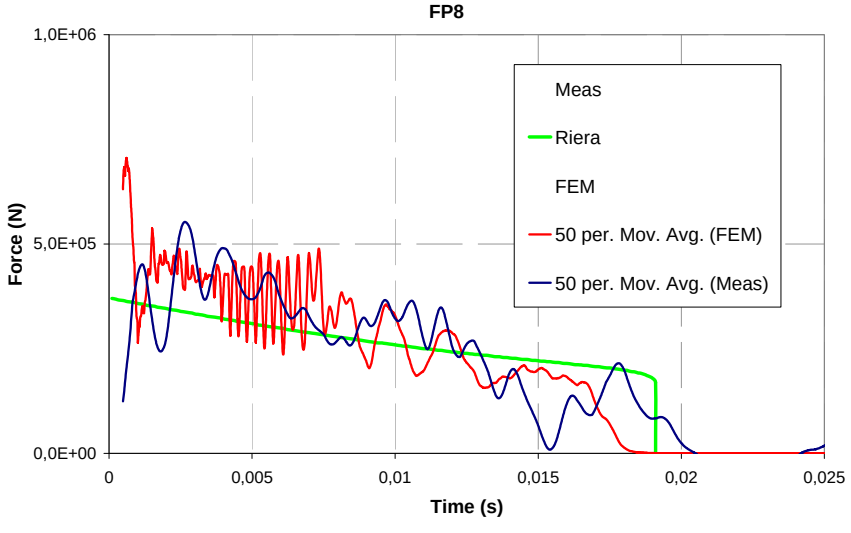

Figure 13. Averaged force-time curves of test FP8 according to test measurements, Riera method and FE simulations.

Numerical studies on Test TF11

The reinforced concrete wall is simply supported on all the four edges. The span width is 2 m and the thickness of the wall is 15 cm. This slab is reinforced using bars with a diameter of 6 mm and a spacing of 50 mm. The amount of reinforcements (on both faces) is 0.000565 m^2/m. The effective thickness *d* of the slab is $0.15 - 0.018 = 0.132$ m. The reinforcement ratio is in this case

$\rho_b = A_s/h = 0.38\%$. The amount of shear reinforcement is 0.00548 m^2/m^2. The uniaxial behaviour of concrete in tension and in compression is shown in Figure 14. The fracture energy, G_f, corresponds to the area under the stress strain curve after cracking. In this case the fracture energy is assumed to be 200 N/m.

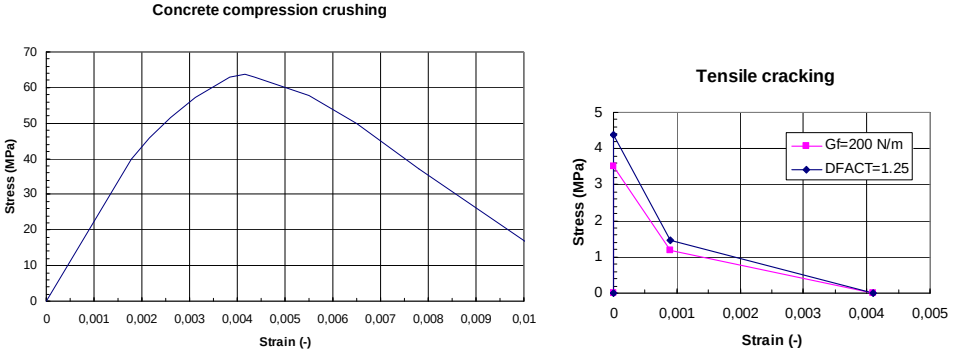

Figure 14. Behaviour of concrete under compression and tension.

Test TF11 was carried out using a stainless steel missile shown in Figure 10. The mass of the missile was 50.5 kg and the impact velocity was 108 m/s. The force time function was calculated by the Riera formula [2] assuming a visco-plastic folding mechanism. The force time function used as a loading function in numerical analyses is shown in Figure 15.

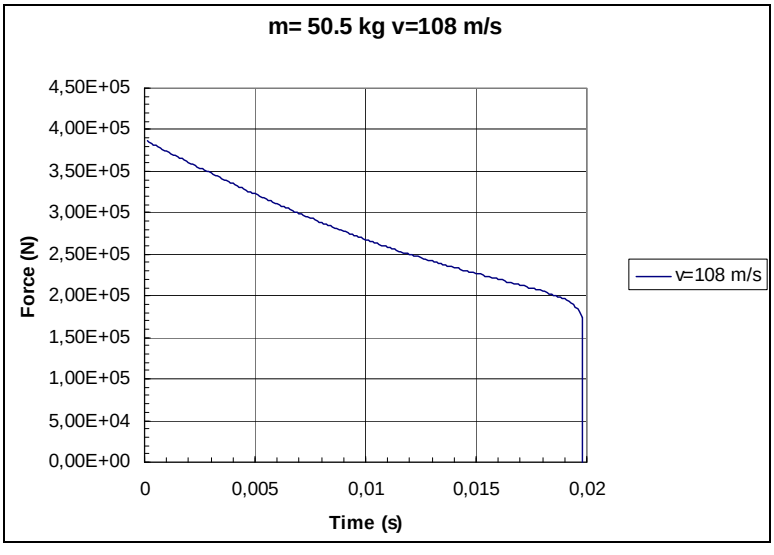

Figure 15. Load function for test TF11.

Simplified method

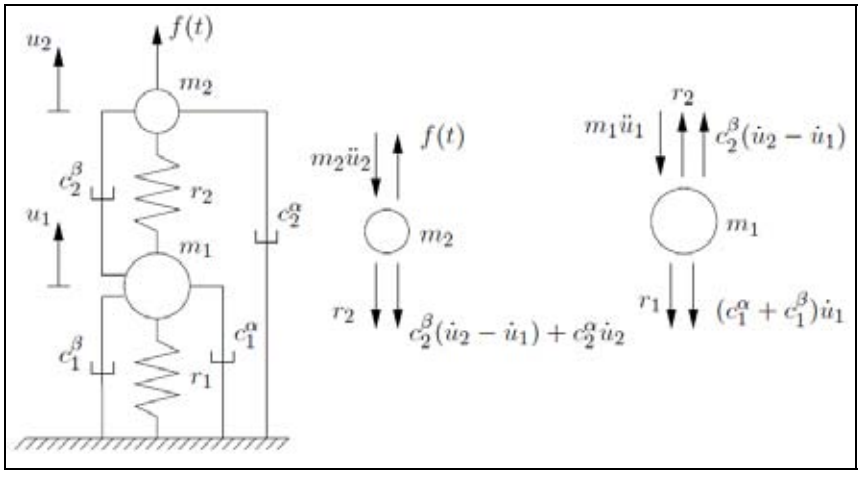

Figure 16. Two degree of freedom impact model with Rayleigh damping.

At least a two degree of freedom model is needed to study both bending and shear failure in a plate impacted by a missile. TDOF model is shown schematically in Figure 16 and it is reported more detailed in [3]. In this model spring 1 and mass 1 are connected with the global bending deformation and spring 2 and mass 2 are used in describing the local shear behaviour at the plate center when the missile impacts.

Dry steel missile test is analysed by a two degree of freedom (TDOF) model assuming a Rayleigh damping and the damping factors $\zeta_1 = 0.1$ and $\zeta_2 = 0.01$ for modes 1 and 2. The shear cone angle is shown in Figure 17.

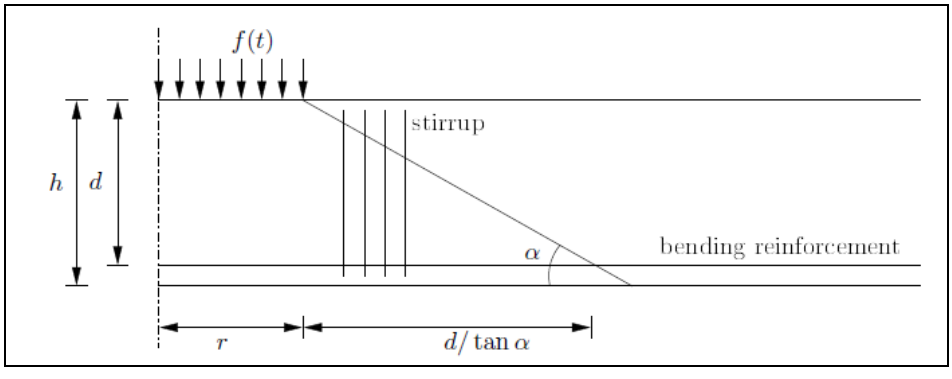

Figure 17. Determination of punching capacity due to stirrups.

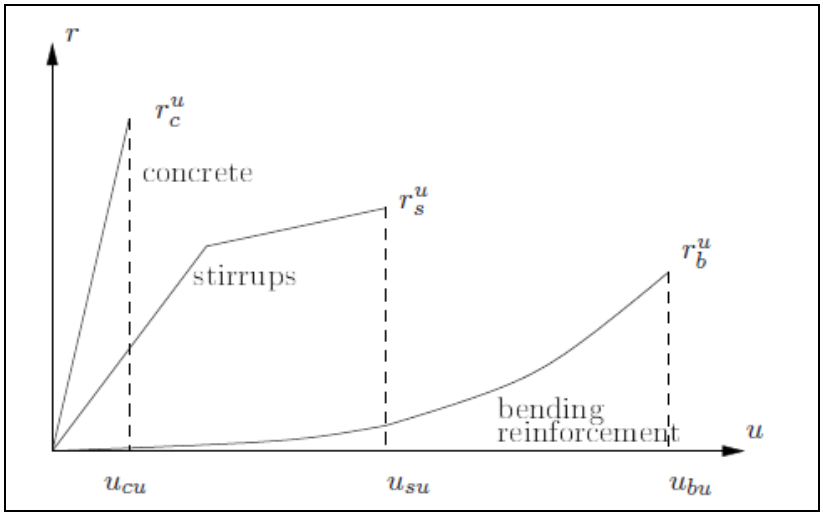

Figure 18. Punching strength due to concrete, stirrups and bending reinforcement.

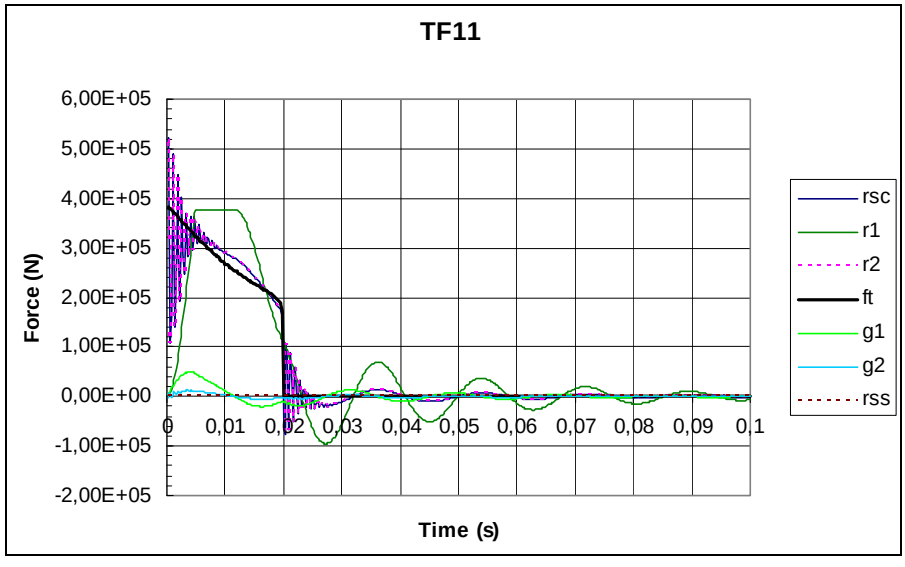

Figure 19. Forces of TDOF model of test TF11, $v_0 = 108$ m/s, $\alpha = 45^o$.

Figure 19 shows various force histories in Test TF11 assuming a shear cone angle of 45°. The internal spring force r_2 (pink dotted curve) consists of the internal force due to the concrete r_{sc} (blue curve). The force acting in the stirrups is small since the punching capacity of concrete is not exceeded. The calculated central deflection as a function of time is presented in Figure 22.

Finite element analyses

The “concrete damaged plasticity” model in Abaqus takes the compression crushing and tensile cracking into account. Damage is associated with cracking and crushing. The uniaxial damage model of concrete is shown in Figure 20. As a default, compression stiffness is recovered after crack closure (w_c = 1) but tensile stiffness is not recovered when tension occurs after compression crushing (w_t = 0).

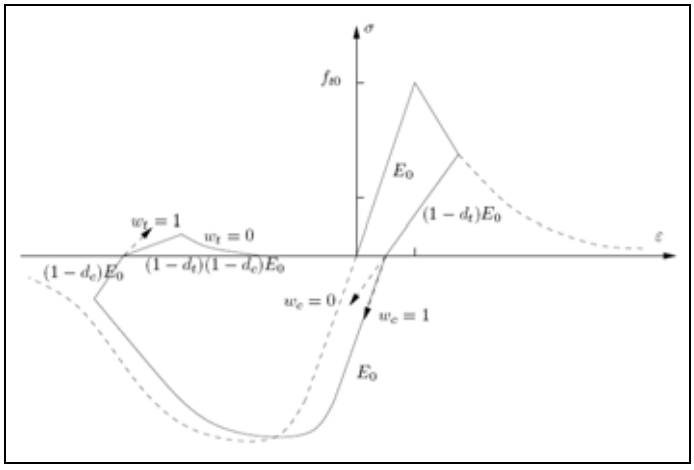

Figure 20. Uniaxial damage model of concrete.

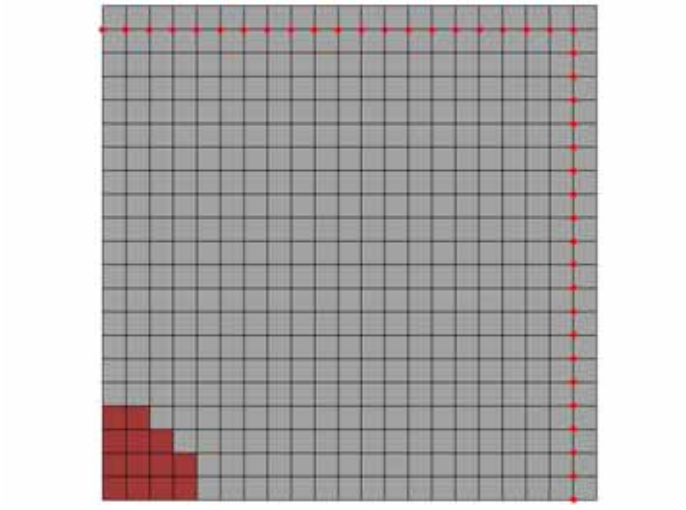

Figure 21. Shell element model, simply supported boundary condition and impact load area indicated with red colour.

Nonlinear finite element analyses were carried out with Abaqus/explicit code [1]. The one quarter finite element model is presented in Figure 21. Due to symmetry, only one quarter of the wall is modelled. The bending reinforcement is modelled as smeared layers. Shear reinforcement is not taken into account. The stress-strain curve used for the reinforcement steel was obtained by static tensile test. The yield strength of reinforcement steel is highly strain rate dependent and increases with the strain rate. This dynamic yield strength was taken into consideration by the Cowper-Symonds formula for uniaxial tension or compression. For mild steel $D = 40$ and $q = 5$ can be used [4].

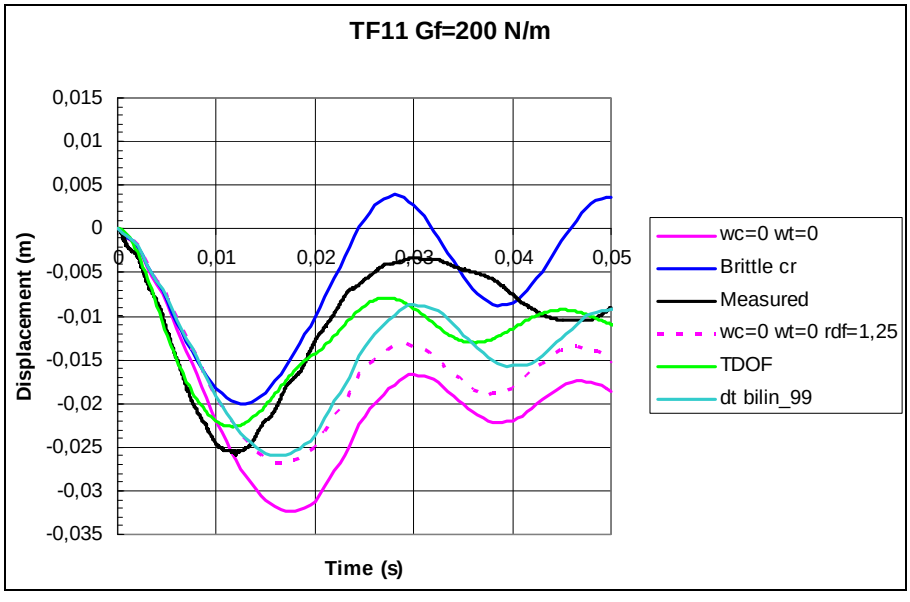

Figure 22. Central deflection as a function of time.

The calculated and measured central deflection values are presented in Figure 22. The blue curve is calculated assuming a “brittle cracking” model. In this case the compression crushing is not taken into account and concrete is assumed to behave elastically under compression. The brittle cracking assumption leads to a slight underestimation of the maximum displacement and the permanent deflection.

The concrete damage model with the assumption of no compression recovery ($w_c = 0$) after tensile cracking overestimated the maximum deflection and the permanent displacement (pink solid curve). High strain rate increases also the tensile strength of concrete.

The effect of the strain rate dependency on tensile cracking behaviour was studied by assuming an increased tensile strength. This was obtained simply by multiplying the tensile strength values with a factor of 1.25. This modified tensile cracking stress-strain curve is also shown in Figure 14. Deflection calculated by using the increased tensile strength assumption is presented with the pink dotted line.

The deflection calculated by the TDOF model is presented with the green curve. This simplified model predicts well the dynamic behaviour of the impact loaded reinforced concrete wall.

Numerical studies on hard missile tests

Missile impacts are usually classified as either “hard” or “soft” according to the missile’s deformability. They may give rise to phenomena of localized target damage like punching as well as to global dynamic flexural response of the target. Three hard missile tests successfully conducted at VTT (referred as A1, AT and AT2) where the dominant failure mode was punching are presented here with numerical simulation results. The target is a 0.25 m thick square slab with a span of 2 m, simply supported on its four edges. It was reinforced with longitudinal bending bars (with a diameter of 10 mm and at 90 mm intervals, on both faces and in both directions). In two of those tests (namely AT and AT2), also transverse shear reinforcement was applied by means of so-called T-headed bars (with a diameter of 12 mm and at each rebar intersection). The tests are listed in Table 2 together with the impact velocity of the missile and various material property values that are considered below. This type of test is shown for instance in Figure 8. The hard missile dimensional drawing is shown in Figure 10.

Table 2. Hard missile test properties.

Test	Impact velocity	Concrete Young’s modulus	Concrete Compression strength*	Concrete tensile splitting strength	Concrete density	Rebar steel yield strength	Rebar steel ultimate strain
	[m/s]	[GPa]	[MPa]	[MPa]	[kg/m^3]	[MPa]	[%]
A1	102	26.5	58	4.00	2212	550	15
AT	100	32.5	54	3.00	2302	550	15
AT2	140	26.8	60	3.90	2231	534	15

* cubic strength in test hall conditions at the testing age

The numerical dynamic analyses, were the target slab, its reinforcement bars and the missile were all modelled separately and explicitly, were conducted with Abaqus/Explicit finite element (FE) code version 6.9-2 [1]. The concrete slab (shown in Figure 1) is modelled with solid 3D elements with 8 nodes, reduced integration and size of 12.5 mm. There are 20 element layers through the thickness of the wall. In a punching case like this with element erosion, the solution gets more accurate with larger amount of elements and for example 50 element layers would give better results. One issue is the number of element layers in the concrete cover. The spalling and scabbing is not modelled very reliably with only two element layers outside the outer rebars as in this study. The total numbers of elements and nodes for the slab are 128 000 and 137 781, respectively.

The model is a 3D quarter model (first quarter seen from the front side) utilizing symmetry conditions. This is reasonable, since the whole structure is nearly symmetric both horizontally and vertically and the missile is assumed to hit the centre of the slab at a straight angle. Only the span width of the wall is modelled and the support conditions are simplified to merely restraining the displacements of the back surface edge nodes in the impact direction. The supporting frame is not included. The boundary conditions have a negligible effect on the main damage modes in this case.

The bending reinforcement bars (shown in green colour in Figure 23) and T-headed bars (shown in yellow colour in Figure 23) are modelled with linear beam elements with 2 nodes and a element length of 12.5 mm. The rebars are embedded rigidly inside the concrete, in the exact location they are initially in relation to the concrete elements. There is not any really accurate interaction, such as bond slipping, between the bars and concrete. The rebar ends also have symmetrical boundary conditions. The rebars are also shown in Figure 25. The missile, shown in Figure 23 and in Figure 25, is modelled with solid 3D elements with 8 nodes, reduced integration and approximate size of 10 mm. An initial velocity shown in Table 1 is given to the missile.

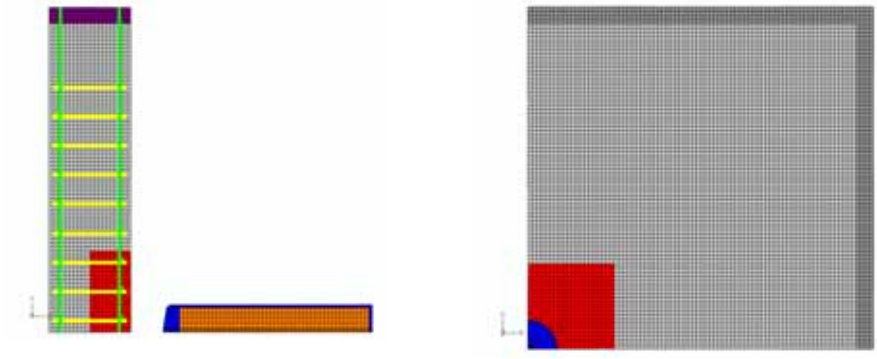

Figure 23. FE model of the target slab and the missile (side view and back view).

The constitutive law for all the steel materials in the model is an elastic-plastic material model with von Mises yield surface and isotropic hardening. The strain rate dependency is taken into account by Cowper-Symonds formula. The tested static ultimate strain values varied between 17.9% and 20.4%, but in every simulation, failure criteria of both 15% plastic shear and ductile tensile strain are applied. After reaching that level, the rebar elements are removed from the model. Figure 24 (on the right) shows the stress-plastic strain curve for zero plastic strain rate for all the steel materials in the model. Young's modulus, Poisson coefficient and density for all the steels were 200 GPa, 0.3 and 7 850 kg/m^3, respectively.

The constitutive law for concrete is much more difficult and arguable question. Abaqus provides couple of models developed especially for concrete, but they do not allow element erosion. "Concrete brittle cracking" model allows erosion in a certain way, but it is not adequate for highly dynamic case with separately modelled rebars. Since deep penetration and even perforation take place, element erosion has to be included. All the concrete elements have a material model with von Mises yield surface and isotropic plastic hardening. Figure 24 (on the left) shows the stress-plastic strain curve for zero plastic strain rate for the concrete materials in different tests. The tensile behaviour is taken into account only by the erosion criterion explained below. The strain rate dependency is taken into account by defining multiplication factors for the stress-plastic strain curve for different strain rates. For instance, at strain rate of 10, the curve is multiplied by 1.95.

The failure criteria depend on the part of the slab. The impact zone indicated by red colour in Figure 23 has an erosion criterion of 21% compressive plastic

strain. That is by no means based on any real consistent and universal physical behaviour of the concrete in compression. This parameter was adjusted to attain a right kind of compression crushing behaviour. The support zone has no element erosion. The other parts of the concrete have a hydrostatic tensile stress erosion criterion of which magnitude is the splitting tensile strength multiplied by 5. The splitting tensile strength for the concrete materials used in the tests is approximately 4 MPa (shown in Table 2), but high strain rates increase it considerably. It is assumed that wherever there is high tension, the strain rate is also high.

The constitutive law for the missile steel is the same as that used for the reinforcement steel, but without any element erosion. The light weight concrete inside the missile shell is modelled in the same way as the concrete in the slab, but without element erosion and with much lower strength.

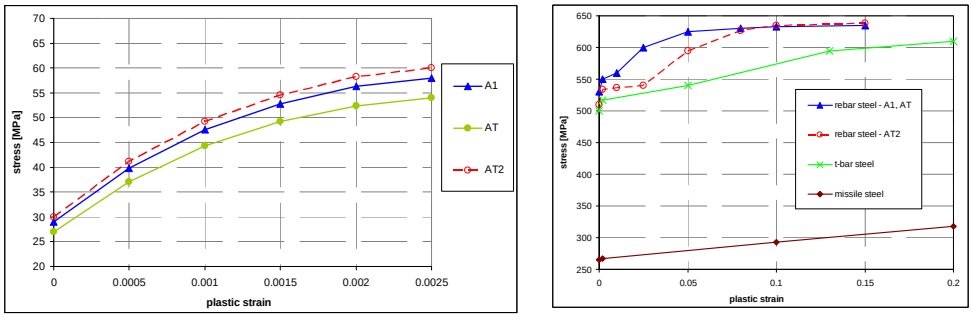

Figure 24. Stress – plastic strain curves for concrete (left) and steel (right) materials.

There is a general contact between every free element facet in the model, thus everything that would have a contact in reality, also has a contact definition in the model. Friction coefficients of various magnitudes are used for contacts in tangential direction. Contact in normal condition is mainly hard, i.e. the pressure-overclosure relationship is without physical softening, but some softening between the missile steel and the outer surface of concrete is applied.

The analysis time for each analysis is 20 ms. The impact starts after 1 ms. The time increment size was approximately $3 \cdot 10^{-7}$ s. Figure 25 shows the induced damage to the target walls in the simulations (on the left) and tests (on the right). The deformed FE model is partly transparent and shows where the concrete elements have eroded. Perforation in test AT2 is simulated in a realistic way. Figure 26 shows the measured and simulated slab displacements in test AT2.

The locations of the displacement sensors (horizontal distance in [mm] from the slab centre) are also shown. The corresponding vertical distance is 230 mm. The maximum measured and simulated values are 13.1 mm and 7.4 mm, respectively. The oscillation frequency is higher in the simulation. Figure 27 shows the position [m] of the missile front in every test in impact direction. The impact takes place in zero-position, and consequently, perforation in -0.25 m position.

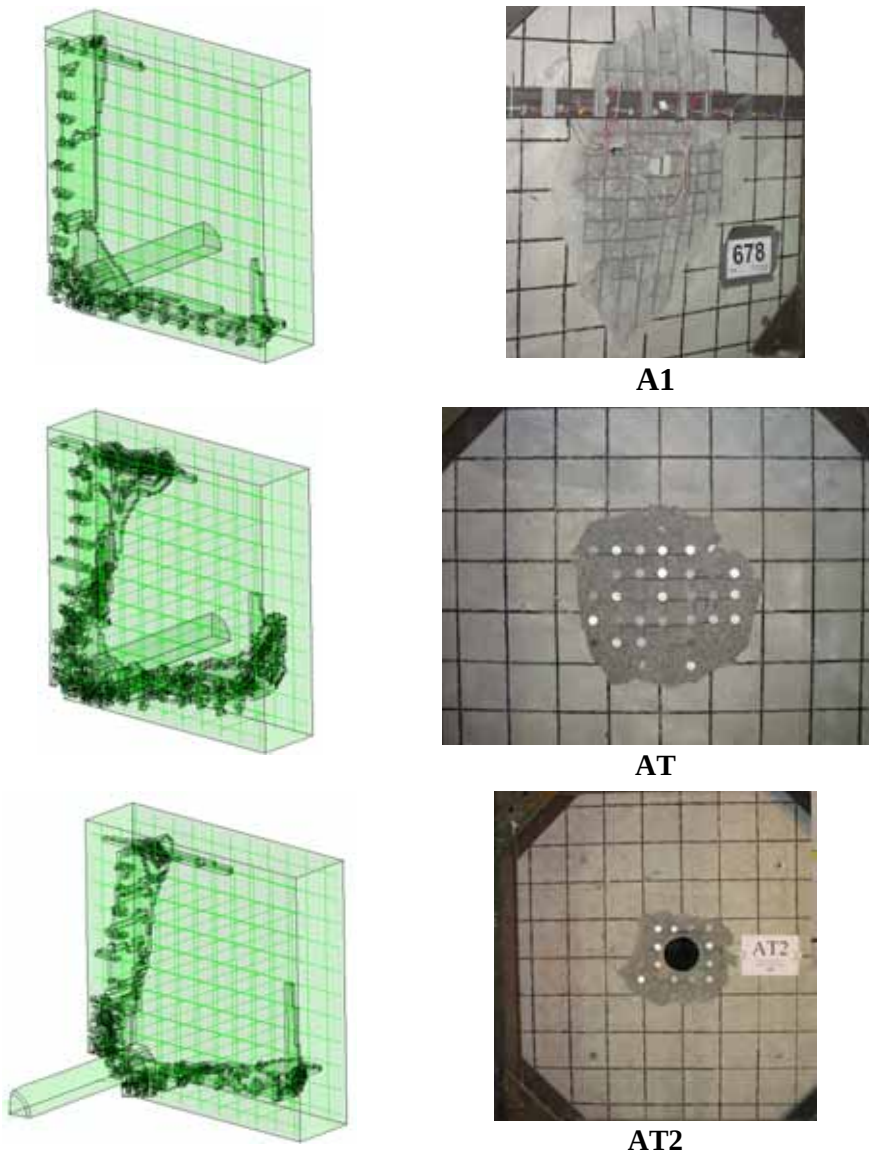

Figure 25. Damage to the target walls in the simulations (on the left) and tests (on the right).

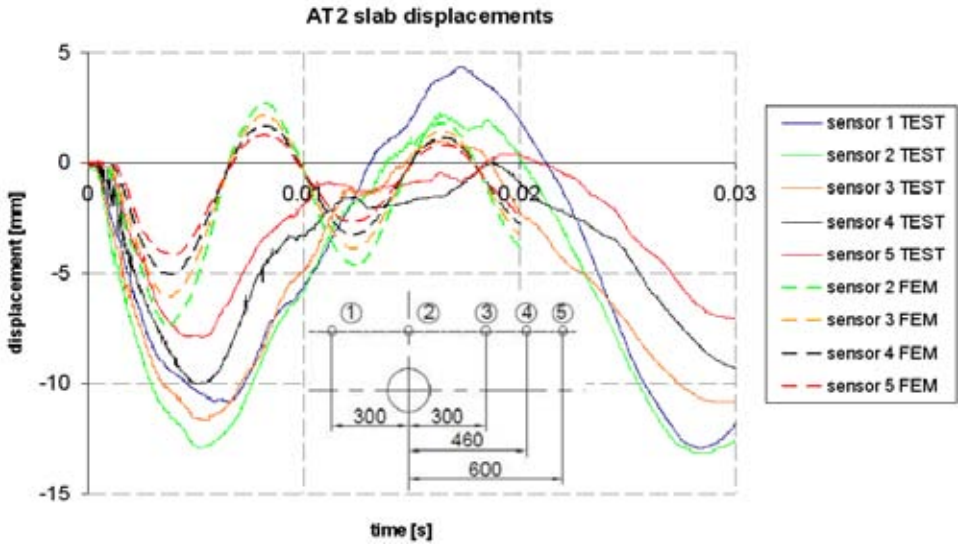

Figure 26. Measured and simulated slab displacements [mm] in test AT2.

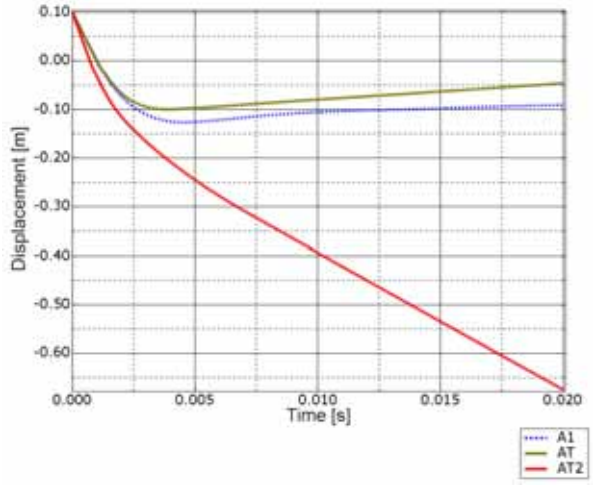

Figure 27. Position [m] of the missile front in every test in impact direction.

Table 3 shows that there is a good correlation between the main measurement and simulation results even though the impact velocity, reinforcement, material properties and the realized damage mechanisms were variable. The simulations somewhat overestimated the penetration depth, but on the contrary, underestimated the residual velocity in case of perforation.

Table 3. Main measurement and simulation results.

Test	Impact velocity	Penetration depth TEST	Penetration depth FEM	Residual velocity TEST	Residual velocity FEM
	[m/s]	[mm]	[mm]	[m/s]	[m/s]
A1	102	120	130	Bounce	Bounce -1
AT	100	38	100	Bounce	Bounce -3
AT2	140	perforation	perforation	45	28

Jet fuel dispersion

Liquid dispersal study

The liquid spread phenomena have been studied in the IMPACT tests both experimentally and numerically. The goals of the study were to get both qualitative and quantitative information of the liquid dispersion phenomena under impact conditions, to measure some of the most important input parameters needed for numerical simulations, and to take in use and to validate simulation methods for the determination of fuel spread and fires.

Because the IMPACT project has been mainly focused on structural aspects, it was necessary to develop relatively cost-effective methods for measuring liquid dispersal phenomena. As in the previous SAFIR programme, the speed and direction of liquid spray coming out from a ruptured missile and the propagation velocity of spray front were measured using high-speed video cameras (500–1 000 fps). Extent of liquid spray was roughly estimated according to wetted area on the floor of the test hall. Size of falling droplets was photographted and measured from the oil-coated collection plates located on the floor. Because the earlier drop-size measurements of flying droplets were partly unsuccessful and because the droplet size is an important input paramemer needed for numerical simulations, special efforts were directed to measurements of drop size of flying droplets using a high-speed video camera and stroboscope for backlightning illumination.

The results of new measurements confirmed the earlier observations that the initial discharge speed of liquid spray was relatively high. The ratio of liquid discharge speed to the impact velocity of liquid container (missile) was mostly

as high as 2–2.5. This result did not indicate any remarkable sensitivity to the impact velocity and initial liquid mass under consideration.

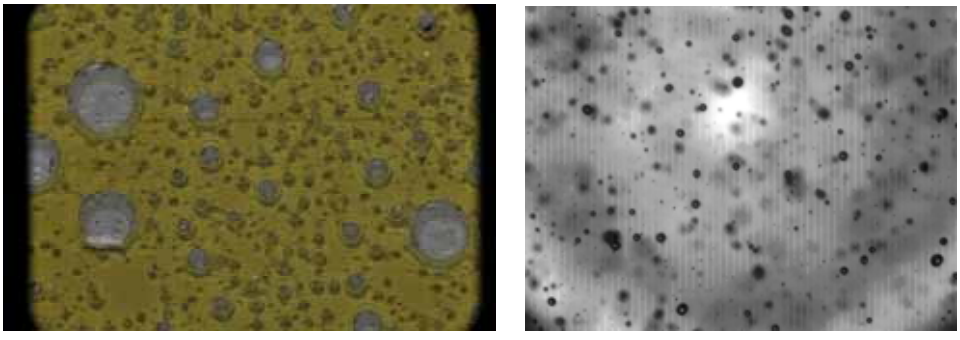

Figure 28. Photographs of drop size measurements: droplets on floor (left) and flying droplets (right). Impact velocity 108 and 135 m/s, initial liquid mass 26 and 25 kg, respectively.

Some results of drop size measurements of landed and flying droplets are show in Figure 29 taken from two different IMPACT tests. Size distributions of landed droplets are plotted in three different measurement locations (distance). Arithmetic mean diameter of landed droplets was about 280–350 µm, whereas the mean diameter of flying droplets was around 80–170 µm in the tests under consideration. The corresponding Sauter mean diameters were 420–540 µm and 140–220 µm, respectively. Note that the flying droplets were measured at 2 m distance from the impact target, whereas the oil-coated collection plates were located on the floor at 3.8–7.8 m distance from the target. General trend of the IMPACT measurements was that the drop size of landed droplets was higher than that of flying droplets. Earlier laboratory studies have indicated that water droplets maybe coalesced in oil even if the viscosity of the oil was very high. In addition, very small droplets probably evaporated before they penetrated into the oil layer or before the fotographs were taken. Consequently, number of small droplets was probably underestimated in the oil samples. Moreover, some water droplets splashed off the surrounding structures and impinged the collection plate affecting the size distribution on the plates. The “splash effect” was minimized in the drop-size analyses by filtering away the largest drops of the samples on the collection plates on the floor.

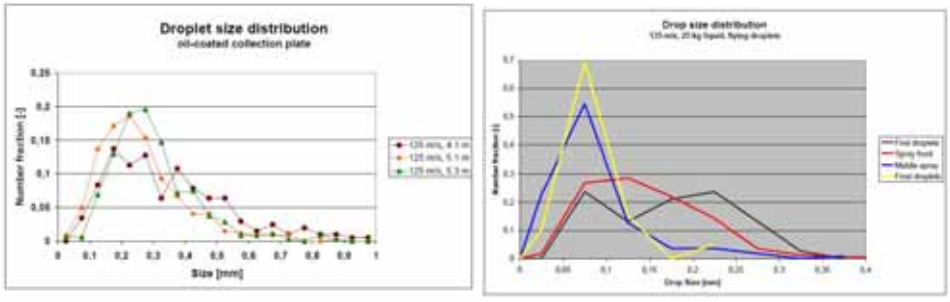

Figure 29. Measured drop size distribution in two different IMPACT tests: droplets on floor (left) and flying droplets (right). Image width 15 mm. Impact velocity 125 and 135 m/s, initial liquid mass 37 and 24 kg, respectively.

The Fire Dynamics Simulator (FDS) program was taken in use in earlier SAFIR programme, and testing and validation of the program continued for the determination of fuel spread and fires. The program was also used to estimate the fraction of the aircraft fuel that accumulates into pools and to examine the heat exposures resulting from a large-scale kerosine release.

Spray computations for 10 tn of kerosine

CFD simulations of the liquid fuel and the resulting fireball during an aircraft impact were performed using the Fire Dynamics Simulator (FDS) code. The simulations were used to investigate the fraction of the fuel that is accumulated into the pools on the ground and the thermal exposures from the initial fireball.

In FDS, the fluid motion is computed using weakly compressible Large Eddy Simulation (LES)-based solver [5]. This model can not predict the increase of pressure by detonation. The two-phase flow of consisting of air and fuel/water is computed using Eulerian-Lagrangian concept where the liquid droplets have zero volume in Eulerian space. This means that the liquid-liquid interactions, that may have importance in dense sprays and early phase of the impact, can not be taken into account. Three modifications were implemented into FDS during the current project: a breakup model for the prediction of the final droplet size distribution, a drag reduction model, and a droplet-CFL condition for the numerical stability and accuracy. See FDS Technical Refrence Guide for more information on the other physical sub-models and numerical implementation.

Before the actual jet fuel simulations, the choice of boundary conditions for the simulation of fuel released from a full scale aircraft impact was examined

and overall performance validated by carrying out simulations of the Sandia Phantom F-4 experiment where five tons of water was released from the tanks of a military aircraft hitting the concrete wall at speed of 215 m/s [6, 7]. The validation can be considered as semi-quantitative because it was mostly based on comparison of water cloud shape and size between video recordings and FDS computations. The simulations were able to reproduce the main qualitative features of the water cloud.

Figure 30 shows a snapshot of the simulated water cloud shape. A reasonable agreement was also found between the predicted and simulated cloud sizes and water front speeds.

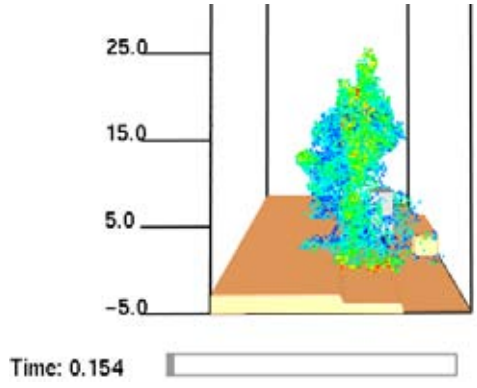

Figure 30. Simulated water cloud in the Sandia Phantom F-4 test.

The jet fuel simulations were performed for a 10 ton of heptane released within a 0.1 s impact at initial speed of 250 m/s. The fuel was ignited immediately on the impact. Damage to the building resulting from the mechanical forces was ignored. The main results from the study were the fraction of the fuel that did not burn in the air, but reached the ground forming burning pools, and the thermal exposure in the vicinity of the impact.

The results indicated that the fraction of the accumulated fuel depends strongly on the choice of the droplet size distribution and the height of the impact location. The mass of the released fuel had also some effect. Figure 31 shows the fraction of fuel accumulated in pools as a function of the initial median droplet diameter of the fuel droplets when the impact height was 15 m from the ground. The pooling fraction is shown to decrease steeply when the median diameter is decreased below 100 μm. The effect of the impact height is

shown in Figure 32 which indicates that practically all the fuel is burned in the fire ball when the impact takes place at height of 30 m from the ground or above.

Figure 33 shows instantaneous temperature fields in a vertical plane cutting through the impact point. Highest temperatures are observed between two and three seconds from the impact, and the main fire ball leaves the 150 m high computational domain in about 10 s. Electrical cables were used as indicators of the severity of the thermal exposure. Based on the simulation results, damages could be expected within a 60 m distance from the impact location.

The current results highlight the importance of physical modelling the droplet size distribution. More work should be done to validate the current breakup model using the data collected from the impact scenarios.

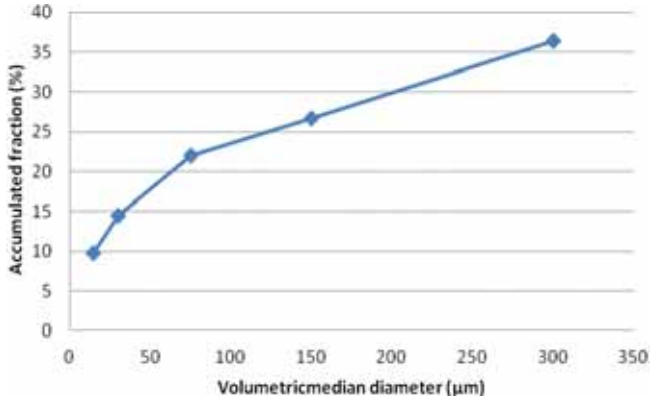

Figure 31. Effect of initial droplet size on the pooling fraction of the fuel.

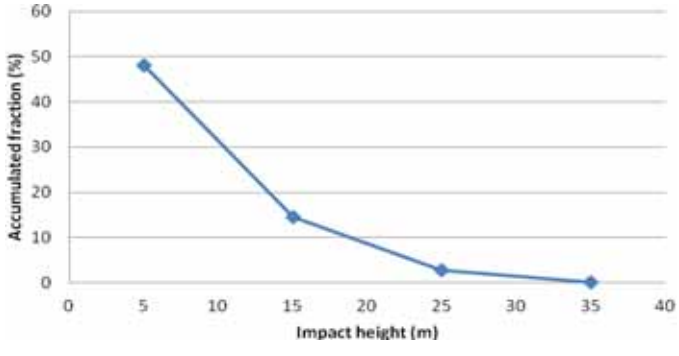

Figure 32. Effect of the impact height on the fuel pooling fraction (d_m = 30 µm).

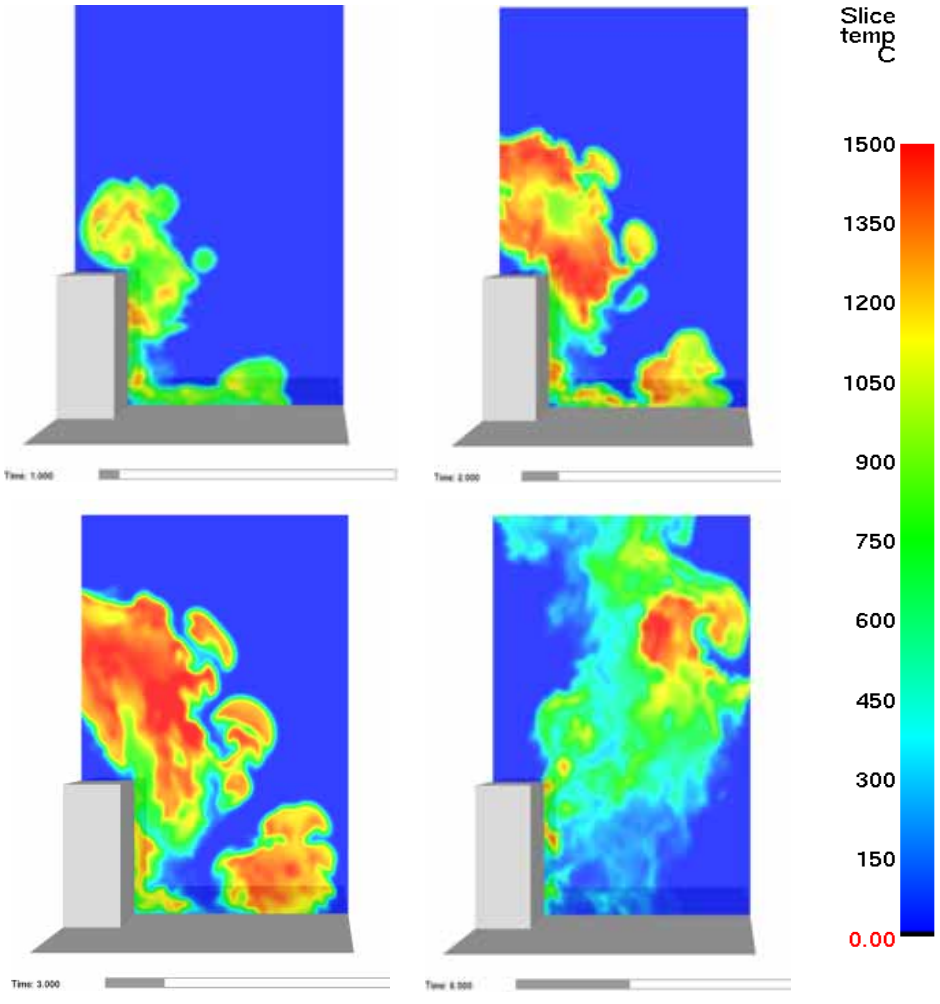

Figure 33. Instantaneous temperature fields in the simulation.

Conclusions

Many tests have been done successfully with the Impact test facility and the test campaign is now moving towards more complex and more elaborate wall and missile configurations. The second phase of the international test campaign is going on.

Bending and shear failure of a reinforced concrete slab subjected to a projectile impact can be simply modelled with a two mass system. The two mass system is, however, sensitive to the assumed angle of shear cone. Determination

of damping parameters requires carefully conducted tests. Nonlinear analyses of reinforced concrete structures are quite sensitive for material parameters. Assumed tensile cracking properties of concrete dominate the calculated maximum deflection value. Tensile damage assumptions affect the dynamic vibration behaviour of the damaged wall. Also the assumption of the compression recovery after tensile cracking seems to affect remarkable the bending vibration frequency and the permanent displacement of the wall.

In the hard missile studies there is a good correlation between the main measurement and simulation results even though the impact velocity, reinforcement, material properties and the realized damage mechanisms varied in different tests. However, the finite element model was developed in such an artificial way that it is able to describe the assumed behaviour, and it is thus not universally applicable to all types of cases, especially if they are beforehand unknown. The used complex analysis method is able to predict the mechanical behaviour of reinforced concrete structures subjected to hard missile impact, such as tunneling, perforation, scabbing and global slab oscillation, but it is very sensitive to certain parameters which may not necessarily have any physical relevance. The methods, codes and computational capacity allow very sophisticated and detailed simulations, but more experience, stronger command of these varying methods and deeper understanding of the physical phenomena is still needed.

Liquid dispersal study has given new qualitative and quantitative experimental information on the phenomena affecting liquid spread, and on important input parameters such as spray speed, propagation direction and drop size needed for numerical simulation. The Fire Dynamics Simulator (FDS) program has been applied both in liquid spreading and fuel burning analyses in impact.

References

1. Abaqus Theory Manual, version 6.10-1. Dassault Systemes, 2010.

2. Riera, J.D. On the stress analysis of structures subjected to aircraft impact forces. Nuclear Engineering and Design 1968, Vol. 8, pp. 415–426.

3. Saarenheimo, A., Calonius, K., Tuomala, M. & Hakola, I. Soft Missile Impact on Reinforced Concrete Wall. Journal of Disaster Research 2010, Vol. 5 No. 4.

4. Jones, N. Structural Impact. Cambridge University Press. 1989.

5. McGrattan, K., Hostikka, S., Floyd, J., Baum, H. & Rehm, R. Fire Dynamics Simulator (Version 5) Technical Reference Guide. National Institute of Standards and Technology, MD. USA. NIST Special Publication 1018-5, 2007. 86 p.

6. von Riesemann, W.A., Parrish, R.L., Bickel, D.C., Heffelfinger, S.R., Muto, K., Sugano, T., Tsubota, H., Koshika, N., Suzuki, M. & Ohrui, S. Full-Scale Aircraft Impact Test for Evaluation of Impact Forces. Part 1: Test Plan, Test Method, and Test Results. 1989. Trans. 10th International Conference on Structural Mechanics in Reactor Technology, Vol. J. Pp. 285–299.

7. Sugano, T., Tsubota, H., Kasai, Y., Koshika, N., Orui, S., von Riesemann, W.A., Bickel, D.C. & Parks, M.B. Full-scale aircraft impact test for evaluation of impact force. Nuclear Engineering and Design 1993, Vol. 140, pp. 373–385.

31. Challenges in Risk-informed Safety Management (CHARISMA)

31.1 CHARISMA summary report

Ilkka Karanta
VTT

Abstract

The CHARISMA (CHAllenges in Risk-Informed MAnagement) project consists of research tasks related to the use of probabilistic safety assessment (PSA) in decision making, developing assessment methods for nuclear plant operation and maintenance, and developing solutions to problem areas within PSA. In addition to the research tasks, advancement of skills, transfer of skills to the new generation and international cooperation are achieved within CHARISMA. The topics include risk-informed decision making, human reliability analysis, reliability of automation and level 2 & 3 PSA.

Introduction

Challenges in risk-informed management are two-fold: the use of risk information as a support for decision making, and the problem areas within the PSA itself. The use of risk information in decision making is challenging, because PSA is a complex field integrating different kinds of statistical and subjective information into a probabilistic model. The concurrent use of both deterministic and probabilistic safety analyses as the basis for decision making is the subject of ongoing discussion. Proper documentation of the assumptions behind both the analysis and the probability model enhances the transparency of

the PSA model and supports interpretation of the results. Communications process between the PSA experts and other experts is crucial for drawing conclusions on the risk significance of different components in the risk analysis.

Due to a nuclear power plant's nature as a complex socio-technical system the challenges in its risk assessment are numerous:

- Identification and screening of hazards to be modelled. Recent issues here include the identification of internal and external hazards (e.g. severe weather phenomena) and their impact on plant safety functions.
- Identification of dependencies and interactions between systems and processes. This includes e.g. dependencies between human interactions, I&C systems and power supply systems.
- Reliability modelling of dynamically behaving systems. Recent issues include digital I&C systems and accident phenomena in level 2 PSA.
- Estimation of probabilities for events and issues where statistical data is rare or totally missing. This includes e.g. estimation of human error probabilities, software error probabilities and frequencies for rare external events.

Main objectives

The main objectives of the project were to develop risk-informed decision making methods integrating results from risk and reliability analyses with other expertise in the problem domain, to develop assessment methods for plants' operation and maintenance to enhance planning of activities and acting in situations, to develop methodologies in the problem areas of PSA, to advance skills in risk analysis, to assure competence transfer to the new generation and to participate in international co-operation.

Risk-informed decision making

PSA-related safety goals

The outcome of a probabilistic safety assessment (PSA) for a nuclear power plant is a combination of qualitative and quantitative results. Quantitative results are typically presented as the Core Damage Frequency (CDF) and as the frequency of an unacceptable radioactive release. In order to judge the acceptability

of PSA results, criteria for the interpretation of results and the assessment of their acceptability need to be defined. The goals are intended to define an acceptable level of risk from the operation of a nuclear facility. However, safety goals usually have a dual function, i.e., they define an acceptable safety level, but they also have a wider and more general use as decision criteria. The exact levels of the safety goals differ between organisations and between different countries. There are also differences in the definition of the safety goal, and in the formal status of the goals, i.e., whether they are mandatory or not.

The Nordic project has explored the issue of probabilistic safety goals for nuclear power plants and provided guidance related to the resolution of some of the problems identified, such as the problem of consistency in judgement, comparability of safety goals used in different industries, the relationship between criteria on different levels, and relations between criteria for level 2 and 3 PSA [1, 2, 3]. In parallel, additional context information has been surveyed by contributing to and benefiting from an international activity related to PSA criteria within the OECD/NEA Working Group Risk [4]. Figure 1 gives an overview of some (but not all) of the concepts that are involved when defining and applying probabilistic safety criteria, using criteria for core damage and unacceptable release as an example.

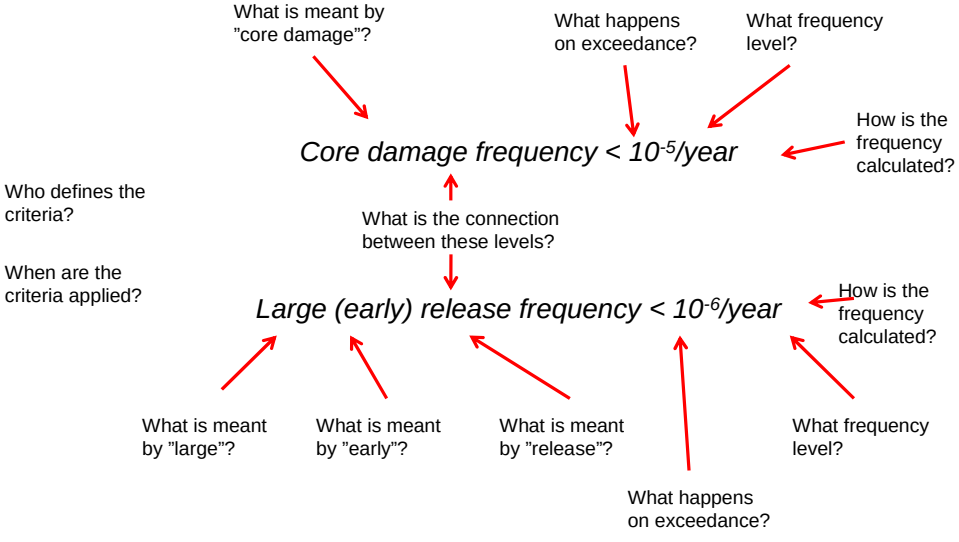

Figure 1. Concepts and questions related to probabilistic safety criteria.

Risk-informed defence-in-depth

The concept of defence-in-depth (DID) is fundamental to safety of nuclear power plants. It calls for multiple successive methods or barriers to radioactive release to the environment. A methodology to assess the DID levels using a plant-specific PSA has developed in this subtask. The work included: 1) mapping of conditions that should be considered for the DID levels, and 2) definition of quantitative measures that should be considered for the defence in depth levels [5]. The approach was studied using loss-of-coolant accidents (LOCA) as examples. The focus was on DID levels 1 and 2, i.e., prevention of abnormal operation and failures and control of abnormal operation and detection of failures, since typically they are not explicitly modelled in PSA-studies.

Risk evaluation of technical specification conditions

The use of risk informed methods in daily operation at nuclear power plants as well as for long term evaluation and definition of rules and regulations is increasing. Risk informed methods have been applied on a case by case basis during the past few years, but it is expected that these methods will be applied in a quite different manner in the coming years.

A literature study and interviews with representatives of the Swedish and Finnish utilities and authorities were carried out on the use of risk-informed approaches to evaluate Technical Specifications (TS). According to the interviews, there is a reasonable agreement on the existing TS evaluation methods on a general level. However, there is no common agreement on the basis for the TS analyses, e.g. types of initiating events and risk measures to be studied. Further, especially concerning the risk-informed approaches for evaluating allowed outage times, the Finnish and Swedish views are diverging.

The report [6] summarises the interviews and provides a short background to the current TS and to the role of PSA in the TS evaluation process. Methods, discussions and comments with regard to surveillance test interval and allowed outage time analyses respectively are presented. In a second phase of the study, to be started in 2009, the aim is to develop guidance to facilitate the use of PSA in interpretation and evaluation of TS criteria.

Human reliability

Risk-informed management of fire situations

In the subtask the analysis of the management of a fire situation as a functional and cooperative whole has been developed further [7, 8, 9]. The specific conditions of decision-making and co-operation and their influence on the control room crews' and fire brigades' action possibilities during fires have been analyzed in order to identify the essential components of the controllability of a situation. The potentials of the approach in safety management and human reliability analysis (HRA) at the plants have been considered.

Co-operation of CHARISMA and FIRAS projects has been started in order to integrate the different methodological approaches to fire safety and management of fire risks. The combination of the qualitative and the quantitative approach has been used for modeling of operational actions in a fire scenario, as part of probabilistic risk assessment.

Emerging human reliability analysis

The subtask aims at reviewing different new approaches to HRA. The work has been carried out by international collaboration. In the international empirical study of HRA methods organised by the OECD/NEA Halden Reactor Project [10], simulator runs were run for two scenarios relevant in PSA context. Several HRA teams from different countries analysed the scenarios with their own HRA methods, and the approaches will be compared. VTT is one of the HRA teams using a method called the enhanced Bayesian THERP (Technique for Human Reliability Analysis) [12]. VTT also participated in another Nordic-German co-operation project, EXAM-HRA. Overall aim of the EXAM-HRA project is to develop best practices guidance for Nordic and German power plants. For a more in-depth description of the work, see the article "EXAM-HRA Project Phase 1: Survey of HRA Practices in Nordic and German PRAs" in this SAFIR-2010 final report or the summary report of the project [11].

Reliability of automation

Digital protection and control systems are appearing as upgrades in older nuclear power plants (NPPs) and are commonplace in new NPPs. To assess the risk of NPP operation and to determine the risk impact of digital system upgrades on NPPs, quantitative reliability models are needed for digital systems. Due to the

many unique attributes of these systems, challenges exist in systems analysis, modeling and in data collection. Currently there is no consensus on reliability analysis approaches. Traditional methods have clearly limitations, but more dynamic approaches are still in trial stage and can be difficult to apply in full scale probabilistic safety assessments (PSA). The number of PSAs worldwide including reliability models of digital I&C systems are few.

Reliability of distributed control systems

In current PSAs, distributed control systems are analysed and modelled very simply. The subtask aims at bringing the analysis of digital systems reliability to the systems architecture level. A survey on reliability assessment of computer-controlled systems has been performed [14]. Dynamic methodologies, such as dynamic flowgraph methodology (DFM) and Markov models, can provide a more accurate representation of probabilistic system evolution in time than the traditional fault tree approach. These methods included unique features that make them suitable for specific applications, but they do not solve the problem of software reliability. The main application case of the subtask has been the feedwater system of a boiling water reactor, and the method used the dynamic flowgraph methodology (DFM) [16]. Computational complexity of DFM has also been analyzed [15]; it turns out that the computational effort of DFM is, in the worst case, exponential, and is quite sensitive to small changes in the model. Importance measures for DFM models have been considered [13]; measures based on the analysis of prime implicants and measures developed for Markov models were found to hold most promise. An alternative DFM approach based on interpreting the DFM model as a binary decision diagram has been developed at VTT; a software implementation based on BDD, Yadrat, has been developed in a separate project. A comparison between two DFM software was performed [17].

Guidelines for reliability analysis of digital systems in PSA context

A comparison of Nordic experiences and a literature review on main international references have been performed [18]. The study shows a wide range of approaches, and also indicates that no state-of-the-art currently exists. The study shows areas where the different PSAs agree and gives the basis for development of a common taxonomy for reliability analysis of digital systems. It is still an open matter whether software reliability needs to be explicitly modelled in the

PSA. The most important issue concerning software reliability is proper descriptions of the impact that software-based systems have on the dependence between the safety functions and the structure of accident sequences. In general the conventional fault tree approach seems to be sufficient for modelling reactor protection system kind of functions. The following focus areas have been identified for the further activities: 1. Develop a taxonomy of hardware and software failure modes of digital components for common use, 2. Develop guidelines regarding level of detail in system analysis and screening of components, failure modes and dependencies, 3. Develop approach for modelling of CCF between components (including software).

Level 2 and 3 PSA

Modelling of phenomenological uncertainties

The Master's Thesis [19] surveyed how phenomenological uncertainties are modeled in level 2 PSA. The methods were applied to a study case of Loviisa nuclear power plant. The accident scenario is a small loss-of-coolant accident where in addition the emergency core cooling is lost. A dynamic PSA modeling tool, STUK PSA [20], was used to modify Loviisa containment event tree. The dynamic modeling approach was compared to the conventional event tree-fault tree modeling. The results show that delay in taking the safety actions has impact in several phenomena. Probabilistic models are constructed that take the delay into account. To support probability quantification, accident simulations are performed using a MELCOR [21] model of Loviisa. The delay is sampled, and the results are presented as distributions in order to quantify the uncertainty of the results. The dynamic approach enables more detailed modeling. Uncertainty analysis is simpler to perform than with the conventional point estimate approach.

Level 3 PSA

Long duration release

In the off-site consequence model ARANO [22], it is assumed that weather is constant during the whole release duration. But during a long release it can be expected that dispersion conditions can be changed. To evaluate significance of weather changes on off-site doses, the existing calculation model was modified to calculate consequences on an hourly base. Then each release phase of one hour can have different weather.

Test calculations indicate that not remarkable differences are expected when calculations are done with hourly based weather data compared with the preliminary approach of constant weather during the release [23, 24].

ASAMPSA2

ASAMPSA2 (Advanced Safety Assessment Methodologies: Level 2 PSA) is a EU-project aiming to develop best practice guidelines for the performance of Level-2 PSA methodologies with a view to harmonization at EU level and allowing a meaningful and practical uncertainty evaluation in a Level-2 PSA. The draft guidelines document [25, 26, 27], is under review by the end users at the moment of writing this paper. For more information, see the homepage of the project http://www.asampsa2.eu/.

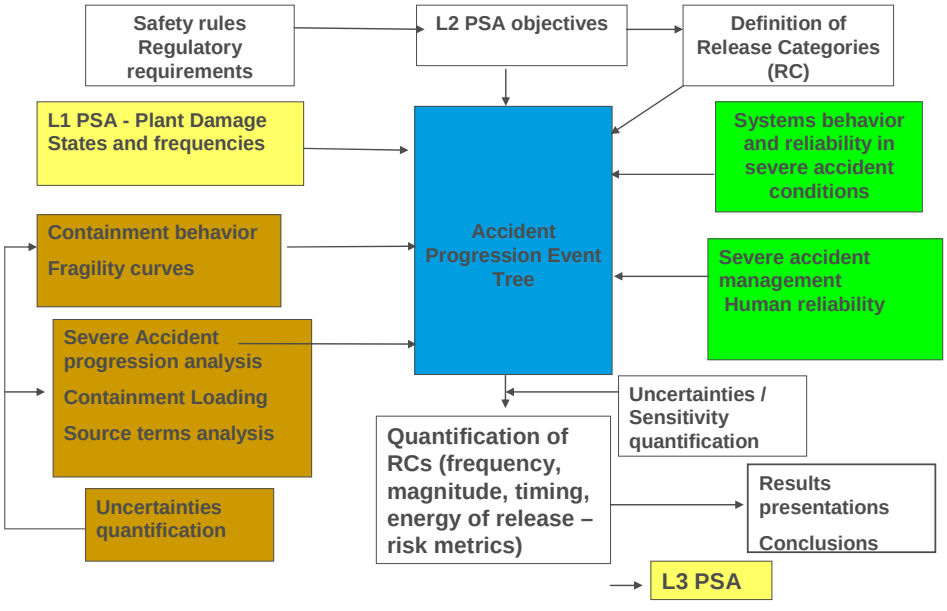

Figure 2. Elements of level 2 PSA [25].

Conclusions

Challenges in risk-informed management are two-fold: the use of risk-information as a support for decision making, and the problem areas within the PSA itself. The PSA safety goals usually have a dual function, i.e., they define an acceptable safety level, but they also have a wider and more general use as

decision criteria. The use of risk informed methods in daily operation at nuclear power plants as well as for long term evaluation and definition of rules and regulations is increasing. Risk informed methods have been applied on a case by case basis during the past few years, but it is expected that these methods will be applied in a quite different manner in the coming years. An example is the assessment of the defence-in-depth as demonstrated in CHARISMA.

Methods for human reliability analysis can be tested by benchmarking them against simulator studies. For dynamically behaving systems, other reliability modelling methods than static event tree-fault tree approach may be needed. Alternative methods have been tested for modelling of digital I&C systems and accident phenomena in level 2 PSA. International collaboration has initiated to develop guidelines for the reliability analysis of digital systems in PSA context. Interdisciplinary collaboration with FIRAS project has been conducted in the development of an integrated modeling approach to support fire PSA.

CHARISMA project has been also active in international co-operation through e.g. OECD/NEA Working Groups Risk (WGRISK), Nordic Nuclear Safety Research (NKS), Nordic PSA Group (NPSAG), Halden reactor project and ASAMPSA2 project in the EU FP7 programme. Results have been presented internationally at the most important conferences in this field.

References

1. Holmberg, J.-E. & Knochenhauer, M. Probabilistic Safety Goals. Phase 1. Status and Experiences in Sweden and Finland. SKI Report 2007:06, Statens kärnkraft-inspektion (SKI), Stockholm, 2007.

2. Holmberg, J.-E., Björkman, K., Rossi, J., Knochenhauer, M., He, X., Persson, A. & Gustavsson, H. Probabilistic Safety Goals. Phase 2. Status Report. NKS-172, Nordic nuclear safety research (NKS), Roskilde, 2008.

3. Holmberg, J.-E. & Knochenhauer, M. Probabilistic Safety Goals. Phase 3. Status Report, NKS-195 Nordic nuclear safety research (NKS), Roskilde, 2009.

4. Probabilistic Risk Criteria and Safety Goals, NEA/CSNI/R(2009)16, OECD, Nuclear Energy Agency, Committee on the Safety of Nuclear Installations, 2009, Paris.

5. Holmberg, J.-E., Nirmark, J. & Männistö, I. Risk-informed assessment of defence in depth, LOCA example. Phase 1. Mapping of conditions and definition of quantitative measures for the defence in depth levels. SKI Report 2008:33, Swedish Nuclear Power Inspectorate (SKI), Stockholm, 2008.

6. Bäckström, O., Häggström, A. & Simola, K. NPSAG/NKS: Interpretation and Evaluation of the Technical Specification Criteria. Roskilde, NKS. NKS-171. 33 p.

7. Hukki, K. Conditions of operational actions in nuclear power plant fire situations. Factors influencing the controllability of a situation. VTT, Espoo, 2010. Research report VTT-R-04230-10. (In Finnish.)

8. Hukki, K. A Holistic and network-based approach to analyzing and improving operational safety at nuclear power plants. European Safety and Reliability Conference, ESREL2010. Rhodes, Greece, 5–9 Sept. 2010. Ale, Papazoglou & Zio (Eds.): Reliability, Risk and Safety – Back to the Future. European Safety and Reliability Association, ESRA, London, 2010.

9. Hukki, K. & Holmberg, J.-E. Systemic Approach to Development of Risk-Informed Management of NPP Fire Situations. In: Proceedings of the Joint 8th Conference on Human Factors and Power Plants and 13th Annual Workshop on Human Performance / Root Cause / Trending / Operating Experience / Self Assessment, Monterey, California, August 26–31, 2007.

10. Lois, E., Dang, V.N., Forester, J., Broberg, H., Massaiu, S., Hildebrandt, M., Braarud, P.Ø., Parry, G., Julius, J., Boring, R., Männistö, I. & Bye, A. International HRA empirical study – pilot phase report. Description of overall approach and first pilot results from comparing hra methods to simulator data, Report HWR-844, OECD Halden Reactor Project, Halden, Norway, April 2008.

11. Johanson, G., Becker, G., Fritzson, L. & Männistö, I. Evaluation of existing applications and guidance on methods for HRA – EXAM-HRE. Eskonsult, Stockholm, Sweden, January 2011.

12. Holmberg, J.-E., Kent Bladh, K., Oxtrand, J. & Pyy, P. Enhanced Bayesian THERP – Lessons learnt from HRA benchmarking. Proc. of PSAM 10 – International Probabilistic Safety Assessment & Management Conference, 7–11 June 2010, Seattle, Washington, USA, IAPSAM – International Association of Probabilistic Safety Assessment and Management, Paper 52.

13. Karanta, I. Importance measures for the dynamic flowgraph methodology. VTT, Espoo, 2011. VTT-R-00525-11,

14. Karanta, I., Björkman, K., Holmberg, J.-E. & Maskuniitty, M. Reliability assessment of computer controlled systems, SIAS 2010 – The 6th International Conference on Safety of Industrial Automated Systems. Tampere, 14.–15.6.2010 SIAS 2010 Proceedings. Suomen Automaatioseura, 2010. 6 p.

15. Karanta, I. & Kuusela, P. On the computational effort of the dynamic flowgraph methodology. VTT, Espoo, 2010. VTT-R-00831-10.

16. Karanta, I. & Maskuniitty, M. Reliability of digital control systems in nuclear power plants – Modelling the feedwater system. VTT, Espoo, January 2009. VTT-R-01749-08,.

17. Björkman, K. & Holmberg, J.-E. Comparison of two dynamic reliability analysis tools to solve dynamic Flowgraph method models. VTT, Espoo, 2010. VTT-R-00775-10,

18. Authén, S., Björkman, K., Holmberg, J.-E. & Larsson, J. Guidelines for reliability analysis of digital systems in PSA context – Phase 1 Status Report, NKS-230 Nordic nuclear safety research (NKS), Roskilde, 2010.

19. Suopajärvi, A. Modeling of Phenomenological Uncertainties in Level 2 Probabilistic Safety Assessment of a Nuclear Power Plant. VTT, Espoo, May 2008. VTT-R-03384-08. (Also Master's Thesis at Helsinki University of Technology.)

20. Niemelä, I. SPSA level 2 user's guide. Addendum to SPSA user's guide. Helsinki: Finnish centre for radiation and nuclear safety, 1996. 51 p.

21. U.S. Nuclear regulatory commission. NUREG/CR-6119, MELCOR computer code manuals. Vol. 1 & 2. Washington, DC: Division of systems analysis and regulatory effectiveness, Office of nuclear regulatory research, 2005. SAND2005-5713.

22. Ilvonen, M. Software development of models that simulate the dispersion of atmospheric radioactive releases and predict the resulting radiation doses. Espoo. Master's Thesis, Helsinki University of Technology, Department of Information Technology, 1994. 119 p. (In Finnish.)

23. Rossi, J. Use of hourly weather data in ARANO. VTT, Espoo, November 2008. Research report VTT-R-08408-08.

24. Rossi, J., Presentation of the results calculated from the hourly weather data. VTT, Espoo, November 2008. Research report VTT-R-08409-08.

25. Best-practices guidelines for L2 PSA development and applications. Vol. 1 – General. Technical report ASAMPSA2/WP2&3/ 2010-28, IRSN – Rapport DSR/SAGR/2010-193, draft, December 2010. (Limited distribution.)

26. Best-practices guidelines for L2 PSA development and applications. Vol. 2 – Best practices for the Gen II PWR, Gen II BWR L2PSAs. Extension to Gen III reactors. Technical report ASAMPSA2/WP2&3/ 2010-28, IRSN – Rapport DSR/SAGR/2010-193-3, draft, December 2010. (Limited distribution.)

27. Best-practices guidelines for L2 PSA development and applications. Vol. 3 – Extension to Gen IV reactors. Technical report ASAMPSA2/WP4/ 2010-D4, CEA – DEN/DER/ SESI/LSMR/NT DO 8 26/10/10, draft, December 2010. (Limited distribution.)

31.2 EXAM-HRA Project Phase 1: Survey of HRA practices in Nordic and German PRAs

Ilkka Männistö and Jan-Erik Holmberg
VTT

Abstract

The research activities and findings of the EXAM-HRA project phase 1 are detailed in this special article. EXAM-HRA is a Nordic-German co-operation project for surveying and developing a best practices guideline for performing HRA (human reliability analysis) in Swedish, Finnish and German NPPs (nuclear power plants). Phase 1 work was completed in 1, and included a survey of the current HRA practices and methodologies used in selected Swedish, Finnish and German NPPs. The aim of the research was to develop a method for identifying similar human failure events at the different plants, and subsequently discern the reason for any differences in the analysis. Differences in the HRA analysis mainly come from two sources: differences plant design or operational features, or differences HRA practices used to analyse to human actions. Another objective in this work is to identify good practices in plant operations and HRA analysis. Phase 1 work was done in preparation for Phase 2 starting in early 2011, where the actual guidelines are produced based on the findings of Phase 1. EXAM-HRA is an NPSAG project and VTTs participation in the project was coordinated within the CHARISMA project, which is a part of the SAFIR2010 research program.

Introduction

EXAM-HRA is a Nordic-German co-operation project on the human reliability analysis methodology and guidance development. The overall project objective is to provide guidance for a ”state of the art” HRA for purposes of PRA to ensure that plant specific properties are properly taken into consideration in the analysis. This will also provide means to improve plant features based on HRA and PRA results as well as providing means to improve Nordic and German HRA application for PRA purposes. The project is completed in Phases 0–3.

- Phase 0: Preliminary survey and project program
- Phase 1: Survey and initial assessment to find discrepancies

- Phase 2: Reassessment and actual plant aspects
- Phase 3: Guidance.

This paper details Phase 1 which was completed in 2010. Phase 0 was preliminary work surveying the existing HRA guidance [1], and Phase 1 work surveyed existing HRA practices at Swedish, Finnish and German power plants.

The overall project objective is to provide guidance for a "state of the art" HRA for purposes of PRA to ensure that plant specific properties are properly taken into consideration in the analysis. This will also provide means to improve plant features based on HRA and PRA results as well as providing means to improve Nordic and German HRA application for PRA purposes.

This paper details Phase 1 which was completed in 2010 [2]. Phase 1 work surveyed existing HRA practices at Swedish, Finnish and German power plant. A methodology for comparison of the HRA practices was developed and was applied to a set of example scenarios. As the HRA analyses considered come from different NPPs it is important to distinguish between differences resulting from plant design and operational differences, and those that result from differing HRA analysis assumptions and practices. This is reflected in the evaluation methodology development in the project.

The project will also draw from other HRA related projects as a source for development of the best practices guide in Phase 3, like the International Empirical HRA Benchmark Study [3].

Survey of HRA practices in Nordic and German nuclear power plants

Data collection

Human reliability analysis data was collected from Nordic and German power plants. The objective of the data collection was to include every analysed human failure event, and the relevant features from each analysis. This was done to be able to present the data in a common format to allow comparisons. The resulting list was close to 500 HRA analyses from the Nordic and German NPPs. The main purpose of the collected list is to have a representative collection of human actions from Nordic and German NPPs. All the information from the HRA analyses was not included in the table (nor would it have been possible), but the list allows grouping to similar actions for further evaluation.

Evaluation methodology

The collected HRA data is analysed in order to identify best practices and provide better guidance in later phases of the project. It is essential to capture the relevant features of the performed HRA and also to differentiate how plant features contribute to HRA versus choices in the HRA analysis itself.

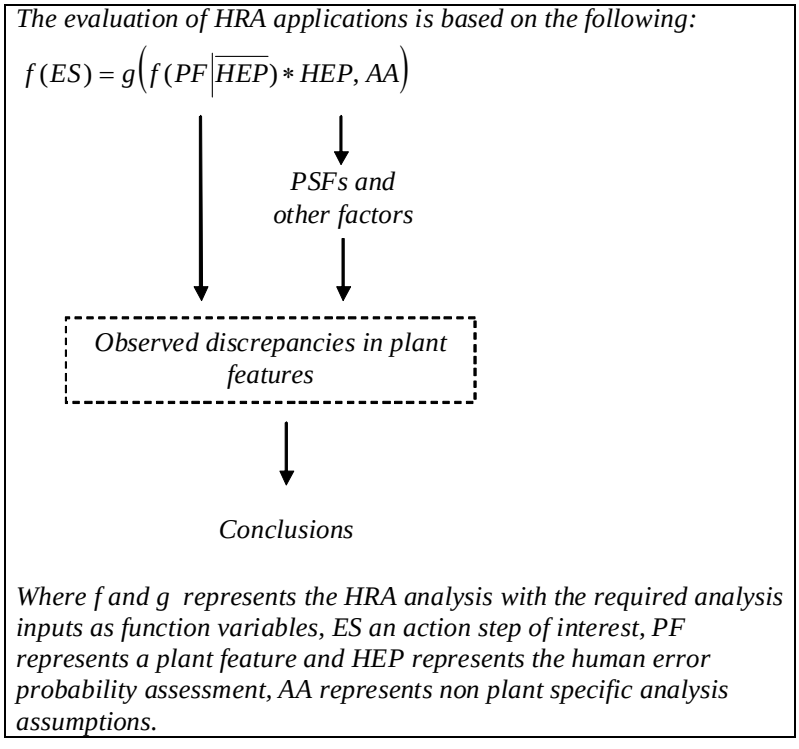

Figure 1. This figure shows the differentiation between plant features and analysis assumptions in the comparison process [5].

In-depth comparison was based on a longer list of specific features and qualities of the HRA analyses. The features were divided under the following headings:

- Level of task
- Context
- Methodology
- Definition/assessment of action
- Resulting data.

The comparison was organized as an excel worksheet. An example of a part of the filled worksheet for the closing of containment air lock during LOCA is presented below:

Table 1. This table contains part of the evaluation worksheet for closing of the containment air lock. The NPPs in the header are KKK = Krümmel, F = Forsmark, OL = Olkiluoto.

GENERAL		KKK	F1, F2 AND F3	OL1/OL2
2.1	**Context**	Small LOCA during shutdown with open airlock	Small LOCA during shutdown with open airlock.	Small LOCA during shutdown with open airlock
2.2	**Strategy for success**	Identification of leak. Three persons are sent to close airlock. Two recoveries: Camera supervision from MCR. Extra person on site.	Identification of leak. One or two persons are sent to close airlock.	Identification of leak. One person ready on location when airlock is open during critical work.
2.3	**Depen-dencies**	No modelled dependencies to previous actions.	No modelled dependencies to previous actions.	No modelled dependencies to previous actions.
2.4	**Other actions**	No.		Equipment blocking the door is considered to result in failure.

The full evaluation worksheet would be too long to be presented in this paper, but can be found in report [4]. As a result of the comparisons

- Differences in HRA due to plant design and operational features
- Differences in HRA due to analysis assumptions and practices used.

Both of these results are likely to prove very useful. Firstly the design and operational features can be used improve practices at the existing plant, and secondly the differences due to HRA analysis assumptions and practices are essential for preparing the guidance document in Phase 3 of the EXAM-HRA project.

Example case studies

The comparison method was tested on three different human failure event HRA analyses. The three selected case studies were closing of containment air lock, restoration of residual heat removal after loss of offsite and manual activation of an external water supply. The purpose of these example studies was to find out what kind of findings and conclusions could be drawn from HRA data with the proposed analysis methodology.

The test scenarios were analysed according the procedure described in the previous section and also an independent report [5]. The example case studies consist of a general description of the scenario that is mostly similar for all plants, another scenario description that is specific to each plant used in the example case and a table that compares selected features of the scenario, plants and the HRA analyses. The example case "closing of containment air lock" is presented in this paper.

Closing of containment air lock

In case of a LOCA (loss of coolant accident) inside containment during an outage, closing of the containment air lock is an important human action. Water will leak out of the primary circuit to the containment building lower drywell, and in cases when the air lock is open, will eventually reach the air lock threshold and flow out of the containment building. Closing of the door will become more difficult if there is a flow through the door opening, meaning that closing of the door is essential to complete in a timely fashion.

In the example air lock example case there were only minor differences in the scenario in terms of initiating event and technical plant differences. Features of emergency response and the HRA analyses varied more significantly. At Olkiluoto 1 & 2 NPP a person tasked with closing the air lock door in case of a LOCA is present during critical outage work. In Krümmel and Forsmark NPPs plant personnel are directed to close the door once LOCA is identified visually by personnel on site, or in the control room alarms are triggered.

Important conclusions drawn from the comparison:

- Olkiluoto 1 and 2 having a supervisor for quickly closing the door was identified as a good practice.
- Krümmel analysis included unnecessary conservatism, as the time available was based on the water flow of a large LOCA even for smaller LOCAs.

- Krümmel was the only action where recoveries were credited
- All the HRA analyses were based on modifications to the Swain Handbooks THERP methodology. Forsmark and Olkiluoto methods are very similar, but for actions during outage Olkiluoto method omits performance shaping factors in favour of specialized time correlation curves.

Conclusions

Results of the Phase 1 were deemed to be satisfactory as the basis for continued work in Phase 2. The collected database of HRA analysis is usable for identifying similar actions for further comparison analysis using the evaluation methodology. The evaluation methodology itself was tested using the three example study scenarios described in this paper.

The evaluation of the example case already identified a good operating practice during outages from Olkiluoto 1 and 2 NPP – one person is stationed near the air lock door during critical outage work – and this should also be considered for implementation in other NPPs. On the HRA analysis side of the comparison it was noted that the Olkiluoto and Forsmark analysis apply time correlation curves, while the Krümmel analysis relies more on the modelling of recoveries. One possible deficiency identified in the HRA analyses was that a possible conflict of interest was indentified, but not explicitly modelled. People working inside the containment were mentioned as a factor that might delay closing of the door, because the people ordered to close the door might delay the action until they are sure that the containment is evacuated (however, it is possible to exit the containment through the upper personnel air lock).

It is also notable that the human error probabilities calculated for the same task in different NPPs yielded roughly similar quantitative results.

References

1. Fritzon, L. et al. EXAM-HRA – Evaluation of Existing Applications and Guidance on Methods for HRA – Phase 0 Reporting, Eskonsult, November 2009.

2. Johanson, G., Becker, G., Fritzson, L. & Männistö, I. Evaluation of existing applications and guidance on methods for HRA – EXAM-HRA. Eskonsult, Stockholm, Sweden, January 2011.

3. Lois, E., Dang, V.N., Forester, J., Broberg, H., Massaiu, S., Hildebrandt, M., Braarud, P.Ø., Parry, G., Julius, J., Boring, R., Männistö, I. & Bye, A. International HRA empirical study – pilot phase report. Description of overall approach and first pilot results from comparing hra methods to simulator data, Report HWR-844, OECD Halden Reactor Project, Halden, Norway, April 2008.

4. Männistö, I. & Fritzson, L. EXAM-HRA Case Study 1 Closing of Containment Airlock, VTT, Espoo, Finland, February 2011.

5. Fritzson, L. Guide for Evaluation of Operator Actions in PSA with Regard to Plant Specific Features. Eskonsult, Stockholm, Sweden, January 2011.

32. Implementation of Quantitative Fire Risk Assessment in PSA (FIRAS)

32.1 FIRAS summary report

Simo Hostikka, Terhi Kling, Johan Mangs and Anna Matala
VTT

Abstract

Implementation of Quantitative Fire Risk Assessment in PSA (FIRAS) project aimed at application of flame spread modelling on real NPP situations, integration of the quantitative fire risk assessment methods into the NPP fire PRA, and carrying out fire simulations related to but outside OECD PRISME-project aiming to (i) guidance for the design of experiments and (ii) validation of the developed fire models. The main results include the improved and validated capabilities to predict flame spread on solid materials, methods to estimate the model parameters from small scale experiments, a quantitative method for the assessment of human actions affecting the safe-shutdown probability, and the assessment of fire spreading and second sub-system failures in a real NPP cable tunnel.

Introduction

The recent developments in numerical fire simulation and computer capacity allow the use of fire simulation as a predictive sub model for the fire-PRA of NPPs. In the previous NPP fire safety projects, promising results were obtained for both the deterministic methods for fire spread simulation and the probabilistic methods allowing risk estimation. The usability of the methods has been shown by applying them on some relatively simple geometries. In FIRAS project, the

fire spread simulations were further developed by utilizing new experimental information and co-operation with the plant personnel and fire brigades to estimate the effectiveness of the active fire safety measures.

The long term objective is the comprehensive assessment and management of fire risks. In 2008, a co-operation with the CHARISMA-project was started to integrate the quantitative fire simulation method (FIRAS) with the systemic approach of risk-oriented decision making in CHARISMA. As a result, a new stochastic operation time model for the computation of the time dependent probability of successful suppression by fire brigade was formulated, utilizing the methods of Human Reliability Analysis (HRA).

VTT transforms new information from the international fire research community into Finland, utilizing the good contacts with NIST/USA, NRC/USA, IRNS/France and GRS/Germany. Within FIRAS project, VTT participated in the OECD PRISME project concerning the spreading of heat and smoke within enclosure fires.

Main objectives

(1) Application of modelling of fire development and spread to fires involving cables and other fire loads found at NPPs, including the potential fire loads during shut down and refuelling outages and reconstruction periods.

(2) Integration of the quantitative fire risk assessment methods into the NPP fire PRA, which will be initiated through a study of fire-risk relevant rooms with potential to comprehensive testing of the models. The work will be carried out in close co-operation with the personnel involved in safety and PRA work of the NPPs.

(3) Carrying out fire simulations related to but outside OECD PRISME-project aiming to (i) guidance for the design of experiments and (ii) validation of the developed fire models.

Results

Development of Fire Dynamics Simulator and simulation methods

VTT participates in the development and maintenance of the Fire Dynamics Simulator program [1] in co-operation with the National Institute of Standards and Technology (NIST), USA. FIRAS contributions were mainly related to modelling of condensed phase materials [2] and the verification and validation

(V&V) activities [3]. Continuous V&V of an open-source software is an essential part of the FDS development process, providing instant feedback to the developer community about the intended and un-intended effects of the committed code changes. The V&V also provides metrics for the code accuracy in the intended application.

In the FIRAS project we have developed methods for the model parameter estimation for the simulation of the pyrolysis and flame spread processes [4, 5]. As the needed parameters include both true physical properties (e.g. density, specific heat) and model-specific parameters (e.g. kinetic reaction coefficients), the methods combine direct measurements with stochastic estimation methods that try to find the optimal set of parameters minimizing the error between experimental results and model predictions in a selected set of tests. The experimental methods included Thermogravimetric analysis (TGA), Differential Scanning Calorimetry (DSC), Simultaneous Thermal Analysis (STA) and Cone calorimetry (air and nitrogen). The estimation methods were implemented as a PyroPlot tool that can be downloaded from http://code.google.com/p/pyroplot/. The estimation process [6] is illustrated in Figure 1.

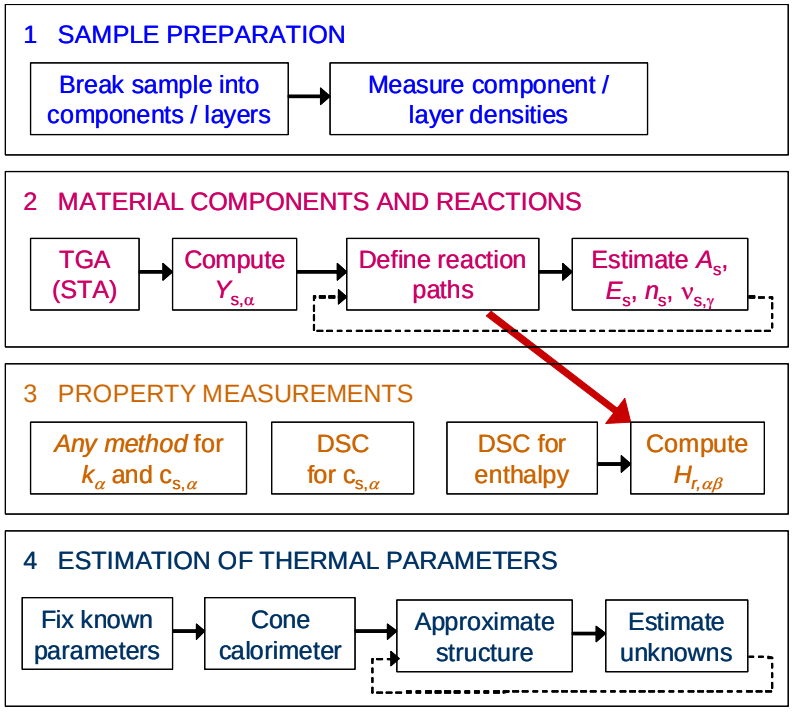

Figure 1. Parameter estimation process for pyrolysis modelling.

Flame spread experiments, ageing effects

To increase the understanding of flame spread physics and to provide validation data for the simulation models, flame spread experiments were performed on well-characterized reference materials (birch wood) and electrical cables. A new experimental apparatus has been developed for the implementation of flame spread tests at different ambient temperatures [7]. The purpose is to obtain a continuous preheated air supply throughout the experiment to be able to measure flame spread velocity at different initial temperatures, starting from ordinary room temperatures up to temperatures near auto-ignition level. Main parameters of the apparatus are: sample length 2 m, diameter at maximum less than 100 mm, and initial temperature at maximum 400°C.

During the years 2007 and 2008, start-up tests of the test rig were performed to ensure consistent flow and temperature conditions, and to characterize the temporal and spatial variations of temperature. Actual flame spread tests were performed for birch wood and PVC-cable MMJ. During the years 2009 and 2010 flame spread experiments were continued on power installation cable MCMK 0.6/1 kV with PVC sheath and PVC insulation. The samples studied differed in outer diameter and age. Two cable types studied in 2009 were MCMK 4x1.5 +1.5 mm2, nominal diameter 13 mm and MCMK 4x6 + 6 mm^2, nominal diameter 18.5 mm. These cable samples were delivered to VTT by TVO as "new" samples off the reel.

The influence of aging on the fire performance properties of cables is interesting as experiments on thermally aged cables indicate that aged samples show a reduced flammability compared to unaged samples of the same cable [8]. In FIRAS project, the "old" sample was MCMK 3x2.5+2.5 mm^2 delivered to VTT by TVO in 1995, and studied in 2010. It is not known at the moment of writing how old this sample was when delivered. The exact formulations of the cable materials were unknown by the authors for both "old" and "new" samples.

Table 1 presents essential features of the MCMK flame spread experiments. The observed flame spread rates as a function of ambient temperature are presented in Figure 2. The "old" cables studied here were rather young compared to the thermally aged cables in [8] with equivalent 40 years life at temperatures 52...82°C. Small scale experiments with STA and standard cone calorimeter were also carried out on old and new cables and cable materials. Small differences between "old" and "new" samples were found, but it could not be concluded whether these were due to ageing or other factors. The present study gave thus no clear indications of changes in fire performance during this period of ageing.

For the validation of flame spread simulations, the birch wood and PVC cable material models were implemented in FDS, and simulations of vertical flame spread at different ambient temperatures were performed. The early models for the PVC cable did not yield good results but the inclusion of combustible additives (softeners) as relatively low-temperature pyrolyzates to the pyrolysis model improved the agreement between simulation and 2-m experiments significantly [9].

Table 1. Essential features of MCMK PVC cable samples and flame spread results.

Sample	**Nominal outer diameter (mm)**	**Flame spread rate (mm/s)**	**Temperature range (°C)**
4x1.5 mm^2 "new"	13	4.2 ... 22.9	23 ... 176
4x6 mm^2 "new"	18.5	3.4 ... 23.7	23 ... 190
3x2.5 mm^2 "old"	12.6	2.1 ... 18.2	22 ... 177

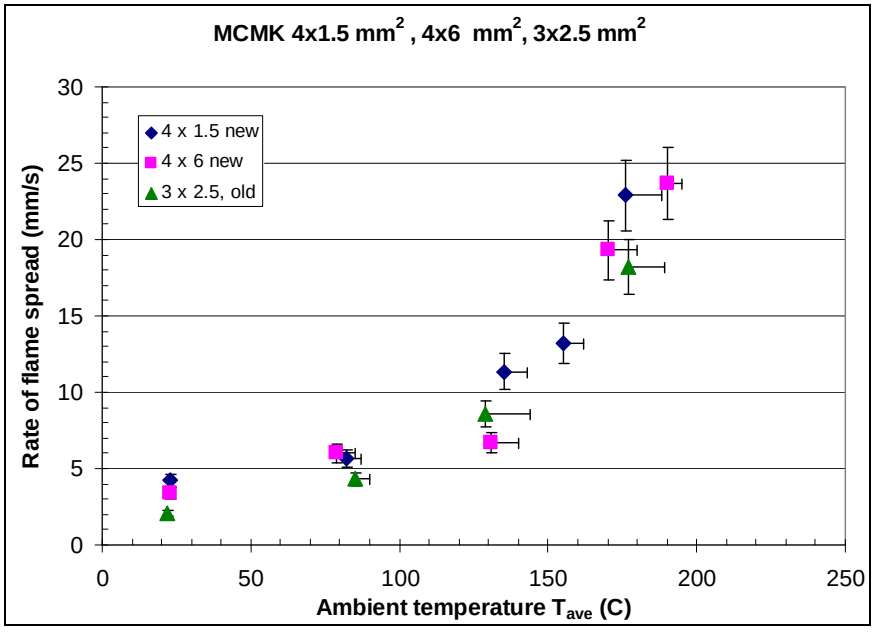

Figure 2. Rate of flame spread as a function of ambient temperature for MCMK cable samples.

Integration of quantitative fire risk assessment into NPP PSA systems

A new quantitative approach was developed to integrate the fire risk assessment by probabilistic fire simulation methods and the Human Reliability Analysis (HRA) methods. In the approach, a fire scenario is first determined including the definition of a fire-induced damage, which can cause a risk to the NPP operation. On the other hand, a scenario is determined for the operational actions aiming at fire suppression before the target damage.

The probabilistic fire simulation of the fire scenario can be performed using FDS and the Probabilistic Fire Simulator (PFS) –tool developed in earlier projects [10]. Fire simulations are used to estimate the time between ignition and the target damage, activation times of smoke detectors and sprinklers and the conditions inside the fire compartment.

An integrated approach containing HRA methods was developed and tested years 2008–2009. Human reliability analysis (HRA) of the probabilistic safety assessment (PSA) includes identifying human actions from safety point of view, modelling the most important of them and assessing their probabilities [11]. The crucial human actions include those of the control room staff, the security centre and the fire brigade after the detection of the fire. A simplified analysis was made in 2008 concerning the cable-room fire scenario to test the idea and to define the necessary data to be able to carry out the analysis of a real case. At the same time, a detailed model for calculation of NPP fire brigade operational actions was developed.

As a combination of the previous models, a stochastic operation time model Fire-HRA was formulated 2009–2010 for the computation of the time dependent probability of a successful suppression by fire brigade. The time between the ignition and the successful suppression of the fire is a sum of time delays due to following actions:

- Detection of the fire
- Confirming the fire
- Making the alarm
- Arrival of the fire brigade
- Co-operation between the fire brigade and the control room
- Preparation of fire suppression
- Fire suppression.

A group of experts was assembled to specify both the operational actions aiming at a suppression and the data on the related time delays. The data was analyzed and utilized in the development of the Fire-HRA -model. The model describes the scenario as a stochastic process containing distributions of the time delays and links to the fire model. The possibility and influence of human errors can be taken into account as well as the effect of so-called performance shaping factors (PSF), which in the case of an NPP could be things like resources, experience, education, instructions, hurry, stress, etc. An example calculation of 10 000 realizations gives the results shown in Figure 3.

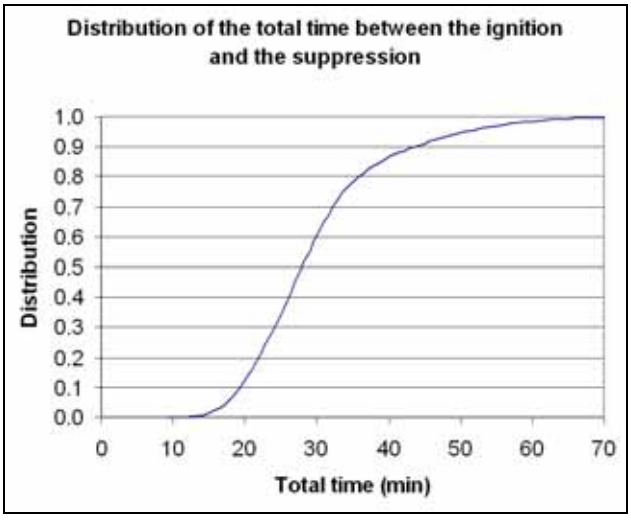

Figure 3. Results of the example calculation of 10 000 realizations of operational actions aiming to suppression of a fire in a cable room.

To be able to perform and analyze nested Monte Carlo simulations, a new version of the PFS-tool was developed (http://code.google.com/p/pfs-fire/downloads/list). The combined approach will be applied in real plant situation later, when the probabilistic simulation results of the cable failures within the target room will be available. The long term objective is the comprehensive assessment and management of fire risks.

International activities

Within FIRAS, VTT has participated in the planning, steering and utilization of OECD PRISME programme. This programme aims at analysing the mechanisms

governing smoke and heat propagation from the room containing the fire to adjacent rooms. The following propagation modes were investigated: through a door; along a ventilation duct that crosses the room containing the fire and that ventilates an adjacent room; along a ventilation duct when flow is reversed within; through leakages between several rooms. A series of integral tests was performed to analyze the effects of smoke damper activation, fire suppression and fire spreading on cables. Temperature induced electrical failures in cables were examined for a large set of different cables supplied by the international project participants. The PRISME tests are performed by IRSN/France.

Formally outside PRISME, there is a parallel benchmarking exercise (BE) to validate the fire models. VTT has participated by FDS simulations. Figure 4 shows an example of BE results: a comparison of model sensitivity measures using Full Factorial Design for sensitivity study and three different fire models [12]. Additionally, a comparison between FFD and full Monte Carlo –simulation was performed, indicating that FFD can provide the same sensitivity information as full Monte Carlo, but may lead to spurious results if the fire behaviour within the selected parameter range is very non-linear.

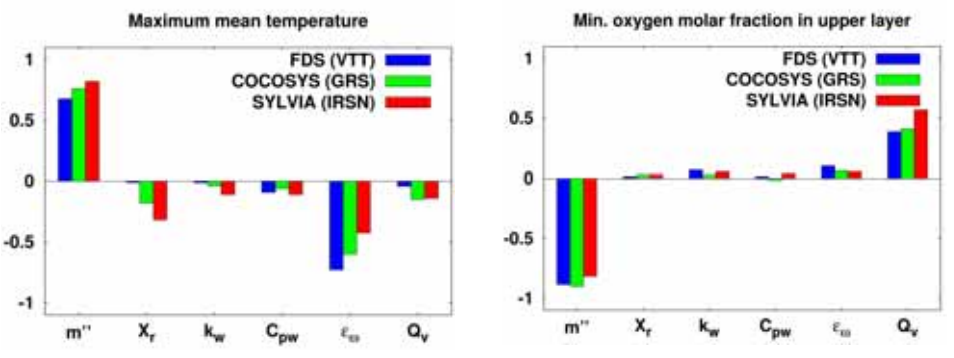

Figure 4. Examples of FFD analysis using three different fire codes.

Applications

The developed simulation techniques were used to study the cable fires, their consequences and the efficiency of water-based suppression systems in a cable tunnel of a real NPP. The objective was two find out the failure probabilities of second sub-system when two of the four sub-systems are paired, i.e. placed in the same space, and to estimate the effectiveness of the water sprinkler systems in the protection of the adjacent trays. A cross section of the tunnel with a

snapshot of the simulated water sprays is shown in left part of Figure 5. The fire load consists of power cables on the few uppermost cable trays. For modelling, a material model of NOKIA AHXCMK 10 kV 3 x 95/70 mm^2 cable (Figure 5 right) was created. Two different water suppression systems were studied.

The simulation results indicate that using either suppression system decreased the heat release rate in the tunnel to less than 10% of the non-sprinklered case. Without fire suppression, the cables of the second sub-system were damaged in almost all fires, but when either of the studied water suppression systems was used, the probability of the cable failures was decreased to less than 1%. This result indicates that in current scenario, the probability of loosing both sub-systems is determined directly by the suppression system unavailability.

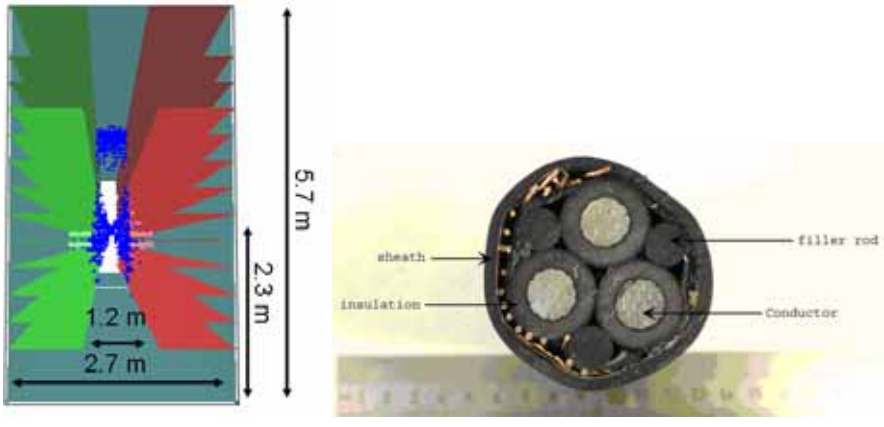

Figure 5. Cross-section of the cable tunnel (left) and the power cable used as fire load (right).

Conclusions

Several aspects of the fire safety analysis methods have been studied on the way towards better integration and utilization of fire simulation methods in the quantitative Fire-PRA. The methods used for predicting the fire spread and heat release rate have been studied both experimentally and by developing the analysis methods. A new 2-m test apparatus has been developed for studying the effect of ambient temperature on the flame spread rate on thin objects, such as electrical cables. Techniques for estimating the pyrolysis model parameters from small scale experiments have been developed. The techniques are based on genetic algorithms and have been demonstrated and successfully applied in real cable tunnel simulations.

New methodology for integration of quantitative fire simulations and the human reliability assessment has been developed and implemented in the Probabilistic Fire Simulator -tool. It can be used to estimate the probability of safe shutdown in fire situations and to identify the dominating factors for human operation success.

Monte Carlo simulations of real cable tunnels indicated that using a suppression system decreased the heat release rate in the tunnel to less than 10% of the non-sprinklered case. Without fire suppression, the cables of the second sub-system were damaged in almost all fires, but when either of the studied water suppression systems was used, the probability of the cable failures was decreased to less than 1%. This result indicates that in such a scenario, the probability of loosing both sub-systems is determined directly by the suppression system unavailability.

References

1. McGrattan, K.B., Hostikka, S., Floyd, J.E., Baum, H. & Rehm, R. Fire Dynamics Simulator (Version 5): Technical Reference Guide. NIST SP 1018-5. NIST Special Publication 1018-5. October 2007. Building and Fire Research Laboratory. National Institute of Standards and Technology.

2. McGrattan, K., McDermott, R., Mell, W., Forney, G., Floyd, J., Hostikka, S. & Matala, A. Modeling the burning of complicated objects using Lagrangian particles. Conference Proceedings of the Twelfth International Interflam Conference. 2010. Pp. 743–753.

3. Hostikka, S. Modern V&V of Fire Dynamics Simulator. Fire Protection Engineering Conference – EUROFIRE 2009, 24–25 September 2009, Belfry Bruges, Belgium, International partnership representing manufacturers, installers, fire brigades, insurances and association. 22 p.

4. Matala, A., Hostikka, S. & Mangs, J. Estimation of pyrolysis model parameters for solid materials using thermogravimetric data. Fire Safety Science 2009, 9, pp. 1213–1223. doi:10.3801/IAFSS.FSS.9-1213.

5. Matala, A. & Hostikka, S. Fire modelling of flame retardant electrical cable. 12th International Fire & Materials conference. 31 Jan. – 2 Feb. 2011, San Francisco.

6. Hostikka, S., Matala, A. Modelling the fire behaviour of electrical cables. 11th International Seminar on Fire Safety in Nuclear Power Plants and Installations. Post-Conference Seminar of the 20th International Conference on Structural Mechanics in Reactor Technology (SMiRT 20), August 17–19, 2009. Helsinki, Finland, the Radiation and Nuclear Safety Authority STUK.

7. Mangs, J. A new apparatus for flame spread experiments. VTT, Espoo, 2009. VTT Working Papers 112. 51 p. + app. 28 p. http://www.vtt.fi/inf/pdf/workingpapers/2009/W112.pdf.

8. Nowlen, S.P. The impact of thermal aging on the flammability of electric cables. NUREG/CR-5619, SAND90-2121. Sandia National Laboratories, Albuquerque, New Mexico 1991. 25 p.

9. Mangs, J. & Hostikka, S. Experiments and numerical simulations of vertical flame spread on charring materials at different ambient temperatures. To appear in: Fire Safety Science 10. 2011. International Association of Fire Safety Science, MD.

10. Hostikka, S Development of fire simulation models for radiative heat transfer and probabilistic risk assessment. Espoo, VTT, 2008. VTT Publications 683. 103 p. + app. 82 p. http://www.vtt.fi/inf/pdf/publications/2008/P683.pdf.

11. Pyy, P. Human reliability analysis methods for probabilistic safety assessment. Espoo, VTT, 2000. VTT Publications 422. 63 p. + app. 64 p. http://www.vtt.fi/inf/pdf/publications/2000/P422.pdf.

12. Suard, S., Klein-Hessling, W. & Hostikka, S. Sensitivity Analysis of Fire Models as Part of the Prisme Project. Eurosafe Forum 2010. Nov. 8.–9.2010, Cologne.

32.2 Experiments and numerical simulations of vertical flame spread on charring materials at different ambient temperatures (FIRAS)

Johan Mangs and Simo Hostikka
VTT

Abstract

A new experimental apparatus for measuring flame spread rates at different ambient temperatures is presented. The 2 m long sample is pre-heated with air to desired temperature, ignited from below with a small propane burner, and flame spread is monitored with thermocouples at the surface of the sample. Rate of vertical concurrent flame spread as a function of ambient temperature is determined on cylindrical birch rod samples and on PVC cable samples. Corresponding flame spread scenarios are numerically simulated using axi-symmetric solution of the flow field and a pyrolysis model with parameters estimated from thermogravimetric and cone calorimeter experiments. The simulation model was able to predict the flame spread rates within the uncertainties associated with the experiments and post-simulation analysis of the spread rate.

Introduction

Flame spread has been one of the central topics of the fire safety research of Finnish nuclear power plants [1, 2, 3] due to the risks associated with huge amounts of electrical cables and other solid fire loads. The fire spreading on pre-heated cables is one of the plausible fire scenarios even for those cables consisting of flame-retarded materials because many of the flame retardants degrade at temperature range 200–300°C. Motivated by the need to understand the effect of the ambient temperature on flame spread process, a new experimental apparatus has been developed for the measurement of flame spread at different ambient temperatures [4]. The second goal of the new apparatus is to provide data for the validation of numerical simulation. In the present work, axi-symmetric simulations of the flame spread on birch rods are performed using Fire Dynamics Simulator [5] and a pyrolysis model with parameters estimated from small scale experiments. The simulation results are compared with experiments and the implications for the future applications are discussed.

Experimental

Structure and operational principles of the apparatus

Schematic pictures of the apparatus are shown in Figure 1. The apparatus consists of a heating channel and a test channel (width 300 mm, depth 330 mm, height 2 940 mm), separated from each other by a thin stainless steel sheet and connected to each other at the upper and lower parts of the channels. The system is insulated with a 100 mm thick Kaowool layer between 0.5 mm stainless steel plates. There is a door on the front side to the channels, an air inlet in the upper part of the heating channel and a smoke outlet at top of the test channel. In the upper part of the heating channel is a 7.0 kW heating resistor and a fan for heating and circulating the air. During the pre-heating phase, the air inlet and roof hatches are closed and the sample is heated by hot air circulating inside the cabinet. During the flame spread experiment, the fan draws in fresh air through the intake in the upper part of the heating channel. The air flows through the heater to the test channel, and fire effluents exit through the outlet. The upper opening connecting the channels is closed during the experiment.

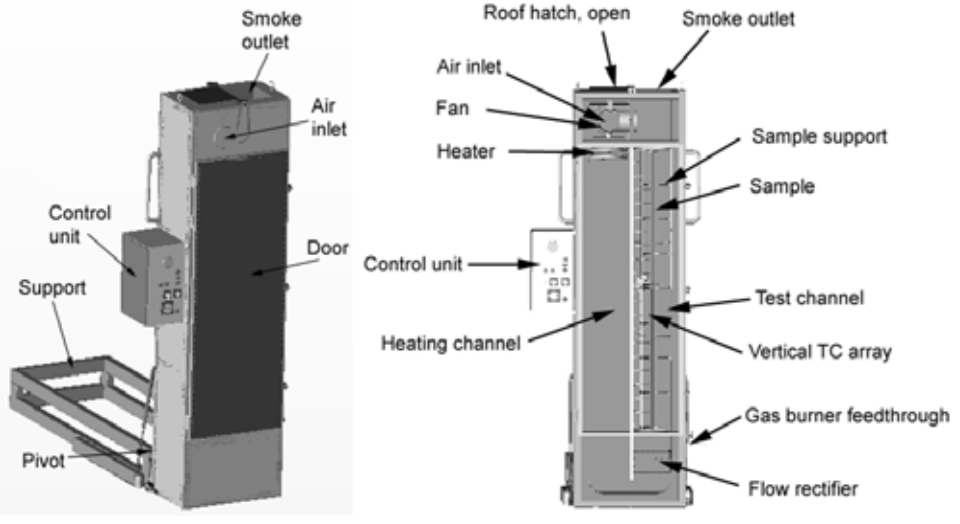

Figure 1. Structure of the flame spread apparatus. Left: general view, right: cross-section with essential features.

The 2 m long sample is suspended from its upper end in a support and kept in place in the centre of the test channel with pins at 250 mm vertical intervals. Gas

temperatures close to the sample surface are measured at 100 mm vertical intervals with 0.25 mm K-type thermocouples T1...T19. The sample is ignited from below with a helical shaped propane burner and a glow wire. When the desired temperature is reached, transition from pre-heating phase to flame spread experiment consists of the following sequence:

1. heating is temporarily turned off
2. the air flow is lowered to 0.3 m/s air flow
3. heating is turned on
4. the heating of glow wire is turned on
5. the propane gas line is opened
6. burner ignition and sample in flame contact
7. the roof hatch is opened.

Maximum gas temperatures in the test channel are measured immediately before turning heating temporarily off and lowering air flow rate. After this the temperatures in the test channel decrease somewhat until the burner is ignited and the lower end of the sample is in flame contact. This temperature drop depends primarily on how fast the operator gets through with the abovementioned sequence, and is typically 5–12°C. The temperature at the start of the flame spread experiment is calculated as the average temperature in the test channel immediately before turning the burner on. The propane burner is on until the thermocouples show that the sample has ignited and flame spread is established. Left side of Figure 2 shows sequential temperature rise as the flame front proceeds along a cylindrical birch rod pre-heated to 197°C.

Rate of flame spread is deduced from the measured surface temperatures by specifying a temperature threshold criterion for the presence of the ignition front. Visual inspection of the temperature-time curves indicated that the temperature rise is steep for most of the curves around 300°C. The propagation of the ignition front to a certain height is thus estimated by determining the moment when the corresponding thermocouple indicated temperature rise above 300°C. Plotting the ignition front height as a function of time (right side of Figure 2), shows that after some time, the flame spread rate approaches constant velocity. Fitting a straight line to this part of the curve gives the steady state rate of flame spread as the slope of the line. The possible influence of the chosen temperature threshold was determined for some experiments using an additional threshold of 400°C. The same slopes were obtained for both thresholds.

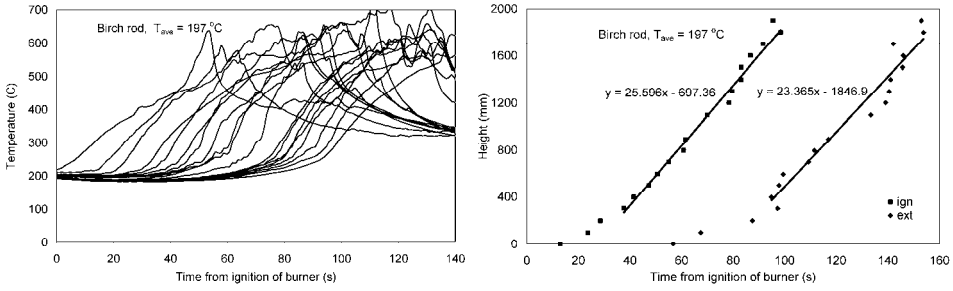

Figure 2. Flame spread on a cylindrical birch sample. Left: temperature –time curves, right: straight line fit to height – time plot for ignition and extinction.

Results from flame spread experiments

Flame spread experiments with cylindrical birch rods and PVC sheathed and PVC insulated cables were carried out. Table 1 lists the samples, temperature ranges and the propane burner output powers and durations. Birch rods were either stored in ordinary indoor conditions (moisture 6 wt. %) or dried. When the undried samples were heated to 97–181°C, their moisture content was reduced to 2.3–2.6 wt. % at time of ignition. Cable experiments were carried out with samples stored in ordinary indoor conditions. A slightly higher burner power output was used in cable experiments to ensure proper ignition, as cable samples do not ignite as easily as wood samples. Deformation of the cable material was observed at temperatures above 200°C, when the samples were heated in a laboratory furnace. Cable experiments were thus not carried out at temperatures above 195°C.

Table 1. Main features of flame spread experiments.

Sample	**Outer diameter (mm)**	**Temperature range (°C)**	**Propane burner**	
			power (W)	**duration (min)**
Birch rod	8	22–271	200	1–1.5
PVC cable MCMK 4 x 1.5 mm^2	13	23–188	520–600	1.7–6.2
PVC cable MCMK 4 x 6 mm^2	18.5	23–195	520–600	1.7–6.2

The dependence of the flame spread rate and length of burning region on ambient temperature are presented in Figure 3. “Error bars” on the right of the markers indicate maximum temperature in the test channel before starting the flame spread experiment. Vertical error bars for PVC cable indicate ± 10% standard deviation as determined for PVC cables. The dependence of flame spread rate on ambient temperature is roughly exponential for both birch rods and PVC cable samples. The result for PVC cable 4 x 6 mm^2 at 131°C seems to be slightly outside the trend, which may be due to uneven flame front propagation. There is no clear difference between the flame spread rates of cables with outer diameters 13 or 18.5 mm.

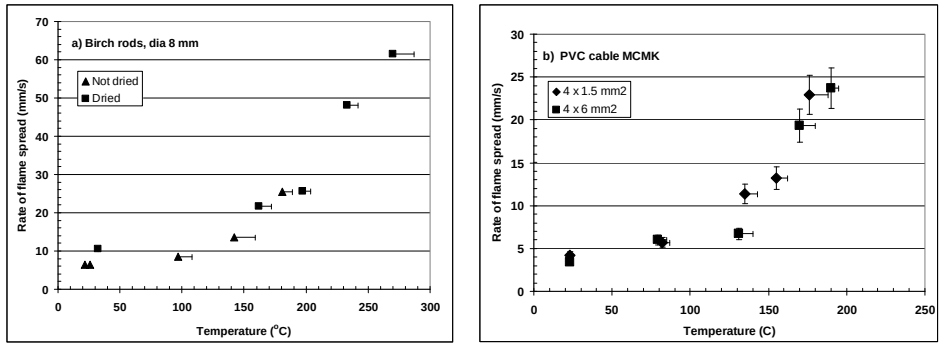

Figure 3. Rate of flame spread on 2 m long samples as a function of ambient temperature.

Numerical simulations

Model description

The numerical simulation tool used here was Fire Dynamics Simulator (FDS) [5]. The birch wood simulations were performed in DNS-mode and the spatial resolution was chosen small enough to resolve the main characteristic length scales of the flow field. The solutions were forced axi-symmetric due to the calculation economics. The details of the hydrodynamic solver can be found from [5]. A global one-step gas phase reaction of fuel and oxygen was assumed with 1% soot yield and 15 MJ/kg heat of combustion. The cell size was 1.0 mm in both horizontal and vertical directions. The computational domain was 0.12 m × 1.8 m and the corresponding grid dimensions 120 × 1 800 (216 000 cells). A sensitivity of the flame spread results to the cell size was studied by performing one simulation with 0.5 mm cell size. The results concerning the flame spread were practically identical to those obtained with 1.0 mm cells.

In the simulations of the experimental apparatus, a constant upward velocity of 0.3 m/s was applied on the bottom boundary and a fixed temperature wall on the outer vertical boundary. Open boundary was specified on the top of the domain. In the simulations of open atmosphere, all three boundaries were specified open. The sample was placed on the central axis of the domain. The simulations were carried out using version 5.4.3 of FDS using the Message Passing Interface (MPI) technique for parallel computing. For this purpose, the computational mesh was divided into six blocks of equal size in vertical direction.

Material model for birch wood

Two parallel reactions were assumed; one converting virgin wood to char and gaseous fuel, and another converting moisture to water vapor. The kinetic coefficients were estimated from thermogravimetric (TGA) experiments [6]. A comparison of experimental and simulated TGA curves for N2 atmosphere and two heating rates is shown in the left part of Figure 4. The heating rates are assumed to be sufficiently slow to allow the sample to remain in thermal equilibrium during the heating. Temperature dependent cs and the heat of reaction were measured with separate DSC experiment. The thermal parameters were estimated from the mass loss rate results of cone calorimeter experiments on birch board at 50 kW/m^2 radiation level in air and N2 atmospheres. The results of the fitted model are shown in the right-hand side of Figure 4. Despite the number of adjustable parameters, the agreement between the model and experiments is only moderate. The ignition times and average burning rates are close to those measured, but the heights of the first burning rate peaks are predicted clearly too high for both atmospheres. Improving the agreement may require model developments considering things like porosity and two-dimensionality by wood grains. The moisture content was set either 1.0 wt.%, or zero in those 2-m simulations where ambient temperature was above 100°C.

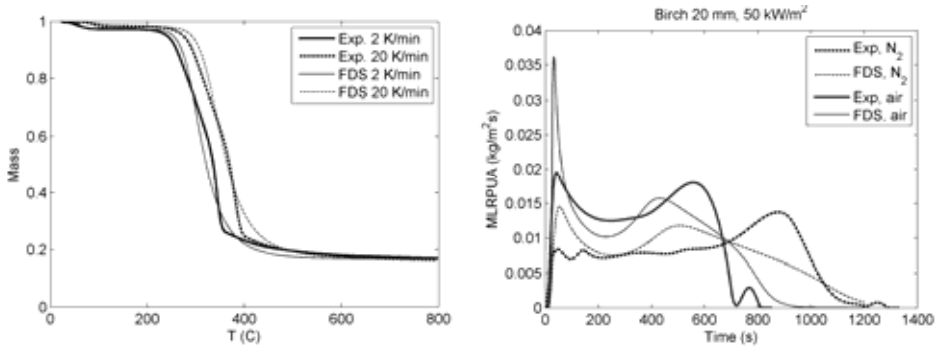

Figure 4. Experimental and material model results for birch. Left: TGA at 2 K/min and 20 K/min heating rates in N2 atmosphere. Right: cone calorimeter mass loss rate MLR at 50 kW/m^2 radiation level.

Results

For the validation of the proposed model, experiments on birch rods were simulated. The position of the upper flame front (upper edge of the pyrolysis region) at each time step was determined as the highest position where the burning rate exceeded 0.001 kg/m^{2}s.

The capability of the model to predict dependence of the flame spread rate on the ambient temperature was studied by carrying out a series of simulations with initial and ambient temperatures ranging from room temperature to 250°C. In each simulation, the initial temperature of the system was specified to be the same as the ambient temperature. Therefore, the simulations cannot capture the possible non-equilibrium starting conditions. Another source of uncertainty is related to the highest ambient temperatures. As shown by Figure 4, the pyrolysis of wood starts around 250°C. In the experiments, the heating rate before the ignition is slow (order of 5 K/min) allowing the progress of pyrolysis before the sample is ignited. In the simulations, the sample is initially in a virgin state regardless of its initial temperature. This may lead to a reaction rate peak in the beginning of the simulation of 250°C ambient temperature.

The predicted flame spread histories at different ambient temperatures are plotted in the left side of Figure 5. Each of the curves shows an initial acceleration phase, after which the flame spread rate slows down a bit, reaching a steady or close-to-steady state. Fitting straight lines to the latter parts of the curves gives us the dependence of the steady flame spread rate on sample diameter. A discontinuity point can be observed in all the curves after the initial

acceleration phase. Similar behavior was not observed experimentally. The steady-state flame spread rates were determined by fitting straight lines to the parts of the curves following the discontinuity, and compared to the experimental results in the right-hand side of Figure 5. The simulation results' error bars reflect the uncertainty of fitting the straight lines. Straight lines fitted well to the data at low ambient temperatures but not as well when $T_\infty \geq 200°C$. For the highest temperatures, better results could be obtained by making a simulation of much taller sample. Considering the experimental and numerical uncertainties, the measured and simulated temperature dependences of the flame spread rate are in agreement.

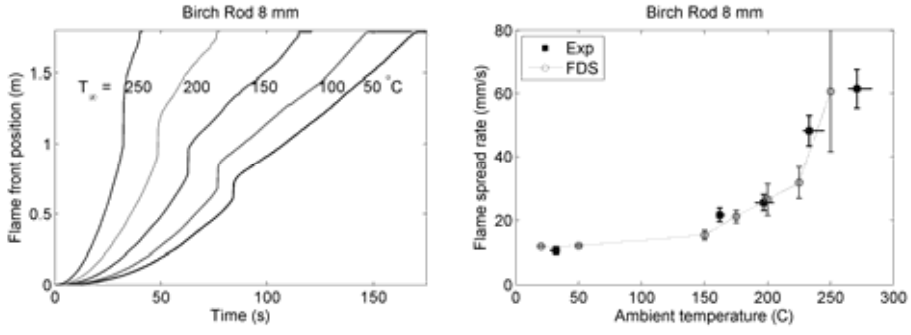

Figure 5. Position of the simulated flame front in simulations at different ambient temperatures (left), dependence of the flame spread rate on the temperature (right).

The good agreement between the flame spread rate predictions and measurements justifies the use of the current model for the validation of pyrolysis models of more complicated samples, and for the research of the sub-grid flame properties to be used in large eddy simulation (LES) of vertical flame spread. The SGS properties could include the components of the flame heat flux, gas temperatures and gas species concentrations.

Conclusions

Features and function of a new apparatus for measuring flame spread on vertical samples at different initial and ambient temperatures is presented together with flame spread experiments on birch wood and PVC cable samples. The temperature dependence of the flame spread rate seems to be roughly exponential for both cylindrical birch wood and PVC cable samples.

Numerical simulations of the vertical flame spread on birch wood were performed using axi-symmetric DNS of the reacting flow, coupled with a pyrolysis model, for which the parameters were estimated from small scale experiments. The agreement between the simulated and experimental flame spread rates was found to be good, with differences being the same order as the uncertainties associated with the experiments and the determination of linear rate from the front location curve. These encouraging results motivate us both for the validation of pyrolysis models of more complicated samples, and for the generation of SGS flame property models to be used in the LES of fire spreading in engineering applications.

Acknowledgements

The authors wish to express their deepest gratitude to Dr. Olavi Keski-Rahkonen, who envisaged and instigated the current research. Protoshop Oy is acknowledged for detail design and construction of the apparatus.

References

1. Keski-Rahkonen, O. & Mangs, J. Assessing of flame spread on NPP cables. In: Y. Zhou, S. Yu & Y. Xu (Eds.). Proceedings of the 18th International Conference on Structural Mechanics in Reactor Technology. SMiRT 18. Atomic Energy Press. Beijing, 2005. Pp. 3972–3983.

2. Keski-Rahkonen, O. & Mangs, J. POTFIS project special report – Experiments and modelling on vertical flame spread. In: Räty, H. & Puska, E.K. (Ed.). 2004. SAFIR, The Finnish Research Programme on Nuclear Power Plant Safety 2003–2006, Interim Report. VTT, Espoo, 2005. VTT Research Notes 2272. Pp. 257–265. http://www.vtt.fi/inf/pdf/tiedotteet/2004/T2272.pdf.

3. Hostikka, S., Matala, A., Mangs, J. & Hietaniemi, J. Implementation of quantitative fire risk assessment in PSA (FIRAS). FIRAS summary report. In: Puska, E.K. (Ed.) SAFIR2010. The Finnish Research Programme on Nuclear Power Plant Safety 2007–2010. Interim Report. VTT. Espoo, 2009. VTT Research Notes 2466. Pp. 495–505. http://www.vtt.fi/inf/pdf/tiedotteet/2009/T2466.pdf.

4. Mangs, J. A new apparatus for flame spread experiments. VTT, Espoo, 2009. VTT Working Papers 112. 51 p. + app. 28 p. http://www.vtt.fi/inf/pdf/workingpapers/2009/W112.pdf.

5. McGrattan, K., Hostikka, S., Floyd, J., Baum, H., Rehm, R., Mell, W. & McDermott, R. Fire Dynamics Simulator (Version 5) Technical Reference Guide. Volume 1: Mathematical Model. National Institute of Standards and Technology, Gaithersburg, MD, October 2007. NIST Special Publication 1018-5.

6. Matala, A., Hostikka, S. & Mangs, J. Estimation of pyrolysis model parameters for solid materials using thermogravimetric data. Fire Safety Science 2009, 9, pp. 1213–1223. doi:10.3801/IAFSS.FSS.9-1213

33. Extreme Weather and Nuclear Power Plants (EXWE)

33.1 EXWE summary report

Kirsti Jylhä, Hanna Tietäväinen, Ari Venäläinen, Milla Johansson, Kimmo Kahma, Hilkka Pellikka, Seppo Saku, Kimmo Ruosteenoja, Jenni Rauhala, Natalia Pimenoff, Aleksi Jokela and Miika Mäkelä
Finnish Meteorological Institute

Abstract

This research comprehensively described the occurrence of extreme weather and climate events and aspects of sea level rise that are relevant from the view point of safety of nuclear power plants. Studies about the frequency, intensity, and spatial and temporal variation of the extreme weather events and their combinations were carried out utilising instrumental meteorological observations, a 1 200-year long preindustrial control simulation and future climate model simulations. In addition to the role of natural climate variability, the study clarified the influence of human-induced climate change on extreme weather events and sea level values. The longest future climate and sea level projections extend to the end of the 21st century. According to them, the daily maximum temperatures and the length of the longest hot spells will clearly increase in Finland. The largest changes, however, are projected for the wintertime minimum temperatures. During summer there will be more intensive precipitation events and during winter more frequent precipitation days. The mean sea level is projected to rise, the change depending on the location along the Finnish

coastline. Uncertainty ranges in the mean sea level scenarios are large mainly due to uncertainties in the future behaviour of the continental ice sheets.

Introduction

The design basis of new nuclear power plants is affected by risks caused by harsh weather conditions and extreme sea level. Some exceptional weather phenomena may also prevent normal power operation of a functioning plant and concurrently endanger its safe shutdown. Extreme weather events may affect, for example, the external power grid connection, emergency diesel generators (blockage of air intakes), ventilation and cooling of electrics rooms and functioning of heat removal chains to the sea.

Due to the influence of anthropogenic greenhouse gas emissions, climate is expected to continue changing during the coming decades. Accompanied with changes in the mean climate, there will be alterations worldwide in the occurrence of extreme weather events and in the global sea level e.g. [1]. Climate is projected to considerably alter in Finland as well [2]. This may have influence on the occurrence of relevant extreme weather events, with possible effects on the nuclear power plants.

The nuclear power plant units now in use, under construction or in design are planned to be operational for several decades, up to the 2070s or so. The risks caused by weather or climate are very often related to very rare situations, e.g. those typically occurring at a specific location once in 50 or 100 years or even less frequently, i.e. having a return (or recurrence) period of 50 years or longer. Because the available time series of weather observations are relatively short, estimation of return periods (or return levels corresponding to a specific return period) of highly unusual phenomena is very challenging. Besides, the on-going climate change may alter the limits of climate extremes. Therefore it is important to use not only past weather observations but also climate model simulations as study material of this project.

Main objectives

The overall objective of this research was to comprehensively analyse extreme weather events and sea level rise that are relevant for nuclear power plant safety in Finland. Studies about the frequency, intensity, and spatial and temporal variation of the extreme weather events and their combinations were carried out utilising instrumental meteorological observations, a 1 200-year long preindustrial

control simulation and future climate model simulations. Literature review and a few case studies were also performed. In addition to the role of natural climate variability, the study aimed to clarify the influence of human-induced climate change on extreme weather and sea levels. The future climate and sea level projections extend to the end of the 21st century.

More specifically, the project aimed to expand the knowledge about the occurrence and probabilities of the following extreme events and danger-causing weather phenomena: very high or low air temperature events having different durations, excess or scanty precipitation, high enthalpy, hail, freezing precipitation, heavy snowfall events in combination with high wind speed, strong winds caused by tornadoes and downbursts, and high sea levels along the Finnish coastline. A review was made about abrupt and nonlinear climate changes that might be triggered in the future by climate warming, with fatal consequences in continental to global scale. These include changes in the Atlantic thermohaline circulation and a significant global sea level rise caused by rapid melting of the continental ice sheets of the West Antarctic and Greenland. Because water level in the Baltic Sea is one of the prime factors from the view point of nuclear power plant safety in Finland, future scenarios were developed for the average and extreme sea level values along the Finnish coastline, as given in detail by [3].

Main results

Within the SAFIR2010/EXWE project in 2007–2010, a number of separate studies were conducted. References to them and their main outcomes have been gathered into a single aggregation report [4] and summarized here.

Extreme temperatures

Aiming at a consistent description of temporal and spatial variations of extreme temperatures in Finland, return levels of low and high temperatures were calculated for 24–30 weather stations located in different parts of the country, and the results were interpolated to a grid covering Finland [5].

Almost everywhere, except of the archipelago and the north-westernmost part of Lapland, the 50-year return level estimates are 31°C or higher for high instantaneous temperature (Figure 1, left). The return levels of the high temperatures are rather uniform geographically. In contrast, the return levels of low temperatures are 10–1°C colder in northern Finland than in the south (Figure 1, right).

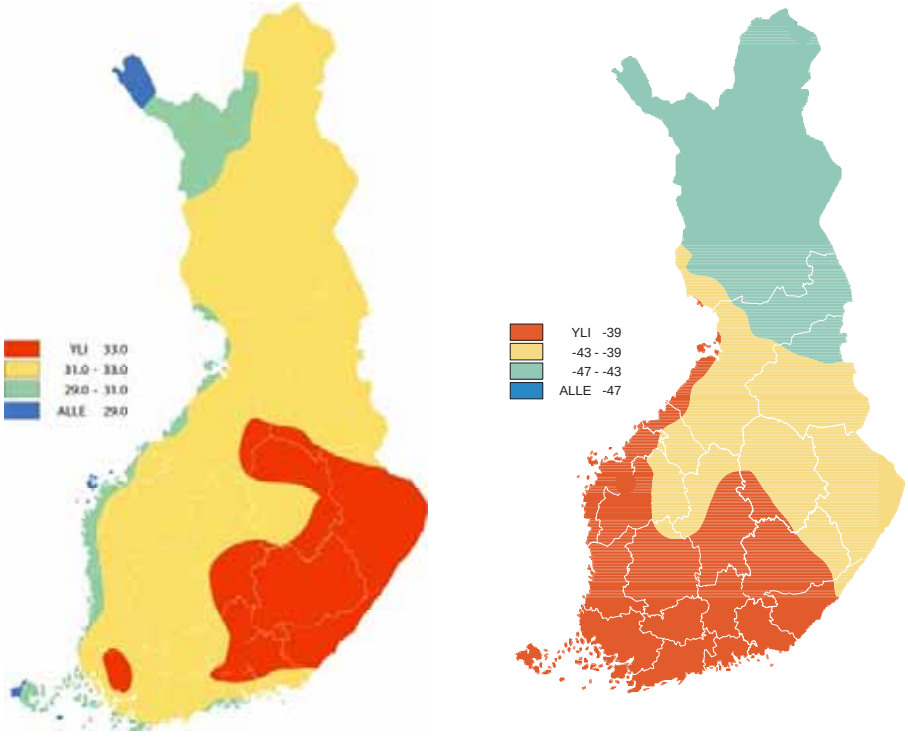

Figure 1. 50-year return level estimates of daily maximum (left) and daily minimum (right) temperatures in Finland. The number of weather stations included is 30 (left) or 24 (right) (adopted from [5]).

In order to extend the extreme event analysis to very rare events (occurring a few times per millennium) and to get better understanding of the natural climate variability, model output from a 1 200-year preindustrial control climate simulation was utilized. After corrections for systematic biases, these millennium-long time series allowed estimation of probabilities for extreme weather events in the current climate in a statistical material much wider than the observed data. To give an example, it was found that the 500-year return level estimate for an extreme 7-day average temperature was 24.0°C (with 95%-confidence interval of 23.6…24.6°C) in July and -30.2°C (-31.1…-29.3°C) in February over a grid box (300 km x 300 km) covering much of southern Finland.

According to future scenarios based on a set of about 20 global climate models, there will be a clear increase in the length of the longest hot spells in Finland. In a typical year, the longest hot spell (consecutive days with daily mean temperature above 20°C) lasts in the present climate less than five days in

southern and central Finland and two days in the north, and even in the warmest summers not more than two weeks. By the 2050s, the length of a typical hot spell is projected to increase on average to eight days in southern and central Finland and five in the north, while in extremely warm summers the longest hot spells can last over a month in southern Finland and up to 20 days in northern Finland.

In a set of three experiments by a regional climate model, daily maximum temperatures occurring on average every fifty years were projected to increase most in south-western Finland. By the end of the 21st century the increase may reach 4–5°C. The largest increases, however, were simulated for wintertime minimum temperatures. The 50-year return levels of cold temperatures may increase by 10°C or more in northern Finland by the end of the 21st century [6].

With temperatures increasing in wintertime, there will be an increase in the freezing point days, with daily minimum temperature below zero, and maximum temperature above zero. Thus, it will mean an increase in the freezing-melting cycles. At first, the freezing point days will become more frequent in the whole country. Towards the end of this century, they continue to increase in the north and east, but start to decrease in the southwest where temperature less frequently drops below zero. The mean annual number of freezing point days will then be larger than currently only locally in northern Finland [2].

Extreme precipitation and drought

Return levels of heavy precipitation events in the past climate were estimated based on observations made at 12 locations in different parts of the country [7, 8]. For monthly precipitation, the 100-year return level varied from 150 to 200 mm between the weather stations, and the 10-year return level between 121–157 mm. For daily precipitation, the 100-year return level was on average around 80 mm, and the 10-year return level around 55 mm. The highest 10-year return level estimates for monthly and daily precipitation amounts were found typically at the southern parts of the country and the lowest estimates in the northern parts.

Future precipitation amounts are projected to be larger than today [2]. The growth will be prominent in winter and weaker in summer. However, the change in precipitation patterns due to climate change is not as clear as in case of temperature. Future increase in wintertime precipitation is a consequence of different factors; besides the increase in the one-day precipitation amounts, the

days with precipitation are also projected to increase and the longest period of dry weather is projected to shorten. In summer, it is quite clear that the one-day precipitation amounts will increase; but on the contrary, the changes in the number of days with precipitation and the length of the longest dry spell are still uncertain [2].

Potentially danger-causing weather phenomena

An extensive overview of potentially dangerous weather phenomena in our country is presented in [9]. In addition, several studies about danger-causing weather phenomena and their occurrence in Finland have been conducted in EXWE [4] and references therein).

A tornado is a rotating column of air that extends from lower surface of a strong cumulonimbus cloud down to the surface of the earth or water and can cause very high winds locally. Only 14% of all tornadoes in Finland can be regarded strong enough to have remarkable influence on constructions (significant tornado, F2 or stronger). During the years 1930–2007 a F2-category or stronger tornado took place on average once in every two years somewhere in Finland. The highest risk over land is in July and over water covered surfaces (including both lakes and sea), in August. Most tornadoes in Finland have been observed in a zone which extends from the Gulf of Finland to the eastern parts of our country.

Downbursts are associated with strong thunderstorms and created by sinking air that hits the ground and spreads out, sometimes causing wind speeds comparable with tornadoes. Most downbursts in Finland occur in June to August, but it is difficult to estimate the probability of a downburst strike on certain area.

Hail cases are usually isolated, short-duration, and small-scale phenomena, and their occurrence depends not only on time of year and time of day but also on geographical location. Most severe-hail case observations in Finland have taken place in southern and western parts of our country because of the longer convective storm season and higher population density there compared to northern and eastern Finland [10]. However, large hail (over 2 cm in diameter) has been observed also as north as near 68.5°N latitude. During the years 1997–2006, an annual average of about 10 cases of severe hail (hail particles larger than 2 cm) occurred during 5 severe-hail days (a day with at least one severe-hail report in Finland). Nonetheless, interannual variation is notable in the number of severe-hail cases and severe-hail days per year.

A supercell is a cumulonimbus cloud that includes a deep rotating updraft called a mesocyclone and has a lifetime of several hours, lasting notably longer than conventional thunderstorms. Most supercells also cause severe weather such as downbursts, large hail or sometimes even tornadoes. Supercells occur in Finland on less than 10 days during a year.

Heavy snowfall events in combination with high wind speeds occur most often during December and January. Most profuse snowfall takes place in an occluded front in a low pressure system.

Freezing precipitation is rain or drizzle that occurs when the precipitation particles are supercooled and in liquid form. Freezing drizzle is typically observed somewhere in Finland about seven times during a year but freezing rain only once a year. About 30% of all cases in Finland are observed in January.

Combined extreme events

Combined extreme weather events were preliminary studied with the aid of the millennium control simulation mentioned above. A negative, statistically significant correlation was found between precipitation sum in June and mean temperature in July. Literature review and synoptic examinations indicated that combinations of extreme weather events are often connected over a large geographical scale and even with contrasting weather events. Their occurrences are greatly affected by anomalies of atmospheric air flows and oscillations like Arctic Oscillation (AO), North Atlantic Oscillation (NAO) and Atlantic Multidecadal Oscillation (AMO).

Sea level on the Finnish coast

A significant global sea level rise because of rapid melting of the continental ice sheets would pose a major threat for the safety of the nuclear power plants. Currently the largest uncertainty concerning the sea level in the Baltic Sea is related to the melting rate and extent of the West Antarctic ice sheet ([3] and references therein).

In the Gulf of Finland, the past declining trend of the mean sea level will probably not continue in the future, because the accelerating rise in the sea level will exceed the land uplift. In the Gulf of Bothnia, the land uplift will dominate over the sea level rise most probably in the near future. According to the average scenario for the year 2100, the mean water level will rise about 45 cm in

Helsinki and about 15 cm at Rauma, relative to the current situation. The uncertainty ranges are wide, however.

The short-term variations in the Baltic Sea level are driven mainly by wind, changes in air pressure and the seiche, the internal oscillation in the Baltic Sea. According to observations, the annual maximum sea levels show a significant increasing trend from the early 20th century up to the present. The extreme sea level values are prone to changes also in the future. Climate change can have an influence on the factors controlling the extreme sea level values, such as prevailing wind patterns or the routes of the low pressure systems. These effects have not been quantitatively studied so far. Thus changes in the extreme sea levels due to the mean sea level change alone have been assessed by [3]. Research studies about changes in global sea level rise are being updated continuously, and it is important to follow the latest results.

Abrupt and nonlinear climate change

Human induced global climate warming might trigger abrupt climate changes that could lead to fatal consequences in continental or even global scale [11, 12]. Abrupt climate changes are especially common when the climate system is being forced to change most rapidly and cross some threshold, a tipping point, triggering a transition to a new stage. The risk of abrupt climate changes grows the higher, the more the global mean temperature rises above the present.

Some of the possible abrupt climate changes could affect the safety of the nuclear power plants. The major concern is the possible abrupt sea level rise which could be triggered by changes in the Atlantic thermohaline circulation or by melting of continental ice sheets. Melting of the Arctic sea-ice would quite likely accelerate the melting of the Greenland ice sheet, too.

In the light of the latest simulations, it is very likely that the Atlantic thermohaline circulation will weaken during the 21st century. In simulations based on the A1B scenario the Atlantic thermohaline circulation would weaken on average by 25% (between 0 and 50% in different simulations). In spite of the reduction of the Atlantic thermohaline circulation the temperatures are projected to rise even in the North Atlantic area because the greenhouse gas induced global warming is so strong.

Both the Greenland and the Antarctic ice sheets have potential for self-amplifying ice loss mechanisms, which makes them particularly important when assessing risks of future sea level rise [11]. Water stored in the Greenland ice

sheet and the West Antarctic ice sheet is sufficient to raise global sea level by several meters [1].

Applications

One of the most important questions related to climate change is the influence of climate change on climate extremes. From the view point of nuclear power plant safety, the results of this study extend the knowledge about external risk caused by weather. Comprehensive information about natural variability of the extremes and their projected changes helps the licensees and authorities to make the current probabilistic safety analyses (PSA) of nuclear power plants more reliable and to identify needs for modifications of the plant and/or operating procedures. Regarding new power plant units, the results can be used for determining the design basis for extreme weather events. In addition to the direct impact on nuclear power plants, the simultaneous effects of extreme weather conditions on the infrastructure should be considered in emergency response planning.

Conclusions

The climate change is altering the occurrence of extreme weather events and levels of sea water. It may also trigger new potentially dangerous weather phenomena or nonlinear and abrupt changes. Though observations and climate models are excellent tools to examine past and future climate and sea level, there are still many research themes that need a large amount of future work.

When preparing oneself for extremities, one has a challenging task in trying to find the golden mean between the realistic yet sufficient preparedness and overestimation of the measures of precaution. For example, hail, snowstorms and freezing precipitation can have severe impacts on society. They can pose threat to power plants or electric power lines and therefore cause difficulties to distribution of electricity. However, studying these and other extreme weather phenomena is far less straightforward than estimating the average climate. Observations of extreme weather events are few in number, which hinders the reliable estimation of the likelihood of those events. Many of the studies conducted within EXWE emphasised particularly the importance of long and homogeneous observation time series as a base of reliable extreme value analysis [4].

Since climate change is likely to change the limits of climate extremes and sea level, it is important to use not only past weather observations but also climate

model simulations as study material. According to them, the daily maximum temperatures and the length of the longest hot spells will clearly increase in Finland. The largest changes, however, are projected for the wintertime minimum temperatures. During summer there will be more intensive precipitation events and during winter more frequent precipitation days. The mean sea level is projected to rise, the change depending on the location along the Finnish coastline. Uncertainty ranges in the mean sea level scenarios are large mainly due to uncertainties in the future behaviour of the continental ice sheets.

Regarding climate models, the use of as many models as possible side by side increases the validity of the future scenarios. A wide range of climate models helps to give more exact uncertainty ranges for the results. The scenarios for the future should be updated regularly, as more research is conducted, accumulating knowledge on the effect of global climate change on average climate, climate extremes and sea levels in Finland.

Acknowledgements

The 1200-year control climate simulation utilized in the EXWE project was run with a coupled atmosphere-ocean climate model ECHAM5/MPIOM at the FMI within the COmmunity earths System MOdelS (COSMOS) co-operation (http://cosmos.enes.org). Expertise and advices of Dr. Petri Räisänen, Dr. Heikki Järvinen and Dr. Johan Silén are acknowledged.

References

1. IPCC. Climate Change 2007. The Physical Science Basis. Contribution ofWorking Group I to the Fourth Assessment Report of the Intergovernmental Panel on Climate Change [Solomon, S.D., Manning, M., Chen, Z., Marquis, M., Averyt, K.B., Tignor, M. & Miller, H.L. (Eds.)]. Cambridge University Press, Cambridge, United Kingdom and New York, NY, USA, 2007.

2. Jylhä, K., Ruosteenoja, K., Räisänen, J., Venäläinen, A., Tuomenvirta, H., Ruokolainen, L., Saku, S. & Seitola, S. Arvioita Suomen muuttuvasta ilmastosta sopeutumis-tutkimuksia varten. ACCLIM-hankkeen raportti 2009 (The changing climate in Finland: estimates for adaptation studies. ACCLIM project report 2009.) Finnish Meteorological Institute, Reports 2009:4. (In Finnish, abstract, extended abstract and captions for figures and tables also in English.)

3. Johansson, M., Kahma, K. & Pellikka, H. Sea level scenarios and extreme events on the Finnish coast. Special report on the EXWE project in this volume.

4. Tietäväinen, H., Hutila, A., Jylhä, K., Johansson, M., Kahma, K., Mäkelä, M., Pellikka, H., Pimenoff, N., Rauhala, J., Ruosteenoja, K., Saku, S. & Venäläinen, A. Extreme weather and nuclear power plants in present and future climate. EXWE Aggregation Report, Finnish Meteorological Institute, 2011.

5. Saku, S., Solantie, R., Jylhä, K. & Venäläinen, A. Äärilämpötilojen alueellinen vaihtelu Suomessa (Spatial variations of extreme temperatures in Finland). Finnish Meteorological Institute, Reports 2011:1. (In Finnish, abstract in English.)

6. Venäläinen, A., Saku, S., Jylhä, K., Nikulin, G., Kjellström, E. & Bärring, L. Extreme temperatures and enthalpy in Finland and Sweden in a changing climate. NKS-194. NKS Secretariat, NKS-776, DK-4000 Roskilde, Denmark, 2009.

7. Venäläinen, A., Saku, S., Kilpeläinen, T., Jylhä, K., Tuomenvirta, H., Vajda, A., Räisänen ,J. & Ruosteenoja, K. Sään ääri-ilmiöistä Suomessa. (Aspects about climate extremes in Finland.) Finnish Meteorological Institute, Reports 2007:4. (In Finnish with abstract in English.)

8. Venäläinen, A., Jylhä, K., Kilpeläinen, T., Saku, S., Tuomenvirta, H., Vajda, A. & Ruosteenoja, K. Recurrence of heavy precipitation, dry spells and deep snow cover in Finland based on observations. Boreal Environment Research, 2009. Vol. 14, pp. 166–172.

9. Gregow, H., Venäläinen, A., Laine, M., Niinimäki, N., Seitola, T., Tuomenvirta, H., Jylhä, K., Tuomi, T. & Mäkelä, A. Vaaraa aiheuttavista sääilmiöistä Suomen muuttuvassa ilmastossa. (Danger-causing weather phenomena in changing Finnish climate) Ilmatieteen laitos, Reports 2008:3. (In Finnish, with abstract in English.)

10. Tuovinen, J.-P., Punkka, A.-J., Rauhala, J. & Hohti, H. Climatology of Severe Hail in Finland: 1930–2006. Monthly Weather Review 2009, Vol. 137, pp. 2238–2249.

11. Levermann, A., Bamber, J., Drijfhout, S., Ganopolski, A., Haeberli, W., Harris, N.R.P., Huss, M., Krüger, K., Lenton, T., Lindsay, R.W., Notz, D., Wadhams, P. & Weber, S. Climatic Tipping Elements with potential impact on Europe. Technical Paper No. 3 to the 'State of the Environment Report 2010' of the European Environmental Agency, 2010.

12. Pimenoff, N., Venäläinen, A., Pilli-Sihvola, K. Tuomenvirta, H., Järvinen, H., Ruosteenoja, K., Haapala, J. & Räisänen, J. Epälineaariset ja äärimmäiset ilmaston muutokset. Selvitys Vanhasen II hallituksen tulevaisuusselontekoa varten. Valtioneuvoston kanslian julkaisusarja 14/2008.

33.2 Sea level scenarios and extreme events on the Finnish coast

Milla Johansson, Kimmo Kahma and Hilkka Pellikka
Finnish Meteorological Institute

Abstract

The global sea level is rising due to thermal expansion of sea water and melting of land-based glaciers. The range of predicted global average sea level rise during this century is 20–200 cm. The uncertainties are large, mainly due to uncertainties in the behaviour of the West Antarctic and Greenland ice sheets in a warming climate. The rise is not geographically uniformly distributed, and the estimated effect on the Finnish coast is 30–150 cm during this century. The actual sea level change on the coast is also affected by postglacial land uplift and changes in the Baltic Sea water balance – controlled by in- and outflow of water through the narrow Danish Straits. Taking all these factors into account, the scenarios predict accelerating sea level rise in the Gulf of Finland. At Helsinki, for instance, the sea level will rise 45 cm up to year 2100 according to the average scenario. The coasts of the Bay of Bothnia will suffer less of the sea level rise, due to stronger land uplift. At Rauma, the sea level will rise 15 cm according to the average scenario. The highest scenarios for the Finnish coast predict a 75 cm higher sea level rise than the average scenario during this century.

The short-term sea level variability in the Baltic Sea is mainly controlled by wind and air pressure changes. An extreme sea level event is always a result of several concurrent factors – a high water amount in the Baltic Sea, low air pressure, and wind blowing towards the coast, as well as a suitably phased internal sea level oscillation in the Baltic Sea. This kind of situation occurred in January 2005, raising sea level to record heights on the Finnish coast of the Gulf of Finland. The extreme sea levels will change in the future – mainly due to changes in the mean sea level, but possibly also affected by changes in the weather phenomena. For instance, the monthly maximum occurring at a rate of 0.01 occurrences/year is currently 142 cm at Helsinki, and will rise to 163 cm in 2050 and 258 cm in 2100.

Introduction

The sea level is an important issue for the safety of the Finnish nuclear power plants, which are all located on the coast. Extremely high or low sea levels may cause problems in the power plant operations, and the probabilities of their occurrence should be taken into account in the safety analyses of the plants. Especially when the design bases for the new power plants are defined, scenarios for sea level during the planned lifetime of the power plant are important.

The sea levels on the nuclear power plant sites have been examined in several studies since the 1990s [1, 2]. In SAFIR2010/EXWE, the mean sea level scenarios as well as probabilities of extreme events were studied [3, 4, 5]. The sea level behaviour on the Finnish coast was studied in more detail in [6], and scenarios for the long-term mean sea level presented in [7].

The mean sea level on the Finnish coast is changing with time. Two factors counteract each other – the sea level rise and the local postglacial land uplift. The global sea level rise is accelerating due to the climate change, and this rise also affects the Baltic Sea, which is connected to the oceans through the narrow Danish Straits. During the last 2–3 years, predictions of high sea level rises, up to 200 cm as a global average in this century, have appeared in the scientific literature. As the sea level rise is currently an area of active research, the scenarios for the Finnish coast should be regularly updated to accommodate the latest scientific knowledge on sea level behaviour in the warming climate. In this study, we present scenarios for the sea level on the Finnish coast up to year 2100.

The short-term sea level variability on the Baltic Sea is mainly controlled by weather phenomena. The occurrence of extreme sea levels, and future changes in their occurrence, are a combination of changes in the mean sea level as well as possible changes in the weather phenomena. In this study, we present probabilities for extremely high sea levels in the future.

Scenarios for mean sea level on the Finnish coast

Global sea level rise and its impact on the Baltic Sea

According to several recent studies, estimates for the global average sea level rise during this century range from 20 to 200 cm (Figure 1). The sea level rise is mainly caused by thermal expansion of sea water and melting of land-based glaciers, both resulting from the global warming. There are still large uncertainties,

especially concerning the behaviour of the continental ice sheets of Greenland and West Antarctica in a warming climate.

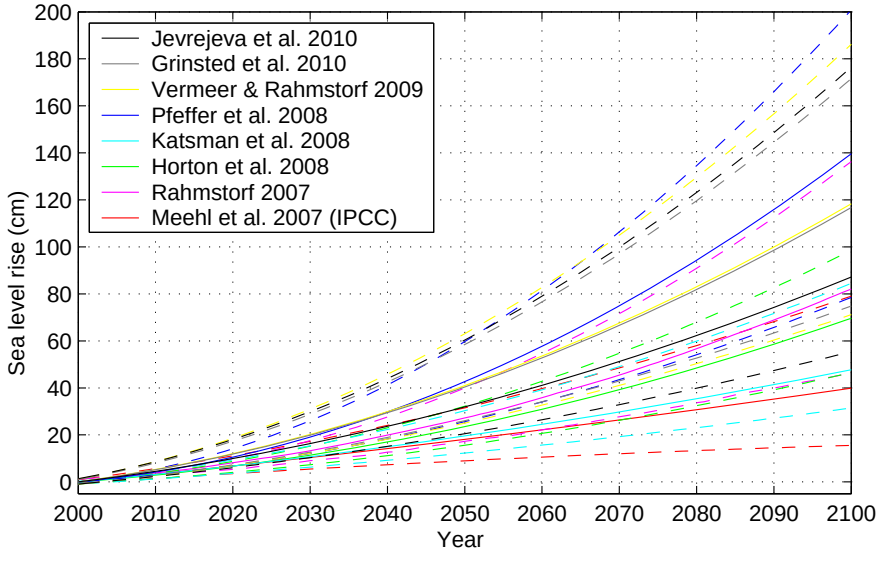

Figure 1. Scenarios for the global average sea level rise, based on recent scientific papers [8, 9, 10, 11, 12, 13, 14, 15].

The sea level rise is not geographically evenly distributed. The effect of thermal expansion varies in different areas. The meltwater from large ice sheets is also unevenly distributed. A large ice mass attracts sea water by gravitation. When the ice mass melts away, the attraction is relieved and sea water retreats away from the melting glacier [16]. Thus, melting of the Greenland ice sheet will not cause a large sea level rise on the Finnish coast – the estimated maximum effect is slightly more than 10 cm up to 2100. On the contrary, melting of the West Antarctic ice sheet would have larger effect on the Finnish coast. We combined the knowledge on these effects and made an expert judgement about the relevance of different scenarios (Figure 1) for the Finnish coast [5]. The predicted effect of the sea level rise will be 30–150 cm up to 2 100, compared to the global average of 20–200 cm. This is a conservative estimate, making worst-case assumptions on some uncertainties. Based on an expert judgement the maximum effect on the Finnish coast will be less than 150 cm. Since a possible overestimation of the risk was considered a safer choice for a nuclear power plant, we chose to use the conservative rather than the best estimate.

Scenarios for the Finnish coast

On the Finnish coast, the sea level rise is counterbalanced by the postglacial land uplift. The rate of land uplift is 30–90 cm in a century on the Finnish coast, being strongest around Vaasa in the Bothnian Sea, and weakest in the eastern part of the Gulf of Finland. Sea level is also affected by changes in the Baltic Sea water balance on a time scale of decades. The amount of water in the semi-enclosed Baltic Sea varies considerably, the variations being caused by in- and outflow of water through the narrow Danish Straits connecting the Baltic Sea to the North Sea.

Taking all these factors into account, sea level scenarios for the Finnish coast were calculated in [5], based on a method from [7]. A few examples of these scenarios are presented in Figures 2 and 3. In the Gulf of Finland, the sea level has been declining in relation to the bedrock during the past decades. In future, the accelerating sea level rise will generally exceed the land uplift, and sea level in relation to the bedrock will rise at an accelerating rate. In the Bay of Bothnia, the land uplift might still balance the sea level rise in the near future, although the highest scenarios predict an accelerating sea level rise even in the Bay of Bothnia.

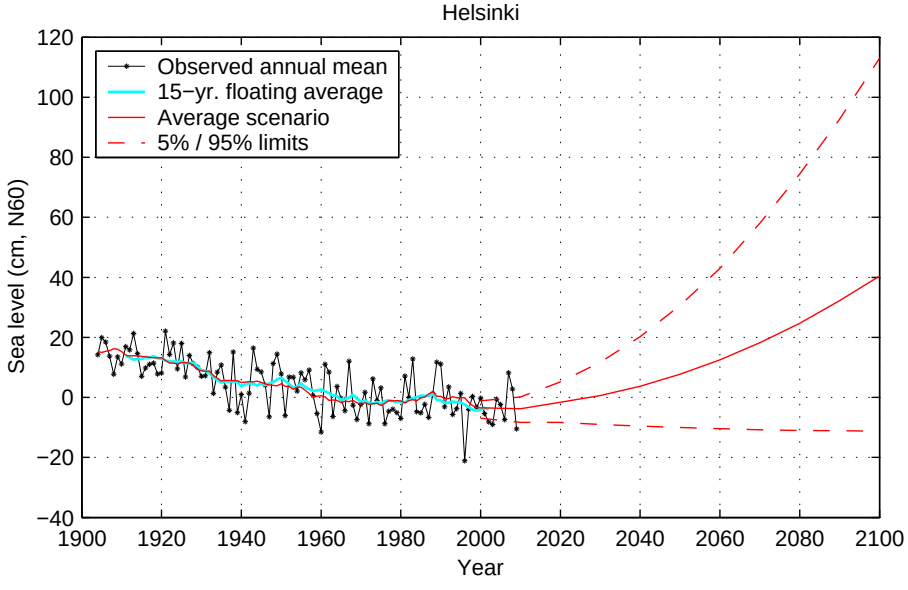

Figure 2. Observed annual mean sea levels in the 20th century and scenarios (conservative estimate) up to 2100 at Helsinki.

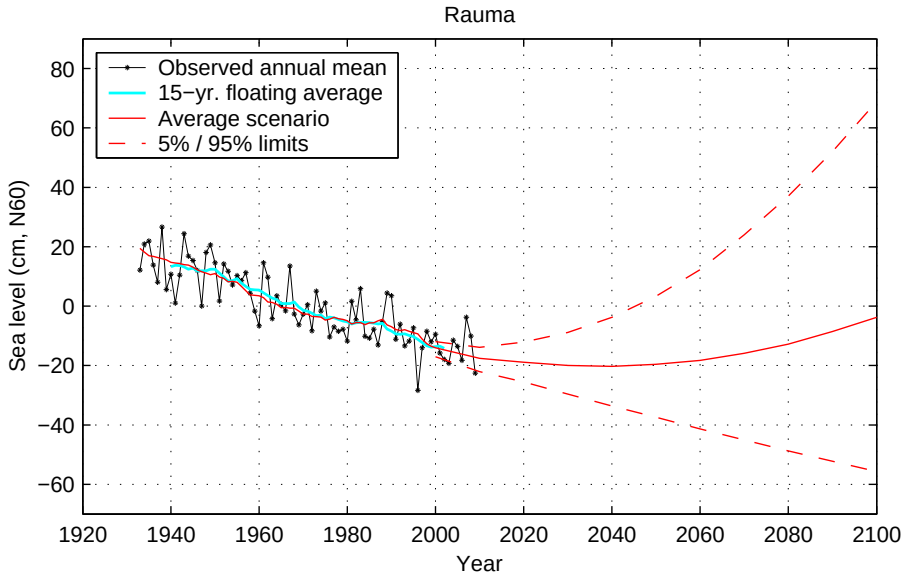

Figure 3. Observed annual mean sea levels in the 20th century and scenarios (conservative estimate) up to 2100 at Rauma.

Extreme sea level events

The short-term sea level variability in the Baltic Sea is mainly controlled by wind and air pressure changes. Winds push water into the gulfs and against coastlines. The sea level rises under a low air pressure. In addition, the sea level oscillates back and forth inside the Baltic Sea, the oscillations being induced by the effects of wind or air pressure. Due to the nature of these effects, most extreme sea levels tend to occur at the closed ends of the Bay of Bothnia and Gulf of Finland. The highest observed sea level at Kemi since 1922 is +201 cm, and at Hamina since 1928 +197 cm, in relation to the theoretical mean sea level. The smallest variability is observed at Föglö in Åland, where the observed maximum is +102 cm since 1923.

An extremely high sea level event is always a result of several concurrent factors – a high water amount in the Baltic Sea, low air pressure, wind blowing towards the coast, as well as a suitably phased internal sea level oscillation. All these factors were acting on January 2005, when a storm passed over the Baltic Sea, raising sea level to record heights on the Finnish coast of the Gulf of Finland. At Helsinki, a sea level of +151 cm was reached, and at Hamina +197 cm.

It is possible that even higher sea levels occur in the Gulf of Finland as a result of a severe storm.

Changes in the extreme events

The sea level maxima have increased from the early 20th century up to the present. For instance at Helsinki, the annual maximum sea levels – in relation to the mean sea level – show an increasing trend of 20 cm in 100 years. The effects of climate change on short-term sea level variability have not yet been studied adequately to assess the possible trends or changes in the future.

Although the future changes in the extreme events themselves are still unsolved, it is apparent that from a land-fast point of view, the extremes are also changing as the mean sea level changes. These changes have been studied based on the mean sea level scenarios presented above.

Probabilities of extreme sea levels on the Finnish coast

The sea level has been recorded on the Finnish coast at 1–4 hour resolution since the late 19th century. These century-long time series allow us to calculate probability distributions for extreme sea levels that occur at a rate of 0.01 occurrences/year or more. When considering the risk estimates of a nuclear power plant, however, extreme events with much smaller occurrence rates are interesting, up to 10-8 occurrences/year. Estimates for such rare events were extrapolated from the observed probability distributions. Figure 4 shows probabilities of extreme sea levels at Helsinki.

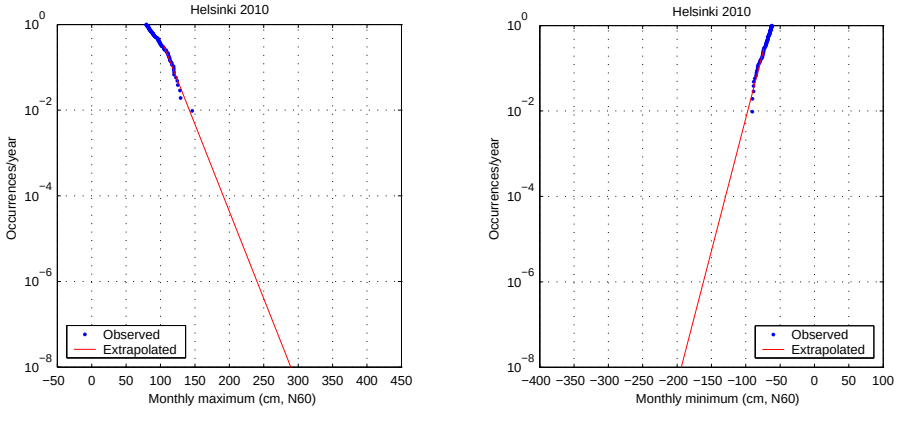

Figure 4. Probability distributions for monthly maximum and minimum sea levels at Helsinki in the present conditions.

The probability distribution of the short-term variability can be combined with the mean sea level scenarios, taking into account the probability of each scenario (5% and 95% limits shown in Figures 2 and 3). This yields combined probabilities for the future occurrence of extremely high sea levels. In Table 1, sea levels occurring with a probability of 0.01 occurrences/year are presented for the Finnish coast in the present situation as well as in the future. The rate of 0.01 occ./year should not be interpreted in such a way that the sea level value would occur once in the next 100 years. Due to the constantly changing situation, the occurrence rates are only applicable for a single year. Further calculations are needed to obtain a sea level that would occur once during a given calendar period.

Table 1. Monthly maximum sea levels corresponding to the probability of 0.01 occurrences/year on the Finnish coast, in the height system N60, for different years [5].

	2010	*2050*	*2100*		*2010*	*2050*	*2100*
Site	*Sea level (cm, N60)*			*Site*	*Sea level (cm, N60)*		
Kemi	182	177	229	Rauma	111	120	203
Oulu	172	169	228	Turku	123	136	223
Raahe	139	135	200	Föglö	102	115	204
Pietarsaari	115	114	183	Hanko	122	139	232
Vaasa	120	115	177	Helsinki	142	163	258
Kaskinen	121	118	183	Hamina	194	213	299
Mäntyluoto	110	113	189				

Conclusions

The postglacial land uplift counteracts the sea level rise on the Finnish coast. On the southern coast, the sea level will rise 30–50 cm during this century, while on the Bay of Bothnia the land uplift still balances the sea level rise, and the sea level will decline up to mid-century and rise back to present sea level or below it up to the end of the century. The uncertainties are large, and the highest scenarios predict a 75 cm higher rise than the average scenarios, while the lowest scenarios remain 55 cm below the average scenario.

We have calculated a conservative scenario, in which the aim is to avoid underestimating the risk of the sea level rise. Thus, it predicts slightly higher sea level rise than the best estimate scenario would. It is applicable for situations

where an underestimation might result to higher costs or damages than an overestimation. Thus, it is a safe choice for the risk estimates of the nuclear power plants.

The extreme sea levels change as the mean sea level changes. There might also be changes in the nature of the extreme events themselves – due to climate change for instance, but these have not been studied adequately. Due to the mean sea level rise, as well as the large uncertainties in the mean sea level scenarios, extremely high sea levels will be more probable in the future than in the present conditions on the Finnish coast.

Our sea level scenarios extend up to year 2100. In the more distant future, the uncertainties especially in the behaviour of the continental ice sheets grow large, and no reliable scenarios can be presented.

References

1. Kahma, K., Alenius, P., Boman, H. & Vuorinen, I. Meriveden korkeus, aallot, lämpötila, suolaisuus ja biologinen kasvusto Loviisan rannikolla seuraavien 20–50 vuoden aikana Merentutkimuslaitos, 1990. (In Finnish.)

2. Kahma, K., Johansson, M. & Boman, H. Meriveden pinnankorkeuden jakauma Loviisan ja Olkiluodon rannikoilla seuraavien 30 vuoden aikana. Merentutkimuslaitos, 2001. (In Finnish.)

3. Johansson, M., Kahma, K., Kangas, A., Pellikka, H. & Boman, H. Meriveden pinnankorkeuden ääri-ilmiöt Loviisan ja Olkiluodon rannikoilla. Merentutkimuslaitos, 2008. (In Finnish.)

4. Johansson, M., Kahma, K. & Pellikka, H. Meriveden pinnankorkeuden skenaariot ja lyhytaikaisvaihtelut. Ilmatieteen laitos, 2010. (In Finnish.)

5. Johansson, M., Kahma, K. & Pellikka, H. Meriveden pinnankorkeuden ja lyhytaikaisvaihteluiden skenaariot Suomen rannikolla. Ilmatieteen laitos, 2011. (In Finnish.)

6. Johansson, M., Boman, H., Kahma, K.K. & Launiainen, J. Trends in sea level variability in the Baltic Sea. Boreal Environment Research 2001, 6, pp. 159–179.

7. Johansson, M.M., Kahma, K.K., Boman, H. & Launiainen, J. Scenarios for sea level on the Finnish coast. Boreal Environment Research 2004, 9, pp. 153–166.

8. Jevrejeva, S., Moore, J.C. & Grinsted, A. How will sea level respond to changes in natural and anthropogenic forcings by 2100? Geophysical Research Letters 2010, 37, 7, L07703.

9. Grinsted, A., Moore, J.C. & Jevrejeva, S. Reconstructing sea level from paleo and projected temperatures 200 to 2100 AD. Climate Dynamics 2010, 34, 4, pp. 461–472.

10. Vermeer, M. & Rahmstorf, S. Global sea level linked to global temperature. Proceedings of the National Academy of Sciences 2009, 106, 51, pp. 21527–21532.

11. Pfeffer, W.T., Harper, J.T. & O'Neel, S. Kinematic constraints on glacier contributions to 21st-century sea level rise. Science 2008, 321, 5894, pp. 1340–1343.

12. Katsman, C.A., Hazeleger, W., Drijfhout, S.S., van Oldenborgh, G.J. & Burgers, G.J.H. Climate scenarios of sea level rise for the northeast Atlantic Ocean: a study including the effects of ocean dynamics and gravity changes induced by ice melt. Climatic Change 2008, 91, 3, pp. 351–374.

13. Horton, R., Herweijer, C., Rosenzweig, C., Liu, J., Gornitz, V. & Ruane, A.C. Sea level rise projections for current generation CGCMs based on the semi-empirical method. Geophysical Research Letters 2008, 35, L02715.

14. Rahmstorf, S. A semi-empirical approach to projecting future sea-level rise. Science 2007, 315, 5810, pp. 368–370.

15. Meehl, G.A., Stocker, T.F., Collins, W.D., Friedlingstein, P., Gaye, A.T., Gregory, J.M., Kitoh, A., Knutti, R., Murphy, J.M., Noda, A., Raper, S.C.B., Watterson, I.G., Weaver, A.J. & Zhao, Z.-C. Global Climate Projections. In: Climate Change 2007: The Physical Science Basis. Contribution of Working Group I to the Fourth Assessment Report of the Intergovernmental Panel on Climate Change [Solomon et al. (Eds.)]. Cambridge University Press, Cambridge, UK and New York, NY, USA, 2007.

16. Mitrovica, J.X., Tamisiea, M.E., Davis, J.L. & Milne, G.A. Recent mass balance of polar ice sheets inferred from patterns of global sea-level change. Nature 2001, 409, 6823, pp. 1026–1029.

Series title, number and
report code of publication

VTT Research Notes 2571
VTT-TIED-2571

Author(s)
Eija Karita Puska & Vesa Suolanen (Eds.)

Title

SAFIR2010
The Finnish Research Programme on Nuclear Power Plant Safety 2007–2010. Final Report

Abstract

Major part of Finnish public research on nuclear power plant safety during the years 2007–2010 has been carried out in the SAFIR2010 programme. The steering group of SAFIR2010 consisted of representatives from Radiation and Nuclear Safety Authority (STUK), Ministry of Employment and the Economy (MEE), Technical Research Centre of Finland (VTT), Teollisuuden Voima Oyj (TVO), Fortum Power and Heat Oyj, Fortum Nuclear Services Oy (Fortum), Finnish Funding Agency for Technology and Innovation (Tekes), Aalto University School of Science and Technology (Aalto, former Helsinki University of Technology) and Lappeenranta University of Technology (LUT). In addition to representatives of these organisations, the Steering Group had permanent experts from the Swedish Radiation Safety Authority (SSM) and Fennovoima Oy (Fennovoima).

SAFIR2010 research programme was divided in eight research areas that were Organisation and human, Automation and control room, Fuel and reactor physics, Thermal hydraulics, Severe accidents, Structural safety of reactor circuit, Construction safety, and Probabilistic Safety Analysis (PSA).

Research projects of the programme were chosen on the basis of annual call for proposals. The annual volume of the SAFIR2010-programme in 2007–2010 has been 6,5–7,1 M€ and approximately 50 person years. Main funding organisations in 2007–2010 have been the State Waste Management Fund VYR with 2,7–3,0 M€ and VTT with 2,4–2,7 M€ annually. In 2010 research was carried out in 33 projects.

The research in the programme has been carried out primarily by VTT Technical Research Centre of Finland. Other research units responsible for the projects solely or in co-operation with other institutions include Lappeenranta University of Technology, Aalto University (previously Helsinki University of Technology), Tampere University of Technology, Fortum Power and Heat Oy (previously Fortum Nuclear Services Oy), Finnish Institute of Occupational Health and Finnish Meteorological Institute. In addition, there have been a few minor subcontractors in some projects.

The programme management structure consisted of the steering group, a reference group in each of the eight research areas and a number of ad hoc groups in the various research areas.

This report gives a summary of the technical results of the SAFIR2010 programme from the entire programme with emphasis on the results achieved during the years 2009–2010. The results obtained during the years 2007–2008 have been reported in detail in the Interim Seminar Report.

ISBN
978-951-38-7689-0 (soft back ed.)
978-951-38-7690-6 (URL: http://www.vtt.fi/publications/index.jsp)

Series title and ISSN	Project number
VTT Tiedotteita – Research Notes 1235-0605 (soft back ed.) 1455-0865 (URL: http://www.vtt.fi/publications/index.jsp)	41204

Date	Language	Pages
February 2011	English	578 p.

Name of project	Commissioned by
SAFIR2010	TEM

Keywords	Publisher
nuclear safety, safety management, nuclear power plants, human factors, automation systems, operating practices, control room technology, nuclear fuels, reactor physics, thermal hydraulics, core transient analysis, steam generators, modelling, accidents, structural safety	VTT Technical Research Centre of Finland P.O. Box 1000, FI-02044 VTT, Finland Phone internat. +358 20 722 4520 Fax +358 20 722 4374

SAFIR2010

Major part of the Finnish public research on nuclear power plant safety during the years 2007–2010 has been carried out in the SAFIR2010 programme. The steering group of SAFIR2010 has consisted of representatives from Radiation and Nuclear Safety Authority (STUK), Ministry of Employment and the Economy (MEE), Technical Research Centre of Finland (VTT), Teollisuuden Voima Oyj (TVO), Fortum Power and Heat Oyj, Fortum Nuclear Services Oy (Fortum), Finnish Funding Agency for Technology and Innovation (Tekes), Aalto University School of Science and Technology (Aalto, former Helsinki University of Technology) and Lappeenranta University of Technology (LUT). In addition to representatives of these organisations, the Steering Group had permanent experts from the Swedish Radiation Safety Authority (SSM) and Fennovoima Oy (Fennovoima).

SAFIR2010 research programme has been divided in eight research areas that are Organisation and human, Automation and control room, Fuel and reactor physics, Thermal hydraulics, Severe accidents, Structural safety of reactor circuit, Construction safety, and Probabilistic Safety Analysis (PSA).

Research projects of the programme were chosen on the basis of annual call for proposals. The annual volume of the SAFIR2010-programme in 2007–2010 has been 6,5–7,1 M€and approximately 50 person years. Main funding organisations in 2007–2010 have been State Waste Management Fund VYR with 2,7–3,0 M€and VTT with 2,4–2,7 M€annually. In 2010 research was carried out in 33 projects.

The research in the programme has been carried out primarily by VTT Technical Research Centre of Finland. Other research units responsible for the projects solely or in co-operation with other institutions include Lappeenranta University of Technology, Aalto University (previously Helsinki University of Technology), Tampere University of Technology, Fortum Power and Heat Oy (previously Fortum Nuclear Services Oy), Finnish Institute of Occupational Health and Finnish Meteorological Institute. In addition, there have been a few minor subcontractors in some projects. This report gives a summary of the technical results of the SAFIR2010 programme from the entire programme with emphasis on the results achieved during the years 2009–2010.

ISBN 978-951-38-7689-0 (soft back ed.)
ISSN 1235-0605 (soft back ed.)
ISBN 978-951-38-7690-6 (URL: http://www.vtt.fi/publications/index.jsp)
ISSN 1455-0865 (URL: http://www.vtt.fi/publications/index.jsp)